

Scientific Award
(Listed in order of presentation)

Brain & Neurorehabilitation

발표일시 및 장소 : 10 월 25 일(금), 13:40 ~ 15:10 , Room A

OPS-1

Effect of Electroencephalography-based Neurofeedback of Upper Limbs in Patients with Stroke

Seungwoo Cha^{1*}, Kyoung Tae Kim², Won Kee Chang³, Nam-Jong Paik³, Hyunmi Lim⁴, Won-Seok Kim^{3†}, Jeonghun Ku⁴

Department of Rehabilitation Medicine, University of Ulsan College of Medicine, Asan Medical Center¹, Department of Rehabilitation Medicine, Keimyung University School of Medicine, Keimyung University Dongsan Hospital², Department of Rehabilitation Medicine, Seoul National University College of Medicine, Seoul National University Bundang Hospital³, Department of Biomedical Engineering, Keimyung University⁴

Objective

The primary aim of this study was to explore the neurophysiological effects of neurofeedback training using EEG, specifically focusing on mu suppression, and to assess its potential benefits in subacute stroke patients.

Methods

Sixteen patients with hemiplegia following subacute ischemic or hemorrhagic stroke were prospectively enrolled in this randomized cross-over study. The study consisted of two experiments: neurofeedback and sham. Each experiment included four blocks: three blocks of resting, grasp, and intervention, followed by one block of resting and grasp. During the resting sessions, participants fixated on a white cross on a black background for 2 minutes without moving their upper extremities. In the grasp sessions, participants were instructed to grasp and release their paretic hand at a frequency of about 1 Hz for 3 minutes while fixating on the same white cross. During the intervention sessions, neurofeedback involved presenting a boxing image corresponding to the mu suppression induced by imagined movement, while the sham condition involved viewing a pre-recorded movie for 3 minutes. EEG data were collected from 19 dry electrodes using a DSI-24 system (Wearable Sensing, San Diego, USA).

Results

During the neurofeedback intervention, significant mu suppression was observed in the ipsilesional hemisphere, a phenomenon not evident during the sham intervention. Additionally, during the grasp sessions following neurofeedback, a progressive strengthening of mu suppression was noted across sessions. In contrast, the sham experiment showed no significant changes in mu suppression during the grasp sessions.

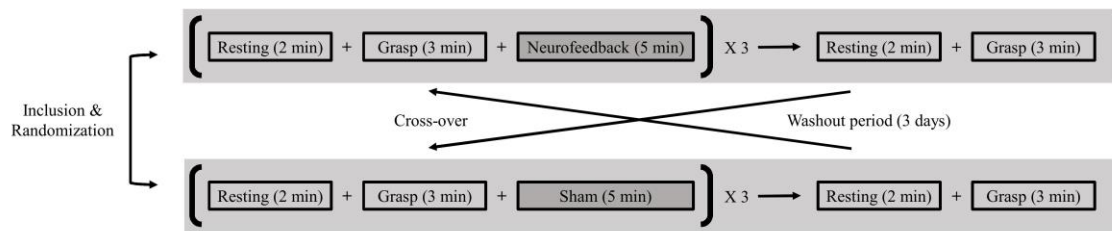
Conclusion

Neurofeedback training elicited substantial mu suppression in the ipsilesional hemisphere of subacute stroke patients, which was sustained during subsequent grasp tasks. This suggests that neurofeedback may enhance motor-related cortical activity, offering a promising adjunctive therapy for motor rehabilitation in stroke patients.

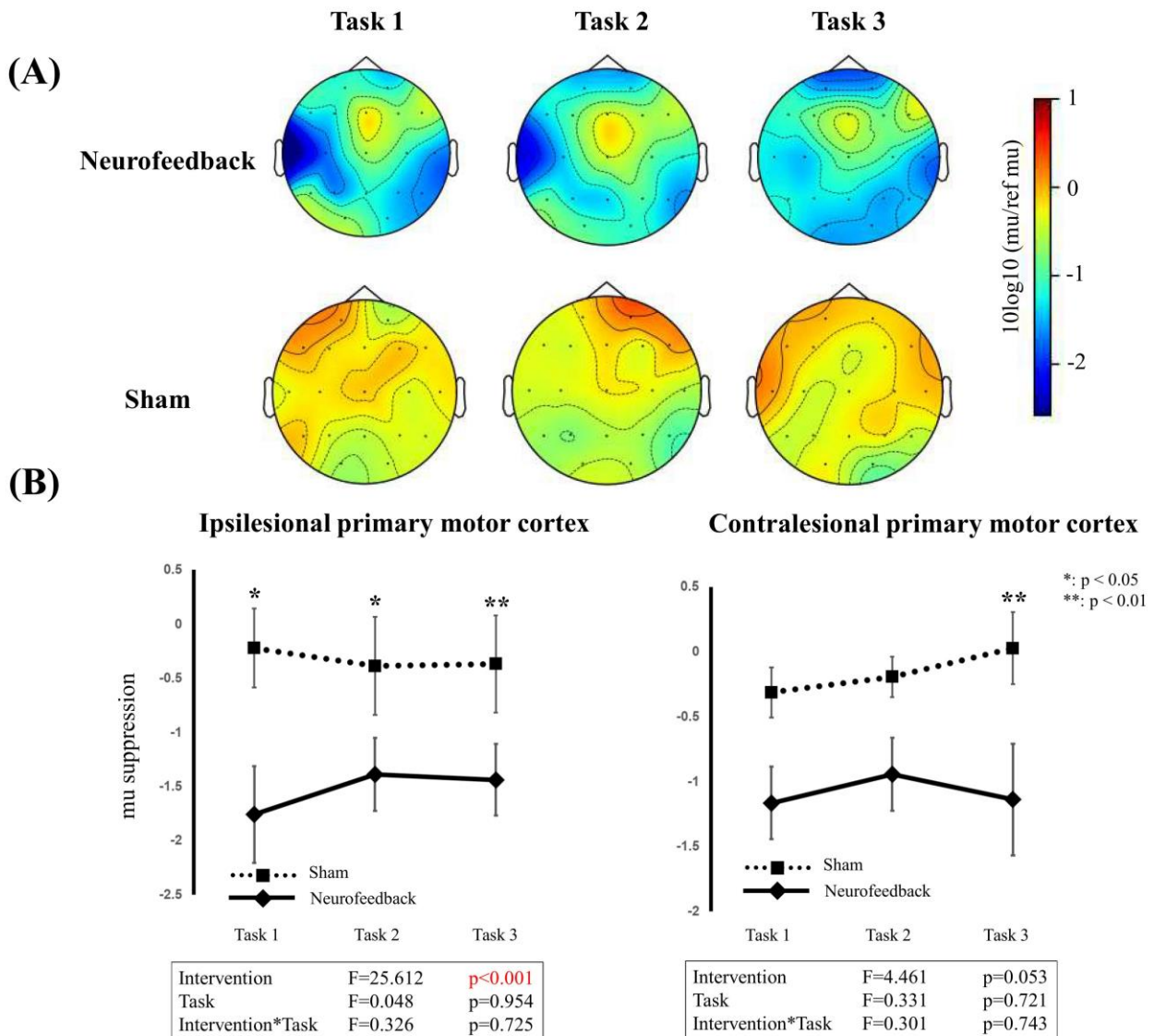
(A)



(B)

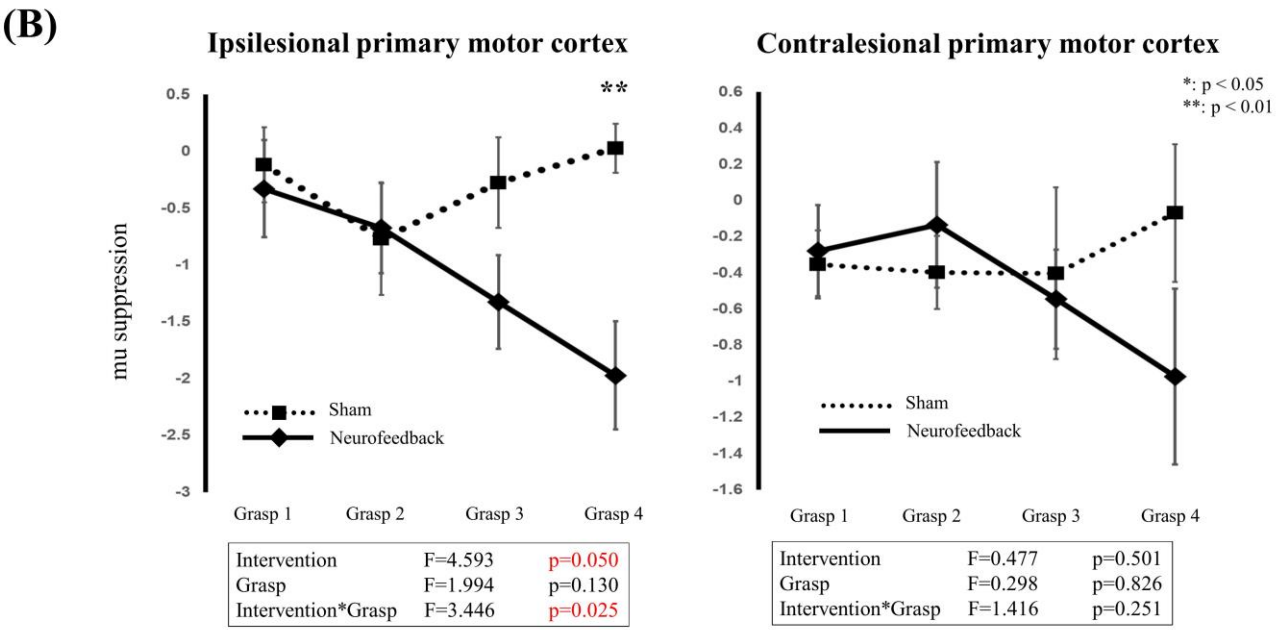
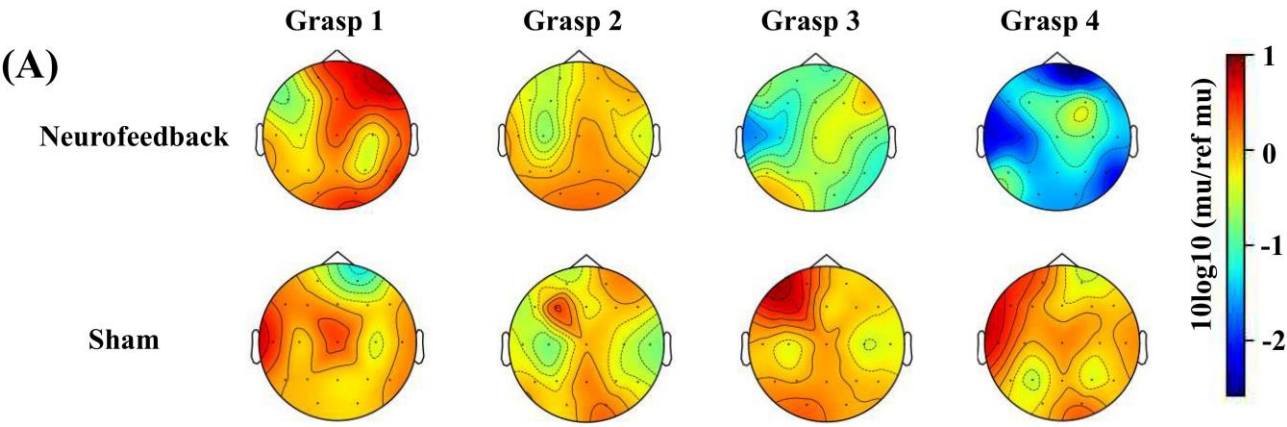


(A) A participant engaged in the neurofeedback intervention. (B) Study design.



(A) Topography of mu suppression in electroencephalography during intervention. (B) Line

charts for mu suppression of ipsilesional and contralesional primary motor cortex during intervention.



(A) Topography of mu suppression in electroencephalography during grasp. (B) Line charts for mu suppression of ipsilesional and contralesional primary motor cortex during grasp.

Brain & Neurorehabilitation

발표일시 및 장소 : 10 월 25 일(금), 13:40 ~ 15:10 , Room A

OPS-2

Efficacy of Robotic Gait Rehabilitation in Chronic Stroke patients: A Study with End-Effector Robot

Jiae Kim^{1*}, Ji Hye Kim¹, Young Hoon Mo¹, Jung Hwa Do¹, Dae Yul Kim^{1†}

Department of Rehabilitation Medicine, Asan Medical Center¹

Background

The clinical efficacy of robotic-assisted gait training (RAGT) in chronic stroke patients remains underexplored despite high rehabilitation needs. Previous studies have established the benefits of RAGT in acute and subacute stroke populations but have shown limited effectiveness in chronic cases. This study aims to evaluate the therapeutic impact of the end-effector robot on gait and lower limb functions in chronic stroke patients compared to conventional rehabilitation therapy.

Methods

This study was a single-center, evaluator-blinded, randomized controlled trial. A total of 44 chronic stroke patients aged 19 years or older, with stroke onset of 6 months or more, and a Functional Ambulatory Category (FAC) score of 3 or less were enrolled. Participants were randomly assigned to a control group, in which patients received conventional rehabilitation therapy, or an intervention group, in which patients received 30-minute sessions of RAGT using end-effector robot, three times a week for 8 weeks, utilizing high-intensity interval training protocols. The primary outcome measure was gait speed assessed by the 10-meter Walk Test (10MWT). Secondary outcome measures included gait ability (FAC), balance (Berg Balance Scale, BBS), walking distance (2-minute Walk Test, 2MWT), lower limb function (Fugl-Meyer Assessment of Lower Extremity, FMA-LE), cardiopulmonary function (VO₂max), activities of daily living (modified Barthel Index, K-MBI), and body composition.

Results

A total of 18 participants in the control group and 19 participants in the robot group completed the study. At baseline, there were no significant differences in age, weight, or stroke onset between the groups. In the robot group, 10MWT significantly improved from 0.38 ± 0.23 m/s to 0.55 ± 0.30 m/s (p

Conclusion

RAGT using end-effector robot significantly enhances gait speed, gait ability, balance, walking distance, and lower limb function in chronic stroke patients compared to conventional therapy. These findings support the integration of robotic rehabilitation into clinical practice for chronic stroke rehabilitation to optimize functional recovery and patient outcomes. Further studies should explore long-term benefits and cost-effectiveness to establish comprehensive rehabilitation protocols.

Acknowledgment This study was supported by the Translational Research Program for Rehabilitation Robots(#NRCTR-EX22003), National Rehabilitation Center, Ministry of Health and Welfare, Korea.

variable		Group		p-value
		Control (n=18)	Robot (n=19)	
age (years)		63.78 ± 9.32	58.16 ± 14.82	0.17
sex (%)	Male	8 (44.4)	14 (73.7)	0.14
	Female	10 (55.6)	5 (27.3)	
weight (kg)		64.7 ± 12.15	61.9 ± 18.31	0.59
Height (cm)		160.0 ± 7.58	167.3 ± 7.2	0.01*
Onset(months)		26.5 [7.7, 45.3]	28 [-18 ,74]	0.22
stroke.etiology n (%)	Infarction	14 (77.7)	8 (42.1)	0.06
	hemorrhage.	4 (22.3)	11 (57.9)	

Table 1. Characteristics of patients . A total of 18 participants in the control group and 19 participants in the robot group completed the study. At baseline, there were no significant differences in age, weight, or stroke onset between the groups. Values are shown as mean ± SD or number (%), and median [IQR]. *p < 0.05. For the statistical analysis, the Chi-square test and t-test were performed.

	Control		Robot		p-value
	Pre	Post	Pre	Post	
10MWT(m/s)	0.48 ± 0.23	0.50 ± 0.25	0.38 ± 0.23	0.55 ± 0.30 (p<0.001*)	<.001**
FAC	2.67 ± 0.69	3.50 ± 1.10 (p<0.001*)	2.32 ± 0.75	3.68 ± 1.42 (p<0.001*)	.033**
BBS	36.72 ± 10.89	40.00 ± 11.75(p=0.005*)	28.42 ± 13.67	35.42 ± 14.42 (p<0.001*)	.018*
2MWT(m)	64.22 ± 32.59	69.28 ± 34.76(p=0.08)	52.89 ± 37.54	71.53 ± 42.02 (p=0.004*)	.012**
FMA-LE	23.06 ± 6.23	24.44 ± 6.08(p=0.01*)	19.42 ± 6.55	25.21 ± 5.74 (p<0.001*)	p<0.001*
VO2max (ml/kg/min)	21.40 ± 10.70	25.79 ± 15.42	12.64 ± 9.77	19.49 ± 9.15(p=.019*)	.499
MBI	76.94 ± 14.80	87.17 ± 14.85 (p<0.001*)	64.79 ± 22.47	76.16 ± 23.02 (p<0.000*)	.669
Lean Body Mass	24.73 ± 6.77	25.77 ± 6.69	27.63 ± 5.10	28.74 ± 6.36	.536

Table 2. Outcome measured pre- and post treatment. In the robot group, 10MWT significantly improved, whereas the improvement in the control group was not statistically significant. FAC, BBS, 2MWT, and FMA-LE showed significant improvements in both groups. Values are presented as mean ± standard deviation. Changes from baseline to follow-up within each group were analyzed using a paired t-test, with significance denoted as * (p < 0.05). Differences in changes between the control and robot groups were assessed with an independent t-test, indicated by ** (p < 0.05).

OPS-3

Identifying gait changes from a CSF tap test using a smart insole in iNPH

Seongmin Hong^{1*}, Wonhee Lee², Seung-Ick Choi³, Hui Woo Yang³, Seok Jong Chung⁴, Jun Kyu Hwang⁵, Na Young Kim^{2,3†}

Department of Medicine, Yonsei University College of Medicine¹, Department and Research Institute of Rehabilitation Medicine, Yonsei University College of Medicine², Department of Rehabilitation Medicine, Yonsei University Yongin Severance Hospital³, Department of Neurology, Yonsei University Yongin Severance Hospital⁴, Department of Neurosurgery, Yonsei University Yongin Severance Hospital⁵

Introduction

Gait disturbance is the earliest and most prominent symptom of idiopathic Normal Pressure Hydrocephalus (iNPH), but it can be improved with cerebrospinal fluid (CSF) shunts. CSF tap test response is a key factor for deciding on surgical treatment. However, detailed assessment of gait is time and resource consuming process. Recent advancement in wireless sensor technology have enabled cost-effective and convenient analysis of gait. We tested whether a sensor-embedded insole could monitor changes in gait before and after CSF tap.

Method

The gait of patients diagnosed with iNPH were evaluated before and after CSF tap test using a smart insole with embedded four pressure sensors and three-axis accelerometers (GDCA-MD®, Gilon, Republic of Korea), as well as conventional tests such as a 10-meter walking test, timed up and go test and berg balance scale. Spatiotemporal features of gait including velocity, step count, cadence, stride length, stride time and swing ratio were computed. We also analyzed the data stream itself to identify the pattern of foot pressure distribution during gait. The peak value of each pressure sensor was extracted and averaged. In addition, assessment of cognitive function and urinary symptoms were performed. Patients were divided into responders and non-responders according to improvement in subjective and objective symptoms after CSF tap. Paired t-tests and Wilcoxon signed-rank tests were conducted for within-group comparisons, and Analysis of Covariance was used for between-group comparisons. A P value

Results

A total of 30 iNPH patients were included (Age = 72.23±10.28, 20 males). Responder group (N=19) showed significant improvement in timed up-and-go test than non-responder group (N=11), but there were no statistically significant changes in other spatiotemporal parameters (Table 1). The mean heel peak pressure significantly increased from before to after CSF tap in both left foot (628.36±89.53 to 654.96±87.08, p = 0.007) and right foot (685.41±48.27 to 710.15±50.51, p = 0.005) in the responder group, while there were no significant changes in either left foot (pre-tap 644.62±73.25 to post-tap 629.01±96.38, p = 0.413) or right foot (pre-tap 675.61±47.24 to post-tap 676.98±53.63, p = 0.830) in the non-responder group (Figure 1). In the seven patients who underwent surgical treatment, mean heel pressure increased after tapping and was maintained post-surgery (Figure 2).

Conclusion

This study indicates that gait analysis using smart insoles can be a supplementary tool in determining surgical treatment in patients with iNPH. Further research could extend this approach to quantitatively analyze and assess gait improvement in patients with various gait disorders using smart insoles.

Acknowledgment This research was supported by a grant from the Korea Health Technology R&D Project through the Korea Health Industry Development Institute (KHIDI), funded by the Ministry of Health and Welfare, Republic of Korea (grant number: RS-2023-00265489) and a faculty research grant of Yonsei University College of Medicine (2024-32-0066).

	Responder (N=19)			Non-Responder (N=11)			Between groups <i>p</i> value
	Pre-tap	Post-tap	Within group <i>p</i> value	Pre-tap	Post-tap	Within group <i>p</i> value	
Neuropsychological test							
MMSE	20.88±6.46	23.25±4.50	0.223	24.00±3.82	25.29±2.81	0.420	0.523
Urinary symptom score							
IPSS	20.89±7.27	16.86±6.76	0.141	15.70±7.89	10.33±7.40	0.030 *	0.162
OABSS	9.33±4.63	9.58±3.63	1.00	5.00±2.94	9.00±0.00	0.317	0.531
Balance and gait parameters							
Timed up-and-go test (s)	20.82±11.77	16.54±6.99	0.003 **	20.01±11.58	20.03±13.25	0.989	0.018 *
Berg balance scale	46.32±7.38	48.58±7.12	0.002 **	43.55±14.69	44.82±14.91	0.040 *	0.268
10-meter walk test (m/s)	0.75±0.23	0.80±0.22	0.221	0.78±0.29	0.81±0.27	0.461	0.785
Step count (n)	13.42±4.86	11.21±2.69	<0.001 **	11.32±3.73	9.86±3.59	0.403	0.584
Cadence (spm)	113.36±12.52	114.06±11.54	0.716	108.46±10.42	114.56±15.82	0.163	0.305
Stride length (m)	1.00±0.22	1.03±0.16	0.317	1.06±0.21	1.03±0.22	0.548	0.403
Stride time (s)	1.08±0.11	1.07±0.10	0.639	1.12±0.11	1.07±0.12	0.119	0.350
Swing ratio (%)	35.06±2.55	34.59±2.61	0.310	34.81±2.04	35.22±2.99	0.614	0.331

Values are presented as mean ± SD; MMSE: Mini-Mental State Exam; IPSS: International Prostate Symptom Score; OABSS: Overactive Bladder Symptom Score; * $P < 0.05$, ** $P < 0.005$

Table 1. Changes in conventional clinical parameters before and after CSF tapping between groups

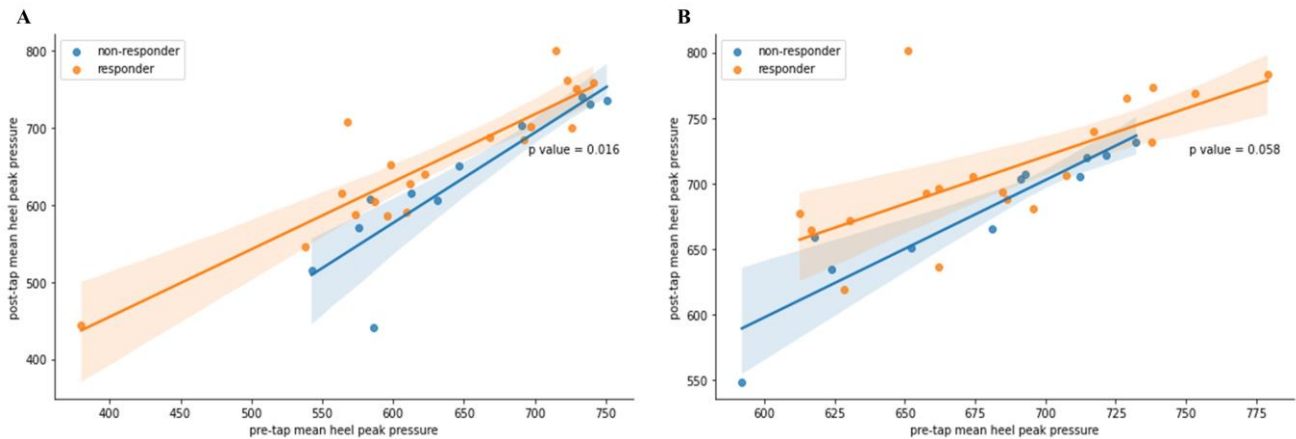


Figure 1. Scatter plot of mean heel peak pressure of the left (A) and the right (B) foot during 10-meter walking test before and after spinal tapping by groups. Mean heel pressure was significantly increased in the responder group (N=19) compared to non-responder group (N=11).

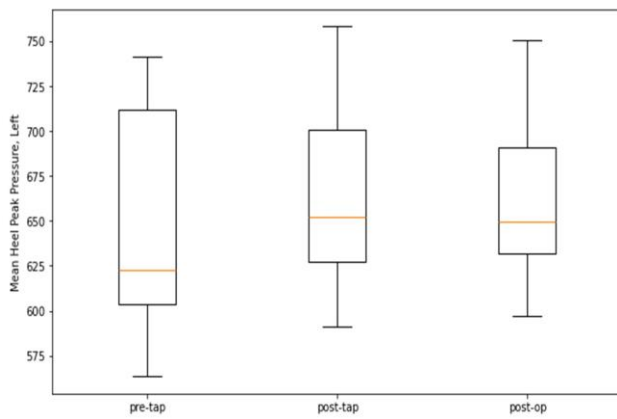
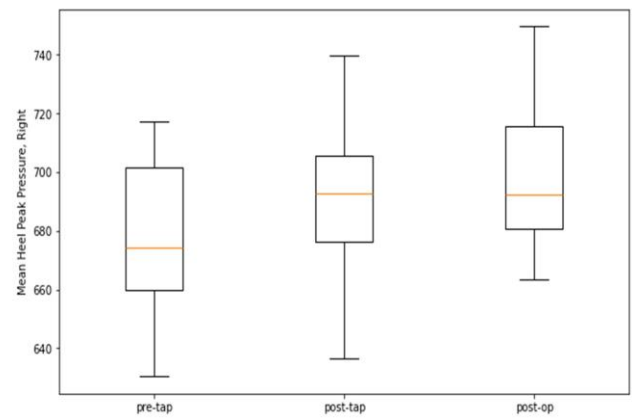
A**B**

Figure 2. Boxplot of mean heel peak pressure of the left (A) and the right (B) foot at pre-tap, post-tap, and post-operative stages for the patients who underwent shunt surgery. Seven patients who showed gait improvement after spinal tapping underwent surgical treatment. Mean heel pressure increased after tapping, and this was maintained after surgery.

Brain & Neurorehabilitation

발표일시 및 장소 : 10 월 25 일(금), 13:40 ~ 15:10 , Room A

OPS-4

Drug delivery through f-BRDP nanoparticles targeting ligand to P-selectin in MCAO rat model

Gi-Wook Kim^{1,3,2**}, Min Ji Sung¹, Suyeon Lee^{3,4}, Seunga Lee^{3,4}, Dongwon Lee^{3,4}, Da-Sol Kim^{1,2}, Yu Hui Won^{1,2}, Sung-Hee Park^{1,2}, Myoung-Hwan Ko^{1,2}, Jeong-Hwan Seo^{1,2}

Department of Physical Medicine and Rehabilitation, Jeonbuk National University Hospital¹, Research Institute of Clinical Medicine - Biomedical Research Institute, Jeonbuk National University Hospital², Department of Bionanotechnology and Bioconvergence Engineering, Jeonbuk National University³, Department of Polymer Nano Science and Technology, Jeonbuk National University⁴

Objective

Drug delivery in stroke has some limitations such as passing the blood-brain barrier (BBB), difficulty maintaining concentration, and non-specificity of the drug. Target-oriented drug delivery research is important and is being studied to overcome these drug delivery systems. P-selectin plays an important role in the occurrence and progression of stroke through thrombus formation and migration of inflammatory cells into damaged blood vessels. Therefore, P-selectin can be a target for drug delivery and therapeutic effects can be achieved by lowering P-selectin. This study aimed to establish an MCAO model and confirm the targeting efficacy of P-selectin-mediated f-BRDP nanoparticles within the infarction lesion of MCAO Rat Models.

Methods

Boronated atRA dimeric prodrug (BRDP) was developed as a self-deliverable antithrombotic nanomedicine with pathological stimuli-activatable therapeutic actions at our laboratory. BRDP could form injectable nanoparticles in the presence of fucoidan which is a sulfated polysaccharide with high affinity to P-selectin overexpressed on the damaged endothelium.

MCAO was induced by inserting a filament through the right common carotid artery to occlude the middle cerebral artery for 60 minutes, followed by reperfusion. Model validation included TTC and H&E staining, alongside MRI. Post-reperfusion, fluorescent BRDP or f-BRDP nanoparticles were intravenously administered, followed by brain harvesting after 24 hours for ex vivo fluorescence imaging.

Results

TTC staining results confirmed ischemic infarction of the white and gray matter of the MCA distribution, while the control model showed uniform red staining (Figure 1-A). H&E staining of MCAO brains revealed pathological features including vacuolation, neuronal loss, lymphocyte infiltration, and enhanced eosinophilic presentation (Figure 1-B). Brain MRI images also showed a high signal change in the MCA area (Figure 1-C). Immunofluorescence staining demonstrated higher P-selectin expression in the ischemic lesion area of the MCAO group compared to controls (Figure 2). Furthermore, fluorescence imaging confirmed precise targeting and localization of f-BRDP nanoparticles within the lesion areas of the MCAO group, whereas BRDP particles showed negligible accumulation (Figure 3). Evaluation of therapeutic effect is ongoing.

Conclusion

This study successfully established and validated a reliable MCAO model through histological and MRI analyses. P-selectin overexpression facilitated precise targeting of f-BRDP nanoparticles to ischemic lesion areas, highlighting its critical biomarker role and potential to enhance therapeutic delivery in ischemic stroke treatments. The demonstrated efficacy of this targeted system, confirmed via fluorescence imaging, suggests significant advancements in stroke therapies by enabling precise drug delivery across the BBB to damaged brain areas.

Acknowledgment This research was supported by the National Research Foundation of Korea (NRF), a grant funded

by the Korean government (MSIT) (No. 2022R1C1C1005770) and by Bio&Medical Technology Development Program of the National Research Foundation (NRF) (No. RS-2023-00236157), and by grants from the Biomedical Research Institute of Jeonbuk National University Hospital, Jeonju, Korea.

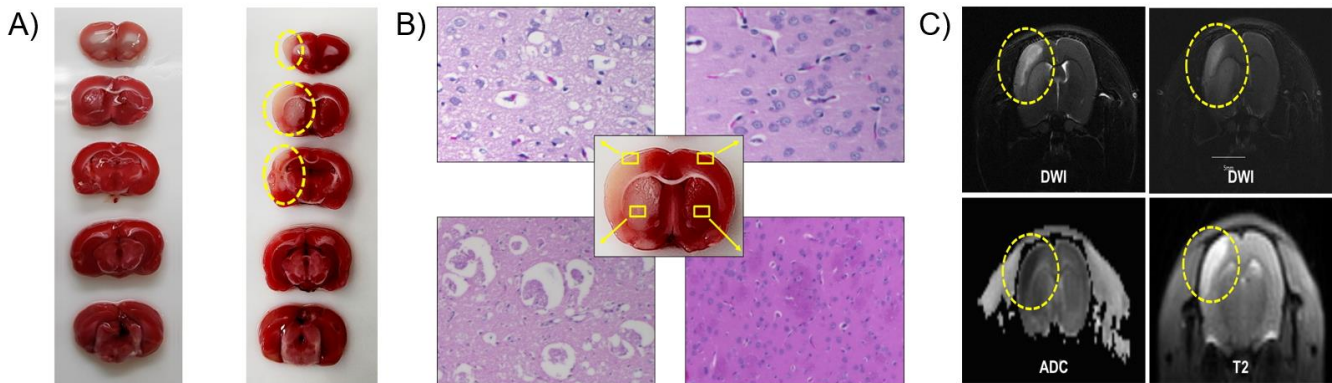


Figure 1. Confirmation and Validation of the MCAO Rat Models – A) TTC stain, B) H&E stain, C) Brain MRI

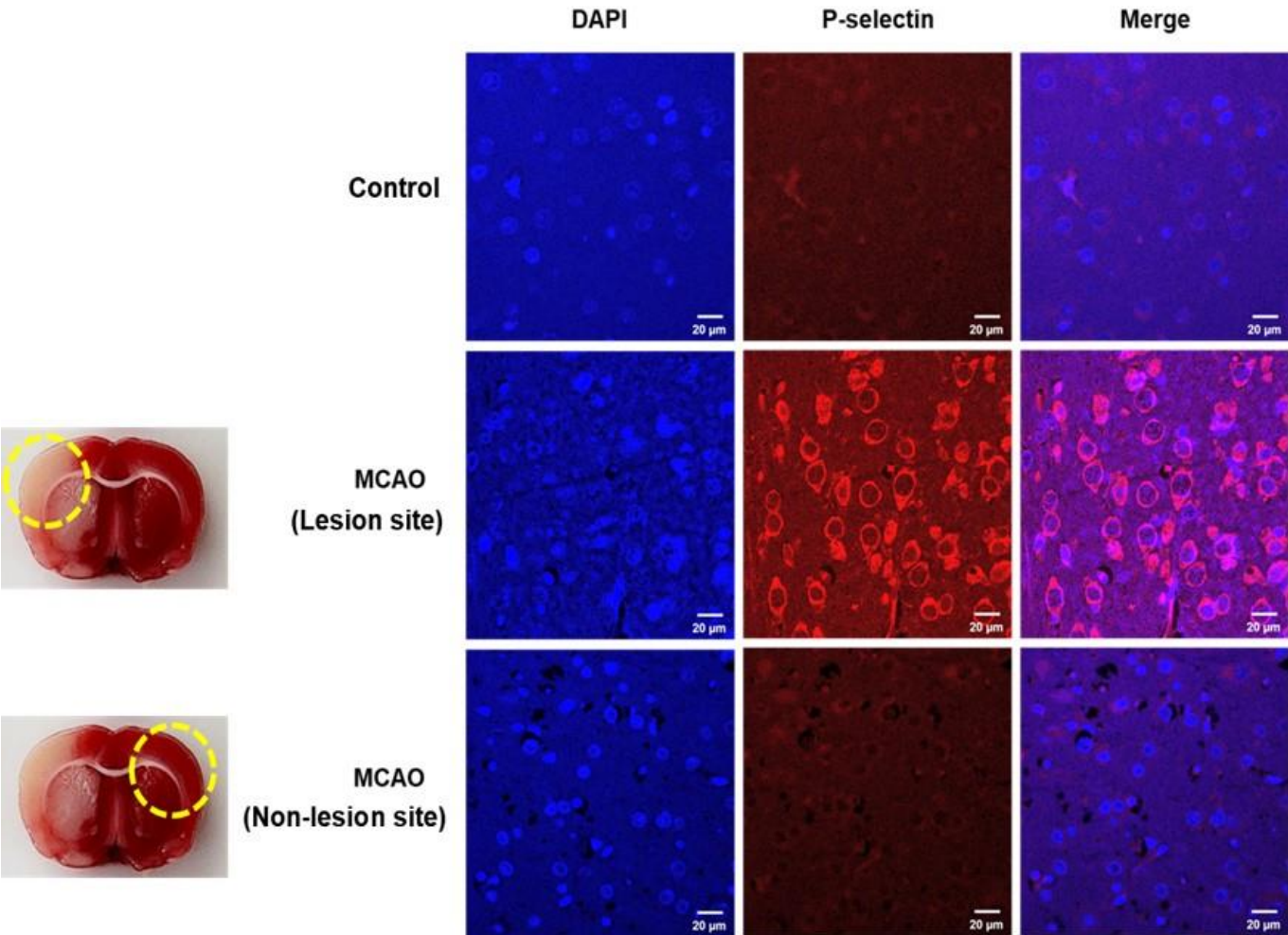


Figure 2. Fluorescence imaging of TRITC-labeled P-selectin antibody in brain tissues

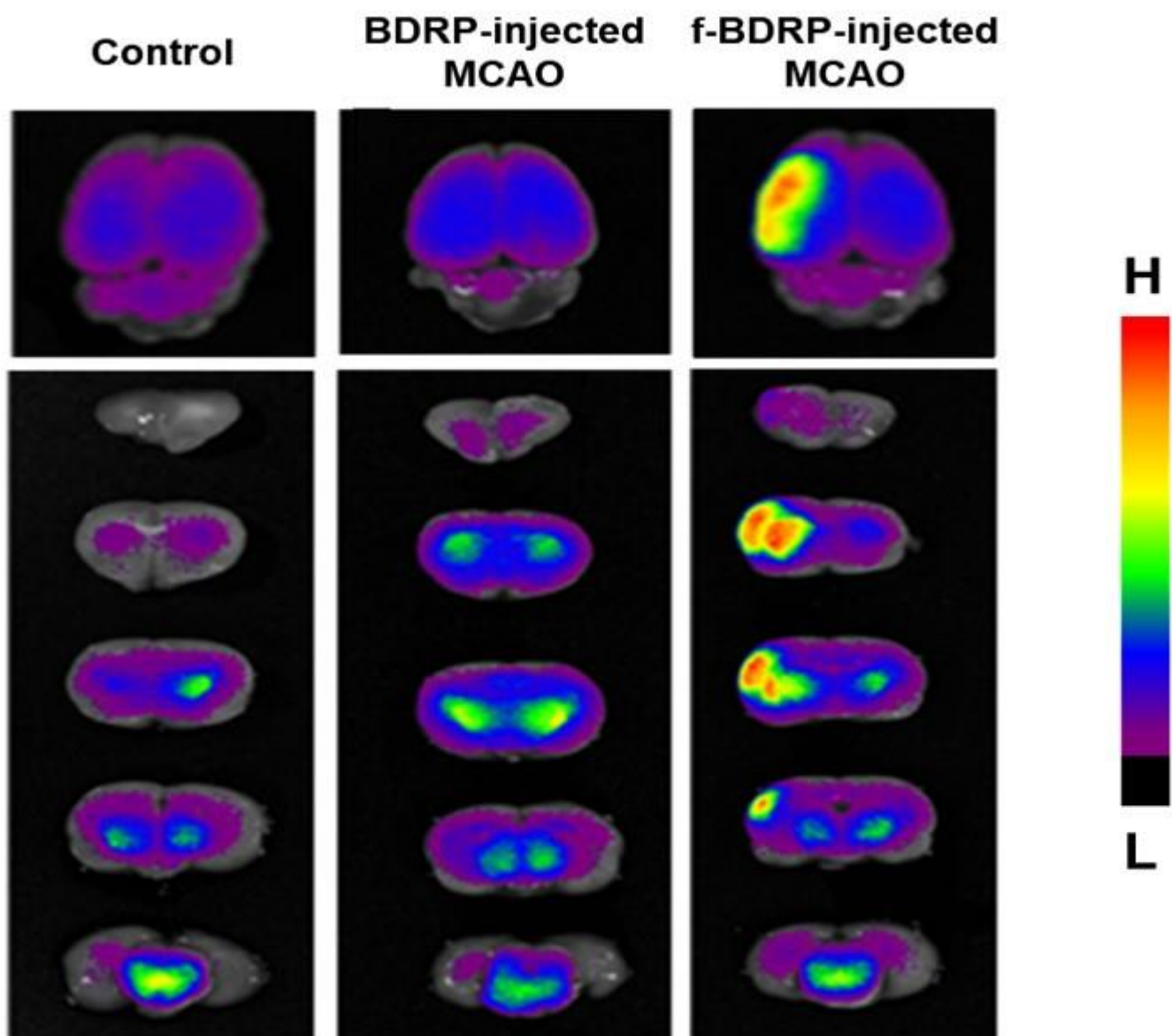


Figure 3. Fluorescence imaging of brains 24 hours post injection of BRDP or f-BRDP nanoparticles

Cancer Rehabilitation

발표일시 및 장소 : 10 월 25 일(금), 13:40 ~ 15:10 , Room A

OPS-5

Towards a simple and painless near-infrared lymphangiography: Lymph-targeted microneedle patch (LMP)

Hwayeong Cheon^{1*}, Hyewon Choi², Hyunsik Yoon^{2,3}, Jae Yong Jeon^{1,4†}

Rehabilitation Research Center, Biomedical Engineering Research Center, Asan Institute for Life Sciences, Asan Medical Center¹, Department of Chemical and Biomolecular Engineering, Seoul National University of Science and Technology², Department of Nano Bio Engineering, Seoul National University of Science and Technology³, Department of Rehabilitation Medicine, Asan Medical Center, University of Ulsan College of Medicine⁴

Purpose

Near-infrared indocyanine green lymphangiography (NIRF-ICGL) is a non-invasive imaging modality that visualizes the superficial lymphatic flow in real-time with high resolution, and it allows for the assessment of both lymphatic drainage and function. These characteristics are useful to evaluate abnormalities in lymphatic drainage or to plan interventional or surgical treatments for lymphedema. However, NIRF-ICGL requires the injection of a fluorescent contrast agent (ICG) intradermally or subcutaneously with a syringe, which is cumbersome and causes pain and discomfort to patients. In this study, we developed a lymph-specific microneedle patch (LMP) with a high capillary force capable of overcoming the increased interstitial pressure caused by lymphedema, and we validated its efficacy for lymphangiography through animal experiments.

Method

We fabricated the LMP using biocompatible polydimethylsiloxane (PDMS) via photopolymerization, designed to gradually increase the capillary force from the drug chamber through millimeter-scale channels, micrometer-scale needles, and nanometer-scale grooves. By adjusting the height, shape, and density of the microneedles, we determined the optimal conditions for maximum drug delivery efficiency while ensuring sufficient tensile strength to penetrate the stratum corneum. Before the in-vivo experiment, the transdermal drug delivery ability and safety during drug application were evaluated in the in-vitro conditions. We then applied LMP to 32 upper limb lymphedema animal models induced by lymph node dissection and radiation exposure to evaluate ICG drug delivery in normal and lymphedema limbs. The results were compared the results with traditional injection methods using 31-gauge needle syringes.

Results

In in-vitro experiments, our developed LMP demonstrated faster drug delivery speed and higher drug capacity compared to existing microneedles. Histological examinations confirmed that the microneedles applied to animal skin penetrated deeply enough to reach the superficial lymphatic vessels. In the drug delivery test, the LMP successfully visualized lymphatic vessels and lymph nodes in normal limbs by ICG injection. We harvested lymph nodes from the upper limbs and identified that ICG delivered via the LMP chamber reached the lymph nodes effectively. Furthermore, the LMP visualized lymphatic drainage even in lymphedema limbs, and we observed the dermal backflow similar to traditional injection methods.

Conclusion

In animal experiments, the LMP demonstrated the ability to deliver ICG from distal to proximal regions comparable to syringe injections, and it successfully visualized lymphatic vessels and lymph nodes in both normal and lymphedema limbs. Considering that microneedles cause less pain compared to syringe needles and the patches are easily applied by attaching to the skin, LMP may be helpful in regular monitoring using NIRF-ICGL for lymphedema in the clinical setting in cancer rehabilitation.

Acknowledgment This work was supported by the National Research Foundation of Korea (NRF) grant funded by the Korea government (MSIT). (RS-2024-00338179, RS-2024-00341884)

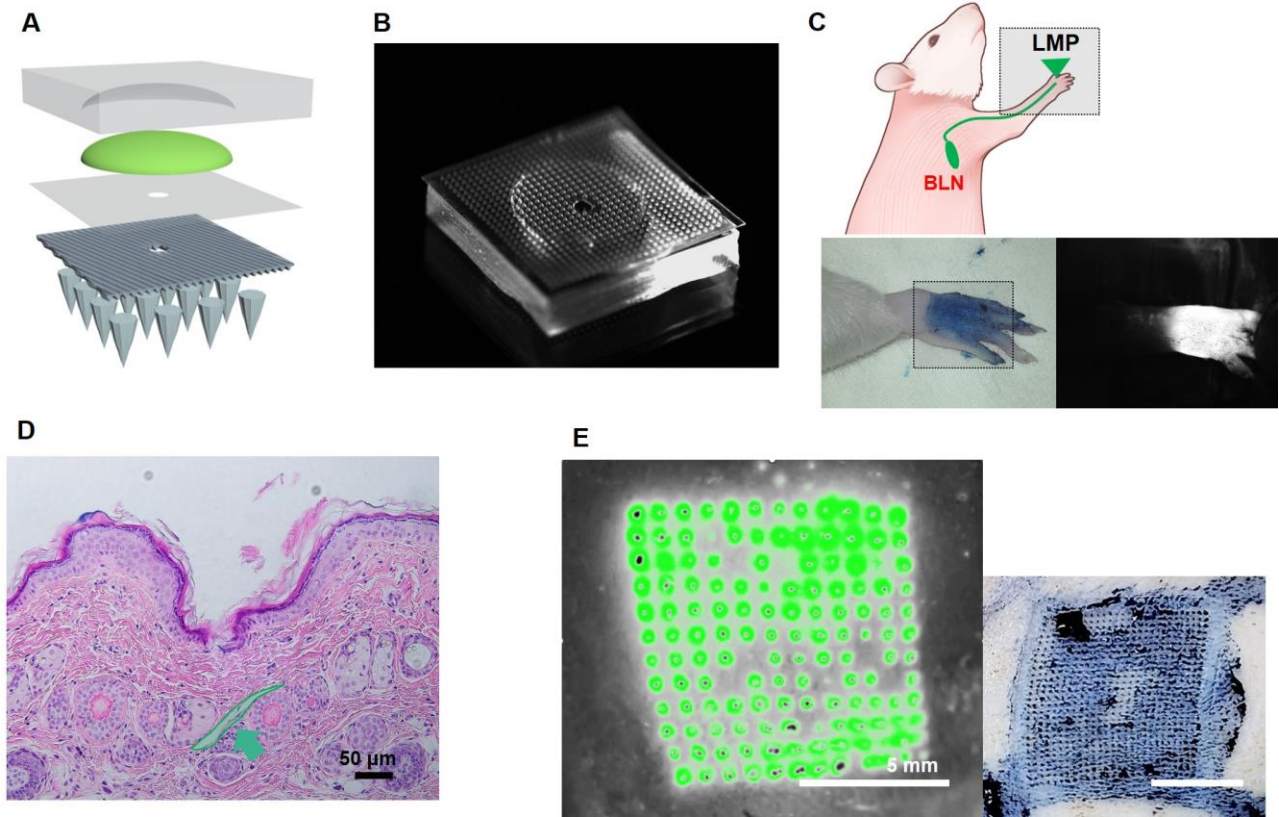


Figure 1. (A) Schematic diagram and (B) photos of LMP. (C) Appearance and NIRF-ICG image applied to the animal's upper limb paw. (D) Cross section of skin with microneedle applied. The stratum corneum is pierced by a microneedle and the epidermal lymphatic vessels immediately below (green arrow). (E) NIRF-ICG image showing ICG absorbed into the skin by applying LMP and visible image using Evans Blue dye.

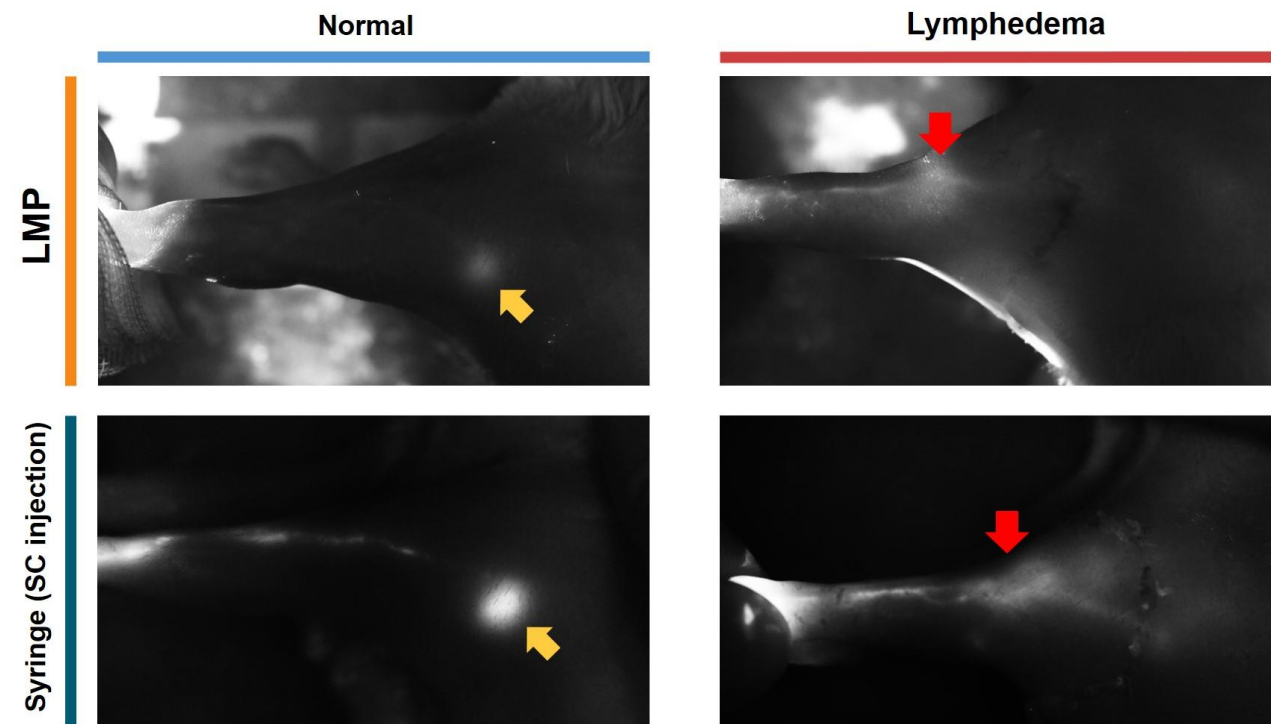


Figure 2. NIRF-ICG image visualizing the lymphatic vessels and brachial lymph nodes (yellow arrows) of the upper limb in animal models using LMP and syringe (intradermal/subcutaneous injection) in normal and lymphedema limbs. Dermal backflow (red arrow) was observed in the lymphedema limb with both LMP and syringe injection.

Cancer Rehabilitation

발표일시 및 장소 : 10 월 25 일(금), 13:40 ~ 15:10 , Room A

OPS-6

Prevalence of Function-limiting Late Effects in Head and Neck Cancer Survivors

Yu Hui Won^{1,2*}, Michael D. Stubblefield^{3,4,5,6†}

Department of Physical Medicine and Rehabilitation, Jeonbuk National University Medical School¹, Research Institute of Clinical Medicine of Jeonbuk National University, Biomedical Research Institute of Jeonbuk National University Hospital², Medical Director for Cancer Rehabilitation, Kessler Institute for Rehabilitation³, National Medical Director for Complex Medical Rehabilitation for the Inpatient Rehabilitation Hospital Division, Select Medical⁴, National Medical Director for ReVital Cancer Rehabilitation , Select Medical⁵, Clinical Professor, Department of Physical Medicine and Rehabilitation , Rutgers New Jersey Medical School⁶

Introduction

Head and neck cancer (HNC) survivors are commonly affected by multiple complex and interrelated long-term and late effects that can adversely affect their function and quality of life.

Objective

To define the prevalence of neuromuscular, musculoskeletal, visceral, oncologic, and other late effects impacting function and quality of life in HNC survivors

Design: Retrospective cohort analysis

Setting: Outpatient cancer rehabilitation clinic

Participants: One hundred and thirty HNC survivors

Interventions: Not applicable.

Main Outcome Measures: Prevalence of neuromuscular, musculoskeletal, visceral, oncologic, and other late effects affecting function and quality of life in HNC survivors.

Results

The majority underwent surgery (53.8%), chemotherapy (22.3%), and radiation therapy (93.8%) as part of their treatment. Neuromuscular complications such as myelopathy (45.4%), radiculo-plexopathy (58.5%), mononeuropathy (84.6%), and myopathy (57.7%) were prevalent. Musculoskeletal impairments included dysphagia (92.3%), dysarthria (60.8%), trismus (40.8%), cervical dystonia (47.7%), and shoulder dysfunction (27.7%). Visceral disorders encompassed lymphedema (86.2%), hypothyroidism (26.2%), and baroreceptor failure (19.2%). Additionally, oncologic complications, including recurrence (18.5%), metastasis (5.4%), and secondary malignancies (8.5%) were observed. Pain (74.6%) and fatigue (31.5%) were reported as major function-limiting impairments. Most survivors (96.9%) were referred to therapy including physical therapy (85.4%), occupational therapy (13.1%), speech-language pathology (84.6%), and lymphedema therapy (72.3%). Most (85.4%) required two or more therapy disciplines.

Conclusion

HNC survivors accessing cancer rehabilitation services commonly present with diverse, complex and interrelated neuromuscular, musculoskeletal, visceral, and oncologic late effects that can severely impact function and quality of life. Comprehensive rehabilitation should include evaluation and management of these complex and interrelated late effects by a rehabilitation team that includes cancer rehabilitation physicians, physical therapists, occupational therapists, lymphedema therapists, and speech-language pathologists, among others.

Acknowledgment This paper was supported by research funds of Jeonbuk National University in 2023.

Table 1. Head and neck cancer survivor demographics

Variable	Number (%)
Total included patients	130
Gender	
Men	101 (77.7%)
Women	29 (22.3%)
Age at diagnosis	53.7 ± 12.3
Location of cancer	
Oral cavity	51 (39.2%)
Tongue	44 (33.8%)
Nasopharynx	16 (12.3%)
Salivary glands	3 (2.3%)
Oropharynx	3 (2.3%)
Larynx	5 (3.8%)
Nasal cavity/paranasal sinus	3 (2.3%)
Hypopharynx	1 (0.8%)
Other†	4 (3.1%)
Cancer type	
Squamous cell carcinoma	120 (92.3%)
Metastatic squamous cell carcinoma	4 (3.1)
Others‡	6 (4.6%)
Head and neck cancer stage at diagnosis	
Stage 1 : 2 : 3 : 4 : unknown	7 (5.4%) : 12 (9.2%) : 27 (20.8%) : 42 (32.3%) : 42 (32.3%)
Treatment	
Surgery	70 (53.8%)
Chemotherapy	29 (22.3%)
Radiation	122 (93.8%)

Age at diagnosis is presented as mean ± standard deviation.

†: neck with unknown primary origin

‡: Acinic cell carcinoma 1, Papillary squamous cell carcinoma 1, Adenocarcinoma 1, Adenoid cystic carcinoma 1, Mucoepidermoid 1, unknown 1

Table 1. Head and neck cancer survivor demographics

Table 2. Prevalence of late effects affecting function in Head and neck cancer survivors

Diagnosis	Number (%)
Neuromuscular	
Myelopathy	59 (45.4%)
Radiculo-plexopathy	76 (58.5%)
Mononeuropathy	110 (84.6%)
Myopathy	75 (57.7%)
Other neurologic	
Cranial nerve dysfunction	101 (77.7%)
CN 3	2 (1.5%)
CN 5	52 (40.0%)
CN 6	2 (1.5%)
CN 7	31 (23.8%)
CN 8	50 (38.5%)
CN 9	74 (56.9%)
CN 10	73 (56.2%)
CN 11	87 (66.9%)
CN 12	73 (56.2%)
Cognitive impairment	12 (9.2%)
Musculoskeletal	
Dysphagia	120 (92.3%)
Dysarthria	79 (60.8%)
Cervical dystonia	62 (47.7%)
Trismus / MIO (mm)†	53 (40.8%) / 17.4 ± 11.4
Cervicalgia	38 (29.2%)
Shoulder dysfunction	36 (27.7%)
Dropped head syndrome	28 (21.5%)
Xerostomia	23 (17.7%)
Dysphonia	14 (10.8%)
Other‡	27 (20.8%)
Lymphedema	112 (86.2%)
Endocrine	
Hypothyroidism	34 (26.2%)
Osteopenia/osteoporosis	3 (2.3%)
Others§	8 (6.2%)
Visceral	
Cardiovascular dysfunction	
Baroreceptor failure	25 (19.2%)
Carotid stenosis	19 (14.6%)
Coronary artery disease	5 (3.8%)
Others¶	5 (3.8%)
Pulmonary dysfunction (aspiration pneumonia)	
Aspiration pneumonia	16 (12.3%)
Functional impairments	
Pain	97 (74.6%)
Fatigue	41 (31.5%)
Dyspnea	5 (3.8%)
Deconditioning	5 (3.8%)
Oncologic	
Recurrence	24 (18.5%)
Metastasis	7 (5.4%)
Secondary cancer¶¶	11 (8.5%)

MIO is presented as mean ± standard deviation.

CN : cranial nerve; PEG : percutaneous endoscopic gastrostomy; MIO : maximal inter-incisal opening

†: 24 patients' data with trismus were included.

‡: osteonecrosis 8, glossodynia 5, dysgeusia 4, odynophagia 4, first bite syndrome 2, dyssosmia 1, mandible fracture 1, jaw dislocation 1, tympanic injury 1

Table 2. Prevalence of late effects affecting function in Head and neck cancer survivors

Table 3. Therapy referrals for Head and neck cancer survivors

Therapy referrals	Number (%)
Any discipline	126 (96.9%)
Two disciplines	27 (20.8%)
Three disciplines	73 (56.2%)
Four disciplines	11 (8.5%)
Two or more disciplines	111 (85.4%)
Physical therapy	111 (85.4%)
Occupational therapy	17 (13.1%)
Speech language pathology therapy	110 (84.6%)
Lymphedema therapy	94 (72.3%)

Table 3. Therapy referrals for Head and neck cancer survivors

Cardiopulmonary Rehabilitation

발표일시 및 장소 : 10 월 25 일(금), 13:40 ~ 15:10 , Room A

OPS-7

The Effect of Exercise on Improving Systemic and Muscular Recovery in Critical Illness Animal Model.

Won Kim^{1*†}, Wonhwa Lee^{2†}, Da Bin Ko^{1,3}, In Ho Woo¹, Jae Hwal Rim¹, Seung Hak Lee¹, Jungbum Kim², Ji Eun Yeom²

Department of Rehabilitation Medicine, Asan Medical Center, University of Ulsan College of Medicine¹, Department of Chemistry, Sungkyunkwan University², Department of Medical Science, AMIST, Asan Medical Center, University of Ulsan College of Medicine³

Objective

Rehabilitation in intensive care units is believed to aid the recovery of critically ill patients. However, there has been no biological investigation into the effects of exercise on their overall and muscular health. Additionally, there is no study on the appropriate intensity of exercise for these patients. Therefore, this study utilized an critical illness animal model and assess the effects of exercise on muscle function and overall health in this setting.

Materials and Methods

A total of 79 mice were divided into normal, control, and exercise groups. The control and exercise groups were subjected to repeated intra-airway administration of LPS optimized to induce critical illness and weakness by maintained acute respiratory distress syndrome (ARDS) for 2 weeks. After the induction of ARDS, the control group was left alone, while the exercise group continued to exercise according to a routine of 25 minutes of exercise, 30 minutes of rest, and 25 minutes of exercise for two weeks. The exercise intensity varied between 50% and 70% of maximum capacity to compare the effects of moderate-intensity and high-intensity exercise. All groups were analyzed at 1 and 2 weeks after the first LPS administration. Before sacrifice, rota-rod and grip strength tests were measured, and blood, skeletal muscle, and lung tissue samples were obtained. Blood samples were used for cell and chemical analyses. Skeletal muscle was subjected to muscle fiber cross-sectional area (CSA) measurement, immunohistochemistry (IHC), and Western blot (WB) analysis for key proteins involved in muscle regeneration, including MyoD, MyoG, Murf-1, and Atrogin-1.

Results

LPS administration induced weight reduction and systemic and lung inflammation compatible with ARDS. Exercise groups showed better grip strength and rota-rod test performance compared to the control group. The moderate-intensity exercise group showed at least similar or better grip strength and rota-rod distance compared to the high-intensity exercise group. In muscle tissue, LPS and exercise intervention resulted in significant changes in muscle fiber CSA and protein expression. IHC and WB analysis revealed differential expression of MyoD, MyoG, Murf-1, and Atrogin-1, with exercise regulating these changes and promoting muscle recovery. In lung tissue, LPS exposure induced significant histological changes and increased IL-4, IL-6, and TNF- α levels. Exercise therapy reduced these inflammatory markers and hydroxyproline levels in BALF, suggesting a reduction in collagen deposition and fibrosis.

Conclusion

The findings demonstrate that exercise can attenuate muscle atrophy and weakness associated with critical illness by reducing systemic and tissue-specific inflammation, and promoting muscle regeneration and lung recovery. Moderate and high intensity exercise were both effective in these regards. These results add biological and scientific evidence of ICU rehabilitation.

Acknowledgment This research was supported by a grant of the National Research Foundation of Korea(NRF) funded by the Korea government(MSIT) (No. 2021R1C1C1010500) and a grant of the Korea Health Technology R&D Project

through the Korea Health Industry Development Institute (KHIDI), funded by the Ministry of Health & Welfare, Republic of Korea (No. RS-2024-00408722).

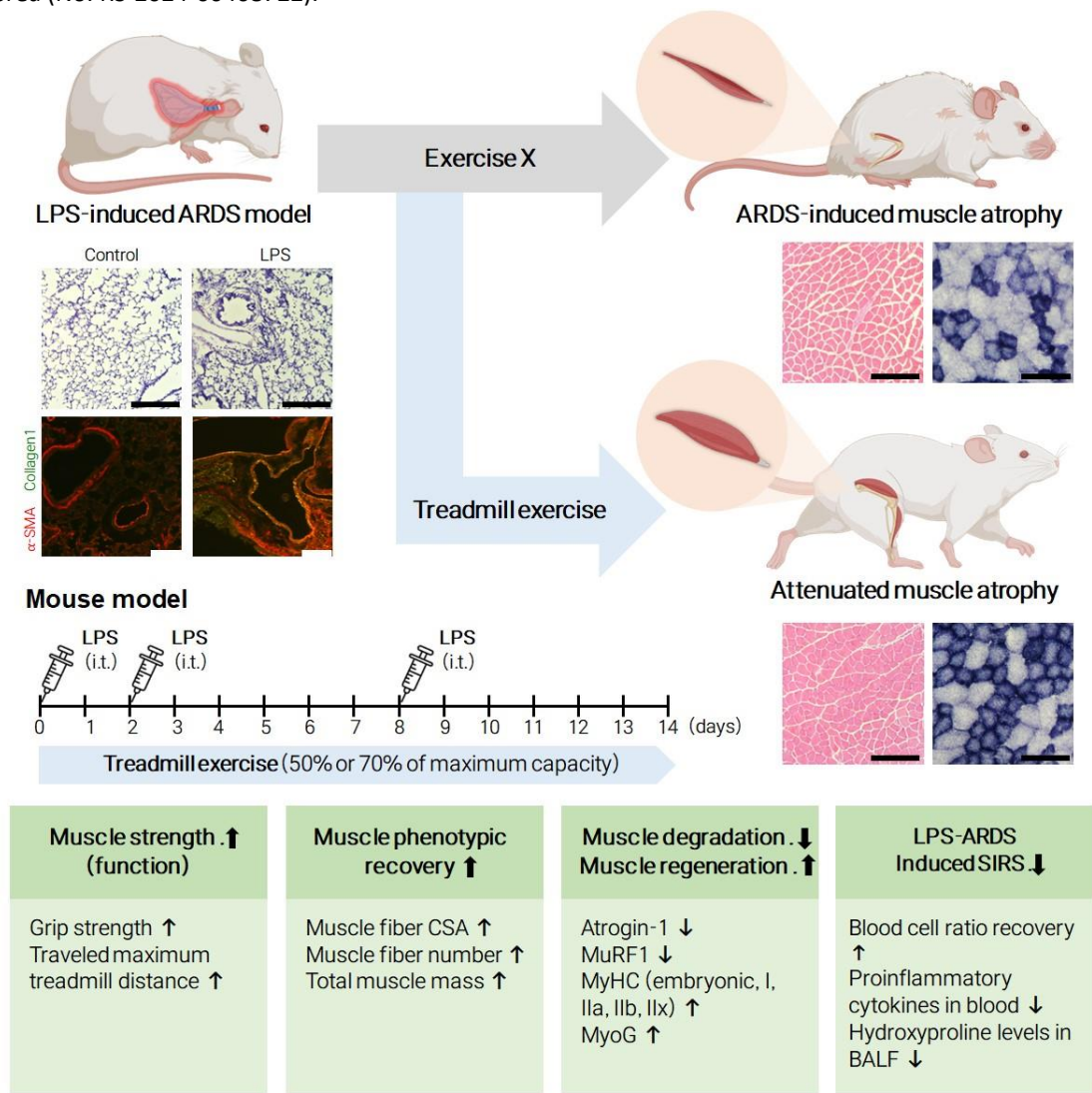


Fig 1. Schematic Experimental Design and Summary of Main Results.

Cardiopulmonary Rehabilitation

발표일시 및 장소 : 10 월 25 일(금), 13:40 ~ 15:10 , Room A

OPS-8

Exercise-induced desaturation during a 6MWT is associated with poor clinical outcome in PAH patients

Byeong-Ju Lee^{1*†}, Myung Jun Shin¹, Jung Hyun Choi², Min Kyung Park¹, Seon Jun Yoon¹, Jae-Hyeong Park³

Department of Rehabilitation Medicine, Pusan National University Hospital, Pusan National University School of Medicine and Biomedical Research Institute¹, Division of Cardiology, Department of Internal Medicine, Pusan National University Hospital, Pusan National University School of Medicine and Biomedical Research Institute², Department of Cardiology in Internal Medicine, Chungnam National University, Chungnam National University Hospital³

Background

The six-minute walk test (6MWT) is an established exercise test for patients with pulmonary arterial hypertension (PAH), affording insight into both exercise intolerance and overall prognosis. Despite the widespread application of the 6MWT, the prognostic implications of exercise-induced desaturation (EID) during this test has been inadequately studied in PAH patients. Thus, we evaluated the occurrence of EID and its prognostic significance in PAH patients.

Method

We analyzed PAH patients in a single-center cohort from April 2016 to March 2021. EID was defined as a reduction in oxygen saturation exceeding 4% from the baseline or to below 90% at any point during the test.

Results We analyzed 20 PAH patients in this cohort, primarily consisting of 16 females with an average age of 48.4 ± 13.3 years. Among them, ten exhibited EID. Baseline characteristics, echocardiographic data and right heart catheterization data were similar between the two groups. However, total distance (354.3 ± 124.4 m vs. 485.4 ± 41.4 m, $P=0.019$) and peak oxygen uptake (12.9 ± 3.2 mL/kg·min vs. 16.4 ± 3.6 mL/kg·min, $P=0.019$) were significantly lower in the EID group. During the total follow-up duration of 51.9 ± 25.7 months, 17 patients had at least one adverse clinical event (2 deaths, 1 lung transplantation, and 13 hospital admissions). The presence of EID was associated with poor clinical outcome (hazard ratio=6.099, 95% confidence interval=1.783–20.869, $P=0.004$).

Conclusions During the 6MWT, EID was observed in a half of PAH patients and emerged as a significant prognostic marker for adverse clinical events

Acknowledgment Not applicable

Table 1 Comparison of baseline characteristics according to exercise-induced desaturation (EID)

Characteristics	Total (n = 20)	EID (+) (n = 10)	EID (-) (n = 10)	P value
Age (year)	48.4 ± 13.3	49.7 ± 14.5	47.0 ± 12.6	0.912
Female sex (%)	16 (80)	7 (70)	9 (90)	0.582
Height (cm)	158.3 ± 7.8	158.6 ± 9.8	158.1 ± 5.6	0.912
Weight (kg)	58.1 ± 7.4	58.7 ± 9.0	57.5 ± 5.8	0.529
BMI (kg/m ²)	23.2 ± 2.7	23.4 ± 3.7	23.0 ± 1.3	1.000
Type of PAH				0.081
Idiopathic PAH (%)	7 (35)	4 (40)	3 (30)	
CHD-associated (%)	5 (25)	0 (0)	5 (50)	
CTD-associated (%)	5 (25)	4 (40)	1 (10)	
Portopulmonary (%)	3 (15)	2 (20)	1 (10)	
WHO functional class 3 and 4 (%)	10 (50)	5 (50)	5 (50)	0.307
Risk at diagnosis				0.666
Low-risk (%)	13 (65)	6 (60)	7 (70)	
Intermediate-risk (%)	3 (15)	1 (10)	2 (20)	
High-risk (%)	4 (20)	3 (30)	1 (10)	
Cardiovascular risk factors				
Hypertension (%)	6 (30)	2 (20)	4 (40)	0.629
Diabetes mellitus (%)	2 (10)	1 (10)	1 (10)	1.000
Echocardiographic data				
LVEF (%)	57.7 ± 4.4	57.4 ± 4.5	57.9 ± 4.5	0.971
Mitral E/e' ratio	10.2 ± 4.0	9.8 ± 3.9	10.5 ± 4.3	0.731
RVSP (mmHg)	68.8 ± 29.9	67.1 ± 27.9	70.4 ± 33.1	0.912
TAPSE (mm)	16.8 ± 4.5	16.6 ± 4.2	17.0 ± 5.0	1.000
Tricuspid annular S' velocity (cm/s)	10.7 ± 2.8	10.5 ± 2.6	10.9 ± 3.0	1.000
RA area (cm ²)	25.3 ± 17.6	27.3 ± 23.4	23.4 ± 9.7	0.739
Right heart catheterization data				
Mean PA pressure (mmHg)	44.0 ± 14.8	43.0 ± 10.6	45.1 ± 19.1	0.780
PCWP (mmHg)	14.7 ± 3.9	13.9 ± 2.6	15.6 ± 5.0	0.604
PVR (WU)	13.0 ± 7.9	12.0 ± 7.5	14.1 ± 8.6	0.605
CI (l/min/m ²)	2.6 ± 0.7	2.8 ± 0.6	2.5 ± 0.8	0.340
Pulmonary function test data				
FVC (L)	2.8 ± 0.7	2.7 ± 0.9	3.0 ± 0.5	0.356
FVC (%)	80.8 ± 15.0	74.6 ± 18.1	87.7 ± 6.1	0.079
FEV1 (L)	2.2 ± 0.6	2.0 ± 0.7	2.3 ± 0.4	0.211
FEV1 (%)	75.1 ± 12.8	69.3 ± 14.7	81.4 ± 6.1	0.035
FEV1/FVC (%)	76.9 ± 7.0	75.9 ± 8.5	78.0 ± 5.3	0.447
DLCO (mL/min/mmHg)	13.6 ± 6.2	11.3 ± 4.8	16.2 ± 6.7	0.156
DLCO (%)	62.8 ± 24.4	52.7 ± 19.2	74.1 ± 25.6	0.079
6-min walk test data				
Total distance (m)	419.9 ± 112.5	354.3 ± 124.4	485.4 ± 41.4	0.019
VO ₂ peak (mL/kg·min)	14.6 ± 3.7	12.9 ± 3.2	16.4 ± 3.6	0.019
HR peak	118.0 ± 21.0	114.1 ± 17.8	121.9 ± 24.2	0.280
VE/VO ₂ slope (mL/min/W)	40.7 ± 12.0	44.4 ± 13.7	37.1 ± 2.9	0.247
BNP (pg/dL)	261.6 ± 290.8	414.7 ± 281.5	165.9 ± 269.2	0.284
Baseline PAH specific medication				
ERA	10 (50)	7 (70)	3 (30)	0.659
PDE5i	5 (25)	2 (20)	3 (30)	1.000
PC	6 (30)	3 (30)	3 (30)	1.000
CCB	1 (5)	0 (0)	1 (10)	0.500

BMI/ body mass index, BNP B-type natriuretic peptide, CCB calcium channel blocker, CHD congenital heart disease, CI cardiac index, CTD connective tissue disease, DLCO diffusing capacity of the lung for carbon monoxide, ERA endothelin receptor antagonist, FEV1 forced expiratory volume at 1 s, FVC forced vital capacity, HR heart rate, LVEF left ventricular ejection fraction, PA pulmonary artery, PAH pulmonary arterial hypertension, PC prostacyclin, PCWP pulmonary capillary wedge pressure, PDE5i phosphodiesterase 5 inhibitor, PVR pulmonary vascular resistance, RA right atrium, RVSP right ventricular systolic pressure, TAPSE tricuspid annular plane systolic excursion, VE ventilatory equivalent of O₂, VO₂ maximal oxygen consumption, WHO World Health Organization

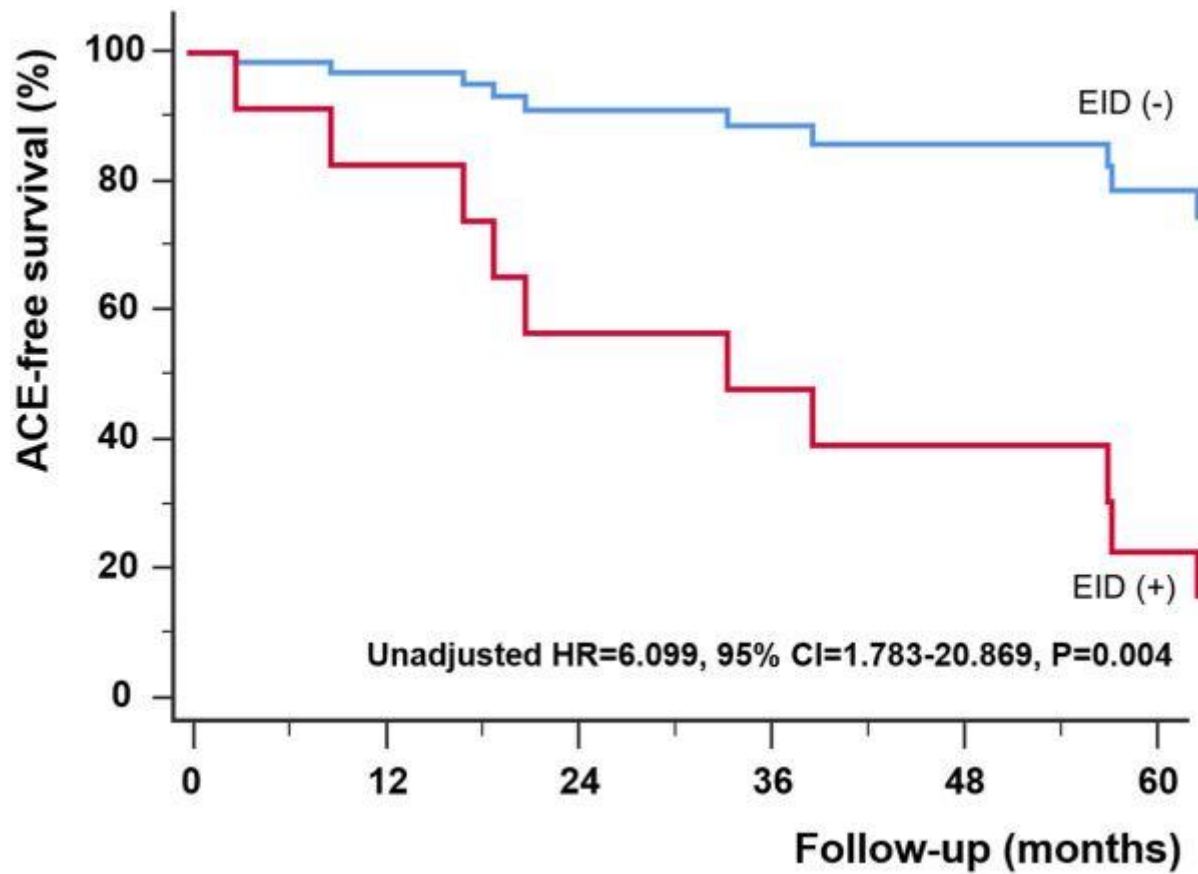
Table 1 Comparison of baseline characteristics according to exercise-induced desaturation (EID)

Table 2 Univariate analysis for prediction of adverse clinical events

Variable	Hazard ratio	95% confidence interval	P value
Age (per 1 year)	1.013	0.965 – 1.062	0.604
Male sex	1.547	0.420 – 5.696	0.512
BMI (per 1 kg/m ²)	1.250	0.966 – 1.618	0.090
WHO functional class 4	0.653	0.084 – 5.102	0.685
High-risk profile	4.745	1.362 – 16.524	0.014
Hypertension	1.869	0.606 – 5.767	0.276
Diabetes mellitus	0.495	0.064 – 3.843	0.502
LVEF (per 1%)	1.001	0.872 – 1.148	0.994
RVSP (per 1 mmHg)	1.012	0.994 – 1.031	0.179
TAPSE (per 1 mm)	0.943	0.819 – 1.085	0.410
Tricuspid annular S' velocity (per 1 cm/s)	0.877	0.683 – 1.126	0.303
RA area (per 1 cm ²)	1.030	0.992 – 1.069	0.120
Mean PA pressure (per 1 mmHg)	1.020	0.984 – 1.057	0.276
PCWP (per 1 mmHg)	1.025	0.904 – 1.163	0.696
PVR (per 1 WU)	1.013	0.931 – 1.103	0.761
CI (per 1 l/min/m ²)	1.000	0.999 – 1.001	0.790
FVC (per 1 L)	0.641	0.236 – 1.745	0.384
FEV1 (per 1 L)	0.410	0.120 – 1.396	0.154
DLCO (per 1 mL/min/mmHg)	0.948	0.850 – 1.058	0.340
Total distance (per 1 m)	0.992	0.986 – 0.998	0.009
VO ₂ peak (per 1 mL/(kg·min))	0.861	0.712 – 1.042	0.125
HR peak (per 1/min)	0.991	0.968 – 1.015	0.465
VE/VO ₂ slope (per 1 mL/min/W)	1.039	0.992 – 1.090	0.108
EID	6.099	1.783 – 20.869	0.004

BMI body mass index, CI cardiac index, DLCO diffusing capacity of the lung for carbon monoxide, EID exercise induced desaturation, FEV1 forced expiratory volume at 1 s, FVC forced vital capacity, HR heart rate, LVEF left ventricular ejection fraction, PA pulmonary artery, PCWP pulmonary capillary wedge pressure, PVR pulmonary vascular resistance, RA right atrium, RVSP right ventricular systolic pressure, TAPSE tricuspid annular plane systolic excursion, VE ventilatory equivalent of O₂, VO₂ maximal oxygen consumption, WHO World Health Organization

Table 2 Univariate analysis for prediction of adverse clinical events



Survival analysis according to the presence of exercise-induced desaturation (EID). Patients with EID have significantly lower adverse clinical event free survival than those of patients without EID.

Pediatric Rehabilitation

발표일시 및 장소 : 10 월 25 일(금), 13:40 ~ 15:10 , Room A

OPS-9

Predictive Factors for Postoperative Outcomes of Cervical Spondylotic Myelopathy in Cerebral Palsy

Su Ji Lee¹, Jihye Hwang^{2*}, Kyung Min Kim¹, Tae Kwon Lee¹, Yusang Jung³, Sung-Rae Cho^{1,2,4†}

Department and Research Institute of Rehabilitation Medicine, Yonsei University College of Medicine,¹ Graduate Program of Biomedical Engineering, Yonsei University College of Medicine,² Department of Pharmacology, Yonsei University College of Medicine³, Brain Korea 21 PLUS Project for Medical Science, Yonsei University College of Medicine⁴

Background

Cerebral palsy (CP) is a non-progressive neurologic disorder, but individuals with CP often face secondary complications, including cervical spondylotic myelopathy (CSM). While conservative treatments for CSM in CP patients are often ineffective, surgical intervention aims to decompress the spinal canal, stabilize the spine, and correct alignment. However, achieving favorable long-term postoperative outcomes is challenging due to factors like the complexity of deformities and involuntary movements. In this study, we aimed to determine the predictive factors associated with postoperative outcomes of CSM in CP patients.

Methods

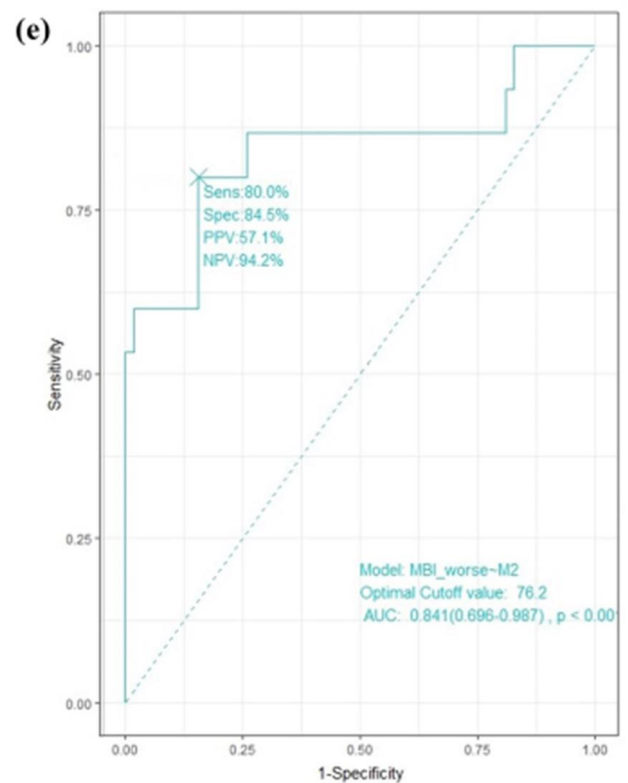
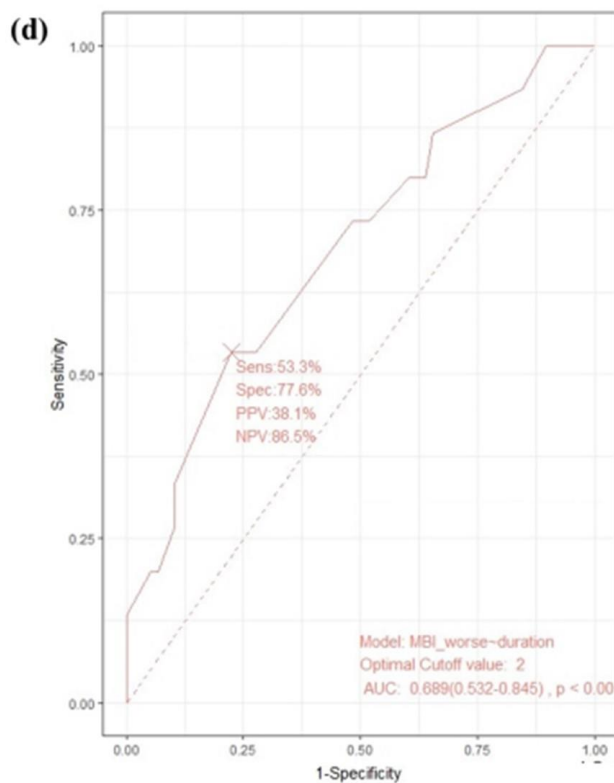
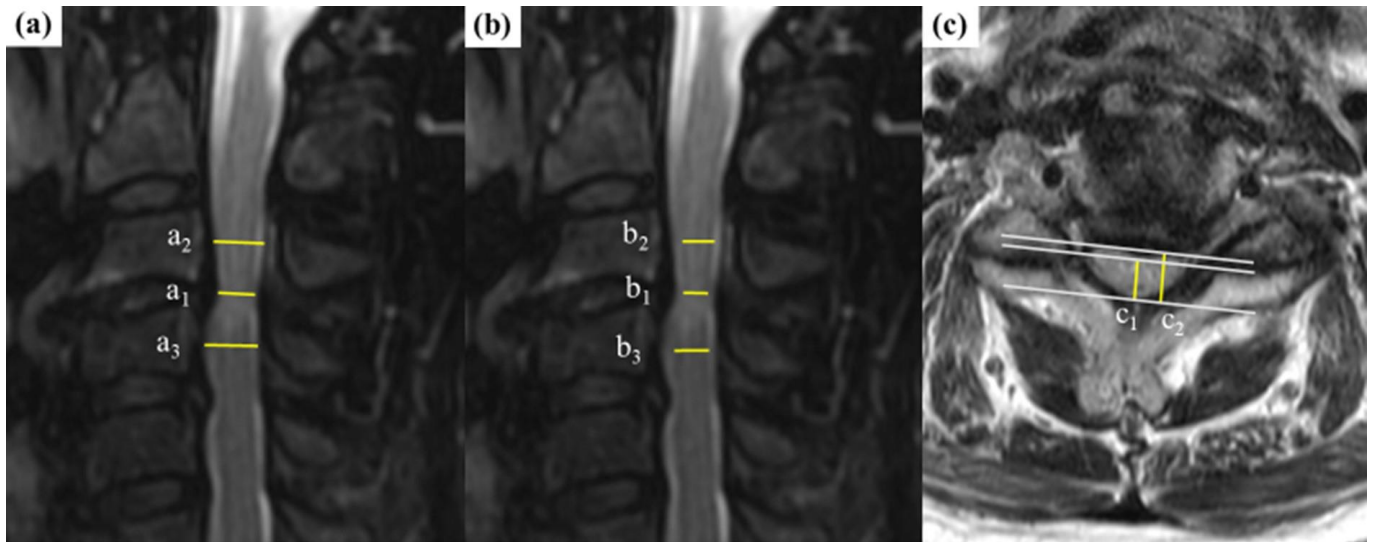
A retrospective cohort study was conducted. Individuals whose postoperative modified Barthel index scores declined by one or more grades were included in the poor outcome (PO) group. Preoperative radiological findings were evaluated using plain cervical radiography and magnetic resonance images. Multivariate logistic regression analysis was performed to assess risk factors for poor postoperative outcomes.

Results

A total of 73 participants were enrolled (15 in the PO group and 58 in the non-PO group) in the study. Duration (years) (odds ratio [OR] 1.99, 95% confidence interval [CI] 1.25–3.65, $P = 0.01$), signal change grade 2 (OR 10.44, 95% CI 1.32–118.01, $P = 0.034$), and spinal cord compression ratio, M2 (OR 0.87, 95% CI, 0.75–0.97, $P = 0.02$) were identified as significant factors associated with the risk of poor postoperative outcomes. Based on the receiver operating characteristic curve analysis, the cutoff values for duration and cord compression metric M2 were determined as 2 years (area under the receiver operating curve [AUC] = 0.689, 95% CI 0.532–0.845) and 76.2% (AUC = 0.841, 95% CI 0.696–0.987), respectively.

Conclusions

Duration of motor weakness, signal change grade, and spinal cord compression ratio on magnetic resonance images predicted poor postoperative outcomes in patients with CSM and cerebral palsy.



The three metrics measured in magnetic resonance images and receiver operating characteristic curve analysis results. (a) M1. M1 was calculated as the canal diameter at the level with the most severe canal stenosis divided by the average of the canal diameters above and below ($a_1/(a_2+a_3) * 1/2$). (b) M2. M2 was calculated as the spinal cord diameter at the level with the most severe spinal cord compression divided by the average of the spinal cord diameters above and below ($b_1/(b_2+b_3) * 1/2$). (c) M3. M3 was calculated by dividing the height at the narrowest point of the spinal cord by the greatest distance along the spinal cord (c_1/c_2). (d) The receiver operating characteristic curve of duration of symptom to poor postoperative outcomes. (e) The receiver operating characteristic curve of spinal cord compression ratio to poor postoperative outcomes..

	Non-PO (n=58)	PO (n=15)	P-value
■ Clinical characteristics ■			
Sex			0.650
Male	31 (53.4%)	9 (60.0%)	
Female	27 (46.6%)	6 (40.0%)	
Type of CP			0.784
Spastic	43 (74.1%)	10 (66.7%)	
Dyskinetic	11 (19.0%)	4 (26.7%)	
Mixed	4 (6.9%)	1 (6.7%)	
HTN			0.504
(-)	56 (96.6%)	14 (93.3%)	
(+)	2 (3.4%)	1 (6.7%)	
DM			0.504
(-)	56 (96.6%)	14 (93.3%)	
(+)	2 (3.4%)	1 (6.7%)	
OP type			1.000
Ant & Post fix	26 (44.8%)	7 (46.7%)	
Ant fix	17 (29.3%)	4 (26.7%)	
Post fix	13 (22.4%)	4 (26.7%)	
Fixation (-)	2 (3.4%)	0 (0)	
Age	45.0 ± 7.9	44.4 ± 8.6	0.729
Duration (years)	0.7 (0.3, 1.4)	2.0 (0.8, 2.8)	0.024*
Height (m)	1.6 (1.5, 1.7)	1.6 (1.5, 1.7)	0.973
Weight (kg)	55.2 ± 10.7	53.4 ± 6.7	0.566
BMI (kg/m2)	21.5 (18.7, 23.7)	20.4 (19.0, 21.0)	0.652
Pre-op MBI	66.0 (34.8, 89.5)	75.0 (61.5, 88.0)	0.235
■ Plain radiograph findings ■			
C0-2 Cobb angle (neutral)	15.9 (8.6, 26.6)	22.7 (16.1, 29.9)	0.243
C2-7 Cobb angle (flexion)	29.4 (17.0, 37.4)	34.2 (19.0, 42.9)	0.390
C2-7 Cobb angle (extension)	23.5 (12.9, 40.3)	34.4 (22.3, 44.9)	0.152
T1 slope	23.4 ± 11.2	19.9 ± 10.4	0.276
C2-7 sagittal vertical axis	21.3 ± 19.7	20.4 ± 22.8	0.868
C2-7 range of motion	-5.3 (-18.8, 18.4)	11.5 (-22.2, 22.2)	0.332
■ MRI findings ■			
T2SI grade			<0.001*
Grade 0	15 (25.9%)	3 (20.0%)	
Grade 1	41 (70.7%)	5 (33.3%)	
Grade 2	2 (3.4%)	7 (46.7%)	
T2SI type			0.228
None	15 (25.9%)	3 (20.0%)	
Focal	26 (44.8%)	4 (26.7%)	
Diffuse	7 (29.3%)	8 (53.3%)	
M1	75.0 (16.0)	64.5 (22.7)	<0.001*
M2	86.9 (9.5)	66.9 (19.1)	<0.001*
M3	72.4 (10.9)	62.4 (11.7)	<0.001*

Clinical characteristics and preoperative radiologic findings of participants.

■ Univariate analysis ■			
Variable	Odds ratio	95% Confidence interval	P-value
Sex			
Male	(reference)		
Female	0.765	0.230 – 2.401	0.650
Type of CP			
Dyskinetic	(reference)		
Spastic	0.937	0.192 – 3.555	0.929
Mixed	N/A		
HTN			
(-)	(reference)		
(+)	2.000	0.089 – 22.371	0.582
DM			
(-)	(reference)		
(+)	2.000	0.089 – 22.371	0.582
OP type			
Ant & Post fix	(reference)		
Ant fix	0.874	0.203 – 3.363	0.847
Post fix	1.143	0.260 – 4.528	0.851
Fixation (-)	N/A		
Age	1.013	0.944 – 1.095	0.724
Duration (years)	1.504	1.094 – 2.161	0.016*
Height (m)	0.742	0.001 – 511.404	0.928
Weight (kg)	0.983	0.925 – 1.039	0.561
BMI (kg/m2)	0.956	0.798 – 1.120	0.602
Pre-op MBI	1.017	0.996 – 1.042	0.146
C0-2 Cobb angle (neutral)	1.017	0.977 – 1.058	0.388
C2-7 Cobb angle (flexion)	1.017	0.972 – 1.067	0.464
C2-7 Cobb angle (extension)	1.019	0.987 – 1.053	0.235
T1 slope	0.969	0.912 – 1.022	0.273
C2-7 sagittal vertical axis	0.998	0.969 – 1.026	0.866
C2-7 range of motion	1.006	0.982 – 1.032	0.614
T2SI grade			
Grade 0	(reference)		
Grade 1	0.610	0.132 – 3.261	0.531
Grade 2	17.50	2.770 – 169.882	0.005*
T2SI type			
None	(reference)		
Focal	0.769	0.150 – 4.343	0.752
Diffuse	2.353	0.563 – 12.264	0.263
M1	0.887	0.819 – 0.940	<0.001*
M2	0.851	0.771 – 0.914	<0.001*
M3	0.874	0.797 – 0.937	0.001*
■ Multivariate analysis ■			
Variable	Odds ratio	95% Confidence interval	P-value
Duration (years)	1.990	1.249 – 3.652	0.009*
T2SI grade 2	10.439	1.316 – 118.006	0.034*
M1	0.981	0.844 – 1.168	0.816
M2	0.854	0.732 – 0.959	0.017*
M3	0.959	0.819 – 1.109	0.582

Univariate and multivariate logistic regression analysis of factors associated with poor outcomes.

Pediatric Rehabilitation

발표일시 및 장소 : 10 월 25 일(금), 13:40 ~ 15:10 , Room A

OPS-10

Quantitative muscle ultrasound: Imaging biomarker in Duchenne muscular dystrophy

Yu Jin Im^{1*}, Yumi Choe², Jong Geol Do¹, Jeong-Yi Kwon^{1†}

Department of Physical and Rehabilitation Medicine, Samsung Medical Center, Sungkyunkwan University School of Medicine¹, Department of Physical and Rehabilitation Medicine, Samsung Medical Center²

Objective

As the era of gene therapy begins, establishing biomarkers that represent the diverse disease state of Duchenne muscular dystrophy (DMD) is crucial for conducting clinical trials. This study explores the potential of quantitative muscle ultrasound (QMUS) as a non-invasive imaging biomarker for DMD. We evaluated the correlation between QMUS in various muscles and clinical functional assessments.

Methods

We used baseline data from a prospective observational longitudinal study in DMD. The study enrolled genetically confirmed DMD male patients aged 5 to 18 years. Participants underwent high-resolution muscle ultrasound scans of various muscle groups, with both qualitative (Heckmatt scale) and quantitative (grayscale level analysis) assessments of muscle echogenicity. Functional capacity was assessed using several tools, including the Vignos scale, Brooke scale, 6-minute walk test (6MWT), North Star Ambulatory Assessment (NSAA), timed function test, Performance of Upper Limb module for DMD (PUL), quantitative muscle strength tests, and respiratory muscle strength tests. Age adjusted partial correlations between QMUS and clinical functional assessments were analyzed using either Spearman's rank correlation test or Kendall's rank correlation test.

Results

Baseline data from 19 genetically confirmed DMD male patients were analyzed (mean age: 11.0 ± 4.0 years). All 19 patients underwent muscle ultrasound scans. Both mean grayscale values of the lower extremity (MGV-LE) and mean grayscale values of the upper extremity (MGV-UE) correlated with functional assessments, including 6MWT (MGV-LE correlation coefficient [CC] = -0.870, $p < 0.001$; MGV-UE CC = -0.850, $p < 0.001$), NSAA (MGV-LE CC = -0.397, $p = 0.021$; MGV-UE CC = -0.481, $p = 0.005$), 4-stair climb (MGV-LE CC = 0.816, $p = 0.001$; MGV-UE CC = 0.715, $p = 0.009$), 10m-walk/run (MGV-LE CC = 0.830, $p < 0.001$; MGV-UE CC = 0.735, $p = 0.006$), rise from floor (MGV-LE CC = 0.726, $p = 0.003$; MGV-UE CC = 0.628, $p = 0.016$). Quantitative muscle strength tests and pulmonary strength tests were not correlated with the MGV of the corresponding muscles.

Conclusion

In conclusion, the results of this study demonstrate that the QMUS is a valuable imaging biomarker for visualizing dystrophic muscle and representing physical function in patients with DMD. In particular, the mean grayscale value of lower extremity muscles from QMUS has the potential to serve as an alternative to comprehensive assessment in patients with DMD. Considering the necessity for repeated assessments, cost-effectiveness, and the risk of radiation exposure, QMUS is a suitable method for assessing dystrophic changes in muscle tissues.

Acknowledgment Financial support was provided by ENCell Co., Ltd., Korea.

Table 1. Demographic and clinical characteristics of participants

Characteristic	All participants (n=19)
Age (year), mean \pm SD	11.0 \pm 4.0
DMD gene mutation type	
Deletion, n (%)	7 (36.9)
Duplication, n (%)	2 (10.5)
Point mutation, n (%)	10 (52.6)
Anthropometric measurement	
Height (cm), mean \pm SD	127.1 \pm 12.6
Weight (kg), mean \pm SD	33.1 \pm 13.2
BMI (kg/m ²), mean \pm SD	19.7 \pm 6.0
Current use of corticosteroids	
Previous use, n (%)	1 (5.3)
Steroid naïve, n (%)	2 (10.5)
On oral steroid, n (%)	16 (84.2)
Ambulation status	
Ambulant, n (%)	15 (78.9)
Non-ambulant, n (%)	4 (21.1)
Comorbidities	
Scoliosis	3 (15.8)
Fragility fracture	3 (15.8)
Congestive heart failure	1 (5.0)

Abbreviations: SD, standard deviation; DMD, Duchenne muscular dystrophy; BMI, body mass index.

Table 1. Demographic and clinical characteristics of participants

Table 2. Age adjusted correlation coefficient between QMUS and functional measurements

Test	N		Mean grayscale value of QMUS											
			MGV-LE	RF	TA	GCM	MGV-UE	D	BB	FCR	M	SCM	GH	DP
6MWT (m)	14	CC	-0.870	-0.454	-0.894	-0.547	-0.850	-0.712	-0.492	-0.779	-0.340	0.094	-0.643	-0.344
		p	<0.001***	0.119	<0.001***	0.053	<0.001***	0.006**	0.087	0.002**	0.256	0.759	0.018*	0.250
NSAA, total score	19	CC	-0.397	-0.062	-0.262	-0.347	-0.481	-0.375	-0.342	-0.397	-0.166	-0.167	-0.253	-0.109
		p	0.021*	0.721	0.129	0.044*	0.005**	0.030*	0.047*	0.021*	0.335	0.334	0.142	0.527
4-stair climb (s)	13	CC	0.816	0.533	0.572	0.426	0.715	0.777	0.365	0.530	0.555	0.329	0.754	-0.025
		p	0.001**	0.074	0.052	0.168	0.009**	0.003**	0.243	0.076	0.061	0.296	0.005**	0.938
10-m walk/run (s)	13	CC	0.830	0.557	0.491	0.583	0.735	0.791	0.457	0.585	0.571	0.493	0.728	0.290
		p	<0.001***	0.060	0.105	0.047*	0.006**	0.002**	0.135	0.046*	0.053	0.103	0.007**	0.361
Rise from floor (s)	15	CC	0.726	0.330	0.675	0.467	0.628	0.580	0.351	0.458	0.062	-0.164	0.482	-0.140
		p	0.003**	0.250	0.008**	0.092	0.016*	0.030*	0.219	0.100	0.834	0.576	0.081	0.634
PUL, total score	19	CC	-0.137	0.072	-0.199	-0.197	-0.308	-0.221	-0.170	-0.390	-0.052	-0.104	-0.226	0.082
		p	0.427	0.675	0.250	0.254	0.075	0.199	0.324	0.024*	0.762	0.546	0.191	0.634

</

0.01≤*p*<0.05 (*), 0.001≤*p*<0.01 (**), *p*<0.001 (***)

Abbreviations: QMUS, quantitative muscle ultrasound; MGV-LE, mean grayscale values of lower extremity; RF, rectus femoris; TA, tibialis anterior; GCM, gastrocnemius; MGV-UE, mean grayscale values of upper extremity; D, deltoid; BB, biceps brachii; FCR, flexor carpi radialis; M, masseter; SCM, sternocleidomastoid; GH, geniohyoid; DP, diaphragm; 6MWT, 6-minute walk test; NSAA, North star ambulatory assessment; PUL, Performance of upper limb module; CC, correlation coefficient.

Table 2. Age adjusted correlation coefficient between QMUS and functional measurements

Table 3. Age adjusted correlation coefficient between strength test and QMUS of the corresponding muscle groups

Test	N	Mean grayscale values of QMUS		
		Muscle	CC	<i>p</i> -value
Quantitative muscle strength test				
Grip strength (kgf)	15	Flexor carpi radialis	-0.370	0.193
Elbow flexion (kgf)	19	Biceps brachii	-0.074	0.771
Knee extension (kgf)	19	Rectus femoris	-0.004	0.987
Ankle dorsiflexion (kgf)	19	Tibialis anterior	0.172	0.495
Respiratory muscle strength test				
MEP (cmH ₂ 0)	17	Diaphragm	0.235	0.398
MIP (cmH ₂ 0)	16	Diaphragm	0.395	0.162

Abbreviations: QMUS, quantitative muscle ultrasound; CC, correlation coefficient; MEP, maximal expiratory pressure; MIP, maximal inspiratory pressure.

Table 3. Age adjusted correlation coefficient between strength test and QMUS of the corresponding muscle groups

Poster Award
(Listed in order of presentation)

Brain & Neurorehabilitation

발표일시 및 장소 : 10 월 25 일(금), 10:00 ~ 10:30 , Poster Room, DID1

PS-1

Neural Protective Effects of Peripheral Nerve Microcurrent Therapy in an Alzheimer's Disease Mouse

Dong Rak Kwon^{1*†}, Eun Ho Kim², Won Seok Lee²

Department of Rehabilitation Medicine, Catholic University of Daegu School of Medicine,¹, Department of Biochemistry, Catholic University of Daegu School of Medicine²

Objective

This research aimed to explore the neural protective effects of peripheral nerve microcurrent therapy (mc) in an Alzheimer's disease mouse.

Methods

Twenty 5xFAD AD mice were randomly allocated to four groups (Figure 1). The procedures included different treatments: Control with untreated to Group 1 (CTL-untreated); Control with mc 6 hours daily for 4 weeks to Group 2 (CTL-mc; 5xFAD with untreated to Group 3 (5xFAD-untreated); and 5xFAD with MC to Group 4 (5xFAD-mc). Behavioral assessments, including the Novel Object Recognition Test (NOR) and Radial Arm Maze Test (RAM), demonstrated improved cognitive function following microcurrent therapy. Histological examination including nissl staining and thioflavin T staining, immunohistochemistry, Immunofluorescence, and western blotting were conducted.

Results

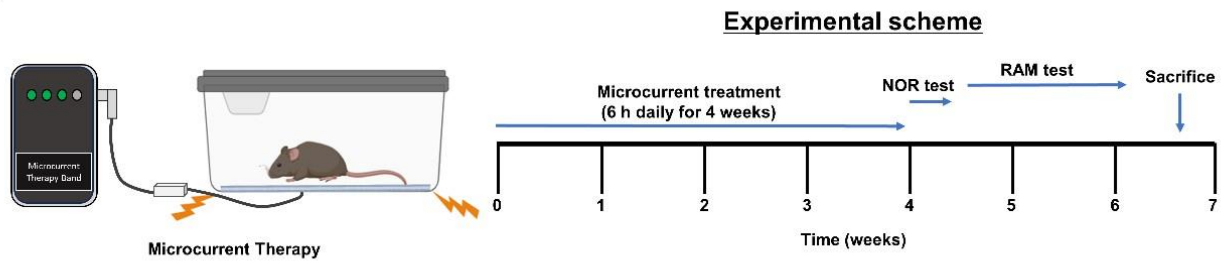
MC therapy attenuates memory impairment and reduces neurodegeneration, as evidenced by improved performance in memory tests and the preservation of the neuronal structure. Additionally, MC therapy significantly decreases amyloid-beta (A β) plaque deposition and inhibits apoptosis, indicating its potential to mitigate AD pathology. This study determined that glial activation is effectively reduced by using MC therapy to suppress the TLR4-MyD88-NF κ B pathway, which consequently causes the levels of inflammatory factors TNF- α , IL-1 β , and IL-6 to decrease, thus implicating TLR4 in neurodegenerative disease-related neuroinflammation

Conclusion

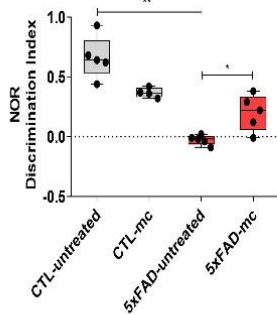
our findings highlight the broad potential of MC therapy in addressing various aspects of AD pathophysiology, including memory loss, neuronal damage, A β accumulation, and synaptic degeneration.

Acknowledgment This work was supported by the grant of Daegu Catholic University Medical Center (RD-23-0030).

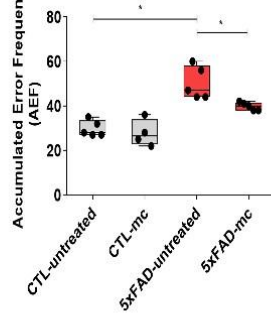
A



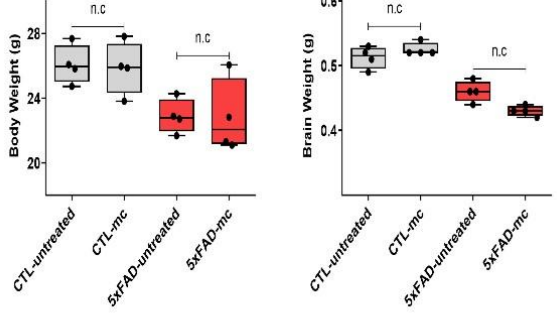
B



C



D



E

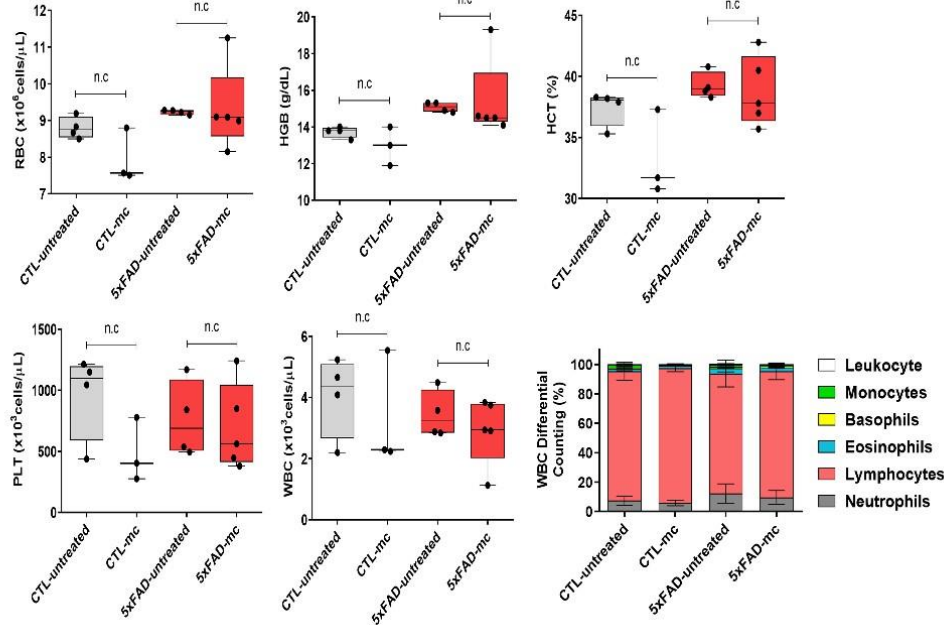


Figure 1. Microcurrent therapy mitigating memory impairment. (A) An illustration of the experimental process. (B) The novel object recognition task was performed on 5xFAD mice (transgenic Figure 1. Microcurrent therapy mitigating memory impairment. (A) An illustration of the experimental process. (B) The novel object recognition task was performed on 5xFAD mice (transgenic mice) and their control group (non-transgenic mice). The discrimination index was computed by determining the percentage ratio of $TB/(TA + TB) \times 100$, with TA referring to the known object and TB signifying the new object. (C) The radial arm maze test was employed to analyze spatial memory (CTL-untreated, 5xFAD-untreated, mc group, $n = 5$, and CTL-mc group, $n = 4$). (D) When the final experiment ended, the weights of the body and brain tissues of the mice were obtained (after 7 weeks) Int. J. Mol. Sci. 2024, 25, 6088 4 of 15 ($n = 5$ mice per group). (E) The hematological parameters for the mice were also determined toward the end of the final experiment ($n = 5$ mice per group). Means \pm SEMs are used to express the data. An ANOVA, followed by Tukey's test, was carried out. * $p < 0.05$ and ** $p < 0.01$ in contrast to the AD model group. The F-value in (B) = 27.8, (C) = 1.638, (D) = 4.939, 5.258, and (E) = 2.407, 2.706, 4.404, 1.223, and 0.6074.

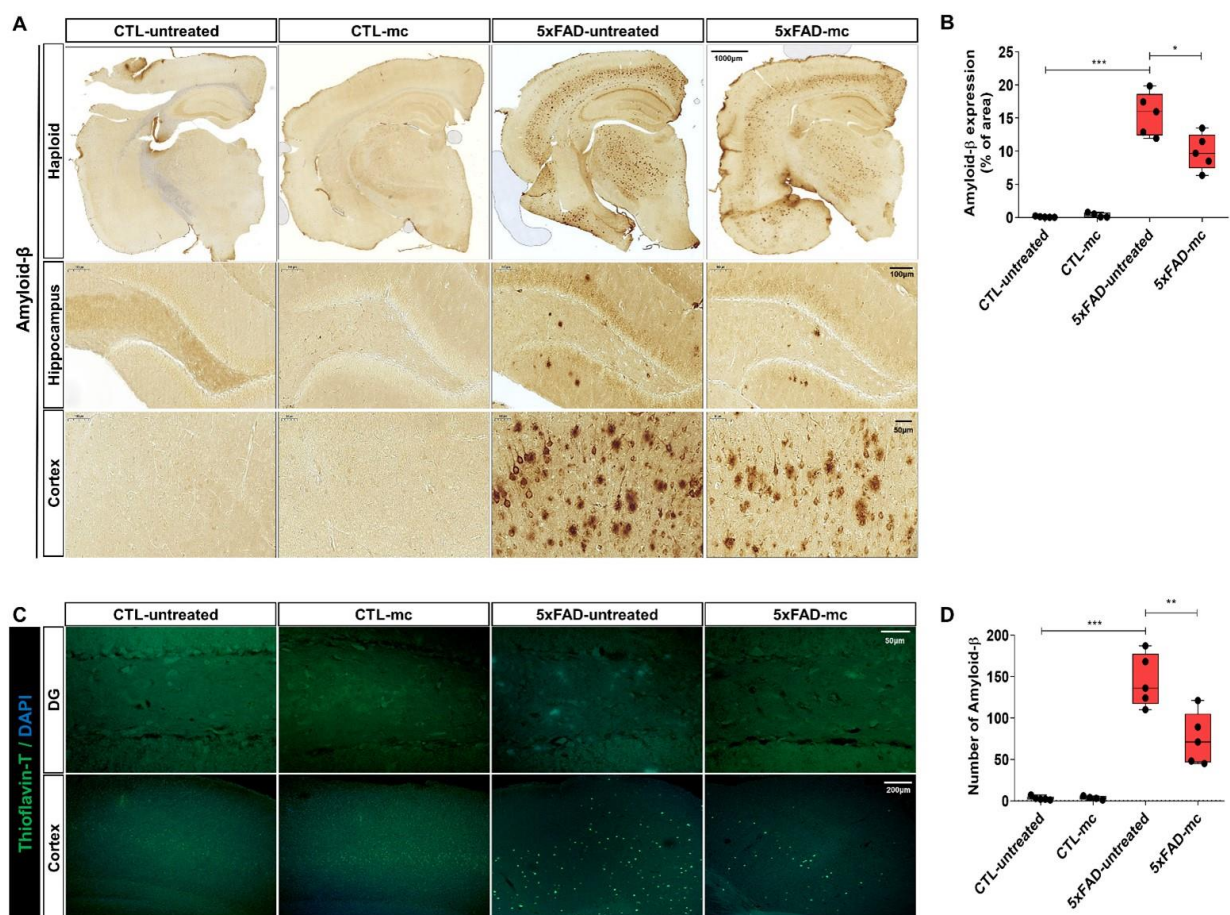


Figure 2. MC therapy reduced brain A β levels and improved the pathology of A β in AD mice. (A) Representative images of A β staining in the cortex, as well as the hippocampus, of every group are shown, for which the scale bar = 1000, 100, 50 μ m. Images with greater magnification are represented with black squares. A β positivity (shown as brown-colored images) was primarily seen in the cytoplasm of neuronal cells, as well as the cytoplasm and membranes of endothelial cells. (B) The amount of A β immunolabeled cells for each view and the extent of A β staining coverage in the brain of every group, with $n = 5$ mice per group. (C) A β plaque immunoreactivity within the cortex and hippocampus of every group is shown, as determined via Thioflavin T staining. Scale bar = 200, 50 μ m. Images with greater magnification are represented with white squares. (D) Quantification of Thioflavin T-positive deposits in both the cortex and hippocampus of four groups, with $n = 5$ mice per group. Means \pm SEMs are used to express the data. An ANOVA, followed by Tukey's test, was employed. * $p < 0.05$, ** $p < 0.01$ and *** $p < 0.001$ in contrast to the AD model group. The F-value in (B) = 2.804 and (D) = 1.158.

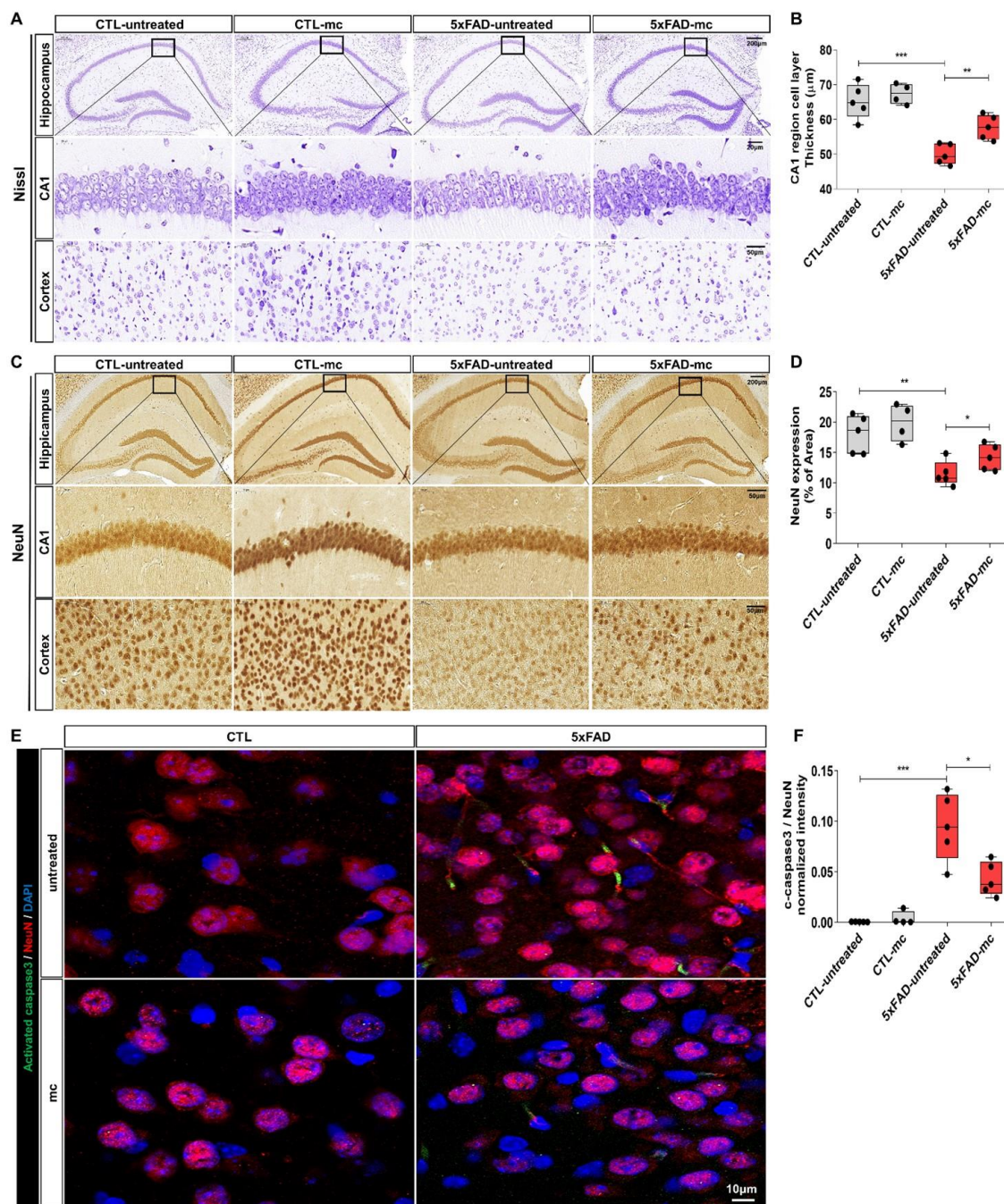


Figure 3. MC treatment compensated for neuronal loss and lowered activated caspase-3 expression levels within the brains of AD mice. (A) Nissl staining images depicting the frontal cortex and hippocampus of the CTL, AD model, MC, and untreated groups. Scale bar = 200, 50, 20 μm. Neuronal loss in the hippocampal CA1 regions was evaluated for the three groups with $n = 5$ mice in each group. (B) Quantification of thickness within the hippocampal CA1 region was determined. (C) Images of NeuN staining in the cortex and hippocampus ($n = 5$ mice per group). Scale bar = 200, 50 μm. (D) Neuronal contents in the cortex and hippocampus were quantified based on NeuN IHC staining outcomes. (E) Co-immunostaining with neuronal markers NeuN demonstrates Caspase-3 activation in the brain of the CTL, AD model, MC, and untreated groups. Scale bar = 20 μm. Images with greater magnification are represented with black squares ($n = 5$ mice per group). (F) The intensity of activated caspase-3 normalized against the neuronal marker NeuN for each view and the extent of activated caspase-3 staining coverage within the frontal cortex of each group are shown with $n = 5$ mice in each group. Means \pm SEMs are used to express the data. An ANOVA, followed by Tukey's test, was employed. * $p < 0.05$, ** $p < 0.01$, and *** $p < 0.001$ in contrast to the AD model group. The F-value in (B) = 13.86, (D) = 8.236, and (F) = 28.29.

Brain & Neurorehabilitation

발표일시 및 장소 : 10 월 25 일(금), 10:00 ~ 10:30 , Poster Room, DID1

PS-2

The LIBRAS Algorithm Determines Balance Recovery After Stroke through Clinical Evaluations

Dong Yun Kim^{1*}, Seulgi Yoon¹, Jae Young Lee¹, Sekwang Lee², Sung-Bom Pyun^{2,3,4†}

College of Medicine, Korea University¹, Department of Physical Medicine and Rehabilitation, Anam Hospital, Korea University College of Medicine², Brain Convergence Research Center, Korea University College of Medicine³, Department of Biomedical Sciences, Korea University College of Medicine⁴

Objectives: This study mainly aims to build an accessible yet accurate prognostic algorithm for balance recovery three months after stroke. We further aim to evaluate if safe balance can lead to recovery of independent walking ability.

Design and methods

66 first-time stroke patients from June 2016 to April 2024 whose initial Berg balance scale (BBS) was lower than 41 were included (Fig. 1). Demographics, stroke characteristics, initial clinical variables (BBS, strength in the hemiparetic hip and ankle muscles, mini-mental state examination, star cancellation test, and Fugl-Meyer assessment), neurophysiological variables (somatosensory evoked potential and motor evoked potential), and neuroimaging variables (fractional anisotropy of the corticospinal tract) were evaluated within a month after the onset. Classification and regression tree (CART) analysis identified factors of significance concerning safe balance (BBS \geq 41) at three months post-stroke, which were priorly selected by simple logistic regressions and Pearson's chi-square tests. The ambulation subscores of the modified Barthel index (MBIa) measured the patient's walking ability, and whether secure balance can guarantee independent ambulation was assessed according to each stage of MBIa.

Results

39 ischemic and 27 hemorrhagic stroke patients were included to the cohort. Twenty-nine of the whole patients had a right-sided stroke, 9 of which experienced visuospatial neglect. Patients with higher initial Medical Research Council grade of hip extensors (\geq 3), or if not (

Conclusions

The LIBRAS is an accurate algorithm that makes use of simple initial assessments to predict whether a patient can accomplish secure balance three months after the stroke. Moreover, the algorithm itself can intactly be extended into predicting the availability of ambulatory ability. The findings of this study emphasize the importance of proper early bedside measures in predicting the recovery of lower extremity functions. Further study is needed to validate this algorithm in a larger, discrete population.

Acknowledgment This work was supported by a National Research Foundation of Korea (NRF) grant funded by the Korean government (MSIT) (No. 2022R1A2B5B02001673).

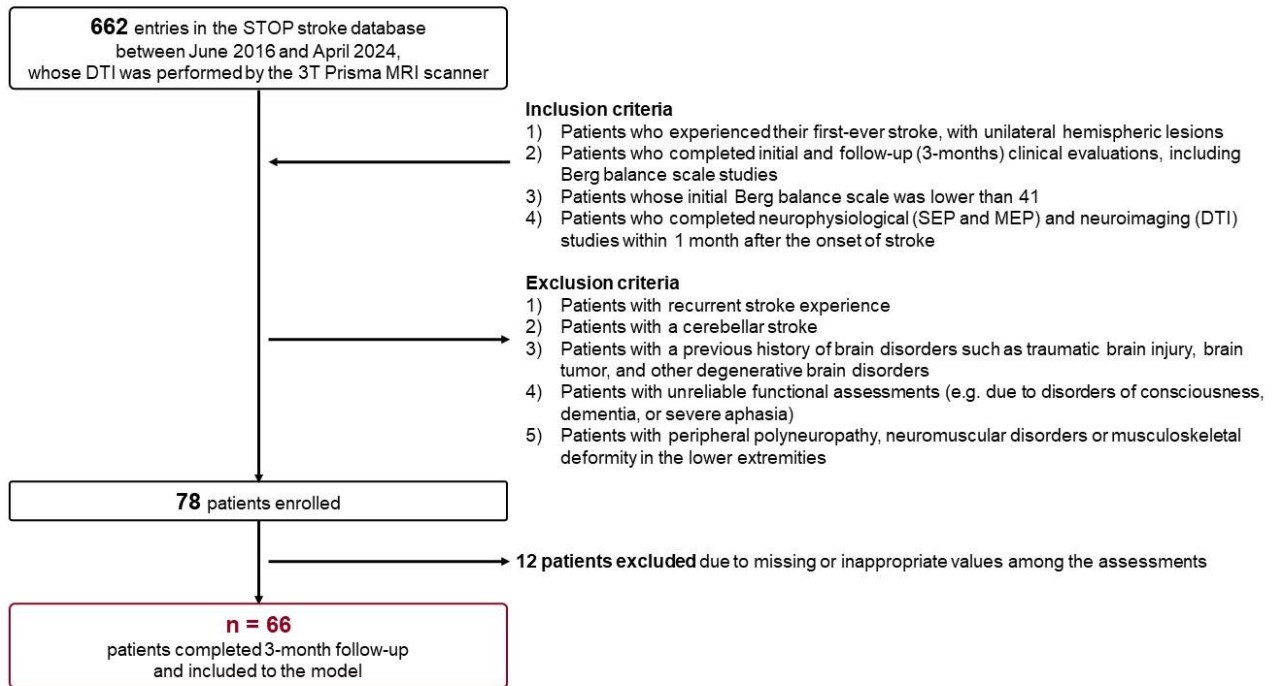


Figure 1. Flowchart of patient inclusion and exclusion.

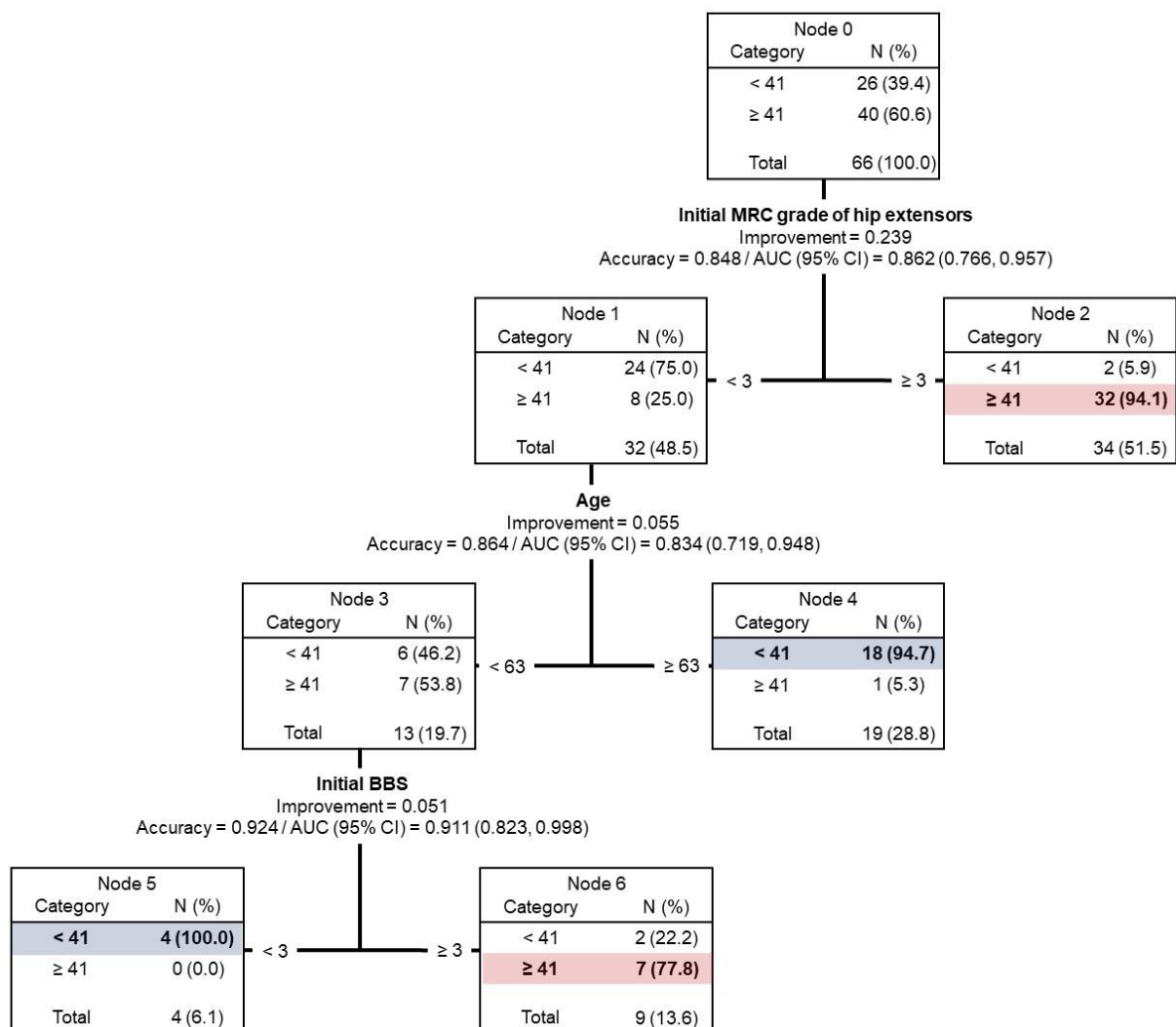


Figure 2. Classification and regression tree (CART) analysis. The analysis identified three factors to predict safe balance

3 months after stroke. The achievement of safe balance can be expected with substantially high accuracy and validity.
 / AUC, area under the curve; BBS, Berg balance scale; MRC, medical research council

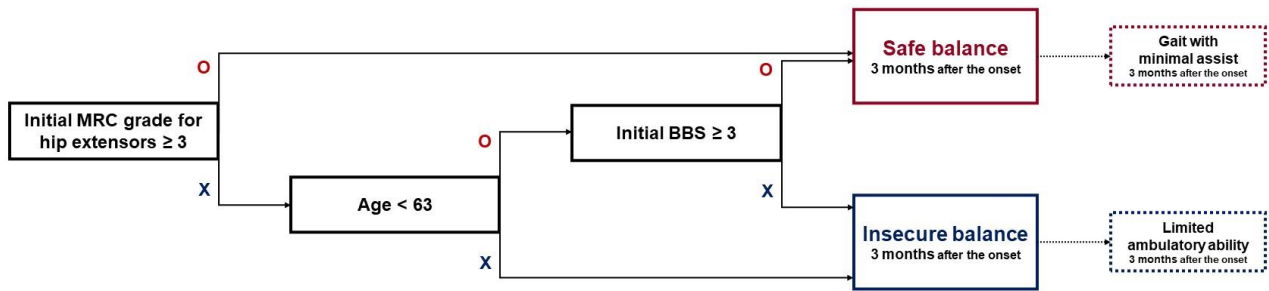


Figure 3. The Levels Indicating Balance Recovery After Stroke (LIBRAS) algorithm. The algorithm predicts if a patient can achieve safe balance and the ability to walk with minimal assist 3 months after stroke. / BBS, Berg balance scale; MRC, medical research council.

Brain & Neurorehabilitation

발표일시 및 장소 : 10 월 25 일(금), 10:00 ~ 10:30 , Poster Room, DID1

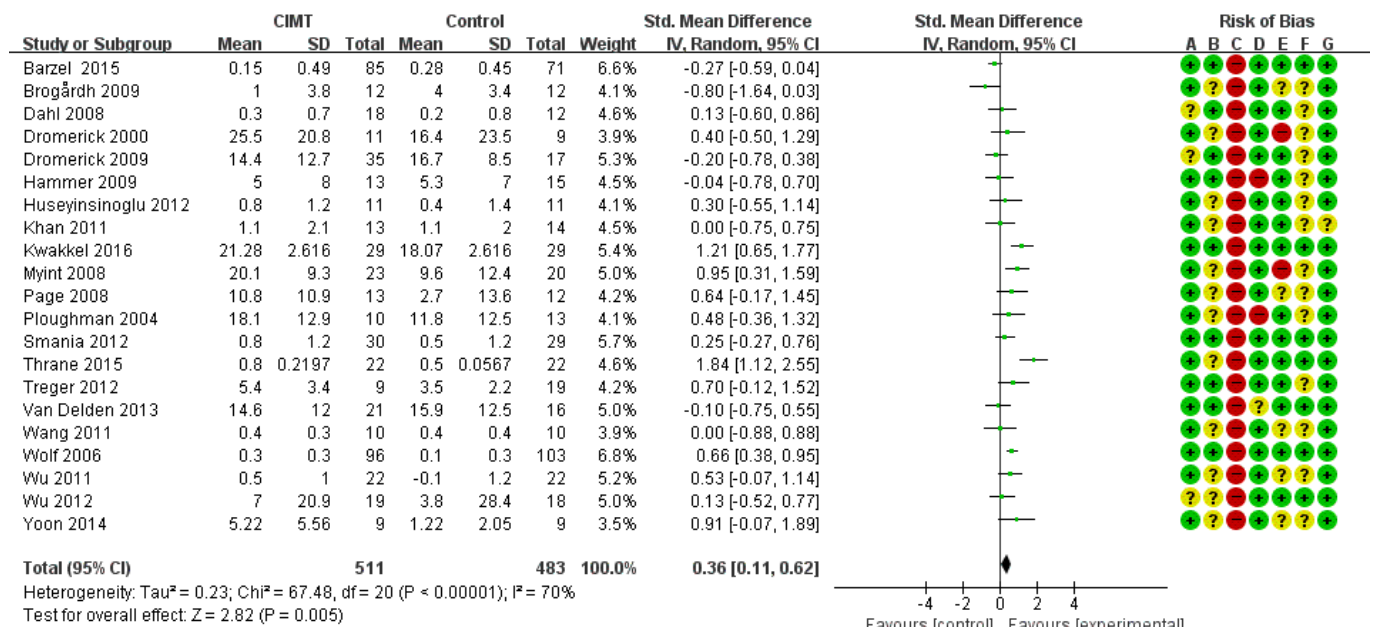
PS-3

The effect of Constraint-induced movement therapy on arm function and ADL in stroke patients

Hyoseon Choi^{1*}, Hyun Jung Kim^{1†}, Su Ho Jun¹

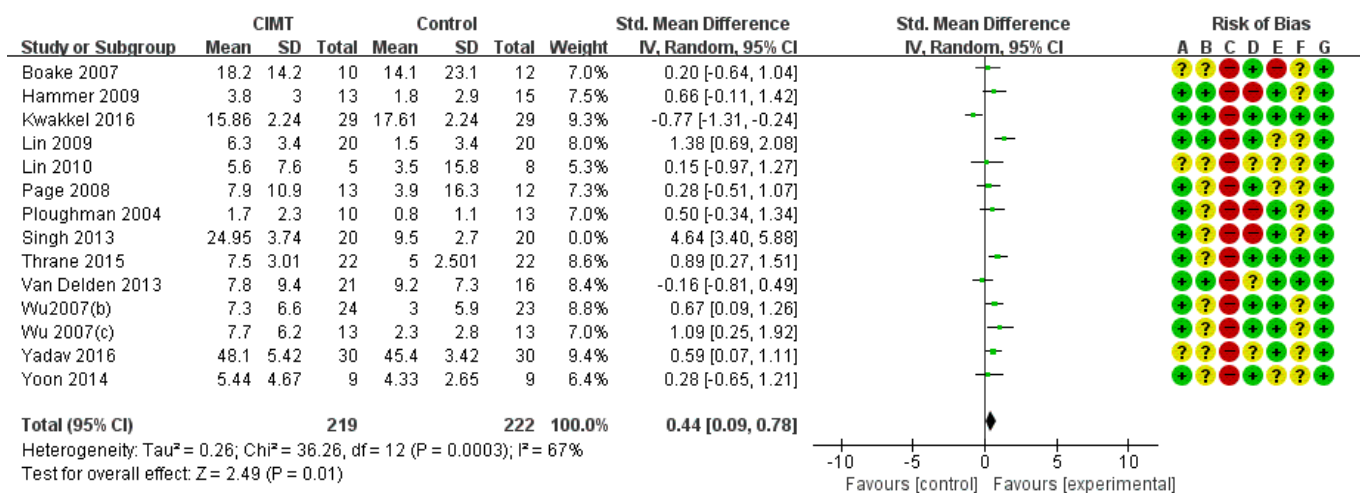
Department of Rehabilitation Medicine, Nowon Eulji Medical Center, Eulji University School of Medicine¹

The principle of Constraint-induced movement therapy (CIMT) is to correct the learned nonuse of the affected upper limb by restricting the movement of the unaffected limb and forcing the use of the affected limb. This meta-analysis included only studies that directly compared conventional rehabilitation therapy with CIMT in stroke patients with hemiplegia. We used 3 international electronic databases: MEDLINE, Embase, and the Cochrane Library. Risk of bias assessment was performed using the Cochrane's Risk of Bias 1.0 tool. The certainty of the evidence was assessed using the Grading of Recommendations, Assessment, Development, and Evaluations method. A total of 34 RCT studies were ultimately selected. In the meta-analysis, 21 RCT studies were included for arm motor function, 13 RCT studies for upper limb motor impairment, and 12 RCT studies for ADL performance. The meta-analysis revealed that CIMT has significant superiority over CT in improving arm motor function, arm motor impairment, and ADL. If CIMT can be implemented considering the strength of the affected upper limb, it is recommended to perform this therapy to improve upper limb function and ADL performance in post-stroke patients with hemiplegia.



Risk of bias legend
(A) Random sequence generation (selection bias)
(B) Allocation concealment (selection bias)
(C) Blinding of participants and personnel (performance bias)
(D) Blinding of outcome assessment (detection bias)
(E) Incomplete outcome data (attrition bias)
(F) Selective reporting (reporting bias)
(G) Other bias

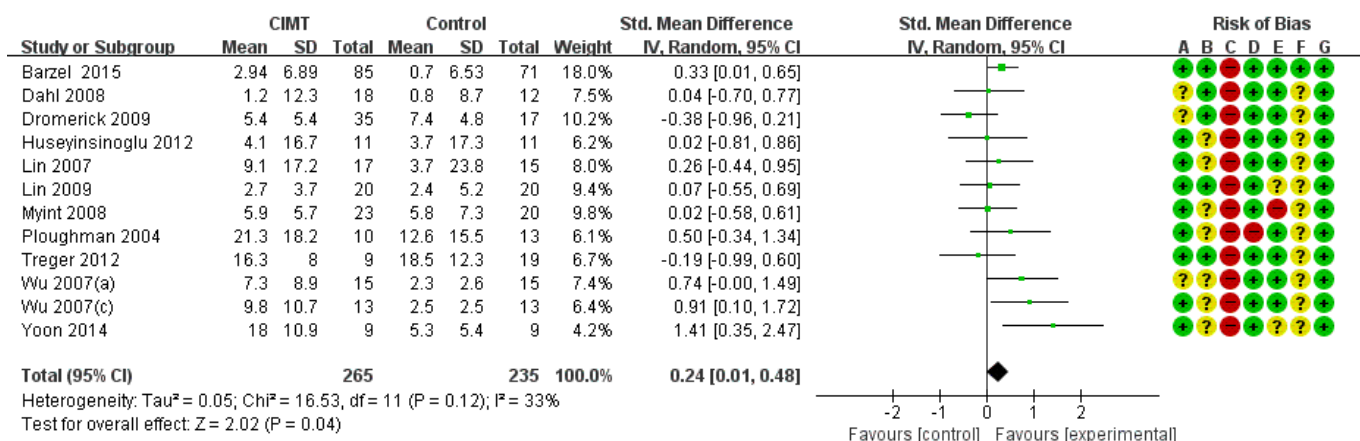
Fig 1. Effect of CIMT on arm motor function



Risk of bias legend

- (A) Random sequence generation (selection bias)
- (B) Allocation concealment (selection bias)
- (C) Blinding of participants and personnel (performance bias)
- (D) Blinding of outcome assessment (detection bias)
- (E) Incomplete outcome data (attrition bias)
- (F) Selective reporting (reporting bias)
- (G) Other bias

Fig 2. Effect of CIMT on arm motor impairment



Risk of bias legend

- (A) Random sequence generation (selection bias)
- (B) Allocation concealment (selection bias)
- (C) Blinding of participants and personnel (performance bias)
- (D) Blinding of outcome assessment (detection bias)
- (E) Incomplete outcome data (attrition bias)
- (F) Selective reporting (reporting bias)
- (G) Other bias

Fig 3. Effect of CIMT on ADL

Brain & Neurorehabilitation

발표일시 및 장소 : 10 월 25 일(금), 10:00 ~ 10:30 , Poster Room, DID1

PS-4

Restless leg syndrome and risk of Parkinson's disease: a nationwide retrospective cohort study

Myeonghwan Bang^{1*}, Dougho Park², Jong Hun Kim³, Tae Soo Lee¹, Hyoung Seop Kim^{1†}

Department of Physical Medicine and Rehabilitation, National Health Insurance Service Ilsan Hospital¹, Medical Research Institute, Pohang Stroke and Spine Hospital², Department of Neurology, National Health Insurance Service Ilsan Hospital³

Introduction

The pathophysiology of Restless Leg Syndrome (RLS) remains unknown, but it is assumed that the dopaminergic mechanism plays an important role. Since both RLS and Parkinson's disease (PD) respond to dopaminergic treatment, many studies have been conducted on the association between the two diseases, but it remains unclear. This retrospective cohort study aimed to explore the possibility that RLS could be deemed as prodromal symptom of PD.

Methods

This was a retrospective cohort study using the Korean National Health Insurance Service Sample Cohort. The subjects were observed for 18 years, from 2002 to 2019. Identifying patients with RLS and PD was based on the 10th revised code of the International Classification of Diseases (ICD-10). We compared the risk of PD in 9,919 subjects with newly diagnosed RLS and 9,919 matched controls based on age, sex, income, region, Charlson Comorbidity index score (Fig. 1.). The association between RLS and the risk of PD was assessed using Cox proportional hazard model. The effect of dopamine agonists(pramipexole, ropinirole) on the risk of PD among RLS patients was also explored.

Results

The mean age at enrollment for the control and RLS groups was 50.1 and 50.3, respectively, and the subjects were predominantly female (62.8%) in both groups (Table 1.). The incidence of PD was higher in the RLS group than that in the control group (1.6% vs 1.0%). A baseline diagnosis of RLS was associated with an increased risk of developing PD (adjusted hazard ratio(aHR) 1.42, 95% confidence interval(CI) 1.08–1.86) (Table 2.). Among RLS patients, the group that did not take dopamine agonists or received them only once had a higher risk of developing PD with an adjusted HR of 1.95, whereas the group that received dopamine agonists two or more times had a lower risk with an adjusted HR of 0.35.

Conclusions

The group with resistance to dopamine agonists in RLS could be considered as having prodromal symptoms of PD, whereas the group responsive to drugs could be seen as less associated with PD. Therefore, this retrospective cohort study suggests that although RLS two subgroups exhibit similar symptoms, they likely differ in pathophysiology and their association with PD.

Acknowledgment The authors did not receive any specific funding for this work and have no acknowledgements to declare.

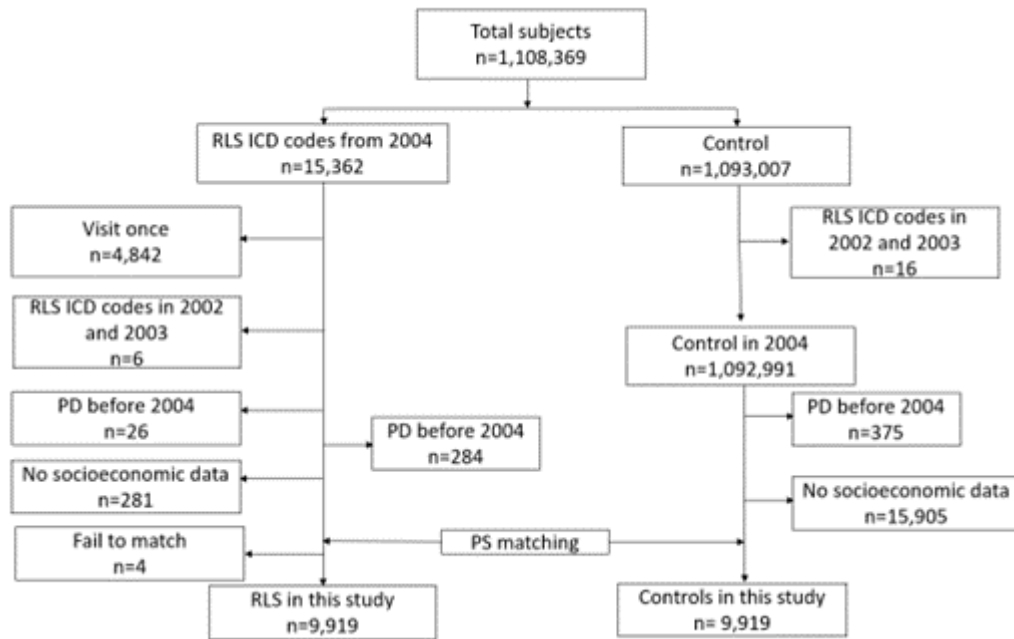


Fig 1. Flowchart of study population selection

	Control group (n=9919)	RLS group (n=9919)	p-value
Age at enrollment (years)	50.10±16.31	50.28±16.00	0.412
Sex			1
Male	3694(37.2)	3694(37.2)	
Female	6225(62.8)	6225(62.8)	
Income level by insurance fee			1
Bottom 0 to 30 th percentile	2390(24.1)	2390(24.1)	
Bottom 30 th to 70 th percentile	3709(37.4)	3709(37.4)	
Bottom 70 th to 100 th percentile	3820(38.5)	3820(38.5)	
Region of residence			1
Rural	5521(55.7)	5521(55.7)	
Urban	4398(44.3)	4398(44.3)	
CCI score			1
BMI			0.012
<18.5	293(3.5)	293(3.3)	
<23	3144(37.3)	3104(35.0)	
<25	2036(24.1)	2190(24.7)	
≥25	2966(35.1)	3278(37.0)	
Smoking			0.333
No smoking	6259(74.3)	6530(73.8)	
Quit	715(8.5)	725(8.2)	
Smoking	1454(17.2)	1599(18.0)	
Alcohol			<0.001
No drinking	5373(63.8)	5959(67.3)	
Drinking	3054(36.2)	2894(32.7)	
Comorbidities			
Sleep disorder ^b	388(3.9)	598(6.0)	<0.001
Iron deficiency anemia	353(3.6)	409(4.1)	0.055

Table 1. Characteristics of the study population

	Diagnosis of PD Cases, n(%)	Cox proportional hazard model			
		Crude HR (95% CI)	p-value	Adjusted HR (95% CI)	p-value
Control group	99(1.00%)	1(reference)		1(reference)	
RLS group	158(1.60%)	1.42(1.11-1.83)	<0.001	1.42(1.08-1.86)	0.012

Table 2. Risk of PD between the RLS and control groups

Cardiopulmonary Rehabilitation

발표일시 및 장소 : 10 월 25 일(금), 10:00 ~ 10:30 , Poster Room, DID1

PS-6

Association between cardiorespiratory fitness and phase angle in heart failure

Young Seok Kim^{1*}, Wonhee Lee¹, Tae Im Yi^{1†}

Department of Rehabilitation Medicine, Yongin Severance Hospital, Yonsei University College of Medicine, Yongin, 16995, Republic of Korea ¹

Introduction

While cardiorespiratory fitness is a pivotal parameter in heart failure, patients often fail to achieve maximal effort due to their frail condition. Recently, the phase angle (PhA) has been recognized as a potential prognostic marker for aerobic fitness. We investigated the association between PhA and cardiorespiratory fitness in heart failure patients.

Methods

This single-center observational study included 83 heart failure patients who simultaneously achieved maximal cardiopulmonary exercise test (CPET) with a respiratory exchange ratio > 1.10 and multifrequency BIA. The primary outcome was the discriminative performance of PhA for aerobic capacity below five metabolic equivalent (MET). We conducted Receiver Operating Characteristic (ROC) curve analysis to define the optimal cut-off point of PhA, and the area under the curve (AUC) with a 95% CI was calculated. Additionally, we evaluated the diagnostic performance of PhA alone and in conjunction with age and body mass index (BMI), and both were combined using DeLong's test to compare the performances of each model. Group comparison was conducted based on the cut-off point of PhA, using 1:1 Propensity score matching (PSM) for covariate balance. Lastly, univariable correlation analysis was conducted between PhA and peak oxygen consumption (Peak VO₂), anaerobic threshold (AT), minute ventilation/carbon dioxide production slope (VE/VCO₂), oxygen pulse, and chronotropic index (%).

Results

ROC curve analysis using PhA alone revealed excellent accuracy with the cut-off level of 4.5 (AUC 0.828, 95% CI: 0.731 – 0.926), and the inclusion of age or BMI increased the AUC slightly to 0.829 (95% CI: 0.731 – 0.928) and 0.864 (95% CI: 0.765 – 0.963), respectively. The addition of age and BMI increased the AUC to 0.877 (95% CI: 0.789 – 0.965), while these incremental improvements in AUC revealed no statistically significant differences. There were moderate to strong positive correlations with Peak VO₂ ($r = 0.62$, $P < .001$; 95% CI, 0.468 – 0.738), AT ($r = 0.55$, $P < .001$; 95% CI, 0.381 – 0.686), and oxygen pulse ($r = 0.65$, $P < .001$; 95% CI, 0.501 – 0.757), indicating that higher PhA was associated with cardiorespiratory fitness. In contrast, a weak correlation with chronotropic index ($r = 0.36$, $P < .001$, 95% CI: 0.158 – 0.536) and a moderate negative correlation with VE/VCO₂ ($r = -0.4$, $P < .001$, 95% CI: -0.571 to -0.207) was observed. After PSM, the low PhA group still showed lower aerobic capacity than the high PhA group.

Conclusions

Phase Angle differentiated patients under 5 MET acceptably with a cut-off value of 4.5 and demonstrated significant linear correlations with key CPET parameters, highlighting its potential as a predictor of cardiorespiratory fitness.

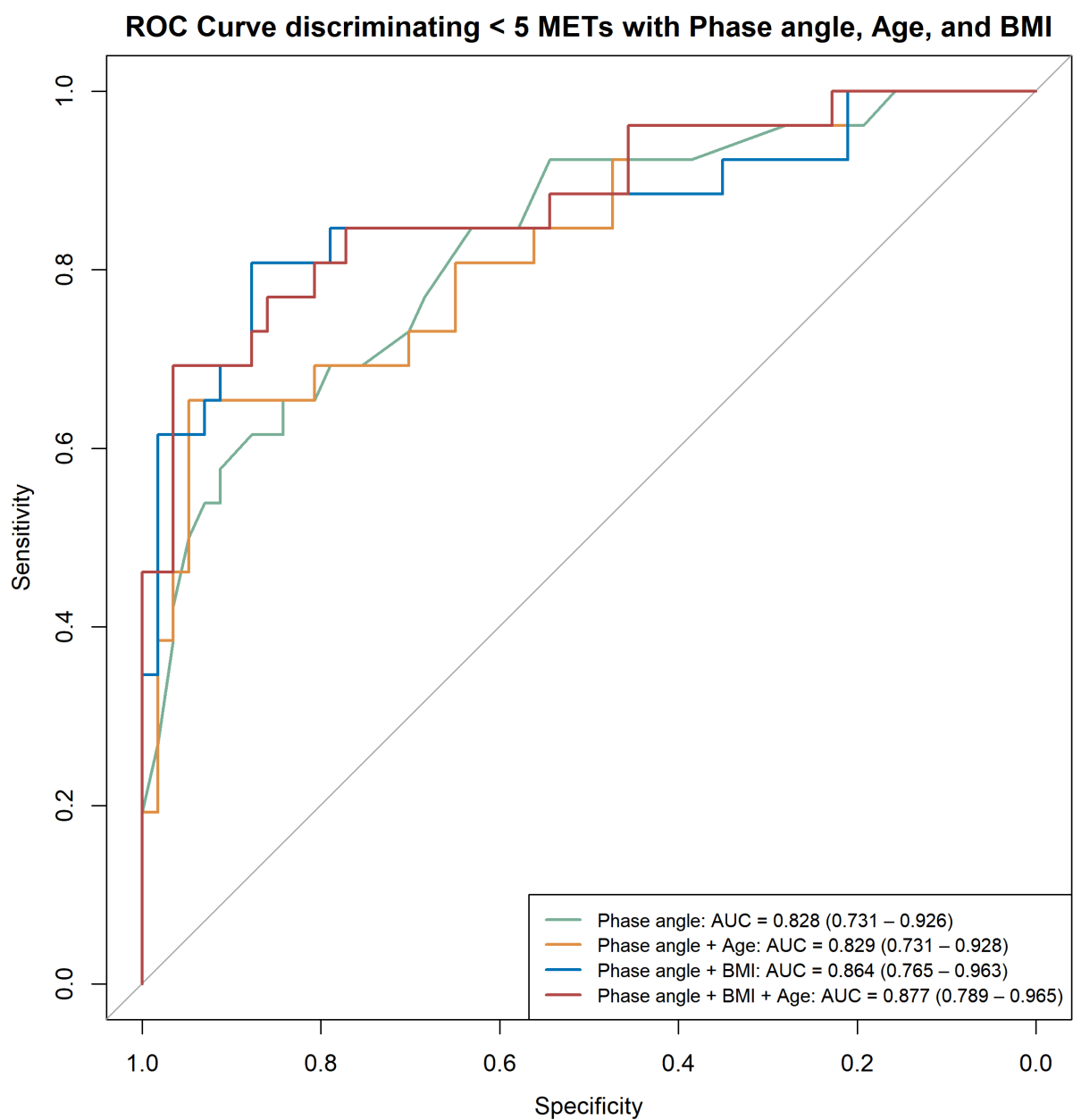


Figure 1. ROC Curve discriminating < 5 METs with Phase angle, Age, and BMI

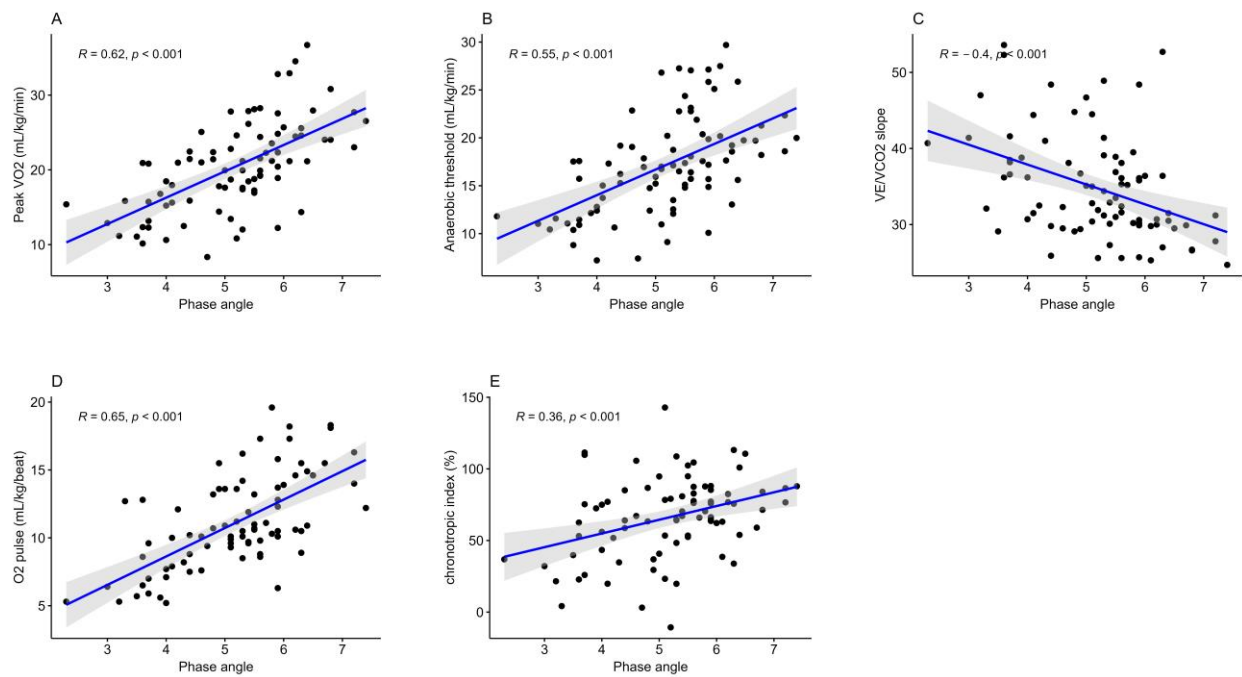


Figure 2. Scatter plot depicting the correlation between (A) Peak VO₂, (B) Anaerobic threshold, (C) VE/VCO₂ slope, (D) O₂ pulse, and (E) chronotropic index

Characteristic	Before Propensity Score Matching			After Propensity Score Matching		
	High PhA (N=60)	Low PhA (N=23)	P Value	High PhA (N=23)	Low PhA (N=23)	P Value
Phase Angle, °	5.7 ± 0.7	3.8 ± 0.5	<.001***	5.5 ± 0.5	3.8 ± 0.5	<.001***
Age, yr	57.2 ± 11.3	65.2 ± 16.4	.039*	63.9 ± 9.4	65.2 ± 16.4	.743
Female	1 (1.7%)	9 (39.1%)	<.001***	1 (4.3%)	9 (39.1%)	.012*
BMI, kg/m ²	26.0 ± 4.0	21.8 ± 3.7	<.001***	23.0 ± 1.8	21.8 ± 3.7	.167
Percentage fat mass, %	26.8 ± 6.0	28.0 ± 8.8	.561	24.3 ± 4.9	28.0 ± 8.8	.089
Current smoker	26 (43.3%)	6 (26.1%)	.233	6 (26.1%)	6 (26.1%)	1
Obesity	32 (53.3%)	4 (17.4%)	.007**	4 (17.4%)	4 (17.4%)	1
Hypertension	53 (88.3%)	22 (95.7%)	.551	21 (91.3%)	22 (95.7%)	1
Diabetes mellitus	27 (45.0%)	6 (26.1%)	.185	11 (47.8%)	6 (26.1%)	.222
Dyslipidaemia	40 (66.7%)	11 (47.8%)	.185	16 (69.6%)	11 (47.8%)	.231
Ischemic heart disease	48 (80.0%)	10 (43.5%)	.003**	20 (87.0%)	10 (43.5%)	.005**
NYHA Functional Class			.093			.403
I	40 (66.7%)	9 (39.1%)		13 (56.5%)	9 (39.1%)	
II	18 (30.0%)	11 (47.8%)		9 (39.1%)	11 (47.8%)	
III	1 (1.7%)	2 (8.7%)		0 (0.0%)	2 (8.7%)	
IV	1 (1.7%)	1 (4.3%)		1 (4.3%)	1 (4.3%)	
Current medications, No. (%)						
ACE inhibitor/ARB	34 (56.7%)	15 (65.2%)	.646	14 (60.9%)	15 (65.2%)	1
β-Blockers	46 (76.7%)	17 (73.9%)	1	15 (65.2%)	17 (73.9%)	.749
Diuretics	30 (50.0%)	21 (91.3%)	<.001***	12 (52.2%)	21 (91.3%)	.009**
Echocardiographic finding, mean ± SD						
LVEF, %	44.6 ± 11.2	41.5 ± 15.6	.398	42.5 ± 11.3	41.5 ± 15.6	.813
E/e'	13.0 ± 5.7	15.9 ± 6.0	.078	13.4 ± 5.3	15.9 ± 6.0	.206
LVMI, g/m ²	96.4 ± 26.6	101.6 ± 23.7	.415	105.0 ± 30.8	101.6 ± 23.7	.676
Cardiopulmonary exercise test, mean ± SD						
Peak VO ₂						
mL/min	1619 ± 461	907 ± 263	<.001***	1398 ± 328	907 ± 263	<.001***
mL/kg/min	22.2 ± 5.7	15.6 ± 3.8	<.001***	21.9 ± 5.0	15.6 ± 3.8	<.001***
% predicted	76.5 ± 18.5	67.1 ± 18.9	.044*	82.6 ± 16.8	67.1 ± 18.9	.005**
AT, mL/kg/min	18.7 ± 4.9	13.1 ± 3.1	<.001***	19.3 ± 4.8	13.1 ± 3.1	<.001***
Metabolic equivalents	6.3 ± 1.6	4.5 ± 1.1	<.001***	6.3 ± 1.4	4.5 ± 1.1	<.001***
VE/VCO ₂ slope	33.6 ± 6.2	38.1 ± 7.5	.006**	34.6 ± 6.8	38.1 ± 7.5	.099
Peak RER	1.16 ± 0.06	1.15 ± 0.06	.316	1.15 ± 0.05	1.15 ± 0.06	1
O ₂ pulse, mL/kg/beat	12.3 ± 3.0	8.0 ± 2.3	<.001***	10.9 ± 2.4	8.0 ± 2.3	<.001***
Chronotropic index, %	70.8 ± 26.9	53.6 ± 28.0	.012*	71.5 ± 24.9	53.6 ± 28.0	.027*

Table 1. Baseline Characteristics of Participants Classified by Phase Angle before and after Propensity Score Matching
Abbreviations: ACE, angiotensin-converting enzyme; ARB, angiotensin II receptor blocker; AT, anaerobic threshold; BMI, body mass index; E, E-wave velocity; e', early mitral annulus velocity (septal); IQR, interquartile range; LVEF, left ventricular ejection fraction; LVMI, left ventricular mass index; NYHA, New York Heart Association; PhA, Phase Angle; RER, respiratory exchange ratio; VCO₂, carbon dioxide production; VE, minute ventilation; VO₂, oxygen uptake

Table 1. Patients Characteristics Classified by Phase Angle before and after Propensity Score Matching

PS-7

Unilateral Hypoglossal Nerve Neurapraxia After Intubation: A Case Report

Jisoo Park^{1*}, Seung Yup Song¹, Dongwook Song¹, Geun-Young Park¹, Hae-Yeon Park¹, Sun Im^{1†}

Department of Rehabilitation Medicine, The Catholic University of Korea Bucheon St. Mary's Hospital ¹

Introduction

Hypoglossal nerve palsy (HNP), though rare, can significantly impact speech and swallowing. Symptoms include tongue deviation, atrophy, and impaired movement, leading to dysarthria and dysphagia. This can occur following procedural airway management during general anesthesia, resulting from various surgeries and airway management techniques. The review of HNP cases indicates the variability in recovery outcomes, highlighting the importance of early diagnosis and intervention to enhance patient prognosis. In this report, we discuss a 65-year-old female who developed focal hypoglossal nerve injury with sudden-onset dysphagia following an operation.

Case Presentation

A 65-year-old female presented with a blow-out fracture sustained on after slipping. Two weeks later, she underwent open reduction and internal fixation with absorbable plate insertion.

Post-operatively, the patient immediately exhibited tongue protrusion impairment and tongue deviation causing disarticulation and facial asymmetry affecting left lip closure. (Fig.1) She experienced dysgeusia, odynophagia with a foreign body sensation in the left pharynx, and difficulty swallowing. Despite no hoarseness, she had trouble with high-pitch phonation. Physical examination showed symmetric shoulder elevation.

FEES and VFSS confirmed symmetrical vocal fold and arytenoid motion. Bolus testing showed that liquid, nectar, and solid foods were tolerable, but the patient reported subjective difficulty in bolus transport of solid foods.

Brain MRI revealed no acute infarction. Viral markers were negative, excluding other causes of cranial neuritis. By laryngoscope, 3mm mass was observed at the left tongue base. (Fig. 2-a) Neck CT indicated mild asymmetric bulging at the left tongue base and oropharyngeal wall. Mouth MRI indicated asymmetric swelling and hyperintense changes in the left hypopharyngeal nerve, but no abnormalities along the XII nerve. (Fig. 2-b) Electromyography performed post 3 weeks of surgery showed left tongue denervation potentials, decreased recruitment, and discrete activity, while the right side was normal. Iowa Oral Performance Instrument (IOPI) measurements also showed unilateral weakness of left tongue. (Fig. 3)

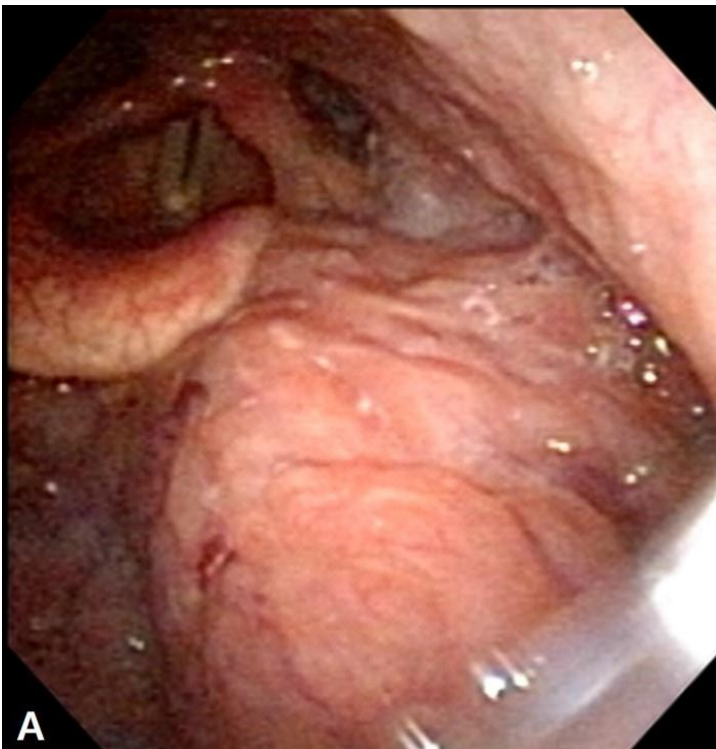
Steroid pulse therapy (Methylpredisolone total 308mg for 9days) was administered. After one month of treatment, the patient's tongue deviation improved, and she reported no discomfort other than a slight feeling of food remaining on the left cheek.

Conclusion

This case illustrates that hypoglossal nerve neurapraxia can rarely result from intubation and emphasizes the need for prompt diagnosis and a comprehensive treatment plan. Early intervention with steroid therapy may contribute to symptom improvement and functional recovery. Additionally, IOPI can serve as an auxiliary measurement tool to evaluate tongue strength in clinical settings.

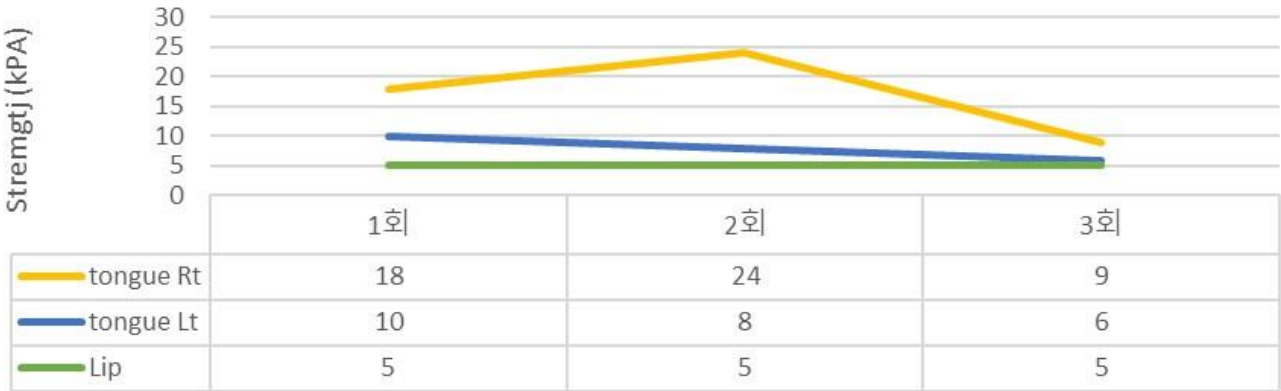


Clinical photo of patient showing tongue protrusion impairment with deviation to left side.



(A) Laryngoscope imaging of patient: 3mm mass was observed at the left tongue base. (B) Axial T1WI with intravenous contrast : Asymmetric swelling, hyperintense change in left tongue is seen.

Iowa Oral Performance Instrument (IOPI)



IOPI measurement results showed asymmetric weakness of left tongue strength.

Intraoperative electromyography monitoring for surgical planning during spinal cord tumor removal

Jinyoung Park^{1*}, Yura Goh¹, Dawoon Kim¹, Hyosik Eom¹, Yejin Lee¹, Joo Eun Park¹, Yoon Ghil Park^{1†}

Department of Rehabilitation Medicine, Gangnam Severance Hospital, Yonsei University College of Medicine¹

Introduction

Intraoperative neurophysiological monitoring for spinal cord tumor surgery has become increasingly common prevent the postoperative neurological complications. However, while evoked potential monitoring are considered as fundamental modalities, intraoperative electromyography (EMG) is often underestimated and less often monitored. Here, we present a clinical case where intraoperative EMG played a crucial role in spinal cord tumor surgery.

Case report

A 79-year-old man presented to a tertiary hospital with radiating pain and progressive weakness in bilateral lower extremities over a period of six months. The motor scores for 10 key muscles in bilateral lower extremities were graded as 4 according to the Medical Research Council scale. His sensory function was normal, and bladder and bowel functions were preserved. Magnetic resonance imaging revealed a cystic spinal cord tumor at the T12-L1 spinal level, and tumor removal surgery was planned with IONM including motor evoked potentials (MEPs), somatosensory evoked potentials (SEPs), free running EMG (fEMG), and triggered EMG (tEMG) (Fig. 1A). The MEPs and fEMG monitored bilateral tibialis anterior (TA) and abductor hallucis (AH) muscles. Bilateral abductor pollicis brevis muscle were also monitored for reference data. Baseline of bilateral tibial SEPs were obtained immediately after intubation, while baselines for MEPs were acquired after the effect of rocuronium had dissipated. During surgery, MEPs and SEPs showed no significant deterioration (Fig. 2A-B).

The surgeon ruptured the tumor cyst, and carefully made internal decompression using cavitronic ultrasonic surgical aspirator. During tumor retraction, fEMG showed B-train were observed in Rt. TA and AH muscle, of which promptly notified to surgeon (Fig. 3A-B). The IONM professional suggested to use of tEMG for identifying spinal nerves, along with the monopolar stimulator. The subdermal needle reference electrode was already inserted into the paraspinal muscles near the surgical site. The surgeon placed a disposable ball-tip stimulator in areas where he suspected the presence of spinal nerves. Stimulation was given with 0.2 – 2.0 mA intensity with 0.3 ms pulse width and 4.7 Hz frequency. During tEMG exploring, compound muscle action potentials were detected in Rt. AH muscle during the tumor removal at conus medullaris lesion (Fig. 3C-D). The frozen biopsy pathology revealed an ancient schwannoma. Consequently, initially planned en-bloc resection was terminated with subtotal removal (Fig 1B). All channels of MEPs showed increased amplitudes compared to the baselines after tumor removal, persisting until the end of the surgery. The patient experienced transient numbness lasting for several days in the right L5 and S1 sensory dermatome without any further weakness.

Conclusion

This study highlights the importance of utilizing fEMG and tEMG in ensuring the safety of spinal cord tumor surgeries involving the spinal nerves.

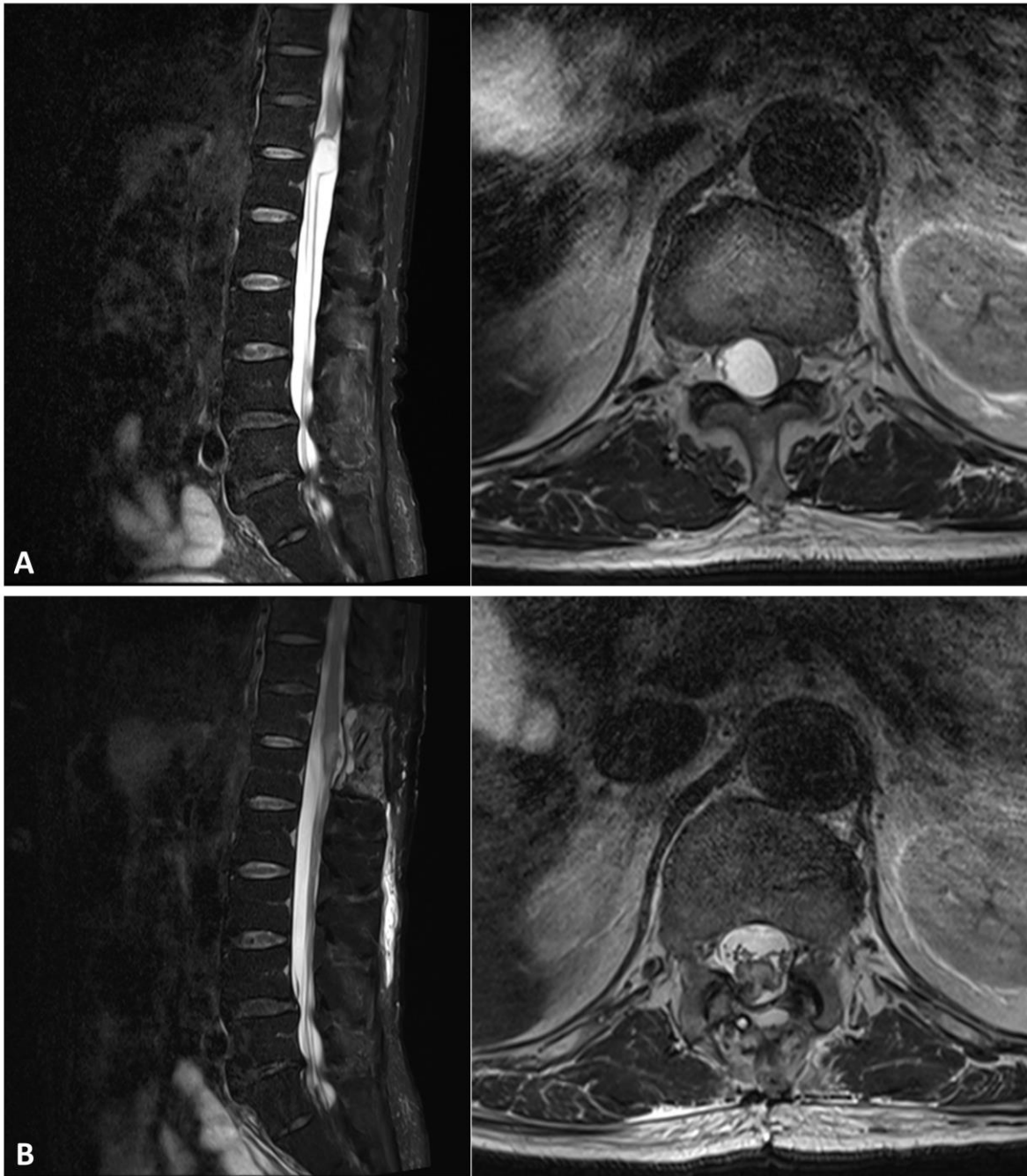


Figure 1. Magnetic resonance images of the spinal cord tumor before and after surgery. The T2-weighted magnetic resonance images before (A) and after (B) tumor removal surgery. The tumor was subtotally removed rather than en-bloc resection.

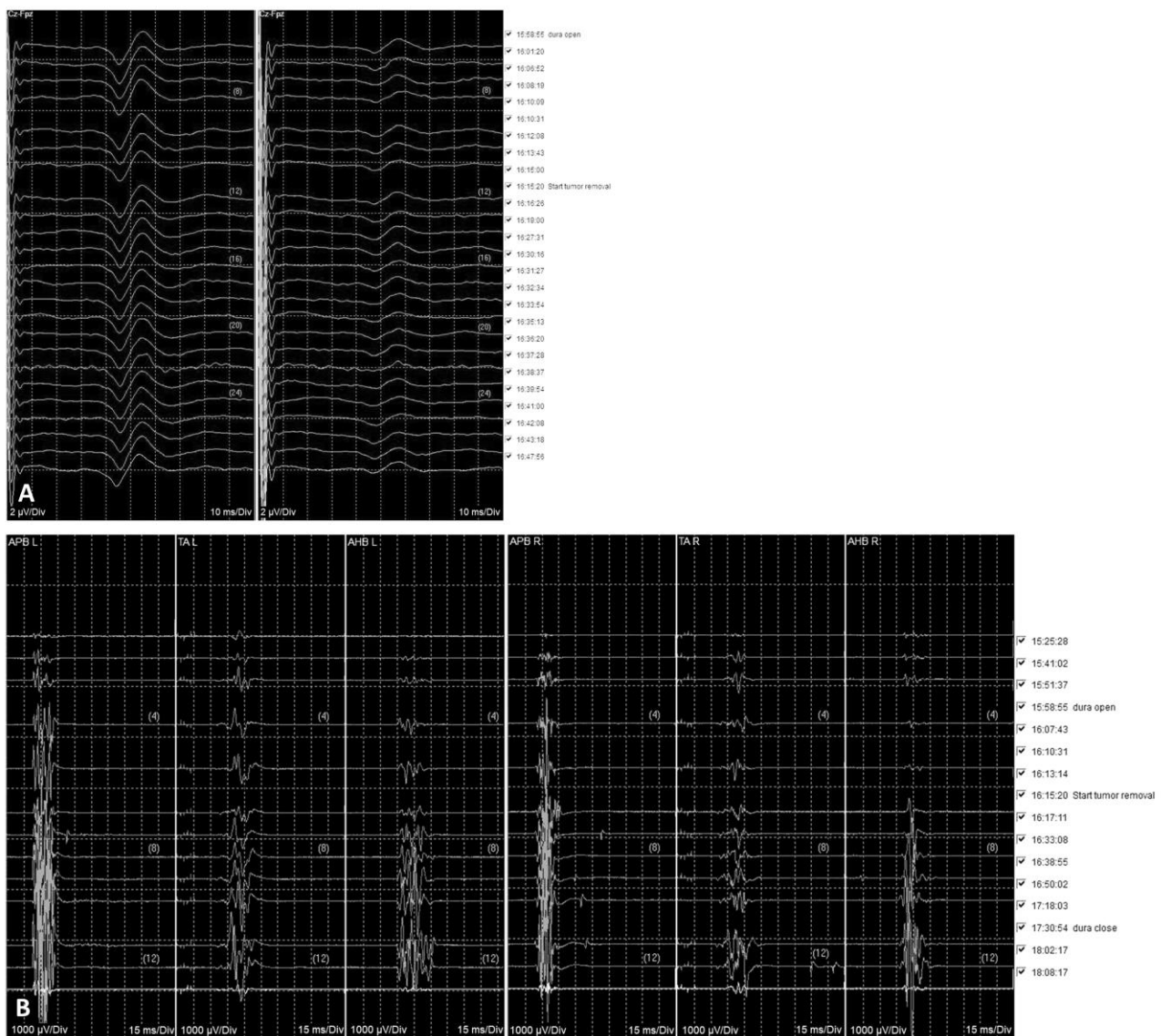


Figure 2. Intraoperative SEPs and MEPs during spinal cord tumor removal. Intraoperative SEPs (A) and MEPs (B) did not exhibit any significant deterioration compared to the baseline. Instead, MEPs in all channels showed increase amplitudes after tumor removal, persisting until the end of the surgery. SEPs, somatosensory evoked potentials; MEPs, motor evoked potentials.

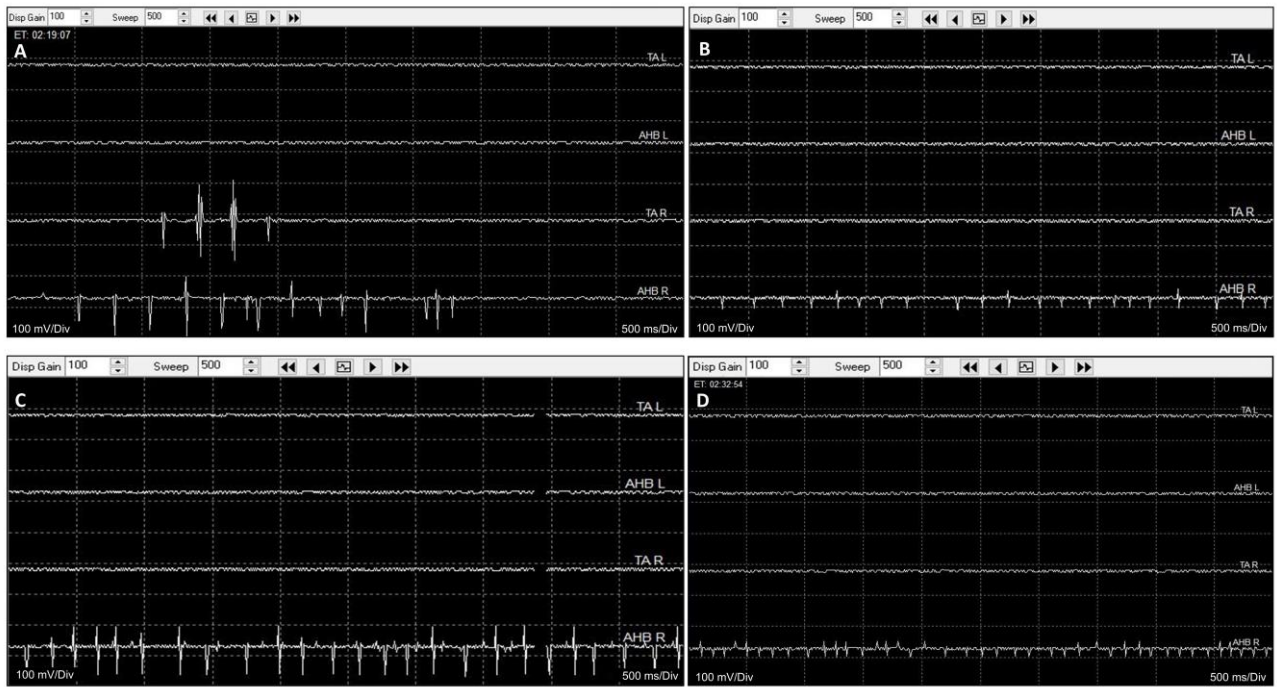


Figure 3. Intraoperative electromyography monitoring during spinal cord tumor removal. The fEMG displayed B-trains in the Rt. tibialis anterior and abductor hallucis muscles (A and B) during tumor retraction. Additionally, the tEMG revealed compound muscle action potentials in the Rt. abductor hallucis muscle during exploration of the spinal nerve at the lesion of the remaining tumor mass (C and D).

Anoctamin 5 muscular dystrophy diagnosed in 2 young male Korean soldiers

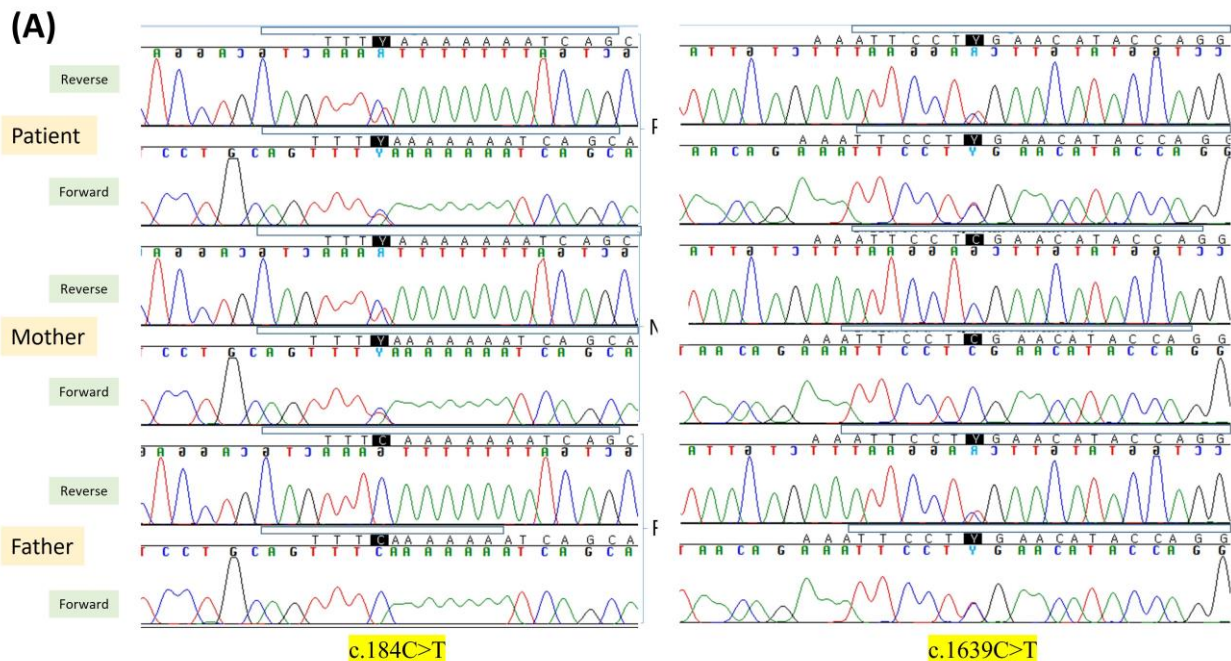
Kyoung-Eun Kim^{1*}, Dae-hyun Jang^{2†}, Hyunjoung Cho³

Department of Rehabilitation Medicine, Armed Forces Capital Hospital¹, Department of Rehabilitation Medicine, , Incheon St. Mary's Hospital, College of Medicine, The Catholic University of Korea², Department of Internal Medicine, Division of Rheumatology, Armed Forces Capital Hospital³

Muscle diseases related to the anoctamin-5 gene (ANO5) exhibit a wide range of muscle phenotypes, from limb-girdle muscular dystrophy and distal myopathy to pseudometabolic myopathy characterized by exercise intolerance and asymptomatic hyperCKemia. These conditions are prevalent in northern European cohorts due to a founder pathogenic variant, but few cases have been reported in the Asian population and none in Korea. We report the first two Korean patients diagnosed with ANO5-related muscular dystrophy, presenting with exercise intolerance during military training.

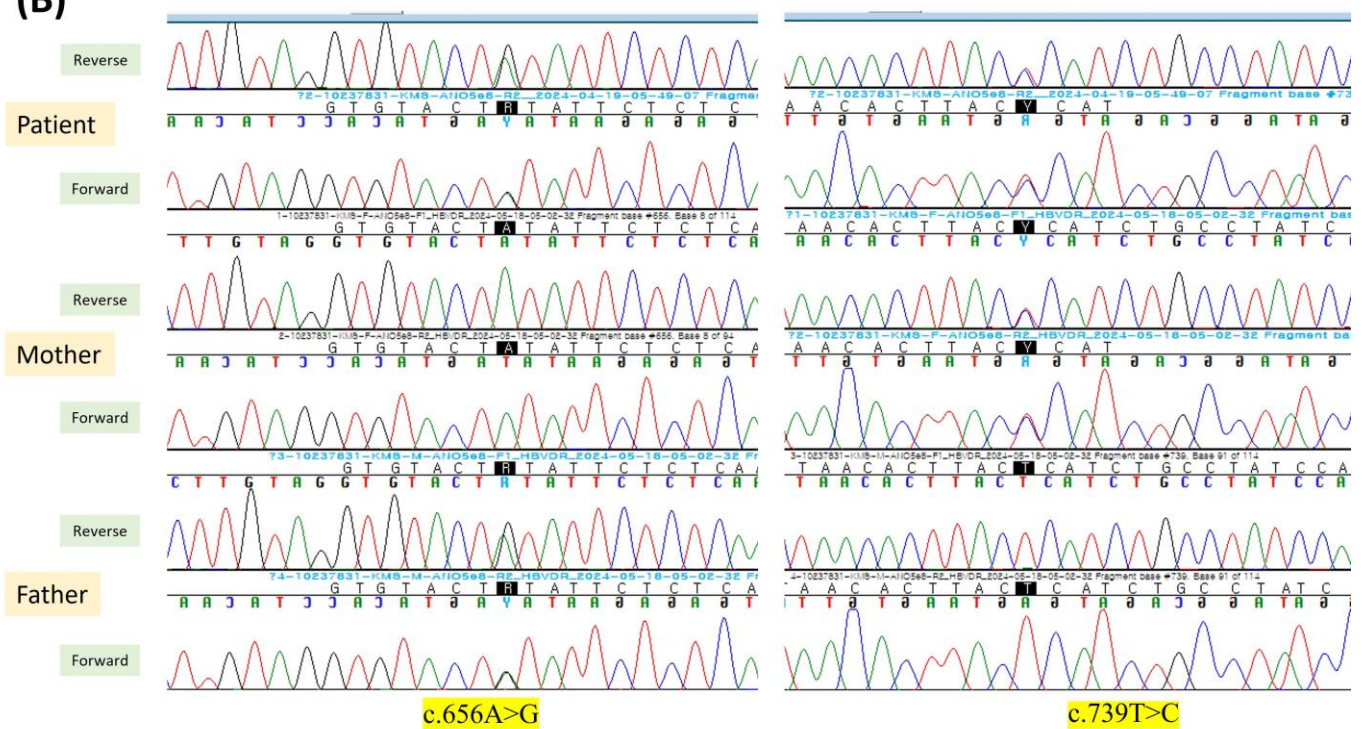
The first case involved a 21-year-old male recruit referred to our clinic for muscle pain and fatigue after training, with persistent hyperCKemia. Genetic testing identified two nonsense heterozygous variants of ANO5, c.184C>T and c.1639C>T. The second case, also a 21-year-old male recruit, presented with elevated serum liver enzymes and CK, and muscle pain after exertional activity. Genetic studies revealed two heterozygous missense variants, c.656A>G and c.739T>C, in trans configuration.

Both patients exhibited similar exercise intolerance and hyperCKemia without definite muscle weakness. These findings suggest underdiagnosis of ANO5-related muscular dystrophy in Korea and highlight the clinical necessity to evaluate this condition in young soldiers experiencing exertional rhabdomyolysis.



DNA sequencing chromatography of ANO5 for the patients and their parents. (A) The first proband had two nonsense variants: c.184C>T from the mother and c.1639C>T from the father.

(B)



(B) The second proband had two missense variants: c.656A>G from the father and c.739T>C from the mother.

Geriatric Rehabilitation

발표일시 및 장소 : 10 월 25 일(금), 10:00 ~ 10:30 , Poster Room, DID2

PS-12

Promoting Rehabilitation with an IoT based Patient Monitoring System in a Smart Hospital

Seung Ick Choi^{1,2*}, Young Seok Kim², Hui Woo Yang², Sung Min Hong², Won Hee Lee³, Na Young Kim^{2,3,4†}

Department of Integrative Medicine Major in Digital Healthcare, Yonsei University College of Medicine¹, Department of Rehabilitation Medicine, Yongin Severance Hospital, Yonsei University College of Medicine², Department of Rehabilitation Medicine, Yonsei University College of Medicine³, Center for Digital Health, Yongin Severance Hospital, Yonsei University College of Medicine⁴

Objective

Evolution of digital technology and wireless network are accelerating the digital transformation of healthcare systems. Wearable sensors and IoT technologies allow real-time monitoring of patient conditions. However, its widespread use in clinical settings is limited. Herein, we set up a digital platform that integrates various information coming from diverse wireless devices based on a 5G network and automatically records it in the EMR in a secondary care hospital. We also tested the feasibility of the system on the two patients admitted for rehabilitation.

Method

IoT network has set based on 5G mobile networks and 5GHz WiFi, as well as 1,136 in-ceiling passive Bluetooth low-energy beacon scanners in a single 17-story building. Data from various digital devices is extracted, transformed, and load on servers in a standardized format (Figure 1A). Report page that integrates information is automatically generated for each patients. Utilized digital solutions were as follows: All inpatients and their caregivers wear a beacon-enabled patient identification tag of real-time location system (Figure 1B). Patients are encouraged to self-report their symptoms using a mobile app (Figure 1C). The quantity and quality of the patient's physical activity is recorded using a smart insole and a band (Figure 1D). For testing the feasibility, patients older than 19 years admitted for rehabilitation were carefully selected.

Results

The first participant was a 59-year-old male patient with right side weakness and aphasia due to a stroke that occurred a week ago. Although he could not describe his physical activity, medical staff were able to objectively determine patients' daily walking time, distance and aerobic exercise intensity using our smart patient care system (Figure 2A). The second participant was a 71-year-old male patient underwent posterior lumbar interbody fusion for osteomyelitis three weeks ago. He still had moderate to severe pain at the surgical site, and suffered from anxiety, sleep disturbance, and depression as a result. Our system allows for rapid interventions, such as medication administration or counseling, when the patient complains of worsening pain or feels anxious. As symptoms improved, the patient was encouraged to increase ambulation. Based on recorded trends in pain, mood, sleep, and physical activity (Figure 2B), it was possible to adjust the dosage of related medications and prescribe appropriate exercise.

Conclusion:

This study presents a smart hospital system that monitors hospitalized patients by combining the patient's vital signs, activity information, and self-reports collected through wireless sensors and mobile apps. We also showed that this system actually helps establish treatment plans and provide appropriate treatment. Specifically, patient participation in rehabilitation was promoted. Future research is needed to integrate more devices and apply them in various clinical cases.

Acknowledgment This research was supported by a grant of the Korea Health Technology R&D Project through the Korea Health Industry Development Institute (KHIDI), funded by the Ministry of Health & Welfare, Republic of Korea (grant number: RS2023-00265489 and RS-2023-KH135442).

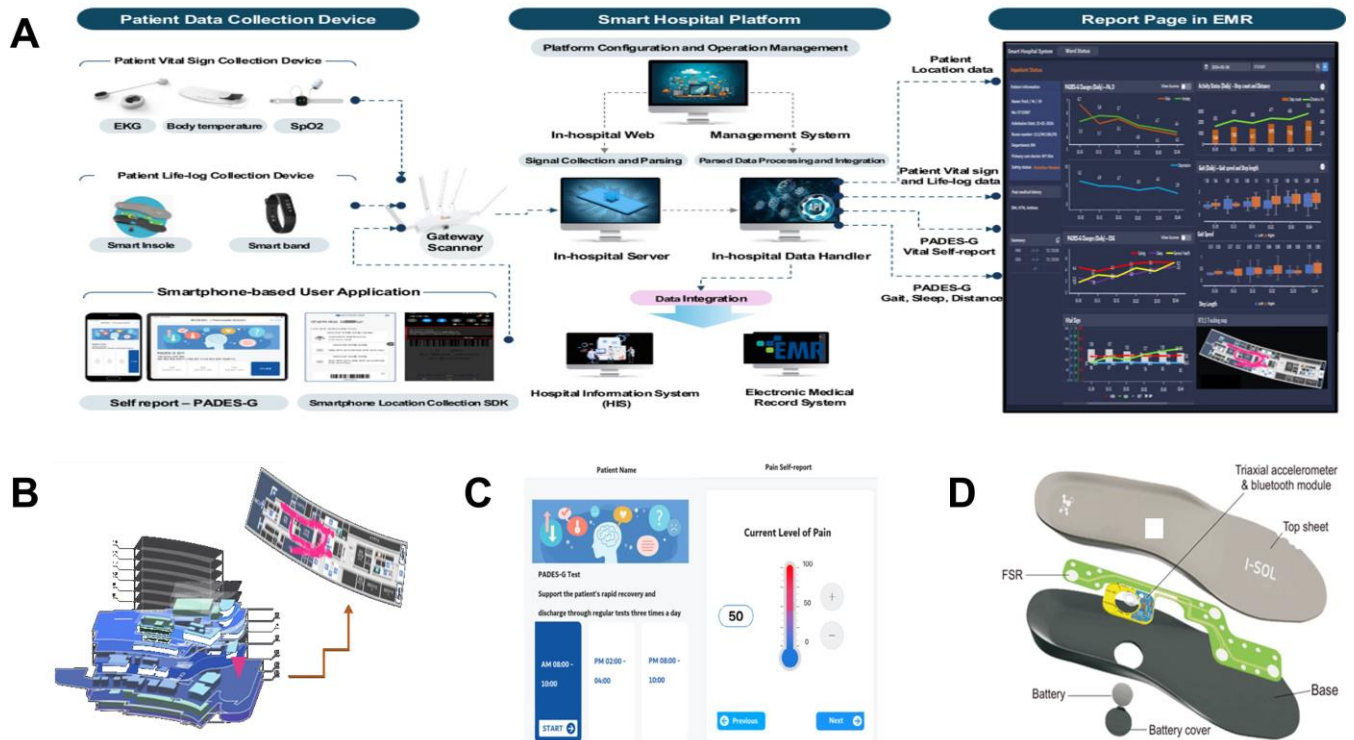


Figure 1. (A) Overview of Smart Hospital System based on 5G network in a secondary care hospital: Data is collected from the wireless sensor to the server through the gateway scanner; Numeric parameters are integrated with hospital information system and electrical medical record (EMR); A report page that displays summary of data for each patient is automatically created. (B) Real-Time Locating Systems based on BLE technology tracks patient movements within the hospital. (C) The mobile app, PADES-G, records self-reported symptoms. (D) Physical activity of patient is recorded by smart Insole with accelerometer and pressure sensors.

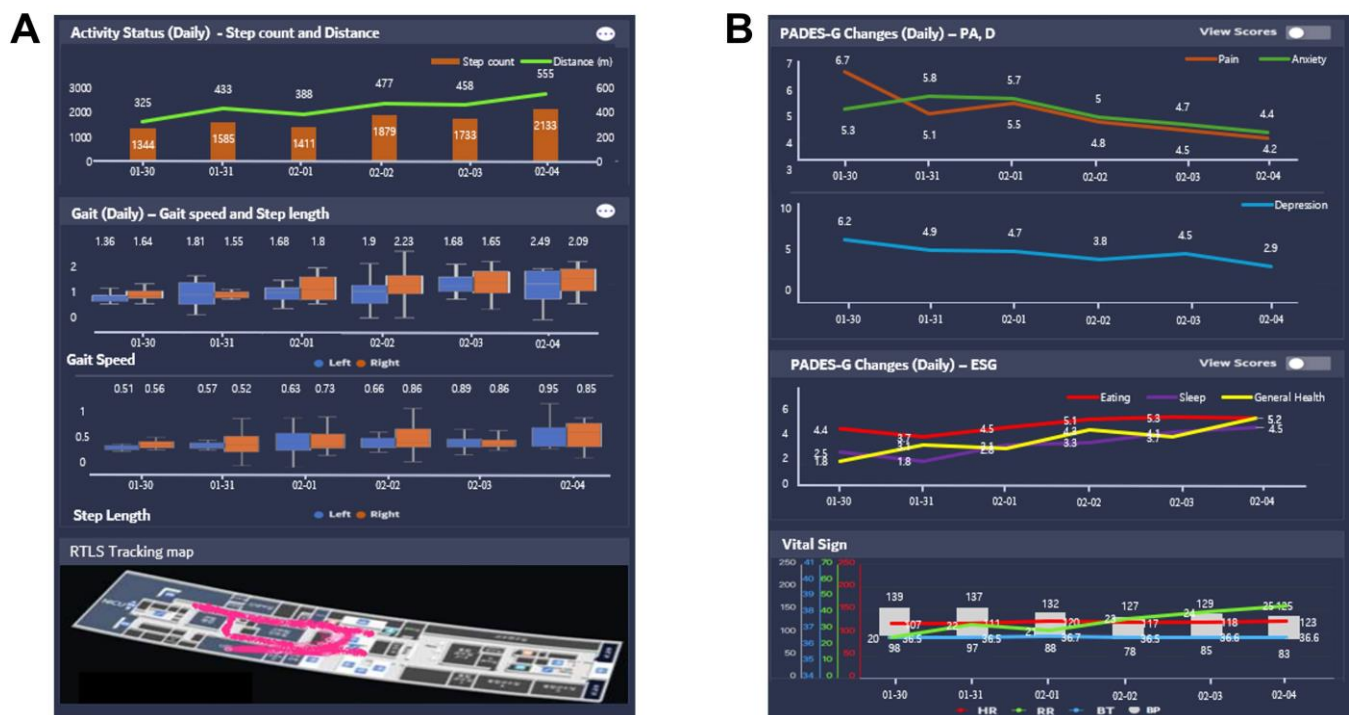


Figure 2. (A) Monitoring gait patterns and action radius assisted in appropriate exercise prescription for the aphasic patients with gait disorders. (B) Monitoring pain, depression, and sleep was helpful in adjusting medications and promoting exercise for the patient after spinal surgery.

Pediatric Rehabilitation

발표일시 및 장소 : 10 월 25 일(금), 10:00 ~ 10:30 , Poster Room, DID2

PS-13

First Report of FLNA Gene Mutation-Associated Lissencephaly and Developmental Delay in South Korea

Myeong Geun Jeong^{1*}, Soyoung Lee^{1†}

Department of Rehabilitation Medicine, Keimyung University Dongsan Hospital, Keimyung University School of Medicine, Daegu, Republic of Korea¹

Introduction

Lissencephaly, a rare brain malformation marked by the absence of normal convolutions in the cerebral cortex, is linked to several genetic mutations, including LIS1, RELN, TUBA1A, NDE1, KTN1, CDK5, ARX, and DCX. FLNA gene mutations, which typically cause disorders like FLNA-related periventricular nodular heterotopia (PVNH), rarely result in lissencephaly without PVNH. This report presents the first known case in South Korea of lissencephaly associated with an FLNA mutation, detailing the neurological and developmental challenges faced by the patient.

Case Report

An 8-year-old girl presented to the rehabilitation department with significant developmental delays and a tip-toeing gait. Born full-term via normal delivery, she exhibited delayed motor development with muscle strength rated as Grade F in the upper extremities, Grade F+ in the right lower extremity, and Grade F- to P in the left lower extremity on the Manual Muscle Test. Her active left ankle dorsiflexion was limited to 0 degrees, and she had a positive Babinski sign on the left side. Her Modified Barthel Index (MBI) was 90/100, and Berg Balance Scale (BBS) was 39. Hand grip strength was significantly reduced at 10.6 kg on the right and 2.7 kg on the left, both below age norms. The Preschool Receptive-Expressive Language Scale (PRES) indicated receptive language at 52 months, expressive language at 41 months, and integrated language at 47 months. Visual perception tests revealed below-average general visual perception and inferior visual-motor integration.

Brain MRI revealed lissencephaly in the entire right hemisphere (Figure 1), prompting genetic testing. Karyotyping, chromosomal microarray, and next-generation sequencing confirmed a mutation in the FLNA gene.

Upon diagnosis, neurodevelopmental treatment was initiated, including cognitive and language rehabilitation and the use of a left ankle-foot orthosis. One year later, at age 9, the patient showed significant motor improvement: muscle strength increased to Grade G to N in the right upper extremity and Grade G in the left, with lower extremity strength at Grade N on the right and Grade G to F+ on the left. Left ankle dorsiflexion improved to 15 degrees. The MBI was 91/100, and the BBS improved to 53. However, hand grip strength remained below average. PRES assessments indicated receptive language at 75 months, expressive language at 49 months, and integrated language at 62 months, showing a developmental delay of about four years.

Discussion

This is the first reported case in South Korea of lissencephaly linked to an FLNA gene mutation without PVNH. The findings underscore the importance of genetic analysis in diagnosing developmental delays and congenital brain anomalies. A precise diagnosis that considers both genetic and symptomatic factors is crucial for setting and achieving targeted rehabilitation goals, and for promoting meaningful functional improvements through precision rehabilitation management.

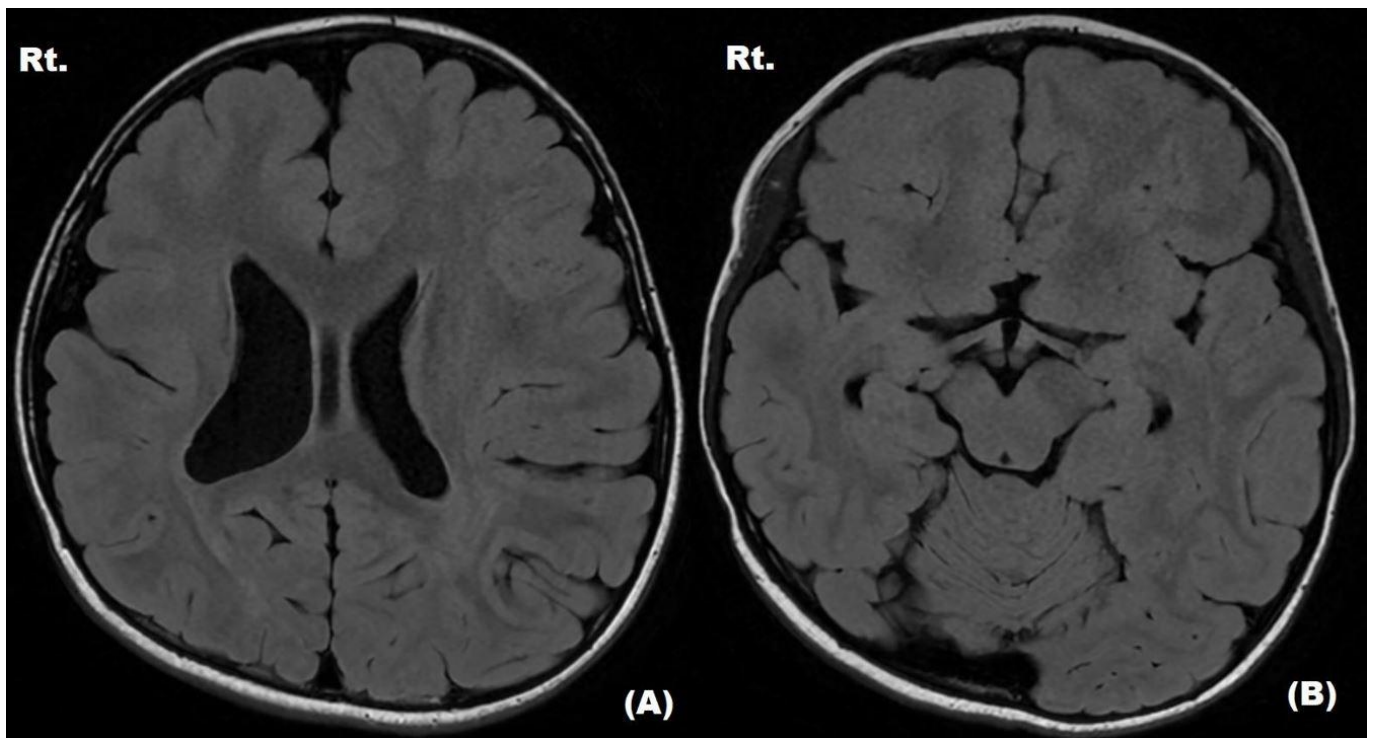


Fig 1. Brain MRI images taken when the patient was 8 years old. A-B) Axial T2-FLAIR images demonstrate diffuse cortical thickening and decreased volume of the right cerebral hemisphere, accompanied by lissencephaly affecting the entire right hemisphere.

Geriatric Rehabilitation

발표일시 및 장소 : 10 월 25 일(금), 13:10 ~ 13:40 , Poster Room, DID1

PS-14

Effect of Exercise combined with Adipose-derived Mesenchymal Stem Cells in a Sarcopenic Rat Model

Dong-Hwa Jeong^{1*}, Min-Jeong Kim¹, Yong-Taek Lee¹, Kyung-Jae Yoon¹, Chul-Hyun Park^{1†}

Department of Physical and Rehabilitation Medicine, Samsung Kangbuk Hospital¹, Medicinal Bioconvergence Research Center, College of Pharmacy, Seoul National University², Department of Physical and Rehabilitation Medicine, Samsung Kangbuk Hospital³, Department of Physical and Rehabilitation Medicine, Samsung Kangbuk Hospital⁴, Department of Physical and Rehabilitation Medicine, Samsung Kangbuk Hospital⁵

Background/Aims

Sarcopenia, characterized by an age-related progressive decline in muscle mass, strength, and function, restricts daily activities and causes functional impairments, thus diminishing the quality of life in the elderly. Exercise intervention is crucial for the improvement of muscle structure and function in sarcopenia. Previous studies have shown that mesenchymal stem cells (MSCs) have a therapeutic potential for sarcopenia. The current study aims to evaluate the combined effects of exercise training and adipose-derived mesenchymal stem cells (ADMSCs) in aged rats induced with sarcopenia.

Methods

18 months-old aged rats were randomly divided into four groups: Control group, exercise (Group Ex), ADMSCs injection (Group MSC), and ADMSCs injection with exercise (Group MSC+Ex). Sarcopenia was induced via hindlimb velcro immobilization for 2 weeks. After immobilization, the ADMSCs were administered via intramuscular injection into the gastrocnemius muscle (GCM), and the exercise groups performed treadmill exercise. To evaluate the effects of each treatment on skeletal muscle, the cross-sectional area (CSA) of the GCM, immunohistochemistry, ultrasound assessment, functional tests, quantitative reverse transcription-polymerase chain reaction, and western blotting were conducted

Results

GCM muscle mass was increased in the Ex, MSC, and MSC+Ex groups compared to the control group, respectively. Although the mean CSA of GCM muscle did not differ significantly between the groups, the size distribution of myofiber shifted towards larger sizes in the Ex and MSC+Ex groups compared to the control. In functional assessment by the rotarod test, group MSC+Ex showed the highest performance compared to the control (p

Conclusions

Present study demonstrated that the combined therapy of exercise and ADMSCs injection was the most efficacious intervention in sarcopenic rats, showing a possibility of synergistic treatment for sarcopenia.

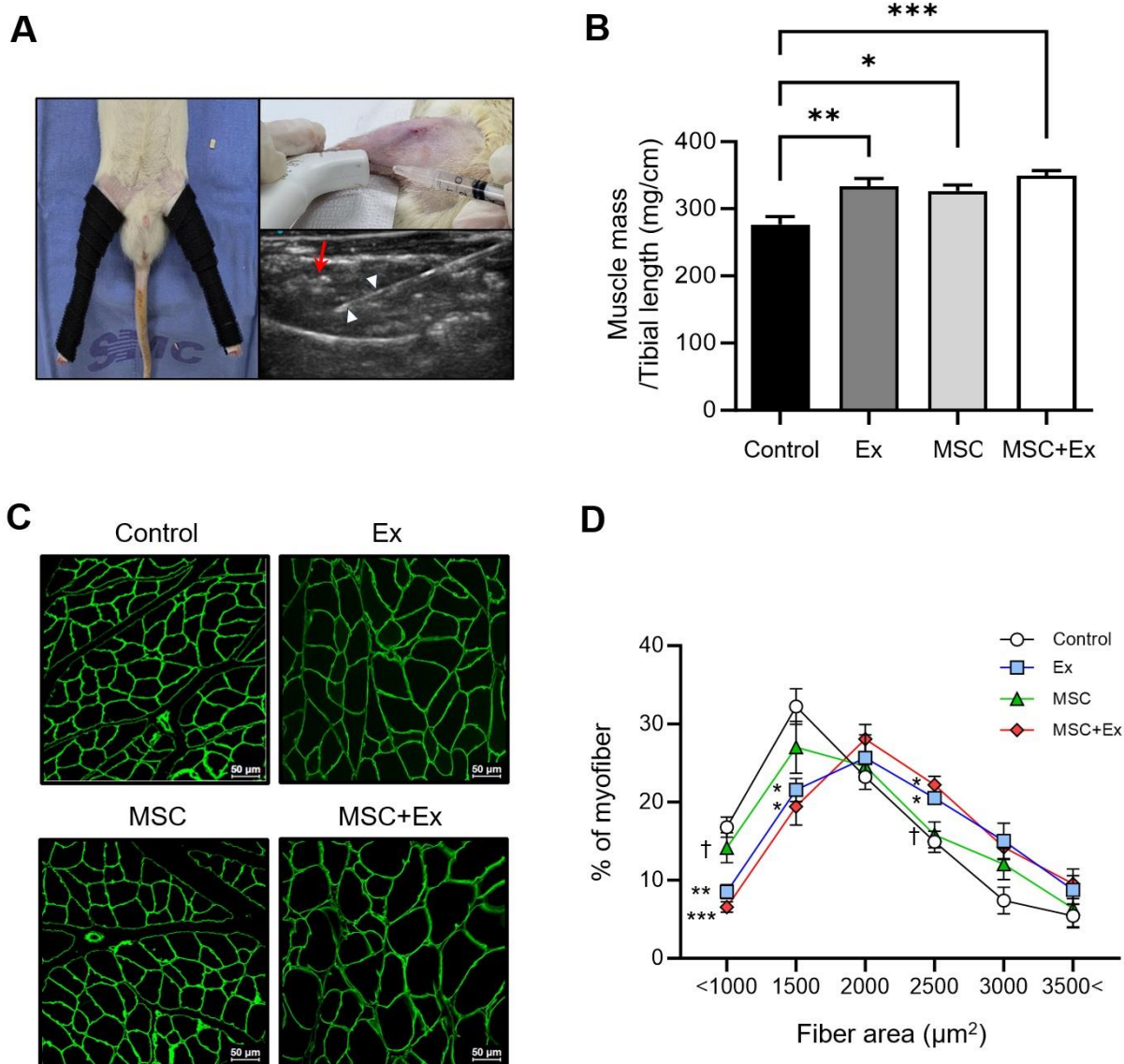


Figure 1. Immobilization-induced atrophy model and comparison of gastrocnemius muscle weight and fiber analysis. (A) Hindlimb velcro immobilization in rats (left). Ultrasound-guided ADMSC injection into GCM muscles (right). The red arrow indicates injected MSC and the white arrowhead shows the syringe needle. (B) The ratio of GCM muscle weight to tibial length ($n = 6$, each). (C) Anti-laminin stained GCM muscles. (D) Frequency distribution of cross-sectional GCM muscle fiber area ($n = 5$, each). Control; Ex, treadmill exercise; MSC, ADMSCs injection; MSC + Ex, ADMSCs injection and treadmill exercise group. All data are presented as mean \pm SEM. * $p < 0.05$, ** $p < 0.01$, and *** $p < 0.001$ compared with control; † $p < 0.05$ compared with group MSC + Ex.

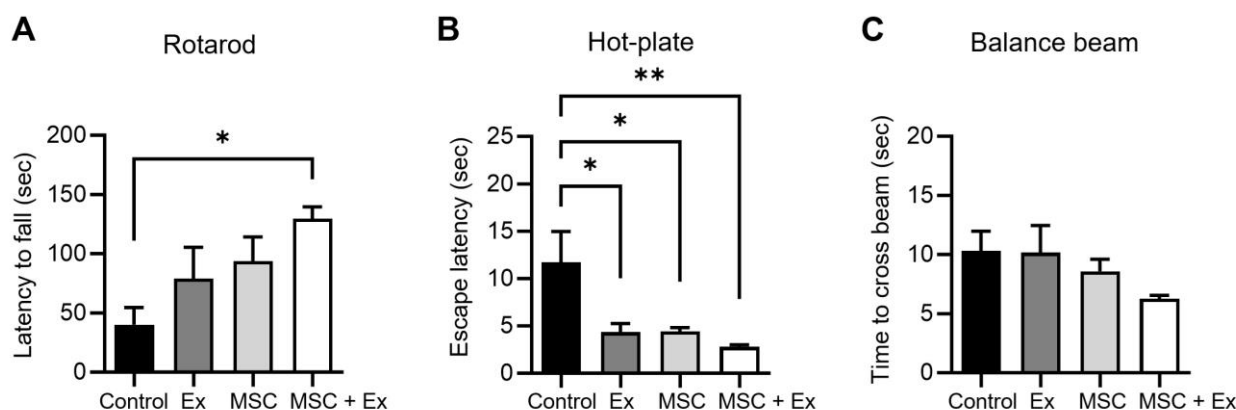


Figure 2. Functional tests of the four groups. (A) Retention time (latency to fall) using rotarod test. (B) Escape latencies in the hot-plate test. (C) Walking time (time to cross beam) from balance beam test. Control; Ex, treadmill exercise;

MSC, ADMSCs injection; MSC + Ex, ADMSCs injection and treadmill exercise group. All data are presented as mean \pm SEM (n = 5 - 6, each). *p<0.05, and **p<0.01 compared with control.

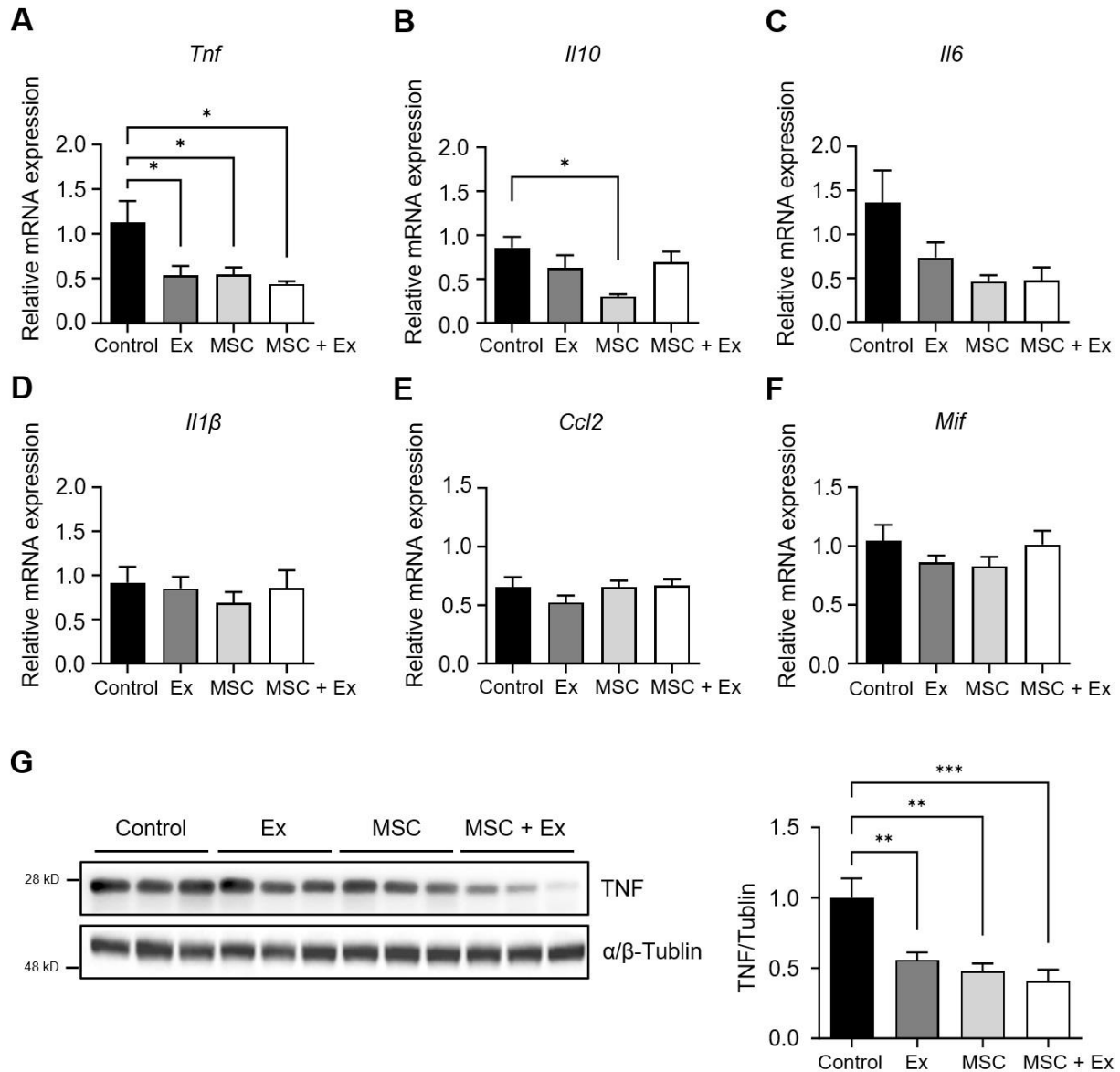


Figure 3. Comparison of levels of pro-inflammatory cytokines. The mRNA expression level of (A) *Tnf*, (B) *Il10*, (C) *Il6*, (D) *Il1β*, (E) *Ccl2*, and (F) *Mif* genes in GCM muscle on Day 28 (n = 5 - 6, each). (G) Relative protein expression of TNF normalized to α/β -Tubulin (n = 6, each). Control; Ex, treadmill exercise; MSC, ADMSCs injection; MSC + Ex, ADMSCs injection and treadmill exercise group. All data are presented as mean \pm SEM. *p<0.05, **p<0.01, and ***p<0.001 compared with control.

Geriatric Rehabilitation

발표일시 및 장소 : 10 월 25 일(금), 13:10 ~ 13:40 , Poster Room, DID1

PS-15

Mitochondrial dysfunction and apoptosis of quadriceps and soleus in long-lasting ovariectomized rats

Kyung Jae Yoon^{1*†}, Min Jeong Kim¹, Yu Rim Hong¹, Yong-Taek Lee¹, Chul-Hyun Park¹

Department of Rehabilitation Medicine, kangbuk samsung hospital. Sungkyunkwan University School of Medicine¹

Background and aim

Estrogen deficiency (esp. Estradiol, E2) in menopause status leads to decrease the skeletal muscle mass (1-3), of which receptor on mitochondria affects mitochondrial function and apoptotic signals (4). However, there was rare studies which skeletal muscle type is more vulnerable among mitochondria-rich fiber and glycolytic fiber in menopausal women. In this experiment, we compare the mitochondrial dysfunction and apoptosis in quadriceps and soleus muscle of long-lasting ovariectomized rats.

Methods

SD rats were randomly assigned to ovariectomized (OVX group) or sham op group (Sham group). Ovariectomy or sham op were done at 18-week old and fed freely at constant temperature for 24 weeks. They were sacrificed at 42-week old. The bloods were sampled to measure the estradiol level with ELISA kit. Quadriceps and soleus muscles were dissected to evaluate the mitochondrial dynamics and apoptosis. P-Opa1 and Drp1 were measured for fusion and fission of mitochondria, respectively. Caspase-3 and Cytochrome c were evaluated for apoptosis.

Results

Estradiol level was significantly lower in OVX group comparing with sham group in quadriceps and soleus muscle. quadriceps weight per body weight was significantly lower in OVX group comparing with sham group. However, soleus weight per body weight was not different between two groups.

In quadriceps muscle, p-Drp1 was significantly higher in OVX group comparing with sham group. However, Opa1 was not different between two groups. In soleus muscle, p-drp1 and Opa1 had no significant difference comparing with two groups.

In quadriceps muscle, Caspase-3 and cytochrome C were significantly higher in OVX group comparing with sham group. In soleus muscle, there were not significantly diff

Conclusions

Estradiol deficiency caused atrophy of quadriceps (mitochondria-rich muscle fiber), which was associated with impairment of mitochondrial dynamics and apoptosis. In contrast, soleus was not affected by estradiol eradication. Post-menopausal sarcopenia might be mainly affected by mitochondria-rich skeletal muscle atrophy.

Acknowledgment This study was supported by Minister of Science & ICT. Fund number is 2022R1F1A1069303.

Geriatric Rehabilitation

발표일시 및 장소 : 10 월 25 일(금), 13:10 ~ 13:40 , Poster Room, DID1

PS-16

How Long Should One Walk to Measure Habitual Gait Speed with Clinical Significance?

Myung Woo Park^{1*}, Ji Myung Han¹, Sun Gun Chung², Jinkyu Lee^{3†}, Keewon Kim^{2†}

Department of Rehabilitation Medicine, Chung-Ang University Hospital¹, Department of Rehabilitation Medicine, Seoul National University Hospital², Department of Rehabilitative and Assistive Technology, National Rehabilitation Center³

Background

In the elderly, usual gait speed is a crucial predictor of morbidity, hospitalization rates, and life expectancy. However, there is no consensus on the distance needed for clinically significant gait speed measurements in a clinical setting. This study aimed to determine 'minimum required distance' for clinically reliable gait speed measurement, with the margin of error not exceeding clinically meaningful differences, using 2D pose estimation algorithm without specialized equipment. Additionally, we analyzed whether 'minimum required distance' was influenced by epidemiologic or clinical characteristics and level of measurement, center of mass (CoM) versus leading foot.

Methods

A total of 24 healthy volunteers aged 65 or older performed a 10-meter gait speed test and the interval from 2 to 8 meters, excluding acceleration and deceleration phases, was recorded using a smartphone camera. Gait analysis was based on 14 key points from pose estimation algorithm. The speed of the CoM was calculated at 0.1-meter intervals, and the variance in gait speed according to measured distance was analyzed using ANOVA. 'Minimum required distance' was defined as the cut-off distance where the range of the 90% or 95% confidence interval of gait speed did not exceed 0.1 m/s, representing the minimal clinically important difference (MCID).

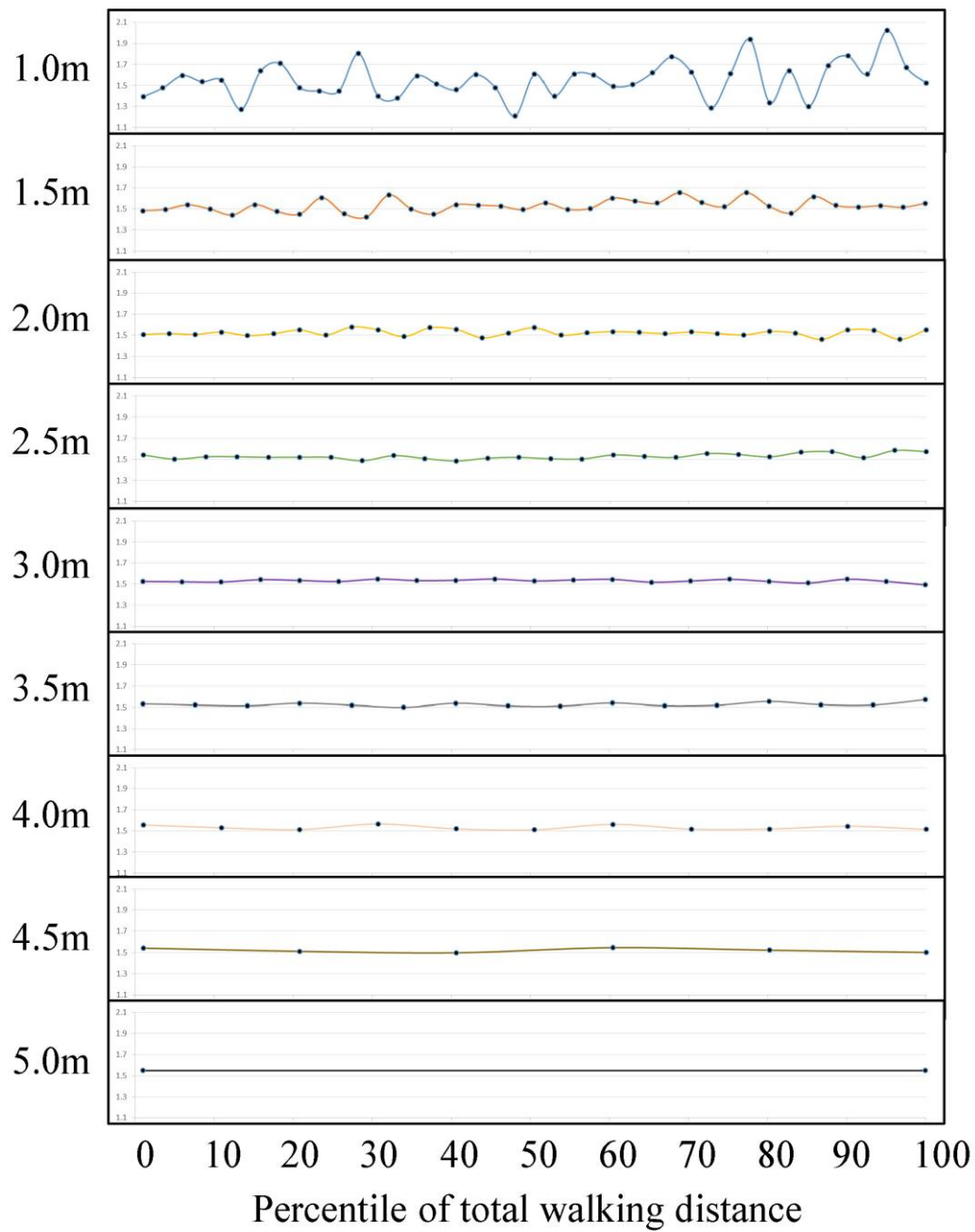
Results

There was no significant difference between manually measured gait speeds and those calculated using the 2D posture estimation algorithm. A minimum distance of 2.1 meters was needed when using the CoM as a reference for gait speed. In contrast, a distance of 4.7 meters was required to maintain a 90% confidence interval within 0.1 m/s when measuring based on the leading foot. Gait speed and lower limb strength showed a positive correlation with speed variance whereas demographic characteristics of the participants did not significantly affect the variance in gait speed.

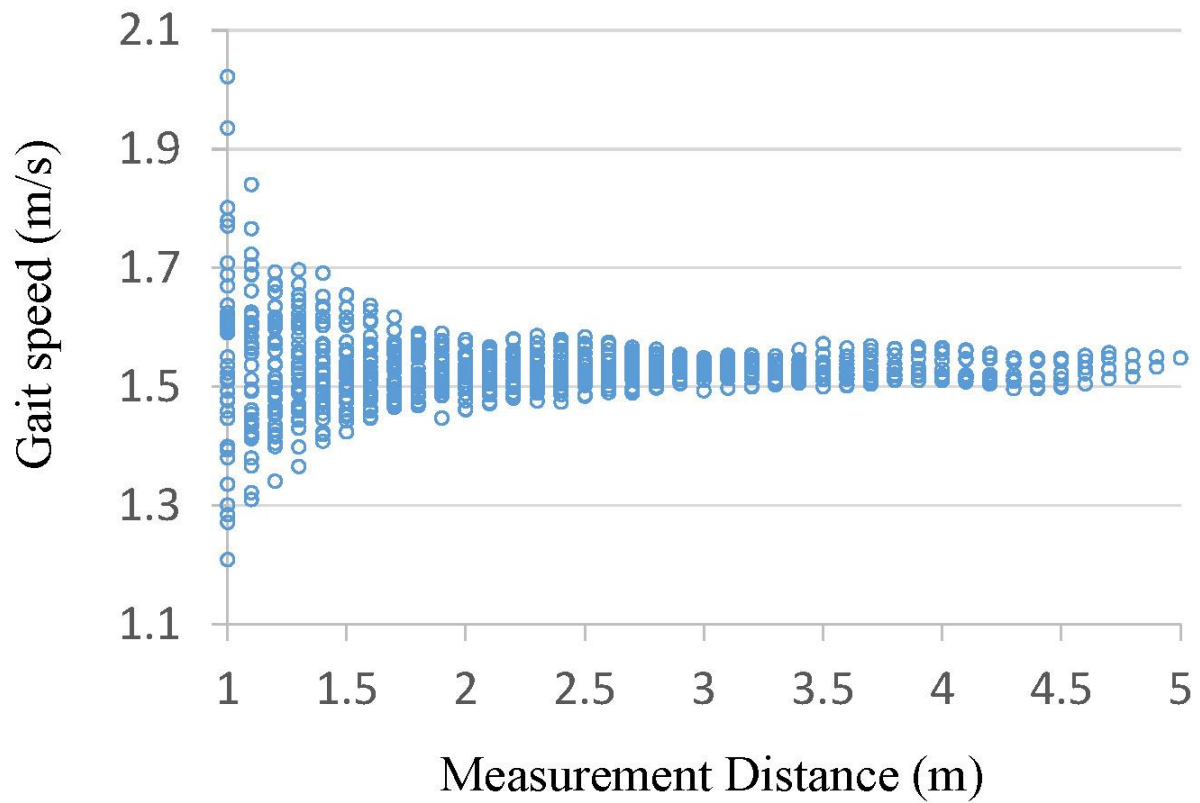
Conclusions

Clinically significant gait speeds can be measured using video-based tracking at a distance exceeding 2.1 meters. When using a walkway approach, the minimum measurement distance increases to at least 4.7 meters. Shorter measurement distances may be required in cases with slower gait speeds or lesser lower limb strength.

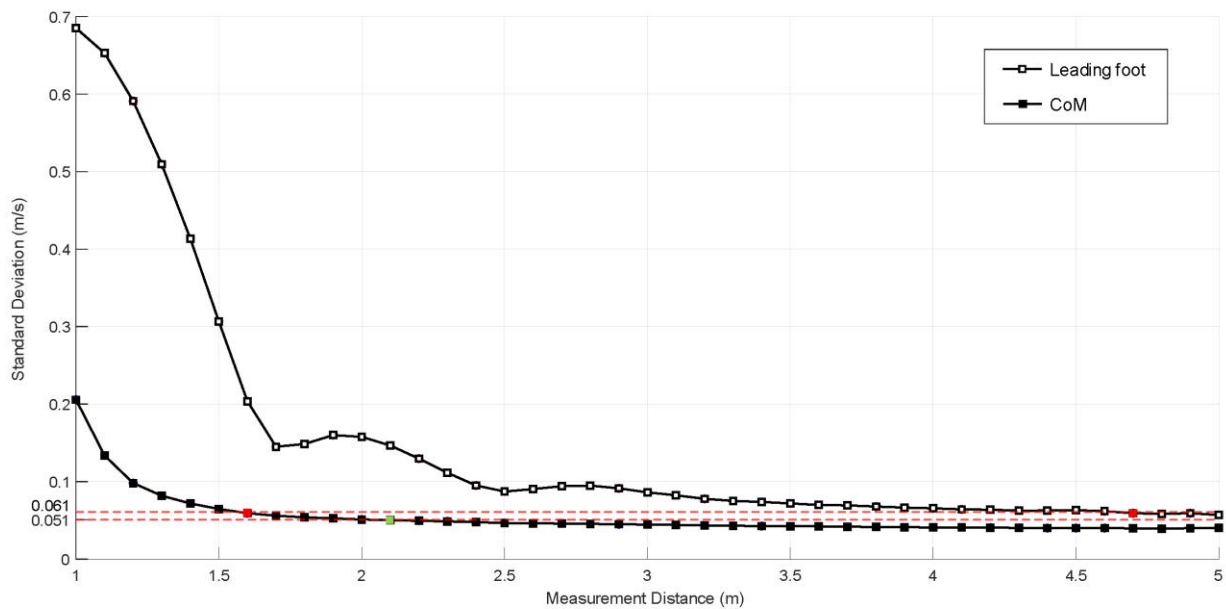
Acknowledgment This research was supported by a grant of Patient-Centered Clinical Research Coordinating Center (PACEN) funded by the Ministry of Health & Welfare, Republic of Korea (grant number : HC21C0064)



[Fig 1] Illustrative case. (a) Gait speed of each segment according to the measurement distance (from 1.0m to 5.0m)



[Fig 1] Illustrative case. (b) Distribution of gait speed according to the measurement distance.



Relationship between the measurement distance and the standard deviation of gait speed. The dashed lines at standard deviations of 0.051 m/s and 0.061 m/s represent the 95% and 90% confidence intervals, respectively. The green points indicate where the measurement values align with the 95% confidence interval, and the red points mark the 90% confidence interval, each in relation to the MCID of 0.1 m/s.

Cancer Rehabilitation

발표일시 및 장소 : 10 월 25 일(금), 13:10 ~ 13:40 , Poster Room, DID1

PS-17

Study of Efficacy of Hyaluronidase Injection for Lymphedema Relief Using Microneedles

Bumchul Kim^{1,2*}, Hwayeong Cheon³, Hyewon Choi⁴, Hyunsik Yoon^{4,5}, Jae Yong Jeon^{1,3†}

Department of Rehabilitation Medicine, Asan Medical Center, University of Ulsan College of Medicine¹, Department of Rehabilitation Medicine, AMIST, Asan Medical Center, University of Ulsan College of Medicine², Rehabilitation Research Center, Biomedical Engineering Research Center, Asan Institute for Life Sciences, Asan Medical Center³, Department of Chemical and Biomolecular Engineering, Seoul National University of Science and Technology⁴, Department of Nano Bio Engineering, Seoul National University of Science and Technology⁵

Purpose

Previous studies have shown that hyaluronidase decomposes hyaluronic acid accumulated in lymphedematous areas, reduces swelling, and promotes antifibrotic immune responses. Transdermal drug delivery using microneedles is a minimally invasive method that minimizes pain and can address the disadvantages of hyaluronidase injection methods, such as pain and infection risk. On the other hand, mast cells play a crucial role in the pathophysiology of lymphedema by participating in the inflammatory and fibrotic processes. In this study, we compared the therapeutic effects of intradermal injection of hyaluronidase using microneedles with those of syringe injection on lymphedema with a focus on mast cell activity and tissue changes.

Methods

We produced upper limb lymphedema models in nine Sprague-Dawley rats using lymph node dissection and 20 Gy radiation. The rats were divided into three groups: control (saline injection using a syringe, n=3), syringe injection (hyaluronidase, n=3), and microneedle injection (hyaluronidase, needle height = 600 μ m, bandage applied for 10 minutes, n=3). Following the hyaluronidase injection in week 1, lymphatic drainage patterns were observed weekly using indocyanine green lymphography, and volume was calculated using the frustum approximation. After 4 weeks, all animals were sacrificed, and histological analysis was performed using Hematoxylin and Eosin (H&E), Masson's trichrome (MT) for fibrosis, and Toluidine blue (TB) staining for mast cell distribution.

Results

Lymphatic flow improved in the hyaluronidase injection groups compared to the control group. Volume change and dermal thickness were significantly reduced in the hyaluronidase injection groups compared to the control group, with a greater reduction observed in the microneedle injection group. MT staining indicated less dense collagen deposition in the hyaluronidase injection groups. TB staining showed increased mast cells with hyaluronidase injection, and the distribution of mast cells was more uniform with microneedle use.

Conclusion

Compared to the control group, both hyaluronidase injection groups significantly reduced lymphedema volume, improved lymphatic flow, resulted in less dense collagen deposition, and increased the number of mast cells. In particular, the microneedle group demonstrated a greater reduction in volume and dermal thickness than the syringe group. This difference between the two injection methods is likely due to the more uniform distribution of mast cells in the microneedle group. The microneedle method may deliver hyaluronidase evenly across the injection area, leading to a more consistent decomposition of hyaluronic acid and promoting mast cell formation. Microneedles potentially become a patient-friendly intervention method that may be used at home because they deliver drugs more effectively than syringes by minimizing patient's discomfort to the dermis layers.

Acknowledgment Acknowledgments This study was supported by a grant from the Asan Institute for Life Sciences and

Corporate Relations of Asan Medical Center, Seoul, Korea and by the National Research Foundation of Korea (NRF) grant funded by the Korea government (MSIT). (2022IF0021, RS-2024-00338179)

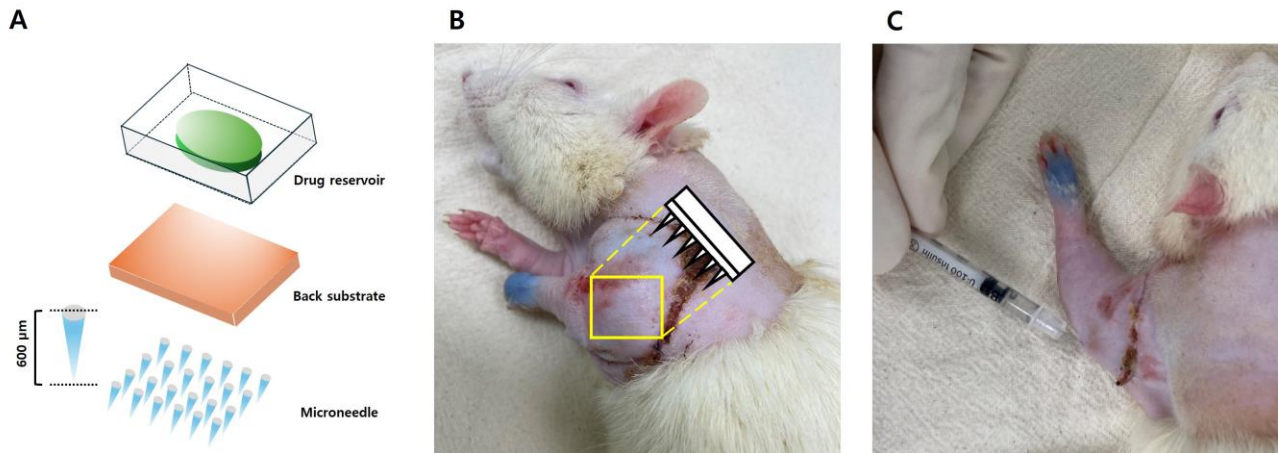


Figure 1. (A) Microneedle device schematic. (B) Hyaluronidase injection area using microneedle (yellow rectangular region; 99.947 mm²). (C) Hyaluronidase injection using a syringe.

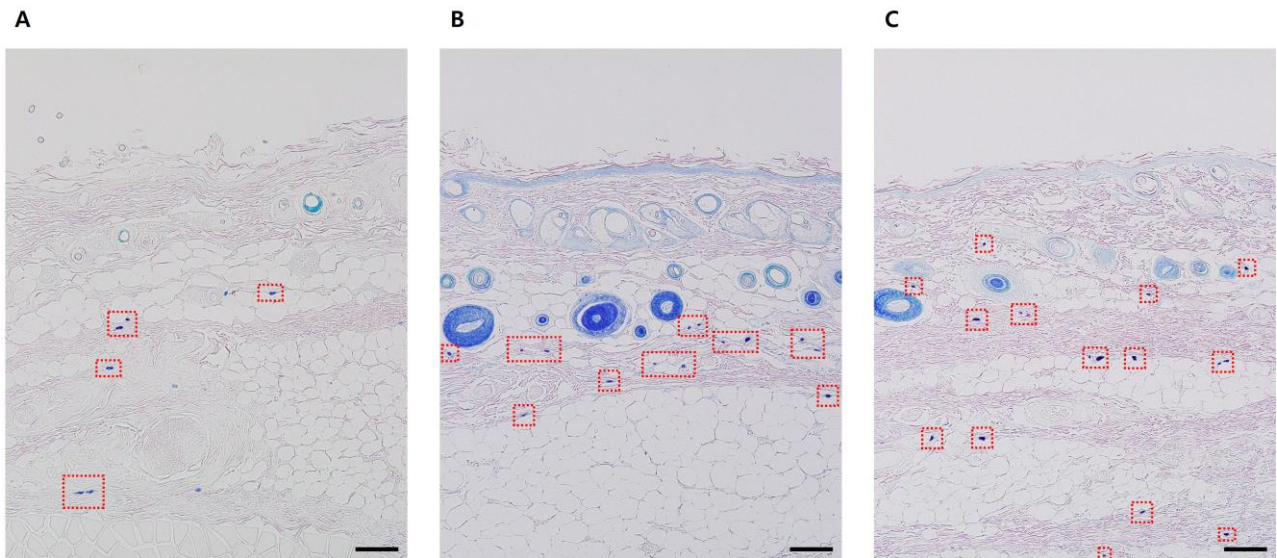


Figure 2. Toluidine blue (TB) staining of mast cells in the upper extremity lymphedema area (red dotted rectangle). (A) Control (saline injection using a syringe). (B) syringe injection (hyaluronidase). (C) Microneedle injection (hyaluronidase, needle height = 600 µm, bandage applied for 10 min). Scale bar = 100 µm.

PS-18

Improvement in functional motor scores in patients with non-ambulatory spinal muscle atrophy

Jin A Yoon^{1,2*}, Yuju Jeong², Jiae Lee², Dong Jun Lee², Kyung Nam Lee², Min Kyung Park², Byung Hoon Lee², Yong Beom Shin^{1,2†}

Department of Rehabilitation Medicine, Pusan National University School of Medicine and Biomedical Research Institute, Pusan National University Hospital¹, Department of Rehabilitation Medicine, Pusan National University Hospital²

Background and Purpose

We analyzed the changes in various motor function and fatigue scores over a four-year period in patients with non-ambulatory spinal muscular atrophy (SMA) during Nusinersen treatment.

Methods

This retrospective single-center study included patients with non-ambulatory SMA who underwent motor function evaluation during intrathecal Nusinersen treatment from March 2019 to May 2023. Patients underwent Hammersmith Infant Neurological Examination (HINE) or Hammersmith Functional Motor Scale Expanded (HFMSE) evaluation before treatment, and approximately every 4 months thereafter. Children's Hospital of Philadelphia Infant Test of Neuromuscular Disorders (CHOP INTEND) or Children's Hospital of Philadelphia – Adult Test of Neuromuscular Disorders (CHOP ATEND), Revised Upper Limb Module, and Motor Function Measure evaluations were performed. Narrative interviews were conducted to explore post-treatment physical improvement regarding activities of daily living (ADLs) and fatigue after ADLs.

Results

A total of 12 patients underwent continuous functional evaluation during Nusinersen treatment. The patients were divided in two groups based on their age at the time of treatment: the children and adolescent (N=7), and adult (N=5) groups. Regarding their functional status, 10 patients (83.3%) were sitters, while 2 patients (16.7%) were non-sitters; in addition, 3 patients (25%) had spinal fusion for scoliosis. Based on the improvement of HFMSE, 9 patients achieved minimal clinically important difference (MCID; HFMSE score change ≥ 3 compared to the baseline value), while the 3 remaining patients, all adults, did not achieve MCID (Patients #5, 7, and 8). Average rates of change (slopes) with corresponding 95% confidence intervals for all assessment tools were in a positive direction. In the children and adolescent group, the most prominent improvement was observed with the CHOP-INTEND (mean slope = 2.215 points/year, 95% CI 0.977–3.527, $p = 0.014$), followed by HFMSE (mean slope = 1.706 points/year 95% CI 0.376–3.066, $p = 0.040$). Improvement of CHOP-ATEND scores were most noticeable for adult patients and exhibited statistical (mean slope = 0.912 points/year, 95% CI 0.345–1.583, $p = 0.013$). A comparison of the differences in slopes between the assessment tools revealed that CHOP-INTEND exhibited significantly higher slopes compared to HINE, RULM, and MFM (p

Conclusions

This study provided insights into the improvement and patterns of change of various functional assessment tools in non-ambulatory SMA after Nusinersen treatment. As demonstrated by our findings, it is necessary to consider various functional aspects to determine the effectiveness of Nusinersen therapy. Additionally, focusing on the improvement of related ADLs is necessary to objectively assess the therapeutic effect.

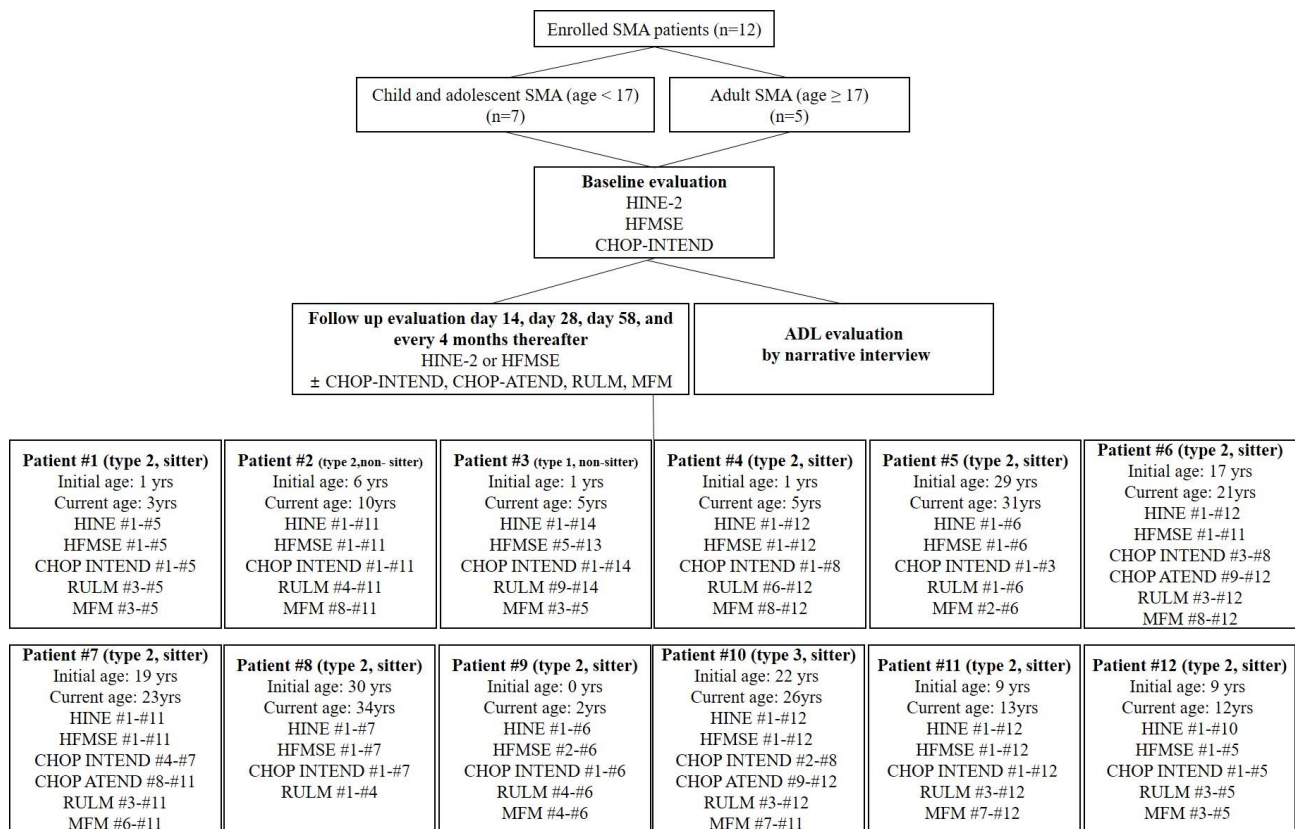


Figure 1. Flow diagram of the study

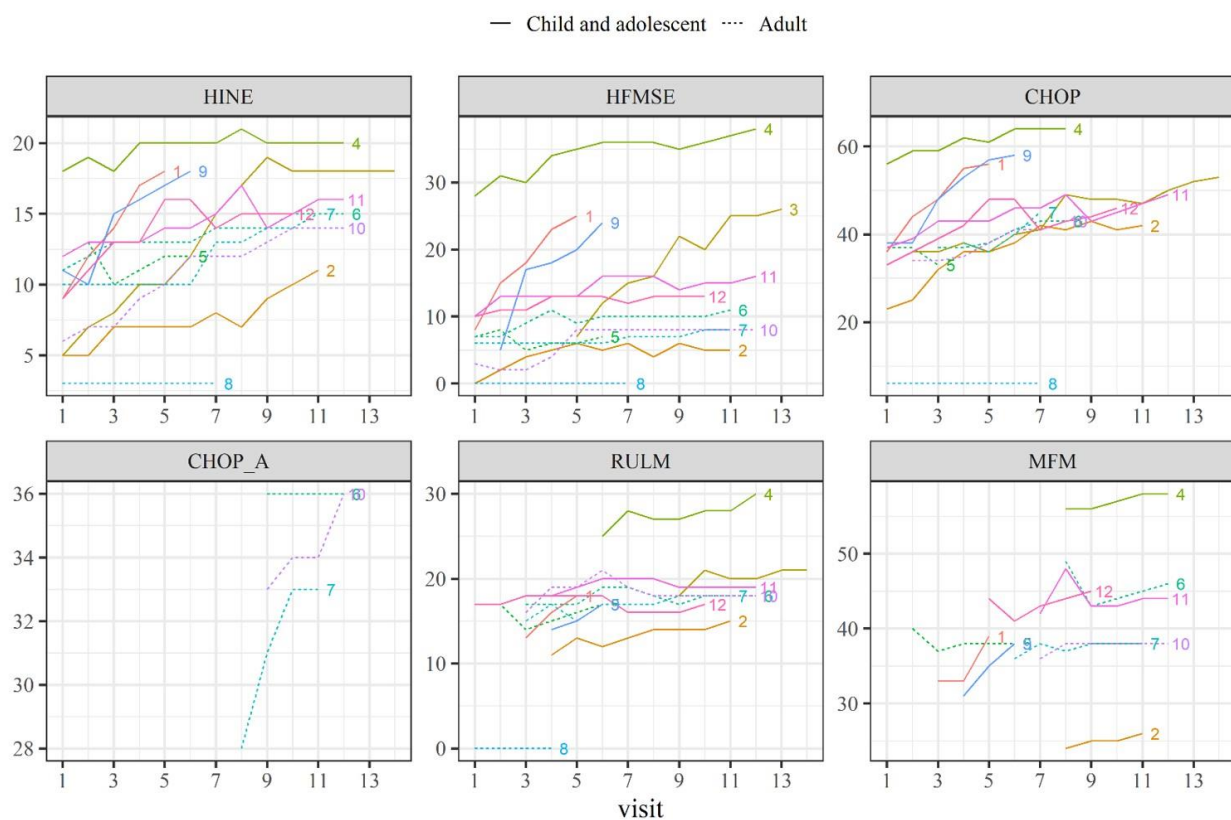


Figure 2. Scatterplot showing the trajectory of each patient based on various assessment tools

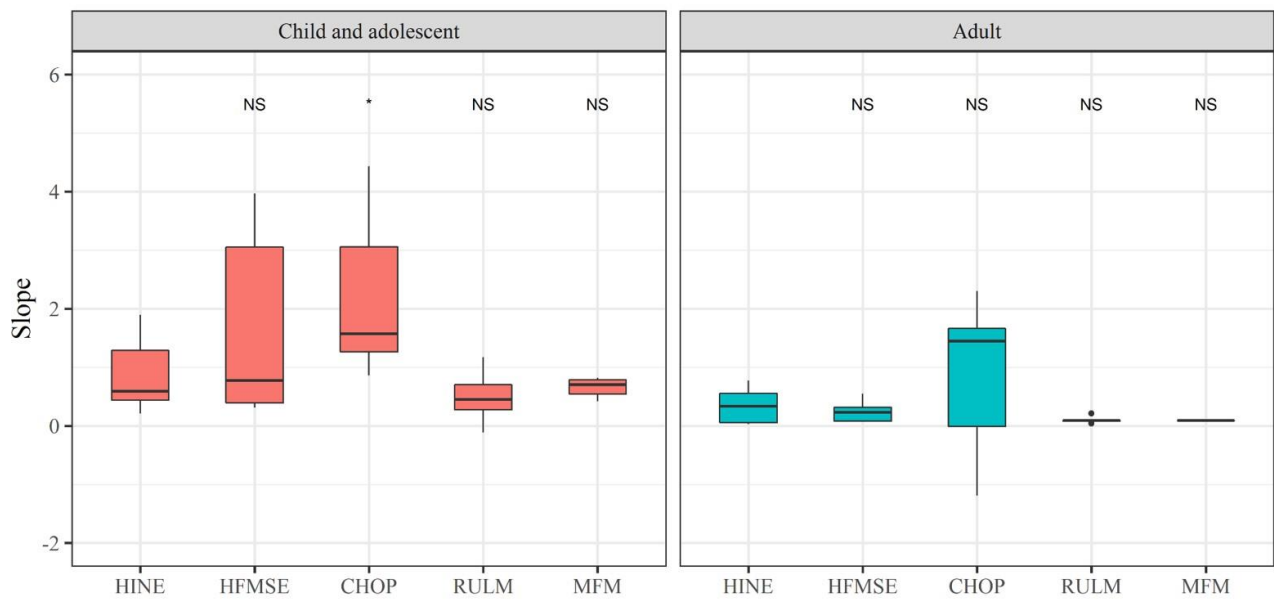


Figure 3. Box plot of slopes showing average annual rate of change using linear mixed model

Pediatric Rehabilitation

발표일시 및 장소 : 10 월 25 일(금), 13:10 ~ 13:40 , Poster Room, DID1

PS-19

Effect of different types of Robot-assisted gait training in children with CP

Shin-seung Yang^{1,2**}, Jayoung Choi^{1,2}

Department of Rehabilitation Medicine, Chungnam National University Hospital¹, Department of Rehabilitation Medicine, College of Medicine, Chungnam National University Hospital²

Purpose

Cerebral palsy (CP) is children's most common developmental motor disorder, causing walking and activity limitations. Recent technological advances suggest robot-assisted gait training (RAGT) as an alternative treatment modality. RAGT can offer repetitive and task-specific training that provides locomotion-relevant afferent input to spinal central circuitries that generate rhythmic stepping behavior. RAGT is classified into trajectory-control and force-control type according to driving method. In addition, depending on the training method, overground walking training or treadmill-tethered RAGT can also be classified. This study aimed to compare the therapeutic effects of different types of RAGT.

Methods/Design

30 children aged 5 to 18 years with cerebral palsy of gross motor function classification system (GMFCS) level II to IV were recruited. Within a single-blinded, randomized controlled trial, each group got RAGT (30 min/session, 3 times/week, 6 weeks) with Walkbot-K (trajectory-controlled, treadmill-tethered gait robot) and Angle legs M20 (torque-assisted, overground walking robot). Outcomes were assessed at baseline (T1, week 0), at starting RAGT (T2, week 6), and at post-RGAT (T3, week 12). Motor function was evaluated using Gross Motor Function Measure-88 (GMFM-88) and Pediatric Balance Scale (PBS); gait ability using a 10-meter walking test (10MWT), Gillette FAQ, and Edinburgh Visual Gait Score (EVGS); and heart rate and energy expenditure monitoring using photoplethysmogram (PPG).

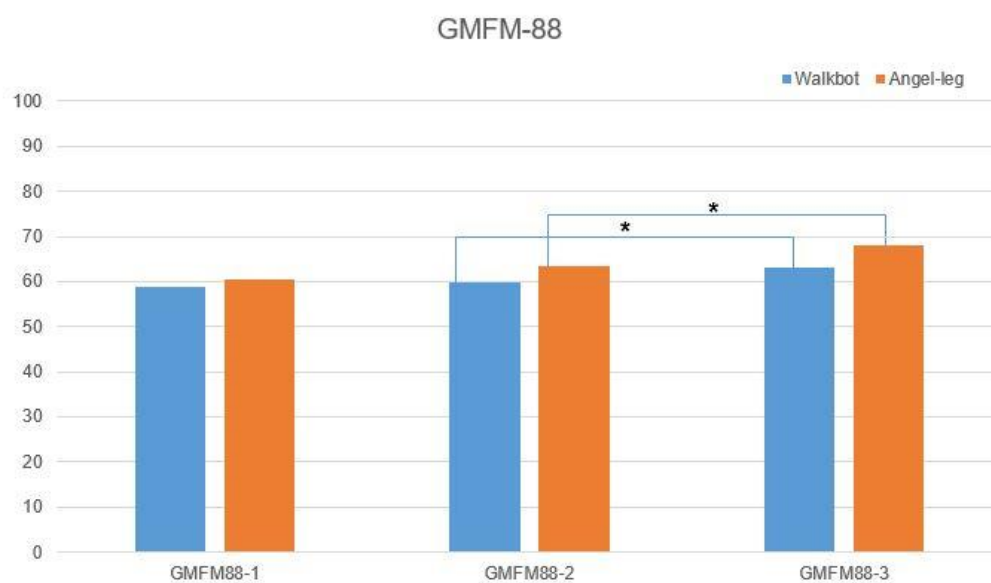
Results

Of the 30 children (mean [SD] age, 7.83 [2.52] years; 29 children (96.7%) completed the intervention. 16 participants (mean [SD] age, 7.47 [2.67] years) and 13 participants (mean [SD] age, 8.31 [2.3] years) were randomly assigned to the Walkbot-K and Angle-leg groups, respectively. GMFM-88 score improved after 6 weeks of RAGT in both groups compared to the period of conventional treatment (Walkbot-K Δ 2.9 \pm 3.1; Angle Leg Δ 2.6 \pm 2.0). Both RAGT groups showed no differences in balance control, and there were no differences in the other gait parameters. During the robotic training period, the increment of heart rate was greater in the Angle Leg group compared to the Workbot group (Walkbot-K Δ 17.29 \pm 8.12; Angle Leg Δ 27.24 \pm 7.04).

Conclusion

This randomized controlled trial provided the individualized RAGT training guide according to the functional status of children.

Acknowledgment Acknowledgment: This study was supported by the Translational Research Program for Rehabilitation Robots (#NRCTR-EX22004), National Rehabilitation Center, Ministry of Health and Welfare, Korea.



1: pretraining, 2: starting RAGT, 3: ending RAGT

Changes of GMFM-88 score



Changes of heart Rate

Pain and Musculoskeletal Rehabilitation

발표일시 및 장소 : 10 월 25 일(금), 13:10 ~ 13:40 , Poster Room, DID2

PS-20

Ultrasound-guided nerve hydrodissection for the carpal tunnel syndrome: A network meta-analysis

KunWook Lee¹, Jong Mi Park^{2*}, Hyewon Ryu², Seo Yeon Yoon¹, Min Seo Kim^{3,4}, Yong Wook Kim¹, Jae Il Shin^{5†}, Sang Chul Lee^{1†}

Department and Research Institute of Rehabilitation Medicine, Yonsei University College of Medicine, Seoul, Republic of Korea¹, Department of Physical Medicine and Rehabilitation, Hallym University Sacred Heart Hospital, Hallym University College of Medicine, Anyang, Republic of Korea², Cardiovascular Disease Initiative, Broad Institute of Harvard and MIT, Cambridge, MA, USA³, Cardiovascular Research Center, Massachusetts General Hospital, Boston, MA, USA⁴, Department of Pediatrics, Yonsei University College of Medicine, Seoul, Republic of Korea⁵

INTRODUCTION

Carpal tunnel syndrome (CTS) is a common neuropathy caused by compression of the median nerve, leading to symptoms like hand numbness, pain, and muscle weakness. Traditional treatments include local steroid injections, but ultrasound-guided hydrodissection, which separates the median nerve from surrounding tissues using injectable solutions, is gaining popularity. This study aims to optimize injectables used in ultrasound-guided nerve hydrodissection for CTS through a systematic review and network meta-analysis.

METHOD

Comprehensive searches of databases including PubMed, MEDLINE, EMBASE, Cochrane, Scopus, and Web of Science were conducted through April 25, 2024. Studies were selected based on predefined inclusion criteria, focusing on randomized controlled trials that reported on the efficacy of different injectables used in ultrasound-guided nerve hydrodissection for CTS. Statistical analyses were conducted using standard mean differences within a random-effects model, and treatment effectiveness was ranked using the surface under the cumulative ranking curve (SUCRA).

RESULTS

Nine studies involving a total of 458 patients with CTS were included in the analysis. Figure 1 shows a network plot of by drug type (1A), by injection volume (1B), by drug type and injection volume (1C). The findings revealed that 5% dextrose was the most effective injectable for improving both the Boston Carpal Tunnel Questionnaire (BCTQ)-Function scores and BCTQ-Symptoms scores, with SUCRA values of 99, 89.8, and 88.8 at 4, 12, and 24 weeks respectively for BCTQ-Function (Figure 2A), and 99.9 at 4 weeks. for BCTQ-Symptoms (Figure 2B). Platelet-rich plasma demonstrated superior long-term symptom improvement, with SUCRA values of 95.7 and 93.9 at 12 and 24 weeks, respectively (Figure 2A). Additionally, the 5-cc injection dose was found to be the most effective for both BCTQ-Symptoms and BCTQ-Function, with SUCRA values of 99.5 for both categories (Figure 2C). The effectiveness of hydrodissection varied depending on the type and dose of medication used (Table1). Electrodiagnostic assessment and ultrasound variables showed significant dependency on these factors, indicating the importance of tailoring the injectable type and volume to the specific needs of the patient.

CONCLUSION

5% dextrose demonstrated superior initial symptom relief and long-term functional recovery compared to other agents, while platelet-rich plasma provided greater long-term symptom improvement. A 5-cc injection dose yielded the best outcomes. Despite these findings, further research is necessary to establish precise treatment protocols that consider disease severity and individual patient characteristics. These recommendations aim to guide clinicians in selecting the most appropriate injectable agents and dosages for ultrasound-guided nerve hydrodissection, ultimately improving patient care and reducing the need for surgical interventions.

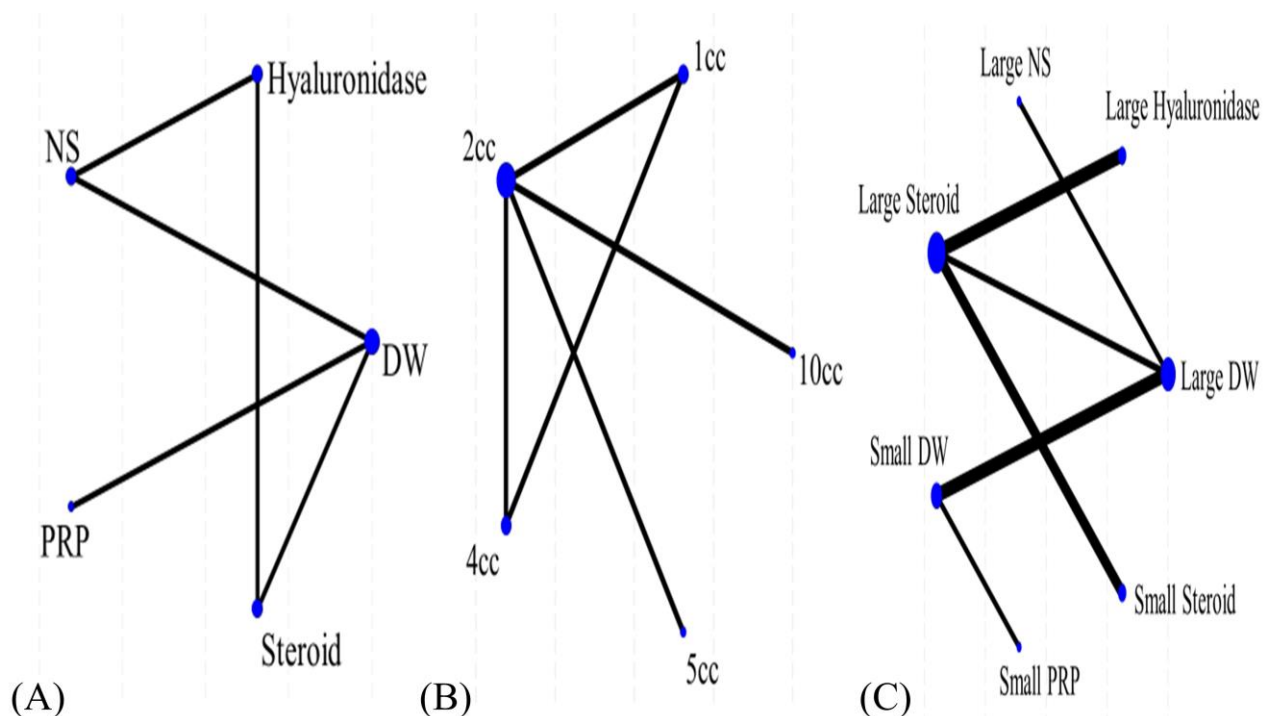


Figure 1. Network plots of ultrasound-guided nerve hydrodissection treatment of Carpal tunnel syndrome (CTS). (A) By drug type (B) By injection volume (C) By drug type and injection volume

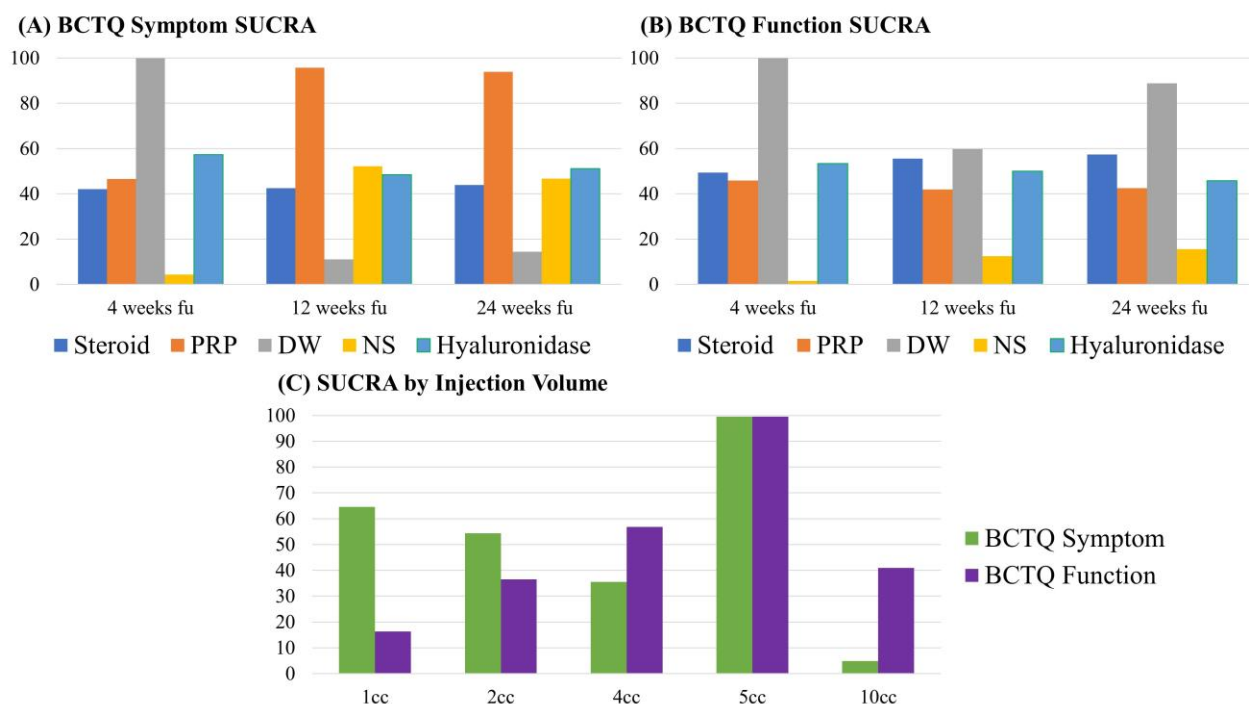


Figure 2. Surface under the cumulative ranking curve (SUCRA) of ultrasound-guided nerve hydrodissection treatment of CTS. (A) Boston Carpal Tunnel Questionnaire (BCTQ) symptom SUCRA change by drug and follow-up period. (B) BCTQ function SUCRA change by drug and follow-up period. (C) BCTQ symptom and function SUCRA changes by injection volume.

Table 1. SUCRA value by drug type and injection volume

	BCTQ symptom	BCTQ function	CSA	SNCV	DML
Small Steroid	61	50.8	38	41.7	42.8
Large Steroid	99.9	63.7	62.5	39.6	91.8
Small DW	30.2	99.8	6.5	71.7	6.4
Large DW	40.5	25.5	67	41.3	17.6
Small PRP	19.5	23.1	45.6	62	67.7
Large NS	33.3	31	76.2	50.9	84.6
Large Hyaluronidase	65.7	56.1	54.3	42.9	39.2

Table 1. SUCRA value by drug type and injection volume

Pain and Musculoskeletal Rehabilitation

발표일시 및 장소 : 10 월 25 일(금), 13:10 ~ 13:40 , Poster Room, DID2

PS-21

Iron-Based Contrast Agent: A Promising Alternative to Gadolinium for Direct Shoulder MR Arthrography

Doyoung Kim^{1*}, Hong Seon Lee², Sanghoon Shin¹, Young Han Lee³, Sungjun Kim^{2,4,5}, Min-Chul Paek¹, Sanghyun Jee¹, Jung Hyun Park^{1,4,5†}

Department of Rehabilitation Medicine, Gangnam Severance Hospital, Yonsei University College of Medicine, Seoul, Republic of Korea¹, Department of Radiology, Gangnam Severance Hospital, Yonsei University College of Medicine, Seoul, Republic of Korea², Department of Radiology, Research Institute of Radiological Science and Center for Clinical Imaging Data Science, Severance Hospital, Yonsei University College of Medicine, Seoul, Republic of Korea.³, Department of Medical Device Engineering and Management, The Graduate School, Yonsei University College of Medicine, Seoul, Republic of Korea⁴, Department of Integrative Medicine, The Graduate School, Yonsei University College of Medicine, Seoul, Republic of Korea⁵

Introduction

The need for alternative MR contrast agents in direct shoulder MR arthrography (MRA) arises from limitations associated with gadolinium-based contrast agents (GBCAs), which are deemed "off-label" for MRA and raise concerns about potential toxicity to joint tissue. This study aims to compare the image quality of iron-based (Figure 1) and GBCA-based direct shoulder MRA.

Method

89 MRAs from 81 patients were analyzed: 39 iron-based MRAs from 31 patients and 50 GBCA-based MRAs from 50 patients. The MRAs were performed at 3.0-T using fast/turbo spin-echo T1- and T2-weighted images with or without fat suppression. Participants underwent MRA for suspected or diagnosed shoulder pathologies between August 2021 and September 2022 by rehabilitation medicine physicians. Quantitative assessments (contrast-to-noise ratio [CNR] and distension measurements) and qualitative evaluations (distension, sharpness, contrast, and overall image quality scores) were conducted by three musculoskeletal radiologists. A visual Turing test (VTT) assessed 39 clinicians (rehabilitation medicine physicians and musculoskeletal radiologists) ability to differentiate between the two contrast agents. Statistical tests included the Shapiro-Wilk test, independent t-tests, and chi-squared test.

Results

The study compared 31 iron-based MRAs (11 females [35.5%], age: 40.0±13.0 years) and 38 GBCA-based MRAs (14 females [36.8%], age: 49.4±18.7 years) within 30 minutes post-injection (Comparison 1), and 8 iron-based MRAs (3 females [37.5%], age: 38.0±7.8 years) versus 12 GBCA-based MRAs (5 females [41.7%], age: 56.2±15.7 years) in the 30-60 minute post-injection timeframe (Comparison 2) (Table 1). Iron-based MRAs demonstrated superior axillary pouch distension and overall image quality in both comparisons (Figure 2). CNR was notably higher with iron-based agents. The VTT showed a 53.3% accuracy in differentiating iron-based from GBCA, similar to random guessing.

Conclusion

Iron-based contrast agents emerge as a promising alternative to GBCAs for direct shoulder MRA, offering superior image quality without the toxicity concerns associated with GBCAs.

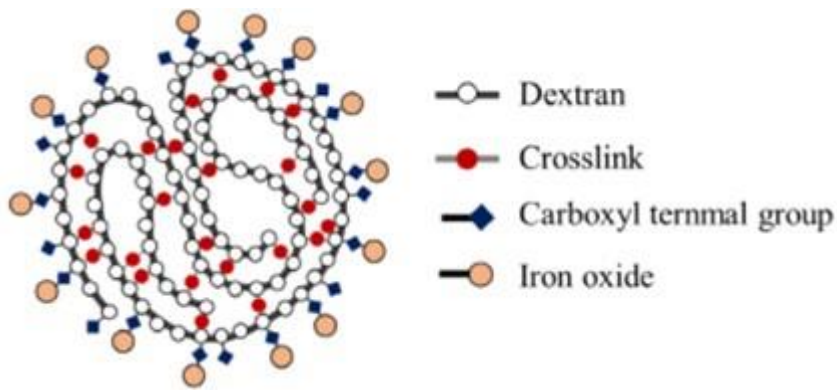


Fig 1. The structure of iron-based contrast agent used in this study

	Comparison 1 (0–30 min)			Comparison 2 (30–60 min)		
	NEMO-103 (n=31)	GBCA (n=38)	<i>p</i> -value	NEMO-103 (n=8)	GBCA (n=12)	<i>p</i> -value
Contrast to noise ratio	112.3±44.6	127.3±41.4	0.154	92.9±26.7	61.5±29.7	0.027
Posterior capsular distension (mm)	13.9±3.6	13.1±2.7	0.311	13.0±4.2	12.4±3.1	0.716
Inferior capsular distension (mm)	10.9±2.6	8.0±5.2	0.004	11.0±2.9	5.8±6.2	0.044
Axillary pouch distension (mm)	9.9±4.6	6.7±4.8	0.006	9.9±3.7	4.5±5.6	0.029
Subjective assessment (range)						
Overall image quality (1-5)	4.7±0.5	4.4±0.5	0.034	4.9±0.2	4.2±0.9	0.020
Distension (1-3)	2.8±0.3	2.6±0.4	0.024	3.0±0.0	2.3±0.9	0.025
Sharpness (1-3)	2.7±0.4	2.5±0.3	0.059	2.8±0.3	2.5±0.5	0.090
Contrast (1-3)	3.0±0.0	2.9±0.2	0.051	3.0±0.0	2.7±0.5	0.039

*Data are presented as mean±standard deviation.

Table 1. Quantitative and qualitative image quality assessment in Comparisons 1 and 2

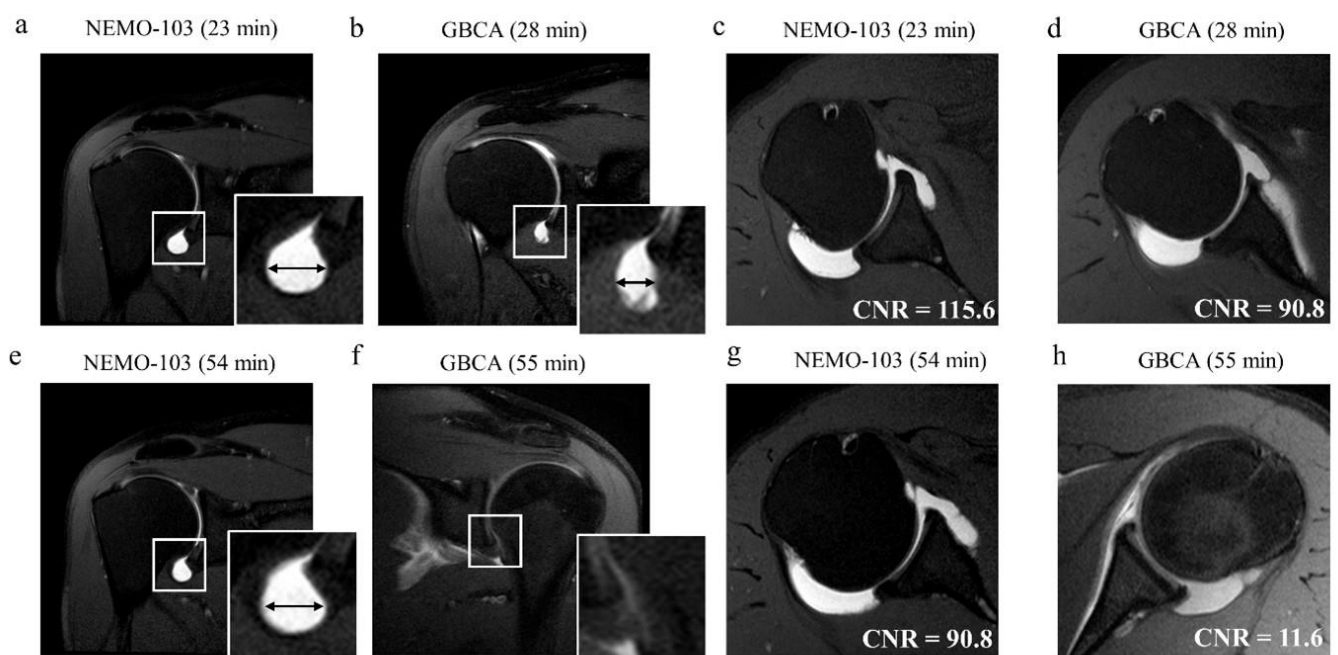


Fig 2. Differences in the distension and contrast-to-noise ratio between the iron-based contrast (NEMO-103) and the GBCA

Pain and Musculoskeletal Rehabilitation

발표일시 및 장소 : 10 월 25 일(금), 13:10 ~ 13:40 , Poster Room, DID2

PS-22

Effects of standing back extension exercise after adopting the lumbar flexion position on hemodynamics and electromyographic signal of the lower back muscle

Mr. Hiroshi Ishida PhD.^{1*†}, Hiroshi Ishida¹, Tadanobu Suehiro¹, Chiharu Kurozumi¹

Kawasaki University of Medical Welfare, .¹

Purpose

Maintaining the trunk in a flexed position may cause partial ischemia in the lower back muscle, inducing muscle fatigue due to metabolite accumulation. Although increased oxygenated hemoglobin and myoglobin (Hb+Mb) levels in the lumbar erector spinae muscle (LES) measured using near-infrared spectroscopy (NIRS) have been observed during trunk extension in standing position, the effects of a standing back extension exercise (SBEE) after holding the lumbar flexion position remain unclear. This study aimed to explore the hemodynamic effects of SBEE after adopting the lumbar flexion position on the LES.

Scope

Sixteen asymptomatic adults (8 males, 8 females; mean age: 20.3 ± 0.5 years) participated in the study.

Method

A two-arm pilot crossover trial design was adopted. Hemodynamics and activities of the LES were measured using NIRS and surface electromyography in prone and Sørensen test positions before and after 5 min of adopting the lumbar flexion position. After adopting the lumbar flexion position, all participants randomly performed 2×3 s of SBEE and maintained a relaxed sitting position (control [CON]) separated by at least a 1-day interval.

Result

After assuming the lumbar flexion position, compared with SBEE, CON was significantly associated with more positive changes in the deoxygenated[Hb+Mb] levels in the prone position ($p=0.028$). Deoxygenated[Hb+Mb] levels in the prone ($p=0.026$) and Sørensen test positions ($p=0.036$) were significantly lower for SBEE than for CON.

Conclusion

Compared with CON, SBEE resulted in lower deoxygenated[Hb+Mb] levels in the LES at rest and during sustained muscle contraction after adopting the lumbar flexion position.

Pain and Musculoskeletal Rehabilitation

발표일시 및 장소 : 10 월 25 일(금), 13:10 ~ 13:40 , Poster Room, DID2

PS-23

The cartilage-generated electric potentials induced by dynamic joint movement; an explorative study

Jae Hyun Lee^{1,2*}, Ye-Seul Jang², Jun Yong Park¹, Jun Won Lee¹, Won-Du Chang^{2†}

Department of Rehabilitation Medicine, Pusan National University Hospital¹, Department of artificial intelligence convergence, Pukyong National University²

Introduction

Excessive loading can damage knee cartilage, making it crucial to assess and measure joint load during therapeutic exercises. However, it remains challenging due to the limitation of present imaging techniques and the indirect nature of simulation analyses. Electroarthrography is a new concept offering a novel, non-invasive approach to observe load-generated potentials of joint cartilage using surface electrodes. While previous studies have shown potentials induced under static pressure, this study aims to explore the potentials induced by dynamic knee joint movements, which involve shift in cartilage contact area.

Methods

We analyzed 20 knees from 20 subjects. Eight surface electrodes were attached around the knee joint (Figure 1) to record electrical signals during both active and passive knee extensions. The signals were captured, filtered and decomposed into five phases: initial flat phase (rest at 90 degrees), activity phase (movement from 90 to 180 degrees), post-activity phase (held at 180 degrees), return phase (return to 90 degrees), and post-return phase (rest at 90 degrees) (Figure 2). Phasic potential differences were statistically compared.

Results

Potential-time graphs from the 20 subjects (mean age 25.0 ± 2.2 years; 5 women) displayed unique characteristics corresponding to different knee kinematic states (Figure 2). At the initial flat phase; no potential changes. At activity phase; generally decreased potentials, with some cases showing increases or fluctuations. At post-activity phase; gradual potential decrease towards baseline. The return and post-return phases exhibited symmetrical topographies, mirroring the activity and post-activity phases in the opposite direction. The mean amplitude of post-activity phase was significantly higher in active extension (2.24 mV) compared to passive extension (1.03 mV) ($p < 0.001$). Similarly, post-return phase amplitudes were higher in active extension (1.70 mV versus 1.06 mV, $p = 0.004$) (Table 1). Subgroup analysis based on electrode channels revealed significant differences in the post-activity phase for Channel 1 (-4.15 vs -1.54, $p = 0.003$) and Channel 4 (-2.32 vs -0.77, $p = 0.008$) (Figure 3).

Discussion

To the best of our knowledge, this study is the first to document the electrical potentials generated by knee joints during dynamic physical activity. Distinct graphical characteristics were identified that correlate with kinematic states of knee joint. Moreover, a viable parameter representing cartilage load was quantified, prioritizing the electrode placement of anterior aspect. Monitoring load through cartilage-generated bioelectric signals could significantly enhance the assessment of physiologic load in daily life, the determination of appropriate rehabilitative exercise regimens, and the mitigation of injury risks. Future studies could focus on innate and covariate factors on this phenomenon to further understand and utilize it in greater detail.

Acknowledgment This work was supported by the National Research Foundation of Korea (NRF) grant funded by the Korea government (MSIT) (No. RS-2024-00334159), and Convergence Medical Institute of Technology R&D project (CMIT2024-00), Pusan National University Hospital.

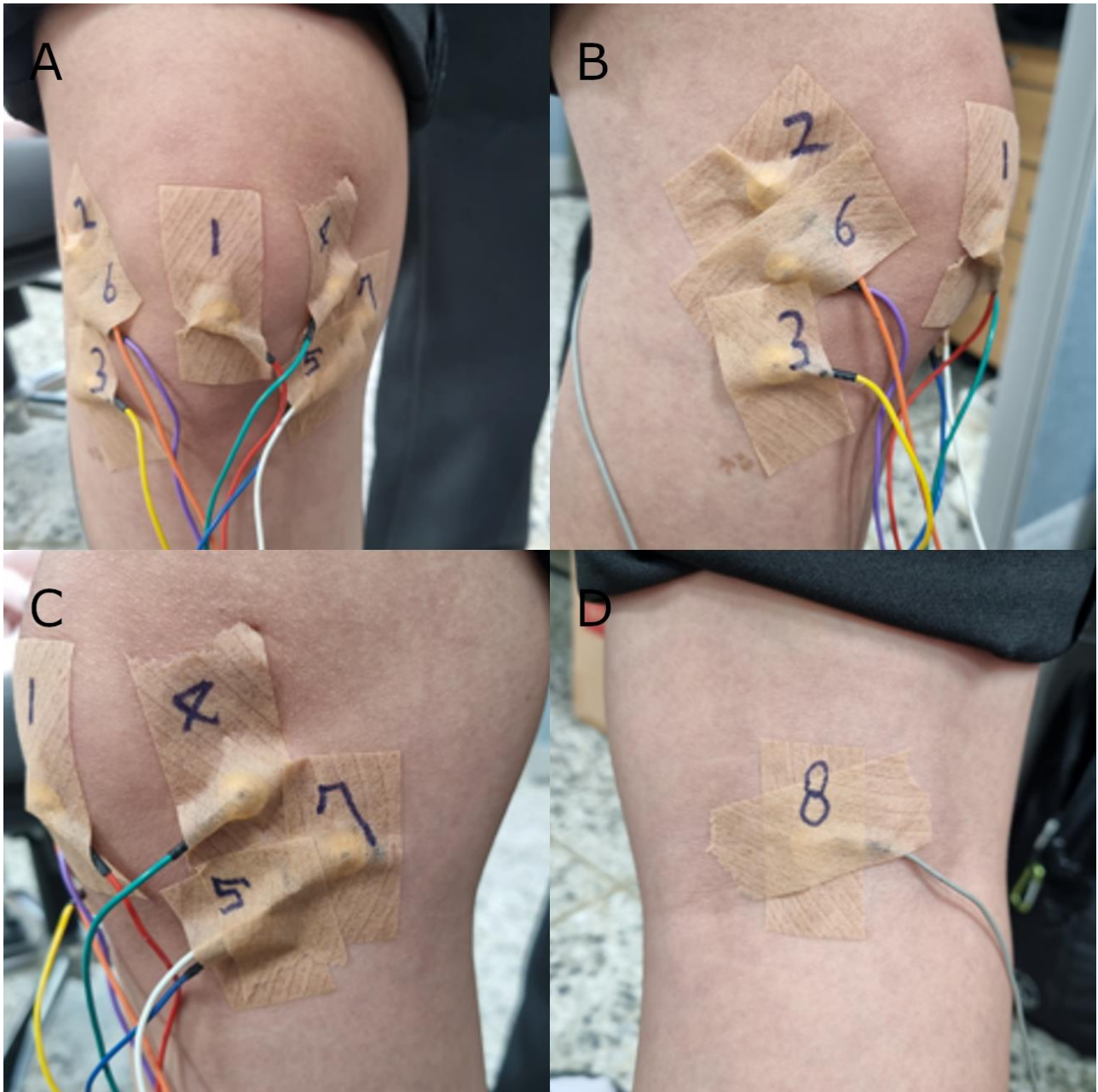


Figure1. Electrode placements on (A) anterior, (B) lateral, (C) medial and (D) posterior side of knee. Electrode positions are demonstrated on subject 5. (A) Electrode #1 is attached to the inferior pole of the patella. (B) Two electrodes (#2-3) are placed on the lateral retinaculum, corresponding to the MPFL and the MPTL, respectively. (C) Two electrodes (#4-5) are placed on the medial retinaculum, corresponding to the LPFL and the LPTL, respectively. Electrodes #6-7 are positioned on the lateral and medial midpoints of the joint line (A, C). (D) Finally, electrode #8 is attached to the midpoint of the posterior popliteal crease. MPFL, medial patello-femoral ligament; MPTL, medial patello-tibial ligament; LPFL, lateral patello-femoral ligament; LPTL, medial patello-tibial ligament.

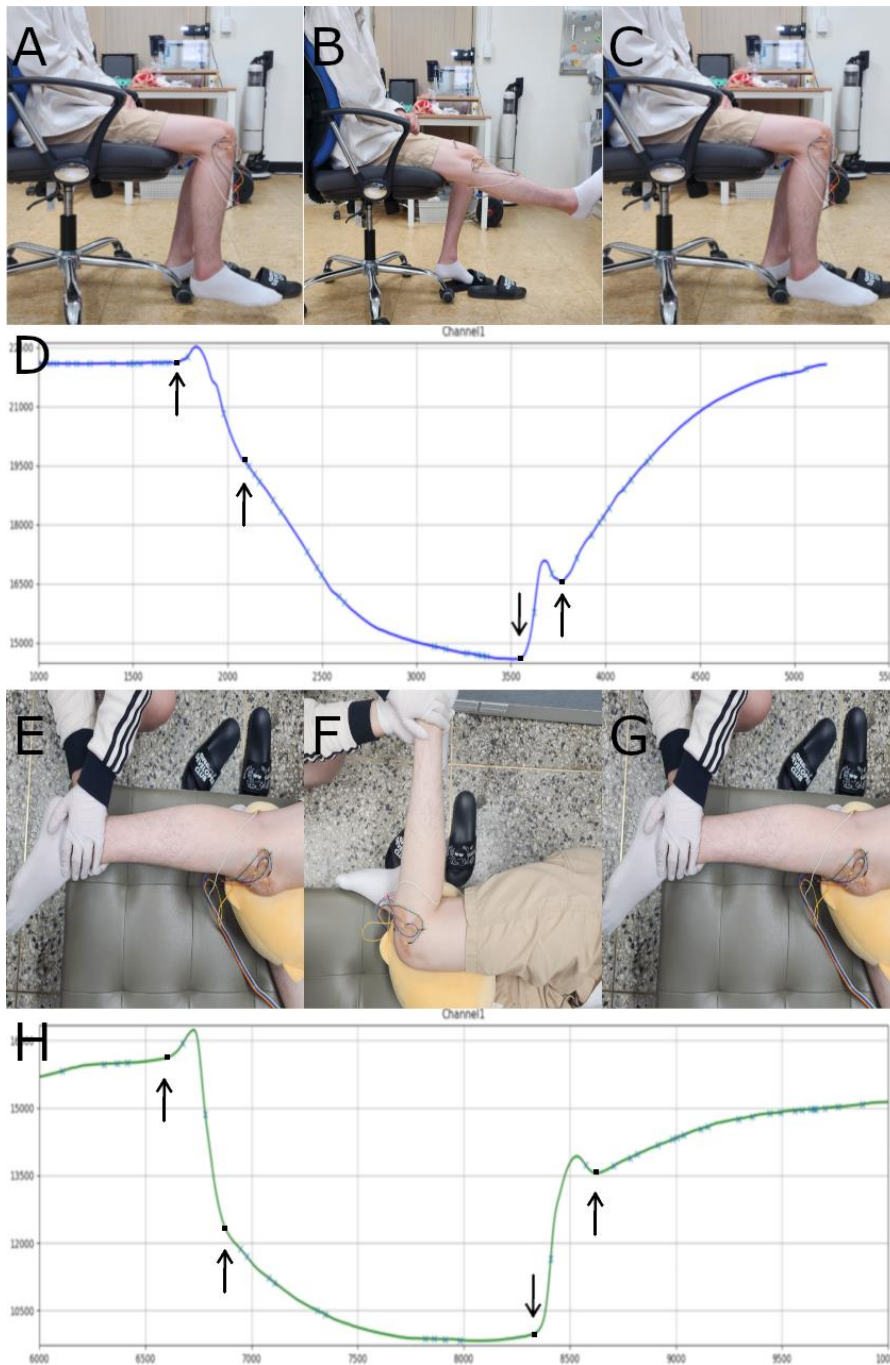


Figure 2. Physical activities and corresponding potential-time graphs depict data from electrode channel 1 for subject #1. (A-C) First row shows the active knee extension in a chair sitting. Participants were instructed to elevate their lower leg while keeping their thigh resting on the seat (A), thus actively extending their knee from 90-degree flexion to its end range (B), then hold for seven seconds before returning to their initial resting position (C). (D, H) Second and last rows shows the corresponding potential-time graphs during active knee extension (D) and passive knee extension (H) with inflection points which of the initiation and end points of the movements (black arrows). (E-G) Third row shows the passive range of motion exercise in a decubitus position. The examiner proceeded to extend the subject's knee from a 90-degree angle (E) to a 180-degree (F), then hold for seven seconds before returning to a 90-degree flexion (G), which mirrors an active extension.

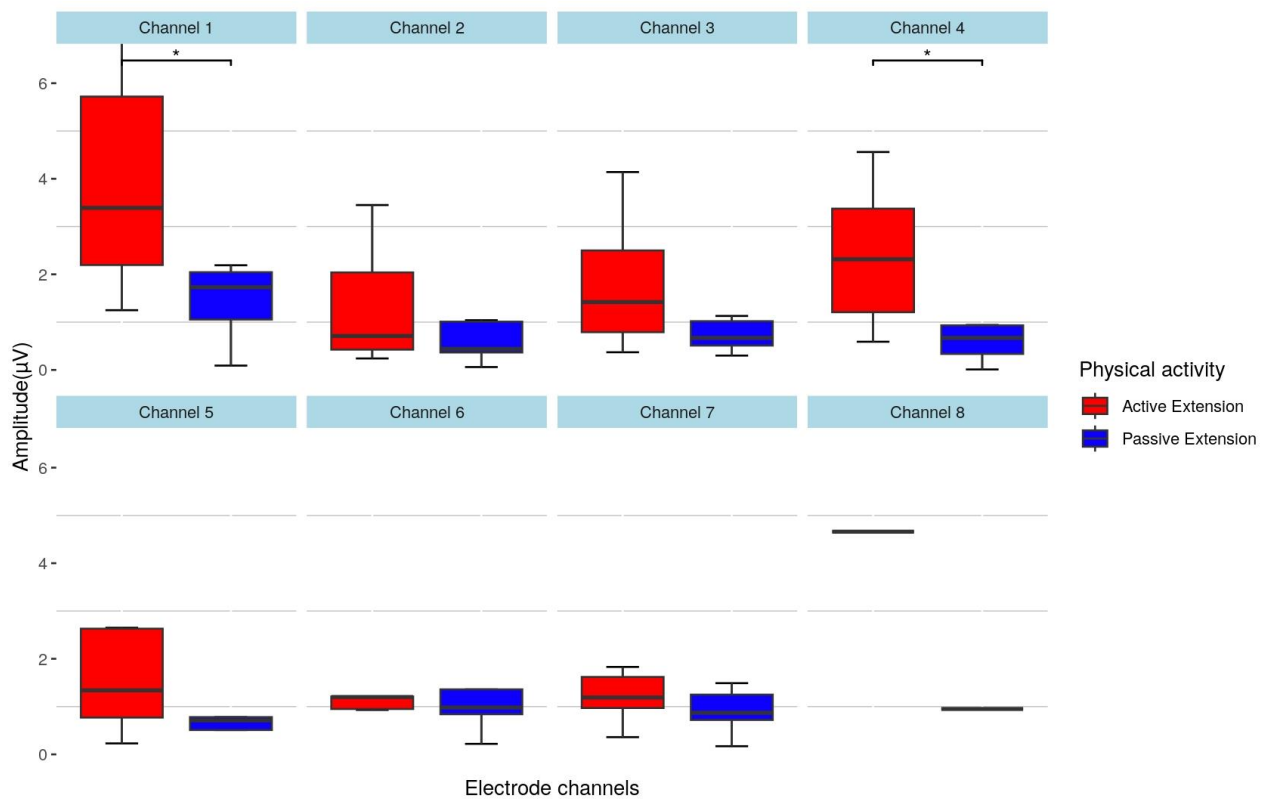


Figure 3. Comparison of active and passive knee extension induced potentials during post-activity phase The active knee extension show the large mean AmpPA across all electrode placements, with channels 1 and 4 demonstrating statistically significant differences. AmpPA, amplitude of post-activity phase; *p<0.05

Orthosis & Prosthesis

발표일시 및 장소 : 10 월 25 일(금), 13:10 ~ 13:40 , Poster Room, DID2

PS-24

Muscle-mimicking shoulder orthosis for Duchenne Muscular Dystrophy: Protocol for a clinical trial

Sungbae Jo^{1*}, JungHyun Kim¹, Eunsu Lee¹, Jeong Min Kim², Yae Lim Lee^{1,3}, Sung Eun Hyun^{1,3}, Hyung-Ik Shin^{1,3}, Cheol Hoon Park⁴, Seong Jun Park⁴, Kyungjun Choi⁴, Hyun-Mok Jeong⁴, Seung Hwan Lee^{1,3}, Woo Hyung Lee^{1,3†}

Seoul National University Hospital, Department of Rehabilitation Medicine¹, PURME foundation NEXON Children`s Rehabilitation Hospital, Department of Physical and Rehabilitation Medicine², Seoul National University College of Medicine, Department of Rehabilitation Medicine³, Korea Institute of Machinery and Materials, Advanced Robotics Research Center⁴

Background

In patients with Duchenne muscular dystrophy (DMD), enhancing upper limb functional movements and minimizing compensatory actions are critical for maintaining independence in daily activities. We developed a protocol to investigate the effect of a novel muscle-mimicking, fabric-type shoulder orthosis (MMFSO) on upper limb functional movements in DMD patients.

Methods

This clinical trial protocol is registered on ClinicalTrials.gov (NCT06363357) and the World Health Organization International Clinical Trials Registry Platform (KCT0009549). Participants will receive education and training on how to properly wear and use the MMFSO before any assessments. To minimize bias caused by fatigue, participants will be randomly allocated to blocks with different assessment orders. Functional movements of the upper limb will be assessed before and after the use of the MMFSO using the Performance of the Upper Limb 2.0, functional workspace, and the Box and Block Test. Additionally, muscle activation levels of the upper limb and compensatory muscles, including the neck, abdominal, and back muscles, will be measured and compared under both conditions.

Results

The study will evaluate the feasibility and effectiveness of the lightweight and user-friendly MMFSO in assisting functional tasks in DMD patients by enhancing shoulder movements. The expected outcomes include improvements in upper limb function as measured by Performance of the Upper Limb 2.0, functional workspace, and the Box and Block Test, as well as a reduction in muscle activation levels in the shoulder and compensatory muscles.

Conclusion

The novel MMFSO has the potential to significantly enhance upper limb function in patients with DMD. The consecutive clinical trial based on this protocol will provide comprehensive data on the feasibility and effectiveness of this innovative orthosis in assisting functional tasks in DMD patients.

Acknowledgment This research was supported and funded by SNUH Lee Kun-hee Child Cancer & Rare Disease Project, Republic of Korea (grant number: 22A-007-0000).

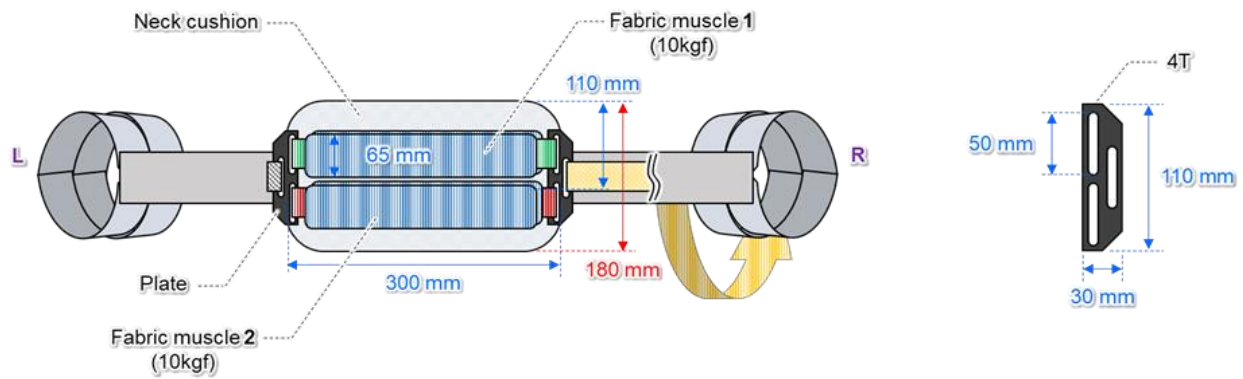


Figure 1. A schematic diagram of the muscle-mimicking, fabric-type shoulder orthosis



Figure 2. The muscle-mimicking, fabric-type shoulder orthosis

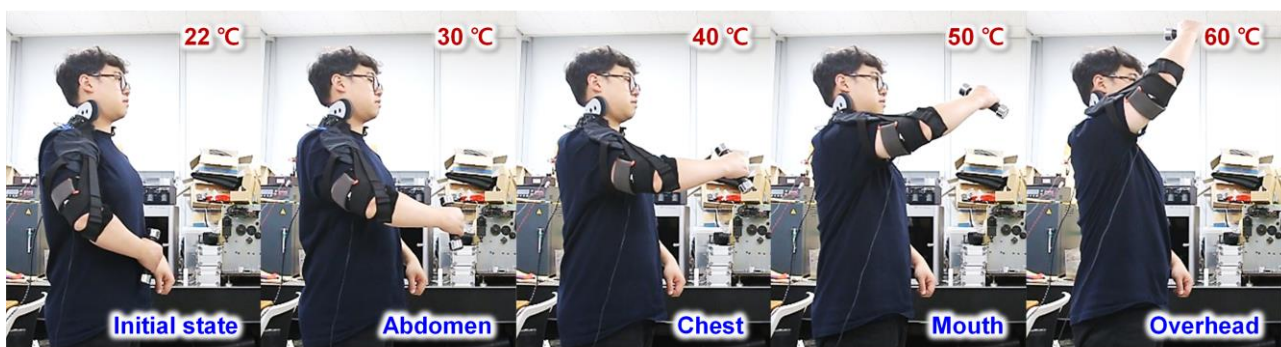


Figure 3. Shoulder assistive performances depending on the electric heating of the muscle-mimicking, fabric-type shoulder orthosis

Orthosis & Prosthesis

발표일시 및 장소 : 10 월 25 일(금), 13:10 ~ 13:40 , Poster Room, DID2

PS-25

Effects of Track-based Stair Climbing Robot on Muscle Activity, Usability, and Psychological Anxiety

Minhee Kim^{1*}, Ki Hoon Kim^{2†}, Sunhae Lee²

Biomedical Research Center, Korea University Ansan Hospital¹, Department of Rehabilitation Medicine, Korea University Ansan Hospital²

Purpose

Stair-climbing robots enhance the functional mobility of individuals with physical disabilities, but research has predominantly focused on an engineering-oriented approach, leaving the user-centered approach largely unexplored. The study aimed to investigate the effects of using a LiftCar-150 track-based stair-climbing robot on muscle activity, usability, and psychological anxiety of users.

Methods: Ten healthy participants and an 80 kg dummy rider were involved in stair climbing tasks at slow (5 m/min) and fast (7 m/min) speeds. Electromyography recorded muscle activity (middle trapezius (MT), erector spinae (ES), multifidus (MF), gluteus maximus (Gmax), gluteus medius (Gmed), and anterior deltoid (AD)). The usability test (safety, efficiency, and satisfaction) was evaluated using a 5-point Likert scale, and perceived psychological anxiety was assessed using a 0 to 10 visual analog scale (VAS).

Results

During stair ascent, the activities of back extensors (ES and MF) and gluteus muscles (Gmax and Gmed) significantly increased compared to those during stair descent. Conversely, during stair descent, the activity of the upper extremity muscle (AD) significantly increased. Usability scores averaged 4.05, 4.1, and 3.7 in terms of stability, efficiency, and satisfaction, respectively. Perceived psychological anxiety scores which evaluated using a 0 to 10 VAS were 4.2 ± 0.3 and 5.4 ± 0.5 under slow speed and 3.5 ± 0.2 and 5.7 ± 0.4 under fast speed during stair ascent and stair descent, respectively.

Conclusions

LiftCar-150 operators agreed with its stability and efficiency in climbing stairs; however, the satisfaction levels remained neutral and activation of specific muscles was increased. These results provide important insights into optimizing the usability of stair-climbing robots.

Acknowledgment This work was supported by the Assistive Technology R&D Project for People with Disabilities and the Elderly, funded by the Ministry of Health & Welfare, Republic of Korea (# HJ20C0058).

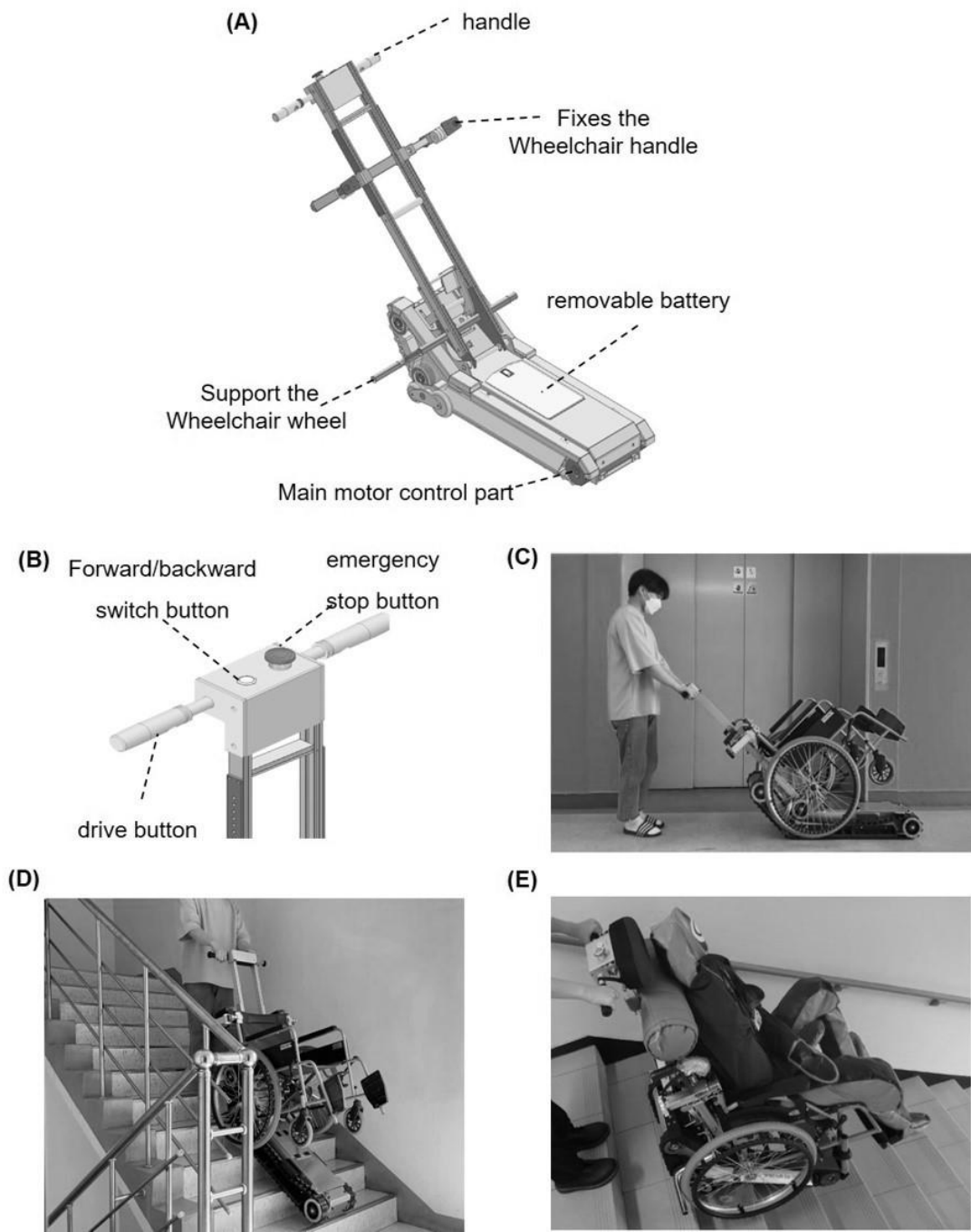


Fig 1. (A) Track based-stair climbing robot LiftCar-150, (B) description of the control button, (C) passive wheelchair joined with LiftCar-150, (D) ascending stair using LiftCar-150, and (E) ascending stair using LiftCar-150 with 80 kg dummy rider.

Muscle	Speed	Stair Ascent	Stair Descent	Z(p) [†]
		Median (IQR)	Median (IQR)	
MT	Slow	9(7.3)	8.0(8.0)	-0.491(0.624)
(% MVC)	Fast	14.5(13)	8.5(14.0)	-1.735(0.083)
	Z(p) [‡]	-1.960(0.05)	-0.357(0.721)	
ES	Slow	16.2(13.1)	7.5(5.7)	-2.666(0.008)*
(% MVC)	Fast	14.2(12.2)	8.0(5.2)	-2.670(0.008)*
	Z(p) [‡]	-0.911(0.362)	-0.957(0.339)	
MF	Slow	21(13.8)	13.5(6.8)	-2.807(0.005)*
(% MVC)	Fast	23.4(14.7)	14.7(10.0)	-2.805(0.005)*
	Z(p) [‡]	-0.654(0.513)	-0.931(0.352)	
Gmax	Slow	12.5(17.2)	5.5(6.5)	-2.606(0.009)*
(% MVC)	Fast	17(13.2)	7.0(7.1)	-2.606(0.009)*
	Z(p) [‡]	-2.371(0.018)*	-0.981(0.326)	
Gmed	Slow	33(34.9)	21.0(25.5)	-2.501(0.012)*
(% MVC)	Fast	32.5(32.5)	22.0(20.8)	-0.339(0.735)
	Z(p) [‡]	-1.724(0.085)	-0.153(0.878)	
AD	Slow	4.7(2.3)	5.5(5.7)	-2.380(0.017)*
(% MVC)	Fast	5.5(5.4)	5.7(5.8)	-0.339(0.735)
	Z(p) [‡]	-2.255(0.024)*	0.524(0.600)	

Table 1. Results of the Wilcoxon signed-rank Tests on % MVC during stair descent and ascent under slow (5 m/min) and fast (7 m/min) speed conditions. Note: All values are % MVC. * indicates significant p-value; $\alpha = 0.05$; [†] indicates the difference between stair ascent and descent; [‡] indicates the difference between slow and fast speed; MT= middle trapezius; ES = erector spinae; MF = multifidus; Gmax = gluteus maximus; Gmed = gluteus medius ; AD = anterior deltoid and IQR = inter-quartile range.

Oral Presentation

(Listed in order of presentation)

Pain and Musculoskeletal Rehabilitation

발표일시 및 장소 : 10 월 25 일(금), 15:40 ~ 17:10 , Room A

OP-1

Mitochondrial Transplantation Mitigates Paraspinal Muscle Atrophy and Neuropathic Pain

Ik-hyun Lim^{1,2*}, Seong-Hoon Kim², Mi Jin Kim³, Chang-Koo Yun³, Yong-Soo Choi^{2,3†}, Kyunghoon Min^{1†}

Department of Rehabilitation Medicine, CHA Bundang Medical Center¹, Department of Bioconvergence Science, CHA University², Department of Biotechnology, CHA University³

Background

Chronic pain after spinal surgery (CPSS) is a disabling chronic pain condition, frequently accompanied by paraspinal muscle atrophy (PMA). PMA leads to biomechanical changes such as loss of lumbar lordosis, contributing back pain through multiple pathologic processes. This study aimed to explore the potential of local plasma-derived mitochondrial (pMT) transplantation and/or vitamin D (Vit D) to counteract PMA, eventually reducing pain behavior.

Methods

pMT was collected from human blood samples. The structure, purity, and function of the pMT were verified, and their mitochondrial respiratory enzyme activity was analyzed. An in vitro model of muscle atrophy was established by treating muscle cells with dexamethasone (Dexa). The pMT (0–25 µg) was delivered to Dexa-damaged muscle cells by centrifugation. Changes in cell proliferation and mitochondrial function were assessed. Then, an in vivo study was conducted using a 2-week rat model of CPSS, created through hemilaminectomy and spinal nerve ligation at the fifth left lumbar vertebra. The rats were assigned to 5 groups, pMT/VitD, pMT, VitD, surgery, and control groups. They were administered intramuscular pMT (50 µg) ± VitD (300 µg) injections according to the assignment. The effects elicited in each group were investigated after 2 weeks via muscle morphology measurement and comprehensive tissue analysis.

Results

The pMT verified for their structure, size, and purity, exhibited mitochondrial respiratory enzyme activity. Two days post-mitochondrial transfer into Dexa-damaged muscles cells, ATP content, cell proliferation, and mitochondrial membrane potential increased and mitochondrial ROS levels decreased ($P < 0.05$). Surgical intervention resulted in a significant reduction in muscle fiber cross-sectional area in rats. However, this reduction was mitigated in the pMT/VitD, pMT, and VitD groups compared to surgery group ($P < 0.01$). pMT ± VitD also increased muscle markers of desmin and myogenin and suppressed apoptosis linked with the AMPK/AKT-regulated FoxO3a signaling pathway. pMT ± VitD demonstrated potential in alleviating surgery-induced muscle atrophy and modulating pain responses. Specifically, treatment with pMT led to a decrease in the levels of pain-related neuropeptides, including Substance P, and a downregulation of genes associated with pain and inflammation. Decreased markers of mitochondrial electron transport chain and PGC1α post-surgery were restored by pMT ± VitD.

Conclusion

Mitochondrial transplantation ± Vit D can be used for muscle regeneration and pain alleviation.

Acknowledgment This study was supported by a grant from the Korea Health Technology R&D Project through the Korea Health Industry Development Institute (KHIDI) funded by the Ministry of Health & Welfare, Republic of Korea (grant no. HI22C0623) and a grant from the Korean Fund for Regenerative Medicine (KFRM) funded by the Korea government (the Ministry of Science and ICT, the Ministry of Health & Welfare) (grant no. 22C0609L1).

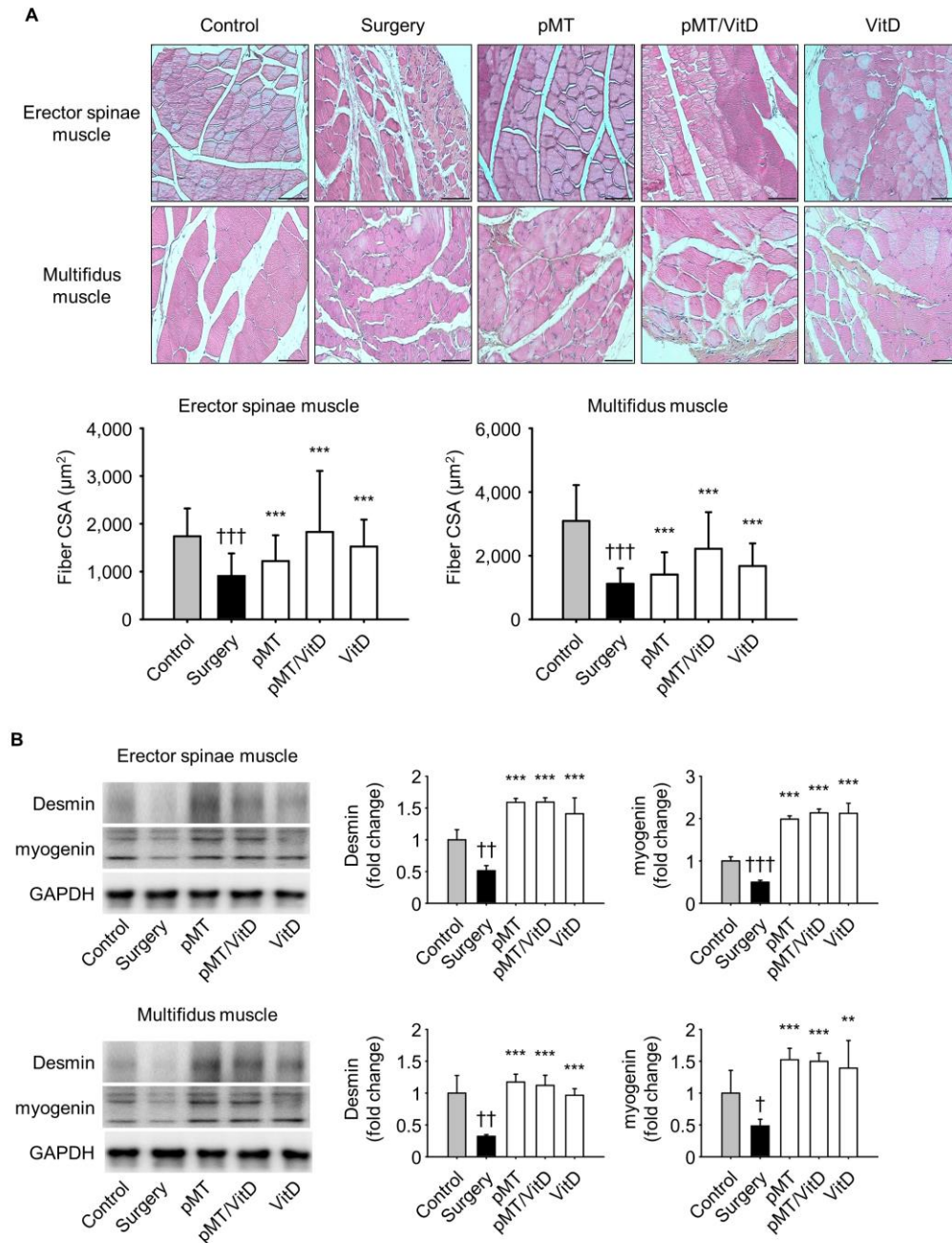
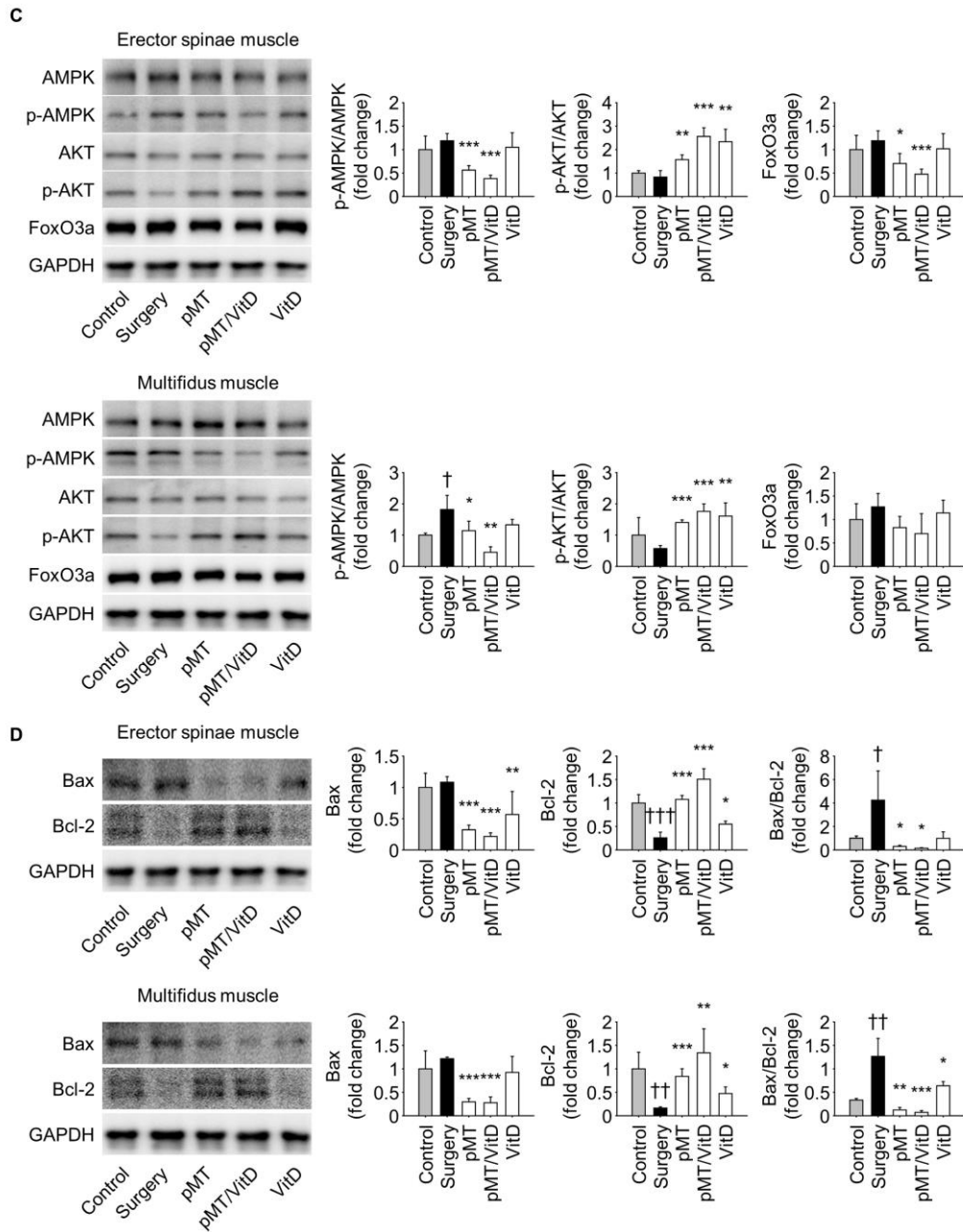
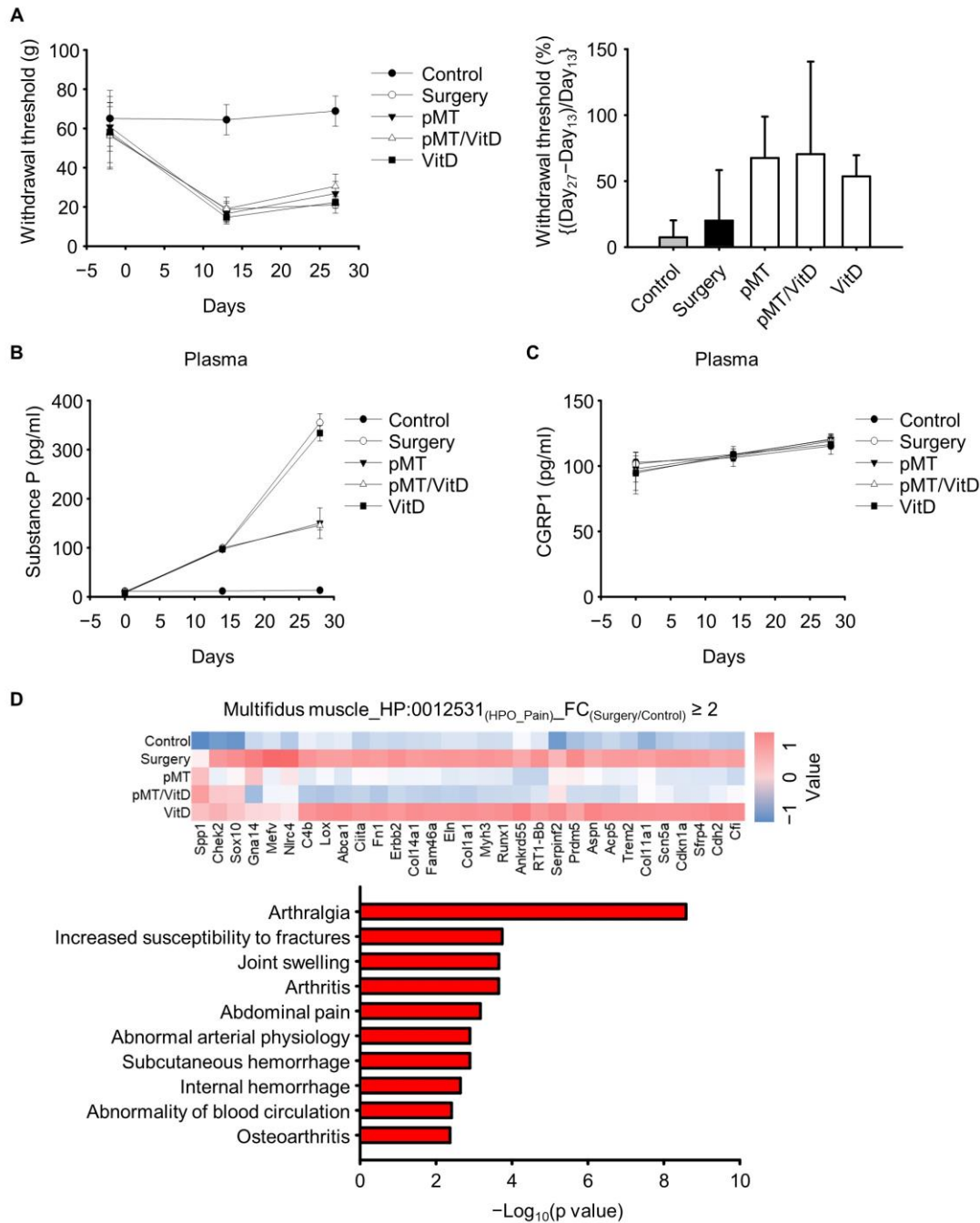


Figure 4. Histological evaluation and protein expression analyses in the paraspinal muscle of a surgery-induced rat atrophy model showed the reversal of surgery induced changes through the administration of pMT \pm Vit D. Erector spinae and multifidus muscles were evaluated separately. (A) Representative images of hematoxylin and eosin (H&E) staining revealing changes in muscle fiber size and quantification of fiber cross-sectional area (CSA). Scale bar = 100 μm . (B) Protein expression levels for muscle-specific markers with representative western blotting and quantified expression levels.



(C) Representative western blotting images quantifying the expression levels of the AMPK/AKT-regulated FoxO3a signaling pathway components in each group. (D) Western blotting analysis for evaluating apoptosis markers Bax and Bcl-2 levels. All data are presented as mean \pm standard deviation. Statistically significant differences are indicated as follows: \dagger $P < 0.05$, $\dagger\dagger$ $P < 0.01$, $\dagger\dagger\dagger$ $P < 0.001$ when compared with control group, and * $P < 0.05$, ** $P < 0.01$, *** $P < 0.001$ when compared with surgery group. AMPK: AMP-activated protein kinase, AKT: Protein kinase B, FoxO3a: Forkhead box O3a, Bax: Bcl-2 associated X protein, Bcl-2: B-cell lymphoma 2



Analysis of pain response in surgery-induced rat atrophy model showed alleviation of pain sensitivity (A) The graph shows the change in paw withdrawal threshold to von Frey filaments before and 2 weeks post-treatment. Analysis of plasma levels of the pain markers (B) Substance P and (C) CGRP1 using ELISA. (D) Human phenotype ontology (HPO) analysis (Top 10 HPO terms) of differentially expressed genes in each group. All data are presented as mean \pm standard deviation. Statistically significant differences are indicated as follows: † $P < 0.05$, †† $P < 0.01$ when compared with control group, and * $P < 0.05$, ** $P < 0.01$, *** $P < 0.001$ when compared with surgery group.

Pain and Musculoskeletal Rehabilitation

발표일시 및 장소 : 10 월 25 일(금), 15:40 ~ 17:10 , Room A

OP-2

Low phase angle is related to poor functional outcome after total knee arthroplasty

Young Seok Kim^{1*}, Seung Ick Choi¹, Jun Young Park², Hui Woo Yang¹, Wonhee Lee¹, Sung-hwan Kim³, Kwangho Chung², Na Young Kim^{1†}

Department of Rehabilitation Medicine, Yonsei University College of Medicine, Yongin Severance Hospital, South Korea¹, Department of Orthopedic Surgery, Yongin Severance Hospital, Yonsei University College of Medicine, Yongin, Republic of Korea², Department of Orthopedic Surgery, Gangnam Severance Hospital, Yonsei University College of Medicine, 211 Eonju-Ro, Gangnam-Gu, Seoul, 130-729, Korea³

Introduction

Phase angle (PhA) has been suggested as a biomarker for muscle quantity, quality, and nutritional status. PhA is associated with disease severity and mortality in various pathophysiological conditions. Although many factors have been found to predict prognosis after total knee arthroplasty (TKA), there is a lack of research on the relationship between postoperative functional status and PhA in patients with knee osteoarthritis. We investigated the association between PhA and physical function in end-stage knee osteoarthritis and its predictive value for functional outcome three months after TKA.

Methods

This single-center prospective cohort study included 199 end-stage knee osteoarthritis patients aged over 55 awaiting TKA (n = 98 for bilateral TKA, n = 101 for unilateral TKA). Patients with traumatic or rheumatic arthritis, severe neurologic diseases, or musculoskeletal diseases were excluded. Demographics, bioelectrical impedance analysis, comorbidities, radiographic severity of knee, handgrip strength, and isokinetic knee strength were collected as covariates. Functional outcomes were measured using 10-meter walk test (10MWT) and Timed up and go test (TUGT). Patients were classified as the low and the high PhA group using cut-off values of 4.95 for males and 4.35 for females. Group comparisons were performed on pre- and postoperative data using two sample t-test and paired t-test. Additionally, analysis of covariance (ANCOVA) was used to adjust postoperative TUGT result for baseline TUGT. A p-value of < 0.05 was considered statistically significant.

Results

The low PhA group (n = 54, 27.1%) was significantly older and had weaker handgrip strength, lower skeletal muscle mass, slower gait speed and longer TUGT result than the high PhA group (n = 145, 72.9%) regardless of the type of operation (Table 1). Isokinetic assessments showed lower peak torque and total work in both extension and flexion in the low PhA group. While significant improvements were observed in 10MWT and TUGT in patients with high PhA after TKA, there was no significant change in patients with low PhA (P = 0.003 vs. P = 0.073 and P = 0.004 vs. P = 0.212, respectively, Table 2).

After adjusting for baseline scores (P < 0.001), ANCOVA revealed a significant difference in follow-up TUGT result between high and low PhA groups (P = 0.033, Figure 1). Adding PhA increased the explained variance in follow-up TUGT result from R² = 0.384 to R² = 0.447. The adjusted R² of the final model is 0.421.

Conclusions

PhA could be a potential predictor of postoperative functional recovery in TKA. Further research is needed to explore the long-term trajectory of muscle strength, function, and PhA in patients with end-stage knee osteoarthritis.

Acknowledgment This research was supported by a grant from the Korea Health Technology R&D Project through the Korea Health Industry Development Institute (KHIDI), funded by the Ministry of Health and Welfare, Republic of Korea (grant number: RS-2023-00265489) and a faculty research grant of Yonsei University College of Medicine (2024-32-0066).

	Bilateral TKA			Unilateral TKA		
	Low PhA (n = 31)	High PhA (n = 67)	P	Low PhA (n = 23)	High PhA (n = 78)	P
Demographics, body composition and comorbidities						
Male	3 (9.7%)	6 (9.0%)	1	3 (13.0%)	18 (23.1%)	.453
Age, yr	74.4 ± 5.8	71.7 ± 6.3	.045*	76.4 ± 7.8	70.7 ± 6.3	.001**
BMI, kg/m ²	26.3 ± 2.9	27.4 ± 3.0	.106	27.2 ± 4.4	28.1 ± 6.1	.534
Percentage body fat, %	41.6 ± 5.5	40.1 ± 5.7	.223	41.9 ± 8.1	39.8 ± 7.3	.256
Obesity	21 (67.7%)	51 (76.1%)	.530	15 (65.2%)	54 (69.2%)	.914
SMI, kg/m ²	6.0 ± 0.7	6.7 ± 0.8	<.001***	6.5 ± 0.9	6.8 ± 1.1	.237
Maximum HGS, kg	19.5 ± 5.0	24.3 ± 5.8	<.001***	21.4 ± 5.2	25.7 ± 7.0	.009**
Sarcopenia	9 (29.0%)	3 (4.5%)	.002**	5 (21.7%)	9 (11.5%)	.368
Whole body PhA, °	4.0 ± 0.3	4.9 ± 0.4	<.001***	4.2 ± 0.3	5.0 ± 0.6	<.001***
10 Meter Walk test, m/s	0.8 ± 0.3	1.0 ± 0.2	.002**	0.8 ± 0.2	1.0 ± 0.2	<.001***
Timed Up and Go test, s	16.7 ± 7.3	12.2 ± 2.8	.002**	15.9 ± 4.9	12.3 ± 3.1	.003**
Isokinetic strength assessment, N•m						
Peak torque extension at 60°/s						
Right / Operated	34.5 ± 14.6	43.0 ± 17.2	.031*	30.6 ± 15.8	41.5 ± 18.6	.013*
Left / Non-operated	30.5 ± 11.2	44.4 ± 27.8	.001**	48.7 ± 18.3	60.7 ± 26.2	.044*
Total work extension at 60°/s						
Right / Operated	161.4 ± 84.2	214.4 ± 101.3	.022*	142.2 ± 78.7	211.2 ± 113.5	.008**
Left / Non-operated	147.5 ± 66.4	229.8 ± 161.0	.001**	244.7 ± 105.3	320.8 ± 164.8	.012*
Peak torque extension at 150°/s						
Right / Operated	24.7 ± 10.2	41.3 ± 76.0	.102	22.2 ± 10.9	29.9 ± 13.3	.013*
Left / Non-operated	22.7 ± 7.9	40.6 ± 58.0	.022*	32.7 ± 14.6	42.2 ± 19.2	.033*
Total work extension at 150°/s						
Right / Operated	348.5 ± 186.1	475.2 ± 216.0	.011*	304.0 ± 162.3	460.1 ± 230.6	.003**
Left / Non-operated	332.8 ± 131.4	518.6 ± 409.9	.002**	489.1 ± 244.9	651.7 ± 305.4	.023*
Peak torque flexion at 60°/s						
Right / Operated	18.1 ± 8.5	27.0 ± 12.6	<.001***	18.6 ± 8.8	24.1 ± 11.9	.044*
Left / Non-operated	17.2 ± 8.4	25.5 ± 14.1	.001**	23.0 ± 8.7	31.0 ± 14.2	.002**
Total work flexion at 60°/s						
Right / Operated	84.4 ± 50.4	123.7 ± 71.6	.013*	75.8 ± 48.5	110.5 ± 69.5	.029*
Left / Non-operated	75.0 ± 52.1	113.1 ± 62.4	.008**	105.7 ± 58.1	164.0 ± 85.8	.001**
Peak torque flexion at 150°/s						
Right / Operated	17.0 ± 6.6	21.2 ± 8.5	.029*	16.0 ± 6.8	21.1 ± 8.7	.014*
Left / Non-operated	16.3 ± 7.4	21.7 ± 11.5	.010*	19.1 ± 7.2	24.7 ± 9.9	.014*
Total work flexion at 150°/s						
Right / Operated	192.4 ± 122.4	266.1 ± 147.6	.028*	169.4 ± 106.8	259.0 ± 162.1	.004**
Left / Non-operated	174.9 ± 128.6	249.1 ± 134.3	.019*	214.3 ± 136.9	349.1 ± 194.8	.003**
Charlson's comorbidity index	1.9 ± 0.9	1.7 ± 0.8	.191	2.0 ± 1.2	1.8 ± 1.0	.392
IPAQ			.173			.259
1	15 (50.0%)	46 (69.7%)		21 (91.3%)	59 (75.6%)	
2	14 (46.7%)	19 (28.8%)		2 (8.7%)	18 (23.1%)	
3	1 (3.3%)	1 (1.5%)		0 (0.0%)	1 (1.3%)	
KL grade, Right / Operated			1			.113
1	0 (0.0%)	0 (0.0%)		0 (0.0%)	0 (0.0%)	
2	1 (3.2%)	1 (1.5%)		2 (8.7%)	5 (6.4%)	
3	6 (19.4%)	24 (35.8%)		7 (30.4%)	43 (55.1%)	
4	24 (77.4%)	42 (62.7%)		14 (60.9%)	30 (38.5%)	
KL grade, Left / Non-operated			1			.015*
1	0 (0%)	0 (0%)		4 (17.4%)	19 (24.4%)	
2	1 (3.2%)	6 (9.0%)		8 (34.8%)	46 (59.0%)	
3	13 (41.9%)	21 (31.3%)		9 (39.1%)	12 (15.4%)	
4	17 (54.8%)	40 (59.7%)		2 (8.7%)	1 (1.3%)	

Table 1. Patients Characteristics Stratified by Phase Angle and Type of Operation

Note: Values are presented as mean ± standard deviation or number (%). "Right / Operated" refers to the Right leg for Bilateral TKA and the Operated leg for Unilateral TKA, while "Left / Non-operated" refers to the Left leg for Bilateral TKA and the Non-operated leg for Unilateral TKA. *P<.05, **P<.01, ***P<.001

Abbreviations: BMI, body mass index; HGS, handgrip strength; IPAQ, International Physical Activity Questionnaire; KL, Kellgren Lawrence; PhA, phase angle; SMI, skeletal muscle index; TKA, total knee arthroplasty

Table 1. Patients Characteristics Stratified by Phase Angle and Type of Operation

	Low PhA (n = 15)			High PhA (n = 31)		
	Baseline	Follow-up	P	Baseline	Follow-up	P
Male, n						
Total	2 (13.3%)			4 (12.9%)		1
Bilateral	1 (11.1%)			3 (23.1%)		.878
Unilateral	1 (16.7%)			1 (5.6%)		1
Age, yr						
Total	72.8 ± 6.3			70.0 ± 6.6		.179
Bilateral	72.3 ± 4.1			69.1 ± 5.8		.160
Unilateral	73.5 ± 9.1			70.7 ± 7.3		.445
BMI, kg/m ²						
Total	27.8 ± 3.0			27.1 ± 3.5		.505
Bilateral	27.7 ± 3.0			27.8 ± 3.1		.958
Unilateral	28.0 ± 3.3			26.7 ± 3.8		.442
SMI, kg/m ²						
Total	6.53 ± 0.65	6.43 ± 0.76	1	6.58 ± 0.81	6.49 ± 0.85	.125
Bilateral	6.4 ± 0.8	6.2 ± 0.9	.554	7.0 ± 0.8	6.8 ± 1.0	.129
Unilateral	6.7 ± 0.2	6.8 ± 0.3	.632	6.2 ± 0.6	6.2 ± 0.6	.842
ECW ratio						
Total	0.407 ± 0.01	0.409 ± 0.01	.085	0.397 ± 0.01	0.399 ± 0.01	.052
Bilateral	0.409 ± 0.01	0.411 ± 0.01	.376	0.399 ± 0.01	0.400 ± 0.01	.055
Unilateral	0.403 ± 0.002	0.407 ± 0.005	.048*	0.396 ± 0.004	0.399 ± 0.01	.072
Phase angle, °						
Total	4.04 ± 0.41	4.06 ± 0.64	.904	4.85 ± 0.33	4.71 ± 0.39	.032*
Bilateral	3.9 ± 0.5	4.0 ± 0.7	.624	4.9 ± 0.4	4.7 ± 0.4	.008**
Unilateral	4.3 ± 0.2	4.2 ± 0.4	1	4.8 ± 0.3	4.7 ± 0.4	.435
10 Meter Walk test, m/s						
Total	0.89 ± 0.21	0.96 ± 0.19	.073	1.03 ± 0.16	1.13 ± 0.17	.003**
Bilateral	0.86 ± 0.21	0.94 ± 0.15	.052	1.04 ± 0.18	1.17 ± 0.18	.053
Unilateral	0.93 ± 0.22	1.00 ± 0.24	.448	1.02 ± 0.15	1.10 ± 0.17	.025*
Timed Up and Go test, s						
Total	13.9 ± 4.0	13.0 ± 3.2	.212	11.9 ± 2.2	10.7 ± 1.7	.004**
Bilateral	13.9 ± 4.2	13.1 ± 3.56	.301	11.1 ± 1.9	10.1 ± 1.8	.096
Unilateral	13.8 ± 4.1	12.9 ± 2.7	.506	12.4 ± 2.3	11.1 ± 1.6	.022*

Table 2. Comparison of Bioimpedance Analysis and Functional Outcomes before and 3 Months after Surgery Stratified by Phase Angle and Type of Operation

* $P < .05$, ** $P < .01$

Abbreviations: BMI, body mass index; PhA, phase angle; SMI, skeletal muscle index; ECW, extracellular water

Table 2. Comparison of Bioimpedance Analysis and Functional Outcomes before and 3 Months after Surgery Stratified by Phase Angle and Type of Operation

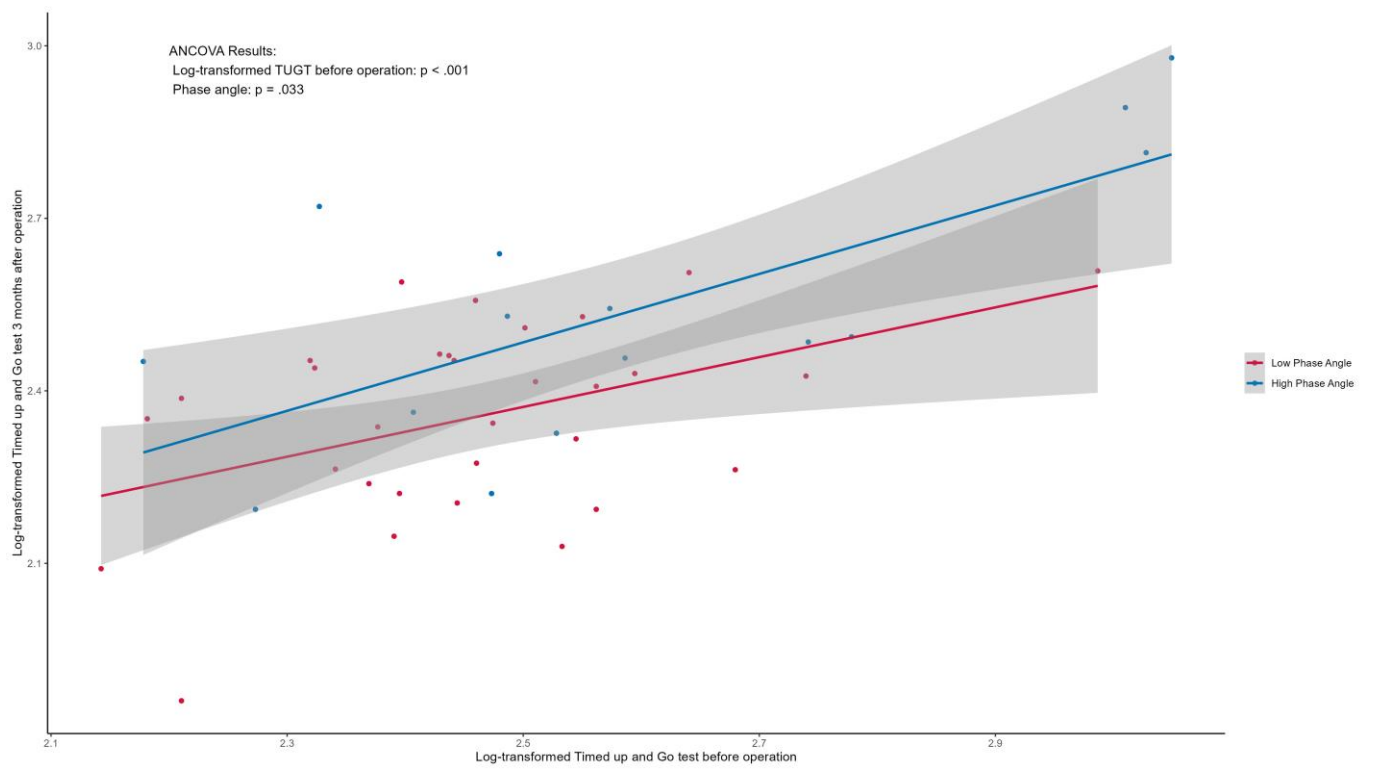


Figure 1. Scatter Plot of Log-Transformed TUGT result before and 3 Months after Operation with ANCOVA

Pain and Musculoskeletal Rehabilitation

발표일시 및 장소 : 10 월 25 일(금), 15:40 ~ 17:10 , Room A

OP-3

Enhanced Elbow Rehabilitation for Baseball Pitchers Using Pneumatic Artificial Muscle

Dr. Muhammad Umair Ahmad Khan PhD. ^{1*†}, Muhammad Umair Ahmad Khan¹, Hashir Ali Hassan¹, Areesha Azam¹, Eshaal Malik¹

Department of Biomedical Engineering UET Lahore Narowal Campus, .¹

Scope

The device operates in two modes: an Intent-Sensing Assistance Mode that uses surface electromyography (sEMG) to identify movement intentions and assists in carrying out the movements, and an Automated Repetitive Motion Mode that performs repetitive limb flexion and extension. The device is portable, lightweight, and easy to use, with a focus on accommodating natural joint movements to minimize the need for precise alignment. Its ergonomic design enhances comfort and facilitates home rehabilitation.

Method

The upper limb soft rehabilitation robot is designed with two pneumatic artificial muscles (PAMs), an EMG sensor, a wearable acrylic sheet covered with soft padding, and a portable air compressor. The device provides continuous flexion and extension with different speeds as set by the user. The PAMs are constructed using a 2D braided mesh approach with polypropylene fibers. SolidWorks is used to design lightweight aluminum molds for producing these fibers, which are then braided into a flexible structure. The PAMs contract upon inflation, generating substantial force to drive movement in the robot's joints.

Result

In this study, two healthy male participants were involved, providing written and informed consent. The device was attached to the elbow, and sEMG electrodes were positioned to evaluate muscle activity. The rectified EMG signal from the biceps muscle captured during the device's continuous passive movement mode demonstrated the activation and contraction of the biceps muscle. The device reduced muscle activity by more than 25 percent in healthy baseball pitchers, indicating its efficiency in supporting movement with minimal physical exertion.

Conclusion

The pneumatic artificial muscle (PAM) in the soft robotic-based rehabilitation device offers significant benefits for upper limb rehabilitation. Its precise control of pressurized air, guided by EMG sensor feedback, ensures accurate and effective muscle activation and movement. The use of lightweight materials and thoughtful design ensures comfort and practicality, making it valuable for stroke patients and athletes, such as baseball pitchers, in rehabilitation. The observed reduction in muscle activity indicates its efficiency, leading to better energy conservation and less fatigue during exercises. This device marks an important development in rehabilitation robotics.

Spinal Cord Injury Rehabilitation

발표일시 및 장소 : 10 월 25 일(금), 15:40 ~ 17:10 , Room A

OP-4

The effect of the Lokomat Free-D module on gait ability in individuals with spinal cord injuries

Su Ji Lee¹, Seongeun Park¹, Min Cheol Ha^{1*}, Wonkyu Min², Ji Cheol Shin^{1†}

Department and Research Institute of Rehabilitation Medicine, Yonsei University College of Medicine¹, Department of Rehabilitation Therapy, Yonsei University Health System²

Background

Robot-assisted gait training, specifically the Lokomat (Hocoma AG, Switzerland), is known to be effective in improving the locomotor ability of individuals with spinal cord injury (SCI). The previous Lokomat system restricts pelvic motion, whereas the Lokomat with the optional Free-D module (FDM), guides the lateral translation and transverse rotation of the pelvis. This study aims to investigate the effect of the FDM on the gait ability of individuals with SCI.

Methods

Twenty-seven individuals aged 19 to 85 years with SCI and classified as AIS scale C or D within 6 months of onset were prospectively recruited and randomly assigned to one of three groups: control group, without Free-D module (wo-FDM) group, and with Free-D module (w-FDM) group. Outcomes were measured using LEMS, AMI, BBS, WISCI-II, SCIM-III, SCIM-III-mobility, and proprioception scores. Intra-group analysis was conducted using the Wilcoxon rank-sum test, while inter-group analysis was performed using the Kruskal-Wallis test. Subgroup analysis was performed according to the AMI. Since there is no established cutoff value for whether the AMI is low or high, we referred to previous literature and set the criterion based on the average AMI value of 52% for ambulatory SCI individuals. Therefore, we established the criterion as 52% of the total 30, which equals 15.6.

Results

In the intragroup analysis, all three groups showed improvements in BBS (Table 1). Additionally, improvements in AMI and WISCI-II were observed in the w-FDM group. The inter-group analysis revealed differences in AMI and SCIM-III-mobility. Post-hoc analysis showed a significant difference in AMI between the control group and the w-FDM group (Table 2, Figure 1). In the low AMI group, there was a significant difference in the changes of LEMS and AMI between the control and w-FDM groups. In the high AMI group, there were no significant differences among the control, wo-FDM, and w-FDM groups.

Conclusions

Lokomat with FDM positively impacts locomotor ability of individuals with incomplete SCI. In particular, when the AMI was below 15, the w-FDM group showed a significant improvement in lower limb strength. However, when the AMI was 15 or higher, there were no significant differences among the three groups.

Table 1. Gait abilities at entry (T0) and the end (T1) of the treatment.

	T0	T1	P-value
Control			
LEMS	29.0 (16.5)	32.0 (23.3)	0.458
AMI	14.5 (10.0)	15.0 (12.3)	0.787
BBS	4.0 (2.3)	8.0 (8.0)	0.04979*
WISCI-II	0 (0.3)	0.5 (1.3)	0.332
SCIM-III	16.5 (8.8)	28.5 (12.0)	0.074
SCIM-III--mobility	1.0 (3.0)	4.5 (4.8)	0.303
Proprioception	9.0 (6.0)	9.0 (6.0)	1.000
wo-FDM			
LEMS	24.5 (8.0)	31.0 (9.3)	0.06
AMI	13.5 (6.0)	17.5 (7.3)	0.17
BBS	3.5 (2.0)	7.5 (19.8)	0.04997*
WISCI-II	0 (0.3)	3.5 (7.8)	0.105
SCIM-III	21.0 (18.3)	41.0 (36.0)	0.091
SCIM-III--mobility	0 (5.0)	12.0 (9.5)	0.079
Proprioception	6.0 (3.5)	8.5 (5.3)	0.414
w-FDM			
LEMS	27.0 (8.0)	34.0 (8.5)	0.091
AMI	13.0 (3.0)	20.0 (9.5)	0.048*
BBS	4.0 (1.0)	21.0 (28.5)	0.003*
WISCI-II	0 (1.0)	8.0 (10.0)	0.019*
SCIM-III	24.0 (25.5)	37.0 (30.5)	0.101
SCIM-III--mobility	3.0 (6.0)	12.0 (9.0)	0.052
Proprioception	12.0 (6.0)	12.0 (6.0)	0.768

*P value < 0.05

Gait abilities at entry (T0) and the end (T1) of the treatment.

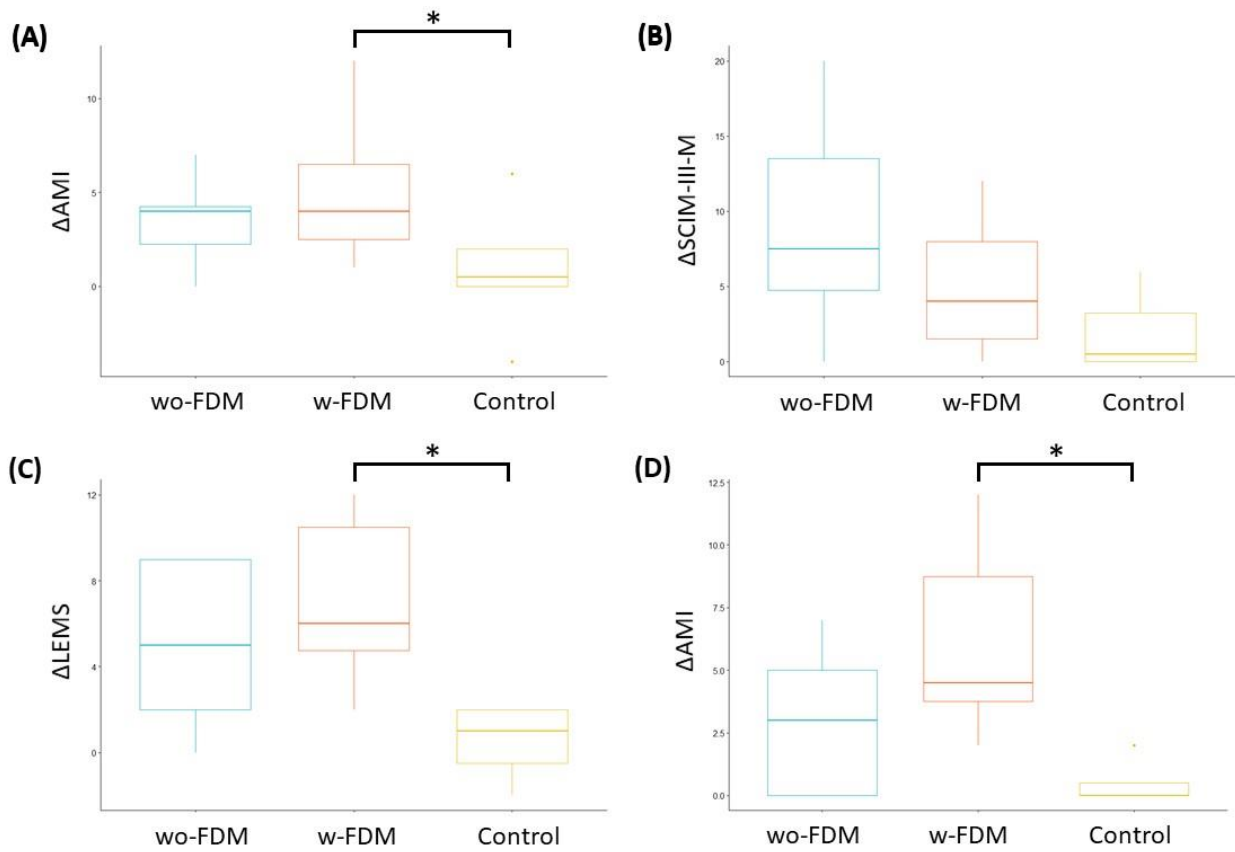
Table 2. Inter-group analysis of motor scores and gait abilities.

	V5	V6	Control	P-value	Post-hoc analysis		
					V5 vs V6	Control vs V5	Control vs V6
Overall							
ΔLEMS	6.0 (2.5)	5.0 (5.5)	2.0 (4.3)	0.144			
ΔAMI	4.0 (2.0)	4.0 (4.0)	0.5 (2.0)	0.037*	0.501	0.146	0.042*
ΔBBS	3.5 (17.8)	13.0 (26.0)	4.0 (3.3)	0.313			
ΔWISCI2	3.0 (7.8)	7.0 (9.5)	0.0 (1.0)	0.101			
ΔSCIM3	22.0 (13.3)	9.0 (15.0)	9.5 (9.3)	0.149			
ΔSCIM3-mobility	7.5 (8.8)	4.0 (6.5)	0.5 (3.3)	0.045*	0.213	0.074	0.165
ΔProprioception	0.0 (2.8)	0.0 (0.0)	0.0 (0.0)	0.162			
Low AMI†							
ΔLEMS	6.0 (2.5)	5.0 (5.5)	1.0 (2.5)	0.030*	0.338	0.197	0.038*
ΔAMI	4.0 (2.0)	4.0 (4.0)	0.0 (0.5)	0.025*	0.230	0.230	0.030*
ΔBBS	3.5 (17.8)	13.0 (26.0)	2.0 (4.5)	0.122			
ΔWISCI2	3.0 (7.8)	7.0 (9.5)	0.0 (0.25)	0.328			
ΔSCIM3	22.0 (13.3)	9.0 (15.0)	9.0 (12.3)	0.812			
ΔSCIM3-mobility	7.5 (8.8)	4.0 (6.5)	0.0 (0.3)	0.124			
ΔProprioception	0.0 (2.8)	0.0 (0.0)	0.0 (0.0)	0.380			
High AMI†							
ΔLEMS	6.0 (2.5)	5.0 (5.5)	2.0 (4.3)	0.085			
ΔAMI	4.0 (2.0)	4.0 (4.0)	0.5 (2.0)	0.358			
ΔBBS	3.5 (17.8)	13.0 (26.0)	4.0 (3.3)	0.818			
ΔWISCI2	3.0 (7.8)	7.0 (9.5)	0.0 (1.0)	0.125			
ΔSCIM3	22.0 (13.3)	9.0 (15.0)	9.5 (9.3)	0.052			
ΔSCIM3-mobility	7.5 (8.8)	4.0 (6.5)	0.5 (3.3)	0.046*	0.150	0.150	0.480
ΔProprioception	0.0 (2.8)	0.0 (0.0)	0.0 (0.0)	0.311			

*P value < 0.05

†Since there is no established cutoff value for whether AMI score is low or high, we referred to previous literature and set the criterion based on the average AMI value of 52% for ambulatory SCI individuals. Therefore, we established the criterion as 52% of the total 30, which equals 15.6.

Inter-group analysis of motor scores and gait abilities.



Box plot of inter-group analysis for each group. (A), (B) Overall analysis. (C), (D) Subgroup analysis of individuals with low AMI.

Cancer Rehabilitation

발표일시 및 장소 : 10 월 25 일(금), 15:40 ~ 17:10 , Room A

OP-6

Lymph-specific magnetic resonance (MR) lymphangiography for evaluation of lymphedema

Hwayeong Cheon^{1*}, Dong Cheol Woo^{2,3}, Kyung Won Kim⁴, Jae Yong Jeon^{1,5†}

Rehabilitation Research Center, Biomedical Engineering Research Center, Asan Institute for Life Sciences, Asan Medical Center¹, Department of Convergence Medicine, Asan Medical Center, University of Ulsan College of Medicine², Convergence Medicine Research Center, , Asan Institute for Life Sciences, Asan Medical Center³, Department of Radiology and Research Institute of Radiology, Asan Image Metrics, Clinical Trial Center, Asan Medical Center, University of Ulsan College of Medicine⁴, Department of Rehabilitation Medicine, Asan Medical Center, University of Ulsan College of Medicine⁵

Purpose

Magnetic resonance lymphangiography (MRL) allows for non-invasive visualization of deeper lymphatic flow using a contrast agent such as gadolinium-based contrast agents (GBCAs), facilitating a comprehensive evaluation of the lymphatic system from various angles in multiple planes. It is highly useful for evaluating lymphedema and assessing its treatment efficacy in cancer rehabilitation. However, GBCAs have a critical limitation: they cannot distinguish between blood and lymphatic vessels, and have a short retention time in the lymphatic vessels. This study aims to propose a new lymph-specific MRL using an iron-oxide-based contrast agent to overcome the current limitations of MRL and validate its technical efficacy compared to near-infrared lymphangiography (NIRF-ICGL) results in lymphedema animals.

Method

The experiment used 29 male Sprague–Dawley rats with lymphedema after lymph node dissection and radiation exposure. These rats were utilized to obtain INV-MRL and NIRF-ICGL images (n=26) and to study the excretion of agents from the body (n=3). The images were compared within the same individual and analyzed at the same anatomical location. The images from both modalities were classified into five stages depending on the changes in dermal backflow patterns, and it was verified whether the staging differed according to the imaging method within the same animals. The area ratio enhanced by the contrast agent within the total region of interest was defined as the threshold area ratio (TAR). The TAR was calculated for each image to quantitatively assess the severity of lymphedema. The consistency of the TAR with the qualitative staging results was then evaluated using Pearson's correlation test.

Results

INV-MRL successfully showed a dermal backflow pattern, which is the appearance of the collateral pathway, dilatation of lymphatic vessels, and diffused area in lymphedema limbs. This was completely different from visualizing only the lymphatic vessels and lymph nodes in the normal limbs. Even though the stages were classified using different criteria for INV-MRL and NIRF-ICGL respectively, the overall classification into similar stages was observed. The TAR, which is a quantitative value, increased with higher severity stages of lymphedema in both imaging modalities. Notably, the qualitative and quantitative results of dorsal NIRF-ICGL had higher concordance with that of INV-MRL.

Conclusion

In conclusion, we successfully demonstrated that INV-MRL is a suitable technique for visualizing lymphatic flow and assessing lymphedema by animal experiments, and it is appropriate for clinical trials as a lymph-specific MRL. Furthermore, we established a staging criterion for the INV-MRL to assess lymphedema and proposed quantitative parameters. These results showed significant concordance with those obtained from NIRF-ICGL depending on the dermal backflow.

Acknowledgment This work was supported by the National Research Foundation of Korea (NRF) grant funded by the Korea government (MSIT). (2022M3A9G1014476, RS-2023-00227084, RS-2024-00338179)

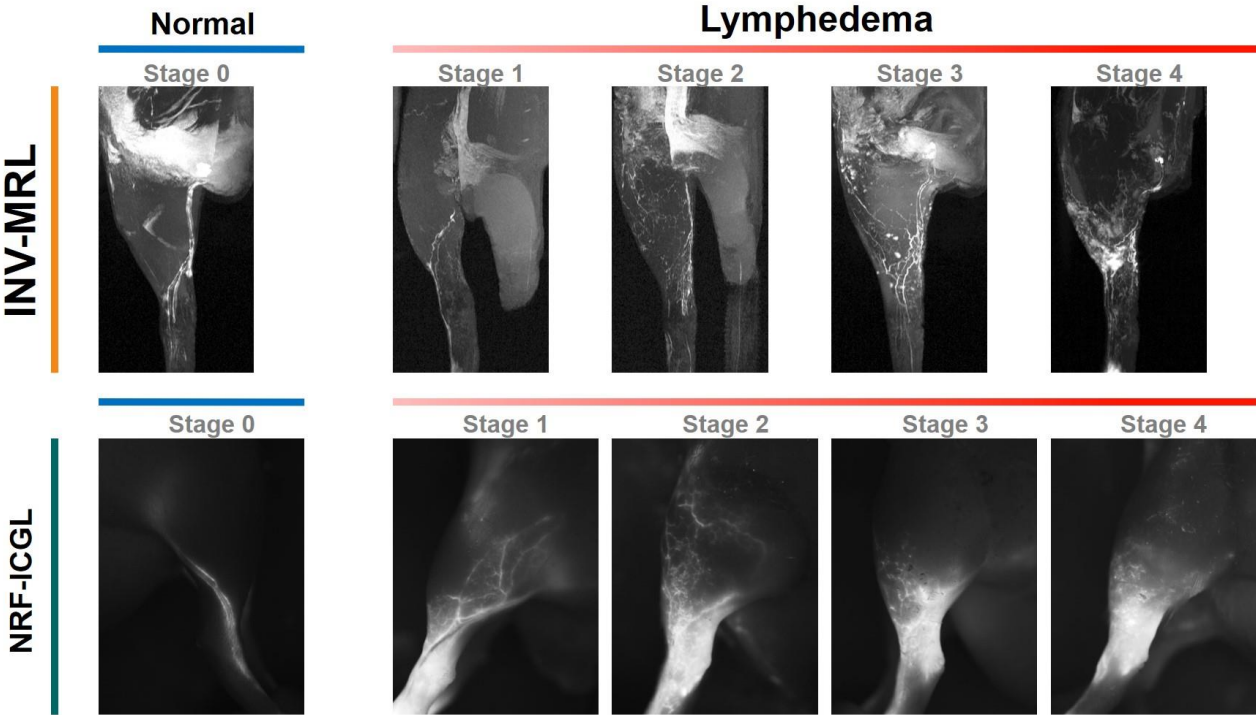


Figure 1. The representative INV-MRL and NIRF-ICGL images of normal and lymphedema limbs in animals. The lymphedema stages were classified based on each modality criteria. The INV-MRL and NIRF-ICGL images for each stage depict the same limb of the same animal.

Cancer Rehabilitation

발표일시 및 장소 : 10 월 25 일(금), 15:40 ~ 17:10 , Room A

OP-7

Prediction of unilesional neuropathic pain 4 months after mastectomy with lymph node resection

Asall Kim^{1*}, Ui-Jae Hwang², Chunghwi Yi², Jaewon Beom^{1†}

Department of Rehabilitation Medicine, Seoul National University Bundang Hospital¹, Department of physical therapy, Yonsei University²

Background

Risk factors for unilateral neuropathic pain after mastectomy with immediate breast reconstruction and lymph node resection are unknown. This study was aimed to identify whether the early physical examination and symptoms factors were able to predict neuropathic pain at 4 months postoperative. We hypothesized a directional correlation between the number of lymph node resection and pectoralis muscle tightness.

Methods

Fifty-seven breast cancer survivors were included in this study between August 2021 and May 2022. Unilesional neuropathic pain was defined as Pain-Detect questionnaire (PDQ) score over 13 at 4 months postoperative. Independent variables were patient characteristics, physical function, and self-reported symptoms at 1 month postoperative. Pectoralis minor length index (PMI) is a normalized index of the pectoralis muscle length divided by height.

Results

On average, 7.5 of lymph nodes were resected. PMI at 1 month was 9.93 ± 0.44 and PDQ at 4 months was 12.19 ± 6.20 out of 35. Univariate logistic regression identified two significant predictors. Multivariate logistic regression established a prediction model with PMI and systemic therapy side effect (subjectively reported symptoms such as dry mouth, hair loss, or headache), which is the sub-score from EORTC BR23, ($\chi^2 = 15.466$) (Table 1). Receiver operating curve analysis reported cut-off values of 9.82 and 26.19 point for PMI and systemic therapy side effect, respectively (Figure 1). PMI was negatively correlated with the number of lymph node resection (Spearman's $\rho = -0.203$) (Table 2). Correlation coefficients were significant in patients who underwent implant-based reconstruction, sentinel lymph node biopsy, radiation therapy, and hormone therapy ($\rho = -0.349, -0.317, -0.548, \text{ and } -0.345$).

Conclusion

Neuropathic pain, which is the major influencing factor for upper limb disability after breast cancer surgery, can be predicted by careful physical examination. Our findings would help clinicians to plan a specific rehabilitation intervention for post-surgery neuropathic pain.

Table 1. Results of multivariate logistic regression

Predictors	B	EXP(b) (<i>p</i> -value)	95% CI
Systemic therapy side effect	0.054	1.055 (0.007)	1.015 – 1.097
Pectoralis minor length index	-1.654	0.191 (0.033)	0.042 – 0.877
χ^2 (<i>p</i> -value)	15.466 (< 0.001)		
Classification accuracy	82.5%		

Significant factors (*p*-value < 0.05) were included in multivariate logistic regression, Enter method was conducted.

* and ** indicates *p*-value < 0.05 and 0.01, respectively.

Results of multivariate logistic regression

Table 2. Correlation between number of lymph node resection and shoulder mobility index at 1-month postoperative.

Group	N	Flexion	Abduction	External rotation	Internal rotation	Center of rotation	PMI	
All	57	0.005 (0.485)	-0.097 (0.238)	0.296* (0.013)	-0.080 (0.277)	0.271* (0.021)	-0.203 (0.065)	
Type of mastectomy	NSM	44	0.020 (0.448)	-0.108 (0.242)	0.252* (0.049)	-0.043 (0.392)	0.149 (0.167)	-0.151 (0.163)
	SSM	9	-0.143 (0.357)	-0.176 (0.325)	0.286 (0.228)	-0.513 (0.079)	0.605* (0.042)	-0.403 (0.141)
	TM	4	0.600 (0.200)	0.800 (0.100)	0.800 (0.100)	0.000 (0.500)	0.800 (0.100)	0.000 (0.500)
Type of reconstruction	ABR	25	-0.067 (0.375)	-0.179 (0.196)	0.259 (0.105)	-0.155 (0.230)	0.149 (0.239)	-0.080 (0.352)
	IBR	32	0.072 (0.347)	-0.016 (0.465)	0.299* (0.048)	-0.032 (0.431)	0.363* (0.021)	-0.349* (0.025)
Type of lymph node dissection	SLNB only	44	-0.076 (0.313)	-0.068 (0.332)	0.330* (0.014)	0.141 (0.181)	0.230 (0.067)	-0.317* (0.018)
	ALND only	5	-0.564 (0.161)	-0.718 (0.086)	0.051 (0.467)	-0.718 (0.086)	0.462 (0.217)	-0.051 (0.467)
	ALND + SLNB	8	0.119 (0.389)	0.048 (0.455)	0.190 (0.326)	-0.024 (0.478)	-0.048 (0.455)	-0.143 (0.368)
History of chemotherapy	No	28	0.065 (0.372)	0.091 (0.323)	0.462** (0.007)	-0.048 (0.405)	0.366* (0.028)	-0.286 (0.070)
	Yes	29	0.019 (0.460)	-0.159 (0.205)	0.054 (0.391)	-0.198 (0.151)	0.146 (0.225)	-0.071 (0.358)
History of radiation therapy	No	41	-0.051 (0.376)	-0.144 (0.184)	0.351* (0.012)	-0.009 (0.477)	0.316* (0.022)	-0.074 (0.322)
	Yes	16	0.284 (0.144)	0.111 (0.341)	0.334 (0.103)	-0.344 (0.096)	0.204 (0.224)	-0.548* (0.014)
History of hormone therapy	No	20	-0.001 (0.499)	-0.130 (0.293)	0.712** (< 0.001)	-0.336 (0.074)	0.685** (< 0.001)	0.043 (0.429)
	Yes	37	-0.026 (0.439)	-0.071 (0.338)	-0.015 (0.464)	0.155 (0.180)	-0.122 (0.236)	-0.345* (0.018)

As the directional-hypothesis was established, one-tailed correlation was examined.

PMI, Pectoralis minor length index; NSM, Nipple-sparing mastectomy; SSM, Skin-sparing mastectomy; TM, Total mastectomy; ABR, Abdominally based reconstruction; IBR, Implant-based reconstruction; SLNB, Sentinel lymph node biopsy; ALND, Axillary lymph node dissection

* and ** indicates *p*-value < 0.05 and 0.01, respectively.

Correlation between the number of lymph node resection and shoulder mobility index at 1-month postoperative

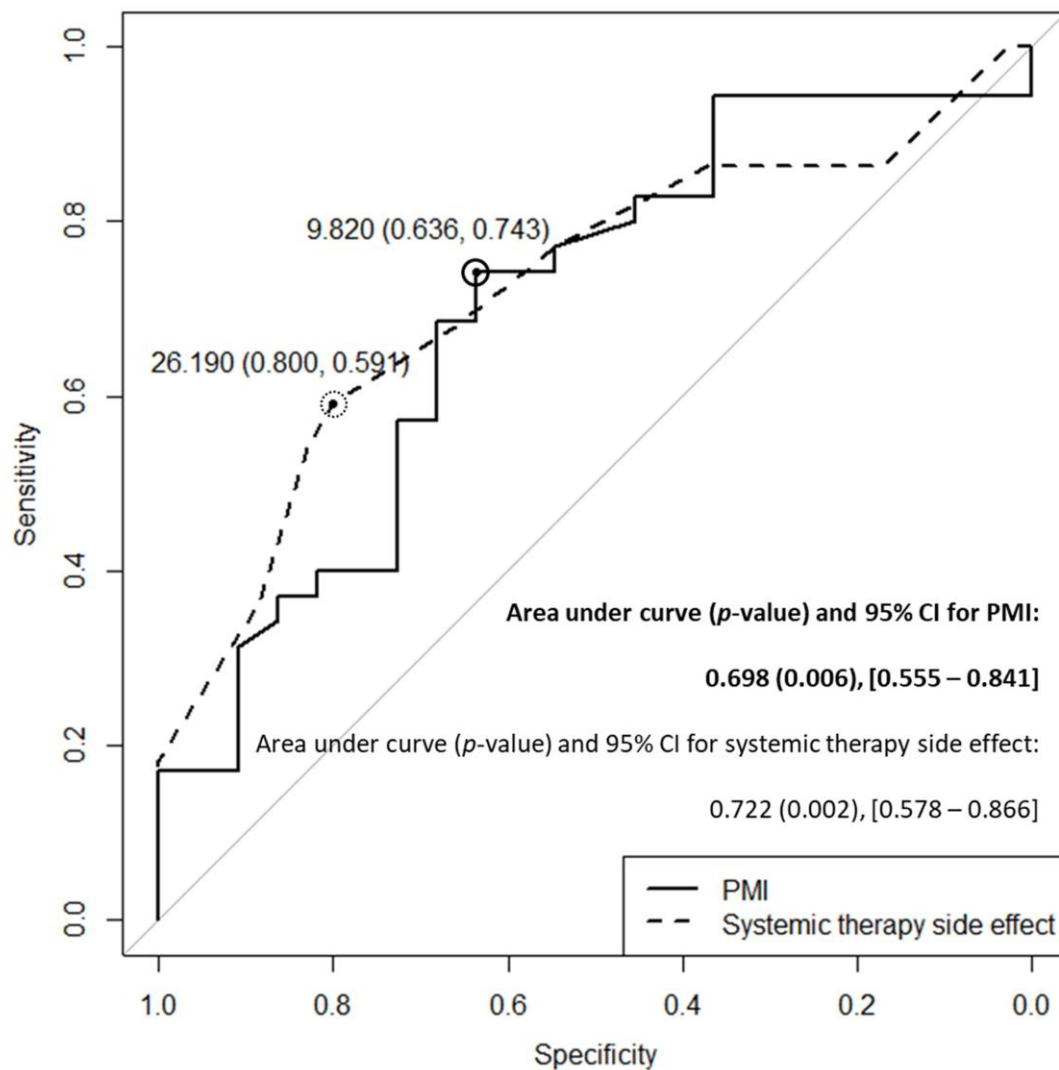


Figure 1. Cut-off value for PMI was 9.820 cm/cm with specificity and sensitivity of 0.636 and 0.743, respectively. Cut-off value for systemic therapy side effect was 26.19 point with 0.800 and 0.591, respectively. PMI, pectoralis minor length index.

Cut-off values of predictors for neuropathic pain

Pediatric Rehabilitation

발표일시 및 장소 : 10 월 25 일(금), 15:40 ~ 17:10 , Room A

OP-8

Can AI-Based Video Analysis Differentiate Hand Posture During Grasp Task in Children?: A Pilot Study

Sunyoung Joo^{1*}, Eun Jae Ko^{1†}, Yong Hoe Koo¹, Tae Won Kim², June-Goo Lee², Su Min Kim¹

Department of Rehabilitation Medicine, Asan Medical Center¹, Department of Biomedical Engineering, Asan Medical Center²

Objective

When we assess the fine motor skills of the young children, we evaluate them with clinical assessments, such as Quality of Upper Extremity Skills Test (QUEST). The aim of this study was to develop a novel AI-based video analysis to qualitatively analyze hand postures during tasks of “Grasp of Cube” and “Grasp of Cereal” item in the QUEST, and evaluate the efficiency of it.

Method

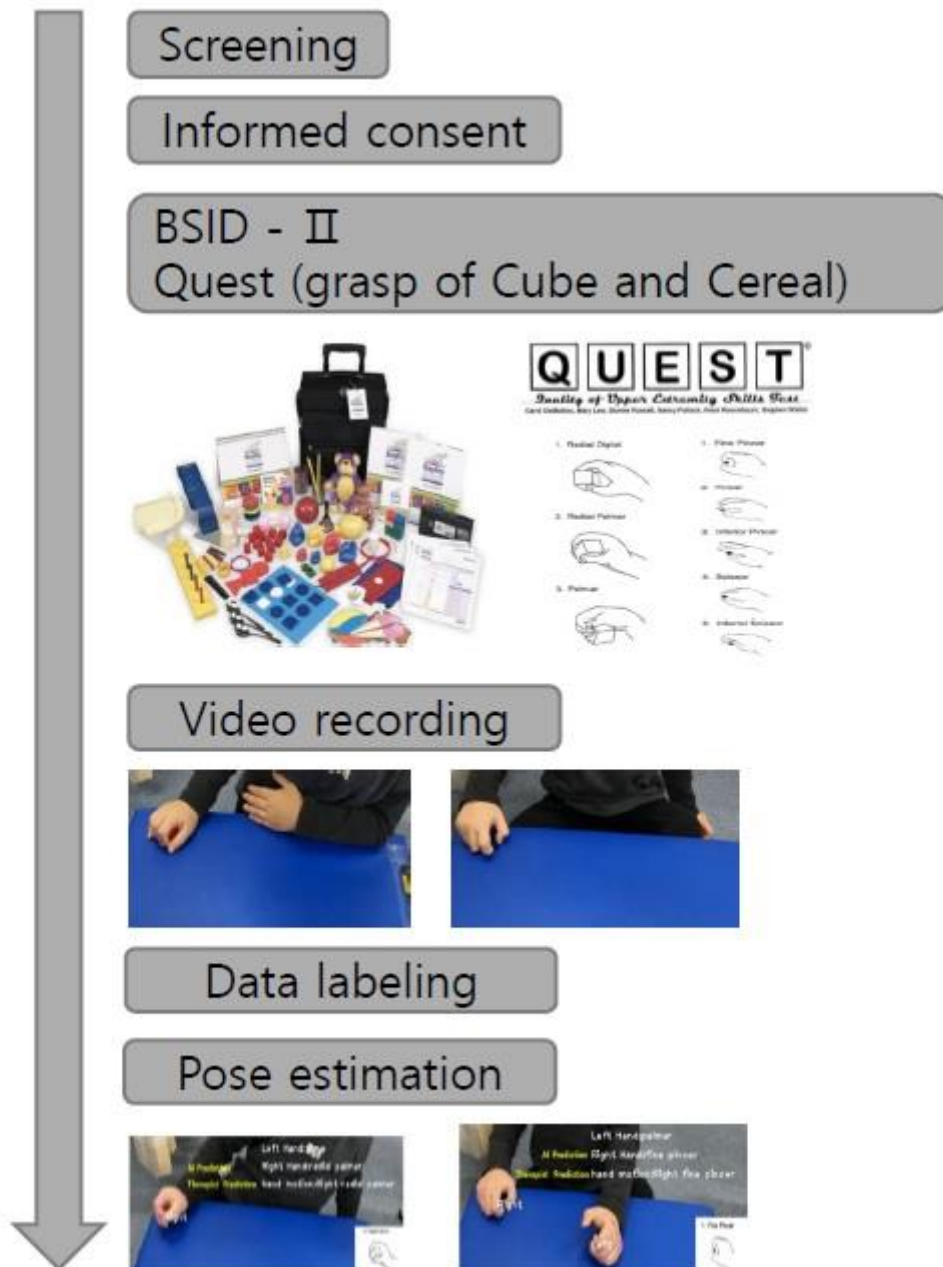
A prospective cohort pilot study was conducted between March 2023 and February 2024. Children aged between 18 and 42 months, who were referred to the Department of Rehabilitation Medicine for suspected developmental delay, were enrolled. Bayley Scales of Infant Development (BSID-II) was administered to the enrolled children to evaluate their general development. QUEST was also administered to them and their performance of the tasks, “Grasp of Cube” and “Grasp of Cereal” in the QUEST were video recorded and analyzed with this novel tool, trying to differentiate among radial digital grasp, radial palmar grasp, palmar grasp, fine pincer, pincer, inferior pincer, scissor, and inferior scissor (Figure 1). The sensitivity and specificity of the novel tool were determined by comparing the results compared to those of the standard QUEST assessment administered by therapists.

Results

Total 19 children with mean age of 29.5 months were enrolled (Table 1). This novel tool for “Grasp of Cube” task and “Grasp of Cereal” task (Figure 2) showed high sensitivity and specificity. It could automatically differentiate right hand from left hand of a child, and it could also differentiate the hands of the children from the hands of the investigators.

Conclusion

The novel deep learning-based diagnostic novel tool demonstrated high predictive accuracy for “Grasp of Cube” and “Grasp of Cereal” item of the QUEST in young children. The results indicate the potential utility of deep learning-based software for detecting different hand postures during performing tasks in children and for assessing fine motor skills of them in the future.



Study Timeline



AI-based Video Anlysis Differentiating Hand Postures of (A) Radial Palmar Grasp and (B) Fine Pincer Grasp

Table 1. Baseline characteristics of the study population (n=19)

Variables	
Gestational age	
<28 weeks	2 (10.5)
28 ≤GA<32 weeks	4 (21.0)
32 ≤GA<37 weeks	6 (31.2)
>37 weeks	7 (36.8)
Birth weight (g)	1939.4 ± 854.8
Age (at the time of participation, months)	29.5 ± 8.0
Sex (Male : Female)	7 (36.8) : 12 (63.2)
BSID-II: Mental developmental index	91.3 ± 24.1
BSID-II: Psychomotor developmental index	83.9 ± 21.9
QUEST: Grasp of Cube	
Right Radial digital : Radial palmar : Palmar : Fail	13: 4 (21.0) : 0 : 2 (10.5)
Left Radial digital : Radial palmar : Palmar : Fail	13: 4 (21.0) : 0 : 2 (10.5)
QUEST: Grasp of Cereal	
Right Fine pincer : Pincer : Inferior pincer : Scissor : Inferior scissor	2 (10.5) : 15 (79.0) : 0 (0.0) : 0 (0.0) : 2 (10.5)
Left Fine pincer : Pincer : Inferior pincer : Scissor : Inferior scissor	2 (10.5) : 16 (84.2) : 0 (0.0) : 0 (0.0) : 1 (5.3)

Values are mean ± SD or number (%). BSID: Bayley Scales of Infant Development ; QUEST: Quality of Upper Extremity Skills Test.

Baseline characteristics of the study population (n=19)

Pediatric Rehabilitation

발표일시 및 장소 : 10 월 25 일(금), 15:40 ~ 17:10 , Room A

OP-9

Identification of Cerebral Palsy-Related Genes using Meta-analysis

Jeeln Choi^{1,2}, Taesic Lee^{3,4}, Seyoung Shin^{1,5}, MinYoung Kim^{1,2,5*†}

Department of Rehabilitation Medicine, CHA Bundang Medical Center¹, Rehabilitation and Regeneration Research Center, CHA University², Department of Family Medicine, Yonsei University Wonju College of Medicine³, The Study of Obesity and Metabolic Syndrome, Korean Academy of Family Medicine⁴, Department of Medical Science, CHA University School of Medicine⁵

Objective

Cerebral palsy (CP) is a complex neurodevelopmental disorder with a multifactorial etiology, including genetic factors. As the elderly pregnant women population has increased over the past decade, the incidence of neonatal brain diseases, including CP caused by an inadequate supply of nutrients and oxygen to the brain due to premature birth or various issues during pregnancy, has also risen. Most affected individuals experience lifelong disabilities; nevertheless, there is currently no effective therapy for CP because of a lack of understanding regarding the exact pathophysiologic mechanism. By integrating public dataset analysis with experimental validation using an hypoxic-ischemic encephalopathy (HIE) animal model, this study aimed to identify and confirm potential genetic markers associated with CP.

Methods

A multi-disciplined team consisting of a pediatric rehabilitation specialist, a data scientist, and a laboratory expert researcher conducted a comprehensive study (Figure 1.1). The study involved literature review, dataset acquisition, normalization, bioinformatics analysis, and experimental validation. Public datasets relevant to HIE mouse model and CP in the clinic were obtained from the Gene Expression Omnibus (GEO) repository (Figure 1.2). These datasets underwent normalization using limma or DESeq2 to ensure consistency and comparability across samples. Then, we performed meta-analysis to find candidate genes for CP.

This step also aimed to confirm the gene expression patterns observed in the candidate genes identified from the public datasets (Figure 1.3). An in-vivo HIE mouse model was established, representing CP. The in-vivo HIE model was induced by common carotid artery (CCA) ligation. Three brains from control mice and three from HIE-induced mice were collected. Tissues were extracted from the ipsilateral brain regions of these samples.

Results

A meta-analysis was conducted by integrating gene expression data from the public data sets of HIE animal models with CP patients' blood samples (Figure 2). This comprehensive analysis identified 164 CP-related candidate genes. To validate these genes and select the CP-related genes, the microarray analysis of established the in-vivo HIE animal model confirmed the expression patterns of the candidate genes identified from the meta-analysis. Among these, four genes, PRPH2($p=0.03$), TLR2($p=0.03$), SUSD4($p=0.01$), and ZNF467($p=0.02$), exhibited significant changes in expression, consistent with the CP phenotype (Figure 3).

Conclusions

Although the pathological mechanisms remain unclear, this study successfully identified gene groups that change in response to HIE the representative cause of CP. The four genes we discovered could serve as therapeutic targets for directly treating CP and as a basis for future diagnostic or therapeutic strategies.

Acknowledgment a grant of the Korea Health Technology R&D Project through the Korea Health Industry Development Institute (KHIDI), funded by the Ministry of Health & Welfare, Republic of Korea (grant number : HI16C1559)

Overview of CP-related meta-gene identification.

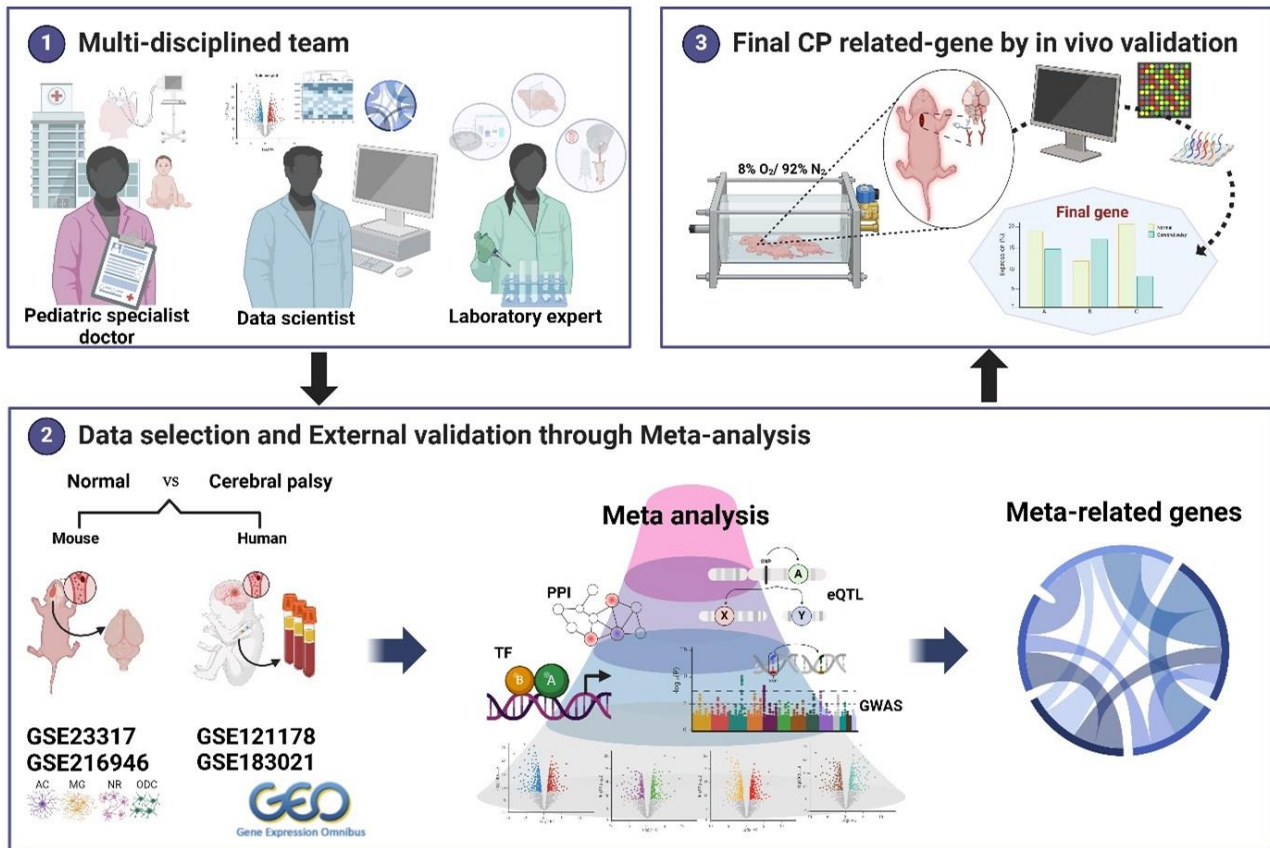


Figure 1. Schematic plot summarizing the overall design of the current study to identify cerebral palsy (CP)-Meta genes. (1) A multi-disciplined team including a pediatric rehabilitation specialist doctor, data scientist, and laboratory expert researcher conducted the literature. (2) Public data sets for cerebral palsy were obtained from a Gene Expression Omnibus (GEO). GSE23317 was obtained from HIE mouse brain and GSE216946 was from variable cell types including astrocyte (AC), microglia (MG), neuron (NR), and oligodendrocyte (ODC) in HIE rat brain. GSE121178, GSE183021 datasets were from human blood with cerebral palsy. The disease-related genes were identified from PPI, TF, eQTL, and GWAS which the domain knowledge obtained from the disease. (3) Pre-clinic sampling for validation of public datasets in cerebral palsy. The hypoxic-ischemic encephalopathy mouse model was operated on through CCA ligation. Each of the three brains which were the control group and HIE group were collected and tissues extracted from ipsilateral brain regions. Each brain tissues were profiled for 41,345 transcript genes. PPI, protein-protein interaction; TF, transcription factor; eQTL, expression quantitative trait loci; GWAS, genome-wide association study; CCA, common carotid artery; HIE, hypoxic-ischemic encephalopathy

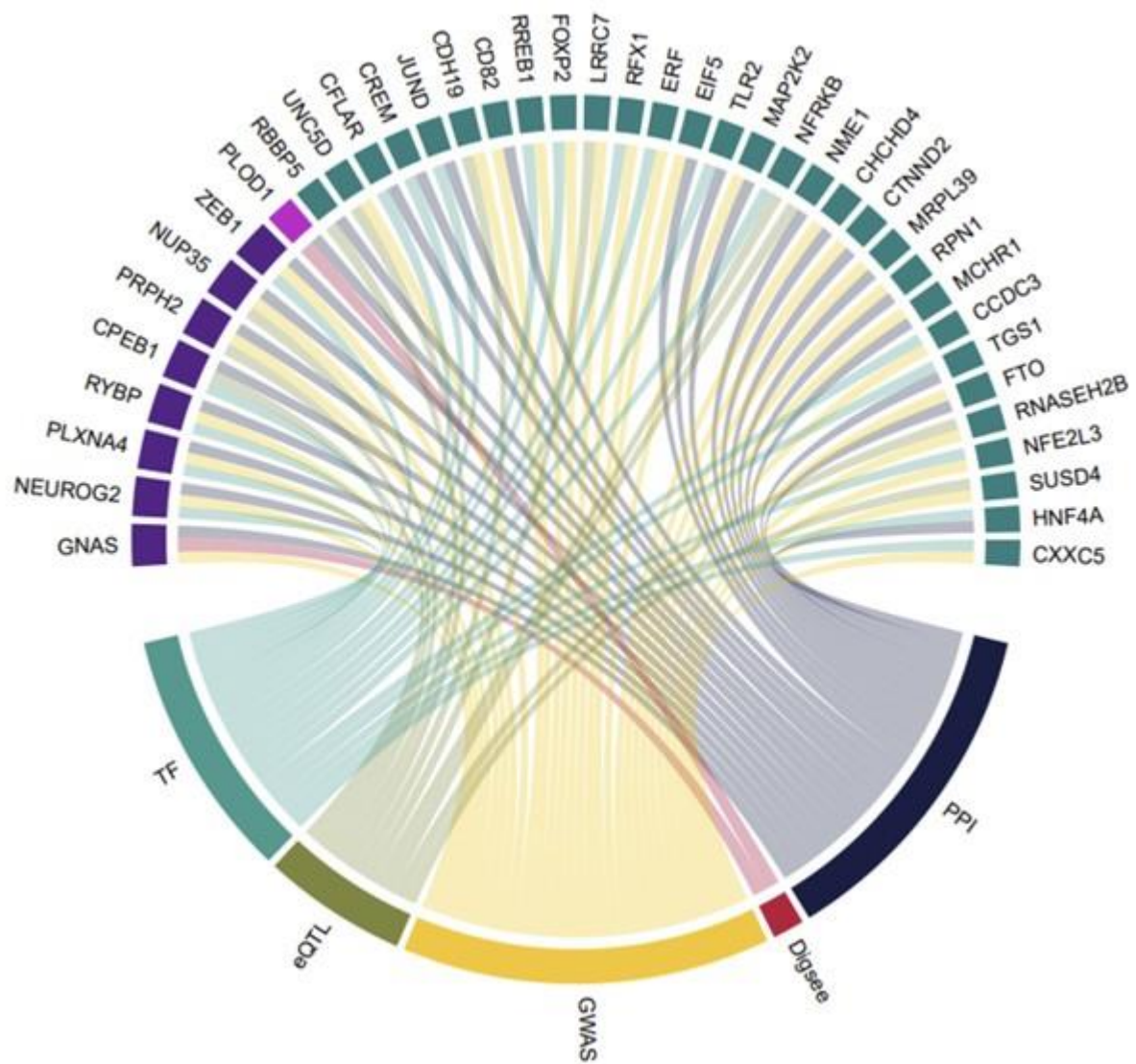


Figure 2. Identification of the upstream CP meta-genes based on the Bayes approach. Cells placed in the lower panel indicate the prior knowledge for screening the upstream genes, including the human TF catalog, brain eQTL database, CP-related SNPs, disease-gene database (Digsee), and protein interactome.

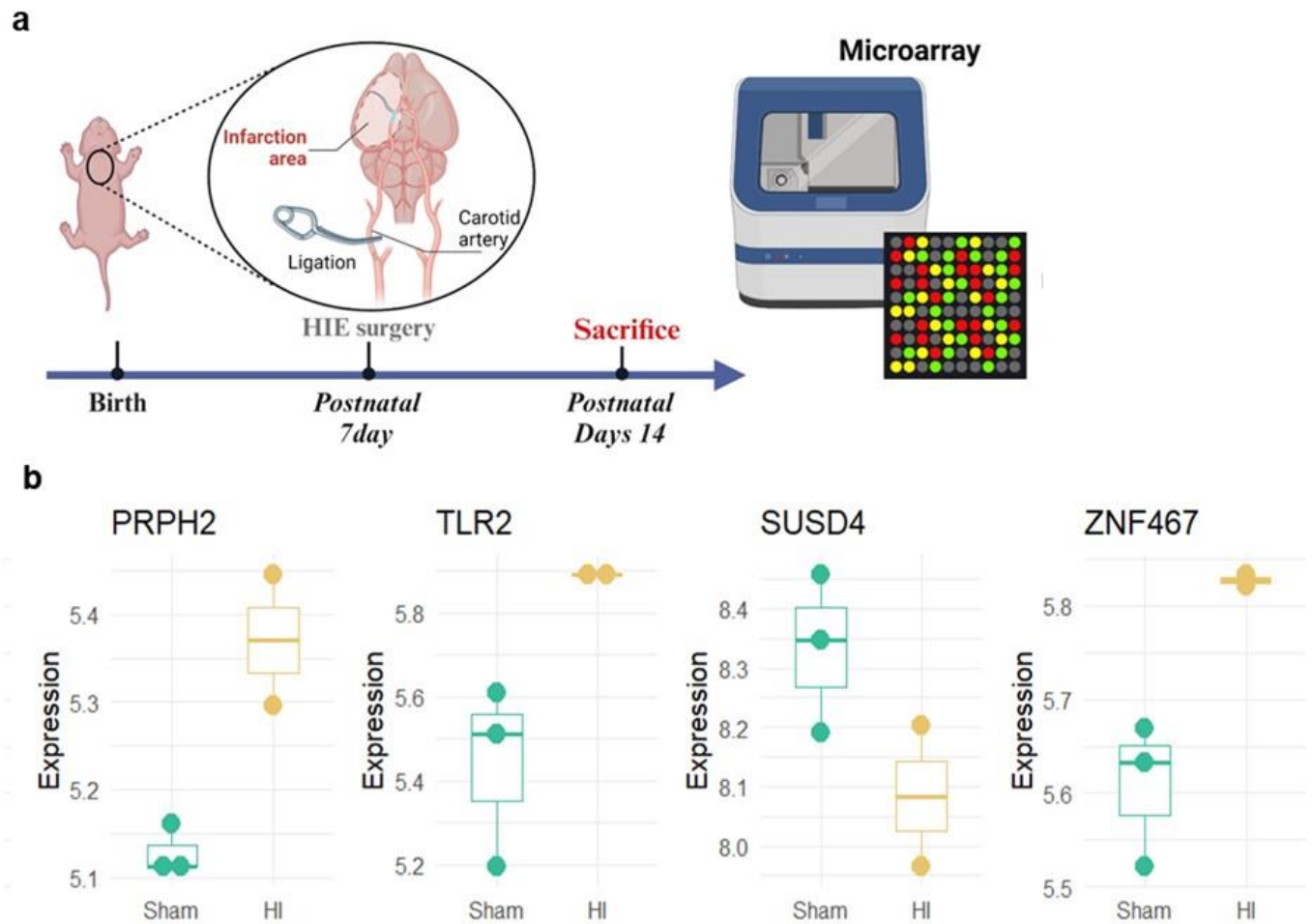


Figure 3. Final meta-gene identification incorporating public datasets with validation in an in vivo HIE model. (a) Present a method for establishing HIE model representing CP and an experimental design. (b) Expression patterns of final CP-related candidate genes verified in the HIE model

Rehabilitation Policy

발표일시 및 장소 : 10 월 25 일(금), 15:40 ~ 17:10 , Room A

OP-10

Why the elderly ceased to drive: A nationally representative cross-sectional study in South Korea

Jaehong Yoon^{1,2*}, Ga-In Shin^{1,2}, Yoonjeong Choi^{1,2}, Hyunji Lee³, Ja-Ho Leigh^{1,2,3†}

National Traffic Injury Rehabilitation Research Institute, National Traffic Injury Rehabilitation Hospital¹, Department of Rehabilitation Medicine, Seoul National University Hospital², Department of Rehabilitation Medicine, National Traffic Injury Rehabilitation Hospital³

Background

According to the aging population, the number of older with a driving license has increased. Although driving is necessary for mobility among the elderly, there might be a risk of driving for older people due to a lack of cognitive skills and physical ability. Previous studies about examining predictors for driving cessation among the elderly focused on physical and cognitive functions, not environmental elements. The comprehensive mobility framework was suggested to be aware of the complexity of factors that influence mobility.

Objective: This study aimed to investigate the predictors for driving cessation among the elderly based on a comprehensive framework and to examine the relative contribution of the predictors.

Methods

We analyzed 2,921 people who were 65 years or older and have driven from the 2020 National Survey of the Elderly. Driving cessation was defined as people who ceased driving after 65 years. According to comprehensive mobility framework, twenty-five variables in six domains (demographic factors, financial factors, psychosocial factors, physical factors, cognitive factors, and environmental factors) were considered as potential predictors for driving cessation. We used forward stepwise logistic regression to select the explanatory variables for final logistic regression. Furthermore, we estimated the relative contribution of explanatory variables for driving cessation across ages (early elderly: 65-74 years and late elderly: 75 years or more) by using dominance analysis.

Results

The results of stepwise regression reported that thirteen variables (age, education attainment, marriage, work, household income, perceived income level, social activities, depressive symptoms, contacts with children, muscle strength, MMSE, and accessibility to hospital and public transit) was selected predictors for final model and the area under the receiver operating characteristic curve of the final model was 86.3. For the early elderly, age most important variable that contributed to 36.5% of the explained variation in driving cessation followed by work (28.2%), household income (6.9%), depressive symptoms (6.8%), and social activities (5.7%). However, for the late elderly, in terms of their relative impact on driving cessation, the factors can be ranked in the following order: work (31.0%), perceived income (10.6%), accessibility to the hospital (8.4%), education attainment (7.9%), and contact children (7.5%). In dominance analysis for the domain, demographic factor, financial factor, and psychosocial factor contributed more than 10% of driving cessation among both the early and late elderly, additionally, environmental factor have an important role in the late elderly.

Conclusions

The results of this study imply that the provision of guaranteed non-driving transportation options can facilitate a reduction in driving risks among older adults by encouraging self-regulation of driving behavior while preserving their mobility.

Acknowledgment This research was supported by Technologies for Future-oriented National Citizen Security Services Program through the Korea Institutes of Police Technology (KIPoT) funded by the Korean National Police Agency (No. PR09-02-000-22).

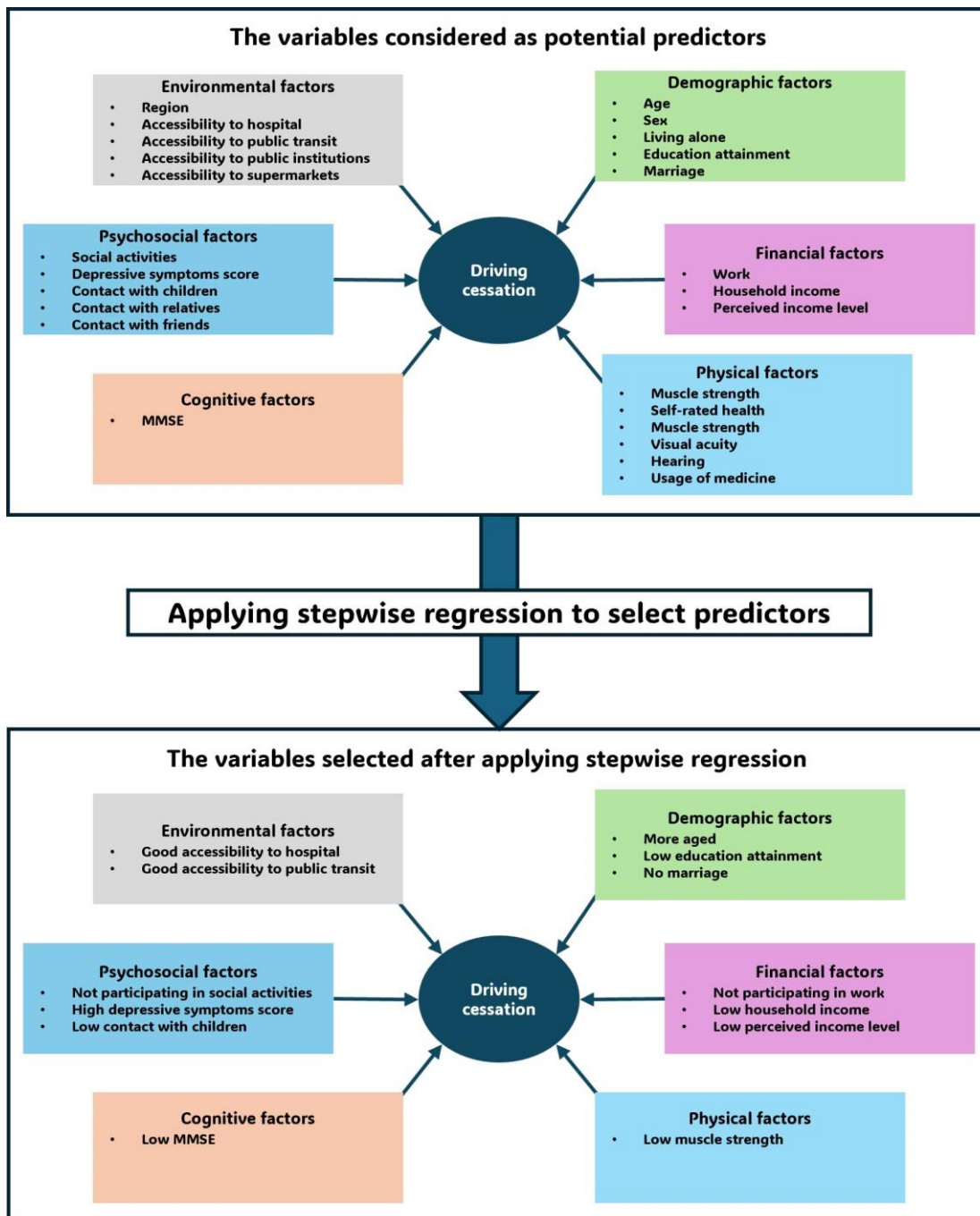


Figure 1. The potential predictors and selected predictors as final model

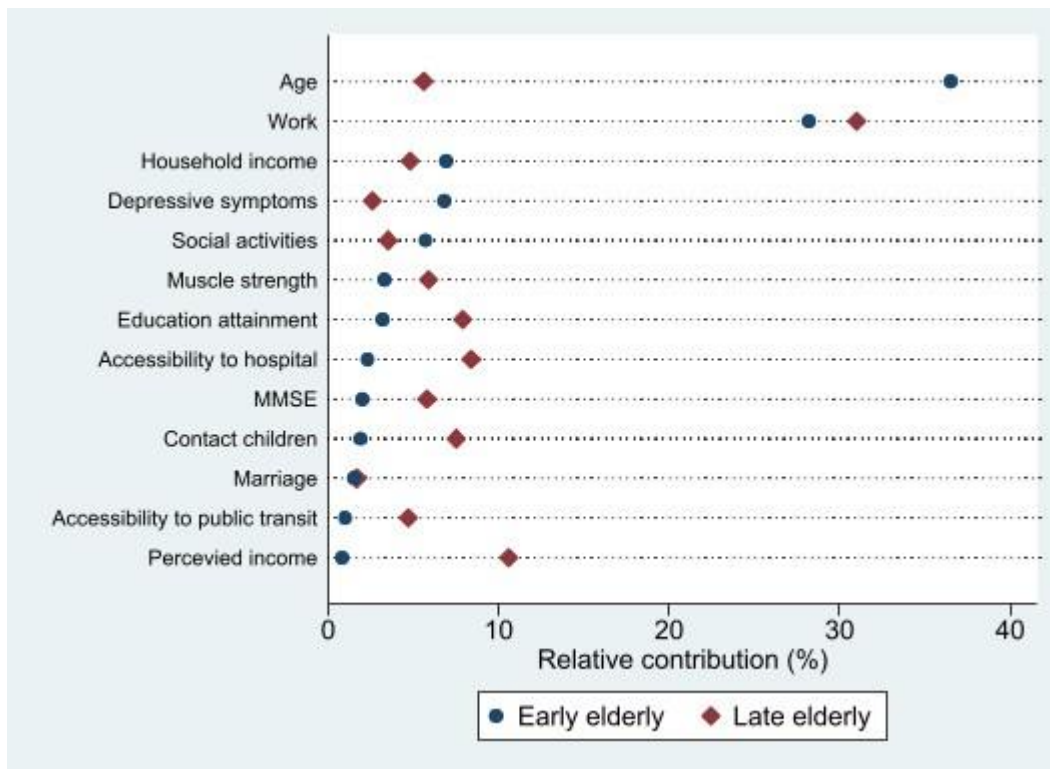


Figure 2. Relative contribution of each predictor associated with Driving Cessation

Early elderly			Late elderly		
Rank	Domain	Relative contribution (%)	Rank	Domain	Relative contribution (%)
1	Demographic factor	41.2	1	Financial factor	46.4
2	Financial factor	35.5	2	Demographic factor	15.0
3	Psychological factor	14.6	3	Psychological factor	13.6
4	physical factor	3.5	4	Environmental factor	13.1
5	Environmental factor	3.1	5	physical factor	6.0
6	Cognitive factor	2.2	6	Cognitive factor	6.0

Table 1. Relative contribution of domain associated with Driving Cessation

OP-11

Effect of left DLPFC electric field magnitude on tDCS-induced resting brain connectivity changes

Eunkyung Kim^{1,2*}, Seo Jung Yun^{1,3,4}, Byung-Mo Oh^{1,3,5}, Han Gil Seo^{1,3†}

Department of Rehabilitation Medicine, Seoul National University Hospital¹, Biomedical Research Institute, Seoul National University Hospital², Department of Rehabilitation Medicine, Seoul National University College of Medicine³, Department of Human Systems Medicine, Seoul National University College of Medicine⁴, Institute on Aging, Seoul National University⁵

Introduction

Although transcranial direct current stimulation (tDCS) is effective for modulating cortical activity, there is considerable variability in response and lack of understanding how resting state functional connectivity (rsFC) changes. This study aimed to investigate how variations in electrical field magnitude (E-field) applied to the target area of tDCS, which was the L-DLPFC, affect L-DLPFC-based rsFC changes in healthy adults.

Methods

A double-blind, sham-controlled, counterbalanced cross-over design was applied on 21 healthy individuals (37.6±8.6y). Participants received either constant 2 mA anodal or sham tDCS during 10 min (wash-out period; at least 3 d). The resting-state fMRI (3-T) was acquired before and after stimulation. The L-DLPFC was localized in each individual and E-field (V/m) was estimated. A spherical region of interest (ROI) surrounding individual peak of the L-DLPFC was generated to construct seed-based rsFC.

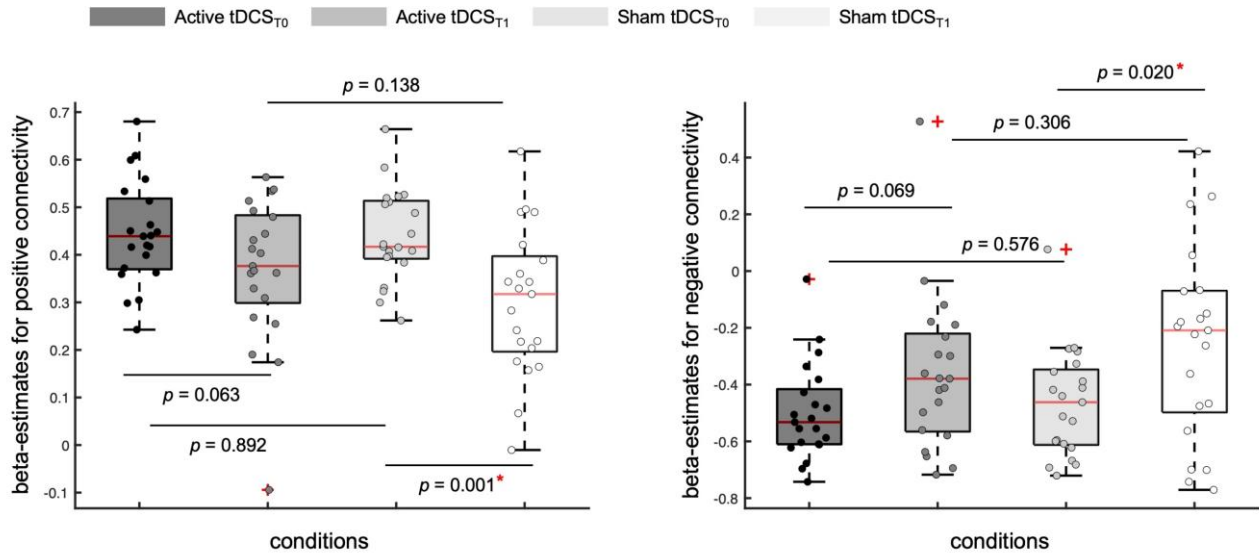
To examine alterations in overall L-DLPFC rsFC after active and sham tDCS, average beta-estimates for both positive and negative L-DLPFC rsFC were extracted from the subject-level regression coefficients (COPEs) images within each condition. Repeated measure of analysis of variance and paired-sample t-tests was conducted to test the significance of difference using MATLAB. To assess locally distributed L-DLPFC rsFC changes, mixed-effect analysis was conducted using FSL FLAME1, treating participants as random effects. Pairwise post-hoc comparison was also performed. The relationship between the E-field delivered to the L-DLPFC and changes in L-DLPFC rsFC was investigated. The positive connectivity map of active tDCST0 (cluster-extent based thresholding $z>3.1$, FWE p

Results

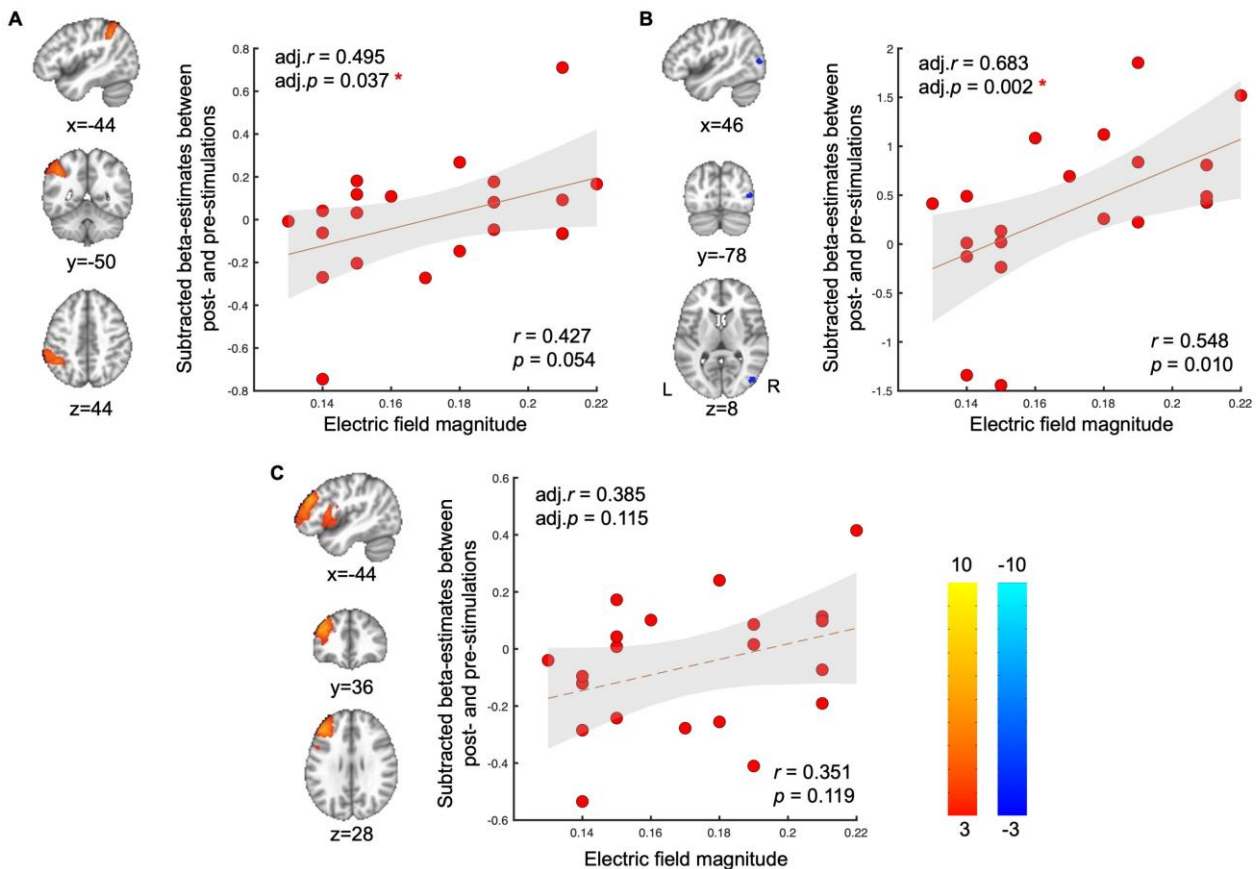
Overall rsFC significantly decreased after sham (positive and negative connectivity, $p = 0.001$ and 0.020 , respectively), with modest and non-significant changes after active tDCS ($p = 0.063$ and 0.069 , respectively)(Fig1). No significant differences in local rsFC were observed among the conditions. Correlations were observed between the E-field and rsFC changes in the L-DLPFC ($r = 0.385$), left inferior parietal area ($r = 0.495$), and right lateral visual area ($r = 0.684$)(Fig2).

Conclusions

TDCS may help to maintain overall rsFC while sham induced reduced rsFC. The impact of single-session active tDCS was subtle t **Acknowledgment** o change local connectivity of L-DLPFC. Nevertheless, E-field applied on the target area is associated with changes in rsFC, observed in proximal and distally connected brain regions with L-DLPFC.



Alterations in the overall L-DLPFC connectivity after active and sham tDCS. (A) Post hoc analyses results for positive connectivity and (B) negative connectivity. The X-axis of the box plots represent active tDCST0, active tDCST1, sham tDCST0, and sham tDCST1 from left to right. The Y-axis indicates beta estimates for the positive and negative connectivity in each case. L-DLPFC, left dorsolateral prefrontal cortex; tDCS, transcranial direct current stimulation.



The regions of interest demonstrating the relationship between the changes in the L-DLPFC connectivity after tDCS and electric field magnitude. (A) The left inferior parietal area, (B) right lateral visual area, and (C) left middle frontal area show correlations with the electric field magnitude ($|r| > 0.3$). The X-axis represents subtracted beta estimates between the active tDCST1 – active tDCST0, while the Y-axis represents the electric field magnitude. The r - and p -values at the bottom right of the regression line indicate the raw correlation, while the values above the regression line are the adjusted values, after adjusting for age, sex, and instances where subject incorrectly identified active tDCS as sham. L-DLPFC, left dorsolateral prefrontal cortex; tDCS, transcranial direct current stimulation.

A Predictive Algorithm for Aspiration Pneumonia in Post-Stroke Patients

Jong Weon Lee^{1,2*}, Hyun-Joung Lee³, Hyeon Ju Jang¹, Kyung-Min Kim^{1,2}, Deog Young Kim^{1,2†}

Research Institute of Rehabilitation Medicine, Yonsei University College of Medicine¹, Department of Rehabilitation Medicine, Yonsei University College of Medicine², Department of Speech-Language Pathology, Wonkwang Digital University³

Introduction

Aspiration pneumonia is one of critical complications following a stroke, with incidence estimated between 5% and 30%. Post-stroke pneumonia extends hospital stays, increases medical costs, and raises morbidity and mortality rates. Since defense mechanisms against aspiration are multifaceted, including protection during swallowing, cough reflexes, nutrition, and cognition, comprehensive evaluation is necessary to identify patients at risk. This study aims to determine an integrative algorithm predicting post-stroke pneumonia.

Methods

328 stroke patients with dysphagia symptoms were recruited at a single tertiary hospital from May 2019 to January 2024. Exclusion criteria included aspiration pneumonia, or those requiring oxygen due to dyspnea, IICP, and head and neck disorders at admission. Videofluoroscopic swallowing study (VFSS), a modified cough reflex test (mCRT), MMSE, baseline blood tests and neurologic exams were performed at admission. In the mCRT, capsaicin concentrations of 7.8uM and 31.25uM were administered via nebulizer for 15 seconds, with cough frequency and peak cough flow measured over the subsequent 30 seconds. Patients were followed for four weeks, and the incidence of pneumonia, based on the Mann criteria, was recorded. Classification and regression tree (CART) analysis was used to identify factors predicting pneumonia.

Results

28 patients (8.5%) were diagnosed with pneumonia. Pneumonia group had significantly lower MMSE scores, a higher proportion of tracheostomy and Penetration-Aspiration Scale (PAS) higher than 6 in VFSS, lower cough frequency in both 7.8uM and 31.25uM mCRT, and lower albumin levels compared to non-pneumonia group (p<0.05). Factors associated with pneumonia in the logistic regression analysis were included in the CART analysis, which accurately predicted pneumonia in 90.12% of stroke patients with an AUC of 0.885 (95% CI 0.815-0.955) (Figure 1). For patients without tracheostomy, 1.35% incidence of pneumonia was detected if PAS was lower than 6. If PAS was 6 or higher, an albumin level below 3.5g/dL indicated 62.50% risk of pneumonia, while an albumin level of 3.5g/dL or higher indicated 10.0% risk. For patients with tracheostomy, none developed pneumonia if the cough frequency at 7.8uM mCRT was 3 or higher. If the cough frequency was below 3, an MMSE score below 6 indicated 50% risk of pneumonia, while an MMSE of 6 or higher indicated 18.75% risk.

Conclusion

This novel algorithm could accurately predict the incidence of pneumonia in post-stroke patients. Assessments with VFSS, mCRT, MMSE and albumin may help identify the risk of aspiration pneumonia in stroke, allowing for early preventive interventions.

Acknowledgment The authors declare that they have no competing interest.

Table 1. Baseline characteristics of the study population.

	Total (n=328)	Pneumonia (+) (n=28)	Pneumonia (-) (n=300)	p
Age	63.4 ± 14.4	67.5 ± 12.1	63.0 ± 14.6	0.120
Women	133 (40.5%)	8 (28.6%)	125 (41.7%)	0.251
MMSE	17.5 ± 10.6	8.2 ± 9.4	18.4 ± 10.3	<0.001
Tracheostomy status	48 (14.6%)	15 (53.6%)	33 (11.0%)	<0.001
Death	1 (0.3%)	1 (3.6%)	0 (0.0%)	0.137
Involved hemisphere				<0.001
Hemi side	240 (73.2%)	10 (35.7%)	230 (76.7%)	
Both sides	88 (26.8%)	18 (64.3%)	70 (23.3%)	
Stroke type				0.627
Ischemic	183 (55.8%)	16 (57.1%)	167 (55.7%)	
Hemorrhagic	140 (42.7%)	11 (39.3%)	129 (43.0%)	
Both	5 (1.5%)	1 (3.6%)	4 (1.3%)	
Tentorial region				0.240
Supratentorial	261 (79.6%)	20 (71.4%)	241 (80.3%)	
Infratentorial	52 (15.9%)	5 (17.9%)	47 (15.7%)	
Both	15 (4.6%)	3 (10.7%)	12 (4.0%)	
VFSS PAS ≥ 6	90 (27.6%)	20 (71.4%)	70 (23.5%)	<0.001
Cough reflex test				
Frequency @7.8μM	4.1 ± 4.5	1.6 ± 2.5	4.3 ± 4.6	<0.001
PCF@7.8μM (L/min)	56.9 ± 105.0	43.1 ± 105.8	58.2 ± 105.0	0.467
Frequency @31.25M	6.0 ± 5.6	2.7 ± 3.6	6.3 ± 5.7	<0.001
PCF@31.25μM (L/min)	78.9 ± 127.8	45.0 ± 74.4	82.0 ± 131.3	0.028
O ₂ saturation (%)	97.9 ± 1.4	97.5 ± 1.7	98.0 ± 1.4	0.096
WBC (x10 ³ /μL)	7.2 ± 2.1	7.4 ± 1.5	7.2 ± 2.2	0.406
Neutrophil (x10 ³ /μL)	4.7 ± 1.9	5.0 ± 1.3	4.7 ± 1.9	0.175
Lymphocyte (x10 ³ /μL)	1.7 ± 0.6	1.5 ± 0.4	1.7 ± 0.6	0.004
NLR	3.2 ± 2.1	3.8 ± 1.9	3.2 ± 2.1	0.160
CRP (mg/L)	8.1 ± 15.1	13.1 ± 11.4	7.6 ± 15.3	0.062
Albumin (g/dL)	4.0 ± 0.4	3.6 ± 0.4	4.0 ± 0.4	<0.001

MMSE, mini-mental state examination; VFSS, videofluoroscopic swallow study; PAS, penetration-aspiration scale; PCF, peak cough flow (L/min); O₂, oxygen; WBC, white blood cell; NLR, neutrophil-to-lymphocyte ratio; CRP, C-reactive protein.

Table 1. Baseline characteristics of the study population.

Table 2. Risk factors associated with post-stroke pneumonia: univariate logistic regression analysis.

	Univariable analysis	
	OR (95% CI)	p value
Age	1.024 (0.994-1.055)	0.122
Sex		
Men	referent	
Women	0.560 (0.239-1.312)	0.182
MMSE	0.913 (0.875-0.949)	<0.001
Tracheostomy		
(-)	referent	
(+)	9.336 (4.096-21.648)	<0.001
Involved hemisphere		
Hemi side	referent	
Both	5.914 (2.658-13.881)	<0.001
Stroke type		
Ischemic	referent	
Hemorrhagic	0.890 (0.399-1.983)	0.776
Both	2.609 (0.275-24.770)	0.404
Tentorial region		
Supratentorial	referent	
Infratentorial	1.282 (0.458-3.586)	0.636
Both	3.012 (0.785-11.561)	0.108
VFSS PAS		
<6	referent	
≥6	8.214 (3.587-20.587)	<0.001
Cough frequency @7.8μM	0.795 (0.681-0.929)	0.004
PCF @7.8μM (L/min)	0.998 (0.993-1.003)	0.468
Cough frequency @31.25μM	0.520 (0.766-0.947)	0.003
PCF @31.25μM (L/min)	0.995 (0.989-1.001)	0.135
O₂ saturation	0.835 (0.672-1.038)	0.104
WBC (10³/μL)	1.056 (0.879-1.241)	0.534
Neutrophil (10³/μL)	1.101 (0.901-1.313)	0.307
Lymphocyte (10³/μL)	0.999 (0.999-1.000)	0.050
NLR	1.109 (0.943-1.275)	0.166
CRP (mg/L)	1.015 (0.995-1.035)	0.101
Albumin (g/dL)	0.069 (0.024-0.198)	<0.001

MMSE, mini-mental state examination; VFSS, videofluoroscopic swallow study; PAS,

penetration-aspiration scale; PCF, peak cough flow; O₂, oxygen; WBC, white blood cell; NLR,

neutrophil-to-lymphocyte ratio; CRP, C-reactive protein.

Table 2. Risk factors associated with post-stroke pneumonia: univariate logistic regression analysis.

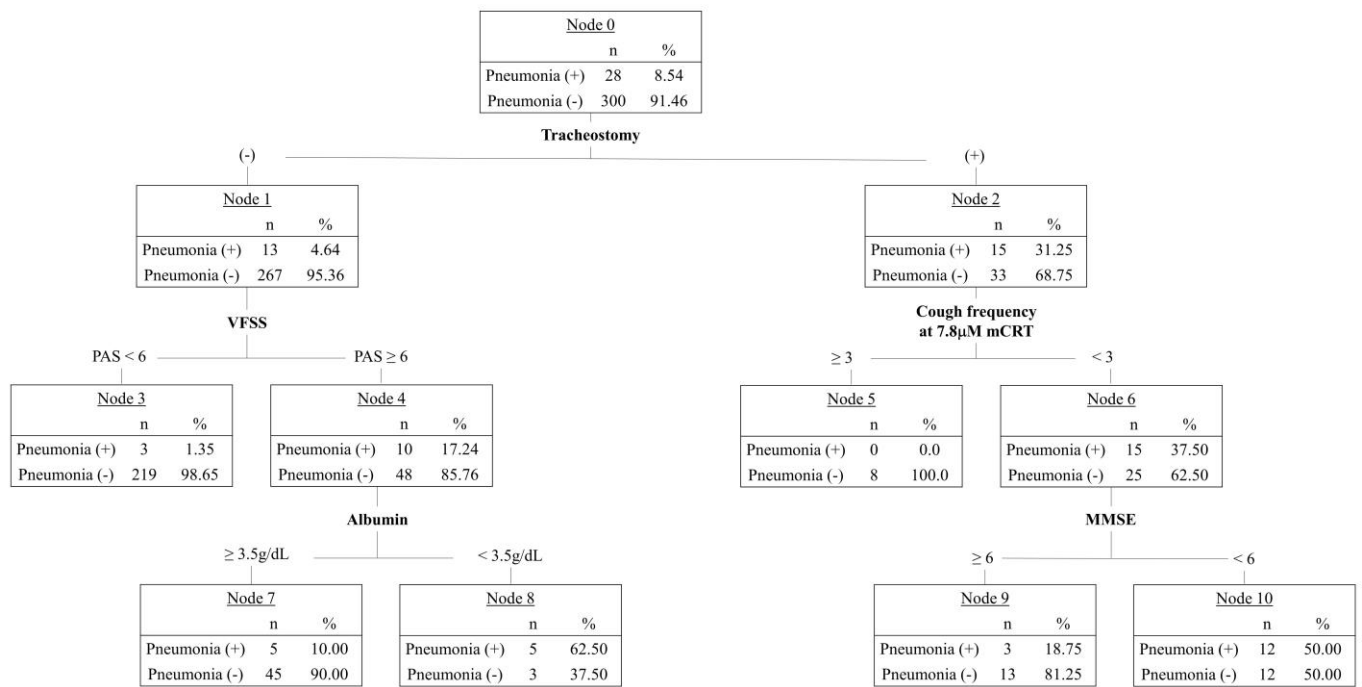


Figure 1. Classification and regression tree (CART) analysis identified factors that predict post-stroke pneumonia.

Effects of Robot-assisted Therapy for Upper Limb Rehabilitation After Stroke: An Umbrella Review

Jong Mi Park^{1*}, Hee Jae Park², Gyu Jin Kim¹, Seo Yeon Yoon², Yong Wook Kim², Jae Il Shin^{3†}, Sang Chul Lee^{2†}

Department of Physical Medicine and Rehabilitation, Hallym University Sacred Heart Hospital, Hallym University College of Medicine, Anyang, Republic of Korea¹, Department and Research Institute of Rehabilitation Medicine, Yonsei University College of Medicine, Seoul, Republic of Korea², Department of Pediatrics, Yonsei University College of Medicine, Seoul, Republic of Korea³

INTRODUCTION

Stroke is a leading cause of disability worldwide, often resulting in hemiplegia or quadriplegia, particularly affecting upper limb function. Recovery from severe upper limb paralysis post-stroke is limited, with only 14% achieving full recovery and 30% partial recovery, significantly impacting daily activities and return to work. Neuroplasticity, the brain's ability to reorganize itself, forms the theoretical basis for rehabilitation. High-dose, intensive, repetitive training is effective in inducing neuroplasticity. Traditional stroke rehabilitation is effective but inefficient, as it requires significant therapist involvement. Robotic rehabilitation therapy offers a promising alternative, delivering high-intensity, high-frequency treatments with real-time progress monitoring and feedback, thereby enhancing neuroplasticity. This study aimed to provide a comprehensive review of meta-analyses on the efficacy of upper extremity robotic rehabilitation therapy in stroke patients.

METHOD

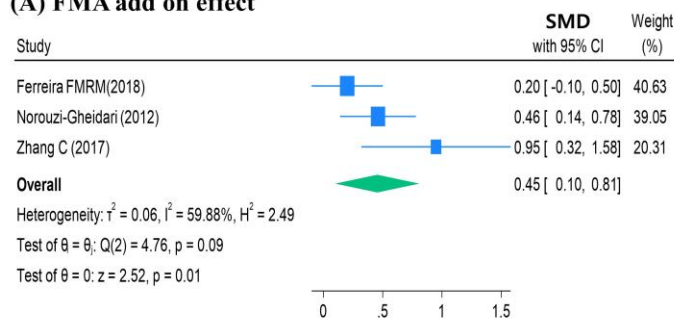
This umbrella review followed PRISMA 2020 guidelines and was registered with PROSPERO (CRD42023465547). A systematic search was conducted across PubMed/MEDLINE, EMBASE, Cochrane, Scopus, and Web of Science from on June 14, 2024. Outcomes focused on clinical efficacy assessed via Fugl-Meyer Assessment, muscle strength, spasticity, and activities of daily living. Meta-analysis was conducted by pooling results from unduplicated individual Randomized controlled trials, using standardized mean differences and 95% confidence intervals. A restricted maximum likelihood random effects model was used due to expected heterogeneity. Subgroup analyses were performed based on robot type, treatment duration, and stroke onset.

RESULTS

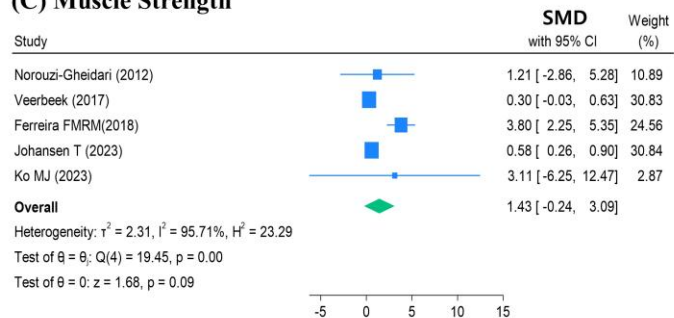
Overall, 16 meta-analyses encompassing 199 individual studies and 19,251 patients were included. The additional effect of robot therapy for Fugl-Meyer assessment was summarized pooled standardized mean differences (SMD) of 0.45 (95% confidence interval, 0.10 - 0.81). Summarized pooled SMD of activities of daily living was 0.29 (0.06 - 0.52). Muscle strength SMD was 1.43 (-0.24 - 3.09). Spasticity SMD was -0.07 (-0.22 - 0.09). In subgroup analysis, the SMD for acute and subacute stroke, chronic stroke, end-effector robot, exoskeleton robot, and unilateral robot were 0.46 (0.19- 0.73). 0.36 (0.20- 0.52), 0.23 (0.09-0.38), 0.39 (0.07-0.71), and 0.32 (0.15-0.50) respectively.

CONCLUSION

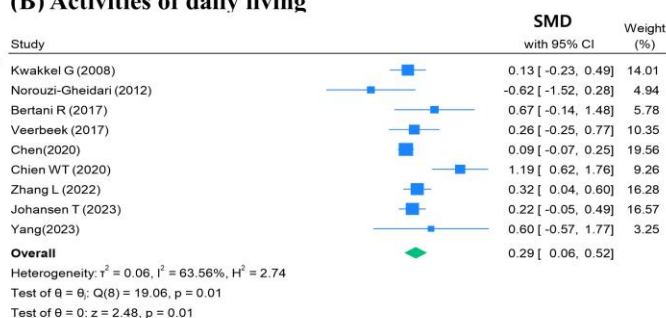
Robot-assisted therapy significantly improves motor function recovery and ADL compared to conventional therapy but does not show significant benefits in muscle strength or spasticity. These improvements are consistent across different stages of stroke and types of robotic devices. The study underscores the potential of robotic therapy as a valuable intervention for stroke rehabilitation. Future research should aim at optimizing robot types and training programs tailored to specific patient characteristics to establish more effective clinical protocols.

(A) FMA add on effect

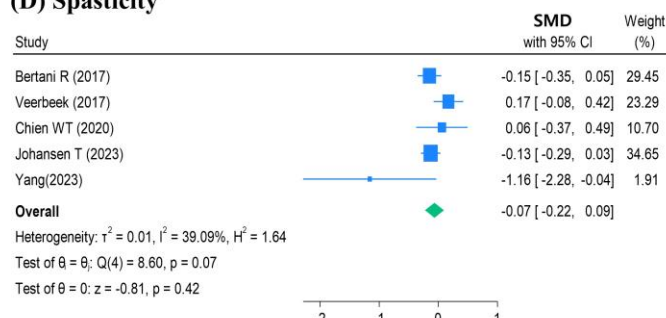
Random-effects REML model

(C) Muscle Strength

Random-effects REML model

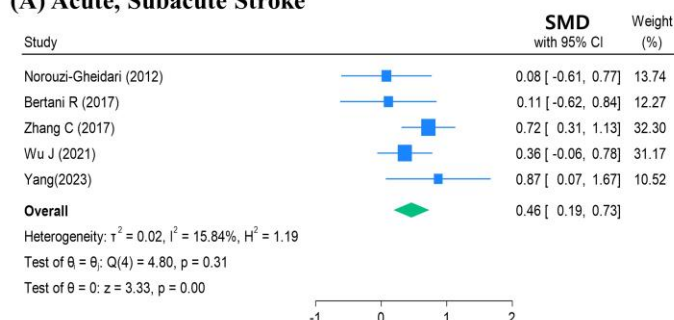
(B) Activities of daily living

Random-effects REML model

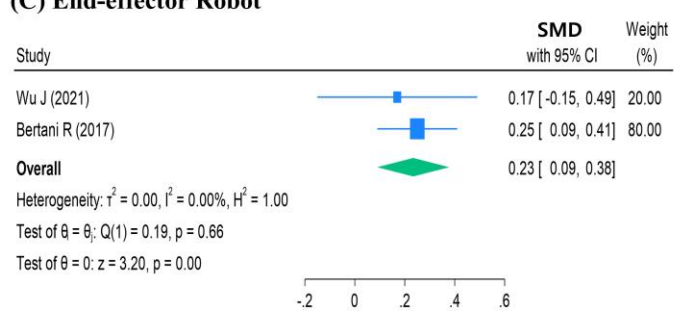
(D) Spasticity

Random-effects REML model

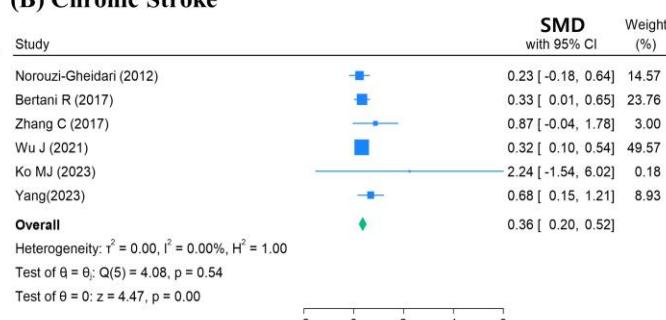
Figure 1. Meta-analysis of the effects of robot-assisted versus conventional therapy in stroke patients (A) Add-on effect in FMA (B) Activities of daily living (C) Muscle strength (D) Spasticity FMA, Fugl–Meyer assessment

(A) Acute, Subacute Stroke

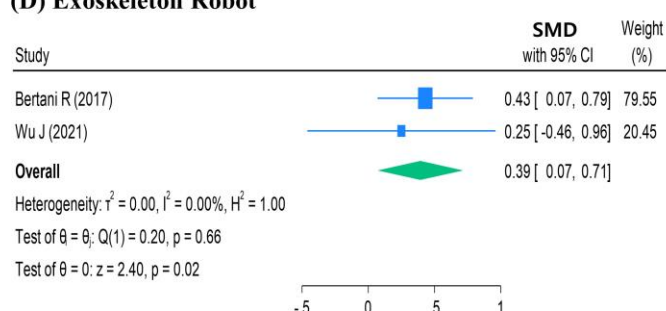
Random-effects REML model

(C) End-effector Robot

Random-effects REML model

(B) Chronic Stroke

Random-effects REML model

(D) Exoskeleton Robot

Random-effects REML model

Figure 2. Subgroup analysis of the effects of robot-assisted versus conventional therapy on FMA (A) Acute, subacute stroke (B) Chronic stroke (C) End-effector robot (D) Exoskeleton robot FMA, Fugl–Meyer assessment

Table 1. Summary of umbrella meta-analysis outcomes.

Outcome	Categories	Re-Analyzed Number of Studies	Re-Analyzed SMD (95% CI)	<i>P</i> value	I ² Statistic	Egger <i>P</i> -value
FMA	RT vs CT	99	0.59 (-0.19, 1.37)	0.14	96.08%	0.392
	Add on RT n vs CT	15	0.45 (0.10, 0.81)	0.01	59.88%	0.297
	Acute, Subacute Stroke	22	0.46 (0.19, 0.73)	<0.001	15.84%	0.628
		45	0.36 (0.20, 0.52)	<0.001	0.00%	0.055
	End-effector Robot	42	0.23 (0.09, 0.38)	<0.001	0.00%	N/A
		10	0.39 (0.07, 0.71)	0.02	0.00%	N/A
	Unilateral	33	0.32 (0.15, 0.50)	<0.001	55.92%	0.018
		14	0.07 (-0.15, 0.28)	0.54	0.00%	0.725
	Bilateral	11	3.60 (-1.75, 8.95)	0.19	92.34%	N/A
		20	2.74 (-1.84, 7.32)	0.24	99.45%	0.170
	Intervention ≤ 4 weeks	28	1.19 (-0.85, 3.24)	0.25	80.17%	N/A
		17	3.06 (-3.14, 9.25)	0.33	89.87%	N/A
ADL	Proximal Training	55	0.29 (0.06, 0.52)	0.01	63.56%	0.299
	Distal Training	30	1.43 (-0.24, 3.09)	0.09	95.71%	0.281
Muscle Strength		30	1.43 (-0.24, 3.09)	0.09	95.71%	0.281
Spasticity		30	-0.07 (-0.22, 0.09)	0.42	39.09%	0.703

CI, confidence interval; FMA, Fugl-Meyer Assessment; RT, Robot-assisted therapy; CT, conventional therapy; ADL, Activities of daily living

Table 1. Summary of umbrella meta-analysis outcomes.

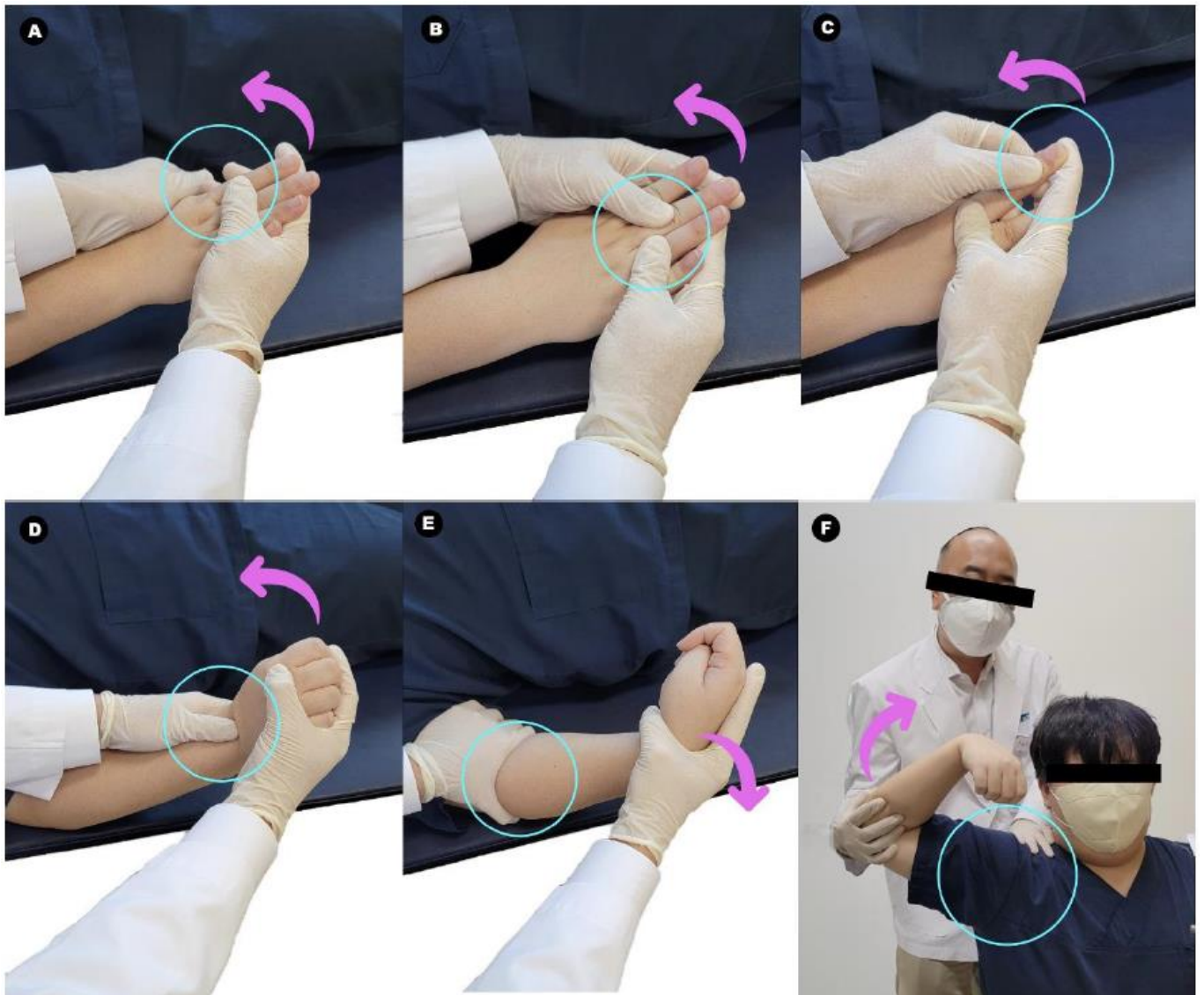
Enhancement of Botulinum Toxin Injections for Post-Stroke Spasticity by Stretching Exercises

Min-Su Kim^{1*†}, In-Su Hwang¹, Jin-Whan Ryu¹, Sol Jin¹, Soo-A Kim¹

Department of Rehabilitation Medicine, Soonchunhyang University Cheonan Hospital¹

Botulinum toxin A (BTX-A) injections play a central role in the treatment of upper limb spasticity in stroke patients. In this study, we proposed structured stretching exercises to enhance the effect of post-stroke spasticity relief of the upper limbs following BTX-A injections. This study aimed to investigate whether these structured stretching exercises plus BTX-A injections can further enhance the long-term effect of BTX-A injections in ameliorating upper limb spasticity after stroke. A total of 43 stroke patients with spasticity of grade 2 or higher on the Modified Ashworth Scale (MAS) in the upper limb muscles were randomly assigned to the intervention group (n=21) or control group (n=22). At predetermined doses, 300 U of BTX-A was injected intramuscularly into the upper limb muscles using electromyography. Patients in the intervention group received assistance with structured stretching exercises after their BTX-A injections for 20 minutes, 5 days per week, for 6 months at the hospital. The patients in the control group conducted self-stretching exercises at home after their BTX-A injections for the same period of time as the patients in the intervention group. The primary outcome measure was the MAS scores of the upper limbs, which were assessed three times: before the intervention (T0), after three months (T1), and after six months (T2). The secondary outcome measures encompassed post-stroke shoulder pain, functional activities of independent daily living, motor function, health-related quality of life, and electromyographic analysis. Significant time and group interaction effects on the modified MAS scores of the elbows, wrists, and fingers were found ($p=0.032$, $p=0.024$, and $p=0.016$, respectively). A between-group analysis showed a significant difference between the groups concerning the change in the modified MAS scores of the elbows, wrists, and fingers at T1 and T2. Similar significant time and group interaction effects were shown on the visual analog scale (VAS) of shoulder pain, the Korean version of the Modified Barthel Index (K-MBI), the EuroQol-5D (EQ-5D), and the root mean square (RMS) index. A post hoc analysis revealed that the patients in the intervention group showed significantly superior improvements in their VAS, K-MBI, EQ-5D, and RMS index scores than those in the control group at T1 and T2. In conclusion, The structured stretching exercises plus BTX-A injections for six months showed a superior effect in relieving post-stroke upper limb spasticity compared to self-stretching exercises plus BTX-A injections and are expected to be helpful in clinical practice for stroke patients with upper limb spasticity scheduled to receive BTX-A injections.

Acknowledgment This research was supported by a grant of the National Research Foundation of Korea (NRF) funded by the Ministry of Education (NRF-2021R1I1A3060949).

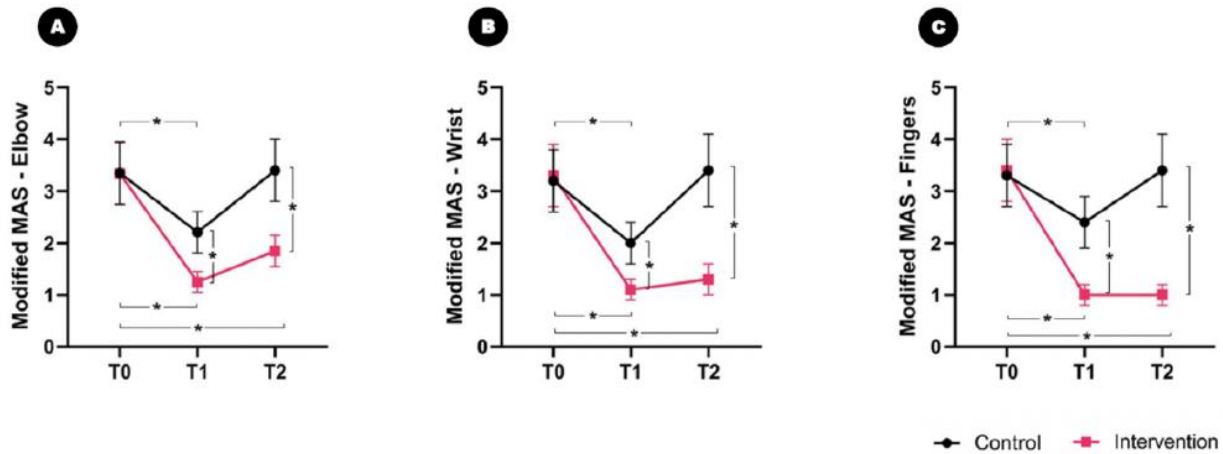


Structured stretching exercises after botulinum toxin A (BONT/A) injection. (Blue circle: Target joints. Pink arrow: Directions for stretching.) The patient is assisted in performing stretching exercises immediately after their BONT/A injections while lying down. Starting with the finger joints, each joint is slowly stretched at a low intensity in the opposite direction of the bend. When the patient reaches the maximum angle at which the pain is tolerable, the position is held for 2 s, and then the muscle is relaxed. Each upper-limb muscle is stretched individually to avoid pain. The physiatrist holds the patient's scapular in place. Then, by slowly rotating the shoulder, the shoulder girdle muscles are stretched clockwise or counterclockwise to an angle that the patient can tolerate. (A) Metacarpophalangeal joint; (B) proximal interphalangeal joint; (C) distal interphalangeal joint; (D) wrist joint; (E) elbow joint; and (F) shoulder joint.

Muscles (BONT/A, UI)	This Study	AbbVie Website	Allergan Delphi Panel
Biceps brachii (BB)	90	60–200	0–50
Brachioradialis (BR)	45	45–75	25–50
Flexor carpi radialis (FCR)	30	12.5–50	50–75
Flexor carpi ulnaris (FCU)	30	12.5–50	25–50
Flexor digitorum superficialis (FDS)	45	30–50	20–60
Flexor digitorum profundus (FDP)	60	30–50	25–75

BONT/A, Botulinum toxin A.

Sites and doses of botulinum toxin A injection.



Comparison of the Modified Ashworth Scale (MAS) scores between the intervention group and the control group over time. Significant time and group interaction effects are found in the modified MAS scores of the elbows, wrists, and fingers. In the between-group comparison, the spasticity relief effect of BONT/A continues until the 6-month time point (T2) in the intervention group of patients. In contrast, the anti-spastic effect of BONT/A is almost lost at 6 months in the control patients. (A) Elbow; (B) wrist; and (C) fingers. * $p < 0.05$.

OP-15

Brachial plexopathy from the perineural spread of malignancies: single-center experience

Yu Jin Im^{1*}, Duk Hyun Sung^{1†}

Department of Physical and Rehabilitation Medicine, Samsung Medical Center, Sungkyunkwan University School of Medicine¹

Introduction

In neuromuscular medicine clinics, it is crucial to differentiate the etiology, distinguishing malignant brachial plexopathy (BP) from other non-malignant causes of BP in patients with a history of cancer. One possible mechanism for the development of malignant BP is the perineural spread (PNS) of malignancy to the brachial plexus. However, there is a paucity of literature on the clinical and neuroradiological aspects of PNS of solid tumors to the brachial plexus. In this study, we aimed to describe the clinical and imaging characteristics of patients with PNS of malignant solid tumors to the brachial plexus.

Method

We retrospectively analyzed the database of neuromuscular clinic and electromyography laboratory from January 2009 to June 2024. Patients with a diagnostic code of both brachial plexus disorder and non-hematologic malignant neoplasm were selected. Patients who met all four brachial plexus MRI criteria were considered to have BP due to PNS of malignancy: 1) enlargement of the brachial plexus on T1-weighted image, 2) increased signal intensity of the brachial plexus on T2-weighted image, 3) enhancement of the brachial plexus, and 4) absence of encasement or external neural compression by a tumor mass.

Results

A total of eight patients with PNS to the brachial plexus were identified. The mean age at diagnosis of BP was 50.3 years (Table 1). All patients initially experienced pain or paresthesia in the affected nerve territory, followed by weakness. The mean time interval from cancer diagnosis to BP symptom onset was 87.9 months. Four patients were in complete remission before BP symptoms began. The most predominant pattern in electrodiagnostic studies was lower trunk plexopathy. Brachial plexus MRI demonstrated extensive T2 hyperintensity and diffuse tubular enlargement in most patients. However, enhancement was predominantly observed in the cervical spinal nerve root and trunk levels, corresponding with increased uptake on F18 fluorodeoxyglucose (FDG) positron emission tomography/computed tomography (PET/CT) scans. Cancer progression was noted in all patients during the diagnostic work-up. The neurological state of seven patients deteriorated, with further intradural extension observed in four patients. Six of eight patients died, with mean survival from PNS diagnosis to death being 27.0 months.

Conclusion

Irrespective of the cancer state, PNS to the brachial plexus should be considered in patients with a history of cancer, particularly those presenting with persistent upper extremity pain or paresthesia followed by motor weakness in the lower cervical myotomes. A comprehensive diagnostic evaluation, including brachial plexus MRI and PET/CT, is essential to ascertain the extent of PNS and any associated cancer progression. Locoregional therapies, such as radiation therapy, may provide pain relief; however, the overall prognosis for patients with PNS is generally poor.

Table 1. Clinical characteristics of patients with PNS of malignancies to the brachial plexus

No	Age /Sex	Primary cancer (Organ / Side)	Clinical presentation of PNS ^a					Interval between cancer diagnosis and onset of symptom (months)	Further treatment for PNS	Survival after diagnosis of PNS (months)
			Side	Pain	Paresthesia	Numbness	Motor weakness ^b			
1	58/F	Breast/Rt	Rt	2 (scapula)	1 (4-5 th finger)		3 (C8, T1*)	84	RTx, CTx	56
2	55/M	Lung/Lt	Rt	2 (scapula, medial forearm)		1 (4-5 th finger)	3 (C7, C8*, T1)	12	OP, CTx	5
3	39/F	Breast/Lt	Lt	2 (scapula)	1 (4-5 th finger, medial forearm)	1 (4-5 th finger, medial forearm)	3 (C8*, T1*)	42	RTx, CTx	Alive (17)
4	37/F	Breast/Rt	Rt	1 (scapula)	2 (hand)		3 (C5*, C6*, C7, C8)	9	RTx	4
5	50/F	Thyroid / Lt	Rt	1 (scapula, axilla, posterior arm)	2 (4-5 th finger)		3 (C8*, T1*)	206	RTx	20
6	50/F	Breast / Rt	Rt		1 (hand)		2 (C8, T1*)	143	RTx, HTx, CTx	Alive (94)
7	50/F	Breast / Rt	Rt	2 (scapula, deltoid)	1 (thumb, 5 th finger)		3 (C5*, C6*, C7*, C8*, T1)	136	RTx, CTx	59
8	63/F	Lung / Rt	Rt	1 (scapula, forearm)	2 (palm)		2 (C8*, T1)	71	RTx, CTx	18

Abbreviations: PNS, perineural spread; F, female; M, male; Rt, right; Lt, left; RTx, radiation therapy; CTx, chemotherapy; OP, operation

^aNumber indicates the chronological order of occurrence of each symptom^bMost affected myotome is indicated by asterisk**Table 1.** Clinical characteristics of patients with PNS of malignancies to the brachial plexus**Table 2.** Diagnostic test findings of patients with PNS of malignancies to the brachial plexus

No	EDX finding	Initial brachial plexus MRI			¹⁸ F-FDG PET/CT		Biopsy	Newly detected cancer progression during diagnostic work-up for PNS	Interval ^a (months)
		Nerve thickening	Neural structure with enhancement	Intradural extension	Affected nervous structure (SUVmax)	Increased uptake pattern			
1	Lower trunk plexopathy	Diffuse tubular	C7, C8 distal root, lower trunk, medial cord	(-)	C8 distal root, lower trunk (2.8)	Linear with skip lesion	NT	LNM (Rt axillary, Rt interpectoral), DM (Lt lung)	9
2	Lower trunk plexopathy	Nodular	C7, C8 root, lower trunk, medial cord	(+) C6-8, T5	C8 root (9.4)	Single dot-like spot	(+) Intradural mass, C8 root	LNM (Rt lower cervical)	12
3	Lower trunk plexopathy	Diffuse tubular	C8 root, lower trunk	(-)	C8 root	Single spot	NT	DM (Rt lung, Lt 1 st rib)	40
4	Pan-plexopathy	Diffuse tubular	C5, C6, C7, C8, T1 root, whole trunk	(-)	NT	NT	NT	LNM (both internal mammary), DM (bilateral rib)	3
5	Lower cervical radiculoplexopathy	Diffuse tubular	C8, T1 root	(-)	C5, C6, C7 root (4.4)	Multiple dot-like spots	NT	LNM (Rt lower cervical, Rt. mediastinal)	4
6	Medial cord plexopathy and median neuropathy	Diffuse tubular	Lower trunk, medial cord,	(-)	Medial cord (2.6)	Linear with skip lesion	NT	Recurrent tumor at Rt chest wall	4
7	Pan-plexopathy	Diffuse tubular	C5, C6 root, upper trunk	(-)	NT	NT	NT	LNM (Rt lower cervical)	7
8	Lower trunk plexopathy	Diffuse tubular	C7, C8, T1 root	(-)	C7, C8 T1 root	Multiple dot-like spots	NT	LNM (Rt lower cervical, bilateral supraclavicular)	8

Abbreviations: PNS, perineural spread; EDX, electrodiagnostic study; MRI, magnetic resonance imaging; FDG, fluorodeoxyglucose; PET, positron emission tomography; CT, computed tomography; SUVmax, maximum standard uptake value; Rt, right; Lt, left; LNM, lymph node metastasis; DM, distant metastasis; NT, not tested

^aInterval between symptom onset and diagnosis of perineural spread**Table 2.** Diagnostic test findings of patients with PNS of malignancies to the brachial plexus

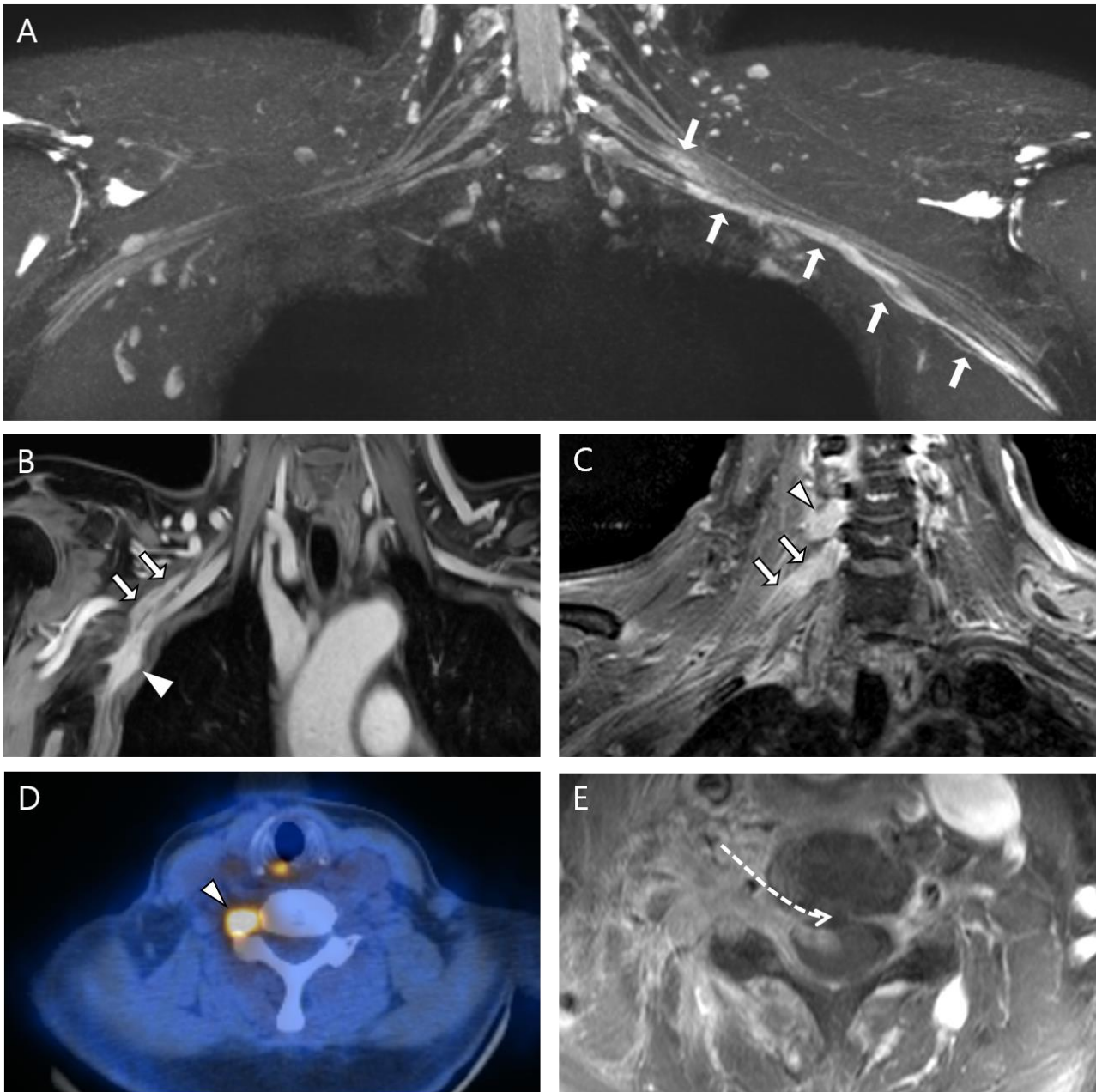


Figure 1. (A) Coronal maximum intensity projection reconstruction images based on T2-weighted imaging of the brachial plexus MRI of patient #3 showed diffuse enlargement and increased T2 signal intensity from the distal C7 and C8 roots to the distal branches of the brachial plexus (arrow). (B) The coronal T1 fat-saturated (FS) gadolinium-enhanced brachial plexus MRI of patient #6 demonstrated a recurrent tumor at the right chest wall (arrowhead) and noted enhancement of the medial cord and lower trunk (arrow). (C) Seven months after the diagnosis of perineural spread in patient #5, a coronal T1 FS enhanced brachial plexus MRI image demonstrated further perineural spreading to the right C6 and C7 spinal nerve roots (arrow), and (D) increased uptake of the right C6 nerve root was noted on an F18-FDG PET-CT scan. (E) Sixteen months after the diagnosis of perineural spread in patient #5, a follow-up cervical spine MRI T1 FS axial post-gadolinium image depicted intradural extension at the C4-5 level.

Cardiopulmonary Rehabilitation

발표일시 및 장소 : 10 월 26 일(토), 08:30 ~ 10:00 , Room A

OP-16

Changes in physical function after lung transplantation

Jong Yoon Chang¹, Jun Hyeok Lee², Geon Woo Kim², Sang-Bum Hong³, Ho Cheol Kim^{3†}, Won Kim^{1†*}

Department of Rehabilitation Medicine, Asan Medical Center, University of Ulsan College of Medicine, Seoul, Republic of Korea¹, Asan Institute for Life Sciences, Asan Medical Center, Seoul, Republic of Korea², Department of Pulmonary and Critical Care Medicine, Asan Medical Center, University of Ulsan College of Medicine, Seoul, Republic of Korea³

Introduction

Patients often experience a slow recovery of physical function post-transplantation not only due to preoperative physical decline from lung disease, but also because of prolonged hospitalization, low physical activity, immunosuppressant, and transplant rejection after surgery. However, there is limited knowledge about changes in physical function following lung transplantation, particularly beyond six months post-surgery. This study aims to investigate the recovery of physical function in lung transplant recipients by comparing outcomes at 6 and 12 months. By examining recovery patterns, we hope to gain a better understanding of their prognosis and identify the impact of extracorporeal membrane oxygenation (ECMO) use on their physical recovery.

Method

Data was obtained retrospectively from patients aged 18 years or older who underwent lung transplantation between August 2018 and August 2023. Physical function was evaluated using the 6-minute walk test (6MWT), grip strength, knee extensor strength, maximal inspiratory pressure (MIP), and forced expiratory volume in one second (FEV1), functional ambulatory category (FAC), 5 times sit-to-stand test (5tSTS), gait speed. We compared physical function at 6 and 12 months postoperatively. Additionally, by stratifying patients into groups based on ECMO use, we examined differences in changes in the 6MWT and grip strength between these groups.

Results

A total of 84 patients were included in the study. The baseline characteristics of the patients are presented in Table 1. The ECMO group had a higher proportion of men and a higher BMI at the time of lung transplantation surgery. There were significant differences between the ECMO and non-ECMO groups in preoperative and postoperative ICU days and total length of hospital stay. Overall, 6MWT, grip strength, knee extensor strength, MIP, FEV1, FAC, 5tSTS, and gait speed improved at 12 months compared to 6 months (Table 2). When grouped by ECMO use, there was a significant improvement in both 6MWT and grip strength within each group, but no significant difference in the changes between the two groups (Table 3). Grip strength was higher in the non-ECMO group compared to the ECMO group at 6 and 12 months, but when adjusted for age and sex, there was no significant difference. The mean distance of the 6MWT showed no significant difference between the two groups at 6 and 12 months. However, the proportion of patients who were able to walk more than 400 meters in the 6MWT was higher in the non-ECMO group, especially at 6 months, although this difference was not statistically significant.

Conclusion

Recovery after lung transplantation can take up to 12 months, necessitating rehabilitation treatment to improve physical function. The recovery of gait function appears to be slower in the ECMO group by 6 months, but most physical functions showed no significant difference between the ECMO and non-ECMO groups at 12 months.

Acknowledgment This research was supported by a grant of the Korea Health Technology R&D Project through the Korea Health Industry Development Institute (KHIDI), funded by the Ministry of Health & Welfare, Republic of Korea (grant number : RS-2024-00408722).

Table 1. Baseline characteristics of the study population.

	Overall (n=84)	ECMO group (n=50)	Non-ECMO group (n=34)	P-value
Age, years (mean (SD))	54.73 (11.06)	55.94 (10.01)	52.94 (12.38)	0.225
Male, n (%)	35 (41.7)	26 (52.0)	9 (26.5)	0.02*
Diagnosis, n (%)				0.017*
Interstitial lung disease	57 (67.9)	40 (80)	17 (50)	
Bronchiolitis obliterans	1 (1.2)	0 (0)	1 (2.9)	
Pulmonary vascular disease	5 (6)	1 (2)	4 (11.8)	
Others	21 (25)	9 (18)	12 (35.5)	
Types of transplantation, n (%)				0.887
Single-lung	4 (4.8)	2 (4)	2 (5.9)	
Double-lung	78 (92.9)	47 (94)	31 (91.2)	
Heart-lung	2 (2.4)	1 (2)	1 (2.9)	
BMI, kg/m² (mean (SD))	22.29 (4.06)	23.20 (3.93)	20.95 (3.93)	0.012*
Preop ICU, days (median [IQR])	7.50 [0.00, 18.00]	16.00 [8.00, 26.75]	0.00 [0.00, 1.00]	<0.001*
Postop ICU, days (median [IQR])	17.00 [12.75, 26.25]	21.00 [14.00, 30.75]	13.50 [10.00, 20.00]	0.001*
ICU others, days (median [IQR])	0.00 [0.00, 0.00]	0.00 [0.00, 3.00]	0.00 [0.00, 0.00]	0.464
Hospital stay, days (median [IQR])	70.50 [43.50, 127.75]	104.00 [65.50, 152.00]	46.50 [30.00, 69.75]	<0.001*
Duration of ECMO, days (mean (SD))	10.29 (16.36)	17.28 (18.14)	0	<0.001*
Number of readmissions, n (median [IQR])	1 [0, 2]	1 [0, 2]	1 [0, 3.75]	0.096

For continuous data, a two-sample t-test or Wilcoxon rank-sum test was used. For categorical data, a Chi-square test was used, and n (%) were reported. ECMO, extracorporeal membrane oxygenation; SD, standard deviation; BMI, body mass index; IQR, interquartile range.

*p-value<0.05

Table 1. Baseline characteristics of the study population.

Table 2. Physical function data at 6-month and 12-month follow-ups.

	At 6-month	At 12-month	Changes from 6 to 12 months	
	Mean (95% CI)	Mean (95% CI)	Difference (95% CI)	P-value
6MWT, m	378.1 (343.8, 412.3)	458.7 (424.0, 493.3)	80.6 (45.7, 115.5)	<0.001*
Grip strength, kg	21.2 (18.9, 23.4)	26.2 (23.9, 28.5)	5.1 (3.8, 6.3)	<0.001*
Knee extensor strength, kg	18.2 (15.4, 21.1)	23.7 (20.8, 26.6)	5.5 (3.6, 7.4)	<0.001*
MIP, cmH₂O	58.7 (53.1, 64.3)	70.2 (64.2, 76.2)	11.5 (5.8, 17.2)	<0.001*
FEV1, %predicted	63.3 (58.9, 67.7)	68.7 (64.2, 73.2)	5.4 (2.7, 8.1)	<0.001*
	n (%)	n (%)	Risk difference (95% CI)	P-value
6MWT ≥ 400m	34 (45.3%)	41 (67.2%)	0.228 (0.100, 0.357)	<0.001*
FAC ≥ 4	51 (67.1%)	57 (93.4%)	0.263 (0.159, 0.367)	<0.001*
5tSTS < 12 s	34 (48.6%)	42 (76.4%)	0.297 (0.170, 0.423)	<0.001*
Gait speed ≥ 1 m/s	30 (42.3%)	41 (74.5%)	0.304 (0.176, 0.432)	<0.001*

Linear mixed-effects models with random intercepts were used to account for repeated measures within the patient for 6MWT, grip strength, knee extensor strength, MIP, and FEV1.

Generalized estimating equations analyses were used to account for repeated measures within the patient for 6MWT, FAC, 5tSTS, and gait speed.

CI, confidence interval; 6MWT, 6-minute walk test; MIP, maximal inspiratory pressure; FEV1, forced expiratory volume in one second; FAC, functional ambulatory category; 5tSTS, 5 times sit-to-stand test.

*p-value<0.05

Table 2. Physical function data at 6-month and 12-month follow-ups.

Table 3. Changes in 6MWT and grip strength, stratified by ECMO use.

		ECMO group		Non-ECMO group		Group difference (Unadjusted)		Group difference (Adjusted for age and sex)	
		Mean (95% CI)	P-value	Mean (95% CI)	P-value	Difference (95% CI)	P-value	Difference (95% CI)	P-value
†6MWT, m	6 months	357.1 (311.3, 403.0)		404.9 (354.5, 455.3)		-47.8 (-115.9, 20.4)	0.165	-13.6 (-76.4, 49.2)	0.665
	12 months	441.3 (397.8, 484.9)		485.5 (429.8, 541.1)		-44.1 (-114, 26.5)	0.215	-12.0 (-76.7, 52.7)	0.711
	Changes from 6 to 12 months	84.2 (38.4, 130.0)	<0.001*	80.6 (26.5, 134.6)	0.004*	3.6 (-67.2, 74.5)	0.918	1.6 (-69.4, 72.6)	0.964
†Grip strength, kg	6 months	18.4 (15.7, 21.2)		25.3 (21.9, 28.7)		-6.9 (-11.2, -2.5)	0.003*	-2.6 (-5.7, 0.5)	0.101
	12 months	23.5 (20.7, 26.3)		30.4 (26.9, 34.0)		-6.9 (-11.4, -2.4)	0.004*	-2.9 (-6.2, 0.4)	0.083
	Changes from 6 to 12 months	5.1 (3.5, 6.7)	<0.001*	5.1 (3.0, 7.3)	<0.001*	0.0 (-2.7, 2.7)	0.982	-0.3 (-2.9, 2.4)	0.823
		Proportion (95% CI)	P-value	Proportion (95% CI)	P-value	Difference (95% CI)	P-value	Difference (95% CI)	P-value
†6MWT ≥ 400m	6 months	0.364 (0.221, 0.506)		0.581 (0.407, 0.754)		-0.217 (-0.441, 0.007)	0.058	-0.169 (-0.375, 0.037)	0.108
	12 months	0.615 (0.463, 0.768)		0.773 (0.598, 0.948)		-0.157 (-0.390, 0.075)	0.184	-0.135 (-0.345, 0.075)	0.208
	Changes from 6 to 12 months	0.252 (0.073, 0.430)	0.006*	0.192 (-0.005, 0.389)	0.056	0.060 (-0.206, 0.325)	0.66	0.034 (-0.220, 0.288)	0.791

†Linear mixed-effects models with random intercepts were used to account for repeated measures within the patient.

*Generalized estimating equations analyses were used to account for repeated measures within the patient.

6MWT, 6-minute walk test; ECMO, extracorporeal membrane oxygenation; CI, confidence interval.

*p-value<0.05

Table 3. Changes in 6MWT and grip strength, stratified by ECMO use.

Cardiopulmonary Rehabilitation

발표일시 및 장소 : 10 월 26 일(토), 08:30 ~ 10:00 , Room A

OP-17

Risk of major adverse cardiovascular events and all-cause mortality by stages of CKD

Yookyung Lee^{1*}, Kyeongil Min¹, Doo Woong Lee², Ye Seol Lee³, Sung Hoon Jeong^{4,5}, Hyunmi Oh^{4,6}, Sujin Kim⁷, Hyang-Lim Lee⁷, Ja-Ho Leigh^{4,5,6†}

Department of Physical and Rehabilitation Medicine, Chung-ang University Gwang-Myeong Hospital¹, Department of Public Health, Yonsei University², Department of Long-term Care Benefits, National Health Insurance Service³, Department of Rehabilitation Medicine, Seoul National University Hospital⁴, National Traffic Injury Rehabilitation Research Institute, National Traffic Injury Rehabilitation Hospital⁵, Department of Rehabilitation Medicine, National Traffic Injury Rehabilitation Hospital⁶, Department of Nephrology, National Traffic Injury Rehabilitation Hospital⁷

Objective

The aim of the present study was to assess the risk of cardiovascular disease (CVD) and all-cause mortality based on the chronic kidney disease (CKD) stage in Korean patients with CKD using nationally representative data.

Participants and method

This was a population-based cohort study using the Korean National Health Insurance data spanning from January 1, 2016, to December 31, 2020. A total of 51,351 participants with first diagnosis of CKD were included, and the incidence rates of CVD and all-cause mortality were calculated according to CKD stages. CKD stage was determined using ICD-10 clinical codes: Stage 1 (N18.1), Stage 2 (N18.2), Stage 3 (N18.3), Stage 4 (N18.4), and Stage 5 (N18.5). As a primary outcome of this study, the incidence of major adverse cardiovascular events was determined based on ICD-10 clinical codes, with requirement that the event occurred during an inpatient visit. The specific events and codes were as follows: Acute MI (I21; inpatient case only), hemorrhagic (I61-62; inpatient case only), ischemic stroke (I63; inpatient case only), unstable angina (I20, I24.0, and I24.8; inpatient case only), and heart failure (I09.9, I11.0, I13.0, I13.2, and I50). Kaplan-Meier survival curves were used to examine the cumulative incidence curves of MACE and all-cause death, and a stratified log-rank test was conducted to compare the Kaplan-Meier curves across different CKD stages.

Results

The CVD risk in stage-5-CKD patients with dialysis was 3.24-fold higher than that in stage-1-CKD patients (Adjusted Hazard Ratio [HR]=3.24, 95% confidence interval [CI]=3.03-3.49, p-value

Conclusion

The risk of MACE and all-cause mortality increased in higher CKD stages compared to CKD stage 1. Notably, the increased risk of death was more pronounced among women and younger individuals. Therefore, active surveillance of CKD, with a specific focus on women and younger individuals, is required to reduce the risk of MACE and mortality.

Acknowledgment This study was supported by a grant from the Ministry of Land, Infrastructure, and Transport Research Fund (NTRH RF-2023001).

Sports Medicine

발표일시 및 장소 : 10 월 26 일(토), 08:30 ~ 10:00 , Room A

OP-18

Comparing a new cadence-based index and oxygen cost indices across varied gait environments

Juntaek Hong^{1*}, Jehyeon Yu¹, Juyeon Lee¹, Dain Shim², Tae Young Choi³, Ye Bin Cho¹, Jeehee Lee¹, Taekyung Lee¹, Dong-wook Rha^{1†}

Department and Research Institute of Rehabilitation Medicine, Yonsei University College of Medicine¹, Department of Exercise Rehabilitation & Welfare, Gachon University, and Research Institute of Rehabilitation Medicine², Department of Rehabilitation Medicine, Yonsei Roi Rehabilitation Clinic³

Background

Walking is a fundamental aspect of daily life and exercise, with clinical benefits for cardiovascular health and muscle strength. However, accurately measuring energy efficiency during walking poses challenges due to equipment and spatial constraints. In this study, we proposed the cadence-based energy expenditure index (cEEI) and analyzed its correlation with the previously proposed index for measuring energy expenditure under various gait conditions.

Methods

We enrolled 16 healthy participants and conducted an experimental protocol on a treadmill to measure the following energy expenditure-related indices: oxygen cost index (OCI), energy expenditure index (EEI), and cEEI. The participants underwent stages of walking at different speeds and inclinations that comply with the modified Bruce protocol while their heart rate, oxygen uptake, and cadence were recorded. Moreover, we categorized gait conditions into two groups based on the walking-running transition cadence of 140 or below: the "walking condition" and the "whole gait condition" including all cadence values. Under each condition, we conducted comparative analyses of the correlations and agreements between three indices using Pearson's correlation analysis and intraclass correlation.

Results

Participants showed significant increases in heart rate, oxygen uptake, and cadence with higher walking speeds and inclinations. (Table 1) Correlation analysis revealed strong associations between cEEI and OCI, especially during walking condition. (Figure 1) Bland-Altman plots and interclass correlation coefficient analysis demonstrated a favorable agreement between cEEI and OCI, outperforming EEI under two gait conditions. (Table 2)

Conclusion

This study proposes cEEI as a reliable metric for estimating energy expenditure during walking by proving a strong correlation and agreement with OCI across various gait conditions. This suggests the potential for cEEI to provide real-time, individualized feedback on energy expenditure during walking, facilitating more personalized exercise prescriptions.

Acknowledgment This work was supported by the National Research Foundation of Korea (NRF) grant funded by the Korea government (MSIT)(No.2022R1A3B1077880).

Stage	Speed (m/min)	An gle (%)	Total interval (n, %)	HR (beats)	<i>P</i> value	Cadence (steps/min)	<i>P</i> value	Normalized cadence (steps/min)	<i>P</i> value	VO2 (mL/kg/min)	<i>P</i> value
1	45.0	0	288 (100)	102.66 ± 15.48		88.23 ± 12.96		89.78 ± 12.51		7.73 ± 3.35	
2	45.0	5	288 (100)	107.45 ± 14.16	< 0.01	85.85 ± 11.43	0.01	87.33 ± 10.43	0.01	12.15 ± 3.89	< 0.01
3	45.0	10	288 (100)	117.11 ± 14.64	< 0.01	83.94 ± 12.04	0.05	85.34 ± 10.90	0.02	16.18 ± 4.54	< 0.01
4	66.6	12	288 (100)	136.59 ± 17.55	< 0.01	96.54 ± 14.08	< 0.01	98.14 ± 13.30	< 0.01	22.48 ± 5.25	< 0.01
5	90.0	14	270 (96.42)	161.30 ± 14.69	< 0.01	115.60 ± 21.27	< 0.01	117.16 ± 18.74	< 0.01	30.32 ± 6.47	< 0.01
6	111.6	16	155 (55.36)	181.57 ± 12.38	< 0.01	173.61 ± 53.96	< 0.01	177.34 ± 53.53	< 0.01	37.27 ± 9.38	< 0.01
Total			1577 (91.26)	130.16 ± 30.40		101.61 ± 34.09		103.34 ± 34.03		19.55 ± 10.92	

Independent t-test was used by comparing each dataset with that of the previous stage. HR, heart rate; VO2, oxygen uptake

Table 1. Information table on the walking environment by stage and collected data

Gait condition	Index	ICC (95% confidence interval)	F test with true value 0			
			Value	df1	df2	<i>P</i> value
Total	Scaled c-EEI - OCI	0.76 (0.73–0.78)	4.1	1576	1576	< 0.01
	Scaled EEI - OCI	0.65 (0.61–0.69)	2.9	1576	1576	< 0.01
Cadence140	Scaled c-EEI - OCI	0.86 (0.85–0.88)	7.4	1445	1445	< 0.01
	Scaled EEI - OCI	0.67 (0.63–0.70)	3	1445	1445	< 0.01

Multiple random raters (ICC 2:k) were used in this table. cEEI, cadence-based energy expenditure index; EEI, energy expenditure index; OCI, oxygen cost index

Table 2. Interclass correlation coefficient (ICC) of two indices (c-EEI and EEI) compared to OCI under two gait conditions: whole gait and walking conditions

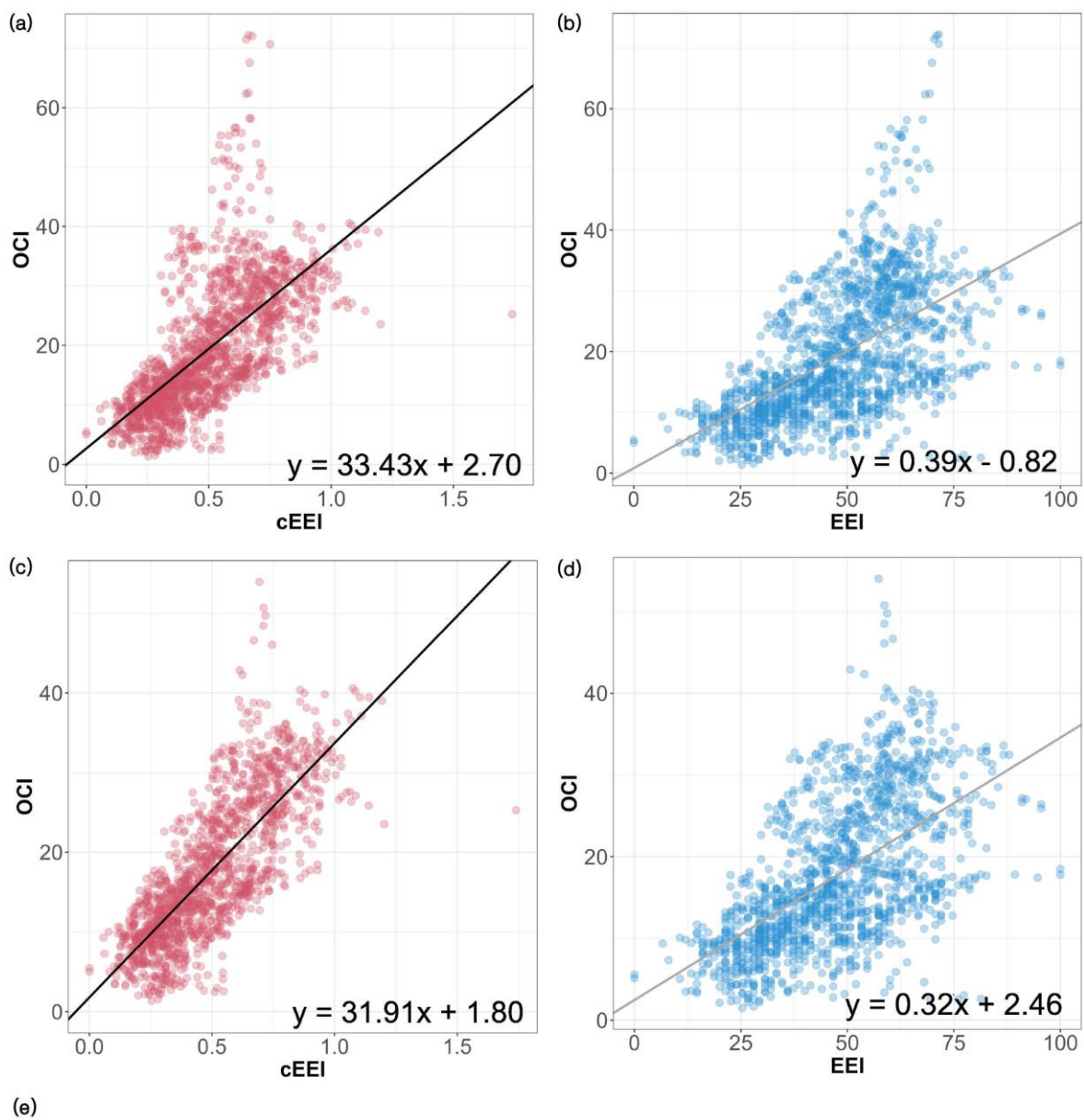


Figure1. Correlation analysis between two indices (cEEI and EEI) compared to OCI under two gait conditions: whole and walking conditions

Sports Medicine

발표일시 및 장소 : 10 월 26 일(토), 08:30 ~ 10:00 , Room A

OP-19

Joint specific kinematic, moment analysis in different aerobic exercises

Yong Jae Na^{1*}, Yujin Kwon^{3,4}, Jeemyung Han⁴, Kanghyeon Lee³, Woojin Yoon³, Gwanseob Shin³, Won Kim^{2†}

Department of Rehabilitation Medicine, Chung-Ang University Gwangmyeong Hospital¹, Department of Rehabilitation Medicine, Asan Medical Center, University of Ulsan College of Medicine², Department of Biomedical Engineering, Ulsan National Institute of Science and Technology³, Department of Rehabilitation Medicine, Seoul National University Hospital⁴, Department of Rehabilitation Medicine, Chung-Ang University Hospital, Chung-Ang University College of Medicine, Seoul Korea⁵

OBJECTIVE

Many patients with knee pain experience worsening symptoms or increased severity, making it difficult to perform aerobic exercise. There is also concern that the weight-bearing and mechanical load occurring during aerobic activities may exacerbate the severity of symptoms in patients with joint pain. Specifically, studies have reported that cartilage in knee osteoarthritis can negatively react to load-bearing activities, potentially accelerating disease progression. Therefore, it is necessary to conduct foundational research to determine the impact of different aerobic exercises on joints. This research aims to calculate the impulse and angular impulse on joints during aerobic exercises at the similar aerobic intensity.

METHODS

One healthy male (age: 35yrs, height: 1.83m, weight: 84kg) participated in the study. The participant conducted fast walking, jogging, and jumping jack trials while maintaining similar heart rate levels ($140 \text{ bpm} \pm 10\%$). Ground reaction forces (GRF) of the right foot was measured with a force plate (AMTI OR6, Advanced Medical Technology Inc., Watertown, MA, USA) at 1,000 Hz, and lower limb kinematics was synchronously measured with a 3-dimensional motion capture system (OptiTrack, NaturalPoint Inc., Corvallis, OR, USA) at 100 Hz. GRF and motion data were imported to OpenSim, a musculoskeletal simulation software, for inverse kinematics and inverse dynamics analysis. Joint angles were calculated and filtered at 15 Hz to calculate knee joint moments in the sagittal plane. Then, the moment data were integrated to generate angular impulse data. All data analysis were conducted using a custom-written code in Matlab (MathWorks Inc., Natick, MA, USA).

RESULTS

An analysis was conducted on a well-trained, healthy adult subject. When performing jogging, fast walking, and jumping jacks at a heart rate of approximately 140, the integration of ground reaction force per step (impulse) normalized by time was highest for for jumping jacks (0.810 BW), followed by jogging (0.408 BW) and fast walking (0.398 BW) being similar .

The peak ground reaction force values were highest for jogging (2.112 BW), followed by jumping jacks (1.791 BW), and then fast walking (1.472 BW).

After integrating the moment (angular impulse) occurring at the knee and normalized by time, jogging (0.422 Nm/kg) was the highest, followed by jumping jacks (0.382 Nm/kg) and fast walking (0.298 Nm/kg).

CONCLUSION

In different exercises at similar aerobic intensity, the impulse was similar for jogging and fast walking, while jumping jacks had the highest value. The peak ground reaction force was highest for jogging, followed by fast walking, and then jumping jacks. The angular impulse was highest for jogging and lowest for fast walking. These results should be considered when selecting the appropriate aerobic exercise for various joint pathologies.

Acknowledgment This work was supported by the National Research Foundation of Korea(NRF) grant funded by the Korea government(MSIT) (No.RS-2024-00346048) and a grant (2024IE0014) from the Asan Institute for Life Sciences, Asan Medical Center, Seoul, Korea.

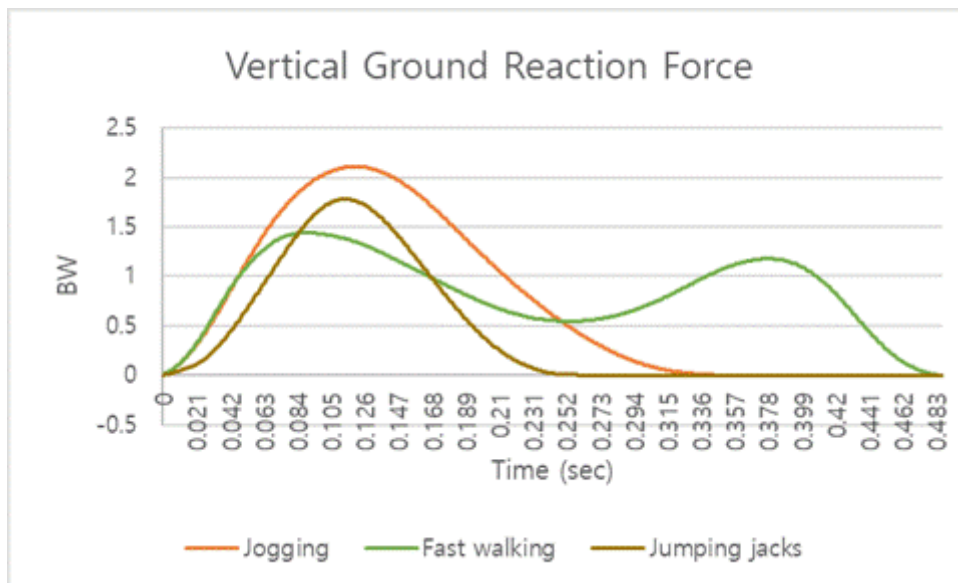


Fig 1. Vertical ground reaction force of different aerobic exercises (orange: jogging, green: fast walking, brown: jumping jacks)

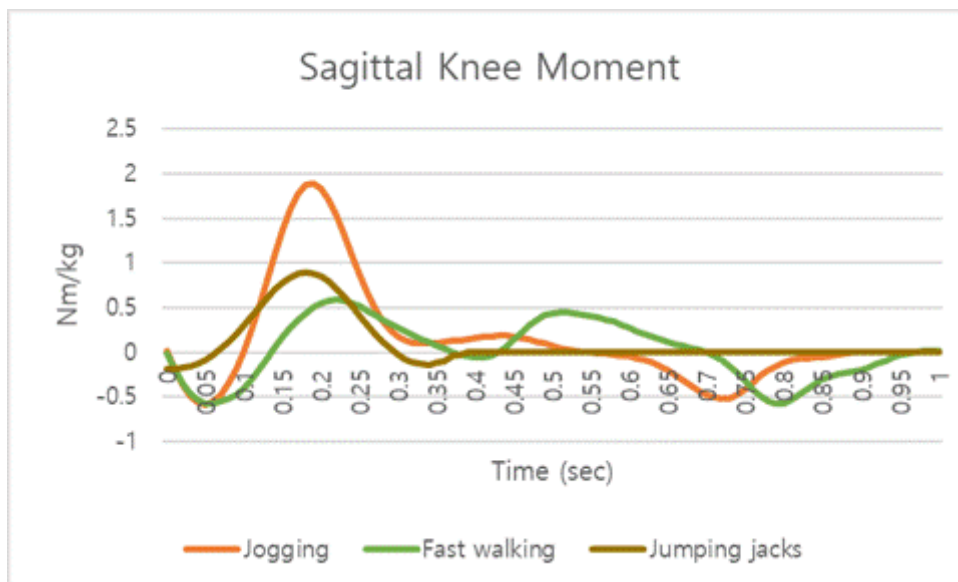


Fig 2. Sagittal knee moment of different aerobic exercises (orange: jogging, green: fast walking, brown: jumping jacks)

Table 1

	Jogging	Fast walking	Jumping jacks
Mean Impulse (BW)	0.408	0.398	0.810
Peak GRF (BW)	2.112	1.472	1.791
Mean Angular Impulse (Nm/kg)	0.422	0.298	0.382

Table 1. Presentation of the mean impulse, peak ground reaction force (GRF), and mean angular impulse for jogging, fast walking, and jumping jacks.

Geriatric Rehabilitation

발표일시 및 장소 : 10 월 26 일(토), 08:30 ~ 10:00 , Room A

OP-20

Validation of Digital Senior Fitness Test System for Assessing Physical Function in Older Adults

Hyun-Ho Kong^{1,2*†}, Dong-Seok Yang³, Hye-Young Gu¹, Hyeon-Seong Joo⁴, Hyun-Chul Shon^{5,6}

Department of Rehabilitation Medicine, Chungbuk National University Hospital¹, Department of Rehabilitation Medicine, Chungbuk National University College of Medicine², Technology Strategy Center, Neofect³, Department of Physical Therapy, Daejeon University⁴, Department of Orthopaedic Surgery, Chungbuk National University Hospital⁵, Department of Orthopaedic Surgery, Chungbuk National University College of Medicine⁶

Background

Frailty is becoming an important health issue for older adults as life expectancy increases and the population of older adults grows. In particular, physical frailty is known to be associated with several health problems such as falls, fractures, and hospitalizations. Several physical function tests are available for the assessment of physical frailty by trained physical therapists, but there are several limitations to their use in clinical settings. Therefore, we have newly developed the Digital Senior Fitness Test (DSFT) system, which automatically measures the multi-domain physical functions of older adults, with a single digital device based on a depth camera. The purpose of this study is to verify the clinical applicability of the DSFT in assessing physical function compared to conventional manual tests.

Methods

This is a cross-sectional study in which community-dwelling healthy older adults were recruited between November 2022 and July 2023. Participants were tested by both manual and automated (using the DSFT system) measurement methods for the following multi-domain physical functions: muscle strength (30-second chair stand test, 30CST), balance (timed-up-and-go test, TUGT), flexibility (shoulder active range of motion), cardiopulmonary endurance (2-minute step test, 2MST), coordination (Figure of Eight Walk Test, F8WT). Intra-class correlation coefficient (ICC) and Bland-Altman analysis were performed to assess the agreement between the results of the two measurement methods.

Results

A total of 61 participants (age of 71.0±4.5 years) were included in the analysis. In the analysis of the agreement between the two measurement methods using ICC, the automated physical function measurement with the DSFT system showed excellent agreement (ICC ≥ 0.75) with the manual measurement for all test items except shoulder external rotation (ICC = 0.72 to 0.79). In particular, some items such as shoulder flexion and F8WT (ICC = 0.94, respectively) showed high ICC values. In the Bland-Altman analysis, the results of the multi-domain physical frailty assessment using the DSFT system were within the clinically acceptable range for all tests compared with the results of the manual test.

Conclusion

The DSFT system demonstrated excellent agreement with conventional manual tests in assessing multi-domain physical function in older adults. The DSFT system shows promise as a reliable and clinically applicable tool for assessing physical frailty in community-dwelling healthy older adults.

Acknowledgment This research was supported by the Medical Device Technology Development Program (grant number: 20014701, modular quantitative aging assessment and care service based on multiple sensors for aging in-home) funded by the Ministry of Trade, Industry, and Energy (MOTIE, Sejong, Republic of Korea).

Table 1. Comparison of the results of manual or automated measurements of physical functions

Variables	Manual measurements	Automated measurements	Bland-Altman bias (95% LoA)	ICC	Correlation coefficient
30-second chair stand test	17.4±4.9	16.3±4.6	1.1 (-4.4 to 6.7)	0.89 (0.80-0.94)	0.82
Shoulder AROM, degree					
Flexion (Rt)	161.0±8.8	158.9±7.5	2.1 (-7.2 to 11.5)	0.89 (0.79-0.94)	0.84
Flexion (Lt)	156.1±10.6	156.1±9.5	0.1 (-9.5 to 9.6)	0.94 (0.90-0.96)	0.89
Abduction (Rt)	168.9±8.0	167.1±5.7	1.8 (-10.1 to 13.8)	0.75 (0.57-0.85)	0.65
Abduction (Lt)	169.0±7.5	166.6±5.8	2.4 (-7.4 to 12.1)	0.81 (0.64-0.90)	0.75
External rotation (Rt)	69.9±10.6	71.0±11.8	-1.1 (-19.5 to 17.4)	0.79 (0.65-0.87)	0.65
External rotation (Lt)	72.8±10.2	72.4±11.1	0.4 (-19.2 to 20.0)	0.72 (0.54-0.83)	0.56
Timed up and go test, sec	6.2±1.1	6.7±1.1	-0.48 (-1.68 to 0.71)	0.87 (0.55-0.95)	0.85
Figure of eight walk test, sec	28.6±4.7	29.7±5.1	-1.0 (-5.0 to 3.0)	0.94 (0.88-0.97)	0.92
2-minute step test	92.8±18.1	85.8±20.7	7.0 (-21.7 to 35.7)	0.81 (0.63-0.89)	0.72

LoA, limits of agreement; ICC, intraclass correlation coefficient; AROM, active range of motion.

Table 1. Comparison of the results of manual or automated measurements of physical functions

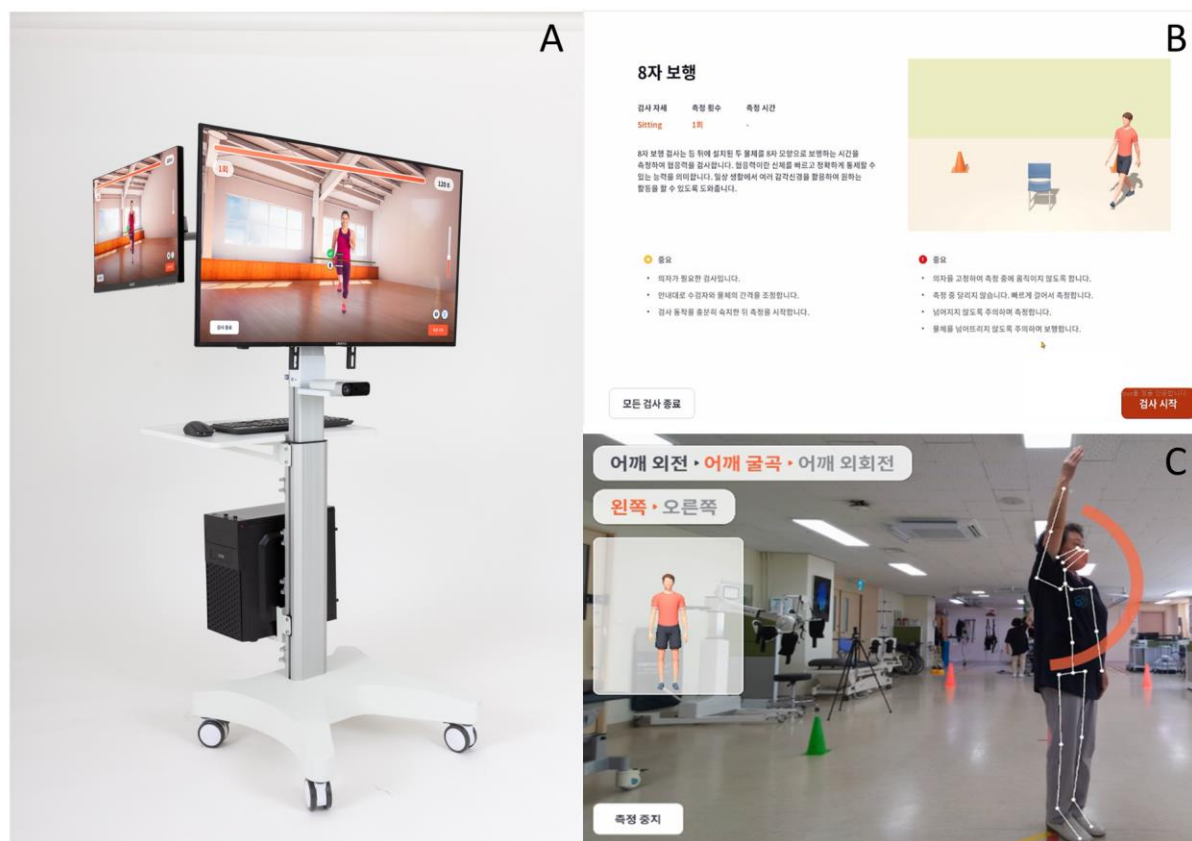


Figure 1. Digital Senior Fitness Test System

E-Poster

(Listed in order of topic)

Predicting Long-term Prognosis of Poststroke Dysphagia with Machine Learning

Minsu Seo^{1*}, Seokjoon Hwang¹, Taeheon Lee¹, Bum Sun Kwon¹, Ho Jun Lee¹, Kiyeun Nam¹, Jin-woo Park^{1†}

Department of Physical Medicine & Rehabilitation, Dongguk University College of Medicine¹

Introduction

Poststroke dysphagia is a common condition that can lead to complications such as aspiration pneumonia and malnutrition, significantly affecting the quality of life. Most patients recover their swallowing function spontaneously, but others persist beyond six months, can we predict this in advance? On the other hand, there have been recent attempts to use machine learning to predict disease prognosis. Therefore, this study aims to investigate whether machine learning can be used to predict the long-term prognosis for poststroke dysphagia using early videofluoroscopic swallowing studies (VFSS) data.

Materials and Method

Data from VFSS performed within 1 month of onset and swallowing status at 6 months were collected retrospectively in patients with dysphagia who experienced their first acute stroke at a university hospital. We selected 14 factors (lip closure, bolus formation, mastication, apraxia, tongue-to-palate contact, premature bolus loss, oral transit time, triggering of pharyngeal swallow, vallecular residue, laryngeal elevation, pyriform sinus residue, coating of the pharyngeal wall, pharyngeal transit time, and aspiration) from the VFSS data, scored them, and analyzed whether they could predict long-term prognosis using five machine learning algorithms: Random Forest, Naïve Bayes, Extra Trees Classifier, Extreme Gradient Boosting, and Logistic Regression. These algorithms were combined through an ensemble method to create the final model.

Results

In total, we collected data from 206 patients, of which 80% were used for training, 10% for validation, and 10% for testing. The model was evaluated using accuracy, precision, recall, F1-score, and Area Under the Receiver Operating Characteristic Curve (AUC), resulting in values of 0.95, 0.89, 0.95, 0.95, and 0.89, respectively.

Conclusion

Machine learning models using early VFSS data have shown very high accuracy and predictive power in predicting the long-term prognosis of patients with post-stroke dysphagia and are likely to provide very useful information for clinicians.

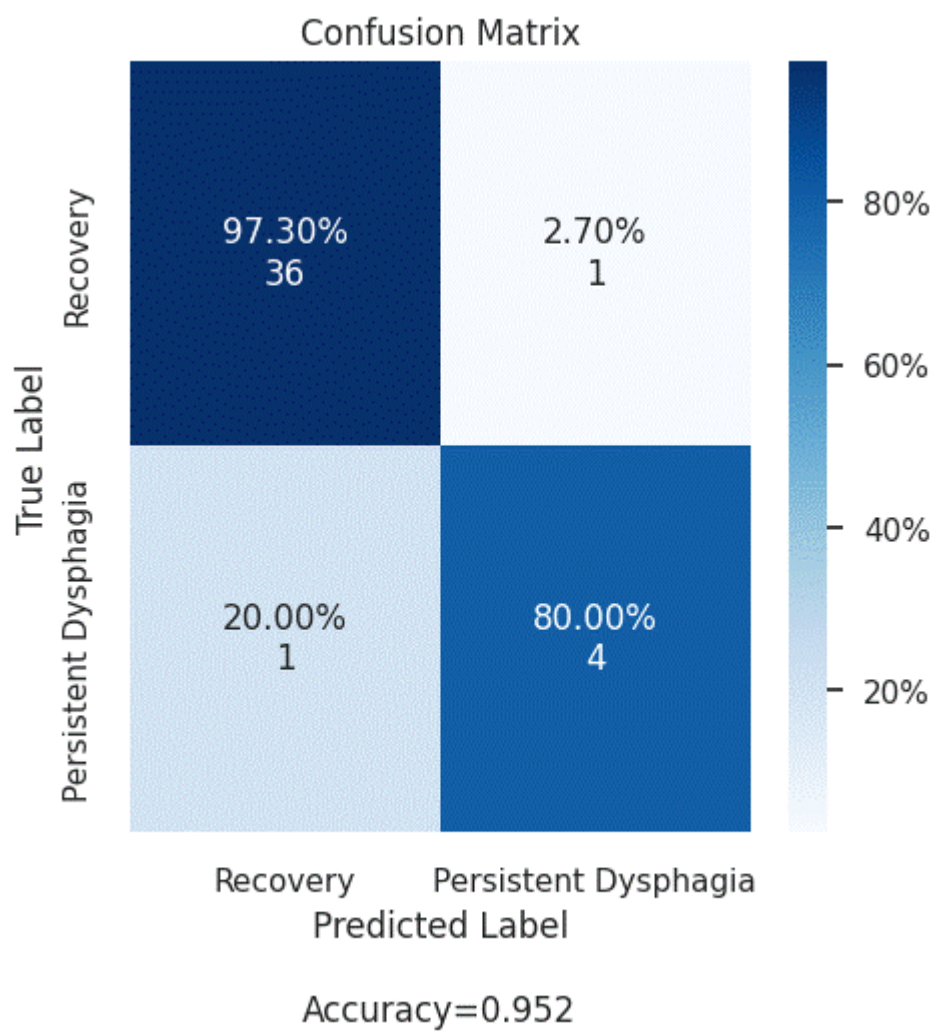


Fig 1. Confusion matrix for model

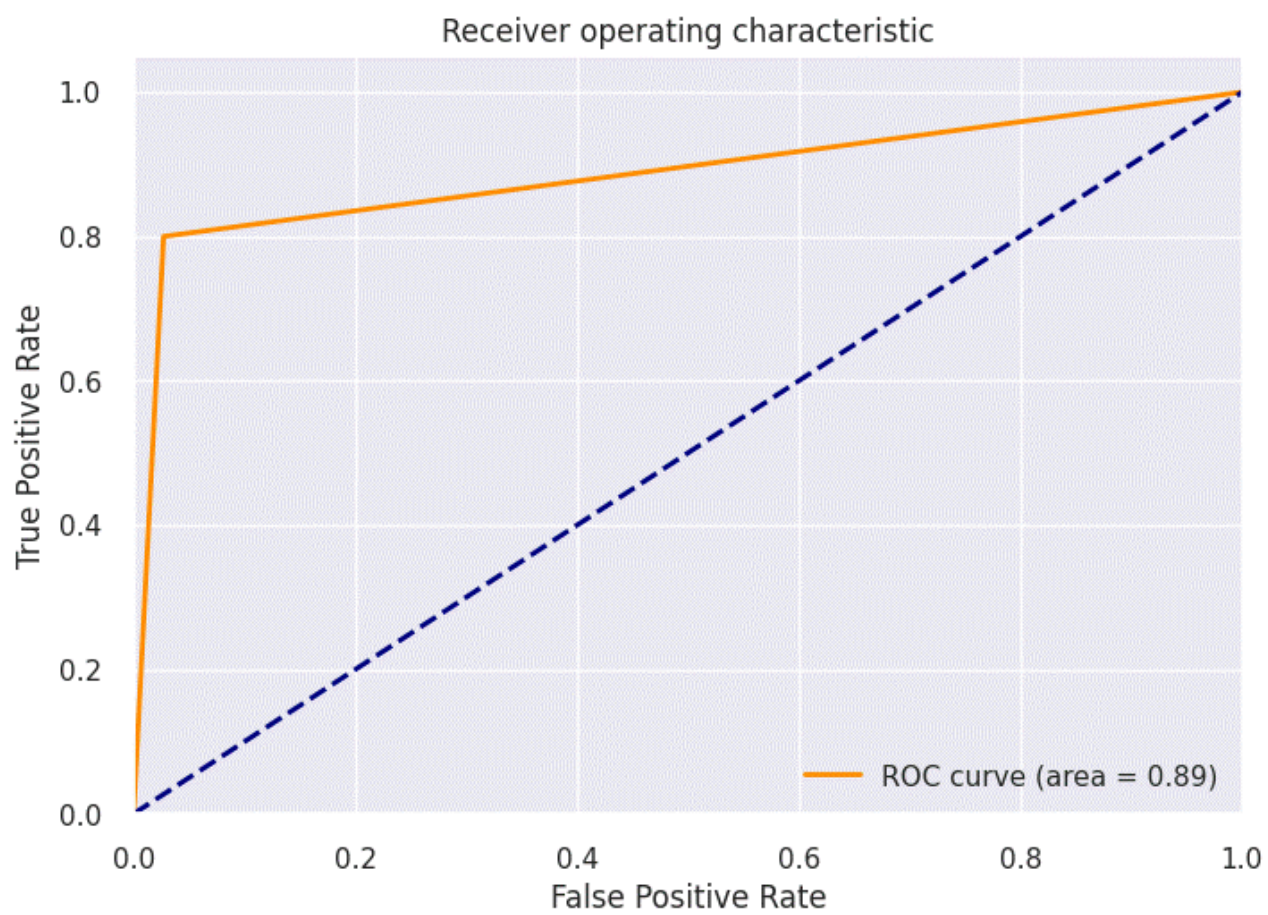


Fig 2. AUC-ROC curve

Effects of Lower Limb CIMT using an Exoskeletal Wearable Device in Chronic Stroke Patients

Ho Seok Lee^{1*}, Soyoung Lee¹, Seung-min Baik¹, Dae Hyun Kim¹, Won Hyun Chang^{1,2†}

Department of Physical and Rehabilitation Medicine, Samsung Medical Center¹, Department of Health Science and Technology, Department of Medical Device Management and Research, Sungkyunkwan University²

Objective

Lower Limb Constraint-Induced Movement Therapy (LL-CIMT) has been proposed as a potential intervention to improve gait function in patients with chronic stroke. LL-CIMT presents a significant challenge due to the necessity of the patient's active involvement, which requires continuous intervention by the therapist. Recently, an exoskeletal rehabilitation robot has been developed with the objective of reducing the reliance on therapists. The aim of this study was to investigate the effects of lower limb constraint-induced motor therapy (LL-CIMT) using the robotic rehabilitation device on ambulatory function in chronic stroke patients.

Methods

A total of 15 chronic stroke patients (9 male, mean age 59.5 ± 12.9 years, mean stroke duration 4.1 ± 4.5 years) were recruited. The treatment comprised 5 robot-assisted gait training sessions over a 2-week period, followed by 10 lower limb CIMT sessions utilizing a torque-assisted exoskeleton (ANGEL LEGS M20, Angel Robotics, Co., Ltd.) over a 3-week interval. The crossover study design entailed the sequential performance of robot-assisted gait training and lower limb CIMT with an exoskeleton. The primary outcome parameters were time in the timed-up-and-go test (TUG), while the secondary outcome parameters were the Fugl-Meyer Assessment-Lower Extremity (FMA-LE). Additionally, spasticity of the affected lower extremity was assessed using the Modified Ashworth Scale (MAS). Data were assessed at baseline (T0), at crossover (T1), at the end of treatment (T2), and 3 weeks after the end of treatment (T3).

Results

A total 14 out of 15 chronic stroke patients were able to complete the 5-week of exoskeleton training. One patient withdrew from the robot-assisted gait training sessions due to discomfort associated with the exoskeleton. During the 5-week period of exoskeleton treatment, no adverse effects or accidents were observed in any of the participants. Only the TUG test demonstrated a statistically significant improvement following robot-assisted gait training (T0 to T1, p

Conclusion

The results of this study indicate that robot-assisted gait training and exoskeleton-based LL-CIMT may represent promising therapeutic avenues for enhancing gait function in individuals with chronic stroke. Nevertheless, in comparison to robot-assisted gait training, exoskeleton-based LL-CIMT may exert an additional effect on the improvement of lower limb motor function in chronic stroke patients. Further studies with a larger number of participants are required to elucidate the benefits of exoskeleton-based LL-CIMT in chronic stroke patients.

Acknowledgment This work was supported by the Korea Medical Device Development Fund grant funded by the Korea government (the Ministry of Science and ICT, the Ministry of Trade, Industry and Energy, the Ministry of Health & Welfare, the Ministry of Food and Drug Safety (Project Number: RS-2021-KD000003)).

Neural Correlates of Visuomotor Function after Supratentorial Stroke

Eunjin Park^{1*}, Youngkook Kim^{1**}

Department of Rehabilitation Medicine, Yeouido St. Mary's Hospital, The Catholic University of Korea¹

Background: Poststroke visual impairment affects functional abilities, such as visual perception, performing motor activities, balancing, navigating complex visual environments, reading, and driving, which may ultimately lower the quality of life. Of those, visuomotor function contributes to performing precise movements using visual feedback. This study aims to explore potential neuroimaging biomarkers representing the poststroke visuomotor function.

Methods

Twenty patients with supratentorial stroke who underwent diffusion tensor imaging were included. The visuomotor function was evaluated by the copying task of the Rey Complex Figure Test (RCFT). The fractional anisotropy (FA) values were extracted for the bilateral optic radiation, superior longitudinal fasciculus, and inferior longitudinal fasciculus: Each white matter tract is responsible for the primary source of visual information to the visual cortices, spatial perception, and object perception, respectively. We assessed the relationship between the FA values of the white matter tracts and the copy score of the RCFT using Spearman correlation analysis.

Results

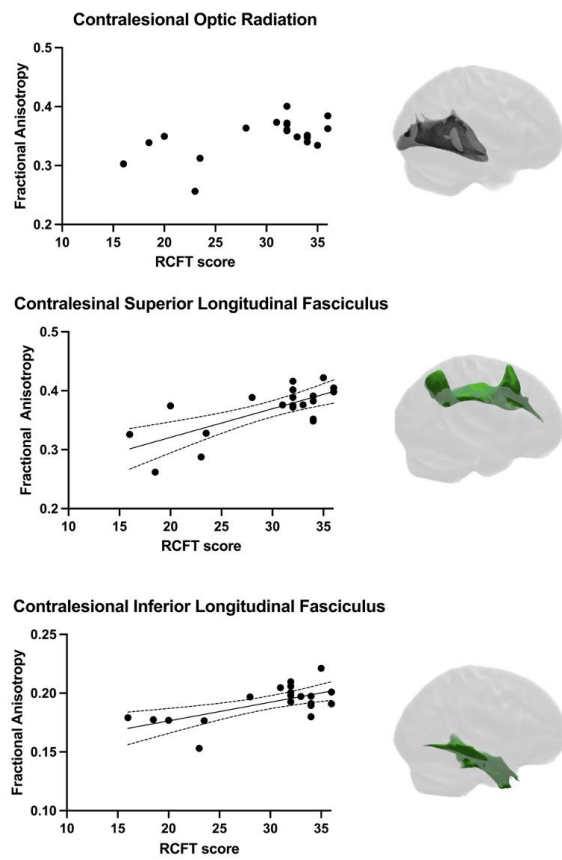
The mean NIHSS score at stroke onset was 8.80 ± 4.06 , and the mean Mini-Mental State Exam score was 23.45 ± 7.00 . The FA values of the contralesional superior longitudinal fasciculus and inferior longitudinal fasciculus were positively correlated with the copy scores of the RCFT (Spearman's rho for the superior longitudinal fasciculus = 0.631, $p = 0.003$; for the inferior longitudinal fasciculus = 0.460, $p = 0.041$)(Figure 1).

Conclusion

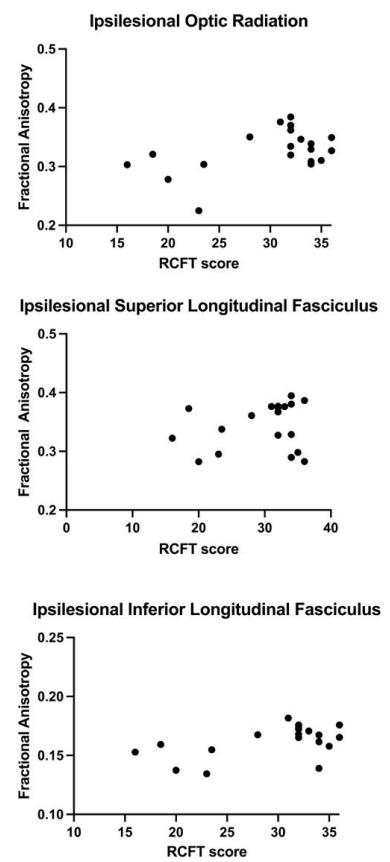
The structural integrity of the contralesional superior longitudinal fasciculus and inferior longitudinal fasciculus contributes to poststroke visuomotor function.



Acknowledgment None.

Contralesional hemisphere



Ipsilesional hemisphere



 *significant correlation*
 *no correlation*

AI (Artificial Intelligence) Classification of Rehabilitation Exercises for Stroke Patients

Hyeon Hong^{1,2*}, Bibalaev Shokhrukh Rustamovich³, Kyuwon Lee^{1,2}, Yeji Jeong^{1,2}, Jeong Hyun Kim^{1,2}, Aeon Lee^{1,2}, Shi Uk Lee^{1,2†}

Department of Rehabilitation Medicine, Seoul National University College of Medicine¹, Department of Rehabilitation Medicine, Seoul National University Boramae Medical Center², Software Engineering Team, RBIOTECH Corporation³

Objective

Stroke patients face a range of impairments in physical, cognitive, and sensory functions, significantly impacting their daily activities and quality of life. Continuous rehabilitation therapy is crucial for maintaining a functional level of these patients. With the use of human activity recognition (HAR) devices, including IMUs, it is possible to guide and monitor home-based exercises. With the collaboration of recently developed AI technology, it is possible to support stroke patients by enabling continuous and accurate monitoring, fostering improved recovery outcomes, and adherence to prescribed home-based rehabilitation exercises. However, there's a lack of studies on how to monitor the exercises done by patients. This study aims to urgently address this gap by developing a deep learning model that can classify stroke rehabilitation exercises, thereby facilitating better monitoring and improving stroke patients' recovery.

Method

IMU sensor data were collected from 49 healthy individuals (24 males, 25 females, age range 19-53 years) to train a deep learning model. Participants performed 33 types of stroke rehabilitation exercises on both sides, each repeated ten times. The exercise classification algorithm was primarily based on a Gated Recurrent Unit (GRU) model. The dataset, comprising 70,640 training samples and 17,660 test samples, was randomly split into 80% for training and 20% for testing.

Results

The deep learning model using GRU achieved an overall accuracy of 98.04%. The training and validation accuracy and loss curves indicate good convergence, with training accuracy reaching 0.980 and validation accuracy reaching 0.988. The loss values stabilized at a low value (training loss: 0.062, validation loss: 0.027).

Conclusion

The GRU-based deep learning model demonstrated high accuracy, indicating sturdy generalization to new data, which is crucial for consistent exercise monitoring in stroke patients. The high performance of the GRU model is attributed to its design for handling time series data, effectively considering the sequence and timing of data points, which is vital for accurate classification. This model addresses the gap in continuous rehabilitation for patients without regular therapy access, providing real-time feedback through IMU sensors. For further studies, training should include data from stroke patients to distinguish their better movement patterns from healthy individuals, offering tailored exercise quality assessments and qualitative feedback. Integrating the GRU model into wearable devices or mobile apps can promote autonomous rehabilitation, reduce healthcare burdens, and enhance patient quality of life. Ongoing research with various severity data from stroke patients is essential to improve the model's sophistication and applicability.

Acknowledgment This study was supported by the Translational R&D Program on Smart Rehabilitation Exercises(TRSRE-MD04), National Rehabilitation Center, Ministry of Health and Welfare, Korea.

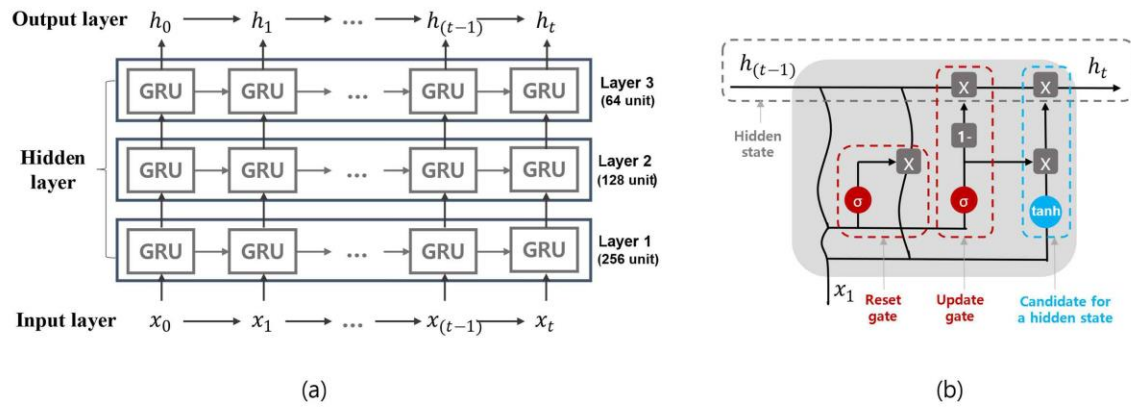


Figure 1. Architecture of GRU; (a) GRU model with three layers (b)Gated structure of a GRU cell

Figure 1. Architecture of GRU; (a) GRU model with three layers (b) Gated struecture of a GRU cell

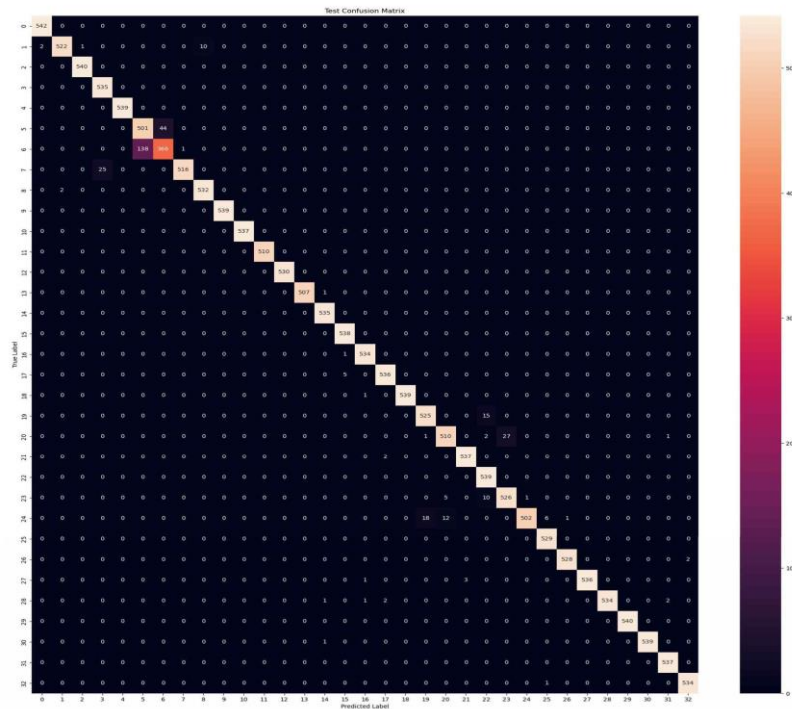


Figure 2. Confusion Matrix of the 33-class exercise classification model

Figure 2. Confusion Matrix of the 33 class exercise classification model

Table 1. Precision, Recall, F1-score, and Support for each exercise

No.	Exercise	Position	Precision	Recall	F1-Score	Support
1	Shoulder rotation 1	Lying down (Prone)	1.00	1.00	1.00	542
2	Shoulder flexion		1.00	0.98	0.99	535
3	Rolling		1.00	1.00	1.00	540
4	Hip flexion		0.96	1.00	0.98	535
5	Hip abduction/adduction		1.00	1.00	1.00	539
6	Bridge		0.78	0.92	0.85	545
7	Bridge with leg cross		0.89	0.72	0.80	505
8	Ankle flexion	Lying down (Supine)	1.00	0.95	0.98	541
9	Lie to sit		0.98	1.00	0.99	534
10	Quadruped positioning		1.00	1.00	1.00	539
11	Kneeling up		1.00	1.00	1.00	537
12	Kneeling walking		1.00	1.00	1.00	510
13	Shifting weight		1.00	1.00	1.00	530
14	Sit to stand		1.00	1.00	1.00	508
15	Shoulder capsule stretching	Sitting	0.99	1.00	1.00	535
16	Shoulder rotation 2		0.99	1.00	0.99	538
17	Shoulder abduction		0.99	1.00	1.00	535
18	Shoulder abduction/adduction with support		0.99	0.99	0.99	541
19	Elbow flexion 1		1.00	1.00	1.00	540
20	Knee lifting		0.97	0.97	0.97	540
21	Leg extension with support		0.97	0.94	0.96	541
22	Stand up with chair support	Standing	0.99	1.00	1.00	539
23	Hip external rotation		0.95	1.00	0.98	539
24	Knee extension		0.95	0.97	0.96	542
25	Ankle dorsiflexion		1.00	0.93	0.96	539
26	Walking in place 1		0.99	1.00	0.99	529
27	Walking in place with a chair		1.00	1.00	1.00	530
28	Squatting with chair		1.00	0.99	1.00	540
29	Wrist flexion (horizontal)	Sitting	1.00	0.99	0.99	540
30	Wrist flexion (vertical)		1.00	1.00	1.00	540
31	Elbow flexion 2		1.00	1.00	1.00	540
32	Inner range quad movement	Standing	0.99	1.00	1.00	537
33	Walking in place 2		1.00	1.00	1.00	535
Average / Total			0.98	0.98	0.98	17660

Table 1. Precision, Recall, F1-score and Supprot for each stroke rehabilitation exercise

Cognitive impairment in patients surviving aneurysmal SAH at 7 days: the KOSCO study

Ho Seok Lee^{1*}, Min Kyun Sohn², Jongmin Lee³, Deog Young Kim⁴, Yong-Il Shin⁵, Gyung-Jae Oh⁶, Yang-Soo Lee⁷, Min Cheol Joo⁸, So Young Lee⁹, Min-Keun Song¹⁰, Junhee Han¹¹, Jeonghoon Ahn¹², Young-Hoon Lee⁶, Dae Hyun Kim¹, Young-Taek Kim¹³, Yun-Hee Kim¹⁴, Won Hyuk Chang^{1†}

Department of Physical and Rehabilitation Medicine, Samsung Medical Center¹, Department of Rehabilitation Medicine, Chungnam National University², Department of Rehabilitation Medicine, Konkuk University School of Medicine³, Department and Research Institute of Rehabilitation Medicine, Yonsei University College of Medicine⁴, Department of Rehabilitation Medicine, Pusan National University School of Medicine⁵, Department of Preventive Medicine, Wonkwang University School of Medicine⁶, Department of Rehabilitation Medicine, Kyungpook National University Hospital⁷, Department of Rehabilitation Medicine, Wonkwang University School of Medicine⁸, Department of Rehabilitation Medicine, Jeju National University Hospital⁹, Department of Physical and Rehabilitation Medicine, Chonnam National University Medical School¹⁰, Department of Statistics, Hallym University¹¹, Department of Health Convergence, Ewha Womans University¹², Department of Preventive Medicine, Chungnam National University Hospital¹³, Department of Physical and Rehabilitation Medicine, Sungkyunkwan University School of Medicine¹⁴

Objective

The aim of this study was to investigate vascular cognitive impairment (VCI) in patients surviving aneurysmal subarachnoid hemorrhage (aSAH) at 7 days after onset.

Methods

This study was a subgroup analysis of patients with aSAH surviving at 7 days from the Korean Stroke Cohort for Functioning and Rehabilitation study. We analyzed 309 patients who completed a face-to-face functional assessment battery and structured self-administered questionnaires at 5 years after onset (Fig. 1). The cognitive function was assessed by the Korean Mini-Mental State Examination (K-MMSE). To assess the functional level regarding activities of daily living (ADL), we measured the Functional Independence Measurement (FIM). All measurements were performed at 3, 6, 12, 24, 36, 48 and 60 months after onset. We defined VCI if the patient had any impairment in the cognitive domain of the K-MMSE. Furthermore, to classify mild and major VCI, we defined the major VCI as the patients who had any impairment in the ADL as measured by the FIM. Impairment in the ADL was defined as having any deficit of the 18 categories comprising the FIM, as measured by a score of 1 to 5. We identified the patients with VCI at 5 years after the onset. we used Kaplan-Meier curve to demonstrate the cumulative incidence of VCI. In addition, among the impaired patients in cognition, we classified the patients with minor and major VCI as defined by the ADL dependence. We identified their cognitive and functional levels during the 5-year follow-up period using the MMSE and FIM.

Results

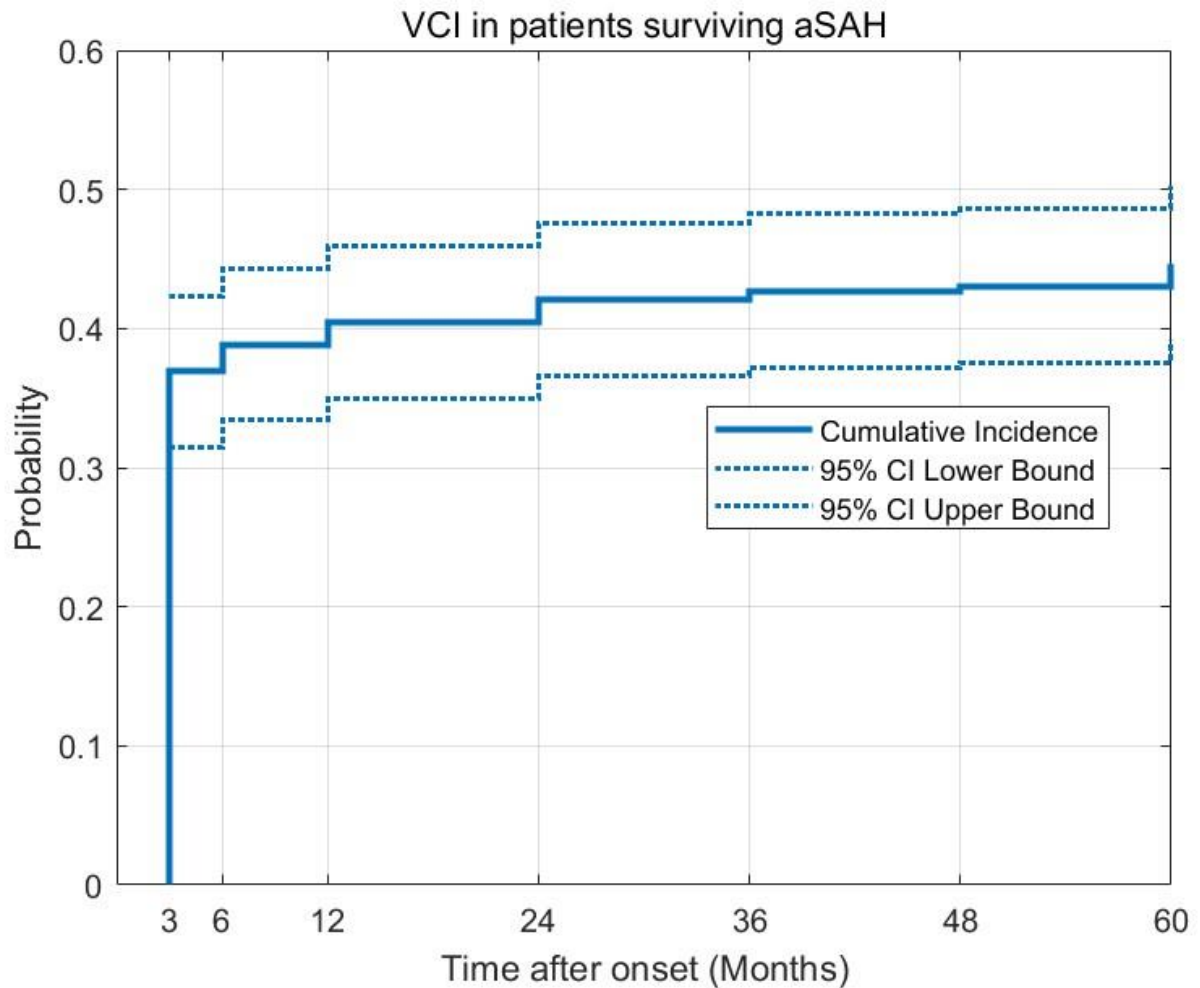
Among the included 309 patients, 36.9% of the patients were identified as having VCI at 3 months after onset. At 5 years after the onset, 138 patients (44.7%) were found to have VCI. The cumulative incidence of VCI is shown in Figure 1. Of the 138 patients suffering from VCI, 90 (65.2%) and 48 (34.8%) were classified as having minor and major VCI, respectively. At 3 months after the onset, the mean (SD) K-MMSE scores of mild and major VCI patients were 24.8±5.7 and 14.6±9.1, respectively. The mean (SD) FIM scores were 118.0±16.3 and 77.2±42.0 in mild and major VCI patients, respectively. At 5 years after the onset, the mean (SD) K-MMSE scores were 26.0±3.9 and 16.8±7.9 in mild and major VCI patients, respectively, while the mean (SD) FIM scores were 125.0±1.6 and 82.9±31.5 in mild and major VCI patients, respectively. The results for K-MMSE and FIM are shown in Figure 2 and 3, respectively.

Conclusion

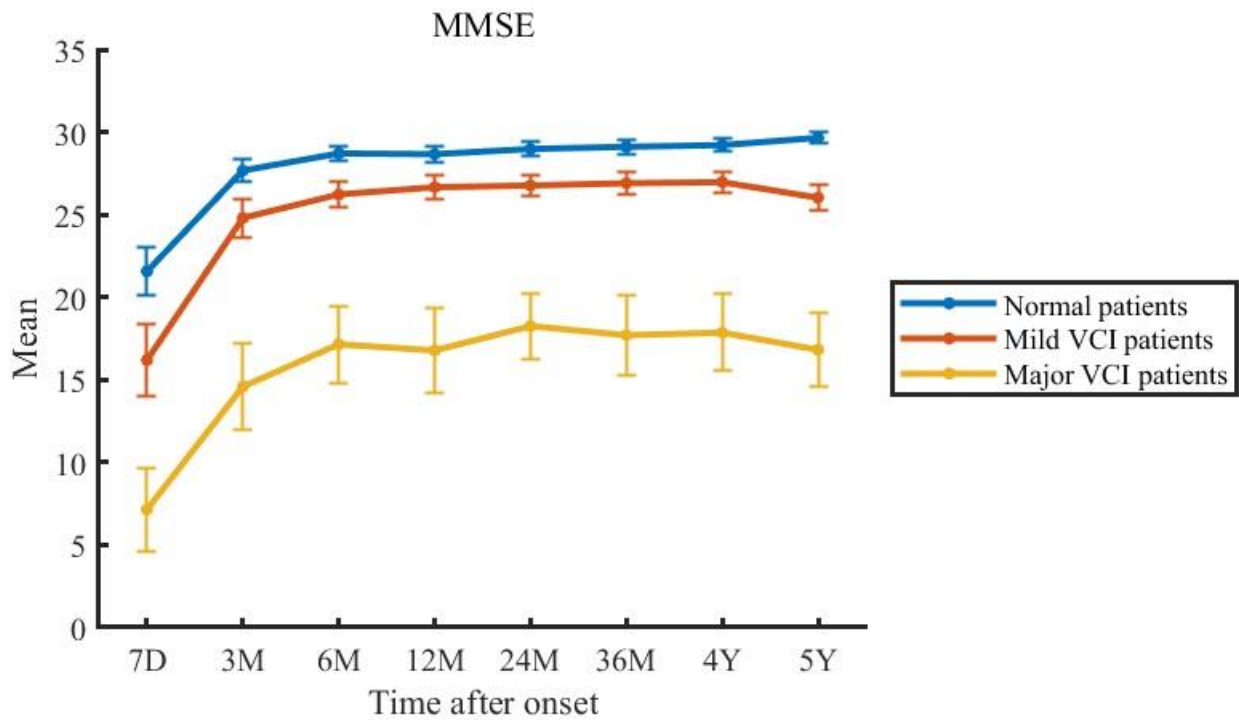
Patients surviving from aSAH are well-known to suffer from cognitive decline. In this study, we demonstrated the longitudinal trend in the incidence of VCI in patients with aSAH. We also identified the proportion of patients who

developed major VCI, or vascular dementia as defined by VCI associated with ADL dependence. These results could provide valuable information for patients and physicians in the management of cognitive impairment following aSAH.

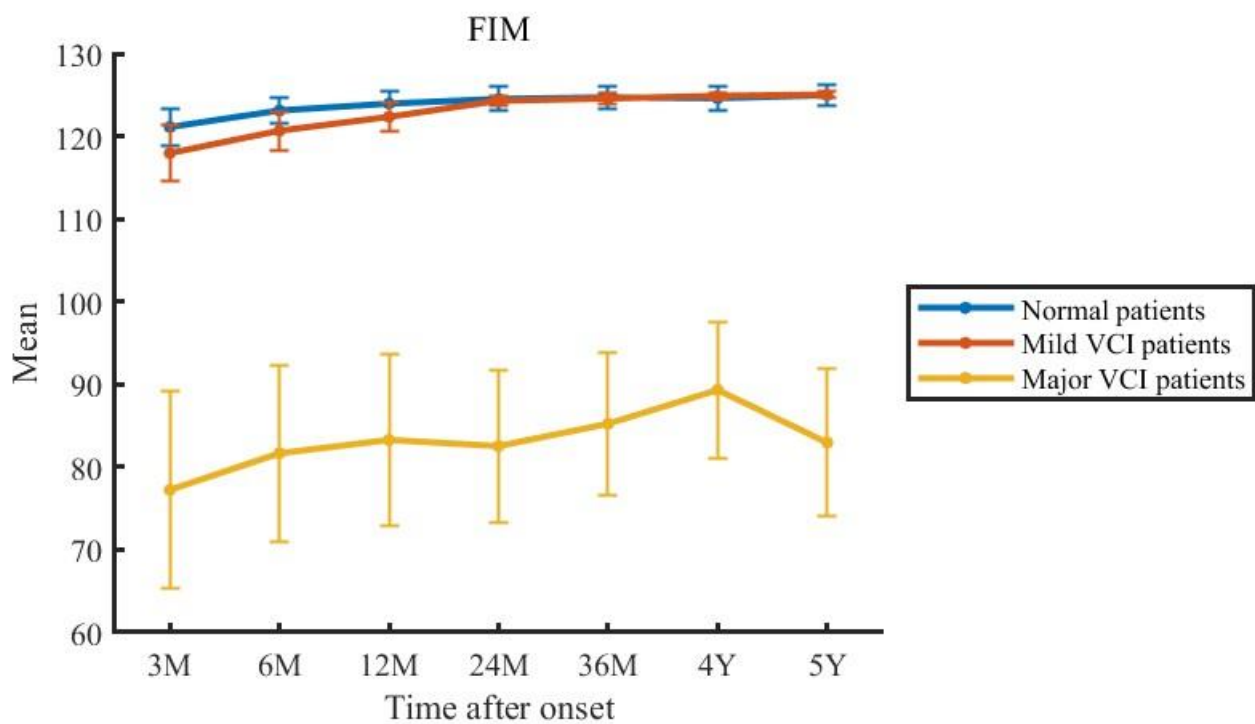
Acknowledgment This work was supported by the Research Program funded by Korea Disease Control and Prevention Agency (3300-3334-300-260-00, 2013-E33017-00, 2013E-33017-01, 2013E-33017-02, 2016-E33003-00, 2016-E33003-01, 2016-E33003-02, 2019-E3202-00, 2019-E3202-01, 2019-E3202-02, 2022-11-006).



The cumulative incidence of vascular cognitive impairment in patients surviving aSAH.



Cognitive levels measured by the K-MMSE in patients surviving aSAH.



Functional levels measured by the by the FIM in patients surviving aSAH.

Safety, Feasibility, and Efficacy of Complex Exercise for Community-Dwelling Stroke Patient

Jung-Lim Lee^{3*}, Yuna Kim³, Yong-Il Shin^{1,2,3}, Sungchul Huh^{1,2,3}, Sung-Hwa Ko^{1,2,3†}

Department of Rehabilitation Medicine, Pusan National University School of Medicine¹, Department of Rehabilitation Medicine, Pusan National University Yangsan Hospital², Research Institute for Convergence of Biomedical Science and Technology, Pusan National University Yangsan Hospital³

Introduction

Stroke is a leading cause of mortality and long-term disability worldwide, with many survivors exhibiting low levels of physical activity post-discharge. A complex exercise program can be a safe method to increase the low levels of physical activity and exercise volume in stroke patients. This pilot study investigates the effectiveness, safety, and feasibility of applying a complex exercise regimen to stroke patients residing in the community after discharge.

Method

This study is a single-group pilot study involving patients who received inpatient rehabilitation for motor impairment after a stroke. Participants performed a tailored complex exercise program, including stretching, aerobic exercise, strength training, and balance exercises, under the guidance of a health exercise specialist in a living lab within the hospital. The program was conducted three to five times weekly, with each session lasting 50 minutes, across a total of 20 sessions. Evaluations pre- and post-intervention included assessments of safety and validity, as well as physical function evaluations such as cardiopulmonary exercise testing (CPET) and various fitness tests (6-minute walk test, timed up-and-go test, chair stand test, figure-of-8 walk test, grip strength test, and sit-and-reach test). Additionally, depression was assessed using the Geriatric Depression Scale (GDS).

Result

A total of 22 subjects were recruited for the study, with one dropout due to fatigue and travel distance, resulting in 21 subjects completing the study. The characteristics of the subjects are presented in Table 1. Among the 21 completers, one subject experienced a mild adverse event (hypoglycemia), which was not a serious adverse event, and the majority of participants completed the study safely, confirming its safety. In the validity assessment, the exercise participation rate was 95.5%, and the exercise adherence rate averaged 95.2%, with all participants who completed the study achieving an adherence rate of over 80% (Table 2). In the CPET, only VO₂ peak showed significant improvement ($p < 0.05$). Fitness assessments demonstrated significant improvements in the 6-minute walk test, timed up-and-go test, chair stand test, figure-of-8 walk test, and grip strength ($p < 0.05$). There was no significant change in GDS scores ($p > 0.05$) (Table 3).

Conclusion

This study demonstrated that the complex exercise program is sufficiently safe and valid for stroke rehabilitation patients. The program significantly improves cardiopulmonary endurance, walking ability, balance, muscle strength, muscle endurance, and coordination.

Acknowledgment This work was supported by the National Research Foundation of Korea(NRF) grant funded by the Korea government(MSIT)(No. 2023M312A1009022)

Table 2. General characteristics in complex exercise group

Variable	Complex Exercise Group (n=21)
Age	59.48±11.38
Height (cm)	166.30±8.04
Weight (kg)	66.73±9.98
Time post stroke (Mon)	28.05±18.79
Sex	
Men	15(71.43%)
Women	6(28.57%)
Stroke type	
Ischemic	15(71.43%)
Hemorrhagic	6(28.57%)
Hemiparetic side	
Left	6(28.57%)
Right	15(71.43%)
Smoking	
Yes	5(23.81%)
No	16(76.19%)
Hypertension	
Yes	8(38.10%)
No	13(61.90%)
Diabetes	
Yes	6(28.57%)
No	15(71.43%)

Values are mean ± s.d.

General characteristics in complex exercise group

Table 2. Frequency of attendance and exercise adherence rate at individual intervention sessions

Participants	Consented to participate (n=22)		
	Total sessions attended	% sessions attended	% Adherence rate for exercise
1	19	95	100
2	20	100	98
3	20	100	96
4	20	100	100
5	20	100	100
6	20	100	95
7	20	100	100
8	20	100	100
9	17	85	100
10	20	100	100
11	20	100	94
12	3 (participant withdrew)	15	60
13	20	100	90
14	20	100	100
15	20	100	100
16	20	100	92
17	18	90	100
18	19 (1 Mild adverse event)	95	85
19	20	100	95
20	20	100	100
21	19	95	90
22	17	85	100

Frequency of attendance and exercise adherence rate at individual intervention sessions

Table 3. Effects of the structured individual complex exercise

Variable	Complex Exercise Group (n=21)		p
	Pre	Post	
VO ₂ peak (ml/kg/min)	25.14 ± 5.42	27.62 ± 5.91	0.000
Peak RER	1.15 ± 0.11	1.18 ± 0.11	0.078
VE/VCO ₂ slope	28.80 ± 6.77	29.45 ± 4.95	0.481
6-Minute walk test (m)	415.74 ± 117.90	508.64 ± 123.93	0.000
Timed up and go (secs)	11.27 ± 4.75	8.27 ± 3.46	0.000
Chair stand test (times)	17.48 ± 4.50	22.14 ± 6.43	0.000
Figure-of-8 Walk Test (secs)	43.58 ± 16.47	32.72 ± 15.04	0.000
Grip strength (kg)	29.06 ± 6.88	34.34 ± 7.73	0.001
Sit and Reach Test (cm)	3.80 ± 9.71	5.81 ± 8.68	0.228
GDS	12.57 ± 8.91	11.48 ± 9.24	0.275

Values are mean ± s.d.

Effects of the structured individual complex exercise

Interactive Multitouch Game Interventions Enhance Prefrontal Activity and Inter-Brain Synchrony

Jinuk Kim^{1*}, Eunmi Kim², Su-Hyun Lee², Gihyoun Lee^{3,4}, Yun-Hee Kim^{2,5†}

Center for Neuroscience Imaging Research, Institute for Basic Science (IBS)¹, Department of Physical and Rehabilitation Medicine, Sungkyunkwan University School of Medicine², Department of Biomedical Engineering, Chonnam National University³, School of Healthcare and Biomedical Engineering, Chonnam National University⁴, Department of Rehabilitation Medicine, Myongji Choonhey Rehabilitation Hospital⁵

Introduction

Digital game-based cognitive interventions can enhance cognitive functions in the elderly population. This study investigated the impact of interactive multitouch game-based cognitive interventions (ICIs) on prefrontal activity and connectivity related to cognitive flexibility as well as inter-brain synchrony among older adults.

Methods

In this single-blind randomized controlled trial, 32 elderly participants (13 men; mean age 74.5 ± 4.3 years) were divided into two groups: ICI group and traditional cognitive intervention (TCI) group. Both groups engaged in 12 sessions of 40-min cognitive training over a period of four weeks. The ICI group participated in gamified tasks on a multitouch screen designed for interactive play using HAPPYTABLE® (Spring Soft Co. Ltd, Seoul, Republic of Korea), whereas the TCI group participated in traditional individual tasks involving the use of paper and pencil. Changes in oxyhemoglobin (oxyHb) concentrations were measured using 20 channels of a functional near-infrared spectroscopy system (NIRScout®, NIRx Medical Technologies, Germany) during the color-word Stroop test before and after the tasks. Inter-brain synchrony was evaluated using the 20-channel topographic map per person through hyperscanning techniques across two participants during the intervention. Correlation analyses were conducted to evaluate intra- and inter-brain synchrony among participants.

Results

Significant improvement was observed in the interference scores and interference ratios of the Stroop test for the ICI group compared with the TCI group after ten sessions. The oxyHb concentration changes in the left dorsolateral prefrontal cortex (dlPFC) and right ventrolateral PFC (vlPFC) during Stroop interference were significantly different between the two groups. Connectivity between dlPFC, vlPFC, orbitofrontal cortex, and frontopolar cortex was also significantly increased in the ICI group after intervention. Remarkably, inter-brain synchrony was significantly greater in the ICI group compared to the TCI group at the dorsolateral prefrontal and orbitofrontal cortices during intervention.

Conclusion

Interactive multitouch game-based interventions improved cognitive flexibility, prefrontal activity and connectivity, and inter-brain synchrony in older adults. These findings might advocate the incorporation of interactive digital games into cognitive training programs as a viable strategy to modulate age-associated cognitive decline.

Acknowledgment This work was supported by the Korea Medical Device Development Fund grant funded by the Korean government (Ministry of Science and ICT, Ministry of Trade, Industry and Energy, Ministry of Health & Welfare, and Ministry of Food and Drug Safety) (KMDF-RS-2022-00140478) and National Research Foundation of Korea (NRF) grant funded by the Korean government (NRF-RS-2024-00343805).

Association between structural integrity of limbic system and cognitive function after MCA stroke

Youngkook Kim^{2†}, Jihye Park^{1*}

Department of Rehabilitation Medicine, Eunpyeong St. Mary's hospital, College of Medicine, The Catholic University of Korea¹, Department of Rehabilitation Medicine, Yeouido St. Mary's hospital, College of Medicine, The Catholic University of Korea²

Background

Post-stroke cognitive impairment (PSCI) is prevalent in patients with middle cerebral artery (MCA) infarctions. We hypothesized that prevalence of PSCI would differ between patients with superficial MCA territory infarctions and those with lenticulostriate artery (LSA) territory infarctions, and that PSCI in patients with MCA infarctions would correlate with the microstructural integrity of the limbic system.

Methods

We retrospectively analyzed the diffusion-tensor imaging (DTI) of 41 patients with stroke in the MCA territory (mean age: 73.6 ± 12.3 years; superficial MCA group, $n=24$; LSA MCA group, $n=17$). All patients underwent clinical evaluation using the NIH Stroke Scale (NIHSS), the modified Rankin Scale (mRS), the modified Barthel Index (MBI) and the Mini-Mental State Examination (MMSE) on the day of MRI examination. We evaluated the microstructural integrity of limbic system, focusing on the cingulum, uncinate fasciculus and fornix (Figure 1). We analyzed the association between the PSCI and the microstructural integrity of the limbic system.

Results

The initial MMSE, NIHSS and MBI were significantly lower in the superficial MCA group compared to the LSA MCA group (Table 1). Among the identified tracts of interest, significant decreases in fractional anisotropy (FA) were observed in the superficial MCA group compared to LSA MCA group in the bilateral cingulum and uncinate fasciculus. No statistically significant FA differences were found in the bilateral fornix. Univariate linear regression analysis showed that all tracts on both sides had a significant correlation with initial cognitive function (p-value

Conclusion

We found evidence that the microstructural integrity of the limbic system in patients with MCA infarctions correlates with initial cognitive function, particularly in the ipsi-lesional uncinate fasciculus. This tract showed the strongest correlation with cognitive function. Additionally, the microstructural integrity of both the cingulum and fornix was also reduced and correlated with initial cognitive function. These findings are considered crucial clues to elucidating the mechanisms underlying cognitive decline in patients with MCA infarctions.

	Lenticulostriate Group	Superficial MCA Group	P-value
Subjects, n	17	24	
Age, years	73.35(14.33)	73.75 (11.05)	0.921
NIHSS	8.35 (2.29)	13.88 (6.19)	<0.001*
mRS	4.06 (0.66)	4.42 (0.78)	0.120
MMSE (0–30)	21.29 (7.14)	9.13 (10.11)	<0.001*
MBI (0–100)	37.12 (21.61)	18.13 (26.42)	0.019*

Abbreviations: NIHSS, National Institutes of Health Stroke Scale; mRS, modified Rankin Scale; MMSE, Mini-Mental State Examination; MBI, Modified Barthel Index.

Values are expressed as the mean (standard deviation).

* Significant correlations are based on P-values of <0.05.

Table 1. Demographic and Clinical Characteristics of the patients with lenticulostriate and superficial MCA territory infarctions.

Models	<i>adjusted R²</i>	Significant variables	Unstandardized		Standardized β	t	P-value
			B	SE			
Uncinate fasciculus	0.675	<i>ipsi</i> -Uncinate fasciculus	114.865	36.963	0.367	3.108	0.004
		Age	-0.286	0.092	-0.338	-3.121	0.004
		NIHSS	-1.003	0.216	-0.546	-4.654	<0.001

Table 2. Multiple Linear Regression Models for initial cognitive functions using FA value of limbic system and clinical values.

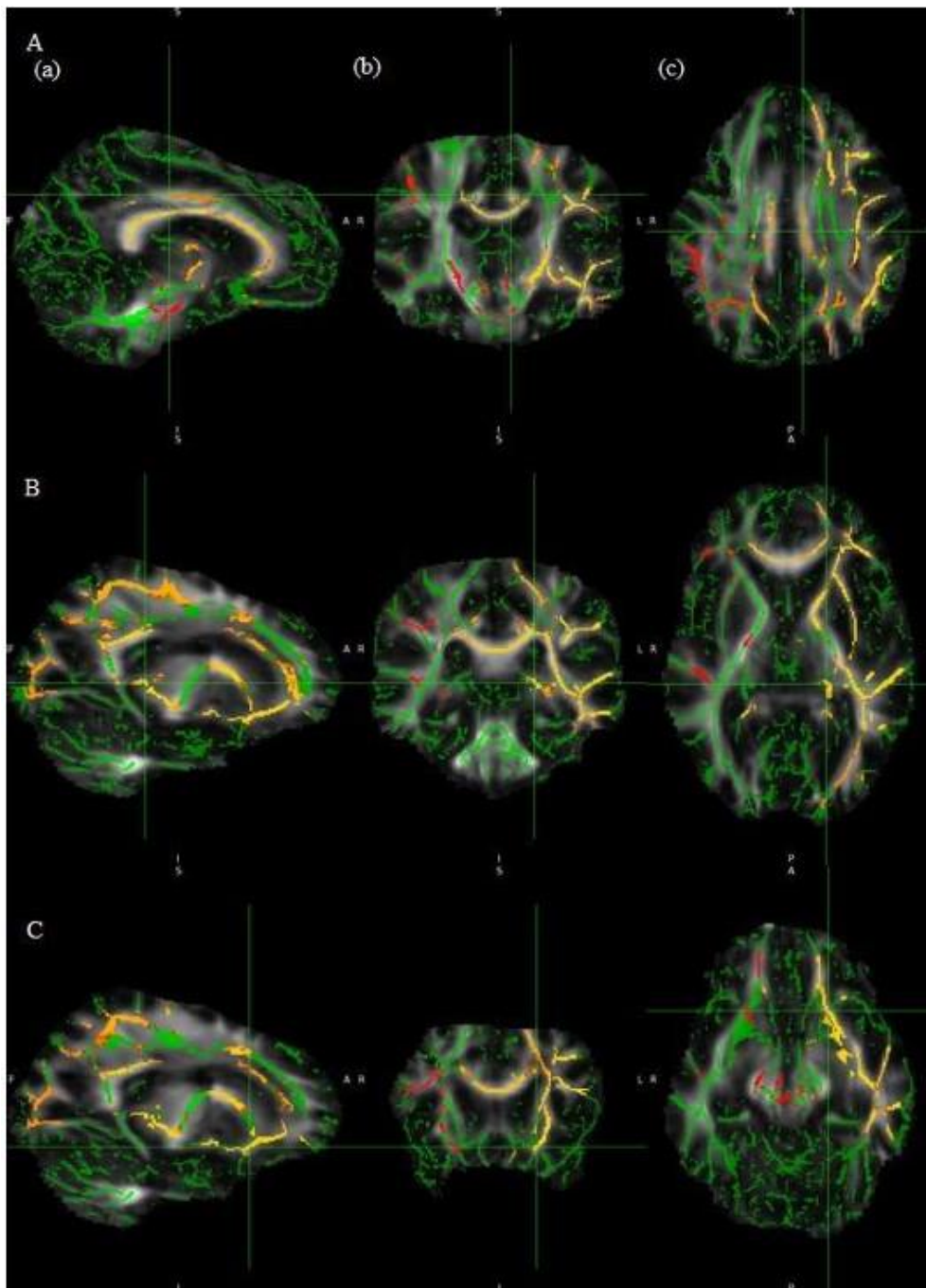


Figure 1. Color fractional anisotropy (FA) maps of diffusion-tensor imaging. (A) Sections for the cingulum; (a) sagittal (b) coronal (c) axial section image. (B) Sections for the fornix. (C) Sections for the uncinate fasciculus.

Investigating Brain Region Selection for Deep Learning-based Alzheimer's Disease Diagnosis

Hyunjin Kim^{1*}, Gyubin Kwon¹, Jungsoo Lee^{1†}

Department of Medical IT Convergence Engineering, Kumoh National Institute of Technology¹

Objective

Alzheimer's disease (AD) is a progressive neurodegenerative disorder characterized by cognitive impairment and significant atrophy of specific brain regions. Previous studies have demonstrated that focusing on specific brain regions as regions of interest (ROIs) can enhance diagnostic performance. This study investigates which brain regions, when utilized in the diagnosis of AD through deep learning methods, result in higher diagnostic performance. By investigating these regions, this study aims to determine whether they can serve as reliable biomarkers for AD diagnosis.

Methods

Four hundred thirty anatomical T1-weighted MRI data (231 cognitively normal (CN) and 199 AD) from Alzheimer's Disease Neuroimaging Initiative (ADNI) were divided into training, validation, and test sets to ensure reliable results. The segmentation tool FreeSurfer was used for ROI extraction. The selected ROIs included the bilateral hippocampus, amygdala, entorhinal cortex, fusiform gyrus, and parahippocampal gyrus, which are commonly utilized in AD research. For each selected ROI, the coordinates encompassing the entire ROI were determined, followed by cropping to extract the volumetric texture. A 3D-ResNet model was employed for AD diagnosis. The model was trained and evaluated using the left, right, and bilateral regions for each ROI, respectively. When bilateral ROIs were used, they were concatenated as different channels for direct input into the deep learning model. Balanced accuracy was used as a metric to measure the diagnostic performance of each ROI when the number of samples per class differed.

Result

The diagnostic performance for selected ROI, separated by left, right and bilateral regions, was as follows: hippocampus (0.759; 0.780; 0.775), amygdala (0.720; 0.747 0.753), entorhinal cortex (0.703; 0.742; 0.791), fusiform gyrus (0.646; 0.630; 0.535), and parahippocampal gyrus (0.710; 0.670; 0.730), respectively. The bilateral entorhinal cortex exhibited the highest performance. It was confirmed that examining both hemispheres simultaneously leads to better diagnostic outcomes.

Conclusion

This study demonstrates that selecting appropriate ROIs can significantly enhance diagnostic performance. Our findings indicate that using bilateral regions results in better diagnostic accuracy compared to unilateral regions. Specifically, the bilateral entorhinal cortex achieved the highest performance among the ROIs, surpassing the unilateral entorhinal cortex and other ROIs. Future work will involve incorporating additional ROIs and evaluating whether performance improvements can be achieved through various combinations of ROIs. Additionally, we plan to utilize data from patients with mild cognitive impairment (MCI) to investigate which ROIs serve as biomarkers for distinguishing between CN and MCI and between MCI and AD.

Acknowledgment This study was supported by the National Research Foundation of Korea (NRF) grant funded by the Korean government (MSIT). (No. RS-2023-00208884, No. RS-2023-00265824).

AI-based Classification of Dysphagia Severity Based on Voice and Cough Sound Analysis

Jeongeun Lee^{1*}, Han Gil Seo¹, Woo Hyung Lee¹, SungEun Hyun¹, Seo Jung Yun¹, Ha Yoon Kim¹, Hyun Mi Oh², Min-Yong Lee², Kiwook Lee³, Byung-Mo Oh^{1†}

Department of Rehabilitation Medicine, Seoul National University Hospital¹, Department of Rehabilitation Medicine, National Traffic Injury Rehabilitation Hospital², Department of Technology, Soundable Health, Inc³

Objective

Dysphagia can lead to serious health outcomes, making early diagnosis crucial. However, the standard diagnostic tests for dysphagia require expensive equipment and skilled operators, which makes them impractical for routine clinical use, especially in home-care setting. This underscores the need for a cost-effective, safe, and easy-to-use bedside screening tool. This study aimed to develop an advanced artificial intelligence (AI) model designed to classify the severity of dysphagia by analyzing patients' vocal and cough sound patterns.

Methods

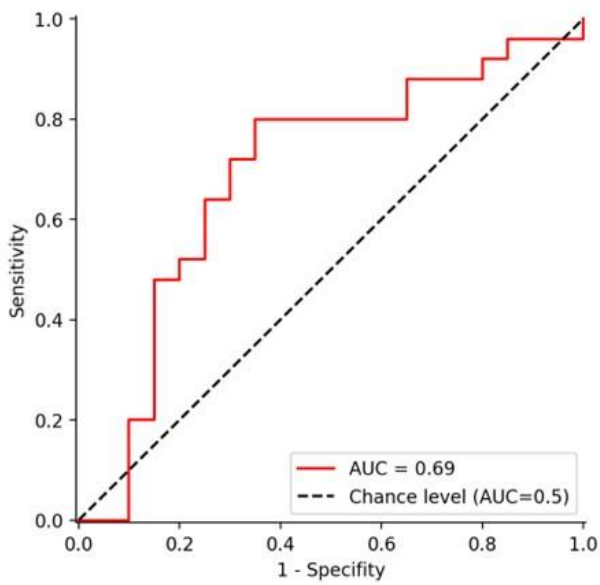
A total of 359 patients with dysphagia from various etiologies were recruited. All patients underwent a videofluoroscopic swallowing study (VFSS). The severity of dysphagia was assessed by clinicians using the Penetration-Aspiration Scale (PAS) and the Videofluoroscopic Dysphagia Scale (VDS). Voice vowels (/a/, /i/, /o/) and cough sounds were recorded using a microphone before and after VFSS. We used an AI modeling technique to determine if it could differentiate between no aspiration (PAS = 1) and aspiration (PAS ≥ 6), as well as between mild (VDS < 25) and severe dysphagia (VDS ≥ 47). Data were randomly divided into training, validation, and test sets with a ratio of 6:2:2. Binary classification models were developed for each outcome. For the vowel sounds, acoustic features with a high correlation to aspiration were selected for machine learning modeling. A deep learning module using cough sounds leverages transfer learning from a cough detection model trained with over 100,000 cough samples. This approach helps module learn the intrinsic characteristics of cough sounds, alleviating the scarcity of labeled dysphagia and cough data pairs. The outputs of these two models were then combined to improve overall predictive performance.

Results

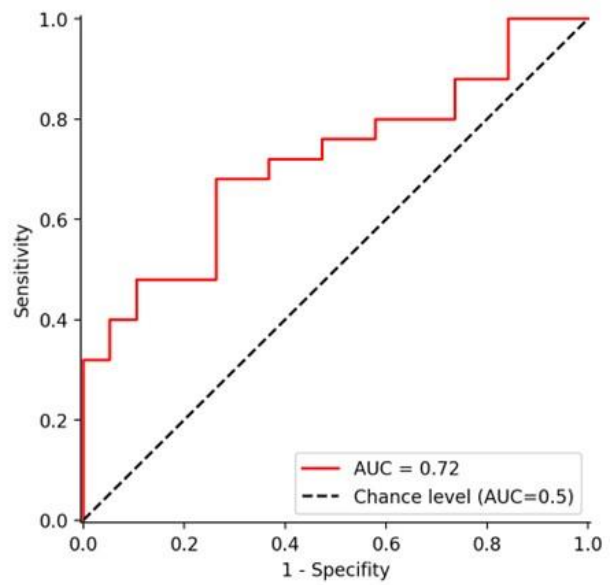
The AI model using pre-VFSS data identified aspiration more accurately than the model using post-VFSS data (area under the curve [AUC] = 0.72 vs. 0.69). For the VDS, the model using post-VFSS data performed better (AUC = 0.76 vs. 0.66) (Figure 1). Using the pre-VFSS voice and cough sounds from 229 patients, the AI model was able to distinguish between no aspiration and aspiration with a sensitivity of 80.0%, specificity of 65.0%, and accuracy of 73.3%. With post-VFSS voice and cough sounds from 194 patients, the AI model was able to distinguish between VDS < 25 and VDS ≥ 47 with a sensitivity of 100%, specificity of 56.5%, and accuracy of 73.0%.

Conclusion

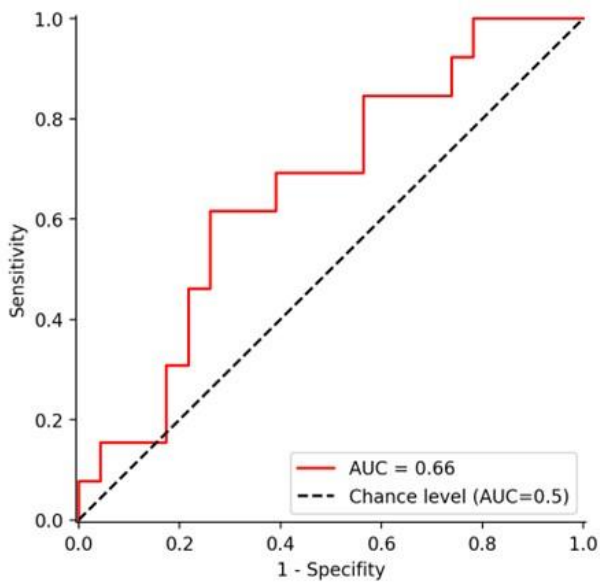
AI modeling using patients' voice and cough sounds appeared to have potential for the screening or monitoring of dysphagia, particularly in long-term care or home-care settings. This approach might help predicting or detecting the presence of aspiration or severe dysphagia.



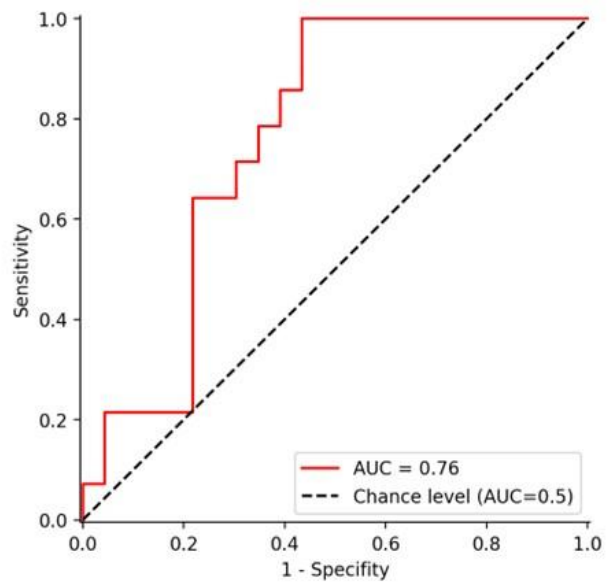
(a) Aspiration (pre-VFSS data)



(b) Aspiration (post-VFSS data)



(c) VDS (pre-VFSS data)



(d) VDS (post-VFSS data)

Figure 1. (a) Area under the curve (AUC) for identifying aspiration using pre-VFSS data, (b) AUC for identifying aspiration using post-VFSS data, (c) AUC for identifying severe dysphagia using pre-VFSS data (d) AUC for identifying severe dysphagia using post-VFSS data

Vascular Risk Factors correlated with Diagnosis of Parkinson's Disease in Patients with Stroke

Hyun Im Moon^{1*}, Joo Won Lee¹, Yong Wook Kim², Sang Chul Lee², Kun Wook Lee², Seo Yeon Yoon^{2†}

Department of Rehabilitation Medicine, Bundang Jeseang Hospital¹, Department and Research Institute of Rehabilitation Medicine, Yonsei University College of Medicine²

Introduction

Parkinson's disease (PD) is the most common and fastest growing neurological disorder and affects around seven million individuals globally. Stroke is the commonest medical problem in the elderly. Autopsy studies have shown that strokes such as cerebral infarction often coexist with PD pathology, and patients clinically diagnosed with PD usually have coexisting cerebral infarction. Given that point of common pathogenesis and shared preventive measure, relationship between PD and stroke could be clinically important. If ischemia is a common underlying factor for stroke and PD, identifying and controlling related risk factors may reduce the incidence of PD to some extent, such as efforts to control various vascular risk factors to prevent recurrence in stroke patients. Therefore, we aimed to find out how various vascular risk factors in patients of stroke are related to the occurrence of PD.

Methods

We used the records of the Korean National Health Insurance Service (NHIS), which is a mandatory health insurance coverage provided by the government to all Korean populations. We selected individuals who were newly diagnosed with stroke, defined as primary diagnosis according to ICD-10 codes (I60-I64) between 2008 and 2016. We only included individuals admitted to the hospital with a diagnosis of stroke based on brain imaging evaluations, such as magnetic resonance imaging or computed tomography. We conducted Cox proportional hazards analyses to evaluate the association of various risk factors, including socioeconomic status, lifestyle factors, and comorbidities, with the incidence of PD in individuals with stroke and estimated the hazard ratio (HR) and 95% confidence interval (CI). Stratified analyses according to sex and stroke type were also performed.

Results

Table 1 shows various risk factors for risk of PD occurrence. In individuals with stroke, former and current smoking showed significant association with reduced risk of PD. Alcohol consumption was also associated with decreased risk of PD in individuals with stroke. Physically active individuals with stroke showed reduced trend for PD occurrence. As for the association between comorbidities and PD risk, PD risk increased only in the DM duration ≥ 5 years group. The association of various factors with PD risk in individuals with stroke stratified by stroke type is presented in Figure 1.

Conclusion Several factors related to PD risk are those reported to be related to PD risk not only in stroke patients but also in the general population. However, since stroke patients already have more vascular risk factors than the general population, and the stroke itself has become a trigger to reduce brain reserves, we think it is a clinically meaningful study to analyze risk factors related to PD risk in the stroke patient group. Lifestyle interventions, including attention to controlling vascular risk factors such as DM, should be encouraged.

		N	PD	Person-years	Incidence rate	Model 1	P-value	Model 2	P-value	Model 3	P-value
Sex	Male	152,472	1,699	758,466.98	2.24	1.00 (0.93-1.07)		1.34 (1.23-1.46)		1.42 (1.30-1.54)	
	Female	132,327	1,575	704,011.1	2.24	1.00	0.9158	1.00	<.0001	1.00	<.0001
Age (years)	40-64	131,539	673	713,849.71	0.94	1.00	<.0001	1.00	<.0001	1.00	<.0001
	≥65	153,260	2,601	748,628.37	3.47	3.67 (3.37-3.99)		3.37 (3.08-3.68)		3.28 (3.00-3.58)	
Smoking	Never	183,093	2,382	954,014.59	2.50	1.00	<.0001	1.00	<.0001	1.00	<.0001
	Former	63,365	623	313,030.67	1.99	0.79 (0.73-0.87)		0.80 (0.72-0.88)		0.80 (0.72-0.88)	
	Current	38,341	269	195,432.82	1.38	0.55 (0.49-0.62)		0.67 (0.58-0.77)		0.66 (0.58-0.76)	
Alcohol consumption	Non	218,484	2,741	1,114,262.02	2.46	1.00	<.0001	1.00	<.0001	1.00	0.0003
	Moderate	55,630	458	291,815.14	1.57	0.64 (0.58-0.71)		0.80 (0.72-0.89)		0.83 (0.75-0.92)	
	Heavy	10,685	75	56,400.92	1.33	0.54 (0.43-0.68)		0.71 (0.57-0.90)		0.74 (0.59-0.94)	
Physically active	No	229,371	2,711	1,171,360.73	2.31	1.00	0.0001	1.00	0.0343	1.00	0.0508
	Yes	55,428	563	291,117.35	1.93	0.84 (0.76-0.92)		0.91 (0.83-0.99)		0.91 (0.83-1.00)	
DM	Normal	136,532	1,463	724,839.74	2.02	1.00	<.0001	1.00	<.0001	1.00	<.0001
	IFG	71,309	781	363,161.31	2.15	1.06 (0.97-1.16)		1.04 (0.95-1.13)		1.03 (0.95-1.13)	
	Incident DM	11,016	126	55,115.6	2.29	1.13 (0.94-1.36)		1.11 (0.93-1.34)		1.12 (0.93-1.34)	
	Duration < 5yr.	24,537	276	127,357	2.17	1.07 (0.94-1.22)		1.04 (0.91-1.19)		1.04 (0.91-1.19)	
	Duration ≥ 5yr.	41,405	628	192,004.43	3.27	1.61 (1.46-1.76)		1.39 (1.26-1.53)		1.38 (1.25-1.52)	
Dyslipidemia	Normal	82,713	1,078	446,979.73	2.41	1.00	0.0005	1.00	0.0012	1.00	0.0003
	Pre-dyslipidemia	46,038	545	257,968.12	2.11	0.88 (0.79-0.97)		0.93 (0.83-1.03)		0.93 (0.83-1.03)	
	Incident dyslipidemia	16,512	158	93,203.06	1.70	0.71 (0.60-0.83)		0.75 (0.63-0.89)		0.75 (0.64-0.89)	
	Controlled dyslipidemia	131,605	1,402	621,024.33	2.26	0.93 (0.85-1.00)		0.87 (0.80-0.94)		0.85 (0.78-0.92)	
	Uncontrolled dyslipidemia	7,931	91	43,302.85	2.10	0.87 (0.70-1.08)		0.91 (0.73-1.13)		0.86 (0.69-1.06)	

Table 1. Cox Proportional Hazard Regression Analysis of the Parkinson's Disease Risk in Individuals with Stroke

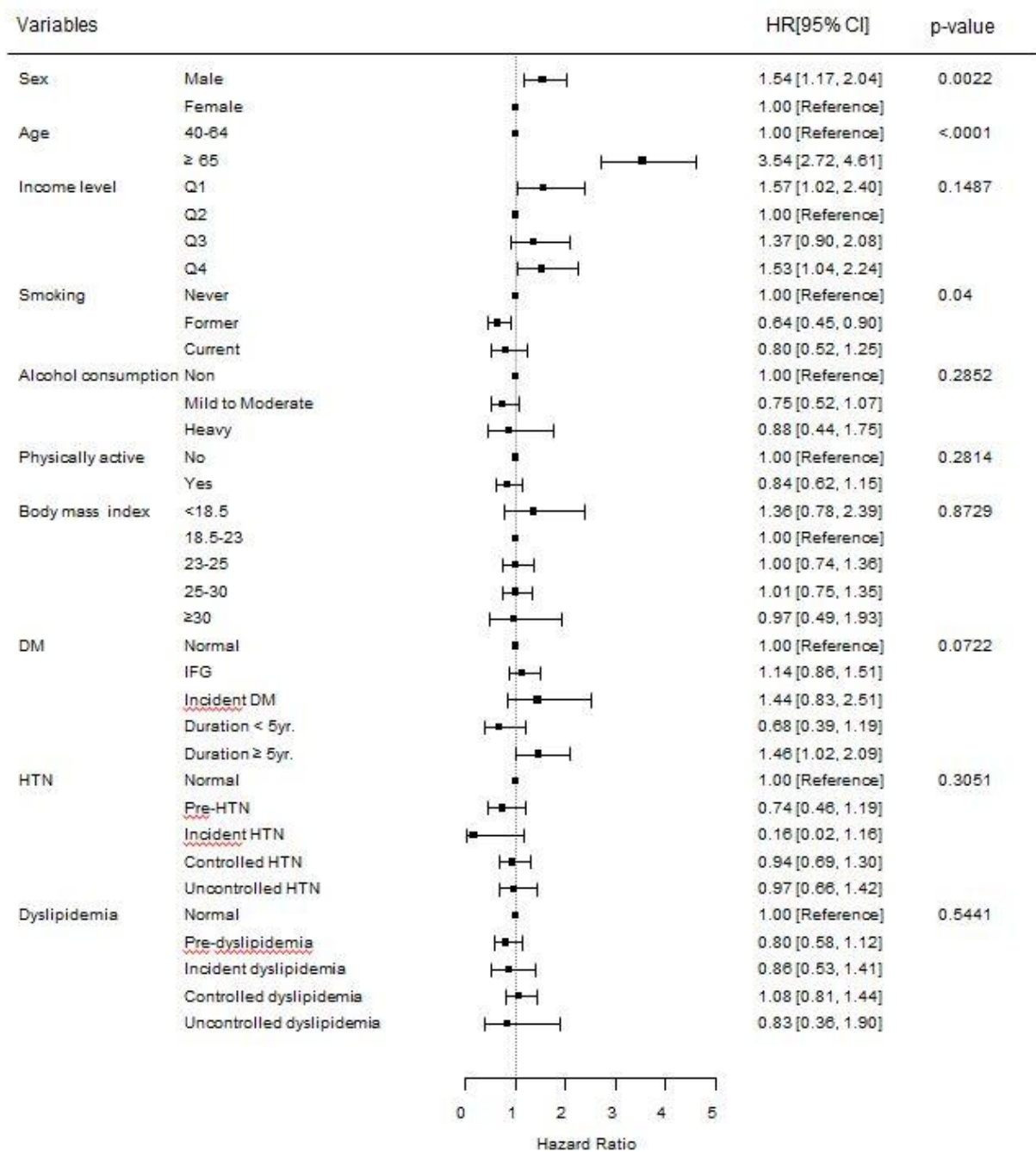


Fig 1. Various factors with PD risk in individuals with hemorrhagic stroke

Motor Tract Integrity Differences Among Gait Pattern Clusters in Chronic Stroke Patients

Jinuk Kim^{1*}, Eunmi Kim², Su-Hyun Lee², Jungsoo Lee^{3†}, Yun-Hee Kim^{2,4†}

Center for Neuroscience Imaging Research, Institute for Basic Science (IBS)¹, Department of Physical and Rehabilitation Medicine, Sungkyunkwan University School of Medicine², Department of Medical IT Convergence Engineering, Kumoh National Institute of Technology³, Department of Rehabilitation Medicine, Myongji Choonhey Rehabilitation Hospital⁴

Introduction

Chronic stroke results in varying degrees of motor impairment leading to different gait patterns. This study aimed to identify distinct gait pattern clusters among chronic stroke patients and compare motor tract integrity across these clusters.

Methods

Sixty-nine chronic stroke patients who had hemiparesis (49 males; mean age: 58.6 ± 11.7 years) but could walk independently participated. Participants underwent gait analysis using a motion capture system and diffusion tensor imaging (DTI) to assess motor tract integrity. A k-means cluster analysis was performed to cluster gait patterns based on 26 angles and moments parameters measured in the hip, knee, and ankle joints on the affected side. Fractional anisotropy (FA) values from DTI were used to evaluate the integrity of various motor tracts across different clusters. The FA maps were non-linearly registered to standard space using the spatial registration algorithm of the tract-based spatial statistics (TBSS) technique. The FA values were calculated by overlapping motor tract templates, including the corticospinal tract (CST) and alternative motor fibers (aMF) on the warped FA maps. Within the CST, additional FA values were extracted for subregions such as the superior corona radiata (SCR), posterior limb of the internal capsule (PLIC), cerebral peduncle (CP), and pyramids, as well as for subtracts originating from the primary motor cortex (M1), supplementary motor area (SMA), dorsal premotor cortex (PMD), and ventral premotor cortex (PMV). A Kruskal-Wallis test was used to examine differences in FA measures between gait pattern clusters. Additionally, a classification and regression tree (CART) analysis identified key factors of motor tract integrity in differentiating the clusters.

Results

A k-means cluster analysis identified four gait pattern clusters among 69 chronic stroke patients. Functional assessments including gait speed revealed significant differences between clusters. Analysis of FA values from DTI also showed significant differences in motor tract integrity across clusters. Specifically, significant differences were observed in the ipsilesional PLIC, CP, and pyramids among the CST subregions ($p < 0.05$). In addition, significant differences were found in the bilateral M1 and aMF, ipsilateral SMA and PMD ($p < 0.05$). The CART analysis identified that FA values of the ipsilesional M1 and pyramid as the primary factors differentiating between the more severe clusters and milder clusters.

Conclusion

This study identified distinct gait pattern clusters among chronic stroke patients and revealed significant motor tract integrity differences across these clusters. Further study is needed to utilize these results for developing individualized rehabilitation strategies in chronic stroke patients.

Acknowledgment This work was supported by the Korea Medical Device Development Fund grant funded by the Korean government (Ministry of Science and ICT, Ministry of Trade, Industry and Energy, Ministry of Health & Welfare, and Ministry of Food and Drug Safety) (KMDF-RS-2022-00140478) and National Research Foundation of Korea (NRF) grant funded by the Korean government (NRF-RS-2024-00343805, NRF-RS-2023-00208884).

Detection of Freezing of Gait in Parkinson's Disease from Foot-pressure Sensing Insoles

Chang-Won Moon^{1,2*}, Jae-Min Park³, Byung Chan Lee⁴, Eungseok Oh⁵, Juhyun Lee⁶, Won-Jun Jang³, Kyeongil Min⁴, Yesung Jung², Yeong-Min Kim², Si-Hyeon Lee³, Kang Hee Cho^{1,2†}

Department of Rehabilitation Medicine, Chungnam National University College of Medicine¹, Department of Rehabilitation Medicine, Chungnam National University Hospital², School of Electrical Engineering, Korea Advanced Institute of Science and Technology (KAIST)³, Department of Physical Medicine and Rehabilitation, Chung-Ang University Hospital⁴, Department of Neurology, Chungnam National University Hospital⁵, Department of Biomedical Institute, Chungnam National University⁶

Backgrounds

Freezing of gait (FoG) is a common and debilitating symptom of Parkinson's disease (PD) that can lead to falls and reduced quality of life. Wearable sensors have been used to detect FoG, but current methods have limitations in accuracy and practicality. In this paper, we aimed to develop a deep learning model using pressure sensor data from wearable insoles to accurately detect FoG in PD patients.

Methods

We recruited 14 PD patients and collected data from multiple trials of a standardized walking test using the pedar insole system. We proposed temporal convolutional neural network (TCNN) and applied rigorous data filtering and selective participant inclusion criteria to ensure the integrity of the dataset. We mapped the sensor data to a structured matrix and normalized it for input into our TCNN. We used a train-test split to evaluate the performance of the model.

Results

We found that TCNN model achieved the highest accuracy, precision, sensitivity, specificity, and F1 score for FoG detection compared to other models. The TCNN model also showed good performance in detecting FoG episodes, even in various types of sensor noise situations.

Conclusions

We demonstrated the potential of using wearable pressure sensors and machine learning models for FoG detection in PD patients. The TCNN model showed promising results and could be used in future studies to develop a real-time FoG detection system to improve PD patients' safety and quality of life. Additionally, our noise impact analysis identifies critical sensor locations, suggesting potential for reducing sensor numbers.

Acknowledgment This research was supported by Chungnam National University Hospital Research Fund, 2021.

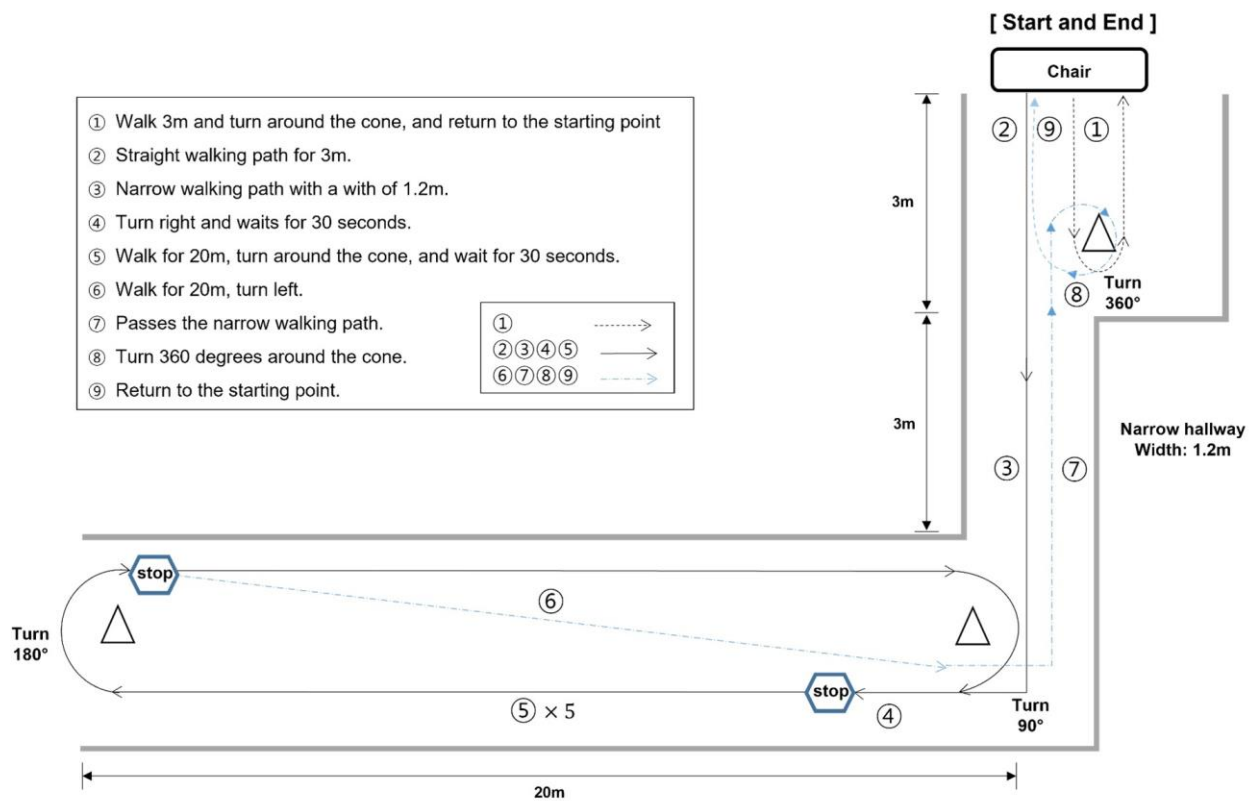


Illustration of the walking test path. The walking path was meticulously designed to incorporate scenarios where each distinct type of FoG could be observed. FoG can manifest in several ways, categorized into five types: 1) start hesitation, 2) turn hesitation, 3) apparent hesitation in tight quarters, 4) destination hesitation, and 5) open space hesitation

Table 1. Comparison of performance metrics across different models and sensor positions for the FoG detection task.

	Model	Raw	Big toe	Forefoot	Heel
Accuracy	LSTM	0.69	0.63	0.63	0.69
	CNN	0.98	0.89	0.77	0.93
	TCNN	0.99	0.90	0.58	0.97
Precision	LSTM	0.04	0.03	0.03	0.03
	CNN	0.36	0.08	0.03	0.01
	TCNN	0.68	0.08	0.03	0.10
Sensitivity	LSTM	0.74	0.76	0.76	0.66
	CNN	0.70	0.54	0.47	0.02
	TCNN	0.88	0.49	0.93	0.14
Specificity	LSTM	0.69	0.63	0.63	0.69
	CNN	0.98	0.89	0.78	0.94
	TCNN	0.99	0.91	0.57	0.98
F1 Score	LSTM	0.07	0.06	0.06	0.06
	CNN	0.48	0.13	0.06	0.01
	TCNN	0.76	0.14	0.07	0.12
TP	LSTM	2,195	2,262	2,260	1,963
	CNN	2,099	1,606	1,401	72
	TCNN	2,623	1,454	2,771	423
FP	LSTM	56,746	67,834	67,426	55,655
	CNN	3,693	19,477	40,046	10,875
	TCNN	1,253	16,868	78,126	3,741
TN	LSTM	125,066	113,978	114,386	126,157
	CNN	178,119	162,335	141,766	170,937
	TCNN	180,559	164,944	103,686	178,071
FN	LSTM	790	723	725	1,022
	CNN	886	1,379	1,584	2,913
	TCNN	362	1,531	214	2,562




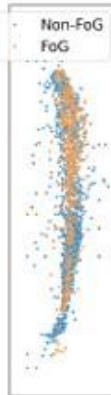


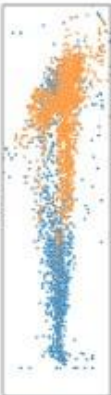

FoG: Freezing of Gait, LSTM: Long Short-Term Memory, CNN: Convolutional Neural Network, TCNN: Temporal Convolutional Neural Network

TP: True Positives, FP: False Positives, TN: True Negatives, FN: False Negatives.

FoG and non-FoG episodes are considered positive and negative, respectively.

Comparison of performance metrics across different models and sensor positions for the FoG detection task.

Table 2. CoP scatter plot and performance of TCNN for individual test datasets.

	ID: 1		ID: 2		ID: 3		ID: 4	
								
Setup	Sensitivity	Specificity	Sensitivity	Specificity	Sensitivity	Specificity	Sensitivity	Specificity
Raw	0.81	0.99	0.68	0.99	1.00	1.00	0.96	1.00
Big toe	0.93	0.83	0.39	0.86	0.90	1.00	0.44	1.00
Forefoot	0.24	1.00	1.00	0.00	0.84	0.82	1.00	0.00
Heel	0.04	1.00	0.57	0.90	0.00	1.00	0.00	1.00

FoG: Freezing of Gait, CoP: Center of Pressure, TCNN: Temporal Convolutional Neural Network.

FoG and non-FoG episodes are considered positive and negative, respectively.

CoP scatter plot and performance of TCNN for individual test datasets.

Development of Assistive Posture for Safe Swallowing in Amyotrophic Lateral Sclerosis

Tae Hoon Kim^{1*}, Mi Jung Kim¹, Ki Wook Oh², Seung Hyun Kim², Jun Yup Kim^{1†}

Department of Rehabilitation Medicine, Hanyang University Medical Center¹, Department of Neurology, Hanyang University Medical Center²

Introduction

Swallowing kinematics has been used in research on various diseases to develop new swallowing assistances. We designed a quantitative evaluation method by modifying previously published kinematic analysis tool that precisely measure swallowing kinematics. Using this, we sought to devise a swallowing assistance posture that could help alleviate hazardous swallowing by correcting anatomical positions of swallowing in amyotrophic lateral sclerosis (ALS).

Methods

A retrospective cross-sectional study was performed by analyzing videofluoroscopic swallowing study (VFSS) of swallowing 10 mL diluted barium solution. As a quantitative analysis tool, modified ASPEKT (mASPEKT), which was derived by adding several combinations of variables to the preexisting analysis tool, ASPEKT, was designed (Figure). One of the both variables for the correlation analyses was each of the amount of airway invasion during swallow reflex, penetration-aspiration scale score during swallow reflex, and total pharyngeal residue area after swallow, which are the swallowing safety-related variables. Another variable for correlation analyses was derived by compositing modifiable kinematic variables in three planes (horizontal-X, vertical-Y, and straight-XY) into one proxy variable using factor analysis (Figure (B)). For correlation analyses, false discovery rate correction by Benjamini-Hochberg method were implemented because of increased Type-I error chance by multiple comparisons.

Results

One VFSS file per subject was obtained from 117 subjects whose video quality was verified and who were diagnosed with ALS without any medical history that could affect swallowing function. 53% were male, 38.5% showed bulbar onset, 33.3% showed airway invasion during swallow reflex, and 91.5% showed pharyngeal residue after swallow. The median (1st quartile - 3rd quartile) was 60 (53-67) years old for onset age, 18 (12-25.3) months for onset duration, 33 (25-37) for ALS functional rating scale-revised (ALSFRRS-R) bulbar score, and 3 (2-3) for ALSFRS-R swallowing score. The amount or depth of airway invasion during swallow reflex did not show a significant Spearman correlation with the modifiable kinematic variables, and the amount of pharyngeal residue after swallow reflex showed significant inverse correlation to the distance between the menton (MT) and anteroinferior corner of the 4th cervical vertebral body (C4) at hyoid burst onset (HYB) and farthest displacement of hyoid bone from C4 (FAR). The correlation coefficients were -0.32 ($P < 0.001$) and -0.28 ($P < 0.01$) at HYB and FAR, respectively. These significances were maintained even in correlation analyses with subjects with only cases of airway invasion or post-swallow existences.

Conclusion

Pushing menton, or chin-tip, during the swallowing reflex has shown potential for reducing amount of post-swallow pharyngeal residues, which is an independent risk factor for development of aspiration pneumonia in ALS.

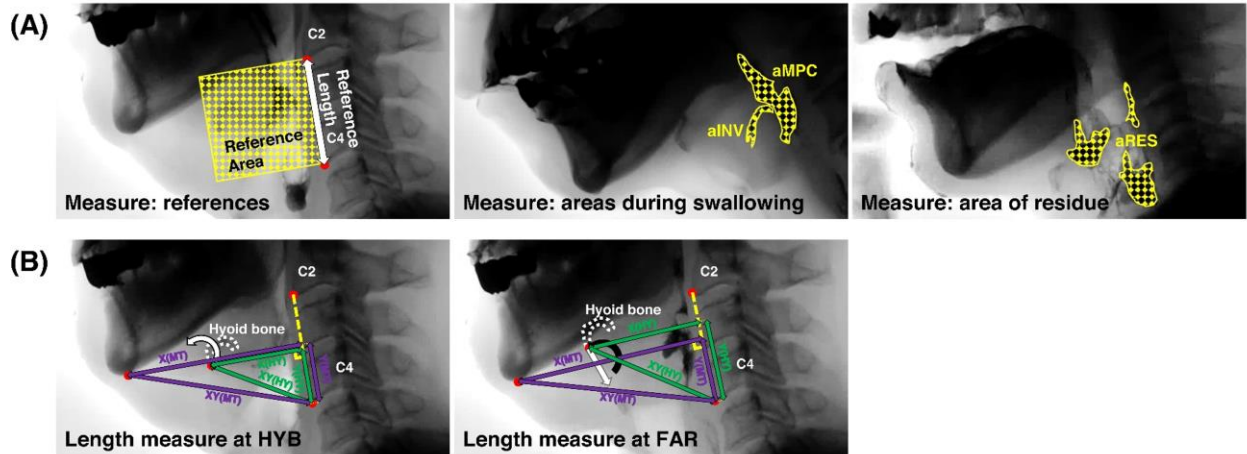


Figure. (A) Measurement of the reference distance, reference area, and area variables of the 'modified ASPEKT (mASPEKT)', **(B)** Measurement of the distances and two events by hyoid bone position

Abbreviations: aINV = area of bolus at maximum airway invasion during swallow; aMPC = area of bolus obliterated at the maximum pharyngeal constriction; aRES = area of post-swallow total residue; FAR = farthest displacement of hyoid bone from C4; HY = anteroinferior corner of the hyoid bone; HYB = hyoid burst onset; MT = menton.

Figure. (A) Measurement of the reference distance, reference area, and area variables of the 'modified ASPEKT (mASPEKT)', (B) Measurement of the distances and two events by hyoid bone position Abbreviations: aINV = area of bolus at maximum airway invasion during swallow; aMPC = area of bolus obliterated at the maximum pharyngeal constriction; aRES = area of post-swallow total residue; FAR = farthest displacement of hyoid bone from C4; HY = anteroinferior corner of the hyoid bone; HYB = hyoid burst onset; MT = menton.

Language network difference between anomic and global aphasia

Kim, KyuJin^{1*}, Yoo, Woo-Kyoung^{1†}

Department of Physical Medicine & Rehabilitation, Hallym University Sacred Heart Hospital¹

Purpose

The language network in the brain is extensively distributed across various tracts, including the arcuate fasciculus, superior longitudinal fasciculus, frontal aslant tract, and middle longitudinal fasciculus. This study aims to investigate whether the structural integrity of these language-related tracts can be linked to the prognosis of patients with aphasia.

Subjects & Methods

In this retrospective study, we compared two groups of patients: those diagnosed with anomic aphasia and those with global aphasia at the time of discharge (approximately four weeks post-onset). All patients underwent diffusion tensor imaging (DTI) during admission. Seven patients were included in anomic aphasia group (age: 57.7 ± 14.1 , M:F=3:4) and 6 patients were global aphasia group (age: 61.5 ± 12.1 , M:F=2:4) classified by K-WAB. The classification of aphasia was carried out using the Korean version of the Western Aphasia Battery (K-WAB). The average K-WAB score for the anomic group was 70.8 ± 22.7 , while the global group scored 2.8 ± 4.5 . All patients had experienced left hemisphere strokes, and we focused on fiber tracts from the left hemisphere only. For tractography, we utilized FSL and FreeSurfer software to acquire parameters including tract volume, average length, fractional anisotropy (FA), mean diffusivity (MD), axial diffusivity (AD), and radial diffusivity (RD) for the arcuate fasciculus (AF), superior longitudinal fasciculus (SLF1, 2, 3), middle longitudinal fasciculus (MLF), and frontal aslant tract (FAT). Comparative analysis of these parameters between the groups was conducted using t-tests, and correlation analysis was performed between the K-WAB scores and diffusion metrics.

Results:

1. The tract volume and average length of tract was not different between groups. 2. FA value of FAT ($p = 0.046$), MLF ($p = 0.049$) and SLF3 ($p = 0.048$) was different between groups, which was larger in anomic group. 3. Correlation between K-WAB and diffusion metrics showed 0.56 only in FAT FA.

Conclusions

The findings of this study suggest that multiple language-related tracts should be assessed to interpret the structural integrity in cases of aphasia. The significant differences in FA values between the anomic and global aphasia groups may indicate that certain tracts play a crucial role in the language recovery process. Further research is needed to explore the implications of these findings on treatment strategies for aphasia rehabilitation.

Effect of Eccentric Resistance Exercise on Chronic Stroke Recovery: A Randomized Trial

Younji Kim^{1*}, Chae Hyeon Lee³, Seung-Lyul Oh⁴, Dae Young Kim⁵, Jae-Young Lim^{2†}

Department of Rehabilitation Medicine, Ewha Womans University Seoul Hospital¹, Department of Rehabilitation Medicine, Seoul National University Bundang Hospital², Department of Rehabilitation Medicine, Seoul National University Hospital³, Department of Rehabilitation Medicine, Aging and Mobility Biophysics Laboratory, Seoul National University Bundang Hospital⁴, Senior Exercise Rehabilitation Laboratory, Department of Gerokinesiology, Kyungil University⁵

Purpose

This study aims to investigate the effects of eccentric contraction-based resistance exercise using a flywheel on functional recovery and muscle strength in chronic stroke patients. Given the potential of eccentric exercises to induce muscle adaptations and enhance physical performance, this research evaluates its efficacy compared to conventional resistance training.

Subjects and Methods

The study employed an 8-week single-center, prospective, parallel-group randomized controlled trial design involving 40 chronic stroke patients with sarcopenia. Participants were randomized into an intervention group (INT, n=20) receiving eccentric overload resistance exercise with a flywheel and a task-oriented home exercise program, and a control group (CON, n=20) undergoing usual care and conventional resistance training. Both groups were assessed at baseline and post-intervention for muscle strength and physical function using isokinetic testing and various physical performance measures. Data analysis included mixed-methods ANOVA and nonparametric tests to evaluate the changes within and between groups.

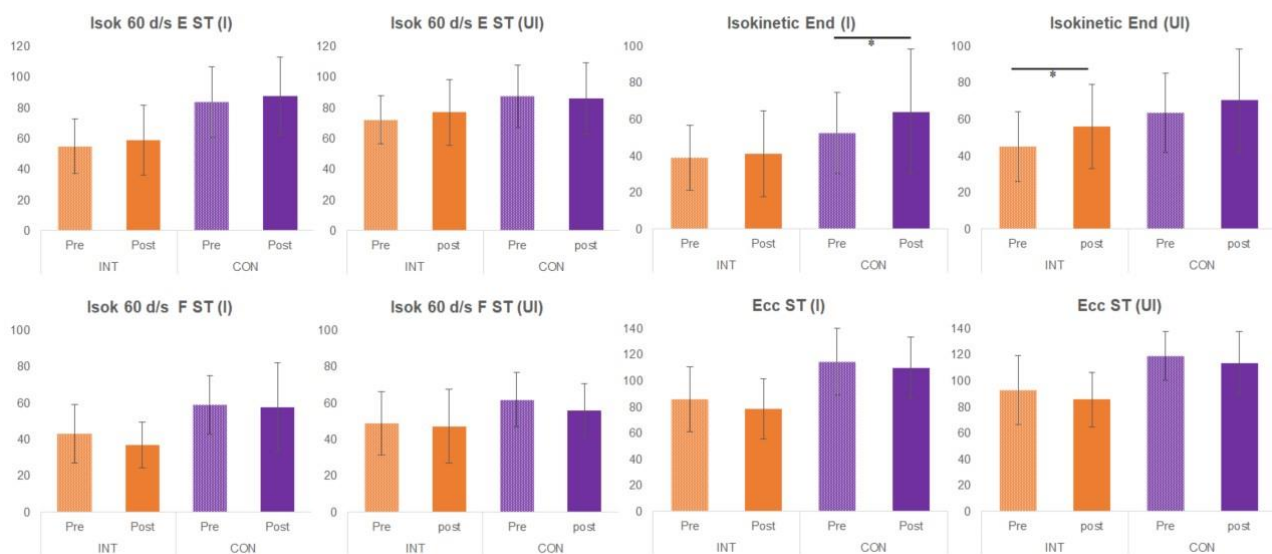
Results

Of the initial 40 participants, 36 completed the study (INT: n=18; CON: n=18). Both groups showed significant improvements in physical function measures such as gait speed, balance, and functional mobility post-intervention. However, no significant differences were observed between the groups in terms of lower extremity muscle strength. Specifically, the intervention group showed a significant increase in isokinetic endurance on the unimpaired side ($p=0.019$), while other measures of lower extremity strength did not show significant differences.

Conclusion

The study demonstrated that both eccentric contraction-based resistance exercise and conventional exercise programs significantly improved physical performance in chronic stroke patients. Despite the absence of significant intergroup differences, the significant within-group improvements highlight the value of structured exercise in stroke rehabilitation. The entrenched neuromuscular adaptations in chronic stroke patients and the short intervention duration likely contributed to these results. Future research with longer durations and larger sample sizes is necessary to fully understand the benefits of eccentric training in this population.

Acknowledgment This study was supported by the Rehabilitation Research & Development Support Program (#NRCRSP-EX20010), National Rehabilitation Center, Ministry of Health and Welfare, Korea.



Primary outcome variables before and after the interventions between the group

Characteristics	Intervention group(n=18)	Control group(n=18)	p-value
Age (years)	68.11±7.15	64.00±8.16	0.117
Gender (M : F)	13:5	14:4	>0.05
Height (cm)	163.72±7.55	165.69±7.20	0.429
Weight (Kg)	64.41±9.40	70.88±9.24	0.045*
BMI (kg/m ²)	24.00±2.91	25.86±3.22	0.078
Duration of stroke (yr)	3.11±3.64	3.33±1.65	0.815
Brain laterality (n)			0.440
Left	4	3	
Right	7	10	
Bilateral	0	0	
Undertermined	7	5	
Stroke type (n)			0.710
Hemorrhagic stroke	4	6	
Ischemic stroke	14	12	
Waist circumference (cm)	87.11±7.90	91.64±6.97	0.077
Hip circumference (cm)	93.78±5.24	97.33±4.79	0.041*
Waist-Hip ratio	0.92±0.05	0.94±0.05	0.447
Thigh circumference (cm)			
Involved side	48.19±3.46	51.65±4.21	0.011*
Uninvolved side	49.44±3.91	51.77±4.60	0.112
Calf circumference (cm)			
Involved side	33.89±2.26	36.78±2.53	<0.001*
Uninvolved side	34.47±2.22	36.78±2.53	0.004*
Body composition			
MM (kg)	40.16±6.69	44.52±6.41	0.054
SMM (kg)	22.85±4.19	25.74±4.05	0.043*
LBM (kg)	42.70±7.05	47.31±6.80	0.054
TFM (kg)	21.71±6.50	23.57±6.05	0.380
PBF (%)	33.48±7.64	33.09±6.82	0.871
ASM (kg)	18.07±3.56	20.31±3.27	0.058
ASMI	6.67±0.85	7.34±0.72	0.015
FAC			0.105
3	3	0	
4	1	0	
5	14	18	
MMSE	28.06±1.59	28.61±1.04	0.223
MBI	105.00 [101.50-105.00]	105.00 [105.00-105.00]	0.226
EQ5D	6.00[5.00-13.00]	7.00 [5.00-8.00]	0.443

BMI, Body mass index; MM, Muscle mass; SMM, skeletal muscle mass; LBM, Lean body mass; TFM, Total fat mass; PBF, Percent body fat; ASM, Appendicular skeletal muscle mass; FAC, Functional Ambulatory Category; MMSE, Mini-Mental State Exam; MBI, Modified Barthel Index; EQ5D, European Quality of Life 5 Dimensions Questionnaire

*P-value < 0.05.

† Values are expresses as mean ±SD or median [Interquartile range].

Baseline characteristics of the participants

Factor	INT (n=18)			CON (n=18)			Change Diff
	Pre	Post	p-value	Pre	Post	p-value	p-value
Physical function							
SPPB (score)	10.50 [5.50-12.00]	11.5 [7.50-12.0]	0.039*	12.00 [9.00-12.00]	12.00 [11.00-12.00]	0.157	0.846
5TSTS (s)	12.00 [10.50-19.48]	12.03 [10.08-17.02]	0.306	11.59±3.66	9.95±2.20	0.013*	0.499
TUG (s)	9.21 [7.70-22.90]	8.67 [7.29-14.00]	0.017*	8.77±2.12	7.99±1.91	0.002*	0.152
6mWT (m)	374.67±167.70	462.50 [299.50-537.25]	0.004*	453.76±71.79	493.65±81.42	<0.001*	0.843
Gait speed (m/s)	0.95±0.42	1.17 [0.72-1.34]	0.035*	1.19±0.21	1.27±0.21	0.047*	0.863
BBS (score)	54.00 [44.00-55.00]	55.50 [50.75-56.00]	0.008	56.00 [52.00-56.00]	56.00 [55.75-56.00]	0.017	0.478

SPPB, Short physical performance battery; 5TSTS, 5-times sit to stand test; TUG, Timed up & go test; 6mWT, 6 minute walk test; 6mGS, ; BBS, Berg balance test

Values are expresses as mean ±SD or median [Interquartile range].

* P-value < 0.05.

† P-values were calculated by independent t-test and Wilcoxon signed rank test

Changes in physical function and muscle strength

Comparative Analysis of Gait Dynamics Using Digital Insoles Through AI Classification

Young-Hwan Lim¹, Chang-Hwan Ahn¹, Yu-Sun Min^{1,2*†}

Department of Rehabilitation Medicine, Kyungpook National University Chilgok Hospital¹, Department of Rehabilitation Medicine, School of Medicine, Kyungpook National University²

Introduction

The Neurogait digital insole is a revolutionary health device designed to measure real-time dynamic plantar pressure and Center of Mass (COM) changes via Bluetooth connectivity to a mobile application. This study aims to leverage the data collected from Neurogait insoles to compare the gait characteristics of stroke patients, Parkinson's patients, and healthy individuals using AI classification techniques.

Methods

Data Collection: The study utilized NeuroGait insoles to gather detailed foot pressure and COM data during walking sessions. The data was collected from three groups: stroke patients, Parkinson's patients, and healthy individuals. Each dataset included variables such as timestamp, pressure values, acceleration, gyroscopic data, and temperature.

Data Preprocessing: The initial data preprocessing involved handling missing values through forward and backward filling methods. Features were extracted based on time (e.g., speed), sensor readings, and pressure distribution. The dataset was then split into training and testing sets, and standardization was applied to normalize the data.

AI Classification: A Random Forest Classifier was chosen for the classification task due to its robustness and interpretability. Cross-validation was employed to evaluate the model's performance, ensuring reliability and preventing overfitting. The classifier was trained on the processed data to distinguish between the three groups based on their gait patterns.

Results

The Random Forest Classifier demonstrated significant accuracy in classifying the gait data into the three groups. Key features contributing to the classification were identified, including specific pressure values, acceleration, and gyroscopic data. The model achieved high cross-validation scores, confirming its effectiveness.

Discussion

The results highlight the potential of using digital insole data combined with AI techniques to distinguish between stroke patients, Parkinson's patients, and healthy individuals. The study underscores the importance of specific gait characteristics that differ among these groups. This approach can aid in developing personalized rehabilitation programs and enhancing the monitoring of patient progress.

Conclusion

This study successfully demonstrates the utility of Neurogait digital insoles and AI classification in analyzing gait differences among stroke patients, Parkinson's patients, and healthy individuals. The findings support the use of advanced digital health devices in clinical settings to improve patient outcomes through precise and individualized care.

Mobile Phone Camera-Based Motion Tracking System for Community Stroke Rehabilitation

Ye Ji Jeong^{1,2*}, Jeong Hyun Kim^{1,2}, Kyu Won Lee^{1,2}, Hyun Hong^{1,2}, Aeh Non Lee^{1,2}, Shi Uk Lee^{1,2†}

Seoul National University, College of Medicine, Department of Rehabilitation Medicine¹, Seoul National University Boramae Medical Center, Department of Rehabilitation Medicine²

Background

Continuous rehabilitation within the community is essential for stroke patients' recovery. Motion detection using smartphone cameras has become feasible owing to techniques such as Human Pose Estimation, which detects joint positions and orientations. We developed a smartphone camera-based training system to guide and monitor stroke patients during rehabilitation exercises, detecting motion via mobile phone cameras and recording performance.

Objective

This study assesses the impact of a community-based rehabilitation exercise system on stroke patients' activities of daily living, balance, and cognitive function. The aim is to determine the effectiveness of this system in improving these outcomes.

Methods

A total of 47 stroke patients were recruited from the Seoul Metropolitan South Regional Disability Health Care Center. Participants used the community-based rehabilitation exercise system for at least 5 days a week over a 28-day period. The system, using a smartphone app, provided real-time feedback and adjusted exercise difficulty based on participants' Functional Ambulatory Category (FAC) scores. FAC scores of 1 indicated low difficulty, 2 or 3 indicated moderate difficulty, and 4 or 5 indicated high difficulty. Post-training, participants' satisfaction with the system was also evaluated.

Participants were divided into two groups based on training duration: more than 7 days (N1=35) and 7 days or fewer (N2=12). Changes in activities of daily living (K-MBI), balance (Short Form Berg Balance Scale), and cognitive function (K-MMSE) were assessed pre- and post-intervention. Data analysis involved paired t-tests for the group that trained for more than 7 days and Wilcoxon signed-rank tests for the group that trained for 7 days or fewer. A post-training satisfaction survey evaluated participants' perceptions.

Results

The >7 days group showed significant improvements in activities of daily living (K-MBI) and balance (Short Form Berg Balance Scale). K-MBI scores increased from 74.97 to 77.29 ($p=.005$), and Short Form Berg Balance Scale scores improved from 18.94 to 20.97 ($p=.005$). K-MMSE scores rose from 26.09 to 26.69, but this was not statistically significant ($p=.068$). The ≤7 days group showed significant improvement only in balance ($p=.015$), with no significant changes in K-MBI or K-MMSE ($p>.05$). The satisfaction survey indicated that 30 out of 47 participants rated the system 4 or 5 out of 5.

Conclusion

The community-based rehabilitation exercise system effectively improved stroke patients' activities of daily living and balance, particularly for those training over 7 days. High satisfaction levels further validate its value. These findings suggest such systems are effective for long-term rehabilitation and reintegration into daily life. Future research should explore larger sample sizes and long-term effects to further validate the system's sustainability and impact.

Table 1. Clinical and demographic characteristics of the participants

Characteristics	Total (N=47)	Group I (N ¹ =35)	Group II (N ² =12)
Age (Mean±SD)	66.4±12.0	67.2±10.0	63.9±16.9
Gender (Male/Female)	30/17	22/13	8/4
Height (Mean±SD)	163.0±7.6	162.7±8.4	163.9±5.0
Weight (Mean±SD)	64.0±11.7	65.4±11.9	60.1±10.4
Diagnosis (Infarction/Hemorrhage/other)	25/21/1	18/17	3/8/1
Affected side (Right/Left/Both)	28/16/3	21/11/3	7/5
Duration of stroke (month) (Mean±SD)	81.0±79.6	93.5±84.5	44.8±49.7
FAC (1/2/3/4/5)	1/13/12/13/8	1/9/9/11/5	0/4/3/2/3
Number of training days (Mean±SD)	13.5±7.4	16.9±5.0	3.4±1.6

SD; standard deviation, FAC; Functional Ambulatory Category.

Table 1. Clinical and demographic characteristics of the participants

Table 2. Comparison of pre- and post- values of K-MBI, SFBBS and K-MMSE results

		Pre (Mean±SD)	Post (Mean±SD)	P
Group I (N ¹ =35)	K-MBI	75.0±16.5	77.3±17.0	<.005*
	SFBBS	18.9±4.6	21.0±5.3	<.005*
	K-MMSE	26.1±3.6	26.7±4.0	.068
Group II (N ² =12)	K-MBI	73.7±16.4	78.8±13.0	.089
	SFBBS	16.3±5.8	21.3±3.8	.015
	K-MMSE	25.3±3.9	25.9±4.1	.165

**p*<.05, K-MBI; Korean version of Modified Barthel Index, SFBBS; Short Form Berg Balance Scale, K-MMSE; Korean Mini Mental State Examination, SD; standard deviation.

Table 2. Comparison of pre- and post- values of K-MBI, SFBBS and K-MMSE results

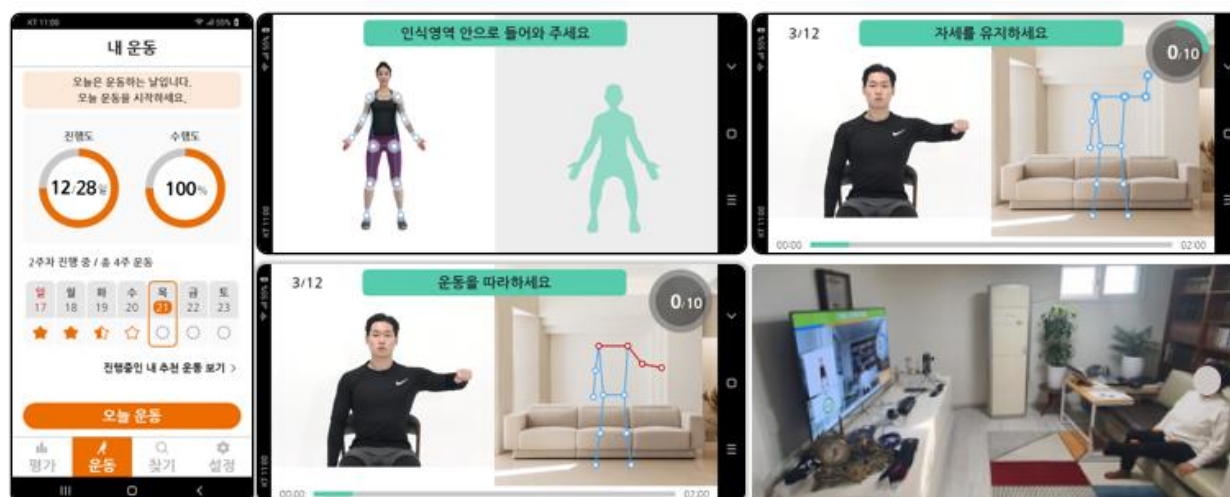


Figure 1. Application Interface and Example of Exercise Execution by Stroke Patients

Enhancing Stroke Rehabilitation: The Impact of Virtual Reality on Upper Limb Recovery

Seyoung Shin^{1*}, Gyoseok Hwang¹, EunYoung Park¹, Jung Rae Cho¹, Hongseok Baek¹, MinYoung Kim^{1†}

Department of Rehabilitation Medicine, CHA Bundang Medical Center, CHA University School of Medicine¹

Objective

The importance of effective rehabilitation therapy for functional recovery after stroke has been consistently emphasized. Adjunctive therapy using a virtual reality (VR) rehabilitation program has emerged as one of the promising methods for improving functions in stroke patients. This study aims to identify the efficacy of VR technology as an adjunctive therapy in stroke rehabilitation.

Methods

Subacute stroke patients admitted to the Rehabilitation Department at CHA Bundang Medical Center from November 2015 to January 2020 were screened retrospectively. Among them, we included 36 patients who received VR training during occupational therapy for their upper extremity rehabilitation (Figure 1). We compared these VR group patients (n=36) to a control group (n=14) who received only conventional rehabilitation during the same duration. The assessment tools were the Mini-Mental Status Examination, modified Barthel Index, Fugl-Meyer Assessment (FMA), Functional Independence Measure, and Motor-Free Visual Perception Test. These tests were assessed before and after each treatment, and the differences in scores between the two time points were measured. Subgroup analysis was done according to the number of VR interventions in the VR group.

Results

In the between-group comparison, there were no significant differences in age, sex, or in-patient rehabilitation duration (Table 1). The change in FMA score was significantly higher in the VR group compared to the control group ($p=0.03$). However, there were no significant differences in other functional changes between the two groups (Figure 2). In the subgroup analysis according to the number of VR sessions (10 times or more vs. less than 10 times), there were no significant differences in all functional changes.

Conclusions

This study suggests that a combination of VR-based rehabilitation and conventional therapy is beneficial for the recovery of upper limb functions in stroke patients. Further studies with randomized controlled designs are needed.

Acknowledgment This research was supported by the IITP grant of Ministry of Science and ICT (2021-0-00742 Development of Core Technology for Whole-body Medical Twin) and supported by a grant of the Korea Health Technology R&D Project through the Korea Health Industry Development Institute (KHIDI), funded by the Ministry of Health & Welfare, Republic of Korea (grant number : HI16C1559).

	VR (N=36)	Control (N=14)	P-value
Sex			1.00
Male	22 (61.11%)	9 (64.29%)	
Female	14 (38.89%)	5 (35.71%)	
Age	56.61 ± 14.21	61.71 ± 16.40	0.28
Days from stroke onset	16.50 ± 7.08	16.21 ± 6.72	0.90
DM, yes	10 (27.78%)	1 (7.14%)	0.23
HTN, yes	17 (47.22%)	5 (35.71%)	0.68
Type			0.10
Ischemic	20 (55.56%)	12 (85.71%)	
Hemorrhagic	16 (44.44%)	2 (14.29%)	
Side			0.97
Right	16 (44.44%)	7 (50.00%)	
Left	20 (55.56%)	7 (50.00%)	
Baseline functional assessments			
MMSE	25.00 [19.50;28.00]	24.50 [20.00;27.00]	0.73
MBI	51.06 ± 18.87	52.50 ± 22.57	0.82
MVPT	40.91 ± 11.63	44.92 ± 10.11	0.28
FIM cognition	28.00 [22.50;30.50]	24.50 [22.00;30.00]	0.51
FIM motor	45.00 [38.00;52.00]	44.50 [29.00;56.00]	0.77
FMA	39.50 [24.50;57.00]	51.50 [23.00;63.00]	0.45

Table 1. Baseline patient characteristics



Figure 1. A display screen capture of virtual reality game

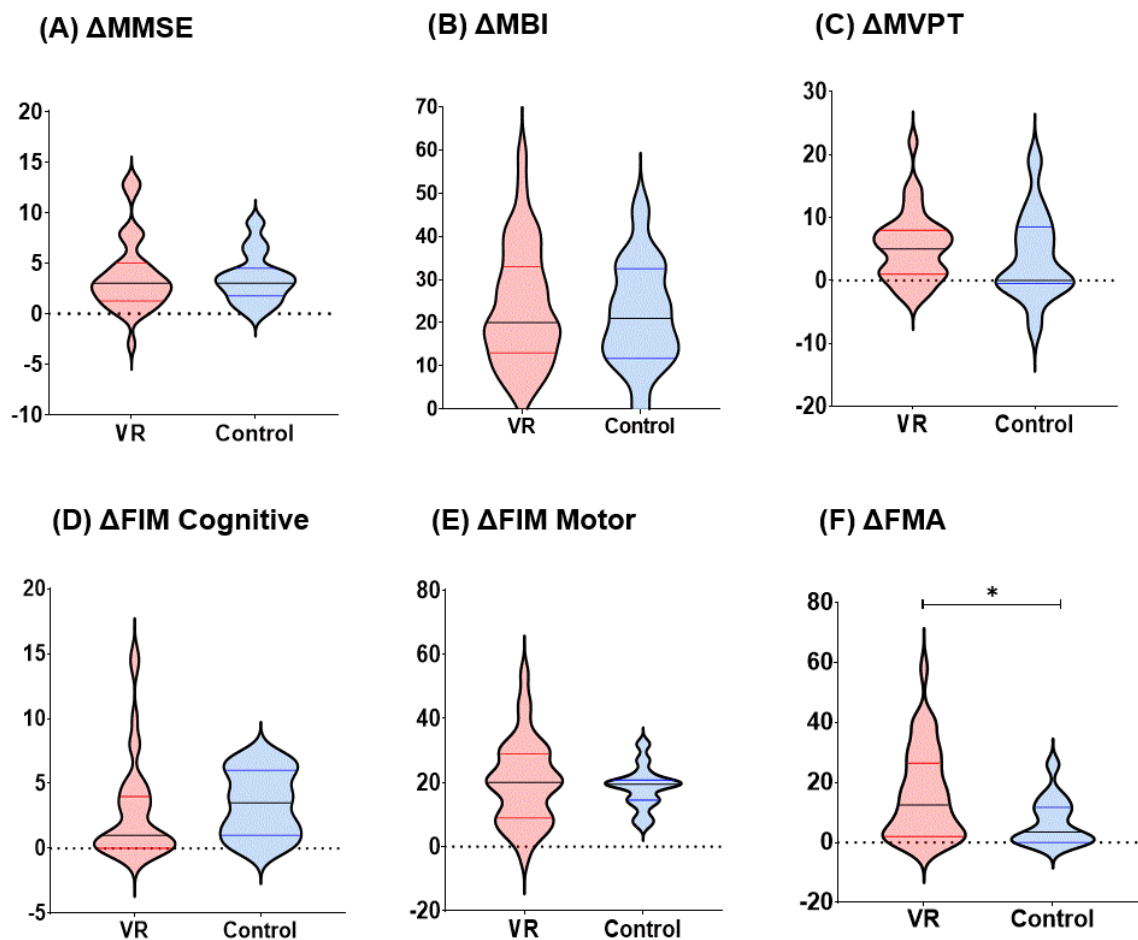


Figure 2. Comparison of functional assessment changes between two groups

The effect of home-based robot rehabilitation in community disabled person

Junhwan Lee^{1*}, Byung-Ju Ryu^{1†}, Seokjoon Hong¹

Department of Physical Medicine and Rehabilitation, Sahmyook Medical Center, Seoul, Korea¹

Introduction

The necessity for appropriate rehabilitation programs for disabled individuals in the community to maintain independent living is increasing. While traditional rehabilitation programs have primarily been based in specialized facilities, disabled individuals often face difficulties accessing these due to their vulnerable health status. This study evaluates the effects of providing the robotic rehabilitation device (Rebless) to disabled individuals and implementing the program at home.

Methods

Initially, 26 patients residing in Dongdaemun-gu participated in the study. Six participants withdrew from the study due to pain, scheduling issues, or dissatisfaction with the program. Thus, 20 patients completed the intervention. Five patients performed elbow exercises, and fifteen patients performed knee exercises. Assessments were conducted by a physician at either the Dongdaemun Health Center or the participants' homes. Participants received the robotic rehabilitation device, transported by the staff. They performed rehabilitation programs for at least 30 minutes, three times a week for eight weeks. Follow-up assessments were conducted after the program. Basic demographics were included. FMA-UE (Fugl-Meyer Assessment for Upper Extremity) was measured for the elbow group, and BBS (Berg Balance Scale), TUG (Timed Up and Go), and 10mWT (10-meter walking test) were measured for the knee group. Additionally, SF-12v2 (Short Form-12v2) was measured for both caregivers and patients, which is divided into two domains: Physical Component Summary (PCS) and Mental Component Summary (MCS), with higher scores indicating a better health-related quality of life. ZBI (Zarit Burden Interview) was measured for caregivers to assess subjective feelings of burden.

Results

The elbow group showed an improvement in FMA-UE scores ($p=0.006$). This aligns with previous research indicating the efficacy of robotic devices in providing repetitive and high-intensity training, which is crucial for motor recovery. The knee group (p

Conclusion

Home-based rehabilitation using robotic devices can be effective, especially for improving upper limb function and reducing caregiver burden. This is particularly valuable for patients who face mobility or accessibility issues. The integration of such programs can enhance overall satisfaction with the rehabilitation process. However, the small sample size and short duration of the study may limit the generalizability of the findings.

Acknowledgment Achilike S, et al. Caregiver Burden and Associated Factors Among Informal Caregivers of Stroke Survivors. *J Neurosci Nurs*. 2020;52(6):277-83. Lynch D, et al. Continuous passive motion improves shoulder joint integrity following stroke. *Clin Rehabil*. 2005;19(6):594-9. Kim JA, et al. The effect of training using an upper limb rehabilitation robot (HEXO-UR30A) in chronic stroke patients: A randomized controlled trial. *Medicine (Baltimore)*. 2023;102(12). Bertani R, et al. Effects of robot-assisted upper limb rehabilitation in stroke patients: a systematic review with meta-analysis. *Neurol Sci*. 2017;38(9):1561-9. Worland RL, et al. Home continuous passive motion machine versus professional physical therapy following total knee replacement. *J Arthroplasty*. 1998;13(7):784-7. Fugl-Meyer AR, Jaasko L, Leyman I, Olsson S, Steglind S. The post-stroke hemiplegic patient: A method for evaluation of physical performance. *Scand J Rehabil Med*. 1975;7(1):13-31. Zarit SH, Reever KE, Bach-Peterson J. Relatives of the impaired elderly: Correlates of feelings of burden. *Gerontologist*. 1980;20(6):649-655. Ware Jr, John E., Mark Kosinski, and Susan D. Keller. "A 12-Item Short-Form Health Survey: construction of scales and preliminary tests of reliability and validity." *Medical care* 34.3 (1996): 220-233. Ware, John E., Susan D. Keller, and Mark Kosinski. SF-12: How to score the SF-12 physical and mental health summary scales. Health Institute, New England Medical Center, 1995.

	Elbow(n=5)	Knee(n=15)	p-value
Sex			0.224
Male	4	10	
Female	1	5	
Mean age(yr)	51.40±13.09	52.20±20.00	0.276
Mean time since injury	5.33±4.27	21.19±16.43	0.054
Injury type			
Ischemic stroke	1	3	
Hemorrhagic stroke	3	6	
Cerebral palsy	0	3	
Spinal cord injury	1	0	
Avascular necrosis of femoral head	0	1	
Kennedy disease	0	1	
Hereditary spastic paraplegia		1	
Neurological level			
Hemiparesis	3	5	
Paraplegia	0	1	
Quadriparesis	2	9	
Other rehabilitation program			0.061
Yes	4	6	
No	1	9	
Modified Rankin Scale	2.6±0.55	3.27±0.88	0.081
Modified Ashworth Scale			0.748
0	1	6	
1	2	8	
2	2	1	

Dermographic data of the participants

	Elbow (n=5)			Knee (n=15)			Total (n=20)		
	Pre	Post	p-value	Pre	Post	p-value	Pre	Post	p-value
FMA-UE	37.20±14.72	43.60±15.75	0.006						
BBS				18.57±19.72	19.57±19.43	0.258			
TUG				27.84±18.21	26.03±16.08	0.074			
10mWT				25.12±14.12	22.59±11.92	0.376			
ZBI	50.25±18.03	44.50±16.82	0.565	31.57±13.25	21.93±10.93	<0.001	35.72±15.98	26.94±15.31	0.001
PCS	30.76±3.24	32.74±9.56	0.697	33.42±8.04	32.17±7.65	0.540	32.75±7.16	32.32±7.90	0.817
MCS	48.13±11.96	46.24±16.64	0.802	51.47±15.61	57.00±13.60	0.126	50.64±14.56	54.31±14.74	0.248
PCS_c	49.12±12.98	45.60±4.83	0.565	50.21±8.65	47.63±11.33	0.353	49.95±9.38	47.16±10.07	0.246
MCS_c	41.90±9.63	41.11±11.39	0.899	51.63±8.56	54.90±9.79	0.117	49.34±9.51	51.66±11.51	0.253

FMA-UE, Fugl-Meyer assessment of upper extremity; BBS, Berg balance scale; TUG, Timed up and go; 10mWT, 10m walking test; ZBI, Zarit burden interview; PCS, Physical component summary; MCS, Mental component summary; PCS_c, PCS score of caregiver; MCS_c, MCS score of caregiver

Clinical outcomes in elbow and knee group pre and post program

Comparative Analysis of Deep Learning Architectures for Penetration and Aspiration Detection in VFSS

Sung-Moon Ryu^{4*}, Chinthala Sreya Reddy³, Jong Taek Lee², Eunhee Park^{1†}

Department of Rehabilitation Medicine, Kyungpook National University Chilgok Hospital¹, Viterbi School of Engineering, University of Southern California², School of Computer Science and Engineering, Kyungpook National University³, Department of Rehabilitation, Kyungpook National University Hospital⁴

This study concentrates on machine learning, specifically deep learning techniques, to automatically detect the presence of aspiration or penetration in videofluoroscopic swallowing studies (VFSS). A comparative analysis is conducted on various deep learning architectures such as 2D Convolutional Neural Networks (2D-CNN), Long Short-Term Memory (LSTM), and 3D Convolutional Neural Networks (3D-CNN). This comparison assesses the performance, network size, and computational speed of the models. In addition, we present findings derived from multi-label and multi-class classification methods. By evaluating the strengths and weaknesses of each technique, we propose the most effective method for detecting penetration or aspiration in VFSS. Our comprehensive evaluation reveals the superiority of 3D-CNN in the automatic detection of penetration and aspiration in VFSS. This research contributes to the development of a clinically viable automatic detection system, offering potential advancements in the care and management of patients with dysphagia.

Comparative Analysis of Automated Segmentation Techniques for Brain Atrophy in Alzheimer's Disease

Gyubin Kwon^{1*}, Hyunjin Kim¹, Jungsoo Lee^{1†}

Department of Medical IT Convergence Engineering, Kumoh National Institute of Technology, Gumi, South Korea¹

Objective

Early diagnosis of Alzheimer's disease (AD) is crucial as it can potentially delay or mitigate the progression of symptoms. Regional brain atrophy is investigated for the diagnosis of AD using anatomical MRI. This study aims to find the optimal automated approach for investigating regional brain atrophy by implementing deep learning-based segmentation models and comparing the regional volumes obtained from the models with a conventional method.

Methods

Anatomical T1-weighted MRI data of Alzheimer's Disease Neuroimaging Initiative (ADNI) dataset, including 231 cognitively normal (CN) individuals, 411 mild cognitive impairment (MCI) patients, and 199 AD patients, were used for this study. The data were divided into training, validation, and test sets in a 6:2:2 ratio. Three deep learning models for segmentation (U-Net, Inception U-Net, and Dilated Inception U-Net) were implemented and compared with a conventional method (FreeSurfer's automatic segmentation). Ten specific regions, such as the hippocampus, amygdala, entorhinal cortex, fusiform gyrus, and parahippocampal gyrus in the left and right hemispheres, were extracted. Regional volumes were statistically compared among CN, MCI, and AD using analysis of variance (ANOVA) and Bonferroni post hoc test.

Result

There were statistical differences in all ten regional volumes obtained from three deep learning-based models among CN, MCI, and AD. On the other hand, nine regional volumes obtained from the traditional method, except for the left fusiform gyrus, had statistical differences. When comparing CN and AD using the conventional method, there were differences in four regional volumes, and when comparing CN and MCI, there were differences in nine regional volumes and eight regional volumes when comparing MCI and AD. Three deep learning-based models showed differences in more regional volumes than the conventional method in CN and AD comparisons and CN and MCI comparisons. On the other hand, in the MCI and AD comparison, the conventional method showed the best results. However, overall, the deep learning-based model was better than the existing method, and the Dilated Inception U-Net showed the best results.

Conclusion

In this study, it was confirmed that deep learning-based segmentation is more accurate than the conventional method in examining brain region atrophy for AD diagnosis. Additionally, while the conventional method requires a significant amount of computation time, the inference phase of deep learning models is considerably faster, making them more practical for real-world applications. Based on this research, we aim to develop an integrated model that can perform brain region segmentation and lesion detection with a single deep learning model, which will be beneficial for patients with AD, stroke, and brain tumors.

Acknowledgment This study was supported by the National Research Foundation of Korea (NRF) grant funded by the Korean government (MSIT). (No. RS-2023-00208884, No. RS-2023-00265824).

Reliability and validity of the Korean version of Moss Attention Rating Scale: A validation study

Sung Hoon Jeong^{1,2,3*}, Ja-Ho Leigh^{1,2,4}, Byung-Mo Oh^{1,2}, Sodam Lee², Hoo Young Lee^{1,2†}

Department of Rehabilitation Medicine, Seoul National University Hospital¹, National Traffic Injury Rehabilitation Research Institute, National Traffic Injury Rehabilitation Hospital², Institute of Health Services Research, Yonsei University³, Institute of Health Policy and Management, Seoul National University⁴

Background

Attention deficits, characterized by an inability to maintain concentration over extended periods and difficulty in organizing conflicting information due to distractibility, are common symptoms following traumatic brain injury (TBI) resulting from road traffic accidents. The Moss Attention Rating Scale (MARS), developed in the United States, is designed as an observational rating scale to provide a valid measure of attention-related behaviors after TBI. However, there is currently no appropriate tool available in Korea to objectively assess the degree of attention deficit due to TBI.

Objective

This study aimed to investigate the reliability and validity of the Korean version of the Moss Attention Rating Scale (K-MARS), a measure of observational evaluation of behavior in patients with attention deficits following traumatic brain injury.

Method

This single-center study translated and modified the original MARS through reverse translation and pilot studies to consider the language and cultural aspects. The translated and adapted K-MARS was administered twice to patients with TBI requiring attention rehabilitation due to cognitive impairment in the general wards of a specialized rehabilitation medical hospital in Korea. We then conducted descriptive statistical analyses of the participants' demographic characteristics and K-MARS scores, and performed internal consistency and test-retest analyses to confirm reliability, as well as convergent validity analysis to confirm validity.

Result

A total of 40 TBI patients participated in this study. The overall internal consistency of the K-MARS was 0.866. The test-retest reliability showed high ICC values ranging from 0.909 to 0.975 for the total score and each subscale. Additionally, the total K-MARS score demonstrated significant positive correlations with Initiation, Consistent/Sustained Attention, K-MMSE, K-MOCA, CNT (forward; forward, t-score; backward; backward, t-score; trail making test-A, t-score), and Auditory CPT (correct response). Significant negative correlations were observed with GDS, CNT (trail making test-A, time), and Auditory CPT (omission error).

Conclusion

The results of this study demonstrate that the K-MARS is a valid and reliable questionnaire for identifying and monitoring the symptoms and severity of attention-related behaviors in various dimensions among Korean TBI patients. By using the K-MARS, clinicians are expected to effectively identify attention deficits in TBI patients' activities of daily living, provide direct attention training, and teach strategies for generalization.

Acknowledgment This study was supported by a grant from the Ministry of Land, Infrastructure and Transport (MOLIT) Research Fund (NTRH RF-2024001).

Table 1. Correlation between K-MARS and existing evaluation tools.

K-MARS	K-MARS [±] (total score)	n
TOTAL_SCORE	1	
FACTOR 1	0.837^{***}	40
FACTOR 2	0.775^{***}	40
FACTOR 3	0.232	40
K-MMSE	0.650^{***}	40
GDS	-0.663^{***}	39
PSQI	-0.184	36
BDI	-0.090	34
BAI	-0.325	35
K-MOCA	0.579^{**}	34
CNT		
Trail making Test-A (Time, seconds)	-0.602^{**}	30
Trail Making Test-A (T-score)	0.592^{**}	30
Trail making Test-B (Time, seconds)	-0.395	22
Trail Making Test-B (T-score)	0.366	22
Digit Span Test: forward (Time, seconds)	0.470^{**}	33
Digit Span Test: forward (T-score)	0.449^{**}	33
Digit Span Test: backward (Time, seconds)	0.536^{**}	33
Digit Span Test: backward (T-score)	0.584^{**}	33
Auditory CPT (correct response)	0.435[*]	33
Auditory CPT (omission error)	-0.435[*]	33
Auditory CPT (commission error)	-0.035	33
Auditory CPT (response time)	-0.120	33

GDS, Global Deterioration Scale; PSQI, Pittsburgh Sleep Quality Index; BDI, Beck Depression Inventory; BAI, Beck Anxiety Inventory; K-MMSE, Korean-Mini Mental Status Examination; K-MOCA, Korean-Montreal Cognitive Assessment.

Factor1: Restlessness/Distractibility; Factor2: Initiation; Factor3: Consistent/Sustained Attention

^{*} This analysis was conducted using Spearman's correlation analysis.

^{*} <0.05, ^{**} <0.01, ^{***} 0.001

Correlation between K-MARS and existing evaluation tools

Table 2. Result of test-retest reliability analysis

Variable	n	Time	Mean	SD	ICC
K-MARS (Total)	30	pre	69.1	13.74	0.958
	30	post	69.8	13.12	
Factor1	30	pre	3.56	0.8	0.909
	30	post	3.58	0.77	
Factor2	30	pre	2.98	0.93	0.979
	30	post	3.00	0.88	
Factor3	30	pre	2.89	0.79	0.952
	30	post	2.89	0.87	

ICC, Intra-class correlation coefficient

Factor1: Restlessness/Distractibility; Factor2: Initiation; Factor3: Consistent/Sustained Attention

Result of test-retest reliability analysis

Table 3. Result of internal consistency

Variable	n	Mean [*]	SD [*]	Cronbach Alpha
K-MARS	40	3.15	1.23	0.866

^{*}This value represents the individual's score for each K-MARS item.

Result of internal consistency

Effect of Soft Wearable Robot for Hip Assistance in Chronic Stroke Patients

Seung-Hyeon Han^{1*}, Jong Weon Lee^{1,2}, Dong-wook Rha^{1,2}, Kyoungchul Kong^{3,4}, Chanyoung Ko³, Sanguk Choi³, Yongtak Yoon⁴, Deog Young Kim^{1,2†}

Research Institute of Rehabilitation Medicine, Yonsei University College of Medicine¹, Department of Rehabilitation Medicine, Yonsei University College of Medicine², Department of Mechanical Engineering, Korea Advanced Institute of Science and Technology³, Angel Robotics, Angel Robotics⁴

Introduction

Post-stroke gait disturbance significantly impacts the patients' independence and quality of life. Recently, soft wearable robots (SWR) have garnered attention as a novel alternative to overcome the limitations of conventional exoskeleton robots. This study aimed to assess the efficacy of an SWR for hip assistance in improving gait ability and patterns in chronic stroke patients.

Methods

Nineteen chronic stroke patients (12 males, 7 females; mean age 58.7±12.0 years) were enrolled. Participants were assessed under three conditions after familiarization trials: SWR worn and activated (Robot On), SWR worn but deactivated (Robot Off), and without SWR (Control). Gait performance was evaluated using the 10-meter walk test and 6-minute walk test. Energy expenditure was measured as oxygen cost (O₂ cost) using a COSMED K5 device (COSMED, Rome, Italy). A 3D motion analysis system (Vicon Motion Systems Ltd., UK) was used to measure the temporospatial, kinematic, kinetic and gait asymmetry. Gait deviation indices, including Gait Deviation Index (GDI), Gait Profile Score (GPS), and Gait Variable Score (GVS), were also calculated. Statistical analysis was performed using SPSS (SPSS Inc., Statics27, USA). The Shapiro-Wilk test was used to assess normality. Repeated measures ANOVA or Friedman test were applied based on normality. Post-hoc analyses employed Bonferroni correction for parametric data and the Wilcoxon signed-rank test for non-parametric data.

Results

The self-selected walking speed in the 10-meter walk test and distance in the 6-minute walk test were significantly increased and oxygen cost significantly decreased in Robot On condition compared to control condition. (p

Conclusion

The soft wearable robot for hip assistance demonstrated improvements in gait speed, endurance, energy efficiency and some gait parameters in chronic stroke patients. The soft wearable robot may be suggested as a novel approach in post-stroke gait rehabilitation. Future studies may be needed for long-term training effects, applicability in real daily living situations and etc.

Acknowledgment This research was supported by the Assistive Technology R&D Project for People with Disabilities and the Elderly funded by the Ministry of Health & Welfare, Republic of Korea (# HJ20C000701).

Table 1. Comparisons of Gait Performance Measures between Three Conditions

	Control	Robot Off	Robot On	P-value
10-Meter Walk Test				
Self-selected (m/s)	0.44±0.27	0.43±0.25	0.55±0.29 ^{*,**}	0.000
Maximum safe (m/s)	0.52±0.31	0.50±0.28 [*]	0.53±0.28 ^{**}	0.009
6-Minute Walk Test (m)	146.50±79.87	144.74±79.45	167.21±83.77 ^{*,**}	0.000

Values are presented as mean±standard deviation;

*p<0.05 vs. control, **p<0.05 vs. Robot off

Table 1. Comparisons of Gait Performance Measures between Three Conditions

Table 2. Comparison of Spatial-temporal Walking Parameters

Parameter	Affected Side				Unaffected Side			
	Control	Robot Off	Robot On	P-value	Control	Robot Off	Robot On	P-value
Cadence (step/min)	70.01±25.01	71.21±20.52	73.83±18.07	0.283	69.95±25.77	70.48±21.18	73.46±16.93	0.320
Walking speed (m/s)	0.36±0.24	0.38±0.22	0.39±0.21	0.092	0.37±0.25	0.38±0.22	0.40±0.21	0.151
Step length (m)	0.28±0.16	0.31±0.14 [*]	0.32±0.13 [*]	0.005	0.30±0.12	0.31±0.11	0.31±0.13	0.607
Step time (s)	1.03±0.55	0.94±0.39	0.87±0.26	0.220	1.03±0.57	0.95±0.41	0.85±0.27	0.810
Step width (m)	0.18±0.04	0.18±0.04	0.18±0.04	0.955	0.17±0.04	0.19±0.03 [*]	0.17±0.04	0.270
Stance duration (%)	68.02±11.05	68.11±9.99	67.04±7.79	0.614	78.08±10.35	77.33±9.91	75.89±8.83 [*]	0.003
Swing duration (%)	31.98±11.05	31.89±9.99	32.96±7.79	0.614	21.92±10.35	22.67±9.91	24.11±8.83 [*]	0.003
Single support duration (%)	21.32±10.15	22.53±8.94	23.92±9.07 [*]	0.003	32.57±10.77	31.27±9.92	33.29±7.72	0.348
Double support duration (%)	46.70±17.61	45.58±14.83	43.12±13.04	0.092	45.51±17.68	46.06±15.63	42.59±12.72	0.110

Values are presented as mean±standard deviation;

*p<0.05 vs. control, **p<0.05 vs. Robot off

Table 2. Comparison of Spatial-temporal Walking Parameters

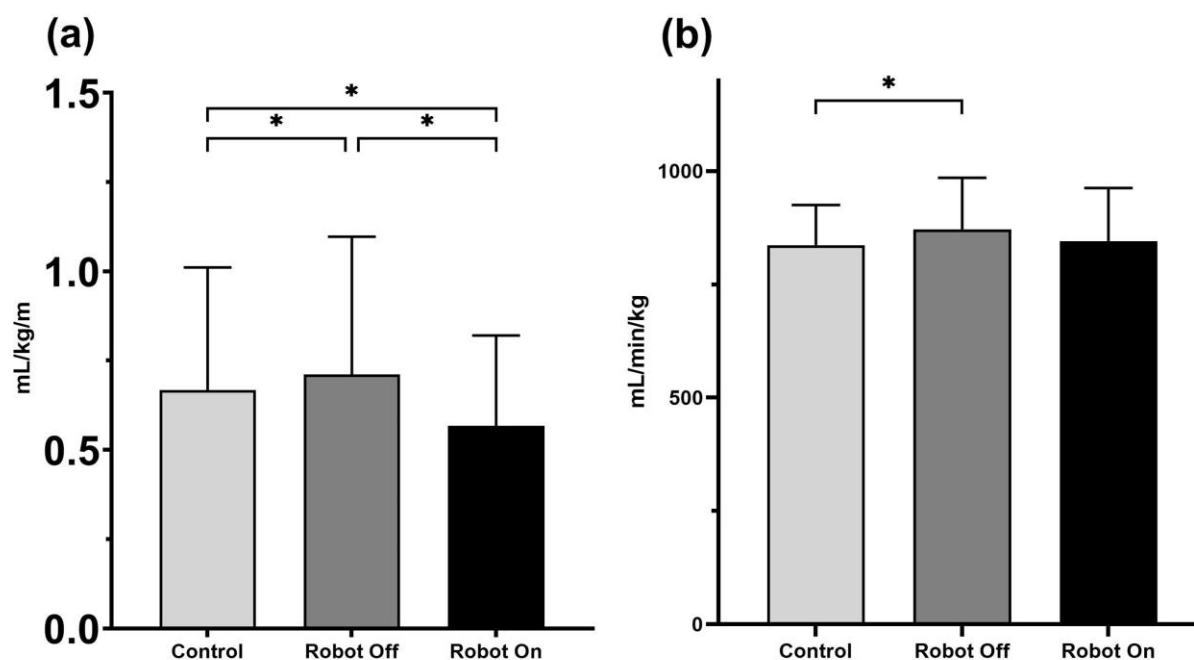


Fig 1. Comparison of Energy Consumption between Three Conditions (a) O₂ cost, (b) O₂ rate. * p-value < 0.05

Characteristics of Postural Instability in Idiopathic Normal Pressure Hydrocephalus

Sung-Moon Ryu^{4*}, Kyunghun Kang², Jong Taek Lee³, Eunhee Park^{1†}

Department of Rehabilitation Medicine, Kyungpook National University Chilgok Hospital¹, Department of Neurology, Kyungpook National University Chilgok Hospital², School of Computer Science and Engineering, Kyungpook National University³, Department of Rehabilitation Medicine, Kyungpook National University Hospital⁴

INTRODUCTION

In patients with idiopathic normal pressure hydrocephalus (iNPH), the characteristics of balance disturbances are not as well understood as those related to gait. This study examines the characteristics of postural instability in quiet standing in these patients.

METHODS

All patients diagnosed with possible iNPH underwent a cerebrospinal fluid tap test (CSFTT). Before CSFTT, we evaluated their center of pressure (COP) measurements on a force plate during quiet standing with eyes opened and closed. Following the COP measurements, we calculated COP parameters using time and frequency domain analysis and then compared them to age- and sex-matched healthy controls using Student's t-test.

RESULTS

A total of 101 patients with iNPH and 28 healthy controls were initially enrolled. In quiet standing with eyes open, there was a significant difference in the base of support (BOS) between iNPH patients and healthy controls. In quiet standing with eyes closed, iNPH patients showed significantly increased COP parameters calculated by time and frequency domain analysis, compared to healthy controls. These included the velocity of COP (vCOP), root-mean-square of COP (rmsCOP), turn index, and base of support (BOS), as well as both the peak and average power spectral density (PSD) values in both the anteroposterior (AP) and mediolateral (ML) directions below 0.5 Hz ($p < 0.05$). Patients with iNPH, the Romberg ratio were higher than in healthy controls.

CONCLUSIONS

Compared to healthy controls, iNPH patients exhibited significant postural instability during quiet standing with eyes closed. Patients with iNPH may need greater reliance on visual input for balance control.

Personalized rTMS to Enhance Ambulatory Function in Parkinson's disease: A RCT protocol

Seo Jung Yun^{1,2,3*}, Ho Seok Lee⁴, Dae Hyun Kim⁴, Sun Im⁵, Yeun Jie Yoo⁶, Na Young Kim⁷, Jungsoo Lee⁸, Donghyeon Kim⁹, Hae-Yeon Park⁵, Mi-Jeong Yoon⁶, Young Seok Kim⁷, Won Hyuk Chang^{4,10†}, Han Gil Seo^{2,3†}

Department of Human System Medicine, Seoul National University College of Medicine¹, Department of Rehabilitation Medicine, Seoul National University Hospital², Department of Rehabilitation Medicine, Seoul National University College of Medicine³, Department of Physical and Rehabilitation Medicine, Center for Prevention and Rehabilitation, Heart Vascular Stroke Institute, Samsung Medical Center, Sungkyunkwan University School of Medicine⁴, Department of Rehabilitation Medicine, Bucheon St. Mary's Hospital, College of Medicine, The Catholic University of Korea⁵, Department of Rehabilitation Medicine, St. Vincent's Hospital, College of Medicine, The Catholic University of Korea⁶, Department of Rehabilitation Medicine, Yongin Severance Hospital, Yonsei University College of Medicine⁷, Department of Medical IT Convergence Engineering, Kumoh National Institute of Technology⁸, Research Institute, NEUROPHET Inc.⁹, Department of Health Science and Technology, Department of Medical Device Management and Research, SAIHST, Sungkyunkwan University¹⁰

Background

Repetitive transcranial magnetic stimulation (rTMS) is one of non-invasive brain stimulations that modulates cortical excitability through magnetic pulses. However, the effects of rTMS in Parkinson's disease (PD) have yield mixed results, influenced by factors including various rTMS stimulation parameters as well as the clinical characteristics of patients with PD. There is no clear evidence regarding which patients should be applied with which parameters of rTMS. The study aims to investigate the efficacy and safety of personalized rTMS in patients with PD, focusing on individual functional reserves to improve ambulatory function.

Methods

This is a prospective, exploratory, multi-center, single-blind, parallel-group, randomized controlled trial. Sixty patients with PD will be recruited for this study. This study comprises two sub-studies, each structured as a two-arm trial (Fig 1). Participants are classified into sub-studies based on their functional reserves for ambulatory function, into either the motor or cognitive priority group. The Timed-Up and Go (TUG) test is employed under both single and cognitive dual-task conditions (serial 3 subtraction). The motor dual-task effect, using stride length, and the cognitive dual-task effect, using the correct response rate of subtraction, are calculated. In the motor priority group, high-frequency rTMS targets the primary motor cortex of the lower limb, whereas the cognitive priority group receives rTMS over the left dorsolateral prefrontal cortex. The active comparator for each sub-study is bilateral rTMS of the primary motor cortex of the upper limb. Over 4 weeks, the participants will undergo 10 rTMS sessions, with evaluations conducted pre-intervention, mid-intervention, immediately post-intervention, and at 2-month follow-up. The primary outcome is change in TUG time between the pre- and immediate post-intervention evaluations. The secondary outcome variables are the TUG under cognitive dual-task conditions, MDS-Unified Parkinson's Disease Rating Scale Part III, New Freezing of Gait Questionnaire, Digit Span, trail-making test, transcranial magnetic stimulation-induced motor-evoked potentials, diffusion tensor imaging, and resting state functional Magnetic Resonance Imaging.

Discussion

The study will reveal the effect of personalized rTMS based on functional reserve compared to the conventional rTMS approach in PD. Furthermore, the findings of this study may provide empirical evidence for an rTMS protocol tailored to individual functional reserves to enhance ambulatory function in patients with PD.

Acknowledgment This research was supported by the K-Brain Project of the National Research Foundation (NRF) funded by the Korean government (Ministry of Science and ICT, MSIT) (No. RS-2023-00265824).

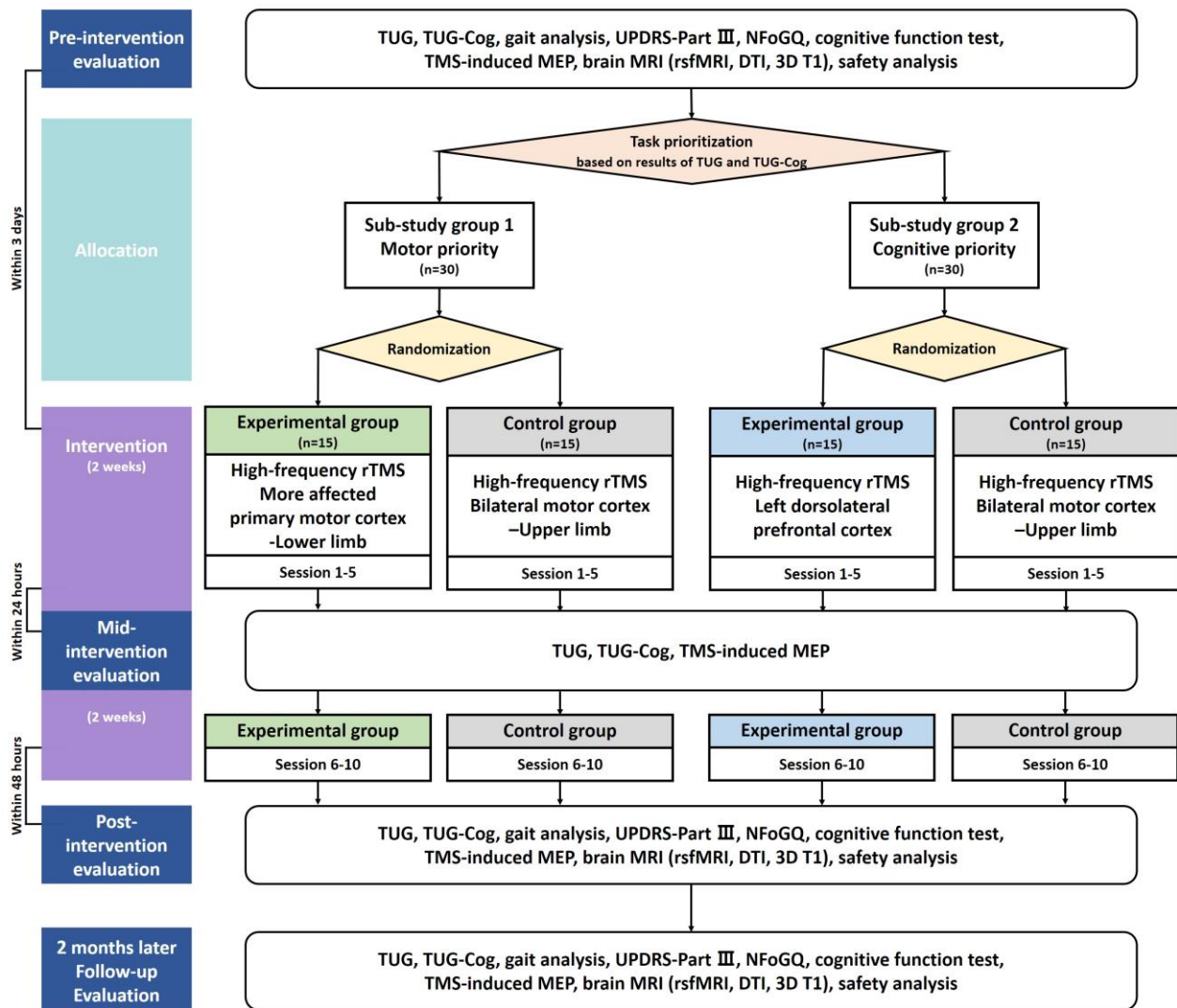


Fig 1. Flowchart through the entire study process

Effect of dual-task exercise on cognitive and physical function in the mild cognitive impairment

Se Hee Jung^{1,2**}, Hee Young Cha¹

Department of Rehabilitation Medicine, Seoul National University College of Medicine¹, Department of Rehabilitation Medicine, Seoul National University Boramae Medical Center²

Background

Dual-task (DT) exercise training is a multidimensional exercise intervention that combines motor and cognitive tasks to affect the motor-cognitive interplay of the brain. Patients with mild cognitive impairment (MCI), which is associated with an increased risk of developing Alzheimer's disease, often need early intervention. We aimed to develop a DT exercise program and investigate whether it improves cognitive and physical function in elderly individuals with MCI.

Methods

Twelve adults aged 65 years or older with MCI were randomized to either the exercise group (n=6) or the control group (n=6). The exercise group underwent 8-week, 3 times a week, 60-minute group exercise sessions, which included moderate-to-high intensity exercise and simultaneous cognitive tasks. The control group performed 60 minutes of light intensity home exercise 4 times a week for 8 weeks. Dual task cost (DTC), cognitive function, physical function, body composition, level of physical activity, and exercise psychology were assessed at baseline and after the intervention.

Results

The exercise group exhibited significant improvements in DTC and cognitive function in the card sorting, verbal learning, Boston Naming, and Stroop Color and Word tests. In terms of physical function, the Short Physical Performance Battery, gait speed, and leg lean mass significantly improved. The exercise group showed significantly greater physical activity and satisfaction with the intervention than did the control group. There were no adverse events during the intervention.

Conclusions

The DT exercise program improved cognitive and physical function in elderly individuals with MCI.

Acknowledgment This study was supported by the Rehabilitation Research & Development Support Program (#NRCRSP-EX20004) and by the Translational R&D Program on Smart Rehabilitation Exercises (#TRSRE-PS01), National Rehabilitation Center, Ministry of Health and Welfare, South Korea.

Toe Grip Strength Is Associated with Improving Gait Function in Patients with Subacute Stroke

Min-Su Kim^{1*†}, Jin-Whan Ryu¹, In-Su Hwang¹, Sol Jin¹, Soo-A Kim¹

Department of Rehabilitation Medicine, Soonchunhyang University Cheonan Hospital¹

Toe grip strength has recently been suggested to play an essential role in maintaining balance and postural stability for ambulatory function in older populations. This study aimed to investigate its association with improving gait function three months after onset in patients with subacute stroke. This longitudinal cohort study included 98 first-ever stroke patients (67 ± 9 years, 56% female) within one month from the onset who could not ambulate independently. Functional outcome indicators, including toe grip strength, hand grip strength, knee extensor strength, Fugl-Meyer Assessment of Lower Extremity (FMA_LE), and the Postural Assessment Scale for Stroke (PASS), were assessed before and three months after the intervention. We analyzed the correlation between participants' gait function using a 10-meter walk test time and various functional indicators. Then, multiple linear regression analysis was used to investigate whether toe grip strength was related to the improvement of gait function. Correlation analysis revealed a significant positive correlation between the 10MWT time and toe grip strength ratio (affected/unaffected side), with a moderate effect size ($r = -0.61$, p

Acknowledgment This research was supported by a grant of the National Research Foundation of Korea (NRF) funded by the Ministry of Education (NRF-2021R11A3060949).



Measurement of toe strength. The patient's toe strength was measured in a sitting position. The ankle was placed in a neutral position and secured with a strap. The first proximal interphalangeal joint was positioned on the grip bar, and the heel stopper was adjusted to fit the heel of each participant. The patient then grabbed the bar of the measuring instrument with maximum force for about 2 seconds using his toes. All patients were measured twice, and the mean value was used as an indicator of the patient's toe strength.

Pearson Correlation Coefficient (r)	Δ 10MWT	Δ Toe Grip Strength, Affected	Δ Toe Grip Strength Ratio	Δ knee Extensor Strength Ratio	Δ FMA_LE	Δ PASS	Age
Δ Toe grip strength, affected	-0.43	-	-	-	-	-	-
Δ Toe grip strength ratio	-0.61 *	0.86 *	-	-	-	-	-
Δ Knee extensor strength ratio	-0.43	0.29	0.51	-	-	-	-
Δ FMA_LE	-0.58 *	0.40 *	0.55 *	0.49 *	-	-	-
Δ PASS	-0.67 *	0.58	0.62 *	0.39	0.33	-	-
Age	-0.49 *	-0.46 *	-0.40	-0.38	-0.34 *	-0.44	-

10MWT, 10 m Walk Test; FMA_LE, Fugl-Meyer Assessment of Lower Extremity; PASS, Postural Assessment Scale for Stroke. *: $p < 0.05$.

Correlation analysis between the walking speed and the functional factors associated with post-stroke gait improvement.

Independent Variable	Unstandardized Coefficient (B)	Standardized Coefficient (β)	t	p-Value	VIF
Δ Toe grip strength ratio	−0.099	−0.113	−2.093	<0.001 *	1.492
Δ FMA_LE	−0.083	−0.142	−1.315	0.004 *	1.601
Δ PASS	−0.166	−0.213	−3.275	<0.001 *	1.883
Age	−0.208	−0.252	−0.159	0.004 *	1.922

FMA_LE, Fugl-Meyer Assessment of Lower Extremity; PASS, Postural Assessment Scale for Stroke. Multiple regression analysis, ANOVA < 0.001, adjusted $R^2 = 0.796$. * $p < 0.05$.

Functional factors associated with the post-stroke gait improvement over 3 months.

A Systematic Review of Cognitive Telerehabilitation in Patients With Cognitive Dysfunction

Hyeonwoo Jeon^{1*}, Doo Young Kim^{1†}, Si-Woon Park¹, Bum-Suk Lee¹, Namjo Jeon¹, Minsong Kim¹, Mingu Kang¹, Suebeen Kim²

Department of Rehabilitation Medicine, International St. Mary's Hospital, Catholic Kwandong University College of Medicine, Incheon 22711, Korea¹, International St. Mary's Hospital, Catholic Kwandong University College of Medicine, Incheon 22711, Korea²

Introduction

One of the possible treatment options for patient with cognitive dysfunction is cognitive telerehabilitation. Previous systematic reviews on cognitive telerehabilitation have focused on specific disease groups and the analysis of intervention methods did not differentiate between traditional face-to-face cognition treatment and usual care. In this systematic review, we aim to analyze randomized controlled trials (RCTs) that compare telerehabilitation with face-to-face treatment or usual care for improving cognitive function in elderly individuals with cognitive dysfunction or patients with acquired brain injury.

Methods

We conducted this systematic review following the guidelines of the Preferred Reporting Items for Systematic Reviews and Meta-Analyses (PRISMA). In this systematic review, we searched 7 electronic databases (PubMed, Cochrane, EMBase, CINAHL, Web of Science, Scopus, KMBASE) to identify relevant studies published through August 31, 2023. We conducted a meta-analysis to assess the quality of the studies and synthesize the evidence. Certainty of evidence was evaluated using the Grading of Recommendations, Assessment, Development, and Evaluation (GRADE) method (Table 1).

Results

Finally, 14 studies were included in the analysis. For comparing telerehabilitation with face-to-face cognition treatment, the meta-analysis included 2 RCTs for global cognition (immediate outcome), 2 RCTs for attention (immediate outcome), 2 RCTs for visuospatial function (immediate outcome). For comparing telerehabilitation with usual care, the meta-analysis included 5 RCTs for global cognition (immediate outcome), 2 RCTs for global cognition (persistence outcome), 4 RCTs for attention (immediate outcome), 3 RCTs for executive function (immediate outcome), 3 RCTs for working memory (immediate outcome), 3 RCTs for visuospatial function (immediate outcome).

Discussion

Telerehabilitation has been shown to be more effective than usual care in improving global cognitive function, and its effectiveness is not inferior to that of traditional face-to-face cognitive treatment. By overcoming the limitations of traditional cognition rehabilitation and providing continuous treatment, telerehabilitation can offer effective treatment in specific situations.

Acknowledgment This research was supported by a grant of the Korean Health Technology R&D Project through the Korea Health Industry Development Institute (KHIDI), funded by the Ministry of Health & Welfare, Republic of Korea (Grant number: RS-2024-00263587).

Table 1. The evidence summaries and GRADEs.

Outcomes	No. of participants / No. of studies	GRADE certainty of evidence (deduction factors)	Statistical methods (IV, Random, 95% CI)	Effect estimates
VS. face-to-face cognition treatment				
Global cognition (immediate)	57 / 2	low (Imprecision -2)	SMD	-0.34 [-0.87, 0.19]
Attention (immediate)	85 / 2	low (Imprecision -2)	SMD	0.10 [-0.32, 0.53]
Visuospatial function (immediate)	85 / 2	low (Imprecision -2)	SMD	-0.26 [-0.75, 0.23]
VS. usual care				
Global cognition (immediate)	158 / 5	moderate (Imprecision -1)	SMD	0.62 [0.17, 1.07]
Global cognition (persistence)	51 / 2	low (Imprecision -2)	MD	0.51 [-2.61, 3.62]
Attention (immediate)	126 / 4	low (Imprecision -2)	SMD	0.24 [-0.11, 0.59]
Executive function (immediate)	109 / 3	moderate (Imprecision -1)	MD	-3.13 [-29.11, 22.85]
Working memory (immediate)	79 / 3	low (Inconsistency of results -1; Imprecision -2)	SMD	-0.02 [-0.56, 0.51]
Visuospatial function (immediate)	79 / 3	very low (Inconsistency of results -1; Imprecision -2)	SMD	0.49 [-0.33, 1.31]

GRADE, Grading of Recommendations, Assessment, Development, and Evaluation; SMD, Standardized mean difference; IV, inverse-variance; CI, confidence interval; MD, mean difference.

The evidence summaries and GRADEs. GRADE, Grading of Recommendations, Assessment, Development, and Evaluation; SMD, Standardized mean difference; IV, inverse-variance; CI, confidence interval; MD, mean difference.

Relationship between Respiratory Muscle Strength and Dysphagia with Parkinsonism

Minjung Kim^{1*}, Byung-Mo Oh^{1†}, Han Gil Seo^{1†}

Department of Rehabilitation Medicine, Seoul National University Hospital, Seoul National University College of Medicine¹

Introduction

In Parkinson's disease, one in three individuals experiences dysphagia. Atypical Parkinsonism also progresses rapidly and leads to dysphagia similar to that in Parkinson's disease. This increases the risk of respiratory complications and potentially fatal conditions such as aspiration pneumonia. Although expiratory muscle strength training has been established as an effective intervention for dysphagia, there is a lack of research on the impact of respiratory muscle strength on dysphagia in patients with Parkinsonism. This study aims to identify the relationship between the respiratory muscle strength and dysphagia severity in videofluoroscopic swallowing studies (VFSS).

Methods

We retrospectively reviewed 96 cases of in which measurements of maximal inspiratory pressure (MIP) and maximal expiratory pressure (MEP) were performed within 3 months. Forty-five cases that were not Parkinsonism were excluded, resulting in a total of 51 cases included. Based on the penetration-aspiration scale (PAS), cases with a PAS score of 6 or higher were classified as the aspiration group, and those with a score below 5 were classified as the non-aspiration group. The Videofluoroscopic Dysphagia Scale (VDS) was scored according to VFSS results. MIP and MEP were assessed with a MicroRPM pressure meter. Three maneuvers were performed for each test, and the maximal value was recorded. Using reference values for average MIP and MEP by gender and age group in healthy Koreans, the measured values were calculated as a percentage of the average values for each corresponding group (normalized MIP and MEP). Patients also completed the Swallowing Disturbance Questionnaire (SDQ). Independent t-tests and Pearson correlation tests were performed.

Results

Among 51 cases, the non-aspiration and aspiration groups comprised 21 and 30 cases, respectively (Table 1). The VDS scores ($P=0.001$) and normalized MEP ($P=0.029$) showed significant differences between the aspiration group and the non-aspiration group (Table 2). Both normalized MIP and MEP showed significant correlations with VDS ($r=-0.540$; P

Conclusion

This study showed that reductions in MIP and MEP are associated with VDS and SDQ scores, which reflect the objective and subjective severity of dysphagia in patients with Parkinsonism. Only reduction in MEP was significantly correlated with PAS, indicating that reduced expiratory muscle strength is associated with higher risk of aspiration. Further large-scale studies are needed to confirm the relationship between respiratory muscle strength and swallowing function in Parkinsonism.

Table 1. Characteristics of cases

	Total (n=51)	Non-aspiratiuon group (n=21)	Aspiration group (n=30)	P value
Age (years)	69.06 ± 9.16	67.76 ± 10.65	69.97 ± 8.01	0.403
Sex (Male/Female)	38/13	16/5	22/8	
Hoehn and Yahr scale	4.10 ± 0.86	4.00 ± 0.89	4.17 ± 0.85	0.251
Disease duration since onset(years)	4.69 ± 2.01	4.57 ± 2.06	4.77 ± 2.01	0.581
Height (cm)	165.76 ± 6.92 (46)	165.23 ± 6.78 (21)	166.21 ± 7.15 (25)	0.636
Diagnosis (n)				
MSA	36	17	19	
PD	10	3	7	
PSP	4	1	3	
VasP	1	0	1	

Non-aspiration group, PAS(2~5); Aspiration group, PAS(6~8); MSA, Multiple system atrophy; PD, Parkinson's disease; PSP, Progressive supranuclear palsy; VasP, Vascular parkinsonism

Table 1. Characteristics of cases

Table 2. Independent T-test between non-aspiration group and aspiration group

	Total (n=51)	Non-aspiratiuon group (n=21)	Aspiration group (n=30)	P value
VDS	43.49 ± 15.32	35.71 ± 12.72	48.93 ± 14.79	0.001*
SDQ score	15.35 ± 7.46	16.18 ± 6.62	14.81 ± 8.03	0.522
MIP (cmHg)	31.57 ± 19.73	33.38 ± 16.38	30.30 ± 21.95	0.569
Normalized MIP (%)	44.76 ± 28.38	53.33 ± 29.65	38.77 ± 26.31	0.078
MEP (cmHtg)	101.81 ± 21.58	101.82 ± 20.91	101.80 ± 22.39	0.997
Normalized MEP (%)	41.54 ± 23.61	50.15 ± 22.94	35.52 ± 22.50	0.029*

VDS, Videofluoroscopic dysphagia scale; SDQ, Swallowing disturbance questionnaire; MIP, Maximal inspiratory pressure; Normalized MIP (%), Value of MIP as a percent of average predicted MIP values by gender and age for Koreans; MEP, Maximal expiratory pressure; Normalized MEP (%), Value of MEP as a percent of average predicted MEP values by gender and age for Koreans
* P value <0.05

Table 2. Independent T-test between non-aspiration group and aspiration group

Table 3. Pearson's correlation

	Pearson	P value
Normalized MIP (%)		
VDS	-0.540	<0.001*
SDQ score	-0.347	0.016*
PAS	-0.210	0.139
Normalized MEP (%)		
VDS	-0.600	<0.001*
SDQ score	-0.317	0.028*
PAS	-0.290	0.039*

Normalized MIP (%), Value of maximal inspiratory pressure as a percent of average predicted maximal inspiratory pressure values by gender and age for Koreans; VDS, Videofluoroscopic dysphagia scale; SDQ, Swallowing disturbance questionnaire; PAS, Penetration-aspiration scale; Normalized MEP (%), Value of maximal expiratory pressure as a percent of average predicted maximal expiratory pressure values by gender and age for Koreans

*P value <0.05

Table 3. Pearson's correlation

Direct Reprogramming of the Central nerve system by OCT4

Han Eol Cho^{1,2**}, Sung-Rae Cho^{1,3}, Won Ah Choi^{1,2}, Hee Jae Park^{1,2}

Rehabilitation Institute of Neuromuscular Disease, Yonsei University College of Medicine¹, Department of Rehabilitation Medicine, Gangnam Severance Hospital², Research Institute of Rehabilitation Medicine, Yonsei University College of Medicine³

Central nervous system (CNS) diseases, particularly neurodegenerative disorders, pose significant medical challenges due to progressive neuronal loss. The landmark 2006 study by Takahashi and Yamanaka introduced induced pluripotent stem cell technology, allowing differentiated cells to revert to a pluripotent state. This has vast implications for CNS disease research and therapy. Recent studies have explored direct reprogramming for CNS repair, transforming one cell type into another without reverting to a pluripotent state. This review explores the potential of OCT4 in revolutionizing CNS disease treatment.

We conducted an extensive search of published scientific literature in databases including MEDLINE, EMBASE, Web of Science, and SCOPUS using the following search strategy until 1 November 2023: (((direct)) OR ((in vivo) OR (in situ)) AND (reprogramming) AND ((brain) OR (spinal cord)) AND ((OCT4))). Only the titles, abstracts, or keywords were searched in SCOPUS. We applied no language restrictions in our search. To identify duplicate entries, we considered factors such as the author, publication year, article title, and the source’s volume, issue, and page numbers. We manually reviewed the bibliographies of selected articles.

Five studies investigated Oct4 as the sole transcription factor for direct reprogramming (Table1). Sim S. et al. overexpressed Oct4 in the dentate gyrus of healthy animals but found no significant results. Javan M.’s team explored Oct4 combined with valproic acid (VPA) and other small molecules, finding that Oct4 with VPA significantly increased neural stem cell markers and reprogrammed endogenous somatic cells, primarily astrocytes, in the brain. In disease models, Oct4 combined with VPA reduced demyelination in mice with optic chiasm demyelination and promoted myelinating oligodendrocytes. Yu et al. demonstrated that Oct4 increased neural stem cells, expanded the oligodendrocyte lineage, and improved motor function in Huntington’s disease mice. Safety assessments reported no teratoma formation up to 100 days post-infection, indicating the safety of Oct4 injections. These studies suggest that Oct4 can effectively promote neural repair and functional recovery in the CNS without significant safety concerns.

Reprogramming Factors	Expression Location	Animal Model /Lesion Model	Animal Age (Time of Reprogramming *)	Delivery Methods		Target Cell (Markers)	Functional Outcome
Oct4	Dentate gyrus	C57BL/6 male mice	8 weeks old	Lentivirus	Stereotactic injection	-	Behavioral test (open field test, elevated plus maze, Y-maze test, contextual fear conditioning paradigm)
Oct4 + VPA	Lateral ventricle	C57BL/6 mice	8~9 weeks old	Lentivirus	Stereotactic injection	Neural stem cell (Pax6, Sox1) Pluripotency marker (Oct4, Nanog, c-Myc, Klf4 and Sox2)	-
Oct4 + VPA	Lateral ventricle	C57BL/6 mice	8~9 weeks old	Lentivirus	Stereotactic injection	Neural progenitor and pluripotency markers (Oct4, Nanog, Klf4, c-Myc, Pax6 and Sox1, SSEA1,Nanog)	
Oct4 + VPA	Lateral ventricle	C57BL/6 mice Optic chiasm demyelination by 1% lysocleithin	not mentioned (1 week before inducing demyelination)	Lentivirus	Stereotactic injection	Myelinating oligodendrocytes	Visual evoked potential
Oct4	Lateral ventricle	R6/2 mice Huntington's disease model	4 weeks old	Adenovirus	Stereotactic injection	Neuron (NeuN (cortex) GAD67, Darpp32 (striatum))	Behavioral test (Rotarod test, Grip strength test)

Table 1. Direct reprogramming study using Oct4.

Impact of COVID-19 on Complications During Stroke Rehabilitation

Cho E Sim^{1*}, Jong Bum Park^{1†}, Yung Jin Lee¹, Mi Jin Hong¹, Dong Jin Chae¹, Seong-Eun Kim¹, Ji-Hwan Kwon¹

Department of Rehabilitation Medicine, Konyang University College of Medicine¹

Objective

The Coronavirus Disease 2019 (COVID-19) first emerged in Wuhan, China, in December 2019, and was declared a pandemic. During the COVID-19 pandemic, prevention and protection measures were implemented to suppress the spread of the disease. These measures have profoundly affected the appropriate treatment of stroke patients. Following a stroke, various complications can occur, including thromboembolic diseases, pneumonia, urinary tract infection (UTI), bowel and bladder dysfunction, pressure injury. The occurrence of these complications can interfere with early rehabilitation and impact recovery.

While several studies have examined the impact of the COVID-19 pandemic on stroke patients, research specifically addressing secondary complications in stroke patients during the COVID-19 pandemic remains limited. Therefore, this study aims to investigate the effects of the COVID-19 pandemic on the occurrence of secondary complications in stroke patients.

Methods

The study was conducted on patients admitted to a hospital with both hemorrhagic and ischemic strokes, divided into two periods: pre-COVID (March 2019 to January 1, 2020) and COVID (March 2020 to January 1, 2021). A total of 604 patients were included in the pre-COVID group, and 554 patients were included in the COVID group. The study aimed to investigate the presence of complications such as UTI, pneumonia, deep vein thrombosis (DVT) or pulmonary thromboembolism (PTE), and pressure injuries. The statistical analysis used was the chi-square test to compare between different categories.

Results

Table 1 presents the comparisons of complication between the two groups. UTI were observed in 20 patients (3.6%) in the COVID group and in 18 patients (2.9%) in the pre-COVID group. Pneumonia was observed in 30 patients (5.4%) in the COVID group and in 24 patients (3.9%) in the pre-COVID group. DVT or PTE occurred in 2 patients (0.3%) in both the COVID and pre-COVID groups. Pressure injuries were observed in 4 patients (0.7%) in the COVID group and in 4 patients (0.6%) in the pre-COVID group.

Although no statistically significant differences were observed between the two groups, there were higher numbers of patients with UTI, pneumonia, DVT or PTE, and pressure injuries in the COVID group.

Conclusion

There were slightly higher incidences of UTI, pneumonia, DVT or PTE and pressure injury among stroke patients during the COVID period compared to the pre-COVID period, although these differences were not statistically significant. This suggests that while there may not be a significant statistical difference, there may be trends indicating a potential impact on certain secondary complications during the pandemic.

Further research with larger sample sizes and longer study durations could provide more insights into these trends and their implications for stroke patient care during global health crises like COVID-19.

	COVID group n=554	Pre-COVID group n=604	p-value*
UTI	20	18	0.5477
Pneumonia	30	24	0.2451
DVT or PTE	2	2	0.931
Pressure injury	4	4	0.9023

* Chi-square test

Table 1. Comparisons of complication between the two groups

Effects of Extracorporeal Shock Wave Therapy on Shoulder Pain Alleviation in Stroke Patients

Heegoo Kim^{1,2*}, Hwang Sean Soon Sung¹, Choi Soyoung¹, Seyoung Shin^{1,2,3}, MinYoung Kim^{1,2,3†}

Department of Rehabilitation Medicine, CHA Bundang Medical Center, CHA University School of Medicine, Seongnam, Republic of Korea¹, Digital Therapeutics Research Team, CHA Future Medicine Research Institute, Seongnam, Republic of Korea², Rehabilitation and Regeneration Research Center, CHA University School of Medicine, Seongnam, 13496, Republic of Korea³

Objectives

Extracorporeal shock wave therapy (ESWT) has been suggested as a non-invasive and alternative treatment for shoulder pain, and the effects of ESWT on various musculoskeletal disorders have been reported. In this present study, we aimed to investigate the effects of ESWT on hemiparetic shoulder pain alleviation in patients with stroke.

Methods

Six stroke patients participated in this double-blind, randomized cross-over study. The inclusion criteria were stroke patients with more than 1 month of onset, numerical rating scale (NRS) over 4 of hemiparetic shoulder pain, age over 20 years, mini-mental scale score (MMSE) over 15. The exclusion criteria were with traumatic hemiparetic shoulder pain, a high risk of bleeding due to severe coagulopathy, hemiparetic shoulder tendon full thickness tear by ultrasound examination. All participants underwent two conditions of ESWT intervention, for 3 days per week, total 6 sessions of intervention within 2 weeks for each condition, separated by 10 days of washout period, in random order of intervention: 1) real ESWT on hemiparetic shoulder, and 2) sham ESWT on hemiparetic shoulder. All participants were asked the standard screening questions suggested in the ESWT guidelines for the exclusion of contraindications or precautions. A total of 3,000 pulse stimulation was delivered to the lesser and greater tubercles of hemiparetic shoulder from 10 to 15 minutes in real condition. Sham stimulation was applied with the same process of real condition with sham probe. Assessments of hemiparetic shoulder pain were administered by NRS and Korean version of shoulder pain and disability index (SPADI) before and after the intervention.

Results

RM-ANOVA showed the significant time × condition interactions of all the measurements of hemiparetic shoulder pain ($p < 0.05$). There were statistical significance in all hemiparetic shoulder pain measurements in real condition ($p < 0.05$). However, in sham condition, significant changes of pain measurements were not showed in all pain measurements.

Conclusion

These results suggested that the application of ESWT on hemiparetic shoulder in stroke patients could alleviate hemiparetic shoulder pain. Consequently, ESWT could be considered one of the therapeutic strategies in pain relief therapy for stroke patients.

Acknowledgment Acknowledgement This research was supported by the IITP grant of Ministry of Science and ICT (2021-0-00742 Development of Core Technology for Whole-body Medical Twin) and supported by a grant of the Korea Health Technology R&D Project through the Korea Health Industry Development Institute (KHIDI), funded by the Ministry of Health & Welfare, Republic of Korea (grant number: RS-2023-00262005).

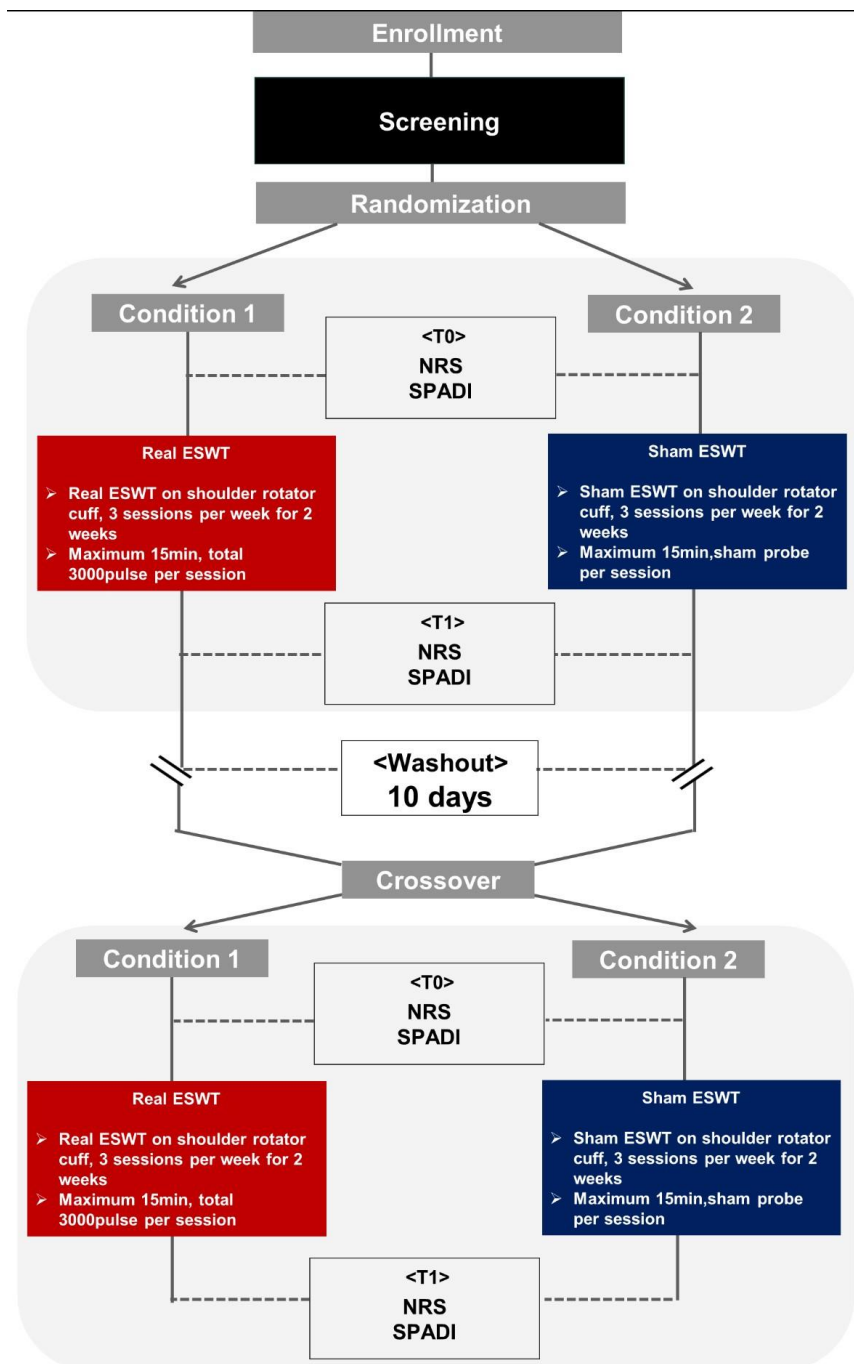


Figure 1. Study design

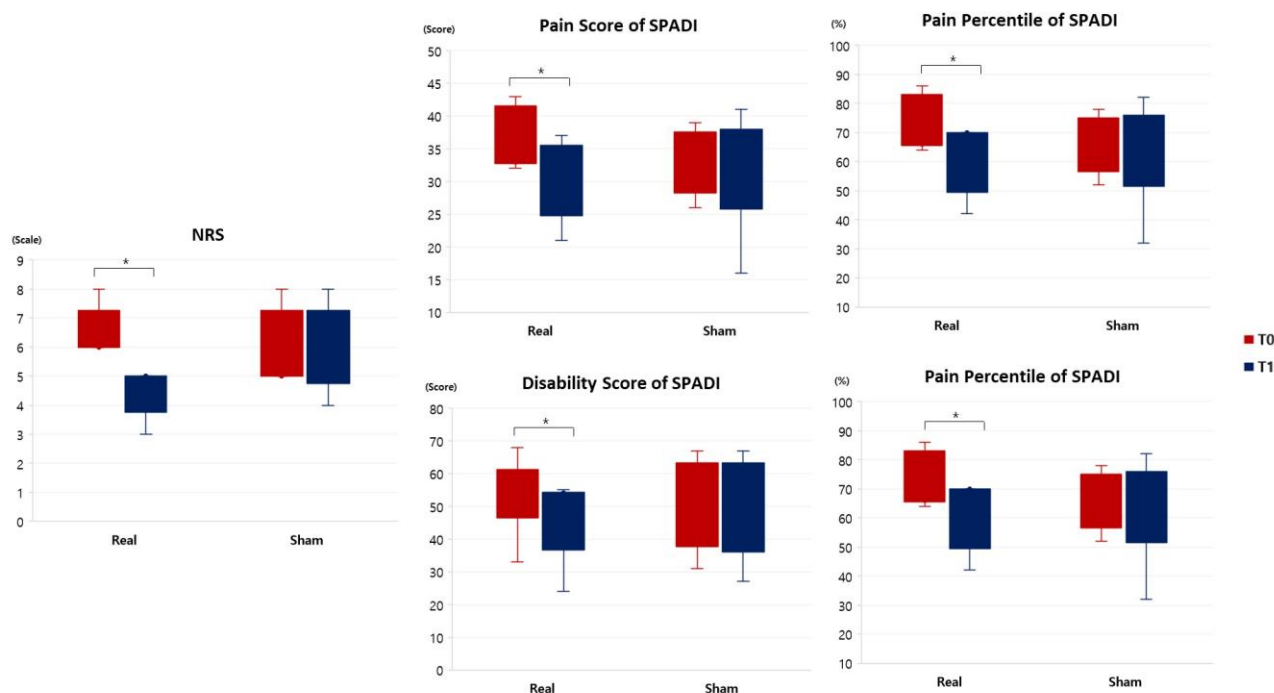


Figure 2. Comparison of pain measurements in real and sham conditions before and after intervention. In all measurements, there were significant time \times condition interactions of hemiparetic shoulder pain ($p < 0.05$). *Significant change before and after intervention (Wilcoxon-signed rank test, $p < 0.05$). NRS, numerical rating scale; SPADI, shoulder pain and disability index, T0, before intervention; T1, after intervention

Subject No.	Initial	Age	Sex	Dx.	Onset duration (days)	Affected side	NRS of hemiparetic shoulder at screening
01	LJI	61	M	Rt. corpus callosum infarction	718	Lt.	7
02	CJU	58	M	Rt. lateral medulla infarction, Lt. Parietal lobe infarction	74	Rt.	6
03	LSH	55	M	Lt. thalamus ICH	475	Rt.	6
04	MJS	53	M	Rt. MCA territory thromboembolic infarction	122	Lt.	8
05	NGS	76	F	Lt. parietal and temporal ICH c Lt SDH, Lt. frontoparietal ICH	46	Rt.	7
06	SSD	65	M	Rt thalamus ICH c IVH	66	Lt.	7
		59.5(54.5-67.8)	M:F = 5:1		98(61.0-535.8)	Rt.:Lt. = 2:3	7(6.0-7.3)

Table 1. Basic Characteristics of Study Participants

Artificial Intelligence-Guided Mobile Telerehabilitation for Subjects with Cognitive Impairment

Namo Jeon^{1*}, Doo Young Kim¹, Taeksoo Jeong¹, Sue Been Kim¹, Bum-Suk Lee¹, Min-Soo Kang², Si-Woon Park^{1†}

Department of Rehabilitation Medicine, International St. Mary's Hospital, Catholic Kwandong University College of Medicine, Incheon, Korea¹, Department of Physical and Rehabilitation Medicine, Seosong Hospital, Incheon²

Objective

To test feasibility and usability of Artificial Intelligence (AI)-guided mobile cognitive telerehabilitation program for patients with stroke or older adults with mild cognitive impairment (MCI).

Methods

This study is a multicenter, uncontrolled, feasibility study. The participants included thirteen subjects with cognitive impairment, defined by a Mini-Mental State Examination (MMSE) score of 26 or lower: 9 subjects with stroke, 4 subjects with MCI. Each participant was given a tablet PC on which AI-guided mobile cognitive rehabilitation program (Zenicog®) was installed, and instructed to go through total 24 sessions of 30-minutes training within 6 weeks. Cognitive assessments included MMSE, digit span, trail making test A & B. Usability questionnaire consisted of equitable and flexibility in use, simple and intuitive use, perceptible information, tolerance for error, low physical effort, size and space for approach and use, overall quality of product and overall satisfaction.

Results

Two participants declined after enrollment due to lack of motivation. Eleven participants completed 24 sessions without drop-out. Participants' mean age was 68.45 ± 8.61 . Eight (72.7%) participants were female and 3 (27.3%) participants were male. Duration of education was 10.73 ± 3.26 years. Three participants had MCI and 8 participants had stroke with the mean duration of 79.63 ± 52.3 days after the onset. The MMSE score was significantly increased from 22.64 ± 3.93 at baseline to 26.18 ± 3.22 after intervention ($p=0.014$). The overall quality of product in the usability questionnaire (Likert scale 1~5) scored 4.00 ± 0.87 , and the lowest score was tolerance for error (3.14 ± 1.1). Female participants and the participants with less than 12 years of education gave lower score in tolerance for error and equitable/flexibility in use, respectively.

Conclusion

AI-guided mobile cognitive telerehabilitation program is feasible and potentially beneficial in improving cognitive function for patients with stroke or older adults with MCI. Special consideration should be given to those who are less familiar with electronic devices to improve its usability.

Acknowledgment This research was supported by a grant of the Korean Health Technology R&D Project through the Korea Health Industry Development Institute (KHIDI), funded by the Ministry of Health & Welfare, Republic of Korea (Grant number: RS-2024-00263587)

Feasibility of Unsupervised Upper Extremity Rehabilitation in Patients with Brain Tumor: Pilot Study

Ho Seok Lee^{1*}, Soyoung Lee¹, Doona Cho¹, Dae Hyun Kim¹, Won Hyuk Chang^{1,2†}

Department of Physical and Rehabilitation Medicine, Samsung Medical Center¹, Department of Health Science and Technology, Department of Medical Device Management and Research, Sungkyunkwan University²

Objective

The objective of this study is to investigate the feasibility and safety of unsupervised upper extremity rehabilitation using a virtual reality (VR)-based planar motion exercise apparatus (Raphael Smart Board™ [SB]; Neofect Inc.) in brain tumor patients.

Methods

A total of five patients with brain tumor (4 male, mean age 55.6±12.7 years,) were recruited. All patients participated in ten sessions, five days per week, over the course of two weeks. Prior to the intervention, the researcher provided the participant with a 30-minute training session on the use of the Raphael Smart Board™ and established the initial task difficulty level. The participants engaged in unsupervised upper extremity rehabilitation using the Raphael Smart Board™ for a daily 30-minute session. Following five sessions of unsupervised upper extremity rehabilitation, the researcher adjusted the task difficulty. Should any issues arise, participants were able to contact the researcher, for example in the event of malfunctions with the device during unsupervised upper limb rehabilitation. The Fugl-Meyer Assessment-Upper Extremity (FMA-UE), 9-hole peg test (9-HPT), and Action Research Arm test (ARAT) were conducted at the outset of the study and at its conclusion. Additionally, the frequency and rationale behind participants contacting the researcher during the course of the intervention were also evaluated.

Results

Four of the five patients with brain tumors completed the two-week course of unsupervised upper extremity rehabilitation. One subject withdrew from the study due to the progression of their brain tumor, which was not related to the intervention. No adverse effects or accidents were reported by the participants. All four patients who completed the intervention demonstrated a statistically significant improvement in FMA-UE, 9-HPT, and ARAT ($p < 0.05$). Over the course of 40 sessions in four patients, there were only two instances where the researcher was contacted. The reasons for these calls were an unrelated headache-induced premature shutdown and a technical error of the Raphael Smart Board™. Both calls could be resolved over the phone without a visit from a researcher.

Conclusion The results of this pilot study indicate that unsupervised upper extremity rehabilitation using a VR-based planar motion exercise apparatus is a feasible and safe approach for patients with brain tumors. However, further investigation with a larger patient cohort is necessary to elucidate the effects of unsupervised upper extremity rehabilitation in patients with brain tumors.

Acknowledgment This research was supported by a grant of the Korea Health Technology R&D Project through the Korea Health Industry Development Institute (KHIDI). funded by the Ministry of Health & Welfare, Republic of Korea (grant number: HI20C1234)

Predictive Value of Cognitive Function and ALT for Functional Ambulation Gain in MCA Stroke Patients

Namo Jeon^{1*}, Doo Young Kim^{1†}

Department of Rehabilitation Medicine, International St. Mary's Hospital, Catholic Kwandong University College of Medicine¹

Background

Cognitive function and routine laboratory biomarkers, such as extremely low alanine aminotransferase (ALT) levels, are emerging as significant predictors of physical recovery in stroke patients. Cognitive impairments can hinder rehabilitation learning, while extremely low ALT levels are associated with frailty and delayed recovery, potentially serving as critical indicators for improving rehabilitation strategies.

Methods

This retrospective study analyzed 87 first-time middle cerebral artery (MCA) stroke patients who began rehabilitation within 30 days at a university hospital from June 2016 to June 2023. Basic group comparisons and multivariate logistic regression were conducted to identify predictors of functional ambulation recovery, considering key covariates like age, sex, NIHSS, BBS, MMSE scores, and extremely low ALT levels.

Results

The study found that female sex, lower MMSE and BBS scores, and extremely low ALT levels were associated with poorer odds of achieving functional ambulation. Specifically, multivariate analysis showed that male sex, higher initial MMSE scores, higher BBS scores, and ALT levels within the reference range significantly increased the likelihood of achieving functional ambulation post-rehabilitation.

Conclusion

Extremely low ALT levels, indicative of frailty, significantly predict poor recovery in MCA stroke patients. This study underscores the importance of routine biomarkers and cognitive assessments in enhancing prognostic accuracy and tailoring rehabilitation strategies to improve patient outcomes.

Acknowledgment This research was supported by a grant of the Korean Health Technology R&D Project through the Korea Health Industry Development Institute (KHIDI), funded by the Ministry of Health & Welfare, Republic of Korea (Grant number: RS-2024-00263587)

Psychological well-being evident in lymphedema treatment in association with weight management

Sang Hee IM^{1*}, Eun Yong Han², Seungeun Park¹, Kye Hee Cho^{3†}

Department and Research Institute of Rehabilitation Medicine, Yonsei University College of Medicine, Severance Rehabilitation Hospital¹, Department of Rehabilitation Medicine, Jeju University School of Medicine², Department of Hospital Medicine, Yonsei University College of Medicine, Yonsei Severance Hospital³

Purpose

Lymphedema is associated with an increased risk of obesity. In obese patients with previous mastectomy, weight reduction alone resulted in a greater decrease in the volume of the affected arm compared to that of the sound side. Additionally, in obese patients, the restriction of lymphatic circulation has shown a significant correlation with lesser efficiency in weight reduction. While fat reduction in conjunction with exercise and nutritional management, is encouraging as a treatment method for obesity, its effectiveness in lymphedema patients has not been established. Therefore, a prospective study was conducted to determine the feasibility of weight control as part of lymphedema therapy through exercise and nutritional management.

Material and Method

A total of 30 breast cancer patients with diagnosed post-mastectomy lymphedema were screened for the study, and 19 of them agreed to participate. During the follow-up, 4 withdrew their consent to participate. The patients were randomly assigned to either a study group on exercise and diet control (n=8) or a control group (n=7). The study group kept 8 weeks of a dietitian-consulted diet log and reported time spent on daily exercise every week. Both groups were exposed to complex decongestive therapy during the study. Laboratory tests, physical function, lymphedema circumference, quality of life questionnaires, and BIA were assessed before and after the intervention. Nonparametric statistics were used for the analysis.

Result

As a result, baseline group differences were not significant between groups. After the intervention, the BBS score significantly differed between groups (P

Conclusion

Although the study group did not show a significant change in lymphedema volume reduction, the consistently positive results in body composition and physical function improvement, psychological distress reduction, and supporting laboratory evidence suggest that weight management should be part of lymphedema treatment. Moreover, this study has shown the benefit of lymphedema treatment in the psychological well-being of lymphedema patients. Further studies with a larger number of participants will help clarify the benefits of weight management concerning body composition and different weight categories in lymphedema.

Acknowledgment This work was supported by the National Research Foundation of Korea(NRF) grant funded by the Korea government(MSIT; Ministry of Science& ICT) (No. 2020R1G1A110314811).

Dysphagia Treatment for Patients with Head and Neck Cancer: A Network Meta-Analysis

MUN SOJEONG^{1*}, Chan Woong Jang¹, Woo Kyoung Yoo¹, Kwang IK Jung¹, Jong Mi Park^{1†}

Department of Physical Medicine and Rehabilitation, Hallym University Sacred Heart Hospital, Hallym University College of Medicine, Anyang, Korea¹

INTRODUCTION

Head and neck cancer treatments often lead to significant dysphagia, affecting patients' quality of life and nutritional status. Dysphagia-related malnutrition and aspiration are common, with implications for patient morbidity and mortality. Various rehabilitation interventions, including swallowing exercises, Neuromuscular Electrical Stimulation (NMES), speech therapy, and telerehabilitation, aim to mitigate these effects and improve outcomes. This network meta-analysis synthesizes current evidence on the effectiveness of these interventions, providing a comprehensive comparison to guide clinical practice and future research. By evaluating multiple treatment modalities, we aim to identify the most effective strategies for preserving swallowing function and enhancing patient recovery during and after cancer treatment.

METHOD

PubMed, MEDLINE, EMBASE, Cochrane, Scopus, and Web of Science were searched through June 6, 2024. Effect sizes for patient-reported swallowing ability, patient-reported quality of life, swallowing tests, and anatomic findings were quantified using standardized mean differences within a random effects model. Effectiveness ranking for each treatment was expressed as the surface under the cumulative ranking curve (SUCRA).

RESULTS

Twenty-two studies involving 1392 participants were included in the final analysis. Figure 1 shows a network plot of patient-reported swallowing ability(1A), patient-reported quality of life(1B), swallowing tests, and anatomical findings (1C). According to SUCRA, NMES with exercise was the most effective option for patient-reported swallowing ability (Figure 2), patient-reported quality of life at 100, and 95.4, respectively. Telerehabilitation was the worst treatment option for patient-reported swallowing ability and patient-reported quality of life, with SUCRA of 12.6 and 15.8, respectively. Based on video fluoroscopic swallow test results and anatomical findings such as mouth opening and hyoid bone migration, usual care was the most effective with SUCRA 69.3, and speech therapy was the least effective with SUCRA 31.4.

CONCLUSION

This network meta-analysis was a comprehensive comparison of different dysphagia treatments for patients with head and neck cancer. The results showed that NMES combined with exercise was superior to other treatments by significantly improving patient-reported swallowing ability and quality of life; however, swallow tests and anatomy showed different results. These results highlight the importance of selecting the appropriate intervention to enhance patient recovery and underscore the need for standardized treatment protocols in clinical practice to ensure optimal outcomes for the management of dysphagia in this patient population.

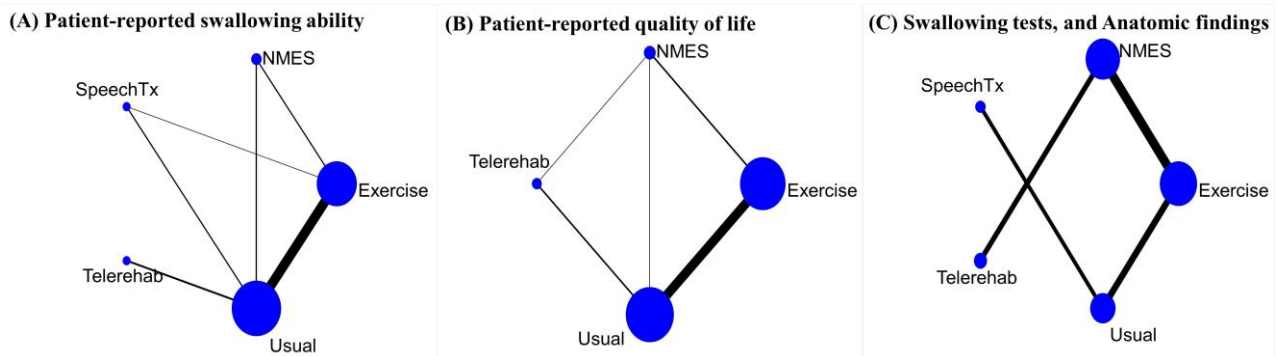


Figure 1. Network plots (A) Patient-reported swallowing ability (B) Patient-reported quality of life (C) Swallowing tests, and Anatomical findings

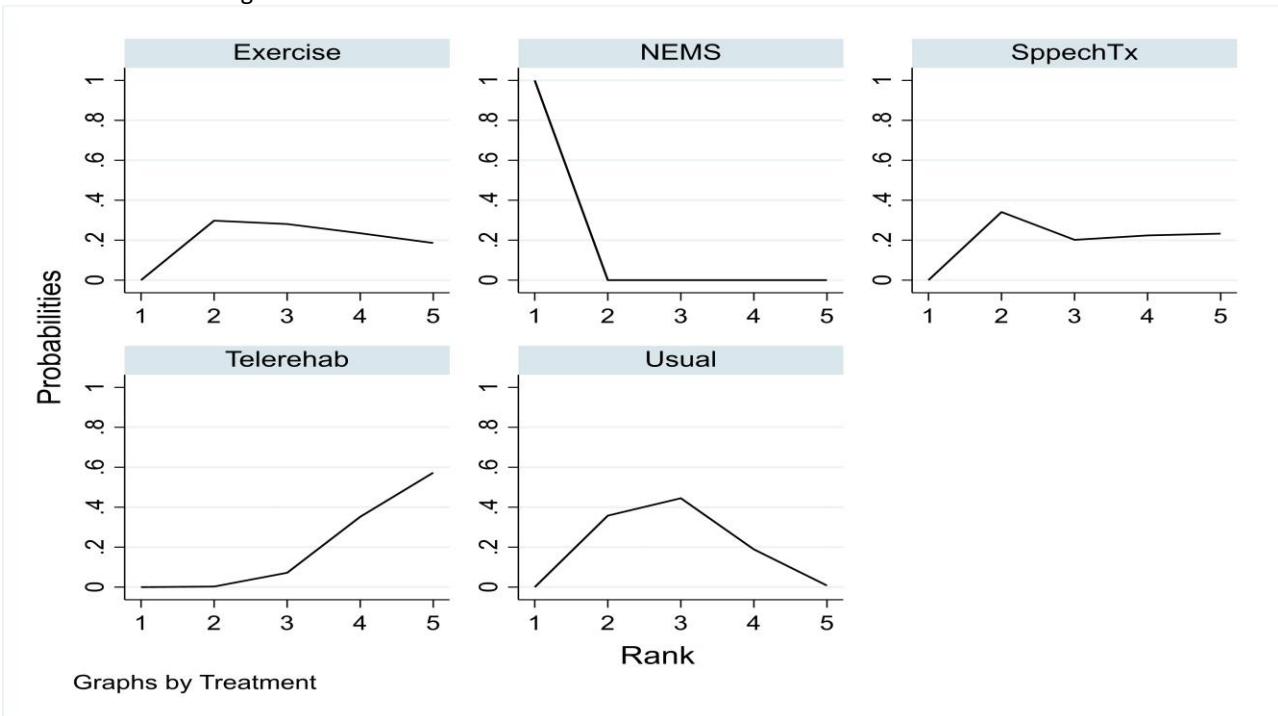


Figure 2. The probability of a given treatment being ranked first, second, third, or fourth in patient-reported swallowing ability.

Table 1. SUCRA value of dysphagia treatment for patients with head and neck cancer.

	Patient-reported swallowing ability	Patient-reported quality of life	Swallowing tests, and Anatomic findings
Usual care	53.8	29.9	69.3
Exercise	42.3	58.9	64.4
NMES	100.0	95.4	37.2
Speech Tx	41.3	-	31.4
Telerehabilitation	12.6	15.8	47.8

SUCRA, Surface under the cumulative ranking curve; NMES, Neuromuscular Electrical Stimulation; Tx, Treatment

Table 1. SUCRA value of dysphagia treatment for patients with head and neck cancer.

Direct effect of lymphatic dynamic transport after low-level laser therapy: a RCT

Jin A Yoon^{1,4*†}, Hasuk Bae², Jae Yong Jeon³, Min Kyung Park⁴, Byung Hoon Lee⁴

Department of Rehabilitation Medicine, Biomedical Research Institute, Pusan National University Hospital, Pusan National University School of Medicine¹, Department of Rehabilitation Medicine, Ewha Womans University Mokdong Hospital, Ewha Womans University College of Medicine², Department of Rehabilitation Medicine, Asan Medical Center, University of Ulsan College of Medicine³, Department of Rehabilitation Medicine, Biomedical Research Institute, Pusan National University Hospital⁴

Objective

This study is aimed to investigate the direct effects of low level laser therapy (LLLT) at different wavelengths on lymphatic motility and local fluid reduction in healthy individuals to further present the most appropriate protocol and effectiveness of LLLT in lymphedema patients.

Methods

A total of 32 healthy participants, including 12 males and 20 females were included and divided into 2 groups. They underwent single session of upper extremity manual lymphatic drainage (UE MLD) to unilateral upper extremity followed by 2 different types of LLLT to ipsilateral axilla region to enhance lymphatic drainage. During each treatment session and resting period, indocyanine green (ICG) lymphography was performed to analyze direct effect of LLLT on lymphatic motility. Extracellular fluid volume and local tissue water amount was also measured before and after the intervention using multiple frequency bioelectrical impedance analysis (MFBIA) and tissue dielectric constant (TDC).

Results

In the analysis comparing the velocity of lymph packets, a significant increase was observed in the velocity during the UE period compared with the resting period in group B. In the case MFBIA values before and after treatment, body water content tended to decrease in both groups after treatment but in the inter-group comparison, there was no significant difference between the two groups. In the case of TDC value, overall patients showed decreased in body water content immediately after UE MLD and LLLT in most measured area. Otherwise, no significant difference in the amount of body water reduction between the two groups after LLLT was confirmed. Intra group analysis comparing the change of velocity and number of lymph packet between each time point showed increased velocity after UE MLD in group B and increased number of packets in both groups. However, number of lymph packet decreased significantly after LLLT compared to resting period in both groups. The Wilcoxon Rank Sum Test comparing velocity of lymph packet during each time points between group A and group B showed no significant statistical difference. In addition, there were no significant differences of lymph packet in all intervention period in intergroup comparison analysis. The linear mixed model result indicated that the increase of velocity of lymph packet during treatment showed significant negative correlation to overall LLLT controlling for other factors. In addition, increase of numbers of lymph packet during treatment showed significant positive correlation with UE MLD and negative correlation with LLLT.

Conclusion

In this study, we quantitatively evaluated the lymphatic motility and tissue water content after different types of LLLT in healthy participants. Based on these data, more clinical evidence should be obtained for appropriate parameters depending on the severity and targeted tissue of lymphedema.

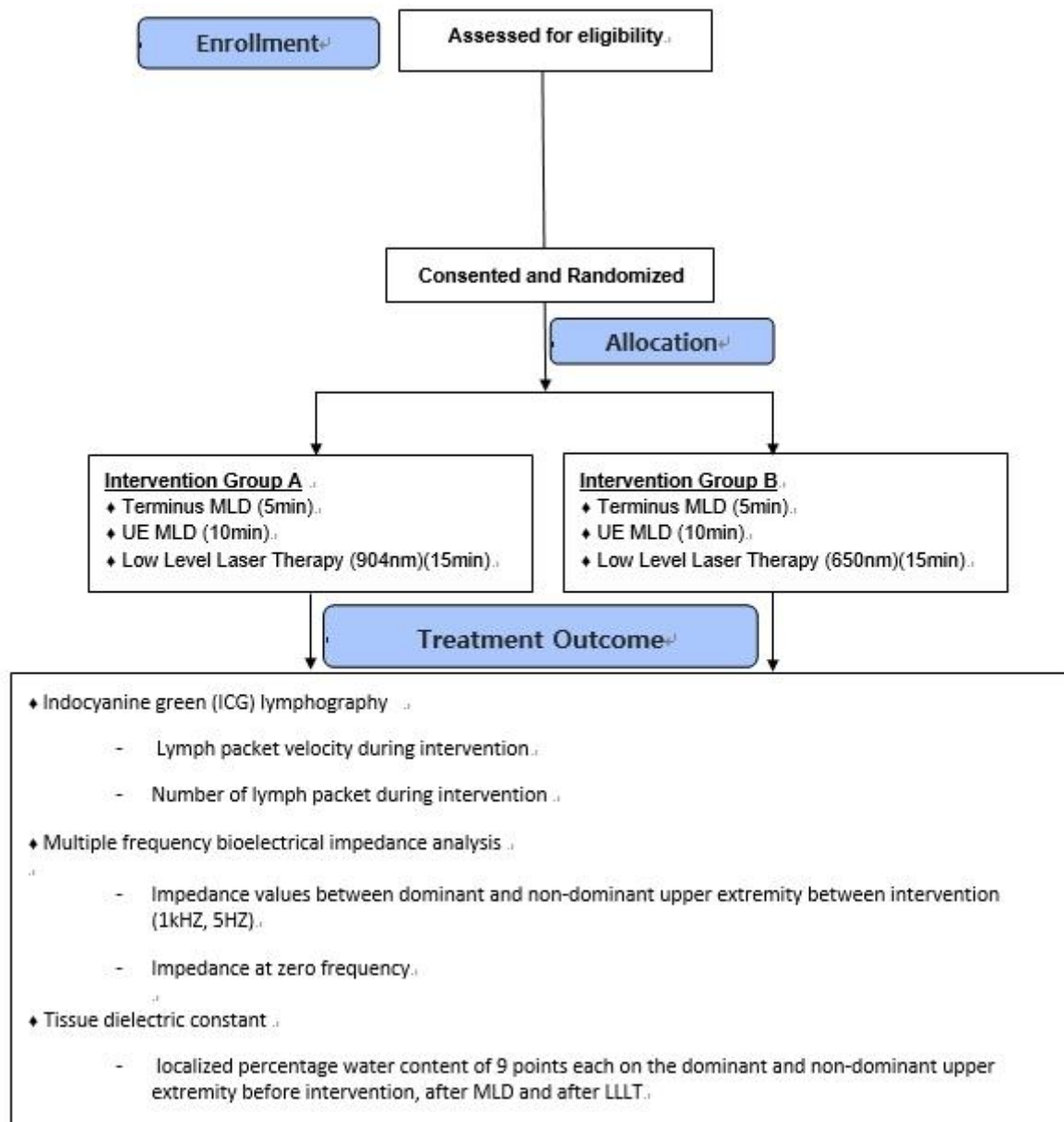


Figure 1. Flow diagram of our study

[Intervention Group A]



[Intervention Group B]

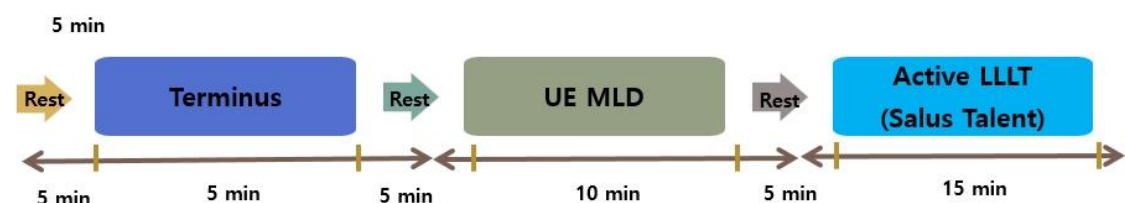


Figure 2. Treatment protocol of two groups used for this study

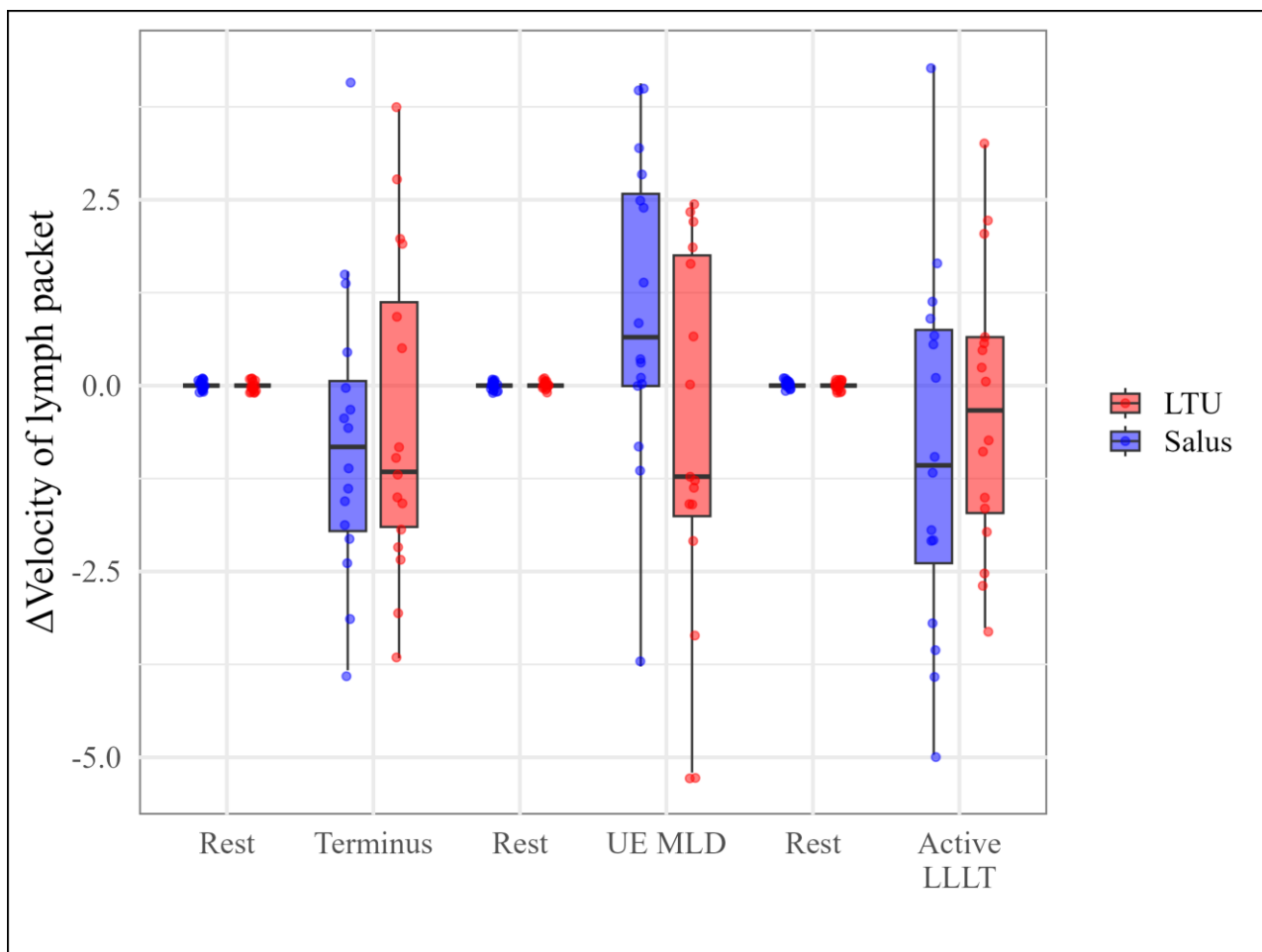


Figure 3. Intra group analysis comparing the change of velocity and number of lymph packet between each time point

Dysphagia after transaxillary robot-assisted thyroidectomy and central compartment neck dissection

Yura Goh^{1*}, Hyeok Jun Yun², Yong Sang Lee², Yoon Ghil Park¹, Jun Sung Lee², Sooin Lee¹, Joo Eun Park¹, Jinyoung Park^{1†}

Department of Rehabilitation Medicine, Gangnam Severance Hospital, Yonsei University College of Medicine, Seoul, Korea¹, Department of Surgery, Thyroid Cancer Center, Institute of Refractory Thyroid Cancer, Gangnam Severance Hospital, Yonsei University College of Medicine, Seoul, Korea²

Introduction

Transaxillary robot-assisted thyroidectomy with central compartment neck dissection (CCND) is increasingly performed due to its advantages, such as avoiding visible neck scars and reducing the risk of neural or parathyroid injury. However, because the transaxillary approach does not involve dissecting the skin of the anterior neck, clinicians tend to neglect the possibility of postoperative dysphagia, depriving patients of the opportunity to address their discomfort. Therefore, this study aims to describe the characteristics of dysphagia in these patients through the analysis of videofluoroscopic swallowing study (VFSS).

Methods

This retrospective observational study screened patients who underwent VFSS due to dysphagia symptoms after transaxillary robot-assisted thyroidectomy with CCND between August 2023 and February 2024 in a single tertiary hospital. The VFSS protocol followed this order: semisolid (International Dysphagia Diet Standardisation Initiative [IDDSI] 3, 1 spoon), semisolid (IDDSI 2, 1 spoon), sesame porridge (IDDSI 4, 1 spoon), small liquid (IDDSI 0, 5 mL), and large liquid (IDDSI 0, 15 mL). If a serious aspiration event without cough reflex occurred, the VFSS was ceased in that step. The severity of swallowing problem was scored using the Videofluoroscopic Dysphagia Scale (VDS), which ranges from 0 to 100, with 0 indicating normal function. The severity of aspiration was rated using the Penetration-Aspiration Scale (PAS).

Results

Fifteen VFSS videos from 15 patients and their medical records were reviewed. The demographic, perioperative, and postoperative characteristics are listed in Table 1. The average period from surgery to VFSS was 1.3 days. By analysis of VFSS video, all patients had no abnormal findings in oral phase of swallowing, however, all 15 patients showed abnormal pattern in pharyngeal phase, resulting in the average VDS score 21.9 (Table 2). Specifically, 14 patients showed decreased laryngeal elevation, 7 patients exhibited pharyngeal wall coating, and 14 and 4 patients had vallecular and piriform sinus residue, respectively. The average PAS score was 2.6, with 3 patients showing penetration and 3 patients showing aspiration (Table 3). The total or subitem scores of VDS were unaffected by the presence of lymph node metastasis, lymphatic invasion, lymphocytic thyroiditis, or adenomatous hyperplasia. However, the approach side affected the average score of the VDS subitem "piriform sinus residue", with higher scores observed when the surgery was approached from the right side (mean [SD]; 3.8 [3.4] for the right, 0.5 [1.5] for the left approach).

Conclusions

Dysphagia following transaxillary robot-assisted thyroidectomy and CCND is frequently underestimated, resulting in clinicians neglecting patient discomfort. This dysphagia is confined to the pharyngeal phase and is notably more prevalent with right-sided approaches. Further data accumulation will aid in developing specific treatment strategies.

Table 1. Patients' characteristics

Characteristics (N=15)	N (%) or mean (SD)
1. Demographic characteristics	
Sex, N(%)	
Male	1 (6.7)
Female	14 (93.3)
Age, yr	37.9 (5.7)
Height, cm	160.2 (6.3)
Weight, kg	62.4 (15.2)
Body mass index, kg/m ²	24.2 (4.9)
2. Perioperative characteristics	
Operation duration, min	110.4 (41.0)
Approaching side	
Right	6 (40.0)
Left	9 (60.0)
3. Postoperative characteristics	
Pathology	2.4 (0.5)
Papillary carcinoma	5 (33.3)
Papillary microcarcinoma	9 (60.0)
Follicular adenoma	1 (6.7)
Combined benign lesion	
Lymphocytic thyroiditis	6 (40.0)
Adenomatous hyperplasia	6 (40.0)
Invasion	
Lymphatic invasion	5 (33.3)
Vascular invasion	0 (0.0)
Lymph node metastasis	6 (40.0)
4. Postoperative characteristics	
Post-surgery to VFSS period	1.3 (0.5)

Table 1. Patients' characteristics

Table 2. Videofluoroscopic swallowing findings

Videofluoroscopic swallowing findings	Score, mean (SD)	No. of dysfunction (%)
Oral phase		
Lip closure	0.0 (0.0)	0.0 (0.0)
Bolus formation	0.0 (0.0)	0.0 (0.0)
Mastication	0.0 (0.0)	0.0 (0.0)
Apraxia	0.0 (0.0)	0.0 (0.0)
Tongue to palate contact	0.0 (0.0)	0.0 (0.0)
Premature bolus loss	0.0 (0.0)	0.0 (0.0)
Oral transit time	0.0 (0.0)	0.0 (0.0)
Pharyngeal phase		
Triggering of pharyngeal swallow	1.8 (2.3)	6 (40.0)
Vallecular residue	2.7 (1.2)	14 (93.3)
Laryngeal elevation	7.8 (3.2)	14 (93.3)
Pyriiform sinus residue	1.8 (2.8)	4 (26.7)
Coating of pharyngeal wall	4.2 (4.6)	7 (46.7)
Pharyngeal transit time	0.0 (0.0)	0 (0.0)
Aspiration	3.6 (5.0)	6 (40.0)
VDS, oral phase subscore	0.0 (0.0)	
VDS, pharyngeal phase subscore	21.9 (11.2)	
VDS, total score	21.9 (11.2)	

Table 2. Videofluoroscopic swallowing findings

Table 3. Aspiration after transaxillary robot-assisted thyroidectomy and central compartment neck dissection

Parameters	N (%)
Penetration-aspiration scale (PAS) score	
1	9 (60.0)
2	1 (6.7)
3	1 (6.7)
4	1 (6.7)
5	0 (0.0)
6	0 (0.0)
7	3 (20.0)
8	0 (0.0)
Aspiration type	
Pre-swallowing aspiration	0 (0.0)
During-swallowing aspiration	6 (100.0)
Post-swallowing aspiration	0 (0.0)
Aspirate	
Solid	0 (0.0)
Semisolid	0 (0.0)
Liquid	6 (100.0)
5 mL	0 (0.0)
15 mL	6 (100.0)

Table 3. Aspiration after transaxillary robot-assisted thyroidectomy and central compartment neck dissection

Cancer Rehabilitation

P-41

A Protocol for Tailored Swallowing Exercises with Telephone Support in Head & Neck Cancer Patients

Min Wook Kim^{1*}, Young Ah Choi¹

Department of Rehabilitation Medicine, Incheon St. Mary's Hospital, The Catholic University of Korea¹

Objective

The primary aim of this study is to establish a protocol for a swallowing management system specifically designed for head and neck cancer patients. Additionally, this study aims to evaluate whether periodic telephone calls can increase adherence to and the effectiveness of dysphagia treatment.

Methodology

This protocol involves a pre-operative swallowing consultation where patients are classified according to their level of dysphagia and the specifics of their surgical intervention. This classification informs the provision of patient education on swallowing physiology and the prescription of tailored exercises, including techniques such as the effortful swallow, the Mendelsohn maneuver, the Masako maneuver, and the Shaker exercises. A randomized controlled trial (RCT), blind to the evaluator, is conducted with two groups: one receiving standard care without telephone follow-up and the other receiving periodic telephone calls twice a month to reinforce adherence.

Outcome Measures

The effectiveness of this protocol is evaluated at baseline, 3 months postoperatively, and 12 months postoperatively. The primary endpoint is the duration of feeding tube dependency one year after operation. Secondary outcomes include Eating Assessment Tool-10, GUSS, Dysphagia Severity Scale (DSS), Functional Oral Intake Score (FOIS), incidence of pneumonia, weight loss, and various patient-reported outcomes such as quality of life, symptom burden, and self-efficacy.

Significance

Establishing a structured and patient-specific swallowing management protocol is crucial for improving the care of head and neck cancer patients. This study not only aims to enhance the clinical outcomes related to dysphagia but also to determine the impact of regular patient engagement through telephone calls on treatment adherence and effectiveness. The findings from this study could significantly influence clinical practices and set new standards for pre- and postoperative care in this patient cohort.

Exploring Quality of life in patients with Breast Cancer-related Lymphedema: Which factors affect?

Ji Young Lim^{1*}, Sun Woo Kim¹, Seonghee Kim¹, Seoyeong Lim¹, Ji Hye Hwang^{2†}

Physical and Rehabilitation Medicine, Sungkyunkwan University School of Medicine¹, Physical and Rehabilitation Medicine, Samsung Medical Center, Sungkyunkwan University School of Medicine²

Objectives

Many studies have reported that breast cancer-related lymphedema (BCRL) is associated with a poor quality of life (QoL) and has physical and psychosocial impacts on patients. In highlighting the importance of QoL, there has been being an emphasis on its regular evaluation and integration into patient care. It enables improving patient satisfaction with treatment by providing comprehensive approaches from the patients' perspective in addition to reducing the size of the lymphedema. There is a need for a better understanding of their QoL through the eyes of the patients living with BCRL in real-world settings. This study aims to investigate the factors affecting lymphedema-specific QoL in BCRL patients through routine electronic patient-reported outcome measure (ePROM) collection.

Methods

A total of 141 patients completed the electronic Korean version of Lymphoedema Quality of Life (LYMQOL) on their mobile phones in an outpatient setting. This outcome measure has been translated and verified by our research team. LYMQOL assesses function, appearance, symptoms, mood, and the QoL domain. Sociodemographic and clinical variables included age, body mass index, residency, lymphedema duration, comorbidities, physical activity, self-care, treatment history for breast cancer and lymphedema, percentage of excessive volume measured by optoelectronic limb volumeter (Perometer®) to classify their lymphedema stage and perceived arm severity in an 11-point scale.

Results

Their characteristics and LYMQOL results are shown in Table 1. According to the multiple regression analysis, their mood and appearance worsened, the number of chemotherapy sessions increased, and the stage of lymphedema was lower, the QoL for patients with BCRL decreased (model explained 47.6% of the QoL variance; $F = 26.471$, $p < .001$).

Conclusions

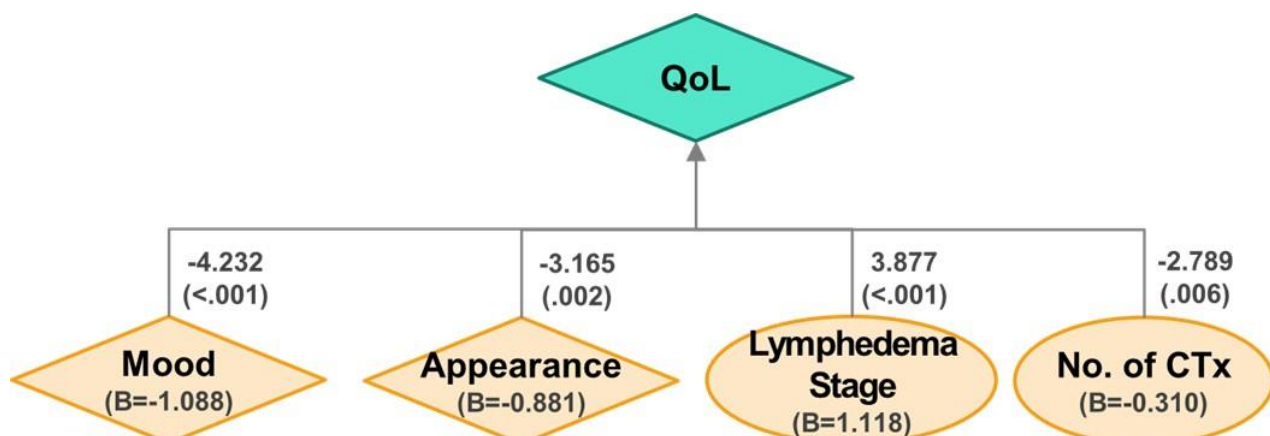
This is the first study to explore the factors influencing QoL in BCRL patients utilizing ePROM collected in clinical practice. These results support previous evidence of the negative effects of arm lymphedema on body image, appearance, and psychosocial well-being. The risk of mild lymphedema progressing to a severe stage may cause psychological stress and increase the burden of management. While other studies reported lymphedema clinical staging or did not include quantitative arm volume, in this study, accurate evaluation of lymphedema might have contributed to finding it as a significant factor. In addition, several times of the chemotherapy across cancer care pathway might have a prolonged impact on their general health conditions and QoL. As regards enhancement of lymphedema-specific QoL, interventions such as an appearance care program or education on coping strategies when increasing their limb volume, and physical/psychological support using digital tools may be included. Further studies on the trajectories of QoL should be also considered to compare patients at the same stage of the BCRL and for better-shared decision-making.

Acknowledgment This research was supported by a grant of the Korean Cancer Survivors Healthcare R&D Project through the National Cancer Center, funded by the Ministry of Health & Welfare, Republic of Korea (RS-2023-CC139237).

Table 1. Demographics of Breast Cancer-Related Lymphedema (N=141)

Characteristics	Values
Sex (female)	141 (100%)
Age (years)	56.20 ± 10.85
Body Mass Index (kg/m ²)	23.68 ± 3.36
Duration of illness (day)	1081.01 ± 1093.38
Place of residence	
- Metropolitan area	98 (69.5%)
- Non-metropolitan area	43 (30.5%)
Number of comorbidities	0.72 ± 0.88
Dominant hand	
- Right	141 (100%)
Side of involvement	
- Right	72 (51.1%)
- Left	69 (48.9%)
Chemotherapy*	
- Yes	130 (92.2%)
- No	11 (7.8%)
Radiotherapy	
- Yes	115 (81.6%)
- No	26 (18.4%)
Treatment for lymphedema (CDT)	
- Yes	52 (36.9%)
- No (including unknown)	89 (63.1%)
Self-care (n=130)	
- Good	52 (40.0%)
- Moderate	2 (1.5%)
- Poor	76 (58.5%)
Physical activity level (n=139)	
- Performance of activities of daily living	134 (96.4%)
- Possible of sports activity	5 (3.6%)
PEV (n=139)	
- Forearm ratio	13.05 ± 11.78
- Whole-arm ratio	13.06 ± 10.98
Lymphedema stage	
- 1 (< whole arm PEV 10%)	73 (51.8%)
- 2 & 3 (≥ whole arm PEV 10%)	68 (48.2%)
LYMQOL domain (score)	
- Function	1.76 ± 0.64
- Appearance	1.90 ± 0.96
- Symptoms	1.95 ± 0.63
- Mood	1.97 ± 0.72
- Quality of Life	5.72 ± 2.22
Perceived arm severity (score)	4.52 ± 2.60

Values are presented as number (%) or Mean ± Standard deviation. *It includes all chemotherapy treatments for breast cancer such as neoadjuvant chemotherapy, adjuvant chemotherapy, and palliative chemotherapy. As of the date of ePRO collection, six patients were receiving chemotherapy. PEV, Percentage of Excessive Volume (measured by optoelectronic limb volumeter); Lymphedema stage, clinical classification; Comorbidity, hypertension, diabetes, hyperlipidemia, BMI: Body Mass Index; Self-care, guideline-compliant compression stocking wear (Good: guideline-compliant, Moderate: occasionally, Poor: not at all); ADL, Activities of Daily Living; CTx, Chemotherapy; RTX, Radiotherapy; CDT, Complex Decongestive Therapy.

Table 1. Demographics of Breast Cancer-Related Lymphedema (N=141)**Fig 1.** Multiple Regression Analysis Results (indicated t and p-value)

Chemotherapy and Breast Cancer-Related Lymphedema: A Nationwide Retrospective Cohort Study

Sung Hoon Jeong^{1,2,3*}, Seong Min Chun⁴, Miji Kim^{2,5}, Hyunji Lee^{2,6}, Ja-Ho Leigh^{1,2,7†}

Department of Rehabilitation Medicine, Seoul National University Hospital¹, National Traffic Injury Rehabilitation Research Institute, National Traffic Injury Rehabilitation Hospital², Institute of Health Services Research, Yonsei University³, Department of Physical Medicine and Rehabilitation, Soonchunhyang University Hospital Seoul⁴, Department of Biostatistics and Computing, Yonsei University Graduate School⁵, Department of Rehabilitation Medicine, National Traffic Injury Rehabilitation Hospital⁶, Institute of Health Policy and Management, Medical Research Center, Seoul National University⁷

Background

Breast cancer mortality has decreased due to improved treatments, making the prevention of complications like breast cancer-related lymphedema (BCRL) crucial for survivors' quality of life. While BCRL risk factors include surgery, chemotherapy, and radiotherapy, the specific impact of chemotherapy on BCRL risk is underexplored and findings are inconsistent.

Objective

This study aimed to investigate the association between chemotherapy and the risk of BCRL in patients with newly diagnosed breast cancer using large representative population-based sample data.

Method

This nationwide, retrospective cohort study utilized data from the Korean National Health Insurance database and the Korea Central Cancer Registry database (2006–2017). Using 1:1 propensity score matching, 41,895 chemotherapy participants and 41,895 non-chemotherapy participants were included in the analysis. Cox proportional hazards regression models were used to examine the association between chemotherapy and BCRL risk.

Result

Compared with patients who did not receive chemotherapy, the risk of BCRL was higher in patients who received chemotherapy (hazard ratio [95% confidence interval], 1.89 [1.75–2.04]). Furthermore, the risk was most pronounced in the taxane therapy group (2.28 [1.83–2.84]), the Distant Staging group (3.83 [3.48–4.22]), the rural residence group (1.97 [1.68–2.32]), and the lowest income group (2.04 [1.74–2.41]).

Conclusion

Chemotherapy after diagnosis of breast cancer increases the risk of BCRL. Therefore, clinicians suggest that BCRL should be monitored more frequently during the follow-up period, especially in patients after taxane, antimetabolite, and anthracycline chemotherapy.

Acknowledgment This study was supported by a grant from the Ministry of Land, Infrastructure and Transport (MOLIT) Research Fund (NTRH RF-2024001)

Table 1. Cox proportional hazards regression analysis of the association between chemotherapy and risk of BCRL in breast cancer patients

Variables		Risk of BCRL			
		HR*	95% CI		
Chemo therapy					
	No	1.00			
	Yes	1.89	(1.75	—	2.04)

BCRL, Breast cancer-related lymphedema; HR, hazard ratio; CI, confidence interval.

*Adjusted for age, region, SEER, Household income level, Health insurance, Disability, Healthcare institution type, CCI, Surgery, Radio therapy, Hormone therapy, Target therapy.

Cox proportional hazards regression analysis of the association between chemotherapy and risk of BCRL in breast cancer patients

Table 2. Results of subgroup analysis examining the effect of chemotherapy on the risk of lymphedema by stratifying by SEER, household income level, and CCI.

Variables		Risk of BCRL				
		HR	HR*	95% CI		
SEER						
	Localized	1.00	1.87	(1.71	—	2.05)
	Regional	1.00	1.96	(1.70	—	2.27)
	Distant	1.00	2.83	(1.80	—	4.47)
	Unknown	1.00	2.29	(1.39	—	3.80)
Region						
	Urban	1.00	1.82	(1.64	—	2.03)
	Sub-urban	1.00	1.94	(1.69	—	2.24)
	Rural	1.00	1.97	(1.68	—	2.32)
Household income level						
	Low	1.00	2.04	(1.74	—	2.41)
	Mid-low	1.00	1.91	(1.64	—	2.22)
	Mid-high	1.00	1.84	(1.54	—	2.20)
	High	1.00	1.82	(1.61	—	2.07)

BCRL, Breast cancer-related lymphedema; HR, hazard ratio; CI, confidence interval; SEER, surveillance epidemiology and end results.

*Adjusted for age, region, SEER, Household income level, Health insurance, Disability, Healthcare institution type, CCI, Surgery, Radio therapy, Hormone therapy, Target therapy.

Results of subgroup analysis examining the effect of chemotherapy on the risk of lymphedema by stratifying by SEER, household income level, and CCI.

Table 3. The association between type of chemotherapy and risk of BCRL in breast cancer patients

Variables	Risk of lymphedema			
	HR ^a	95% CI		
Chemo therapy				
Taxane group	3.83	(3.48	-	4.22)
Anthracycline group	1.28	(1.17	-	1.41)
Antimetabolite group	1.34	(1.17	-	1.54)
None	1.00			

^a **Taxane group:** A group receiving only taxane-based chemotherapy or chemotherapy including taxane; ^b **Anthracycline group:** A group receiving anthracycline-based chemotherapy, either exclusively or in combination with other agents, excluding the Taxane group; ^c **Antimetabolite group:** A group receiving antimetabolite-based chemotherapy, either exclusively or in combination with other agents, after excluding the Taxane and Anthracycline groups; ^d **None:** A group that did not receive any chemotherapy, including taxane, anthracycline, or antimetabolite-based treatments.

^aAdjusted for age, region, SEER, Household income level, Health insurance, Disability, Healthcare institution type, CCI, Surgery, Radio therapy, Hormone therapy, Target therapy.

The association between type of chemotherapy and risk of BCRL in breast cancer patients

Use of Pulmonary Rehabilitation for Lung Cancer Patients in Korea: Analysis of the NHIS Database

Sang Hun Kim^{1*}, Yong Beom Shin^{1†}, Cho Hui Hong⁶, Jinmi Kim³, Jeong Su Cho⁴, Jung Seop Eom⁵, Jae Sik Seo², Seon Jun Yoon²

Department of Rehabilitation Medicine, Biomedical Research Institute Pusan National University Hospital, Pusan National University School of Medicine¹, Department of Rehabilitation Medicine, Biomedical Research Institute Pusan National University Hospital², Department of Biostatistics, Clinical Trial Center, Biomedical Research Institute, Pusan National University Hospital³, Department of Thoracic and Cardiovascular Surgery, Pusan National University Hospital, Pusan National University School of Medicine⁴, Department of Internal Medicine, Pusan National University Hospital, Pusan National University School of Medicine⁵, Biomedical Research Institute, Pusan National University Hospital⁶

Background

Lung cancer is the second most prevalent type of cancer in Korea, with poor prognosis and a 5-year relative survival rate of 34.7%. Although pulmonary rehabilitation (PR) started in Korea in 2016, limited data on its impact on patients with lung cancer remain limited. This study examined the PR trends among patients with lung cancer in Korea from 2017 to 2021 using the National Health Insurance Service (NHIS) database.

Methods

PR prescription trends were analyzed using the insurance codes MM440 and MM290. Statistical analyses included descriptive statistics, t-tests, chi-square tests, and propensity score matching to compare groups with and without PR prescriptions. Annual PR claims, regional distribution, and related physical function evaluations were analyzed.

Results

The prevalence of lung cancer increased from 2017 to 2021, with PR prescriptions (MM440) rising from 1,002 to 3,723. However, the average number of PR sessions per patient was only 2.8. PR recipients were typically older adults, predominantly male, with higher comorbidities, and longer hospital stays. The number of physical function evaluations, such as maximum inspiratory/expiratory pressure and grip strength tests, approximately doubled over 5 years. Geographical analysis indicated higher PR claims in metropolitan areas.

Conclusion

PR for patients with lung cancer in Korea has grown significantly since insurance coverage began, with a 3.7-fold increase over 5 years. Despite this growth, only 2.9% of patients received PR, and the average number of sessions remained low. Greater efforts by healthcare providers, the government, and patients are necessary to improve PR access and adherence.

Acknowledgment This work was supported by the National Research Foundation of Korea (NRF) grant funded by the Korean government (MSIT) [grant number 2021R1C1C1006936].

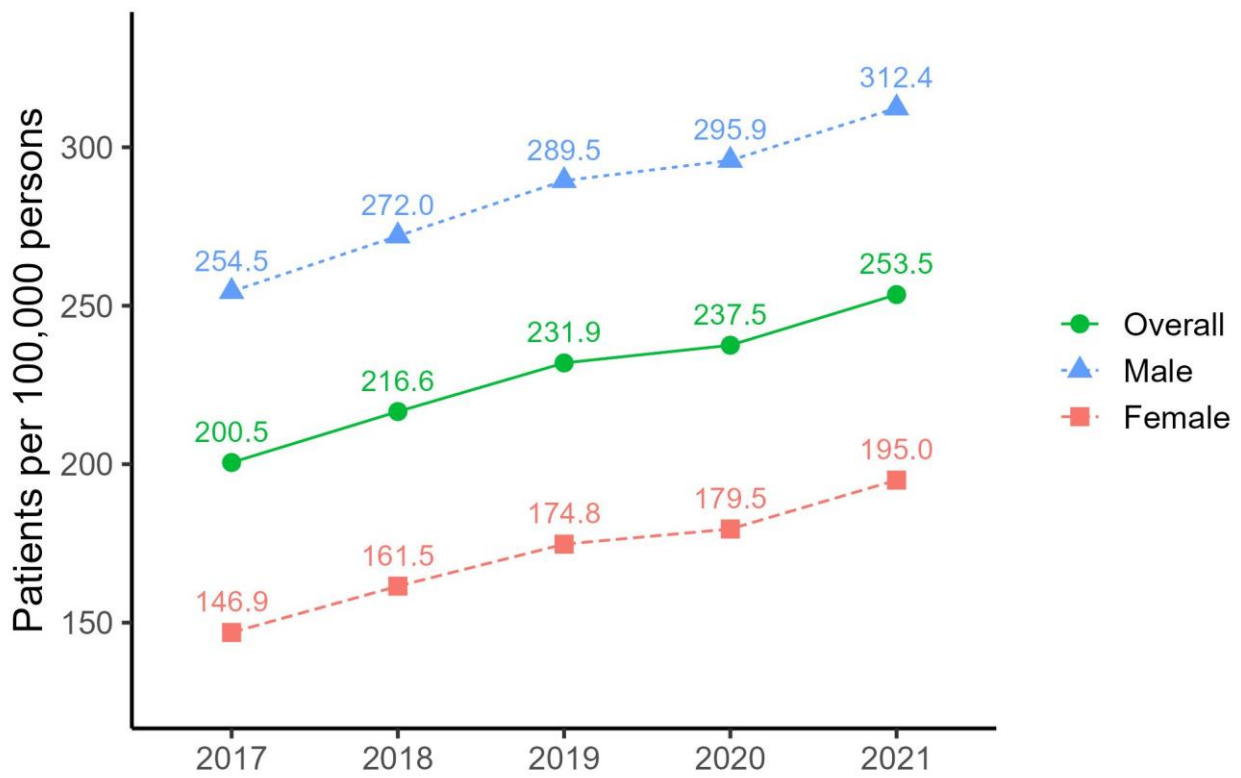


Figure 1. Prevalence of lung cancer in Korea.

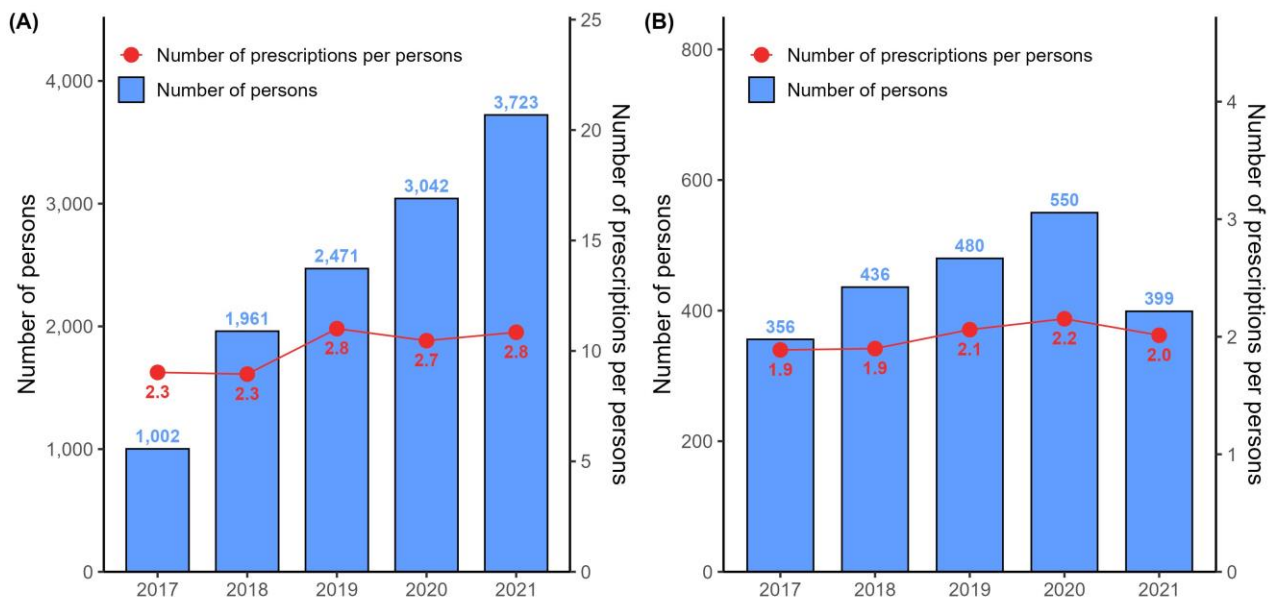
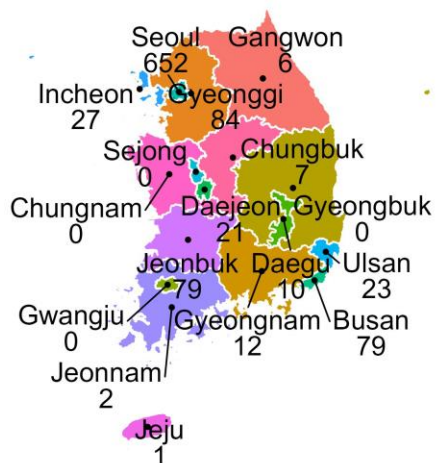


Figure 2. Actual number of persons prescribed (MM440, MM290) and average number of prescriptions per person. (a) MM440, (b) MM290

(A)



(B)

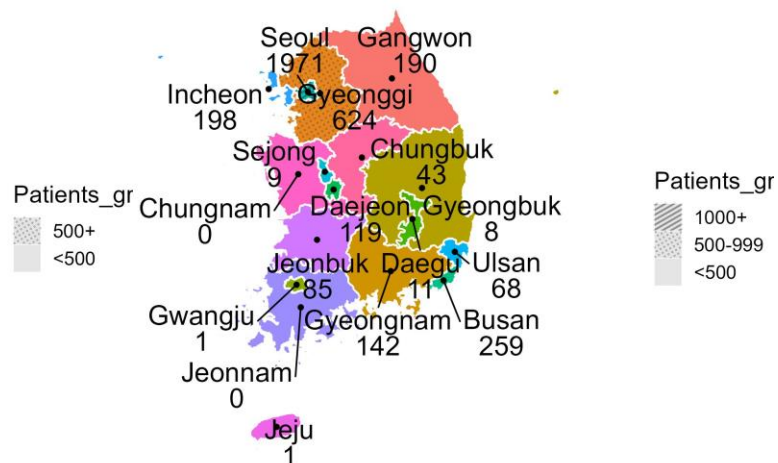


Figure 3. Changes in regional distribution of MM440 implementation rate between (a) 2017 and (b) 2021.

The effects and feasibility of moderate-to-high intensity exercise for people on hemodialysis

Se Hee Jung^{1**}, Jeongwoo Jeon², Jung Pyo Lee³, Jeonghwan Lee⁴, Hamin Bak⁵, Eun Jee Sohn⁵, Ji-Eun Oh⁵

Department of Rehabilitation Medicine, Seoul National University College of Medicine, Seoul National University Boramae Medical Center¹, Department of Physical Therapy, Digital Healthcare Institute, Sunmoon University², Department of Internal Medicine, Seoul National University College of Medicine³, Department of Internal Medicine, Seoul National University Boramae Medical Center⁴, Department of Rehabilitation Medicine, Seoul National University College of Medicine⁵

Despite the importance of exercise interventions in chronic kidney disease (CKD) undergoing hemodialysis (HD), most interventions currently used are low-intensity exercises. Therefore, the purpose of this study was to investigate the effect and feasibility of a moderate-to-high-intensity exercise program in CKD receiving HD. Thirteen CKD patients undergoing HD participated in a moderate-to-high-intensity exercise program (interdialytic exercise) consisting of aerobic and strength training twice a week for 8 weeks. To maintain intensity during exercise, heart rate was monitored in real-time, and the Borg rating scale of perceived exertion was investigated. Outcome measures included cardiopulmonary fitness and physical performance, cognitive and psychological function, health-related quality of life, exercise behavior, bone health, body composition, and laboratory tests. Participants' level of physical activity was also investigated. Measurements were performed at T0 (pre-intervention), T1 (post-intervention), and T2 (follow-up; 8 weeks after the end of the intervention). Our findings showed significant improvements in cardiopulmonary fitness and physical performance (six-minute walk test, timed up-and-go test, short physical performance battery, stair climb power test) as well as muscular strength (isometric strength and sit-to-stand test) after exercise intervention. Moreover, the effectiveness was maintained until the 8-week follow-up. In addition, all participants completed the moderate-to-high-intensity exercise program without any side effects. In conclusion, the current study demonstrated the safety and effectiveness of moderate-to-high-intensity exercise and suggests that this intensity of exercise may be feasible for CKD undergoing HD. Therefore, experts may recommend moderate to high-intensity exercise based on the individual CKD patient's health status.

Acknowledgment This study was supported by the Translational R&D Program on Smart Rehabilitation Exercises (#TRSRE-PS01), National Rehabilitation Center, Ministry of Health and Welfare, Korea.

A Quality Improvement Project for Trauma ICU Rehabilitation in Regional Trauma Center

Jae Sik Seo¹, Jun Yong Park¹, Ho Jeong Shin¹, Bo Kyung Ha³, Yong Beom Shin^{1,2}, Myung-Jun Shin^{1,2†}, Myung Hun Jang^{1,2*}

Department of Rehabilitation Medicine, Biomedical Research Institute, Pusan National University Hospital, Busan, Korea¹, Department of Rehabilitation Medicine, Pusan National University School of Medicine, Busan, Korea², Department of Nursing, Regional Trauma Center, Busan, Korea³

Introduction

Critically ill patients (pts) in the trauma intensive care unit (TICU) often experience long-term disabilities depending on the mechanism of the trauma and require extended rehabilitation (RM). Early RM for critically ill trauma pts helps prevent complications, reduces the length of hospital stay, and improves quality of life. However, the practical implementation of RM for these pts is hindered by various structural and cultural barriers. Effective RM requires efficient inter-professional communication, but there are issues such as limited staff, time constraints, lack of protocols, and insufficient staff training. Effective RM of critically ill pts in the TICU requires multidisciplinary collaboration and active participation from nurses. This study aimed to enhance the efficiency and activation of RM for critically ill trauma pts through several improvement activities: expanding training for healthcare professionals on the necessity of early RM, implementing systems to facilitate effective inter-professional communication, and developing standardized nursing records related to RM.

Method

This study was conducted as part of the 2023 ICU Quality Improvement Program. The quality improvement activities included the establishment of an Electronic Medical Records (EMR) system to share information on safety criteria compliance and RM coverage for trauma pts; the creation of a communication board to facilitate the sharing of treatment plans among multidisciplinary and inter-professional teams (Fig. 1); the implementation of RM education for nurses; the development of an early RM nursing manual for trauma pts; and the development of standardized nursing records for RM. After the improvement activities, we evaluated the rates of RM session implementation, nurse participation, and nursing record performance. Additionally, we assessed changes in nurses' satisfaction with ICU RM using a self-report questionnaire consisting of 10 questions on a 5-point Likert scale.

Result

The RM treatment rate for TICU pts who met the safety criteria improved from 71.43% to 97.44%. The participation rate of nurses in RM sessions increased from 24.59% to 93.81%, and the performance rate of RM treatment nursing records increased from 8.20% to 96.41%. Nurses' satisfaction with early RM among 87 nurses working in three TICUs increased by 46.28%, from an average of 2.96 points to 4.33 points on a 5-point scale (Fig. 2).

Discussion

This study confirmed that the development of a trauma ICU RM manual and education significantly improved nurses' awareness of ICU RM and demonstrated the potential to establish and expand a comprehensive RM system within the ICU. These efforts have shown that it is possible to overcome structural and cultural barriers and to activate trauma ICU RM. By implementing these strategies, we can foster a culture of ICU RM among all ICU staff.

Multidisciplinary Trauma ICU Rehabilitation

오늘날짜: 월 일		HD	POD		
손상부위 & 각종 튜브 위치		수술/시술/검사계획			
Rt.	Lt.	중환자실 퇴실계획			
<p>Bone Organ</p>		재활 협진			
		<input type="checkbox"/> YES <input type="checkbox"/> NO			
		재활 screening 결과			
		<input type="checkbox"/> PASS <input type="checkbox"/> FAIL			
		물리치료 - 운동 (시작일:)			
Mobilization LEVEL 1 LEVEL 2 LEVEL 3 LEVEL 4 LEVEL 5		처방 및 치료 도구 <input type="checkbox"/> Ergometer: U/L <input type="checkbox"/> Thera band <input type="checkbox"/> WALKER <input type="checkbox"/> TENS	치료이력 <input type="checkbox"/> 모니터링 필요	팀간 전달사항	
물리치료 - 호흡 (시작일:)					
치료 목표 <input type="checkbox"/> 무기폐 예방 <input type="checkbox"/> 가동성 증진 <input type="checkbox"/> 객담 배출 <input type="checkbox"/> 폐활량 증진 <input type="checkbox"/> 호흡근 훈련		치료 도구 <input type="checkbox"/> IS (<input type="checkbox"/> 수가 <input type="checkbox"/> 지급) <input type="checkbox"/> Manual hyperinflation (ambu) <input type="checkbox"/> MIE <input type="checkbox"/> VEST <input type="checkbox"/> IMT/PEP (/) <input type="checkbox"/> 기타	호흡물리치료 스케줄/교육 <input type="checkbox"/> 치료 예정 시간 <input type="checkbox"/> 식이 중단 요청 시간 <input type="checkbox"/> 호흡재활 교육동영상	팀간 전달사항	
체위 및 보조기 기타() <input type="checkbox"/> sitting <input type="checkbox"/> Rt. up 30 <input type="checkbox"/> 15 <input type="checkbox"/> 0 <input type="checkbox"/> Lt. up <input type="checkbox"/> Neck collar <input type="checkbox"/> AFO <input type="checkbox"/> Splint <input type="checkbox"/> Velpeau <input type="checkbox"/> TLSO <input type="checkbox"/>		호흡기능 평가 항목 날짜 결과 NIF FVC US PEF Cuff leak		인공호흡기 (weaning, NIV, home ventilator) <input type="checkbox"/> T-piece <input type="checkbox"/> Home-vent <input type="checkbox"/> Lung recruitment	
환자상태 의식 LOC / RASS(/) S5Q(/5) 인공 기도 <input type="checkbox"/> ETT (삽관일: / 발관일:) <input type="checkbox"/> Tracheostomy (시행일:) 식이 종류 & 양: 식이 중단시간: 투약 <input type="checkbox"/> 진정제 <input type="checkbox"/> 승압제		Vocalization <input type="checkbox"/> ACV <input type="checkbox"/> ACV /c Deflation <input type="checkbox"/> ONE WAY VALVE	Dysphagia <input type="checkbox"/> FEES (시행일:) 식이처방: <input type="checkbox"/> NMES	ADL <input type="checkbox"/> ADL <input type="checkbox"/> 개인위생	Cognition <input type="checkbox"/> Multimodal stim <input type="checkbox"/> 인지재활태블릿

Figure 1. Multidisciplinary communication board for Trauma ICU rehabilitation

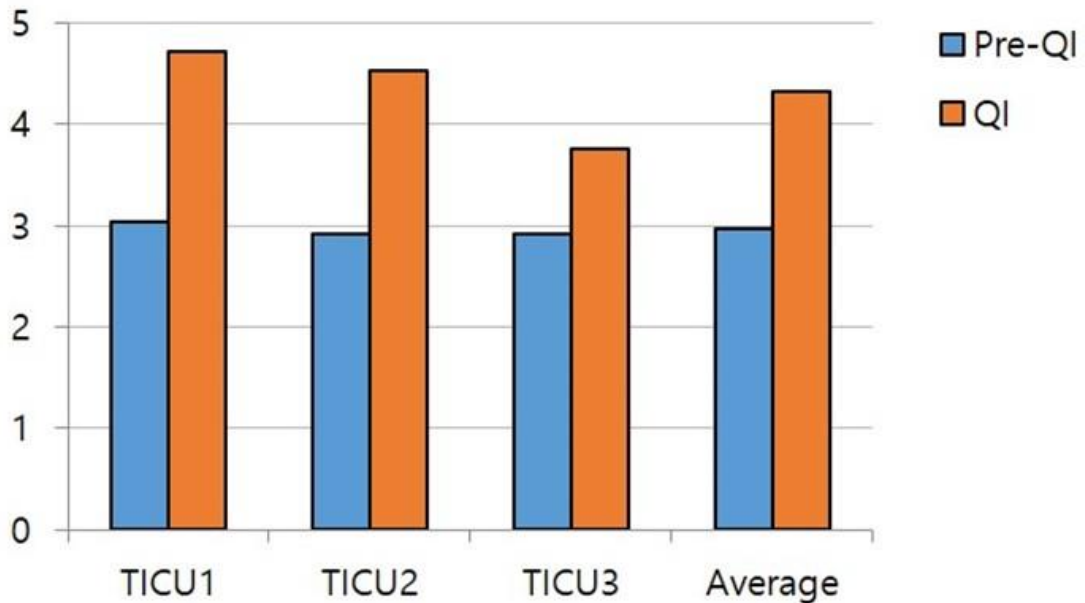


Figure 2. Changes in satisfaction with Trauma ICU rehabilitation across three ICUs

	Pre-QI	QI
Patients who passed the screening (n)	21	117
Patients receiving physiotherapy treatment (n)	15	114
Physiotherapy treatment (n)	61	501
Nurse participation (n)	15	470
Rehabilitation nursing records completed (n)	5	483
Physiotherapy treatment performance rate (%)	71.43	97.44
Nurse participation rate (%)	24.59	93.81
Nursing record performance rate (%)	8.20	96.41

Table 1. Comparison of rehabilitation performance indicators before and after Quality Improvement Activities in Trauma ICUs

Machine Learning for the Accurate and Explainable Prediction of Respiratory Muscle Strength

Sang Hun Kim^{1*}, Myung-Jun Shin^{1†}, Sa-Eun Park², Ki-Hun Kim², Ji Won Jung³, Tae Sung Park⁴, Jun Yong Park⁵, Jun Won Lee⁵

Department of Rehabilitation Medicine, Pusan National University Hospital and Pusan National University School of Medicine¹, Department of Industrial Engineering, Pusan National University², Faculty of Industrial Design Engineering, Delft University of Technology³, Department of Convergence Medical Institute of Technology, Pusan National University Hospital⁴, Department of Rehabilitation Medicine, Biomedical Research Institute, Pusan National University Hospital⁵

Background

The most representative Respiratory Muscle Strength Indicators (RMSIs) are maximum inspiratory pressure (MIP), maximum expiratory pressure (MEP), and peak cough flow (PCF). These indicators serve as major criteria to predict the risk of various respiratory diseases. Some existing studies tried to develop the prediction models for the three RMSIs of healthy adults and then, derive the references of healthy adults based on the prediction models. Nevertheless, these prediction models focused on linear regression, which inherently limit the utilization of the correlated predictors due to the multicollinearity problem and the capturing of non-linear relationships between the three RMSIs and their predictors primarily focusing on demographics (DEMO), and anthropometrics (ANTH).

Objective

To address the limitations, this study aims to develop machine learning (IML) models for accurate and interpretable prediction of the three RMSIs of 353 healthy adults with DEMO, ANTH, and physical functions (PF) predictors known to affect RMSIs, which were not mainly utilized yet in existing studies.

Methods

Various IML models were developed for each RMSI as their prediction target for each subset of DEMO, ANTH, and PF predictors as their predictors. To interpret the developed IML models, TRIAGE and SHAP analysis were used to analyze the predictive uncertainty scores across different predictor subsets and to identify the influence of predictors on the best-performing IML models, respectively. These analyses suggest the optimal sets of predictors for the predictive performance of the IML models

Results

For all RMSIs, the best IML models showed a significant improvement in predictive performances over the linear regression models (e.g., MAE: 2.85% for MIP, 3.48% for MEP, and 4.12% for PCF). In TRIAGE analysis, the predictor set including all predictors had the optimal predictive uncertainty scores for all best IML models. SHAP analysis results suggest the PF predictors are critical for all the best IML models.

Conclusion

These accurate and interpretable predictions of the developed IML models are expected to contribute to more precise and informed references of healthy adults on the RMSIs.

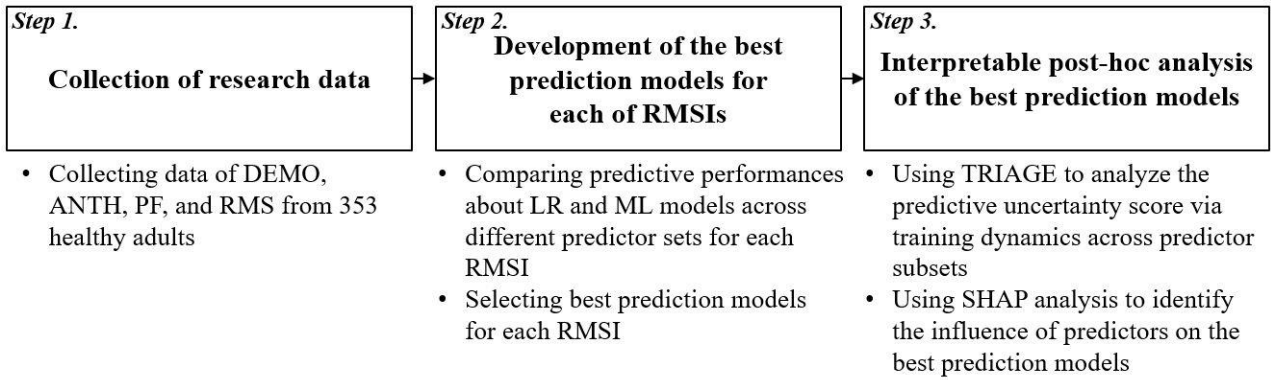


Fig. 1 The overall process of research

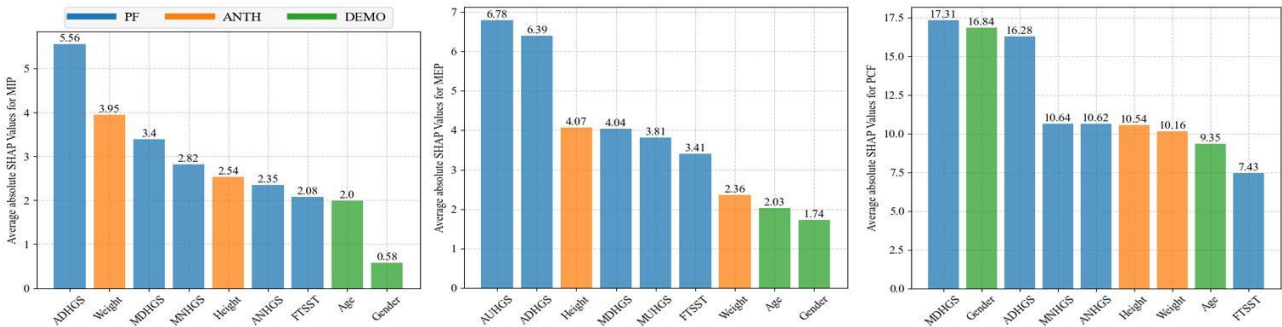


Fig 2. Average absolute Shapley values of predictors for the best MIP, MEP, and PCF prediction models

RMS	Model	Type	R ² †	RMSE‡
MIP	LR	Type A (DEMO)	0.274±0.12	22.87±3.1
		Type B (DEMO + ANTH)	0.338±0.13	21.81±3.0
		Type C (DEMO + ANTH + PF)	0.404±0.13	20.62±2.6
	KNN	Type A (DEMO)	0.288±0.15	22.61±3.4
		Type B (DEMO + ANTH)	0.335±0.14	21.89±3.5
		Type C (DEMO + ANTH + PF)	0.400±0.14	20.69±3.0
	LGBM	Type A (DEMO)	0.292±0.13	22.62±3.7
		Type B (DEMO + ANTH)	0.305±0.11	22.42±3.4
		Type C (DEMO + ANTH + PF)	0.387±0.13	20.95±3.0
	RF	Type A (DEMO)	0.302±0.13	22.87±3.1
		Type B (DEMO + ANTH)	0.316±0.13	22.21±3.3
		Type C (DEMO + ANTH + PF)	0.390±0.14	20.85±2.8
MEP	XGB	Type A (DEMO)	0.266±0.12	23.02±3.3
		Type B (DEMO + ANTH)	0.313±0.13	22.25±3.4
		Type C (DEMO + ANTH + PF)	0.415±0.13	20.45±3.4
	LR	Type A (DEMO)	0.365±0.15	25.68±3.7
		Type B (DEMO + ANTH)	0.368±0.15	25.61±3.6
		Type C (DEMO + ANTH + PF)	0.473±0.15	23.25±3.3
	KNN	Type A (DEMO)	0.385±0.16	25.25±3.9
		Type B (DEMO + ANTH)	0.440±0.13	24.18±4.0
		Type C (DEMO + ANTH + PF)	0.500±0.14	22.71±3.4
	LGBM	Type A (DEMO)	0.383±0.12	25.48±4.2
		Type B (DEMO + ANTH)	0.399±0.12	25.13±4.3
		Type C (DEMO + ANTH + PF)	0.476±0.12	23.35±3.6
PCF	XGB	Type A (DEMO)	0.399±0.13	25.09±4.0
		Type B (DEMO + ANTH)	0.408±0.14	24.88±4.2
		Type C (DEMO + ANTH + PF)	0.481±0.15	23.13±3.5
	LR	Type A (DEMO)	0.385±0.11	25.40±3.8
		Type B (DEMO + ANTH)	0.401±0.12	25.07±4.3
		Type C (DEMO + ANTH + PF)	0.511±0.12	22.51±3.5
	KNN	Type A (DEMO)	0.568±0.09	72.26±8.3
		Type B (DEMO + ANTH)	0.608±0.09	68.78±8.3
		Type C (DEMO + ANTH + PF)	0.606±0.10	68.81±8.7
	LGBM	Type A (DEMO)	0.590±0.09	70.50±8.1
		Type B (DEMO + ANTH)	0.626±0.10	67.10±8.6
		Type C (DEMO + ANTH + PF)	0.618±0.10	67.77±9.3
	RF	Type A (DEMO)	0.595±0.08	70.17±8.2
		Type B (DEMO + ANTH)	0.606±0.09	69.06±8.5
		Type C (DEMO + ANTH + PF)	0.603±0.10	68.19±9.6

RMSIs	Predictor sets	Proportion of characterized observations		
		Under-estimated	Over-estimated	Well-estimated
MIP	Type A	0.141±0.05	0.122±0.04	0.737±0.39
	Type B	0.070±0.04	0.067±0.04	0.863±0.04
	Type C	0.036±0.02	0.040±0.03	0.924±0.04
MEP	Type A	0.136±0.04	0.111±0.04	0.752±0.05
	Type B	0.080±0.04	0.057±0.04	0.863±0.04
	Type C	0.044±0.04	0.038±0.03	0.918±0.04
PCF	Type A	0.140±0.04	0.112±0.03	0.748±0.04
	Type B	0.080±0.04	0.053±0.03	0.867±0.04
	Type C	0.039±0.02	0.037±0.03	0.923±0.03

Predictive performance comparison of the RMSI prediction model

Current Respiratory Management Strategies for Adult Duchenne Muscular Dystrophy in South Korea

Hee Jae Park^{1,2*}, Han Eol Cho^{1,2†}, Won Ah Choi^{1,2†}, Seong-Woong Kang^{1,2}

Department of Rehabilitation Medicine, Gangnam Severance Hospital¹, Research Institute of Rehabilitation Medicine, Yonsei University College of Medicine²

Background

Duchenne Muscular Dystrophy (DMD) is a genetic disorder characterized by progressive muscle degeneration, leading to severe respiratory complications in adult patients. Recent advancements in respiratory care have extended the lifespan of individuals with DMD, necessitating a comprehensive evaluation of their current respiratory management strategies.

Objective

This study aims to investigate the current respiratory management practices and outcomes in adult patients with DMD in South Korea, emphasizing the importance of non-invasive ventilatory support.

Methods: A retrospective analysis was conducted on the medical records of 168 adult patients with genetically confirmed DMD who were treated at the Pulmonary Rehabilitation Center of a tertiary referral hospital. Data on the initiation, type, and duration of respiratory support were collected and analyzed.

Results

Of the 168 patients, 161 (95.8%) required mechanical ventilation, with a predominant reliance on non-invasive ventilation (NIV). The mean age for initiating ventilatory support was 19.8 ± 4.3 years. Most patients using NIV had an average age of 29.6 ± 5.8 years and required it for 15.4 ± 7.0 hours per day. In contrast, 10 patients (6.2%) required invasive ventilation due to severe complications. The effective use of NIV has significantly reduced hospitalization rates and improved survival.

Conclusions

The findings underscore the critical role of non-invasive ventilatory support in managing respiratory complications in adult patients with DMD. Continuous monitoring and timely initiation of respiratory support are essential to enhance the quality of life and extend the lifespan of these patients. Further research is needed to optimize respiratory care protocols and address the challenges associated with long-term ventilatory support.

Association of Physical Activity with Lung Function in COPD Patients: A Comparative Analysis

So-youn Chang^{1**}, Eun Jin Park¹, Ja Eun Koo¹, Eun Joo Lee¹, Youngkook Kim¹, Sun Jae Won¹

Department of Rehabilitation Medicine, Yeouido St. Mary's hospital, College of Medicine, The Catholic University of Korea, Republic of Korea¹

Purpose

Chronic obstructive pulmonary disease (COPD) causes airflow obstruction leading to breathing difficulties and reduced physical activity (PA), though regular PA can improve symptoms and exercise tolerance. Many COPD patients have low PA levels due to breathlessness and fatigue, worsening their health and lung function. This study explored the association between PA levels and lung function in COPD patients compared to normal individuals and those with restrictive lung disease (RLD).

Methods

This cross-sectional study investigated data involving 16,692 participants aged 40 years and older from the Korea National Health and Nutrition Examination Survey (KNHANES) from 2014 to 2019. All participants, the COPD, the RLD patients, and the normal group underwent a pulmonary function test (PFT), measured Forced expiratory volume in one second (FEV1), Forced vital capacity (FVC), and additionally Peak expiratory flow (PEF). Within those groups, through a questionnaire about exercise intensity, type, and exercise time, we further subdivided them into three levels of physical activity: low, moderate, and high. The association between PA level and variables about pulmonary function has been analyzed using ANCOVA. The analysis was adjusted for variables to evaluate potential confounding associations.

Results

Significant differences in FEV1 according to PA level were only observed in the normal and COPD groups, and the effect of PA on FEV1 varied significantly by group (Table 2). Similarly, FVC showed significant differences by PA level in these two groups, with the impact of PA on FVC also varying significantly by group. In contrast, only the COPD group showed significant differences in PEF by PA level, and there was no significant interaction effect of PA on PEF across groups. Table 3 shows associations between adherence in specialized activities and lung function. In adherence to walking, only the normal group demonstrated significant differences in FEV1, FVC, and PEF, based on whether adherence was maintained. Regarding strengthening exercise, the normal and COPD groups showed a significant difference in only PEF. In adherence to aerobic exercise, significant differences in FVC and PEF were noted in the normal group, and significant differences in FEV1, FVC, and PEF were confirmed in the COPD group. The impact of aerobic exercise on FEV1 and FVC demonstrated significant variation across groups.

Conclusions

Our findings indicate that increased physical activity is associated with improved pulmonary function in COPD patients and that aerobic exercise was found to be independently associated with improved lung function in COPD patients. For COPD patients, it is essential to provide a focus on enhancing aerobic exercise through individualized training programs.

	Normal (n=12386)	RLD (n=2013)	COPD (n=2293)	p-value
Age				<.0001 [†]
40 – 49 years	40.1(0.63)	22.4(1.23)	11.7(0.97)	
50 – 59 years	35.3(0.55)	33.8(1.28)	25.6(1.23)	
60 – 69 years	17.0(0.43)	25.0(1.07)	32.8(1.16)	
≥ 70 years	7.6(0.27)	18.9(0.97)	29.9(1.07)	
Sex				<.0001 [†]
Male	43.8(0.46)	59.4(1.22)	74.9(1.02)	
Female	56.2(0.46)	40.6(1.22)	25.1(1.02)	
Dynapenia	5.8(0.27)	9.3(0.76)	8.2(0.63)	<.0001 [†]
Low income	34.8(0.78)	28.4(1.39)	23.0(1.23)	<.0001 [†]
Education				<.0001 [†]
Education years < 12	27.0(0.60)	37.5(1.33)	46.3(1.35)	
Education years ≥ 12	73.0(0.60)	62.5(1.33)	53.7(1.35)	
BMI level				<.0001 [†]
< 18.5	1.8(0.14)	1.6(0.32)	2.3(0.36)	
18.5 ≤ < 23	37.5(0.50)	20.1(1.03)	37.4(1.18)	
23 ≤ < 25	26.5(0.45)	22.9(1.12)	26.4(1.15)	
25 ≤ < 30	30.5(0.48)	45.1(1.34)	31.5(1.19)	
≥ 30	3.8(0.20)	10.3(0.78)	2.4(0.37)	
Smoking				<.0001 [†]
Non-smoker	61.2(0.51)	50.3(1.30)	31.8(1.13)	
Ex-smoker	21.2(0.43)	29.2(1.18)	37.3(1.22)	
Current smoker	17.6(0.45)	20.5(1.11)	30.9(1.21)	
Drinking				<.0001 [†]
Non	25.9(0.47)	28.4(1.20)	27.1(1.08)	
Mild	65.6(0.52)	60.0(1.30)	60.1(1.23)	
Heavy	8.5(0.32)	11.6(0.86)	12.9(0.83)	
Physical activity-intensity				0.0005 [†]
Low	60.6(0.54)	66.3(1.28)	62.9(1.24)	
Moderate	30.0(0.48)	26.2(1.17)	27.7(1.14)	
High	9.5(0.33)	7.5(0.73)	9.5(0.82)	
Physical activity-type				
Walking	38.9(0.55)	39.1(1.32)	38.9(1.22)	0.9903
Strengthening exercise	21.3(0.44)	19.6(1.00)	25.8(1.14)	<.0001 [†]
Aerobic exercise	46.7(0.56)	40.7(1.26)	44.6(1.28)	<.0001 [†]
Comorbidities				
Hypertension	31.2(0.52)	49.7(1.38)	44.9(1.21)	<.0001 [†]
Diabetes mellitus	12.8(0.36)	26.1(1.14)	20.8(0.96)	<.0001 [†]
Dyslipidemia	24.7(0.48)	32.6(1.23)	24.2(1.05)	<.0001 [†]
Asthma	1.5(0.13)	3.1(0.42)	7.2(0.60)	<.0001 [†]
CVD	2.8(0.16)	7.4(0.64)	6.6(0.53)	<.0001 [†]
Depression	4.7(0.21)	4.4(0.51)	3.8(0.50)	0.3190
Waist circumference	82.7±0.10	88.6±0.26	85.7±0.21	<.0001 [†]
Fasting Glucose	101.7±0.25	110.1±0.76	105.6±0.57	<.0001 [†]
Total cholesterol	198.3±0.40	194.7±1.02	188.8±0.95	<.0001 [†]
HDL-C	51.4±0.14	48.3±0.31	47.9±0.29	<.0001 [†]
Triglyceride	117.9(116.3-119.4)	136.1(132.1-140.3)	127.8(124.2-131.4)	<.0001 [†]
FEV1	2.9±0.01	2.3±0.01	2.3±0.02	<.0001 [†]
FVC	3.6±0.01	3±0.02	3.7±0.03	<.0001 [†]
Peak expiratory flow	7.4±0.02	6.7±0.05	6.2±0.05	<.0001 [†]

Table 1. The demographic and clinical characteristics of participants.

	Group	Physical activity level	Model 1 ^a	Model 2 ^b	Model 3 ^c
FEV1	Normal	Low	2.84±0.01	2.81±0.01	2.80±0.01
		Moderate	2.88±0.01	2.82±0.01	2.81±0.01
		High	3.14±0.02	2.86±0.01	2.85±0.01
		<i>p</i> -value	<.0001 [*]	0.0038 [*]	0.0044 [*]
	RLD	Low	2.32±0.02	2.26±0.01	2.25±0.01
		Moderate	2.29±0.03	2.26±0.01	2.25±0.01
		High	2.50±0.05	2.24±0.03	2.22±0.03
		<i>p</i> -value	0.0003 [*]	0.8584	0.8531
	COPD	Low	2.29±0.02	2.24±0.02	2.23±0.02
		Moderate	2.38±0.03	2.31±0.03	2.29±0.03
		High	2.57±0.06	2.31±0.04	2.29±0.04
		<i>p</i> -value	<.0001 [*]	0.0258 [*]	0.0302 [*]
	<i>p</i> -value for interaction		0.0631	0.0408 [*]	0.0404 [*]
FVC	Normal	Low	3.58±0.01	3.59±0.01	3.57±0.01
		Moderate	3.63±0.02	3.60±0.01	3.58±0.01
		High	3.98±0.03	3.67±0.02	3.65±0.02
		<i>p</i> -value	<.0001 [*]	0.0001 [*]	0.0001 [*]
	RLD	Low	2.95±0.02	2.88±0.01	2.86±0.01
		Moderate	2.90±0.03	2.87±0.02	2.85±0.02
		High	3.16±0.06	2.83±0.03	2.81±0.04
		<i>p</i> -value	0.0007 [*]	0.6434	0.6302
	COPD	Low	3.57±0.03	3.47±0.02	3.44±0.02
		Moderate	3.70±0.05	3.56±0.04	3.53±0.04
		High	4.00±0.07	3.62±0.05	3.59±0.05
		<i>p</i> -value	<.0001 [*]	0.0195 [*]	0.0220 [*]
	<i>p</i> -value for interaction		0.0131 [*]	0.0025 [*]	0.0025 [*]
PEF	Normal	Low	7.31±0.03	7.28±0.03	7.26±0.03
		Moderate	7.42±0.04	7.31±0.03	7.29±0.03
		High	8.16±0.07	7.40±0.05	7.38±0.05
		<i>p</i> -value	<.0001 [*]	0.0543	0.0592
	RLD	Low	6.63±0.06	6.31±0.05	6.29±0.05
		Moderate	6.58±0.10	6.34±0.06	6.33±0.06
		High	7.33±0.17	6.40±0.12	6.38±0.12
		<i>p</i> -value	0.0004 [*]	0.7368	0.7223
	COPD	Low	6.02±0.06	5.66±0.05	5.64±0.05
		Moderate	6.25±0.09	5.76±0.08	5.74±0.08
		High	6.99±0.17	5.98±0.14	5.96±0.14
		<i>p</i> -value	<.0001 [*]	0.0353 [*]	0.0426 [*]
	<i>p</i> -value for interaction		0.4769	0.7173	0.7265

Table 2. Association between physical activity level and lung function.

(a) Walking						(b) Strengthening exercise						(c) Aerobic exercise					
	Group	Walking	Model 1 ^a	Model 2 ^b	Model 3 ^c		Group	Strengthening exercise	Model 1 ^a	Model 2 ^b	Model 3 ^c		Group	Aerobic exercise	Model 1 ^a	Model 2 ^b	Model 3 ^c
FEV1	Normal	No	2.88±0.01	2.81±0.01	2.80±0.01	FEV1	Normal	No	2.83±0.01	2.81±0.01	2.80±0.01	FEV1	Normal	No	2.82±0.01	2.81±0.01	2.80±0.01
		Yes	2.87±0.01	2.83±0.01	2.82±0.01			Yes	3.05±0.01	2.84±0.01	2.83±0.01			Yes	2.94±0.01	2.83±0.01	2.82±0.01
		p-value	0.5350	0.0221 [*]	0.0204 [*]			p-value	<.0001 [*]	0.0891	0.1037			p-value	<.0001 [*]	0.0574	0.0769
	RLD	No	2.33±0.02	2.26±0.01	2.25±0.01		RLD	No	2.30±0.02	2.26±0.01	2.25±0.01		RLD	No	2.30±0.02	2.26±0.01	2.25±0.01
		Yes	2.31±0.02	2.25±0.01	2.24±0.01			Yes	2.42±0.03	2.24±0.02	2.23±0.02			Yes	2.36±0.02	2.25±0.01	2.24±0.01
		p-value	0.5292	0.6352	0.6416			p-value	0.0002 [*]	0.9713	0.9777			p-value	0.0798	0.8011	0.8213
	COPD	No	2.34±0.02	2.25±0.02	2.24±0.02		COPD	No	2.29±0.02	2.26±0.02	2.25±0.02		COPD	No	2.26±0.02	2.23±0.02	2.22±0.02
		Yes	2.34±0.03	2.28±0.02	2.26±0.02			Yes	2.48±0.03	2.27±0.03	2.26±0.03			Yes	2.43±0.03	2.30±0.02	2.29±0.02
		p-value	0.9866	0.4908	0.4884			p-value	<.0001 [*]	0.4956	0.4961			p-value	<.0001 [*]	0.0059 [*]	0.0066 [*]
	p-value for interaction		0.9188	0.3819	0.4251		p-value for interaction		0.0125 [*]	0.0497 [*]	0.0496 [*]		p-value for interaction		0.0220 [*]	0.0189 [*]	0.0189 [*]
FVC	Normal	No	3.64±0.01	3.59±0.01	3.57±0.01	FVC	Normal	No	3.57±0.01	3.60±0.01	3.57±0.01	FVC	Normal	No	3.56±0.01	3.59±0.01	3.57±0.01
		Yes	3.62±0.01	3.61±0.01	3.59±0.01			Yes	3.87±0.02	3.63±0.01	3.61±0.01			Yes	3.72±0.01	3.61±0.01	3.59±0.01
		p-value	0.5366	0.0226 [*]	0.0203 [*]			p-value	<.0001 [*]	0.0631	0.0774			p-value	<.0001 [*]	0.0131 [*]	0.0204 [*]
	RLD	No	2.96±0.02	2.88±0.01	2.86±0.01		RLD	No	2.92±0.02	2.88±0.01	2.87±0.01		RLD	No	2.93±0.02	2.88±0.01	2.87±0.01
		Yes	2.94±0.03	2.87±0.02	2.85±0.02			Yes	3.07±0.03	2.83±0.02	2.82±0.02			Yes	2.98±0.03	2.86±0.02	2.84±0.02
		p-value	0.5351	0.6402	0.5912			p-value	<.0001 [*]	0.759	0.7522			p-value	0.1886	0.5791	0.5674
	COPD	No	3.64±0.03	3.49±0.02	3.47±0.02		COPD	No	3.57±0.03	3.49±0.02	3.46±0.02		COPD	No	3.54±0.03	3.45±0.02	3.43±0.02
		Yes	3.65±0.04	3.52±0.03	3.50±0.03			Yes	3.87±0.05	3.56±0.04	3.54±0.04			Yes	3.78±0.04	3.57±0.03	3.55±0.03
		p-value	0.8755	0.392	0.4139			p-value	<.0001 [*]	0.1992	0.1959			p-value	<.0001 [*]	0.0051 [*]	0.006 [*]
	p-value for interaction		0.8888	0.1474	0.3307		p-value for interaction		0.0014 [*]	0.0033 [*]	0.0033 [*]		p-value for interaction		0.0028 [*]	0.0012 [*]	0.0012 [*]
PEF	Normal	No	7.42±0.03	7.28±0.03	7.26±0.03	PEF	Normal	No	7.26±0.03	7.27±0.02	7.25±0.03	PEF	Normal	No	7.24±0.03	7.26±0.03	7.24±0.03
		Yes	7.42±0.03	7.33±0.03	7.31±0.03			Yes	8.04±0.04	7.40±0.03	7.38±0.04			Yes	7.63±0.03	7.34±0.03	7.33±0.03
		p-value	0.9414	0.0177 [*]	0.0169 [*]			p-value	<.0001 [*]	0.0007 [*]	0.0008 [*]			p-value	<.0001 [*]	0.0012 [*]	0.0015 [*]
	RLD	No	6.70±0.06	6.56±0.05	6.54±0.05		RLD	No	6.57±0.06	6.31±0.04	6.30±0.04		RLD	No	6.62±0.07	6.33±0.05	6.32±0.05
		Yes	6.61±0.08	6.27±0.06	6.25±0.06			Yes	7.11±0.10	6.38±0.08	6.36±0.08			Yes	6.75±0.08	6.31±0.05	6.29±0.05
		p-value	0.3227	0.2172	0.2373			p-value	<.0001 [*]	0.2226	0.2108			p-value	0.2097	0.5746	0.5956
	COPD	No	6.15±0.07	5.69±0.06	5.67±0.06		COPD	No	5.98±0.06	5.68±0.05	5.66±0.05		COPD	No	5.95±0.07	5.63±0.05	5.61±0.06
		Yes	6.20±0.07	5.75±0.06	5.74±0.06			Yes	6.73±0.09	5.85±0.08	5.83±0.08			Yes	6.45±0.08	5.82±0.06	5.80±0.07
		p-value	0.6265	0.2172	0.6364			p-value	<.0001 [*]	0.0364 [*]	0.0395 [*]			p-value	<.0001 [*]	0.0182 [*]	0.0199 [*]
	p-value for interaction		0.5468	0.3556	0.1245		p-value for interaction		0.1966	0.6995	0.6931		p-value for interaction		0.0239 [*]	0.1187	0.1161

Table 3. Associations between lung function and adherence to walking (a), strengthening exercise (b), and aerobic exercise (c).

The Frequency and Characteristics of Intratracheal Complications in Patients with Tracheostomy Tubes

Seong-Eun Kim^{1*}, Jong Bum Park^{1†}, Yung Jin Lee¹, Mi Jin Hong¹, Dong Jin Chae¹, Cho E Sim¹, Ji-Hwan Kwon¹

Department of Rehabilitation Medicine, Konyang University College of Medicine¹

Background

Tracheostomy is a surgical procedure to open the trachea below the cricoid cartilage, often performed for upper airway obstruction, trauma, or neuromuscular diseases. It provides a long-term airway solution, avoiding complications from oral or nasal intubation. However, tracheostomy tubes can lead to various complications, including infection, bleeding, tracheomalacia, and tube obstruction. While early complications are well-studied, research on long-term intratracheal complications remains insufficient.

Objective

This study aims to investigate the frequency and characteristics of long-term intratracheal complications in patients with tracheostomy tubes.

Methods

Data were collected by reviewing patient records of those with tracheostomy tubes from the Department of Rehabilitation Medicine at OO University Hospital between June 1, 2016, and November 30, 2023. These patients sought consultations from the Department of Otolaryngology for airway evaluation. They underwent examinations using laryngotracheoscopy, and additional imaging studies such as CT scans were performed when necessary. Patients were evaluated for commonly occurring tracheostomy complications. They were then divided into two groups: one with intratracheal complications and one without complications. To compare the characteristics of the two groups, factors such as sex, age, BMI, MBI, lesion etiology, length of onset, length of tracheostomy, and type of tube were investigated. The T-test, Mann–Whitney U-test and the chi-square test were used to compare the baseline characteristics of the two groups.

Results

This study was performed on 98 patients undergoing tracheostomy. As shown in Table 1, the average age was 60.5 years, and 60.2% of patients were men. The median duration of tracheostomy was 159 days. Out of the 98 patients, 67 were classified into the complication group, while 31 were classified into the non-complication group. Factors such as sex, age, BMI, MBI, lesion etiology, length of onset, length of tracheostomy, and type of tube did not show a significant difference between the two groups (P value

Conclusion

This study determined the rate of late complications in patients with tracheostomy. It is impossible to determine from this sample which factors (sex, age, BMI, MBI, lesion etiology, length of hospitalization and tracheostomy, tube types) are related to tracheostomy complications. Understanding the possible late complications of tracheostomy placement and identifying symptoms of such complications allow for the optimal care of patients.

Table 1. Characteristics of the patient population

Class Variables [Missing]	Overall (N)	Without Complication (N(%))	With Complication (N(%))	P-value
Study population	98	31(31.6)	67(67.4)	
Sex, male [0]	57	20(64.5)	37(55.2)	0.52
Age [0] (average)	60.5	63.8	59.0	0.15
BMI (kg/m2) [0] (average)	21.9	20.6	22.6	0.07
Underweight(<18.5)	18	9(29.0)	9(13.4)	
Normal Weight(18.5-22.9)	47	15(48.4)	32(47.8)	
Overweight (23-24.9)	12	5(16.1)	7(10.4)	
Obese (>25)	19	2(6.5)	17(54.8)	
MBI [2] (average)	9.0	7.4	9.9	1.0
Total~Maximal assist (<50)	93	30(96.8)	63(97.0)	
Moderate~Mild assist (51-90)	3	1(3.2)	2(3.1)	
Minimal assist~Independent (91-99)	0	0(0.0)	0(0.0)	
Lesion etiology [0]				0.98
Brain				
Hemorrhage	63	20(64.5)	42(62.7)	
Infarction	11	3(9.7)	7(10.4)	
Hypoxic brain damage	6	2(6.5)	4(6.0)	
Others	4	0(0.0)	2(3.0)	
Spinal cord injury	5	2(6.5)	3(4.5)	
Neuromuscular	3	1(3.2)	2(3.0)	
Respiratory	6	2(6.5)	4(6.0)	
Length of onset [0] (median)	187	194	173	0.13
Length of tracheostomy [6] (median)	159	157	159	0.15
Type of tube [0]				0.19
Cuffless, fenestrated	50	14(45.2)	35(52.2)	
Cuffed, fenestrated	10	2(6.5)	8(11.9)	
Cuffed, nonfenestrated	36	15(48.4)	20(29.9)	
Others	2	0(0.0)	4(6.0)	

BMI, Body Mas Index; MBI, Modified Barthel Index.

*p < 0.05 by Mann-Whitney U-test, T-test, or chi-Square test.

Table 1. Characteristics of the patient population

Table 2. Intratracheal complications

Complications	N(%)
Granulation tissue	40(40.8)
Bleeding/Crust	34(34.7)
Vocal cord palsy	13(13.3)
Laryngeal swelling	12(12.2)
Tracheal stenosis	8(8.2)
Discharge	5(5.1)
Mucosal abrasion/injection	4(4.1)
Fistula	2(2.0)
Tracheomalacia	1(1.0)
Tracheal wall inversion	1(1.0)
Total	120(122.4)

Table 2. Intratracheal complications

Prehabilitation Research: A Scientometric Review

Eunjee Lee^{1*}, Gyujin Kim¹, Sanghyun Jee², Jung Hyun Park², Myungeun Yoo³, Chan Woong Jang^{1†}

Department of Physical Medicine and Rehabilitation, Hallym University Sacred Heart Hospital¹, Department of Rehabilitation Medicine, Gangnam Severance Hospital², Department of Rehabilitation Medicine, Uijeongbu Eulji Medical Center³

Introduction

Prehabilitation enhances patients' physical conditions before surgery, incorporating nutrition and psychological support; this study analyzes its literature from 2002 to 2022 to provide insights into research trends and global distribution.

Methods

We collected prehabilitation-related publications from the Web of Science Core Collection database, covering over 20,000 peer-reviewed journals. The search used the formula: (TS=(prehabilitation)) AND TS=(exercise OR physical OR nutrition* OR psychol* OR mental), conducted on September 13, 2023, for articles from 2002 to 2022. Only English-language articles were included, with titles, keywords, and author information extracted.

For bibliometric analysis, we used CiteSpace (version 6.2) to perform co-occurrence and co-citation analysis, focusing on data from 2002 to 2022. We selected the 50 most cited items from each year and applied the Pathfinder pruning method. Metrics like betweenness centrality and burst strength identified influential nodes and dynamic research areas. The Mann-Kendall test in R (version 4.3.1) assessed annual trends in publications and citations.

Results

We analyzed 553 research articles referencing 8,007 sources. From 2002 to 2022, there was a significant increase in prehabilitation research publications and citations, with a notable rise in average citations per year (Figure 1). The Mann-Kendall test confirmed this upward trend (publications $P=0.003$, citations P

Prehabilitation articles were classified into 49 disciplines (Figure 2A). Key fields like surgery, oncology, and rehabilitation showed significant collaborative impact and high betweenness centrality values, indicating their role in connecting disciplines. Sports sciences, orthopedics, and rehabilitation had the highest burst strength values, highlighting their influence.

Co-citation analysis revealed 49 clusters, with notable trends in postoperative complications and cancer surgery (Figure 2B). Initially focused on major abdominal surgeries, prehabilitation research has expanded to include thoracic surgeries, such as lung cancer and aortic valve replacement. Preoperative exercise remains central, with growing interest in multimodal prehabilitation and its effectiveness based on patient characteristics.

Geographically, the USA, Canada, England, and the Netherlands were the leading countries in this research. McGill University was the top institution, with significant contributions from Maastricht University.

Conclusion

We analyze prehabilitation research (2002-2022), highlighting rapid growth in North America and Western Europe while emphasizing the need for personalized programs and broader geographic studies to enhance understanding and future research.

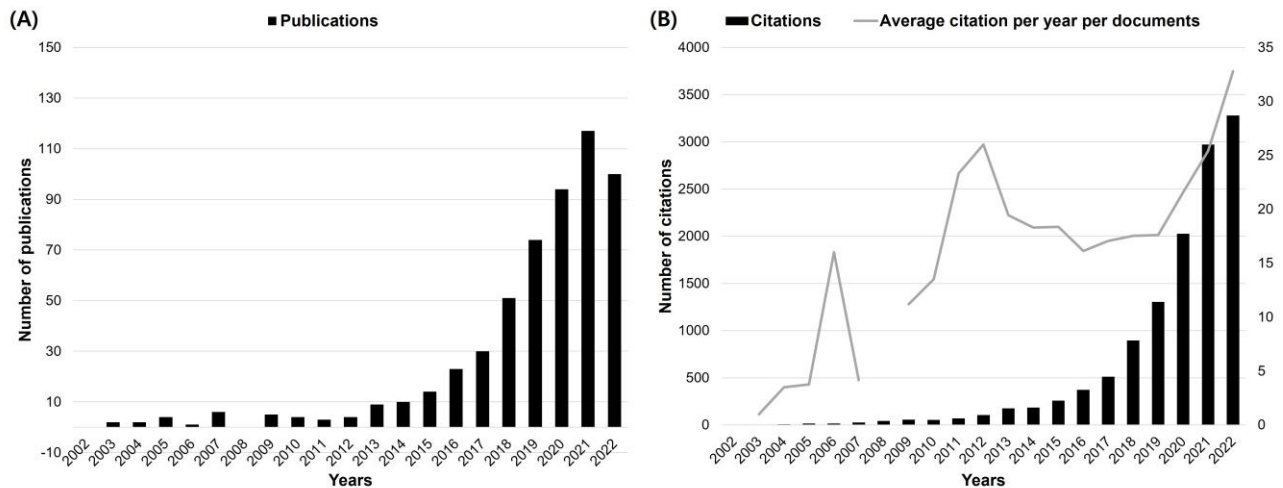


Figure 1. Overview of global trends in prehabilitation research publications (A), citations and average citations per year per documents (B): 2002-2022.

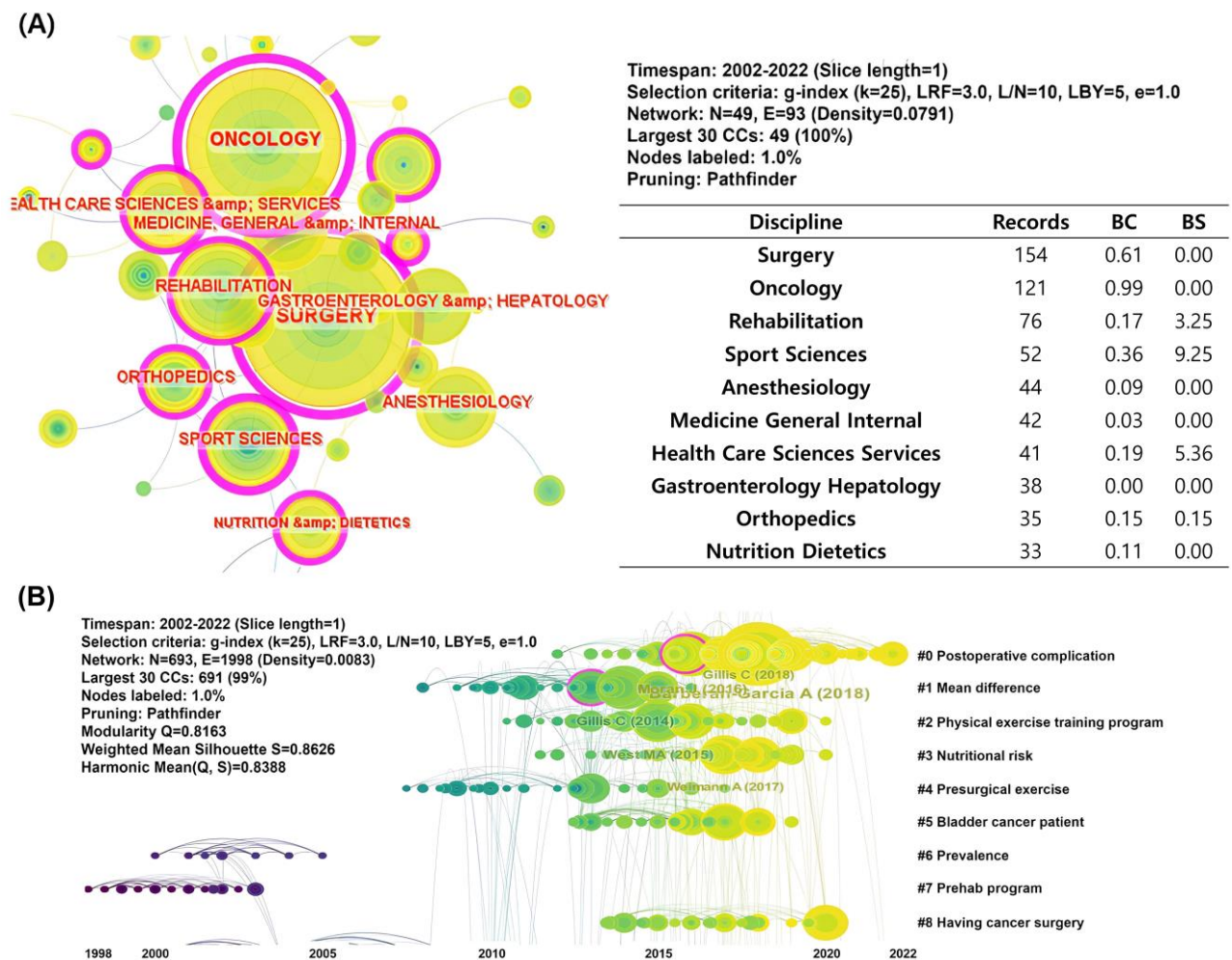


Figure 2. (A) Co-occurrence network of disciplines and (B) timeline view displaying co-citation clusters of research articles on prehabilitation published from 2002 to 2022.

Rank	Country	Counts		Betweenness Centrality	Burst Strength
1	USA	136		0.36	NA
2	Canada	98		0.31	NA
3	England	95		0.19	NA
4	Netherlands	73		0.14	NA
5	Australia	38		0.14	NA
Rank	Institutions	Counts	Country	Betweenness Centrality	Burst Strength
1	McGill University	63	Canada	0.37	NA
2	Maastricht University	24	Netherlands	0.18	NA
3	University of Texas System	18	USA	0.17	NA
4	Harvard University	18	USA	0.17	NA
5	University of Calgary	17	Canada	0.16	NA

Table 1. Top 5 countries and institutions with published research on prehabilitation between 2002 and 2022.

Safety and applicability of a newly developed outdoor cycling device as cardiac rehabilitation

Jin Taek Lee^{1*}, Bo Ryun Kim^{1†}, Young Mo Kim¹, Ho Sung Son², Jae Seung Jung², Hee Jung Kim²

Korea University Anam Hospital, Department of Rehabilitation Medicine¹, Korea University Anam Hospital, Department of Thoracic and Cardiovascular Surgery²

Objective

The purpose of this study is to investigate the safety and applicability of a newly developed outdoor interactive cycling device as home-based cardiac rehabilitation (HBCR) for patients with cardiovascular diseases (CVD).

Methods

CVD patients with low to moderate risk were recruited. These participants first performed a symptom-limited cardiopulmonary exercise test (CPET) using a modified Bruce protocol. After a rest period of 30 to 60 minutes, they rode the outdoor interactive cycling device for 10 minutes with monitoring of gas analysis and ECG.

We compared the results of those tests conducted using the treadmill and cycling device, focusing on key variables such as oxygen consumption (VO₂), heart rate (HR) and metabolic equivalents (METs).

Results

The mean age of a total 20 patients was 56.1 years (± 11.67), and all participants were male. In the CPET conducted using a treadmill, the following values were observed: VO₂ max (28.37 ± 5.60), HR max (152 ± 19.76), and MET max (8.22 ± 1.62). The test conducted using the cycle device showed the following results: VO₂ mean (19.79 ± 5.66), HR mean (134.85 ± 18.44), HR rest (85.55 ± 13.70), and MET mean (5.55 ± 1.40) (Table 1). Except for two participants, the MET values measured using the cycle device were within the therapeutic range (40~85% of MET max) calculated from the treadmill maximal MET values (figure 1). However, there was a difference between the resting heart rate before using the treadmill (76.35 ± 11.76) and the resting heart rate before using the cycle device (85.55 ± 13.70).

Subgroup analysis was performed by dividing patients into those under 60 and those aged 60 and older. Statistically significant differences were observed in VO₂ max, HR max, and MET max, but no statistically significant differences were found in VO₂ mean, MET mean, and HR mean between the two groups. These results imply that the cycle device could provide higher exercise intensity in patients aged 60 and older (Table 1).

No significant cardiac events, such as ST elevation/depression or hemodynamic instability, were observed during cycling.

Conclusion

This study suggests that an outdoor interactive cycling device can provide a therapeutic exercise intensity for HBCR in patients with various CVD. In addition, The outdoor cycling device showed higher intensity exercise effects in patients aged 60 years or older.

	Age group			P-value
	Under 60 (N=11)	Over 60 (N=9)	Total (N=20)	
Age	47.5 (\pm 7.51)	66.6 (\pm 5.20)	56.1 (\pm 11.67)	0.0002 ¹
Height	177.4 (8.21)	170.6 (4.31)	174.3 (7.44)	0.0524 ¹
Weight	81.3 (\pm 11.98)	70.4 (\pm 8.53)	76.4 (\pm 11.69)	0.0524 ¹
BMI	25.8 (\pm 3.03)	24.2 (\pm 2.23)	25.1 (\pm 2.76)	0.2539 ¹
Diagnosis (number)				
Angina	3 (15%)	4 (20%)	7 (35%)	
NSTEMI		2 (10%)	2 (10%)	
STEMI	4 (20%)	1 (5%)	5 (25%)	
Heart failure	1 (5%)		1 (5%)	
Valvular heart disease	1 (5%)	1 (5%)	2 (10%)	
Aortic disease		1 (5%)	1 (5%)	
Infective endocarditis	1 (5%)		1 (5%)	
Cardiomyopathy	1 (5%)		1 (5%)	
Maximal oxygen consumption	31.8 (\pm 4.74)	24.1 (\pm 3.07)	28.4 (\pm 5.60)	0.0008 ¹
Maximal MET	9.1 (\pm 1.35)	7.1 (\pm 1.23)	8.2 (\pm 1.62)	0.0049 ¹
Maximal Heart rate	163.6 (\pm 16.15)	139.6 (\pm 15.58)	152.8 (\pm 19.76)	0.0061 ¹
Rest Heart rate (treadmill)	78.2 (\pm 10.67)	74.1 (\pm 13.26)	76.4 (\pm 11.76)	0.3040 ¹
Mean oxygen consumption	19.6 (\pm 5.01)	20.0 (\pm 6.68)	19.8 (\pm 5.66)	0.9092 ¹
Mean MET	5.6 (\pm 1.41)	5.5 (\pm 1.47)	5.5 (\pm 1.40)	0.8490 ¹
Mean Heart rate	141.3 (\pm 19.08)	127.0 (\pm 15.04)	134.9 (\pm 18.44)	0.0801 ¹
Rest Heart rate (cycle)	87.5 (\pm 12.87)	83.2 (\pm 15.08)	85.6 (\pm 13.70)	0.4698 ¹

¹Wilcoxon rank sum p-value; Values represent mean \pm standard deviation or number (%)

Table 1. Demographic and clinical characteristics of the patients(N=20)

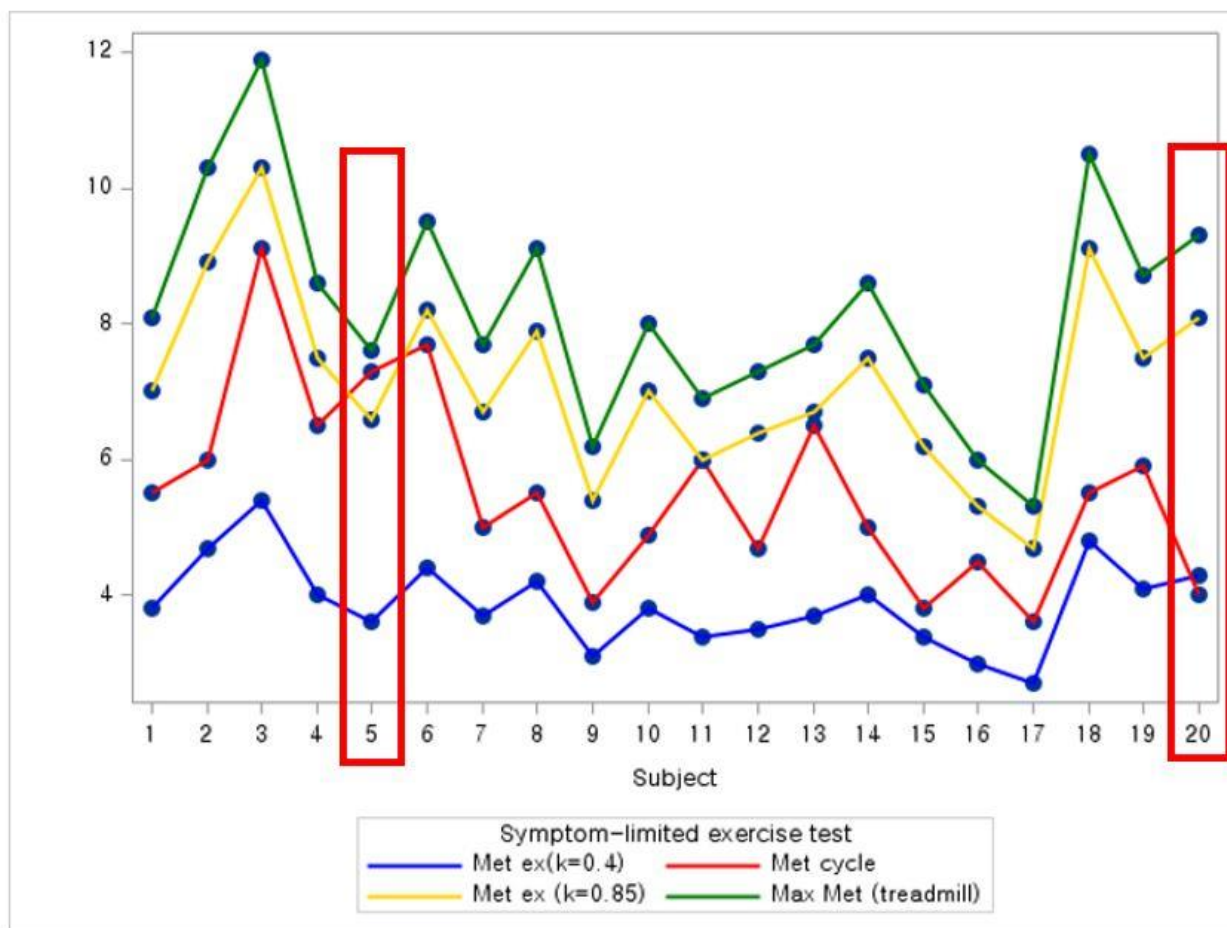


Figure 1. MET Values for Each Patient Measured Using the Cycle Device Relative to the therapeutic range derived from treadmill Maximal MET Values



Figure 2. outdoor Interactive cycling device

Musculoskeletal pain and balance problem in cardiac rehabilitation: prevalence and impact

Ji Hee Kim^{1**}, Min Cheol Joo¹, Eun Sun Lee¹, Jong Joon Lee¹

Department of Physical Medicine of Rehabilitation, Wonkwang University School of Medicine¹

Back ground and objective

Musculoskeletal problem is an important role in participation in cardiac rehabilitation in patients with cardiovascular disease and is a major factor influencing physical inactivity. This study aims to determine the prevalence of musculoskeletal pain in patients with myocardial infarction and the impact of pain on cardiac rehabilitation enrollment and cardiorespiratory fitness.

Methods

Individuals hospitalized for a cardiac event (myocardial infarction, percutaneous coronary intervention) are patients who is referred Cardiac Rehabilitation program from February to MAY 2024. All patients completed a questionnaire regarding musculoskeletal pain and balance problem, and appendicular skeletal muscle mass (ASM) was measured. Exercise capacity variables were measured. Eighty-nine patients were referred, 2 died, and 74 men and 13 women were analyzed.

Results

Musculoskeletal comorbidities affecting movement were reported in 62.1% (58.1% of men, 92.2% of women; $P=0.01$) of patients referred to cardiac rehabilitation. Spinal stenosis (12.7%), Arthritis (10.8%) was the most frequent diagnosis. Musculoskeletal pain sufficient to limit the ability to do walking was reported in 51.7% of the respondents. Balance problem affected 32.2%, with taking painkillers to relieve pain was reported in 24.1%. A total of 66.6% of patients participated in exercise tolerance test for cardiac rehabilitation. Patients with VAS 0, 68.7% participated in the exercise tolerance test, with an average of 22.8 ± 6.3 mL·kg·min, and among patients with VAS 1 or higher, 65.4% participated, with an average of 21.9 ± 6.8 mL·kg·min. In two group, there was no difference in cardiorespiratory fitness ($P=0.60$), showing that the presence or absence of musculoskeletal pain did not affect enrollment. There was no difference in ASM ($P=0.30$) and skeletal muscle mass (SMI) ($P=0.51$), Korean Activity Status Index (KASI) ($P=0.16$) between the two groups.

CONCLUSION

Many of patients referred to cardiac rehabilitation have musculoskeletal and balance problems, and especially common in women. However, patients with MS problem did not have low cardiorespiratory fitness, and there was no difference in enrollment. Accordingly, it is very important to screen for pain from the stage of first referral for cardiac rehabilitation and adjust treatment plans.

	Total	Men	Women	P-value
	N=87	N=74(85.1%)	N=13(14.9%)	
Age (years)	65.5±10.7	64.1±9.7	73.1±13.1	0.014*
Body mass index (kg/m ²)	24.25±3.18	24.4±3.28	23.3±2.4	0.199
Skeletal muscle index	8.0±1.09	8.28±0.9	6.6±0.7	<0.001*
Smoking/ Nonsmoking	38/49	37/37	1/12	0.042*
Education levels (years)	11.6±4.08	12.3±3.67	7.8±4.2	<0.001*
Depression symptoms (PHQ-9 score)	0.49±1.19	0.47±1.26	0.6±0.8	0.133

Table 1. Demographics..

Table 1. Demographics

	N(87)	Men(74)	Women(13)
Intensity of muscle/joint pain	87	74	13
No pain	33(37.9%)	31(41.9%)	1(7.7%)
Pain rated 1–5	34(39.1%)	27(36.5%)	8(61.5%)
Pain rated 6–10	20(23%)	16(21.6%)	4(30.7%)
Effect of pain on ability to perform moderate exercises	87	74	13
No limitation	42(48.3%)	37(50%)	5(38.4%)
Slight limitation	25(28.7%)	22(29.7%)	3(23%)
Moderate limitation	16(18.4%)	12(16.2%)	4(30.7%)
Severe limitation	4(4.6%)	3(4.1%)	1(7.6%)
Pain relief with medications	87	74	13
No pain medication	66(75.9%)	59(79.7%)	7(53.8%)
Pain medications present	21(24.1%)	15(20.3%)	6(46.2%)
	68	56	12
No pain relief	36(53%)	30(53.6%)	6(50%)
Slight pain relief	22(32.3%)	18(32.1%)	4(33.3%)
near total pain relief	10(14.7%)	8(14.3%)	2(16.7%)
Balance problems affecting ability to perform	N(87)	Men(87)	Women(13)
No balance problems	59(67.8%)	52(70.3%)	7(53.8%)
Balance problems present	28(32.2%)	22(29.7%)	6(46.2%)
	28	22	6
No limitation	2(7.1%)	2(9.1%)	0(0.0%)
Slight limitation	20(71.4%)	17(77.3%)	3(50%)
moderate limitation	3(10.7%)	1(4.5%)	2(33.3%)
Severe limitation	3(10.7%)	2(9.1%)	1(16.7%)
Patients who were told by a healthcare professional that they have the following (multiple answers)	102	86	16
Arthritis in the joints	11(10.8%)	9(10.5%)	2(12.5%)
Herniated disk in the back/neck	11(10.8%)	10(11.6%)	1(6.2%)
Inflammatory arthritis	6(5.9%)	6(7%)	0(0.0%)
Osteoporosis	6(5.9%)	3(3.5%)	3(18.7%)
Spinal stenosis	13(12.7%)	11(12.8%)	2(12.5%)
Vertebral or spinal fracture	1(1%)	1(1.1%)	0(0.0%)
Joint swelling	2(2%)	1(1.1%)	1(6.3%)
Neurological problem other than stroke	5(4.9%)	4(4.7%)	1(6.3%)
Not applicable (N/A)	47(46%)	41(47.7%)	6(37.5%)

Table 2. Patient distribution according to musculoskeletal pain screening questionnaire.

Table 2. Patient distribution according to musculoskeletal pain screening questionnaire.

Initial ETT	Musculoskeletal Pain :VAS 0 (N=22)	Musculoskeletal Pain :VAS 1-10 (N=36)	P-value
VO _{2 peak} (mL/kg/min)	22.78±6.39	21.96±6.89	0.665
VE _{peak} (L/min)	58.44±17.82	49.77±22.29	0.115
Peak RER	1.08±0.06	1.03±0.11	0.069
METs(M)	6.51±1.83	6.26±1.96	0.654
Exercise time (sec)	785±155.08	750.5±174.28	0.320

Table 4. Comparison of exercise capacity between patients without Musculoskeletal Pain and patients with Musculoskeletal Pain at initial ETT.

Abbreviations: VO_{2 peak}, peak oxygen consumption; VE_{peak}, volume of air exchanged per minute; RER, respiratory exchange ratio; METs, metabolic equivalent of tasks

* Denotes significant difference between the year group and (*p<0.05).

Table 4. Comparison of exercise capacity between patients without Musculoskeletal Pain and patients with Musculoskeletal Pain at initial ETT.

Association between phase angle and physical function in patients with acute myocardial infarction

Seung Jun Lee^{1*}, So Young Lee^{1†}, Jun Hwan Choi¹, Hyun Jung Lee¹

Department of Rehabilitation Medicine, Jeju National University Hospital¹

Back ground

The phase angle(PhA) of bioelectrical impedance is an important prognostic tool in clinical practice. The aim of this study was to evaluate the associations between PhA and physical function, including sarcopenia, cardiopulmonary function and arterial stiffness, in patients with acute myocardial infarction(AMI).

Methods

We evaluated 66 patients with AMI who entered the Cardiac Vascular Center of this hospital to undergo percutaneous coronary intervention(PCI). Upon admission, the patients' demographic information was recorded. And, Bioelectrical impedance analysis(BIA), brachial-ankle pulse wave velocity(baPWV), ankle-brachial index(ABI) and cardiopulmonary function test were performed within the 4 weeks after PCI.

Results

The mean age of participants was 63.59 ± 11.63 years, 59(89.4%) were males and 7(10.6%) were females. Age, body mass index(BMI), Skeletal muscle mass index(SMI), peak oxygen consumption(VO_{2peak}), oxygen consumption at anaerobic threshold(VO_{2AT}), diastolic blood pressure at rest(DBPrest), rate pressure product(RPP), baPWV and ABI were significant correlation with PhA ($P < 0.05$) in male. In the multivariable linear regression in male, BIA-derived PhA was positively associated with VO_{2peak} ($\beta = 0.493$, $P = 0.002$) and the SMI ($\beta = 0.433$, $P < 0.001$).

Conclusions

According to the present study results, the BIA-derived phase angle was positively associated with the cardiopulmonary function and sarcopenia in male patients with acute myocardial infarction.

Table 1. Demographic and Clinical Characteristics of Study Patients

	Male(n=59)	Female(n=9)	P-value
Age, years	63.22±10.97	66.71±17.04	0.457
STEMI, n(%)	18 (30.5)	5 (71.4)	0.045
LVEF, %	52.84±10.78	51.01±6.75	0.665
Cormorbidity, n(%)			
HTN	26(44.1)	2(28.6)	0.359
Diabetes	11(18.6)	1(14.3)	0.625
Dyslipidemia	8(13.6)	1(14.3)	0.661
Bioelectrical impedance analysis (BIA)			
height, cm	168.90±5.67	154.00±4.00	<0.001
weight, kg	72.86±13.84	61.43±12.34	0.041
Body mass index, kg/m ²	25.45±4.18	25.87±4.83	0.806
Skeletal muscle mass index, kg/m ²	8.23±0.95	6.63±1.03	<0.001
Phase angle, °	6.55±1.18	5.40±0.89	0.016
Cardiopulmonary function test			
VO _{2peak} , mL/kg/min	24.96±6.21	18.09±5.79	0.007
VO _{2AT} , mL/kg/min	18.18±5.30	14.11±4.07	0.055
HR _{rest} , beats/min	144.75±21.67	135.00±37.71	0.526
HR _{peak} , beats/min	73.97±11.63	81.14±18.80	0.155
SBP _{peak} , mmHg	166.34±27.90	170.29±29.40	0.726
DBP _{peak} , mmHg	74.78±12.18	76.86±14.35	0.677
SBP _{rest} , mmHg	121.17±15.31	138.14±19.57	0.009
DBP _{rest} , mmHg	74.15±10.91	77.29±11.72	0.478
RPP	24330.66±6218.79	24513.43±8661.08	0.944
RER	1.03±0.10	0.94±0.14	0.141
Arterial stiffness			
baPWV, m/sec	1448.36±338.67	1827.79±587.55	0.141
ABI	1.03±0.12	1.02±0.12	0.858

STEMI = ST elevation myocardial infarction; LVEF = left ventricular ejection fraction; VO_{2peak} = peak oxygen consumption; VO_{2AT} = oxygen consumption at anaerobic threshold; HR_{peak} = heart rate at peak exercise; HR_{rest} = heart rate at rest; SBP_{peak} = systolic blood pressure at peak exercise; DBP_{peak} = diastolic blood pressure at peak exercise; SBP_{rest} = systolic blood pressure at rest; DBP_{rest} = diastolic blood pressure at rest; RPP=rate pressure product; RER=respiratory exchange ratio; baPWV = brachial-ankle pulse wave velocity; ABI = ankle-brachial index

Table 1. Demographic and Clinical Characteristics of Study Patients

Table 2. Correlation between phase angle and study outcomes in patients with AMI

Variable	Phase Angle	P-value
Age, years	-0.673	0.000
LVEF, %	0.237	0.071
height, cm	0.038	0.774
weight, kg	0.501	0.000
Body mass index, kg/m ²	0.562	0.000
Skeletal muscle mass index, kg/m ²	0.749	0.000
VO _{2peak} , mL/kg/min	0.506	0.000
VO _{2AT} , mL/kg/min	0.447	0.000
HR _{rest} , beats/min	0.248	0.058
HR _{peak} , beats/min	-0.102	0.441
SBP _{peak} , mmHg	0.208	0.114
DBP _{peak} , mmHg	0.146	0.272
SBP _{rest} , mmHg	0.021	0.875
DBP _{rest} , mmHg	0.296	0.023
RPP	0.294	0.024
RER	0.011	0.933
baPWV, m/sec	-0.490	0.000
ABI	-0.470	0.000

Table 2. Correlation between phase angle and study outcomes in patients with AMI

Table 3. Multivariate linear regression analysis for cardiopulmonary function and sarcopenia

	VO _{2peak}			
	β	B	95% CI	p-value
Phase angle	0.493	2.596	0.79	0.002
BMI	-0.405	-0.600	0.2	0.004
age	-0.385	-0.202	0.085	0.021

	Skeletal muscle mass index			
	β	B	95% CI	p-value
Phase angle	0.433	0.349	0.062	0.000
BMI	0.561	0.127	0.017	0.000

Table 3. Multivariate linear regression analysis for cardiopulmonary function and sarcopenia

A Study on Risk Factors in Elderly Drivers and Acceptability of Conditional Driving Licenses Systems

Gain Shin^{1,2*}, Jun Hee Won², Ja-Ho Leigh^{1,2,3,4†}

Department of Rehabilitation Medicine, Seoul National University Hospital¹, National Traffic Injury Rehabilitation Research Institute, National Traffic Injury Rehabilitation Hospital², Department of Rehabilitation Medicine, National Traffic Injury Rehabilitation Hospital³, Institute of Health Policy and Management, Medical Research Center, Seoul National University⁴

Object

To identify the physical, cognitive, and psychological characteristics that elderly drivers experience when driving or ceasing to drive and to assess the acceptance and awareness of a conditional driver's license among elderly drivers in South Korea.

Method

This survey study targeted elderly drivers aged 65 and older living in the community, with a valid driver's license. A total of 900 elderly drivers responded to the survey. Data were analyzed using the JAMOV program, version 2.4.11. Descriptive statistics and frequency analysis were employed to examine the participants' general characteristics and factors making driving difficult. Independent t-tests and one-way ANOVA were conducted to compare driving difficulties and awareness of the conditional driving license system across different age groups, residential areas, and diagnosed disease groups. Pearson correlation analysis was used to determine correlations between variables. The significance level was set at .05.

Result

The study identified various factors contributing to driving difficulties, categorized into human and environmental factors. Human factors included physical, cognitive, visual, and psychological aspects. The most frequently cited difficulties were 'Dazzle/light bleeding' (34%) and 'Lack of confidence in specific driving situations such as long-distance driving, highway driving, or night driving' (34%). Environmental factors encompassed 'type of road', 'driving situation', and 'weather conditions'. Participants reported significant difficulties with 'sudden stopping while driving' (40%) among 'driving situation' factors, and in 'weather conditions' factors, they reported significant difficulties in all items.

Driving difficulty increased with age, showing significant differences among the age groups '65-71', '71-75', and '76 and older'. Additionally, significant differences in driving difficulties were observed across different disease groups. Among participants, 51% were unaware of conditional driver's licenses, while 46% had only a superficial awareness. When considering the implementation of a conditional driving license system to reduce license cancellations or returns among the elderly, the responses were more favorable ('yes') than unfavorable ('no'), excluding neutral responses. The acceptability of the conditional driving license system was generally positive, with the most favorable conditions being 'restrictions on vehicle-mounted functions', 'speed restrictions', and 'time restrictions'.

Conclusion

The predictive model developed in this study could contribute to preventing serious traffic accidents caused by elderly drivers and might assist them in driving safely.

Acknowledgment This research was supported by Technologies for Future-oriented National Citizen Security Services Program through the Korea Institutes of Police Technology(KIPoT) funded by the Korean National Police Agency. (No. PR09-02-000-22)

Factor	Category	Items	Mean±SD	No difficult <i>N</i> (%)	Moderate <i>N</i> (%)	Difficult <i>N</i> (%)
Environmental	Type of road	Highway	2.69±0.92	411(46%)	307(34%)	182(20%)
		Route	2.44±0.80	498(55%)	323(36%)	73(9%)
		Alleyway	2.77±0.95	382(42%)	300(33%)	218(24%)
	Total		2.63±0.79	-	-	-
	Driving situation	Change the lane	2.51±0.84	480(53%)	304(34%)	116(13%)
		Go straight to the non-signal intersection	2.65±0.85	405(45%)	341(38%)	154(17%)
		Turn left at a non-signal intersection	2.73±0.89	382(42%)	328(36%)	190(21%)
		Permitted-unprotected left turn	2.81±0.94	361(40%)	307(34%)	232(26%)
		Turn right at an intersection with heavy traffic	2.72±0.87	383(43%)	337(37%)	180(20%)
		Enter the roundabout	2.73±0.86	374(42%)	348(39%)	178(19%)
		When a vehicle in the next lane cuts in front while driving	2.95±0.97	307(34%)	310(34%)	283(31%)
		When the vehicle in front suddenly stops while driving	3.17±1.03	248(28%)	294(33%)	358(39%)
	Total		2.78±0.78	-	-	-
	Driving climate conditions	Fog	3.41±0.87	138(15%)	306(34%)	456(51%)
		Driving at night	3.34±0.91	184(20%)	272(30%)	444(49%)
		Rain / Hail	3.42±0.91	152(17%)	299(33%)	446(50%)
		Cloudy	3.00±0.87	268(30%)	366(41%)	266(29%)
		Heavy snowfalls	3.71±1.00	126(14%)	208(23%)	566(63%)
		Glare	3.40±0.94	159(18%)	313(35%)	428(47%)
	Total		3.38±0.77	-	-	-
Human	Physical	Decreased in the strength of the limbs	2.47±0.78	477(53%)	346(39%)	77(8%)
		Decreased limb reaction time	2.61±0.84	431(48%)	333(37%)	136(15%)
		Pain	2.72±0.88	391(43%)	326(36%)	183(20%)
		Decreased in joint movement	2.61±0.85	422(47%)	343(38%)	132(15%)
		Hearing loss	2.51±0.81	462(51%)	345(38%)	93(10%)
	Total		2.58±0.72	-	-	-
	Cognition	Maintaining a safe distance	2.36±0.74	525(58%)	332(37%)	43(5%)
		Speed control	2.49±0.81	464(52%)	345(38%)	91(10%)
		Driving in a designated lane	2.50±0.84	475(53%)	315(35%)	110(12%)
		Compliance with traffic laws	2.18±0.79	615(68%)	243(27%)	42(5%)
		Pause at the crosswalk stop line	2.23±0.82	598(66%)	242(27%)	60(7%)
		Predicting dangerous situations	2.90±0.94	303(33%)	347(39%)	250(28%)
		Know the right time to enter the road	2.78±0.89	340(38%)	366(41%)	194(21%)
		Responding correctly to unexpected road traffic conditions	2.96±0.94	301(33%)	329(37%)	270(30%)
		Adequate intervention in lane change	2.75±0.89	359(40%)	357(40%)	184(20%)
		Passing through an intersection	2.59±0.83	404(45%)	384(43%)	112(12%)
	Total		2.57±0.68	-	-	-
	Visual	Vision	2.76±0.81	343(38%)	398(44%)	159(18%)
		Visual Field	2.85±0.80	309(34%)	399(44%)	192(21%)
		Color vision	2.54±0.78	444(49%)	370(41%)	86(10%)
		Contrast sensitivity	2.87±0.82	300(33%)	401(45%)	199(22%)
		Bright/Dark adaptation	3.03±0.86	257(28%)	366(41%)	277(31%)
		Glare/Light blur	3.14±0.89	222(25%)	366(41%)	312(34%)
	Total		2.86±0.70	-	-	-
	Psychological	Difficulty waiting while driving	2.35±0.75	539(60%)	312(35%)	49(5%)
		Being embarrassed and unable to deal with emergencies	2.63±0.83	411(46%)	357(40%)	132(14%)
		Burdensome to judge the situation	3.02±0.92	271(30%)	348(38%)	281(31%)
		Ominous and anxious when driving	2.48±0.81	505(56%)	294(33%)	101(11%)
		Not confident in driving for a particular situation	3.07±0.94	261(29%)	330(37%)	309(34%)
	Total		2.71±0.70	-	-	-

Table 1. Categories and items of environmental and human factors that make driving difficult

Table 2. Category that make driving difficult by age group and disease group (n=900)				
Factor	Category	F	p	Post-Hoc
Environmental	Type of road	22.1	<.001*	Age Group 1 < Age Group 2 < Age Group 3
	Driving situation	25.8	<.001*	Age Group 1 < Age Group 2
	Driving climate conditions	14.1	<.001*	Age Group 1 < Age Group 3
Human	Physical	44.2	<.001*	Age Group 1 < Age Group 2 < Age Group 3
	Cognition	21.0	<.001*	
	Visual	26.3	<.001*	
	Psychological	22.1	<.001*	
* Age Group 1: 65-70, Age Group 2: 71-75, Age Group 3: 76 and over				
Environmental	Type of road	3.83	0.015*	Dx Group 3 < Dx Group 2
	Driving situation	2.23	0.094	-
	Driving climate conditions	1.90	0.143	-
Human	Physical	1.84	0.153	-
	Cognition	3.47	0.020*	-
	Visual	3.95	0.012*	Dx Group 3 < Dx Group 2 Dx Group 3 < Dx Group 4
	Psychological	4.40	0.007*	-
** Dx group 1: Chronic disease, Dx group 2: ophthalmic disease, Dx group 3: spinal and musculoskeletal diseases, Dx group 4: musculoskeletal diseases of limb, Dx group 5: Other diseases				

Table 2. Category that make driving difficult by age group and disease group

Table 3. Opinion on the expected effect of cancellation/return reduction of driver's license due to conditional area when introducing the conditional driving license system					
Conditions	N(%)				
	More favorable	Favorable	Neutral	Unfavorable	More Unfavorable
Time limits	62(6.9)	272(30.2)	364(40.5)	184(20.4)	18(2.0)
Space restrictions	49(5.5)	219(24.3)	414(46.0)	201(22.3)	17(1.9)
Speed limits	66(7.3)	297(33.0)	363(40.3)	160(17.8)	14(1.6)
Road type restriction	51(5.7)	301(33.4)	341(37.9)	186(20.7)	21(2.3)
Vehicle restrictions	65(7.2)	317(35.2)	375(41.7)	126(14.0)	17(1.9)
Personalized restrictions	63(7.0)	235(26.1)	430(47.8)	157(17.4)	15(1.7)

Table 3. Opinion on the expected effect of cancellation/return reduction of driver's license due to conditional area when introducing the conditional driving license system

Importance of Bilateral Hip Assessments in Unilateral Lower Limb Amputees

Seong Jin^{1*}, Chi Hwan An¹, Ho Yong Jeong¹, Woohwa Choi¹, Sun-Won Hong¹, Hoon Ki Song¹, Hyun Sung Kim¹, Yun Kyung Lee¹, Hyo Jung Kang¹, Dong-young Ahn¹, Hea-Eun Yang^{1†}

VHS Medical Center, Department of Rehabilitation Medicine¹

Introduction

Lower limb amputees often experience significant bone loss in the residual limb, increasing their risk of falls and fractures. Osteoporosis in men is frequently underdiagnosed and inadequately treated, despite high morbidity and mortality rates following fractures. Dual-energy X-ray absorptiometry (DXA) is the gold standard for BMD measurement, but BMD discordance between skeletal sites can lead to misdiagnosis and improper management. This study evaluates BMD differences and discordance in veterans with unilateral lower limb amputation, hypothesizing significant discordance between both hips.

Methods

Data were collected from 84 male veterans. BMD was measured using DXA at the lumbar spine, intact hip, and amputated hip. The study assessed discordance between these sites and analyzed factors influencing BMD on the amputated side.

Results

The T-scores for the lumbar spine, intact hip, and amputated hip were -0.27 ± 1.69 , -0.25 ± 1.20 , and -1.07 ± 1.33 , respectively. Osteoporosis and osteopenia were present in 19% and 34.6% of patients, respectively (Table 1). Osteopenia and osteoporosis were most prevalent in the hips on the amputated side (32.1% and 13.1%, respectively), followed by the lumbar spines (22.6% and 8.3%) and the hips on the intact side (17.9% and 2.4%). BMD discordance between the lumbar spine and hip was found in 47.6% of participants, while discordance between both hips was observed in 39.3% (Table 2). Transfemoral amputees had significantly lower BMD at the amputated hip compared to transtibial amputees (-2.38 ± 1.72 vs. -0.87 ± 1.16 , $p < 0.01$). The T-score of the amputated side hip was lower in traumatic amputations compared to vascular amputations (-1.25 ± 1.23 vs. -0.33 ± 1.68 , $p < 0.05$) (Table 3).

Conclusion

Veterans with unilateral lower limb amputation exhibit a high prevalence of osteoporosis and significant BMD discordance, particularly between both hips. The notable difference in BMD between the amputated and intact hips, especially among transfemoral amputees, suggests that amputation level significantly impacts bone health. These findings underscore the necessity for bilateral hip assessments to ensure accurate diagnosis and effective management of osteoporosis in this population. Regular monitoring and tailored interventions are essential to mitigate fracture risk and improve long-term outcomes for lower limb amputees.

Acknowledgment This study was supported by a VHS Medical Center Research Grant (VHSMC 24014), Republic of Korea.

Characteristic	Mean \pm SD / n (%)
Age (years)	69.0 \pm 8.6
Time after amputation (years)	38.4 \pm 18.5
Amputation side (right : left)	43 (51.2%) : 41 (48.8%)
Amputation level (transfemoral : transtibial)	11 (13.1%) : 73 (86.9%)
Height (cm)	165.9 \pm 5.7
Weight (kg)	65.2 \pm 9.0
Body mass index (kg/m ²)	23.7 \pm 2.7
T-score of lumbar spine	-0.27 \pm 1.69
T-score of intact side hip	-0.25 \pm 1.20
T-score of amputated side hip	-1.07 \pm 1.33
Normal : Osteopenia : Osteoporosis	39 (46.4%) : 29 (34.6%) : 16 (19.0%)

n=84

Table 1. Patient Characteristics

Spine vs. Hip		Number of Patients	Observed Prevalence (%)
Concordance		44	52.4
Minor discordance	Lower in hip	16	19.0
	Lower in spine	19	22.6
Major discordance	Lower in hip	2	2.4
	Lower in spine	3	3.6
Between Hips			
Concordance		51	60.7
Minor discordance	Lower in hip	22	26.2
	Lower in spine	2	2.4
Major discordance	Lower in hip	7	8.3
	Lower in spine	2	2.4

n=84, BMD: bone mineral density.

Table 2. Concordance and Discordance in BMD Between Spine, Hip, and Between Both Hips

	Transfemoral (n=11)	Transtibial (n=73)	p-Value	Trauma (n=56)	Vascular (n=11)	p-Value
Age (years)	70.4 \pm 9.3	68.8 \pm 8.6	0.570	69.4 \pm 9.0	70.8 \pm 5.6	0.606
Time after amputation (years)	46.6 \pm 11.0	37.3 \pm 19.1	0.160	43.4 \pm 14.2	4.7 \pm 7.7	0.000*
Height (cm)	165.1 \pm 5.9	166.0 \pm 5.6	0.659	166.1 \pm 5.8	165.4 \pm 6.1	0.734
Weight (kg)	61.3 \pm 8.3	65.9 \pm 9.0	0.124	66.4 \pm 9.6	62.4 \pm 6.7	0.215
Body mass index (kg/m ²)	22.4 \pm 2.3	23.9 \pm 2.7	0.099	24.0 \pm 2.7	22.7 \pm 1.5	0.160
T-score of lumbar spine	-0.84 \pm 1.57	-0.19 \pm 1.70	0.237	-0.32 \pm 1.55	-0.07 \pm 1.10	0.610
T-score of amputated side hip	-2.38 \pm 1.72	-0.87 \pm 1.16	0.000*	-1.25 \pm 1.23	-0.33 \pm 1.68	0.036*
T-score of intact side hip	-0.79 \pm 1.87	-0.17 \pm 1.06	0.111	-0.31 \pm 1.14	-0.26 \pm 1.52	0.881
Transfemoral : Transtibial				10 : 46	0 : 11	0.195

Values are presented as Mean \pm standard deviation. *Statistical significance.

Table 3. Patient Characteristics and T-Scores According to the Level and Cause of Amputation

Suicide risk and associated factors in Parkinson's disease: A nationwide cohort study

Jee Hyun Suh^{1*}, Seo Yeon Yoon², Jin Hyung Jung³, Sang Chul Lee², Kyungdo Han⁴, Kun Wook Lee², Yu Ji Han¹, Yong Wook Kim^{2†}

Department of Rehabilitation Medicine, Ewha Womans University Mokdong Hospital¹, Department and Research Institute of Rehabilitation Medicine, Severance Hospital², Samsung Biomedical Research Institute, Sungkyunkwan University School of Medicine³, Department of Statistics and Actuarial Science, Soongsil University⁴

Introduction

Although increased mortality in patients with Parkinson's disease (PD) is well-documented, studies on suicide-related mortality have yielded conflicting results. Moreover, the impact of comorbidities, socioeconomic factors, and health behaviours as potential risk factors for suicide remains underinvestigated. This study aimed to investigate suicide mortality risk in patients with PD and comprehensively elucidate the association between comorbidities, socioeconomic factors, health behaviours, and suicide in these patients.

Methods

This study is a nationwide population-based cohort study using Korean National Health Insurance Service data from 2009 with a longitudinal follow-up until 31 December 2021. This study included 2,732,294 (PD, n = 4,132; without PD, n = 2,728,162) individuals from the 2009 National Health Screening Program. PD was defined by ICD-10 code (G20) and registration code (V124) in the rare intractable diseases program. Comorbidities were identified using medical history, ICD-10 codes, laboratory data, and prescribed medications. Health behaviours were obtained from a self-reported National Health Screening Program questionnaire. The primary outcome was suicide mortality, determined by ICD-10 codes for intentional self-harm (X60-X84).

Results

Suicide mortality in patients with PD increased by 2.71-fold, and those with both PD and metabolic diseases (diabetes mellitus, dyslipidaemia, and metabolic syndrome) did not show an increased suicide risk. Males with PD had a more than 7-fold higher risk (HR=7.34, 95% CI, 5.25-10.26). Low-income patients with PD had an approximately 5-fold higher risk compared to high-income non-PD individuals (HR=5.10, 95% CI, 3.07-8.46). Patients with PD concomitant with depression (HR=5.00, 95% CI, 3.06-8.16) and alcohol consumption (HR=3.54, 95% CI, 2.14-5.89) also showed increased suicide risk.

Conclusion

Patients with PD have a higher suicide risk, particularly males, younger individuals, those with lower income, depression, or alcohol consumption.

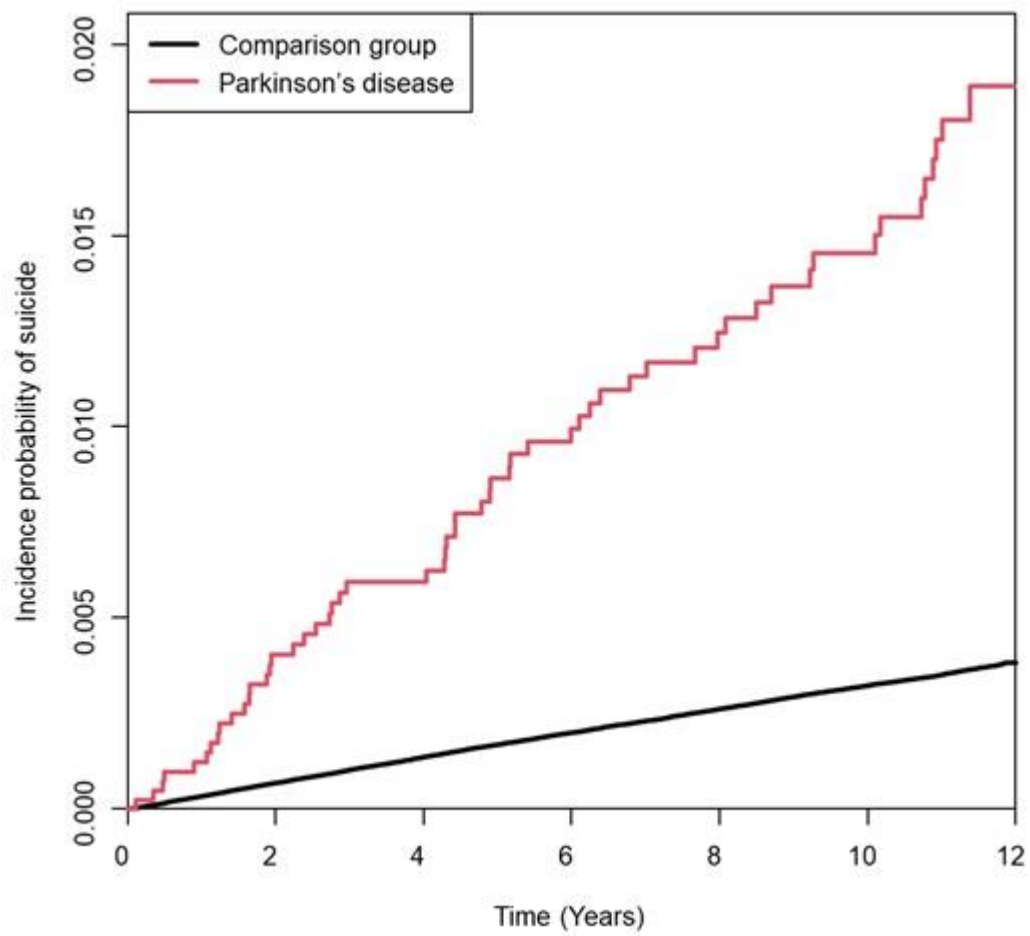


Figure 1. Kaplan-Meier curves of suicide risk in Parkinson's disease and comparison groups.

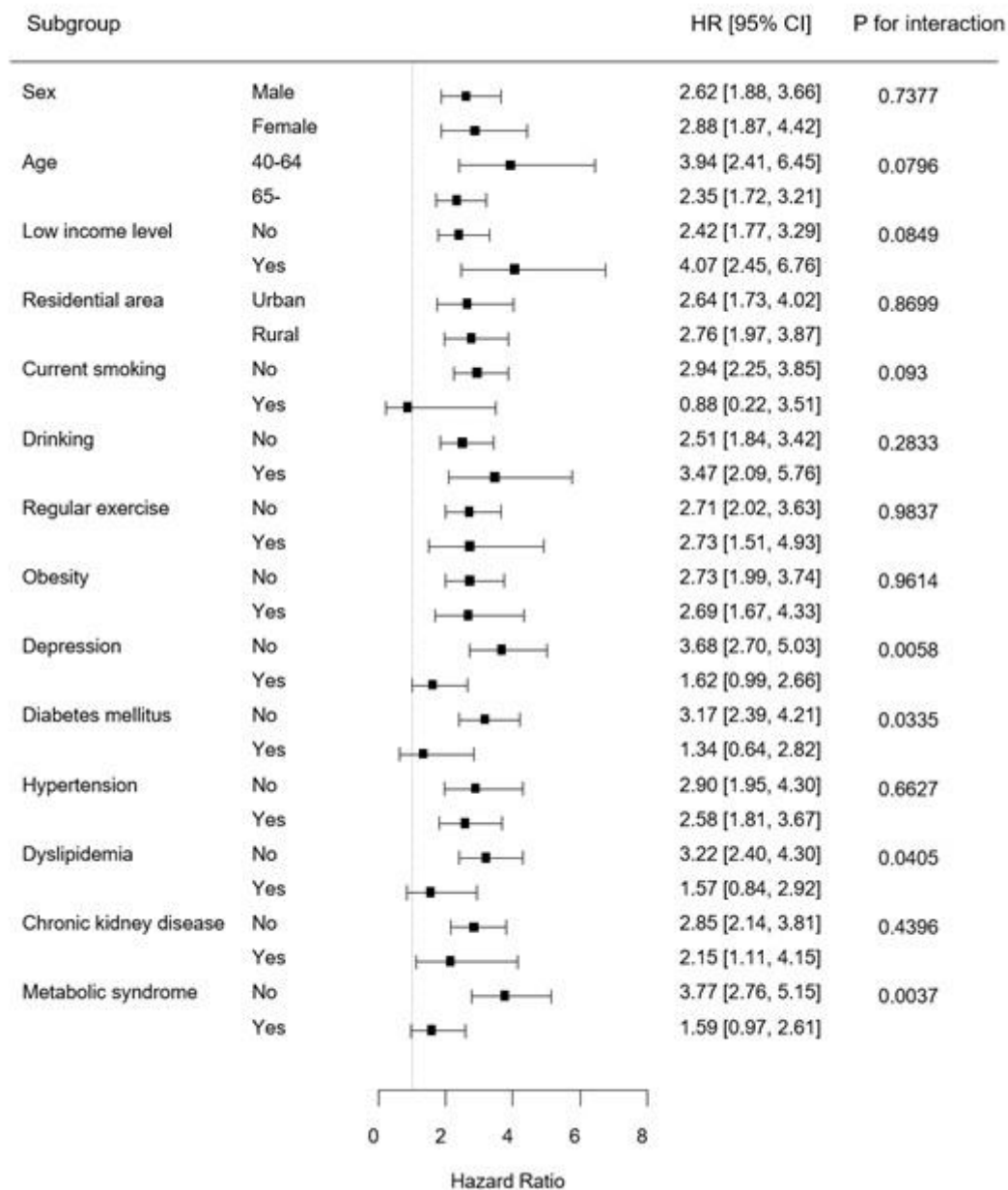


Figure 2. Subgroup analysis of the suicide risk according to Parkinson's disease by sociodemographic, lifestyle factors, and comorbidities

The Effect of Insulin Resistance on Sarcopenic Obesity

Seongmin Choi^{1*}, Yunsoo Soh^{1†}, Jong Ha Lee¹, Dong Hwan Yun¹, Jinmann Chon¹, Myung Chul Yoo¹, Ga Yang Shim¹

Department of Physical Medicine & Rehabilitation, College of Medicine, Kyung Hee University¹

Background

Sarcopenic obesity (SO), characterized by the coexistence of sarcopenia and obesity, poses a significant health risk to the elderly. Sarcopenia involves the loss of skeletal muscle mass and strength, while obesity is defined by excess body fat. The combination of these conditions exacerbates the risk of adverse health outcomes, including increased morbidity and mortality. Insulin resistance, obesity, and sarcopenia have been reported to be a potential bidirectional causal relationship. However, the causal relationship between insulin resistance and SO, particularly whether insulin resistance causes SO, has not yet been investigated. In this study, we aimed to investigate the effect of insulin resistance on SO.

Method

The study population consisted of older adults aged 70-84 years from the Korean Frailty and Aging Cohort Study (KFACS). We included 2,071 (men 1,030; women 1,041) participants in the cross-sectional analysis. In a two-year longitudinal study, individuals who had SO at baseline and were lost to follow-up were excluded, resulting in a final inclusion of 1,580 (men 797; women 783) participants (Figure 1). SO was assessed using the ESPEN and EASO guidelines, with body composition measured by dual-energy X-ray absorptiometry (DXA). Insulin resistance was evaluated by the homeostatic model assessment for insulin resistance (HOMA-IR). The HOMA-IR was determined using the subsequent equation: (glucose in mg/dl × insulin in mU/L divided by 405). Insulin resistance was defined as HOMA-IR > 2.54.

Results

The baseline characteristics of the participants are shown in table 1. The percentage of high HOMA-IR was higher in SO group compared to non-SO group in men. In a cross-sectional study, high HOMA-IR group had a higher risk of SO (OR, 2.75; 95% CI, 1.66-4.58), high fat mass (OR, 2.83; 95% CI, 2.01-3.98), low muscle mass (OR, 2.00; 95% CI, 1.39-2.78) in men after adjusting for confounding factors (Table 2). In a longitudinal study, high HOMA-IR group had a higher incidence of SO in men after adjusting confounding factors (OR, 2.64; 95% CI, 1.38-5.06).

Conclusion

Our results showed that a high HOMA-IR was associated with low muscle mass and high fat mass. Further more HOMA-IR was associated with higher incidence of SO over two years in men. Insulin resistance may be a risk factor of SO, particularly in men.

Bioelectrical Impedance Vector Analysis in Elderly Hip fracture Patients

Seung-Kyu Lim^{1*}, Jin-Whan Ryu¹, In-Su Hwang¹, Sol Jin¹, Jae-Young Lim^{2†}

Department of Rehabilitation Medicine, Soonchunhyang University Cheonan Hospital, Soonchunhyang University College of Medicine¹, Department of Rehabilitation Medicine, Seoul National University Bundang Hospital, Seoul National University College of Medicine²

Background

Hip fracture patients commonly experience interconnected geriatric nutritional issues like undernutrition, sarcopenia, and frailty. Interventions targeting these factors are crucial for improving postoperative outcomes in hip fracture patients. Bioelectrical impedance vector analysis (BIVA) offers an assessment of body composition and hydration status, serving as a valuable tool to guide appropriate interventions. This study aims to assess body composition using BIVA in older adults with hip fractures and compare the findings with those of reference populations.

Methods

This cross-sectional study included 103 hip fracture surgery patients aged 65 years and older. Bioelectrical impedance assessment was conducted, and resistance (R) and reactance (Xc) data were analyzed based on height and plotted on RXc graphs. We used data from age- and BMI-matched community-dwelling South Korean and international populations without hip fractures, as reported in previous studies, as our healthy reference populations. We also included data from a South Korean young population. We compared the data for men and women in our study with these reference populations using confidence ellipses. The individual vectors of our patient group were plotted relative to the tolerance ellipses, representing 50%, 75%, and 95% of the reference values for each population. Vectors were also differentiated on the graphs based on the presence of sarcopenia.

Results

The BIVA confidence ellipse indicated that the men and women with hip fractures were significantly different from reference population groups ($P < 0.001$), showing a noticeable downward displacement and reduction in the Xc component (Figure 1). Only a small proportion of men ($n=2$) and women ($n=10$) with hip fractures but without sarcopenia were located within the 75% tolerance ellipse when compared to community-dwelling South Korean older adults without hip fractures. The majority of men and women with hip fractures were positioned outside the 75% and 95% tolerance ellipses when compared with other reference groups for both men and women, predominantly in the lower right and upper right quadrants. This reflects a loss of body cell mass and water imbalance, suggestive of muscle wasting and dehydration. Both men and women with sarcopenia displayed a greater rightward displacement, indicating more severe muscle wasting and dehydration (Figure 2 and 3).

Conclusions

Hip fracture patients exhibit a distinct BIVA pattern indicative of frailty and malnutrition, which differs from that of community-dwelling adults without hip fractures. BIVA can be an effective tool for screening and early identification of body composition changes in older hip fracture patients, who often face overlapping geriatric nutritional issues such as malnutrition, sarcopenia, and frailty. By providing reliable diagnoses, BIVA facilitates timely, multidisciplinary interventions, including nutritional and rehabilitation support, for these patients.

Acknowledgment This research was supported by a grant of the Korea Health Technology R&D Project through the Korea Health Industry Development Institute (KHIDI), funded by the Ministry of Health & Welfare, Republic of Korea (grant number : HI19C0481, HC20C0157).

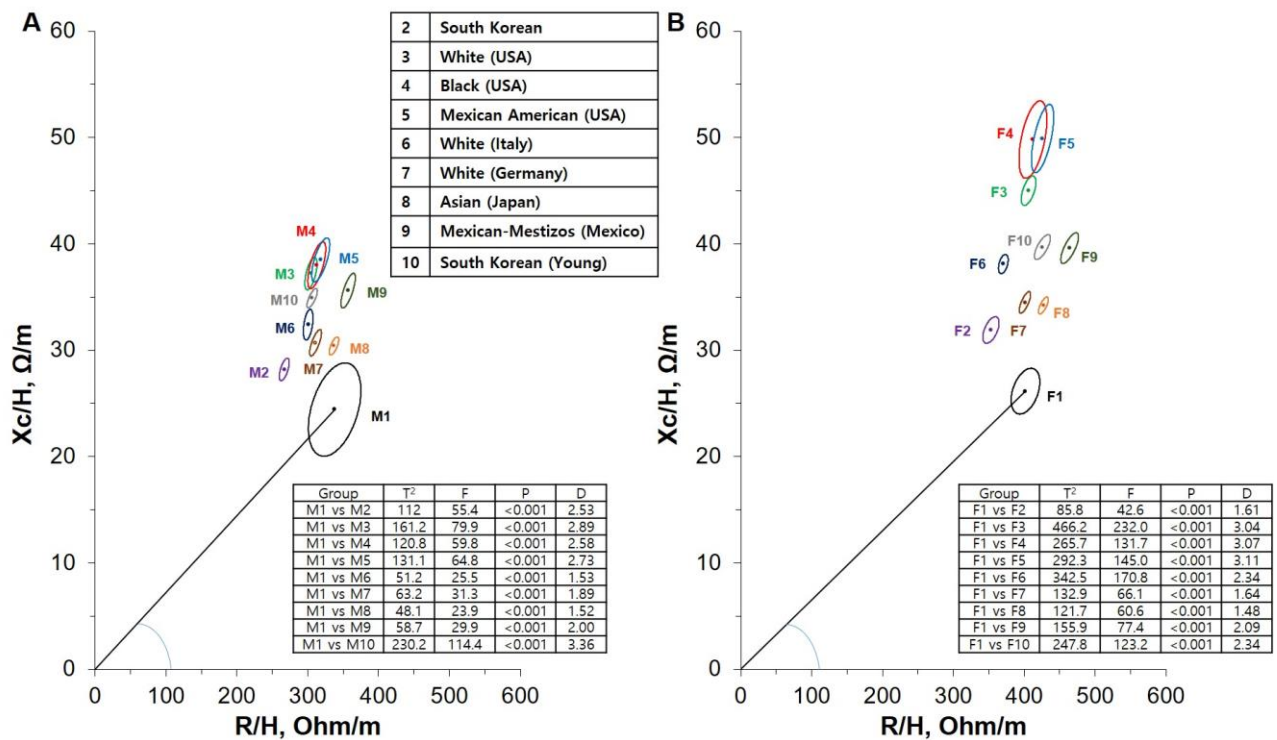


Figure 1. BIA vectographs (R/H and Xc/H) illustrate the relative bivariate vector positioning and confidence ellipses for (A) the male (M1, n=24) and (B) female (F1, n=79) participant study groups. Reference vectors from the male (M2–10) and female (F2–10) populations are also plotted. Full statistical analyses, including Hotelling's T2 test, F and P values, and Mahalanobis distance (D), are conducted and presented in the comparison tables in Figure. The reference dataset details are available in Table 2. ; R/H, resistance/height; Xc/H, reactance/height.

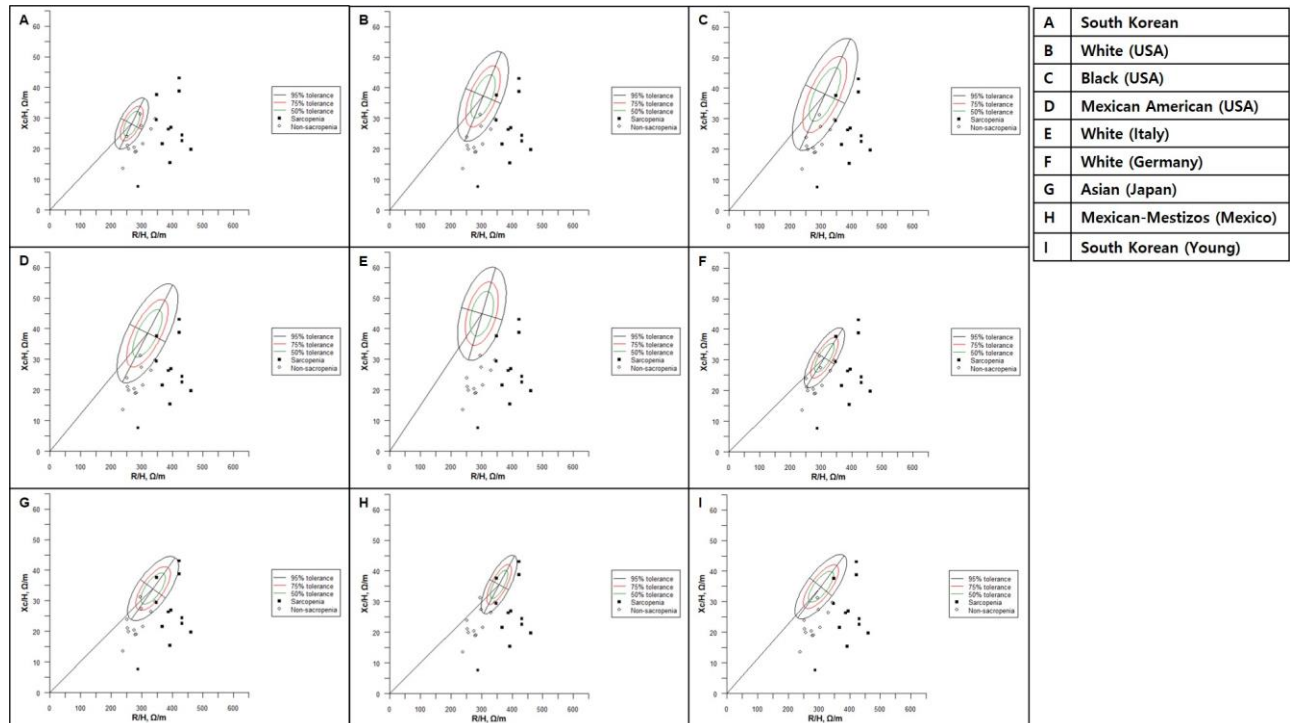


Figure 2. Individual vectors for men are depicted as dots based on sarcopenia classification within the tolerance ellipses (50%, 75%, and 95%) of each reference population (A: F2, B: F3, C: F4, D: F5, E: F6, F: F7, G: F8, H: F9, I: F10).

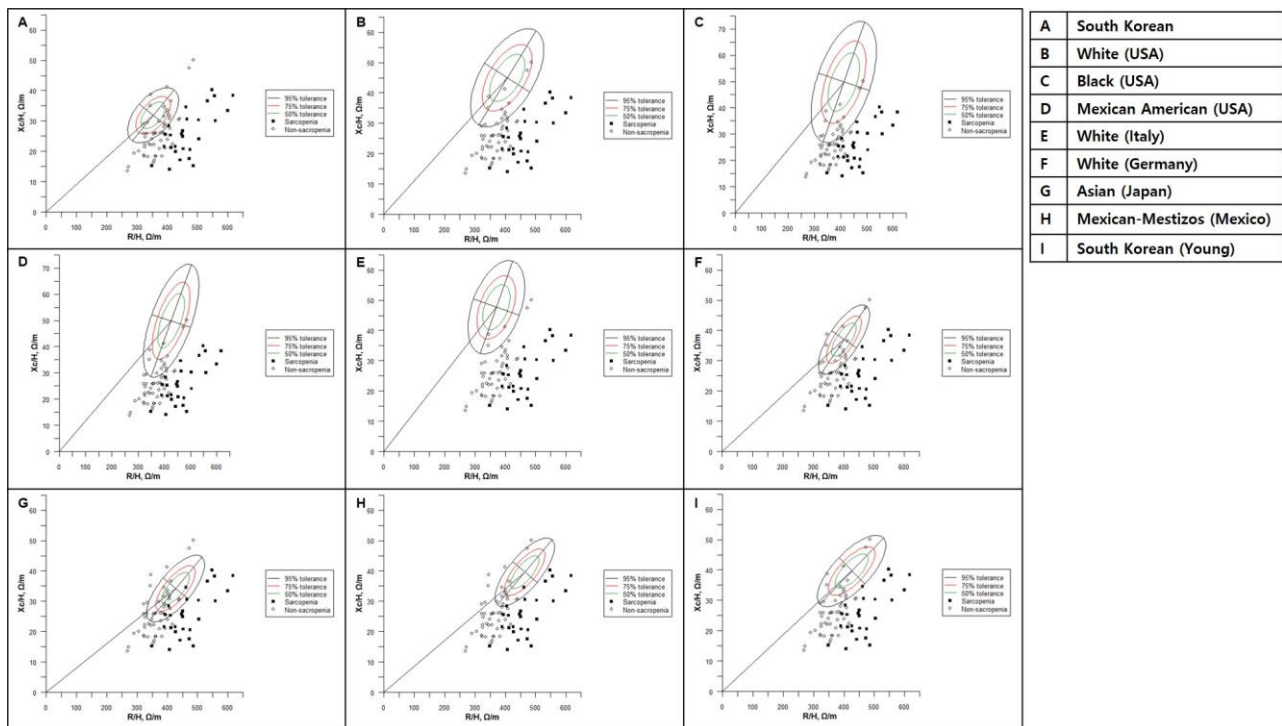


Figure 3. Individual vectors for women are depicted as dots based on sarcopenia classification within the tolerance ellipses (50%, 75%, and 95%) of each reference population (A: F2, B: F3, C: F4, D: F5, E: F6, F: F7, G: F8, H: F9, I: F10).

Low balance confidence as a risk factor for social frailty

Ga Yang Shim^{1*}, Myung Chul Yoo¹, Yunsoo Soh¹, Jinmann Chon¹, Chang Won Won^{1†}

Kyung Hee University Medical Center, Department of Rehabilitation Medicine¹, Kyung Hee University Medical Center, Department of Family Medicine²

Background

Social frailty is a type of frailty that causes disability, death, and other adverse outcomes, making it important to identify risk factors. The aim of this study was to investigate the cross-sectional and longitudinal associations between social frailty and low balance confidence in community-dwelling older adults.

Methods

Data were derived from the first and second wave of the Korea Aging Cohort Study (KFACS). Social frailty was defined based on 5-item questionnaire regarding general resources, social resources, social behavior, and the fulfillment of basic social needs. Balance confidence was assessed using the Activities-specific Balance Confidence Scale.

Results

The study included 2,937 participants, of whom 1355 (46.1%), 1004 (34.2%), and 578 (19.7%) participants were classified as robust, social pre-frailty, and social frailty, respectively. In the cross-sectional analysis, low balance confidence was associated with social pre-frail and frail after multivariate adjustment. In a longitudinal analysis, participants with low balance confidence at baseline had a 1.6 times higher risk of incidental social frailty for 2 years.

Conclusions

We established causal relationship between low balance confidence and social frailty. This suggests that social frailty can be prevented by strengthening interventions for community-dwelling older adults who had low balanced self-confidence.

Acknowledgment This research was supported by a grant from the Korea Health Technology R&D Project through the Korea Health Industry Development Institute, funded by the Ministry of Health and Welfare, Republic of Korea (grant number HI15C3153).

	Robust (n=1355)	Pre-frailty (n=1004)	Social frailty (n=578)	Total (n=2937)	P value
Age	75.7±3.9	76.2±4.0	76.4±3.8	76.0±3.9	<0.001
BMI	24.3±2.9	24.5±3.1	24.6±3.2	24.4±3.0	0.319
Sex					<0.001
Men	743 (54.8%)	417 (41.5%)	238 (41.2%)	1398 (47.6%)	
Women	612 (39.8%)	587 (58.5%)	340 (58.8%)	1539 (52.4%)	
Education, years	9.1±5.1	8.2±5.1	7.3±4.9	8.5±5.1	<0.001
No formal	224 (16.5%)	299 (22.8%)	167 (28.9%)	620 (21.1%)	<0.001
Elementary	365 (26.9%)	257 (25.6%)	157 (27.2%)	779 (26.5%)	
Middle, high	481 (35.5%)	362 (36.1%)	190 (32.9%)	1033 (35.2%)	
College and above	285 (21.0%)	155 (15.5%)	64 (11.1%)	504 (17.2%)	
Low economic status	30 (2.2%)	51 (5.1%)	79 (13.7%)	160 (5.4%)	<0.001
Comorbidities					
Hypertension	757 (55.9%)	599 (59.7%)	344 (59.5%)	1700 (57.9%)	0.261
Diabetes mellitus	306 (22.6%)	199 (19.8%)	134 (23.2%)	639 (21.8%)	0.179
Osteoarthritis	314 (23.2%)	264 (26.3%)	156 (27.0%)	734 (25.0%)	0.071
Depressive disorder	27 (2.0%)	26 (2.6%)	32 (5.5%)	85 (2.9%)	0.001
MMSE	25.7±3.3	25.5±2.9	25.0±3.6	25.5±3.3	0.001
K-IADL	12.4±3.3	11.6±2.9	11.4±2.9	11.9±3.1	<0.001
Physical activity (MET)	3554.2±3853 .8	3076.7±4040 .8	2892.6±4431 .9	3260.8±4045 .4	0.001
ABC score	82.3±18.3	78.0±20.2	74.6±20.4	79.3±19.6	<0.001
Fall history	262 (19.3%)	196 (19.5%)	138 (23.9%)	596 (20.3%)	0.055

Data are presented as mean ± standard deviation or N (%).

BMI, body mass index; MMSE, Mini-mental state examination; K-IAD: Korean instrumental activities of daily living; CCI, ABC, Activities-specific Balance Confidence

Table 1. Baseline characteristics of participants according to the social frailty status

	Model 1			Model 2		
	OR	95% CI	P value	OR	95% CI	P value
Robust	Reference			Reference		
Social pre-frail	1.777	1.474-2.142	<0.001	1.479	1.192-1.834	<0.001
Social frail	2.865	2.092-3.923	<0.001	2.136	1.460-3.127	<0.001

OR, odds ratio; CI confidence interval

Model 1: unadjusted

Model 2: adjusted for age, sex, economic status, education level, depressive disorder, MMSE, K-IADL, physical activity

Bold indicates statistical significance

Table 2. Cross-sectional analysis of association between low balance confidence and social frailty

	Model 1			Model 2		
	OR	95% CI	P value	OR	95% CI	P value
Robust	Reference			Reference		
Social pre-frail	1.768	1.376-2.272	<0.001	1.205	0.909-1.597	0.194
Social frail	2.874	2.077-3.977	<0.001	1.599	1.101-2.321	0.014

OR, odds ratio; CI confidence interval

Model 1: unadjusted

Model 2: adjusted for age, sex, economic status, education level, depressive disorder, MMSE, K-IADL, physical activity

Bold indicates statistical significance

Table 3. Longitudinal analysis of association between low balance confidence at baseline and incidence of social frailty

Assessing the SARC-F Tool for Sarcopenic Obesity Screening in Community-Dwelling Older Adults

Seongmin Choi^{1*}, Jong Ha Lee¹, Dong Hwan Yun¹, Jinmann Chon¹, Yunsoo Soh^{1†}, Myung Chul Yoo¹, Ga Yang Shim¹

Department of Physical Medicine & Rehabilitation, College of Medicine, Kyung Hee University¹

Background

Aging is typically associated with a loss of skeletal muscle mass and function, often coupled with an increase in body fat. This combination leads to the development of sarcopenic obesity (SO), a condition marked by the coexistence of sarcopenia and obesity. SO is a significant risk factor for adverse clinical outcomes, including functional impairment, metabolic diseases, and increased mortality. According to the ESPEN and EASO consensus, the diagnostic process for SO involves three steps: initial screening, diagnostic procedures for those with positive screening results, and staging for those diagnosed with SO. Validating efficient screening tools that can identify individuals needing further diagnostic evaluation is crucial. This cross-sectional study aimed to assess the validity of the SARC-F as a screening tool for SO.

Method

This cross-sectional study utilized data from the Korean Frailty and Aging Cohort Study, recruiting 2,020 community-dwelling older adults (1,016 men and 1,004 women) aged 70-84 years. SO was defined based on ESPEN and EASO criteria. Participants with either a high body mass index (BMI) or waist circumference (WC) and suspicion factors for sarcopenia (e.g., SARC-F, calf circumference (CC), SARC-CalF) were classified as positive screening. The performance of each screening tool, including sensitivity, specificity, positive predictive value (PPV), negative predictive value (NPV), and accuracy, was calculated using MedCalc Software Ltd.'s diagnostic test evaluation calculator (Version 20.210).

Results

Of the 2,020 participants, 1,016 (50.3%) were men, and 1,004 (49.7%) were women. Table 1 presents the performance analysis of each screening assessment. Positive screening, defined by SARC-F (≥ 4) combined with either high BMI or WC, showed low sensitivity (men, 5.68%; women, 17.82%), high specificity (men, 99.03%; women, 94.35%), and high NPV (men, 91.68%; women, 91.09%) for both sexes. Due to the low sensitivity of SARC-F (≥ 4) combined with high BMI or WC, we further analyzed the performance of different SARC-F cut-off values (Table 2). Lowering the cut-off values increased sensitivity but decreased specificity for both sexes.

Conclusion

SARC-F (≥ 4) combined with high BMI or WC is a screening tool for sarcopenic obesity that offers high specificity and high NPV, making it useful for efficiently ruling out sarcopenic obesity in clinical settings. When using SARC-F as a screening tool, considering various cut-off values other than a score of 4 may be beneficial.

Table 1. Screening Assessments Validated against Sarcopenic Obesity

		Sensitivity	Specificity	PPV	NPV	Accuracy
SARC-F (≥ 4) +	Men	5.68	99.03	35.83	91.68	90.91
high BMI or WC [†]	Women	17.82	94.35	26.17	91.09	86.62
CC ^{††} +	Men	34.09	59.48	7.42	90.45	57.27
high BMI or WC	Women	34.65	59.91	8.85	89.08	57.36
SARC-CalF (≥ 11) +	Men	13.64	95.04	20.56	92.12	88.04
high BMI or WC	Women	19.80	86.93	14.55	90.61	80.15

Abbreviations: PPV, positive predictive value; NPV, negative predictive value; BMI, body mass index; CC, calf circumferences; WC, waist circumferences; ref, reference.

Each values are expressed as percentage.

[†] High BMI, ≥ 25 kg/m²; high WC, ≥ 90 cm for men and ≥ 85 cm for women.

^{††} ref, < 34 cm for men and < 33 cm for women.

Table 2. Performance Analyses of Different SARC-F Cut-offs for Sarcopenic Obesity

		Sensitivity	Specificity	PPV	NPV	Accuracy
Sarc-F (≥ 6) +	Men	2.27	99.89	66.77	91.47	91.40
high BMI or WC [†]	Women	8.08	98.45	36.93	90.51	89.32
Sarc-F (≥ 5) +	Men	3.37	99.78	59.82	91.55	91.40
high BMI or WC	Women	15.49	97.79	44.01	91.15	89.47
Sarc-F (≥ 4) +	Men	5.68	99.03	35.83	91.68	90.91
high BMI or WC	Women	17.82	94.35	26.17	91.09	86.62
Sarc-F (≥ 3) +	Men	6.82	98.83	28.67	91.72	90.42
high BMI or WC	Women	24.75	90.03	21.81	91.42	83.44
Sarc-F (≥ 2) +	Men	15.91	95.26	24.23	92.24	88.36
high BMI or WC	Women	42.57	79.96	19.27	92.53	76.18
Sarc-F (≥ 1) +	Men	44.32	83.19	20.08	94.00	79.81
high BMI or WC	Women	59.41	61.02	14.62	93.05	60.86

Abbreviations: PPV, positive predictive value; NPV, negative predictive value.

Each values are expressed as percentage.

[†] High BMI, ≥ 25 kg/m²; high WC, ≥ 90 cm for men and ≥ 85 cm for women.

Differences in correlation of ultrasound parameters with muscle mass and strength in two settings

Ga Yang Shim^{1*}, Jong Bum Kim², Chang Won Won³, Jae-young Lim^{4†}

Kyung Hee University Medical Center, Department of Rehabilitation Medicine¹, TK Orthopedic Surgery Hospital, Department of Rehabilitation Medicine², Kyung Hee University Medical Center, Department of Family Medicine³, Seoul National University Bundang Hospital, Department of Rehabilitation Medicine⁴

Background

The prevalence of sarcopenia is expected to increase as society ages, and simple tools to assess muscle condition are needed. Ultrasound is a non-invasive and easy-to-use technique. However, muscle assessment using ultrasound depends on several factors, and its reliability and validity are still lacking. Therefore, we investigated and compared the correlation between ultrasound parameters and muscle mass and strength in two different settings.

Methods

Subjects were recruited from two different settings. Group A recruited 180 subjects in their 20s to 50s for research purposes, and Group B was derived from a retrospective chart review of with suspected sarcopenia aged 60 years or older who completed ultrasound muscle evaluation in a clinical setting. Both groups acquired longitudinal and transverse images of the rectus femoris (RF), and image analysis was performed using image J for group A and the on-screen calipers for group B to measure muscle thickness (MT), echo intensity (EI), and pennation angle (PA). Muscle mass and strength was assessed by bioelectrical impedance analysis (BIA), and grip strength and knee extensor strength, respectively.

Results

Finally, 180 subjects (age 38.6 ± 12.6) in Group A and 119 subjects (age 79.3 ± 8.6) in Setting B were included. There were significant differences in age, skeletal muscle mass index (SMI), Leg SMI, grip strength, RF MT, PA, and EI between two groups (Table 1). SMI and leg SMI were moderately correlated with RF MT in both Groups, except correlation between leg SMI and RF MT in Group B. Among the ultrasound qualitative muscle parameters, only RF EI had a statistically significant negative correlation with muscle strength in Group A (Table 2). RF MT showed a statistically stronger correlation with leg SMI measured by BIA in Group A than in Group B (Figure 1).

Conclusion

Ultrasound muscle parameters showed a moderate correlation with muscle mass and strength in Group A and a weak to moderate correlation with only muscle mass in Group B. Additionally, correlation coefficients in younger subjects for research purposes were statistically significantly greater than those in older subjects in clinical settings. These suggest that operator-dependent ultrasound has greater variability in the elderly with poor muscle condition. Therefore, further research on standard measurement and analysis methods is required to use of ultrasound for sarcopenia diagnosis in clinical settings.

Acknowledgment This research was funded by the Korean government (the Ministry of Science and ICT, Ministry of Trade, Industry and Energy, Ministry of Health & Welfare, and Ministry of Food and Drug Safety) (No. 1711138173, KMDF_PR_20200901_0101) and funded by the Korean Geriatrics Society.

	Group A (N=180)	Group B (N=119)	P value
Age, yr	38.6±10.9	79.3±8.6	<0.001
Sex			0.143
Men	91 (50.6)	51 (42.9)	
Women	89 (49.4)	68 (57.1)	
Height, cm ²	167.9±9.1	158.9±9.0	<0.001
Weight, kg	64.1±12.7	57.5±10.3	<0.001
BMI, kg/m ²	22.6±3.1	22.7±3.1	0.674
Grip strength, kg	34.0±10.2	18.3±6.8*	<0.001
Knee extensor strength	44.1±17.5 (kg)	45.9±20.7 (Nm) [†]	-
BIA parameters			
SMI, kg/m ²	7.2±1.3	6.1±1.1	<0.001
Leg SMI, kg/m ²	5.5±0.8	4.7±0.8	<0.001
Ultrasound parameters			
RF MT (L), cm	1.9±0.4	1.2±0.4	<0.001
RF MT (T), cm	1.9±0.4	1.3±0.4	<0.001
RF EI	59.4±12.0	142.9±33.1	<0.001
RF PA, °	12.8±3.5	8.9±2.7	<0.001

Abbreviations: BMI, body mass index; BIA, bioelectrical impedance analysis; SMI, skeletal muscle mass index; RF, rectus femoris; MT(L), muscle thickness in longitudinal image; MT(T), muscle thickness in transverse image; EI, echointensity; PA, pennation angle

* 82 subjects had grip strength measured

† 53 subjects had isokinetic knee extensor strength measured

Table 1. Baseline characteristics of subjects

	RF MT (L)		RF MT (T)	
	Group A	Group B	Group A	Group B
SMI	0.549**	0.414**	0.554**	0.416**
Leg SMI	0.613**	0.368**	0.521**	0.354**
	RF EI		RF PA	
Grip strength	-0.499**	-0.084	0.060	0.205
Knee extensor strength	-0.456**	-0.125	0.141	0.076

**p<0.01

Abbreviations: RF, rectus femoris; MT(L), muscle thickness in longitudinal image; MT(T), muscle thickness in transverse image; EI, echointensity; PA, pennation angle; SMI, skeletal muscle mass index

Table 2. Correlation coefficients between ultrasound muscle parameters and muscle mass and strength

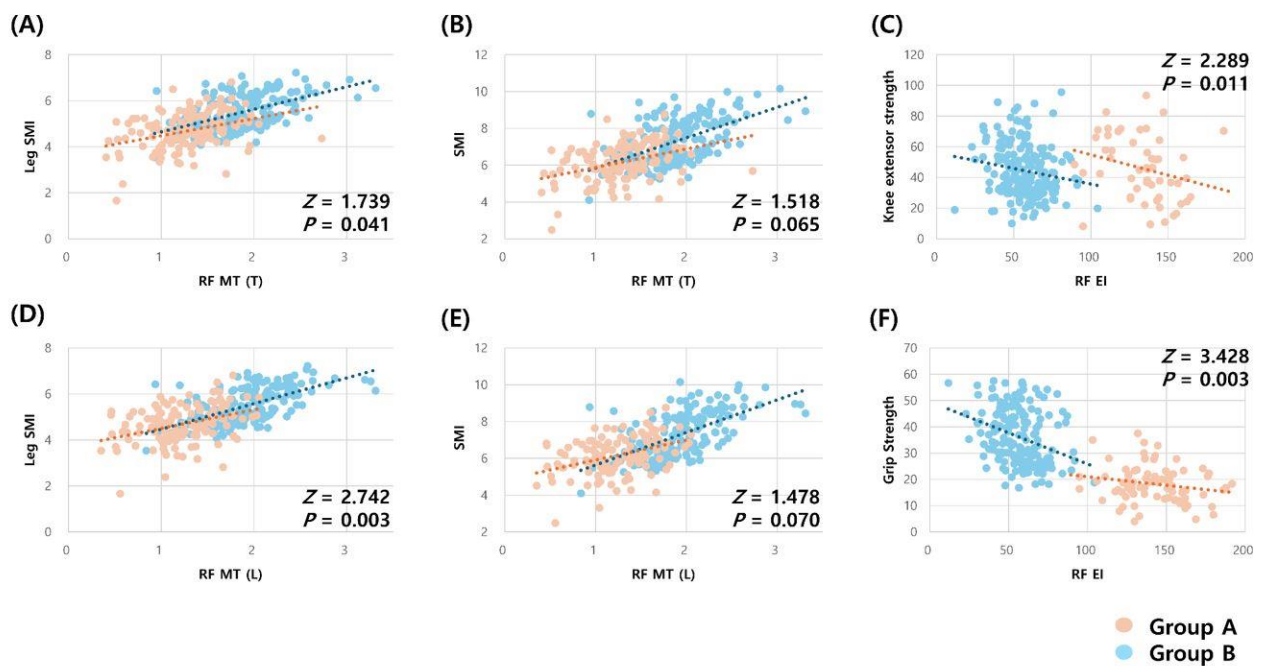


Figure 1. Scatter plots showing correlations of ultrasound muscle parameters with muscle mass and strength, and comparison of correlation coefficients between Groups

The Association between Inflammation and Sarcopenic Obesity

Seongmin Choi^{1*}, Yunsoo Soh^{1†}, Jong Ha Lee¹, Dong Hwan Yun¹, Jinmann Chon¹, Myung Chul Yoo¹, Ga Yang Shim¹

Department of Physical Medicine & Rehabilitation, College of Medicine, Kyung Hee University¹

Background

Sarcopenic obesity (SO), the simultaneous presence of sarcopenia and obesity, significantly impacts the health of the elderly. Sarcopenia is the loss of muscle mass and function, while obesity is characterized by excessive body fat. Circulating pro-inflammatory cytokines, including tumor necrosis factor, interleukin-1, and interleukin-6 are increased, creating a state of low-grade chronic inflammation. All these changes promote fat mass gain and loss of muscle mass. We hypothesized that inflammation may play a role in the development of SO. In this study, we aimed to investigate the negative impacts of inflammation on SO.

Method

This study involved older adults aged 70-84 years from the Korean Frailty and Aging Cohort Study (KFACS). We included 2,071 (men 1,030; women 1,041) participants in this cross-sectional analysis (Figure 1). SO was defined according to the ESPEN and EASO guidelines, with body composition assessed using dual-energy X-ray absorptiometry (DXA). High-sensitivity C-reactive protein (hsCRP), an inflammatory marker that predicts incident stroke and myocardial infarction, was used to determine the state of inflammation. Inflammation was defined as an hsCRP level > 3mg/L.

Results

The baseline characteristics of the participants are shown in table 1. The SO group had a higher hsCRP in women. In a logistic regression analyses, high hsCRP group had a higher risk of SO (OR, 2.65; 95% CI, 1.49-4.58), low HGS (OR, 2.21; 95% CI, 1.36-3.59) in women after adjusting for confounding factors (Table 2). However, in men, high hsCRP was not significantly associated with SO.

Conclusion

In this study, we found that SO was associated with high hsCRP levels in women. Chronic low-grade inflammation was associated with a higher risk of SO, mainly because of its association with muscle strength, especially in women.

Association between Waist Circumference and All-Cause Mortality in Parkinson's disease

Jee Hyun Suh^{1*}, Seok-Jae Heo², Yong Wook Kim³, Sang Chul Lee³, Yu Ji Han¹, Kun Wook Lee³, Seo Yeon Yoon^{3†}

Department of Rehabilitation Medicine, Ewha Womans University Mokdong Hospital¹, Department of Biostatistics and Computing, Yonsei University Graduate School², Department and Research Institute of Rehabilitation Medicine, Severance Hospital³

Introduction

Despite many previous studies on the association between metabolic syndrome and Parkinson disease (PD), only few studies have investigated the association between WC and PD. This study aimed to investigate the association between WC and all-cause mortality in patients with PD.

Methods

Among the whole nationwide population data from Korea National Health Insurance Service, newly diagnosed PD (ICD-10 code: G20), between 2008 and 2017, were selected. All-cause mortality was the primary outcome. Anthropometric data, including WC and body mass index (BMI) were obtained from health screening data. The Cox proportional hazards model was used to assess mortality risk according to WC.

Results

Among the 22,118 patients with PD, 9,179 (41.50%) died during the 10-year follow-up period. WCs

Conclusion

Central obesity is a significant risk factor for mortality in patients with PD after adjusting for BMI. Our results suggest that management of WC is crucial for PD patients and that BMI should be considered in the WC management plan for mortality in PD.

Table 1. Characteristics of Participants

Variables	Waist circumference					p-value
	M <70 F < 65	M 70-80 F 65-75	M 80-90 F 75-85	M 90-100 F 85-95	M >100 F >95	
N (%)	590 (2.7)	4,569 (20.7)	9,819 (44.4)	5,834 (26.4)	1,306 (5.9)	
Age (years)	68.70 ± 11.42	68.17 ± 10.37	68.84 ± 9.00	69.66 ± 8.21	69.98 ± 8.20	<0.001
Sex						<0.001
Male	261 (44.2)	2,013 (44.1)	4,447 (45.3)	2,353 (40.3)	377 (28.9)	
Female	329 (55.8)	2,556 (55.9)	5,372 (54.7)	3,481 (59.7)	929 (71.1)	
Low income level (lower 25%)	110 (18.6)	844 (18.5)	1,650 (16.8)	957 (16.4)	214 (16.4)	0.038
Residential area (urban)	230 (39.0)	1,811 (39.6)	3,878 (39.5)	2,231 (38.2)	484 (37.1)	0.262
Insurance type						<0.001
National health insurance	568 (96.3)	4,456 (97.5)	9,661 (98.4)	5,729 (98.2)	1,274 (97.5)	
Medical aid	22 (3.7)	113 (2.5)	158 (1.6)	105 (1.8)	32 (2.5)	
Charlson comorbidity index	2.73 ± 2.21	2.67 ± 2.20	2.99 ± 2.34	3.28 ± 2.38	3.69 ± 2.44	<0.001
†Hypertension	279 (47.3)	2,299 (50.3)	5,953 (60.6)	4,152 (71.2)	1,025 (78.5)	<0.001
†Dyslipidemia	62 (10.5)	365 (8.0)	734 (7.5)	472 (8.1)	102 (7.8)	0.082
†Pneumonia	202 (34.2)	1,774 (38.8)	4,559 (46.4)	3,105 (53.2)	755 (57.8)	<0.001
†Depression	174 (29.5)	1,173 (25.7)	2,617 (26.7)	1,627 (27.9)	398 (30.5)	0.002
Current smoker	46 (7.8)	345 (7.6)	697 (7.1)	333 (5.7)	67 (5.1)	<0.001
Heavy alcohol drinker	8 (1.4)	108 (2.4)	237 (2.4)	165 (2.8)	23 (1.8)	0.055
Regular exercise	125 (21.2)	1,324 (29.0)	2,902 (29.6)	1,657 (28.4)	282 (21.6)	<0.001
Body mass index (kg/m ²)	18.59 ± 2.40	20.92 ± 2.09	23.46 ± 2.19	25.97 ± 2.39	28.90 ± 3.01	<0.001
Systolic blood pressure (mmHg)	120.09 ± 16.36	123.61 ± 16.24	126.86 ± 15.92	129.25 ± 15.81	131.18 ± 16.16	<0.001
Diastolic blood pressure (mmHg)	74.45 ± 10.26	75.32 ± 10.14	76.93 ± 10.00	77.90 ± 10.10	78.75 ± 10.37	<0.001
Laboratory findings						
Total cholesterol (mg/dL)	176.69 ± 36.16	187.03 ± 38.75	190.55 ± 43.29	192.66 ± 50.29	197.47 ± 83.02	<0.001
Triglyceride (mg/dL)	94.15 ± 44.21	111.67 ± 63.51	131.99 ± 79.02	147.89 ± 82.26	160.57 ± 96.45	<0.001
LDL (mg/dL)	101.18 ± 31.30	111.47 ± 50.75	113.45 ± 49.09	114.78 ± 64.44	116.77 ± 86.03	<0.001
HDL (mg/dL)	56.50 ± 15.62	55.23 ± 25.02	52.11 ± 24.02	50.68 ± 23.23	50.89 ± 27.39	<0.001
Fasting glucose	97.49 ± 24.15	101.60 ± 26.44	104.64 ± 29.53	109.18 ± 33.02	113.80 ± 37.46	<0.001

Values are presented as mean ± SD or number (%).

HDL, high-density lipoprotein; LDL, low-density lipoprotein

†Other co-morbidities not included in Charlson comorbidity index

Table 1. Characteristics of Participants

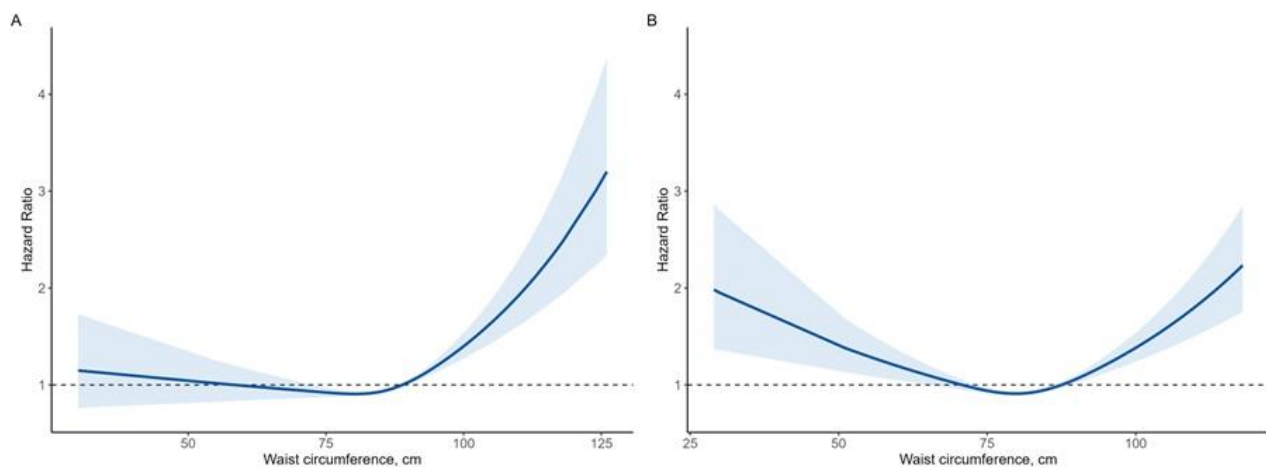


Figure 1. Restricted cubic spline plots of the association between waist circumference (WC) and all-cause mortality in individuals with Parkinson disease (PD). (A) Male and (B) Female

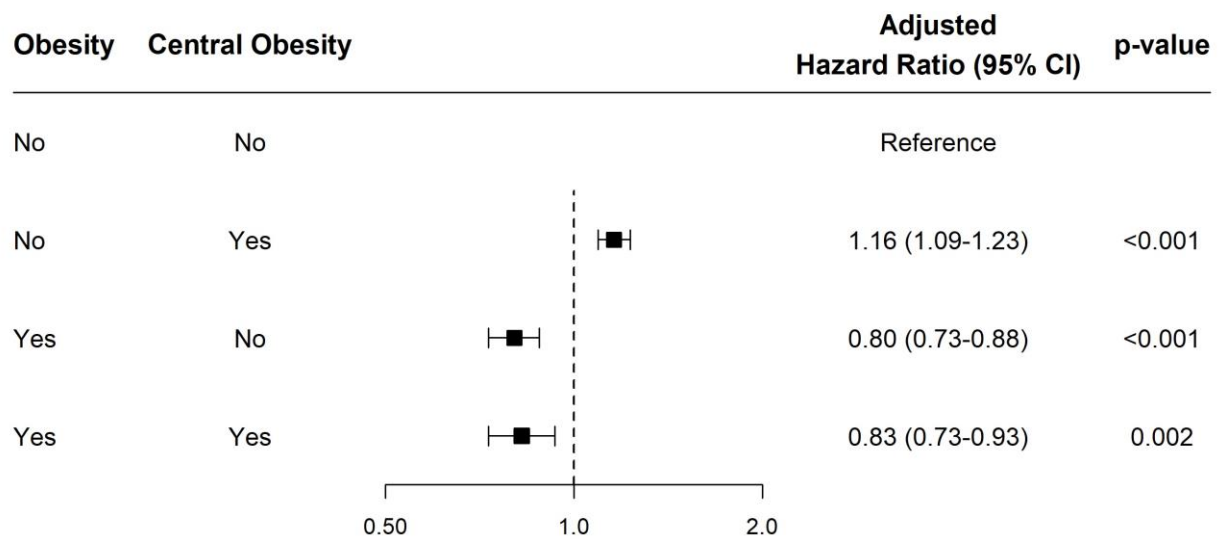


Figure 2. Adjusted hazard ratios with 95% confidence intervals for all-cause mortality in individuals with Parkinson disease (PD) according to obesity and central obesity

Effect of tongue-strengthening home exercise in older adults with sarcopenic dysphagia

Tae-Hyung Yoon¹, Morishita Motoyoshi², Nami Han^{3**}, Ji-Su Park^{4†}

Department of Occupational Therapy, Dongseo University¹, Department of Physical Therapy, Reiwa Health Sciences University², Department of Rehabilitation Medicine, Inje University Busan Paik Hospital³, Research Institute for Korean Medicine, Pusan National University⁴

Objective

This study aimed to investigate the effects of a portable tongue-strengthening home exercise (TShE) tool on swallowing-related oropharyngeal muscles in community-dwelling older adults with sarcopenic dysphagia.

Methods

Forty community-dwelling older adults with sarcopenic dysphagia were enrolled in the study. The participants were randomly assigned to the experimental and control groups. (Fig 1) Maximum tongue strength (1-Repetition Maximum) was measured in the experimental group using the Iowa Oral Performance Instrument, and TShE was performed using a portable tool with an intensity corresponding to approximately 70–80% of the range based on the 1-Repetition Maximum value (30 times/day, 5 days/week, for 8 weeks). The control group did not perform any tongue exercises. The primary outcome measures were tongue strength and thickness. The secondary outcome measure was suprahyoid muscle strength (digastric and mylohyoid muscles).

Results

The experimental group showed significantly greater increases in suprahyoid muscle (mylohyoid and digastric) thickness ($p=0.01$ and 0.011 , $d=1.0$ and 0.55), as well as tongue strength and thickness (p

Conclusion

This study confirmed that TShE using a portable tool is effective in increasing swallowing-related oropharyngeal muscle activity in older adults with sarcopenic dysphagia. Therefore, TShE is recommended as an inexpensive, safe, and easy-to-use therapy for sarcopenic dysphagia in older adults.

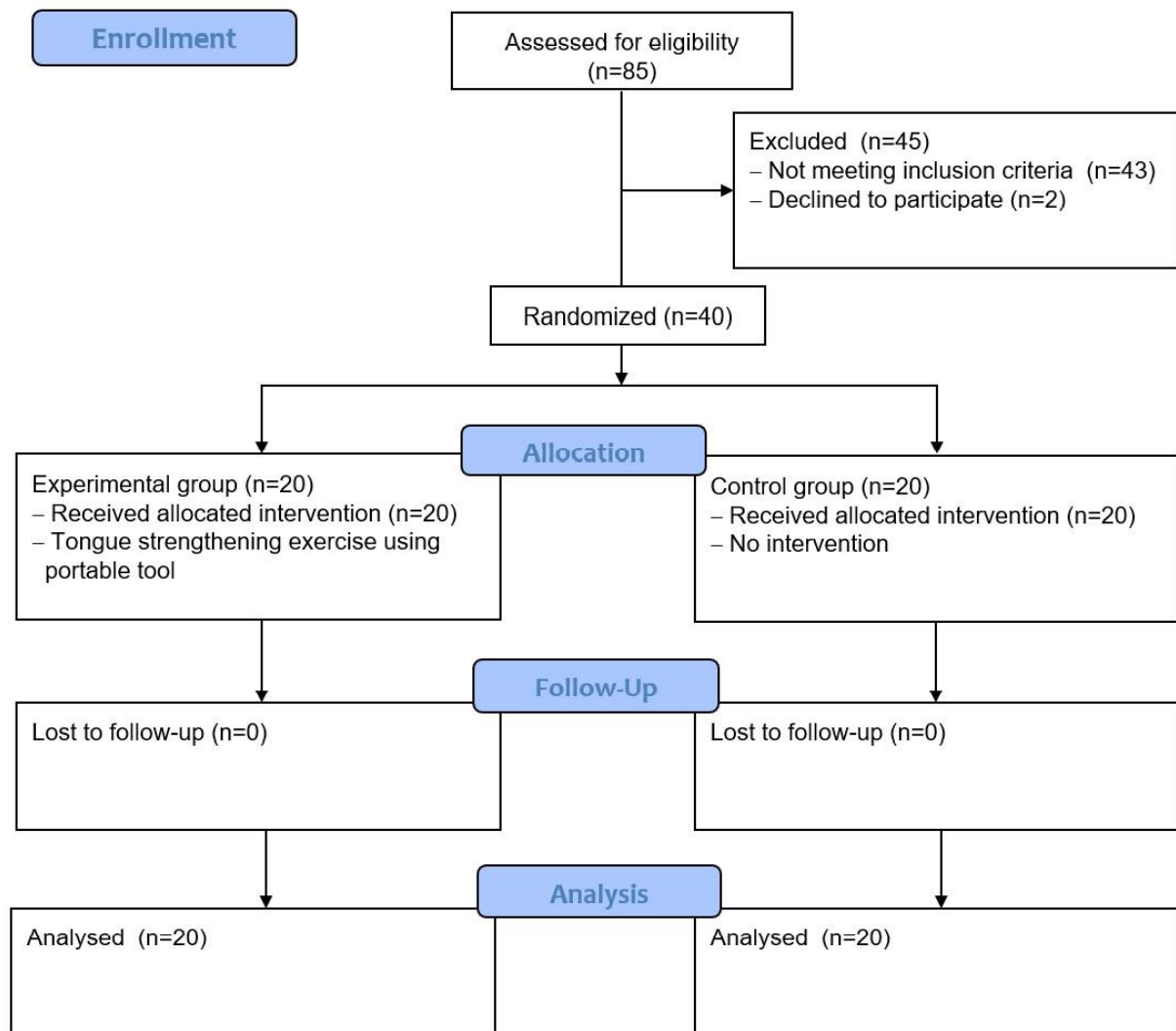


Fig 1. Consolidated Standards of Reporting Trials (CONSORT)

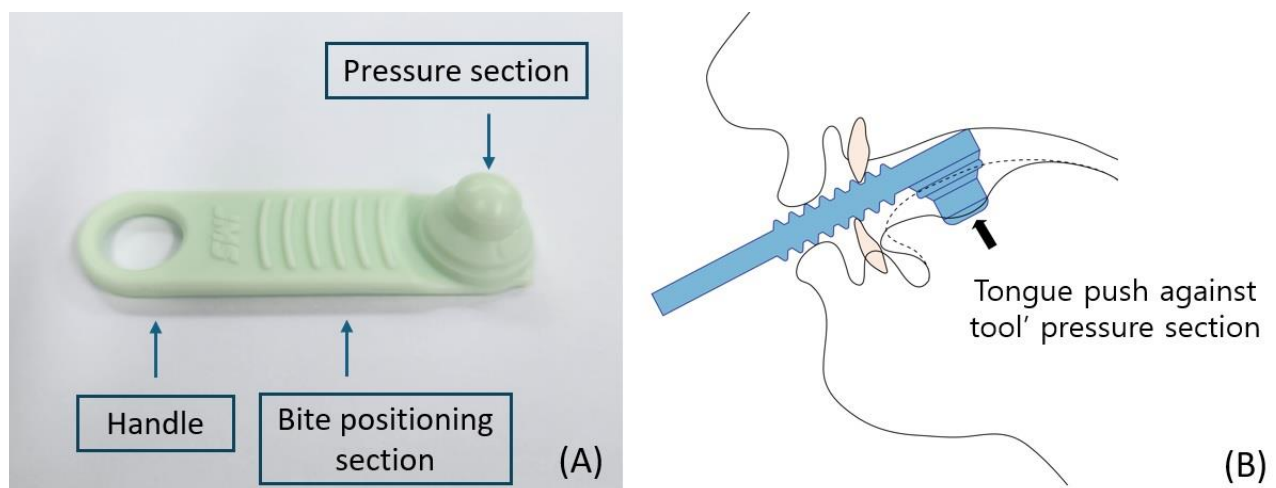


Fig 2. (A) Picture of the used exercise tool. (B) Illustration showing the principle of tool exercise instruction.

Table 1. Change of tongue muscles in parameters pre and post intervention

	Experimental group				Control group				Intergroup <i>p</i> -values
	Pre	Post	change	<i>p</i> -value	Pre	Post	change	<i>p</i> -value	
Tongue strength (unit: kpa)	17.20 (1.60)	22.55 (2.25)	△ 5.35 (1.59) [†]	<.000**	17.35 (1.89)	17.70 (2.15)	△ 0.35 (0.98)	.130	.000 [†]
Tongue thickness (unit: mm)	38.01 (3.12)	39.95 (2.92)	△ 1.95 (1.09) [†]	<.000**	37.51 (2.80)	37.75 (3.19)	△ 0.25 (0.11)	.330	.029 [†]
Mylohyoid muscle (unit: mm)	0.65 (0.05)	0.72 (0.06)	△ 0.07 (0.04) [†]	<.000**	0.66 (0.06)	0.66 (0.07)	△ 0.00 (0.02)	.160	.010 [†]
Digastric muscle (unit: mm)	5.79 (0.44)	6.11 (0.50)	△ 0.31 (0.16) [†]	<.000**	5.64 (0.45)	5.69 (0.48)	△ 0.04 (0.03)	.176	.011 [†]

The values are mean (standard deviation)

p* < 0.05 by Wilcoxon test. *p* < 0.01 by Wilcoxon test. [†]*p* < 0.05 by Mann-Whitney U test.

Table 1. Changes of tongue muscles in parameters pre and post intervention

Predicting functional outcomes after total knee arthroplasty using machine learning algorithms

Jin Taek Lee^{1*}, Bo Ryun Kim^{1†}, Young Mo Kim¹, Seoung Ho Choi², Jun Hwan Choi³, Hye Won Lee⁴

Korea University Anam Hospital, Department of Rehabilitation Medicine¹, Hansung University, College of Liberal Arts Faculty of Basic Liberal Art², Jeju National University Hospital, Department of Rehabilitation Medicine³, Ewha Womans University, Department of Medicine, College of Medicine⁴

Objective

This study aims to develop a predictive model based on preoperative variables to predict functional outcomes three months after total knee arthroplasty (TKA) using machine learning algorithms.

Methods

This retrospective cohort study involved 313 patients who underwent TKA between September 2013 and January 2022.

The analyzed data consisted of demographic & anthropometric variables, clinical characteristics, and functional assessments (Western Ontario and McMaster Universities Osteoarthritis Index [WOMAC] total score, Visual Analogue Scale [VAS] score, EQ-5D total score, Timed Up and Go [TUG], 6-minute walking test [6MWT], stair climbing test [SCT] ascending and descending, peak torque (PT) of knee extensor strength and knee flexor strength. These measurements were taken both preoperatively and 3 months postoperatively.

Five machine learning algorithms were used to predict postoperative functional outcomes including Linear Regression, Poisson Regressor, Tweedie Regressor, Passive Aggressive Regressor, and ARD Regression. External validation was performed using new external data from 7 individuals.

Feature importance was assessed using bar plots to visualize the contribution of each variable to the model's predictions. SHAP (SHapley Additive exPlanations) values were used to interpret model predictions and understand the impact of each feature on the outcome. The 10 most important variables analyzed in each model's SHAP and feature importance, as well as the variables that showed statistically significant results in the multivariate analysis, were comprehensively considered and selected.

Results

The average age of a total of 313 patients was 71.80 (\pm 5.91) years and 49 (15.65% of the total) patients were males (Table 1).

In the analysis conducted to identify key preoperative factors influencing postoperative outcomes, different machine learning models demonstrated the best performance for each factor.

Significantly important variables for predicting postoperative functional outcomes were TUG, SCT ascending and descending, and PT of knee flexors and knee extensors. Detailed findings are listed in Table 2.

Overall, the predictive model incorporating these variables demonstrated strong explanatory power in predicting postoperative functional recovery.

Conclusion

The machine learning models incorporating preoperative variables demonstrated strong explanatory power in predicting postoperative functional recovery after TKA.

Therefore, measuring these key preoperative variables, particularly clinical characteristics and functional assessments, would be crucial for predicting postoperative prognosis and recovery.

Variables	Values
Age (years)	71.81 ± 5.91
Sex, males/females (number)	49(15.7%) / 264(84.3%)
Height	153 ± 7.13
Weight	62.73 ± 9.62
Body mass index (kg/m ²)	26.53 ± 3.43
Clinical characteristics (number)	
KL grade 2 / 3 / 4	1(0.3%) / 51(16.3%) / 261(83.4%)
TKA surgery history	168 (53.7%)
Stroke	5 (1.6%)
Heart disease	17 (5.4%)
Hypertension	205 (65.5%)
Diabetes	55 (17.6%)
Hyperlipidemia	80 (25.6%)

Table 1. Demographic and clinical characteristics of the patients (N=313)

Postoperative outcome	Preoperative variables
WOMAC Total	WOMAC total, SCT ascend, PT of knee flexor
TUG	TUG
6MWT	WOMAC total, TUG, SCT ascend, SCT descend
SCT ascend	TUG, SCT ascend, PT of knee extensor
SCT descend	SCT descend, PT of knee extensor
PT of knee extensor	SCT descend, PT of knee extensor
PT of knee flexor	SCT descend, PT of knee flexor

Table 2. Main preoperative variables predicting postoperative outcomes

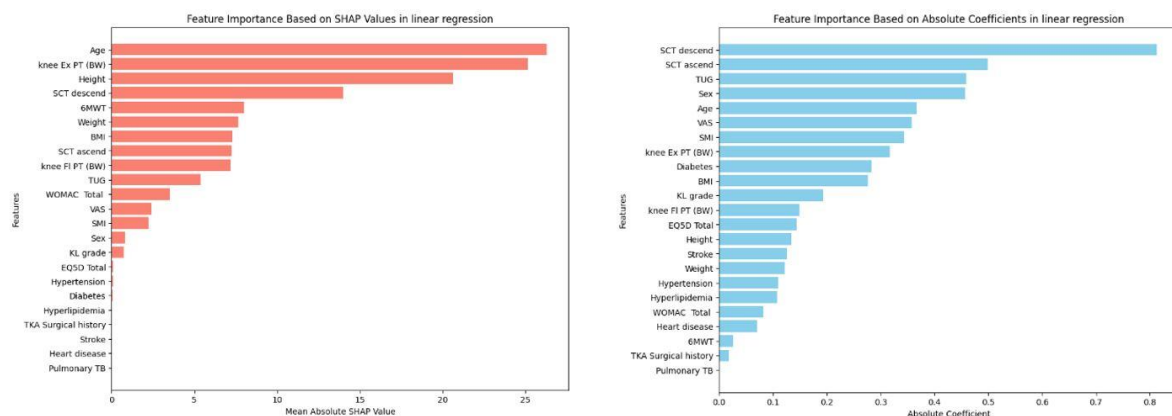


Figure 1. The 10 most important variables analyzed in each model's SHAP and feature importance

Proposing Cut-Off Values for Respiratory Muscle Sarcopenia in Elderly women: A Single Hospital Study

Tae Sung Park^{1,2*}, Jun Yong Park^{2,3}, Jun Won Lee^{2,3}, Sang Hun Kim^{2,3,4}, Myung Hun Jang^{2,3,4}, Byeong Ju Lee^{2,3,4}, Myung Jun Shin^{1,2,3,4†}

Department of Convergence Medical Institute of Technology, Pusan National University Hospital¹, Department of Biomedical Research Institute, Pusan National University Hospital², Department of Rehabilitation Medicine, Pusan National University Hospital³, Department of Rehabilitation Medicine, Pusan National University School of Medicine⁴

Sarcopenia significantly impacts older adults and patients with chronic conditions by reducing muscle mass and strength. Recent studies introduce `respiratory sarcopenia,` where deterioration of respiratory muscles leads to compromised lung function and adverse health outcomes. This study examines the link between respiratory muscle strength, measured by maximal inspiratory pressure (MIP) and maximal expiratory pressure (MEP), and sarcopenia in elderly Korean women. It aims to establish cut-off values for MIP and MEP in sarcopenia screening, highlighting the importance of early detection and management of respiratory muscle health to enhance overall well-being and prevent the progression of sarcopenia.

This study retrospectively analyzed data from women patients over 65 who had their respiratory muscle strength, hand grip strength (HGS), and skeletal muscle index (SMI) measured at Hospital, between December 2016 and June 2022. Out of 125 patients who met the inclusion criteria, those with cardiac or respiratory diseases were primarily included, while those with ambulation difficulties were excluded. For statistical analysis, the study used SPSS Statistics version 19.0. It compared functions between patients with and without sarcopenia using independent t-tests and evaluated the sensitivity and specificity of MIP, MEP, and other tests using receiver operating characteristic (ROC) curves. The area under the ROC curve (AUC) and 95% confidence intervals were calculated to determine the tests' effectiveness, with an AUC of 0.7 or higher considered significant. Optimal cut-off values for identifying sarcopenia were identified using the Euclidean method, and a significance level was set at $\alpha = .05$.

In a study involving 125 women participants over 65, 27 were diagnosed with sarcopenia based on criteria from the Asian Working Group, specifically having HGS below 18kg and muscle mass under 5.7 kg/m² (Table 1). Screening effectiveness was evaluated using the area under the ROC curve AUC. The AUC results showed that HGS and SMI are highly effective for sarcopenia screening, with AUCs of 0.86 and 0.92, respectively. MIP also proved significant with an AUC of 0.76, indicating its potential in respiratory muscle strength assessment for sarcopenia screening. Optimal cut-off points were identified to balance sensitivity and specificity effectively (Table 2) (Figure 1).

This study highlights the effectiveness of including MIP with traditional sarcopenia screening methods like HGS and SMI for older women patients. It validates the use of HGS and SMI through significant AUC values and introduces MIP as a valuable addition to improve sarcopenia detection accuracy. By establishing optimal cut-off points for these metrics, which effectively balance sensitivity and specificity, the study suggests a more comprehensive approach to sarcopenia diagnosis. This could enhance management and intervention strategies for the aging population.

Table 1. General characteristics of the elderly women

Variable	Non-sarcopenic(n=98)	Sarcopenic(n=27)	p value
Age (years)	71.99±5.01	76.37±5.03	0.000*
Height (cm)	153.94±5.24	151.24±5.21	0.019*
Weight (kg)	56.91±8.04	47.91±9.19	0.000*
MIP (cmH ₂ O)	52.24±20.03	35.26±13.74	0.000*
MEP (cmH ₂ O)	70.83±20.96	60.07±24.42	0.025*
HGS (kg)	20.32±4.49	14.52±3.27	0.000*
SMI (kg/m ²)	6.22±0.79	4.93±0.48	0.000*

Mean±SD, * = p<0.05, MIP; maximal inspiratory pressure, MEP; maximal expiratory pressure, HGS; hand grip strength, SMI; skeletal muscle mass index

Table 1. General characteristics of the elderly women

Table 2. Cut-off points, AUC, sensitivity, specificity of muscle strength tests to screening sarcopenia.

	AUC (95%CI)	Cut-off values	Sensitivity	Specificity
MIP (cmH ₂ O)	0.76 (0.66-0.85)	40.50	0.67	0.65
MEP (cmH ₂ O)	0.63 (0.49-0.76)	63.50	0.57	0.58
HGS (kg)	0.86 (0.79-0.92)	17.17	0.79	0.73
SMI (kg/m ²)	0.92 (0.88-0.97)	5.35	0.86	0.85

AUC; area under the ROC curve, MIP; maximal inspiratory pressure, MEP; maximal expiratory pressure, HGS; hand grip strength, SMI; skeletal muscle mass index

Table 2. Cut-off points, AUC, sensitivity, specificity of muscle strength tests to screening sarcopenia.

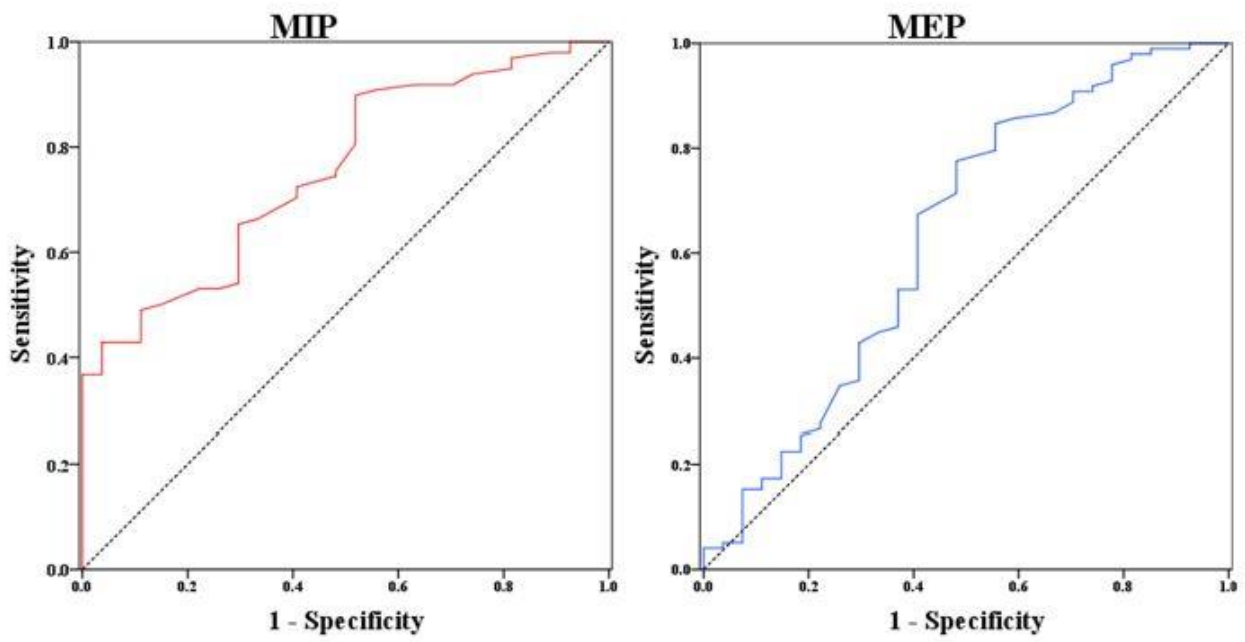


Figure 1. ROC curves for MIP, MEP. ROC curves for MIP [AUC=0.76 (0.66-0.85)], MEP [AUC=0.63 (0.49-0.76)]

Figure 1. ROC curves for MIP, MEP. ROC curves for MIP [AUC=0.76 (0.66-0.85)], MEP [AUC=0.63 (0.49-0.76)]

The Relationship Between Vitamin D Deficiency and Sarcopenic Obesity in Elderly Koreans

Seongmin Choi^{1*}, Jong Ha Lee¹, Dong Hwan Yun¹, Jinmann Chon¹, Myung Chul Yoo¹, Ga Yang Shim¹, Yunsoo Soh^{1†}

Department of Physical Medicine & Rehabilitation,, College of Medicine, Kyung Hee University¹

Background

Sarcopenic obesity (SO) is a growing concern among the elderly, characterized by the loss of muscle mass and function combined with excess body fat. This condition leads to adverse health outcomes, including increased risk of falls, disability, and mortality. Identifying modifiable risk factors is crucial for developing effective prevention and intervention strategies. Vitamin D levels typically decrease due to reduced outdoor activities and a decline in the skin's capacity to produce vitamin D precursors as individuals age. Vitamin D deficiency was defined as having 25-hydroxy vitamin D levels below 20 ng/mL, may be one of modifiable risk factor associated with SO. In this study, we aimed to investigate the association between Vitamin D deficiency and SO.

Method

The study involved elderly individuals between 70 and 84 years residing in the community, who had participated in the Korean Frailty and Aging Cohort Study (KFACS). 2,071 (men 1,030; women 1,041) participants were included in the cross-sectional analysis (Figure 1). We used the ESPEN and EASO guidelines for definition of SO. Vitamin D deficiency was defined as 25-hydroxy vitamin D level < 20ng/ml. Unadjusted and fully adjusted logistic regression models were performed.

Results

The level of Vitamin D was lower in the SO group compared to the non-SO group among men. Vitamin D deficiency group had a higher risk of SO in men after adjusting for confounding factors (OR, 2.33; 95% CI, 1.45-3.76). Additionally, Vitamin D deficiency group had high fat mass (OR, 1.32; 95% CI, 1.01-1.75), abnormal 5 TSTS (OR, 2.19; 95% CI, 1.04-4.59), and low HGS (OR, 1.46; 95% CI, 1.08-1.98) in the unadjusted model (Table 1). However, the results were not statistically significant after adjusting for confounding factors.

Conclusion

Vitamin D deficiency is significantly associated with a higher prevalence of sarcopenic obesity among elderly Korean men, suggesting that maintaining adequate vitamin D levels might be an important factor in preventing sarcopenic obesity among elderly Korean men.

Table 1. Cross-sectional Association of Vitamin D Deficiency and SO

	Model 1		Model 2	
	Men OR (95% CI)	Women OR (95% CI)	Men OR (95% CI)	Women OR (95% CI)
SO	2.25 (1.46–3.48)*	1.25 (0.84–1.86)	2.33 (1.45–3.76)*	1.36 (0.89–2.08)
High fat mass	1.32 (1.01–1.75)*	1.16 (0.91–1.48)	1.34 (0.99–1.81)	1.09 (0.84–1.41)
Low muscle mass	1.05 (0.81–1.37)	0.86 (0.67–1.10)	1.05 (0.80–1.38)	0.81 (0.62–1.05)
Abnormal 5 TSTS	2.19 (1.04–4.59)*	1.05 (0.69–1.61)	1.96 (0.89–4.30)	1.06 (0.68–1.65)
Low HGS	1.46 (1.08–1.98)*	1.13 (0.83–1.53)	1.09 (0.84–1.41)	1.23 (0.88–1.72)

Model 1: unadjusted; Model 2: adjusted for age, high physical activity, depression, high HOMA-IR, high hsCRP, and low FT, hypertension, dyslipidemia, height, cerebrovascular accident, osteoarthritis, diabetes mellitus, osteoporosis, heart disease, liver disease, weight loss, pulmonary disease, alcohol history, smoking history, fall in one year, hospitalization in one year, and MMSE-KC.

Abbreviations: SO, sarcopenic obesity; OR, odds ratio; CI, confidence interval; 5 TSTS, 5 times sit-to-stand chair test; HGS, hand grip strength.

* P<0.05

A Study of Usability of Application-Based Exercise Prescription in the Elderly

So Yeon Jun^{1**}, Seung Nam Yang¹, Changseok Lee²

Department of Rehabilitation Medicine, Korea University Guro Hospital¹, DYPHI Research Institute, DYPHI Inc., Daejeon, Republic of Korea²

Frailty can appear with age, but not all elderly people show frailty. Frailty is characterized by vulnerability to inflammation, decreased metabolism, hormone regulation, proteostasis, complaints of fatigue, and reduced physical activity. Therefore, in the case of an elderly population with frailty, overall socioeconomic costs may increase due to increased medical expenses. As frailty progresses, patients become more avoidant of exercise. However, frailty is by no means the contraindication of physical exercise, and it has been shown that sarcopenia and frailty can be improved through regular physical activity. Importantly, aerobic exercises and progressive resistance exercise prescriptions can have a positive effect on the prevention of frailty. However, it does not mean that all elderly people are assessed with the same degree of frailty and that the same prescription is given to all. There can be significant differences in the degree of frailty depending on the individual, and a customized prescription tailored to the individual's physical situation is needed.

In this study, we evaluated the physical function of participants, including short physical performance battery (SPPB), using an automated physical function evaluation system (Figure 1) and balance ability in a group of smartphone users aged 65 years or older and conducted application-based exercise prescriptions. As an initial evaluation, the cognitive status of all subjects was assessed, static balance, walking speed, sitting, and standing were performed using a fully automated physical function measuring device, and the scores were added to obtain the SPPB score. Application-based exercise was performed 5 times a week for 4 weeks. The SPPB score and balance ability were reevaluated after the exercise period.

19 subjects were recruited in this study, and 17 participants completed the 4-week program. The average program participation rate during 4 weeks was 96.17%, showing a very high level of compliance. The SPPB score showed improvement in the total score and sitting and standing scores. (Table 1)

Through this study, we were able to confirm the improvement in physical function of elderly participants through the 4-week application-based program with the participants' high compliance and ease of use. In addition, since the participants did the exercise in their own living space rather than visiting a hospital, we were able to confirm the advantage of convenient accessibility. In the future, the effectiveness of the application-based program will be able to be reconfirmed through a large number of participants and follow-up over a longer period of participation.

Acknowledgment This research was supported by Korean Academy of geriatric rehabilitation medicine



Figure1. Automated physical function evaluation system

Automated physical function evaluation system

Table1. Improvement of the short physical performance battery score

		Mean (n=17)	p
SPPB score (Total)	Pre	10.0 ± 1.00	0.002*
	Post	11.29 ± 0.99	
SPPB score (Standing balance)	Pre	3.88 ± 0.33	0.560
	Post	3.94 ± 0.24	
SPPB score (Usual gait speed)	Pre	3.71 ± 0.47	0.560
	Post	3.76 ± 0.56	
SPPB score (Repeated Chair stands)	Pre	2.41 ± 1.06	0.002*
	Post	3.59 ± 0.80	

Values are presented as the mean ± the standard deviation.

An asterisk (*) indicates a significant difference, based on the Wilcoxon signed-rank test

The SPPB score showed improvement in the total score and sitting and standing scores

Characteristics of Hip Fracture-related Falls in the Elderly Population: a Systematic Review

Seung-Kyu Lim^{1*}, In-Su Hwang¹, Jinwhan Ryu¹, Sol Jin¹, Jae-Young Lim^{2†}

Department of Rehabilitation Medicine, Soonchunhyang University Cheonan Hospital, Soonchunhyang University College of Medicine, Cheonan¹, Department of Rehabilitation Medicine, Seoul National University Bundang Hospital, Seoul National University College of Medicine²

Background

With the global aging trend, the incidence of falls and hip fractures is projected to rise, leading to an increased associated burden. Over 90% of hip fractures result from falls, yet not all falls cause fractures, suggesting specific fall characteristics may contribute to hip fractures. This review provides insights into fragility hip fracture-related falls among the elderly, aiding in understanding and developing effective fall prevention strategies for this population.

Methods

Searches encompassed PubMed, OVID, EMBASE, Cochrane Library, and Web of Science, supplemented by citation checks. We included non-randomized studies detailing characteristics of fragility hip fracture-related falls in the elderly, with or without a non-hip fracture control. Evaluated fall characteristics included height, location, direction, time, mechanism, activity during the fall, hip impact, protective responses, walking aid use, and impact surface. The quality of these studies was assessed using the revised Risk of Bias Assessment tool for Non-randomized Studies 2 (RoBANS2).

Results

A total of 30 articles were reviewed, comprising 23 non-case control and 7 case-control studies, with a mean age of 75.6 years. Studies presented varied details on fall characteristics. Hip-fracture related falls typically occur indoors at or around standing height during daytime, often involving sideways or backward motions with inadequate protective responses. Slipping is predominant, yet lost balance and weakness/collapse are notable. Walking precedes many falls, but stationary activities (lack of forward motion, changing positions, sitting or standing still, transfer) also contribute. Low usage of walking aids and impact on hard surfaces are common features of these falls. As individuals age, they frequently experience a decrease in walking speed, leg strength, and balance, evident during activities like walking and simple movements such as changing positions. Consequently, they're more likely to fall sideways or backward, leading to direct hip impacts due to inadequate protective responses. Furthermore, decreased shock absorption from muscle atrophy and diminished bone strength increases the risk of hip fractures, even in falls from standing or lower heights. The age-related decline in physical abilities increases susceptibility to falls and hip fractures during walking and indoor activities, reflecting changes in life patterns associated with physical weakness. These attributes serve as early indicators of susceptibility to hip fractures.

Conclusion

This review underscores fall characteristics associated with fragility hip fractures in older adults, highlighting features more aligned with age-related physical frailty than general falls. Each characteristic collectively contributes to the occurrence of hip fractures. Such insights can guide healthcare providers in implementing tailored interventions to reduce hip fractures and related challenges.

Acknowledgment This research was supported by a grant of the Korea Health Technology R&D Project through the Korea Health Industry Development Institute (KHIDI), funded by the Ministry of Health & Welfare, Republic of Korea (grant number : HI19C0481, HC20C0157).

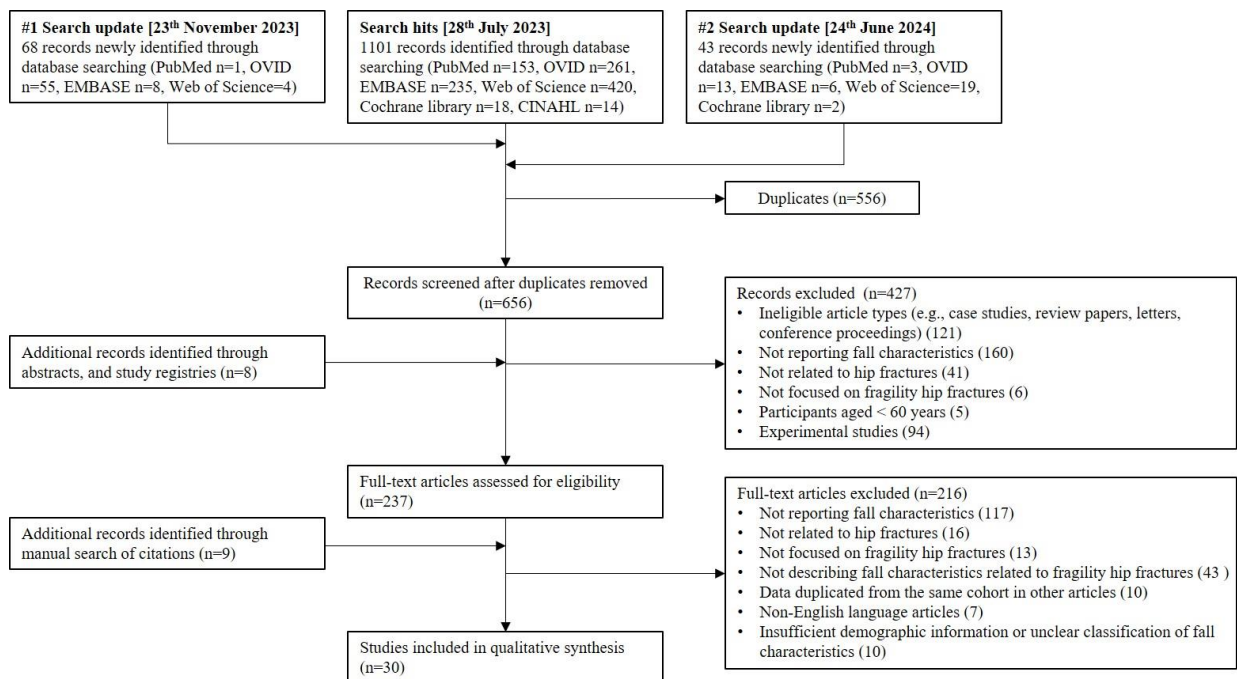


Figure 1. Flow chart of the article inclusion process

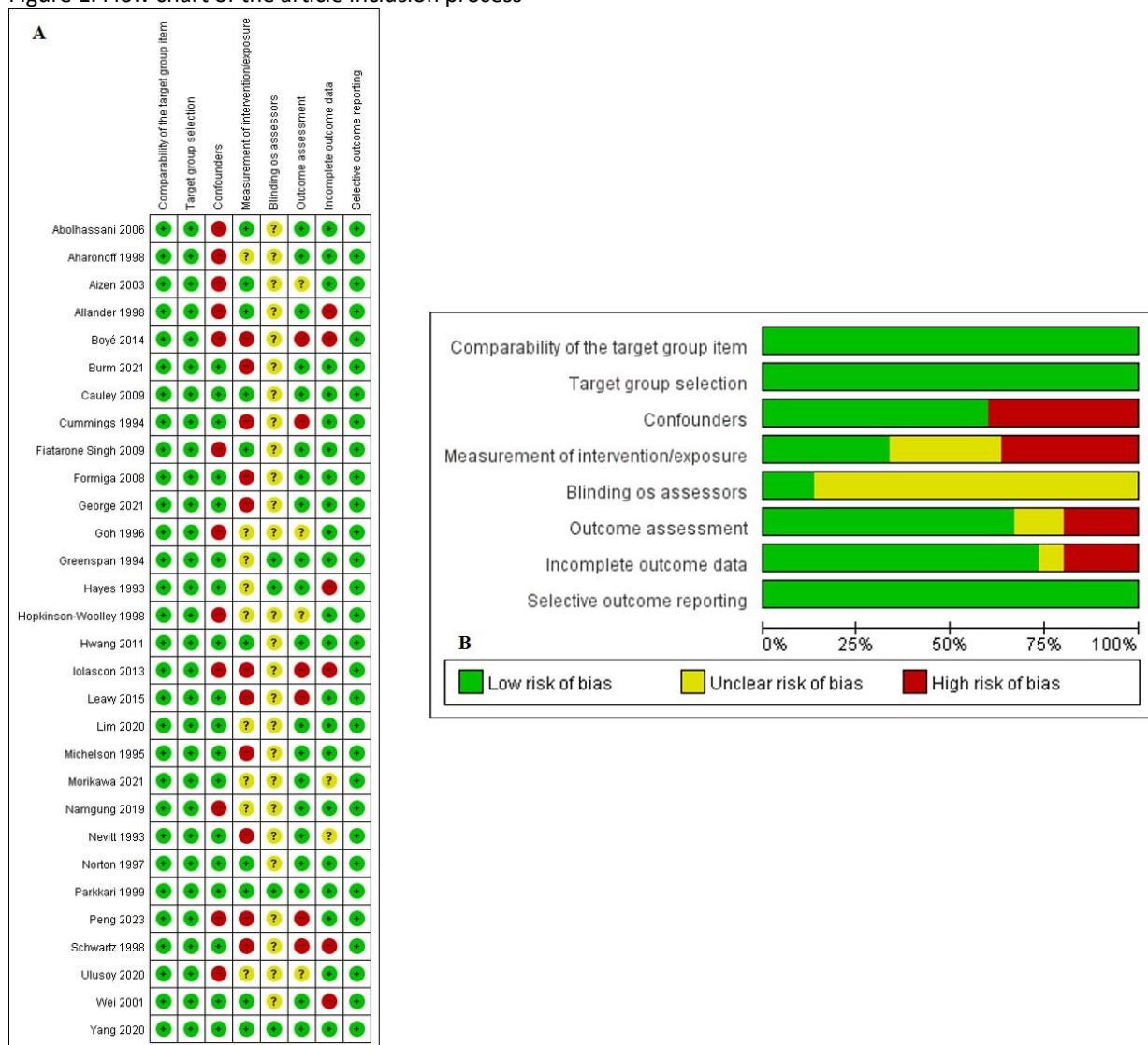


Figure 2. Risk of bias appraisal using RoBANS2. A. Risk of bias summary: review authors' judgements about each risk of bias item for each included study. B. Risk of bias graph: review authors' judgements about each risk of bias item presented as percentages across all included studies.

Differential Impact of Cognitive Subdomains on Motor Skills in the Elderly

Hyunjin Kim¹, Jungsoo Lee^{1†}, Woohee Han^{1*}

¹Department of Medical IT Convergence Engineering, Kumoh National Institute of Technology¹

Objective

Motor and cognitive functions gradually decline over the course of aging. Existing studies have reported that both function levels are related to each other. This study aims to investigate the additional relationships between motor and cognitive functions, including specific motor skills and cognitive subdomains, in the elderly. Furthermore, we aim to investigate how specific cognitive subdomains are related to various motor skills with different movements and complexity.

Methods

One hundred six elderly persons participated in this study. The Korean Mini-Mental State Exam (K-MMSE) and the Seoul Neuropsychological Screening Battery (SNSB-C) were assessed to examine cognitive global and subdomain functions, including attention, language, visuospatial, memory, and executive functions. The 9-Hole Pegboard Test (9HPT), the 10 Meter Walking Test (10MWT) at comfortable and maximum speeds, the 6 Minute Walking Test (6MWT), the Time Up and Go Test (TUG), and the Four Square Step Test (FSST) were assessed to examine specific motor skills for upper and lower limbs. Correlation analysis was used to investigate the significant relationship between cognitive and motor functions, respectively. Furthermore, multiple linear regression was utilized to investigate the role of cognitive subdomain functioning in each motor skill and the difference in the contribution of subdomain for different motor skills.

Results

Global cognitive function (K-MMSE) and all motor skills were correlated with each other. Cognitive subdomains (attention, language, visuospatial, memory, and executive functions) were correlated with all motor skills. The level of correlation with K-MMSE was highest in the order of FSST, TUG, 10MWT at maximum speed, 9HPT, 10MWT at comfortable speed, and 6MWT. Furthermore, in multiple linear regression analysis different cognitive domains contributed according to different motor skills. 9HPT was significantly associated with the memory and executive domains, while the 10MWT at comfortable speed was associated with the visuospatial domain. The 10MWT at maximum speed showed associations with the visuospatial and executive domains. Moreover, the TUG, FSST, and 6MWT were associated with the language domain.

Conclusion

These results demonstrated that motor and cognitive function levels are generally related to each other in various motor skills and global and subdomain levels of cognition. The importance of cognitive contribution was confirmed by examining that the contribution of cognitive function increased as motor skill complexity increased, such as speed and balance. Lastly, cognitive subdomains differently contributed according to upper and lower motor skills, and lower motor skills with different speed or balance. By examining the relationship between cognition and motor function in detail, this study could contribute to establishing strategies necessary to effectively prevent cognitive and motor function decline in the elderly.

Acknowledgment This study was supported by the National Research Foundation of Korea (NRF) grant funded by the Korean government (MSIT). (No. RS-2023-00208884, No. RS-2023-00265824).

Classification of Fall and Non-Fall in Personal Gait Data Using Feed Forward Neural Network

Kyeong-Jun Seo^{1*}, Ji-Eun Cho¹, Jung Hwan Kim^{2†}

Department of Rehabilitation & Assistive Technology, National Rehabilitation Center¹, Rehabilitation Hospital and Research Institute, National Rehabilitation Center²

Individuals with central nervous system damage and the elderly frequently experience falls due to weakened lower limb strength. Repeated falls can lead to physical and psychological losses and significantly diminish quality of life. This study aims to provide foundational research for fall prevention by collecting fall data and analyzing it using artificial intelligence.

Falls can occur due to various situations, such as slipping during walking or tripping over obstacles. In this study, we induced slips during walking to collect data. To achieve this, a surfactant was applied to a PE material film to make it slippery during walking. The subject was a healthy adult who had electromyography (EMG) and Inertial Measurement Unit (IMU) sensors attached to their body, as well as markers to monitor walking movements. Additionally, a harness was attached to the subject's back to prevent injury in case of a fall.

The collected data was preprocessed to remove unnecessary noise and fall and non-fall data were labeled through video analysis. To classify falls and non-falls, a Fully Connected Feedforward Neural Network (FFNN) was used, with a single hidden layer. The dataset was divided into training data (70%), validation data (15%), and test data (15%). The learning process was conducted using three approaches: EMG+IMU, EMG alone, and IMU alone. The accuracy results for each approach were as follows: 82.8% for both EMG+IMU and EMG, and 83.3% for IMU.

Since the study was conducted using data from only one healthy adult, the high accuracy observed may be influenced by this limited sample size. Additionally, the small proportion of fall data within the overall walking data likely impacted the results. Future research should involve a larger number of subjects and a broader range of fall data to enhance and validate the findings.

Acknowledgment This research was supported by a grant (#NRCTR-IN24003) by the Korea National Rehabilitation Center.

Predicting Rehospitalization Rates of Hip Fracture Patients using Survival analysis ML models

Juahn Oh^{1**}, Seung Hoon Kim³, Yong Han Cha¹

Department of Medicine, Eulji University¹, Soon Chun Hyang University Bucheon Hospital, Department of Ophthalmology², Eulji University Hospital, Department of Orthopedic Surgery³

Background

Hip fractures in the elderly pose significant challenges for morbidity, mortality, and healthcare systems globally. As the population ages, hip fracture incidences are expected to increase, requiring innovative strategies to manage high re-hospitalization rates. Re-hospitalization impedes recovery and adds financial strain on healthcare systems, highlighting the need for precise predictive models. This study evaluates advanced survival analysis machine learning models to predict re-hospitalization in elderly post-hip fracture patients, aiming to improve patient outcomes and reduce healthcare system burdens.

Methods

The retrospective cohort study included 718 hip fracture patients January 2020 to June 2022. Data on demographics, clinical characteristics, and rehospitalization dates were collected at 6 weeks, 3 months, 6 months, 12 months, and 24 months. Key variables included sex, age, BMI, BUN, fracture type, ASA score, and comorbidities. Machine learning models, including Cox Proportional Hazards (CPH), Random Survival Forests (RSF), Gradient Boosting survival Model (GBM), and Support Vector Machines (SVM), were developed. The data was split into training (80%) and test (20%) sets, with hyperparameter tuning via cross-validation.

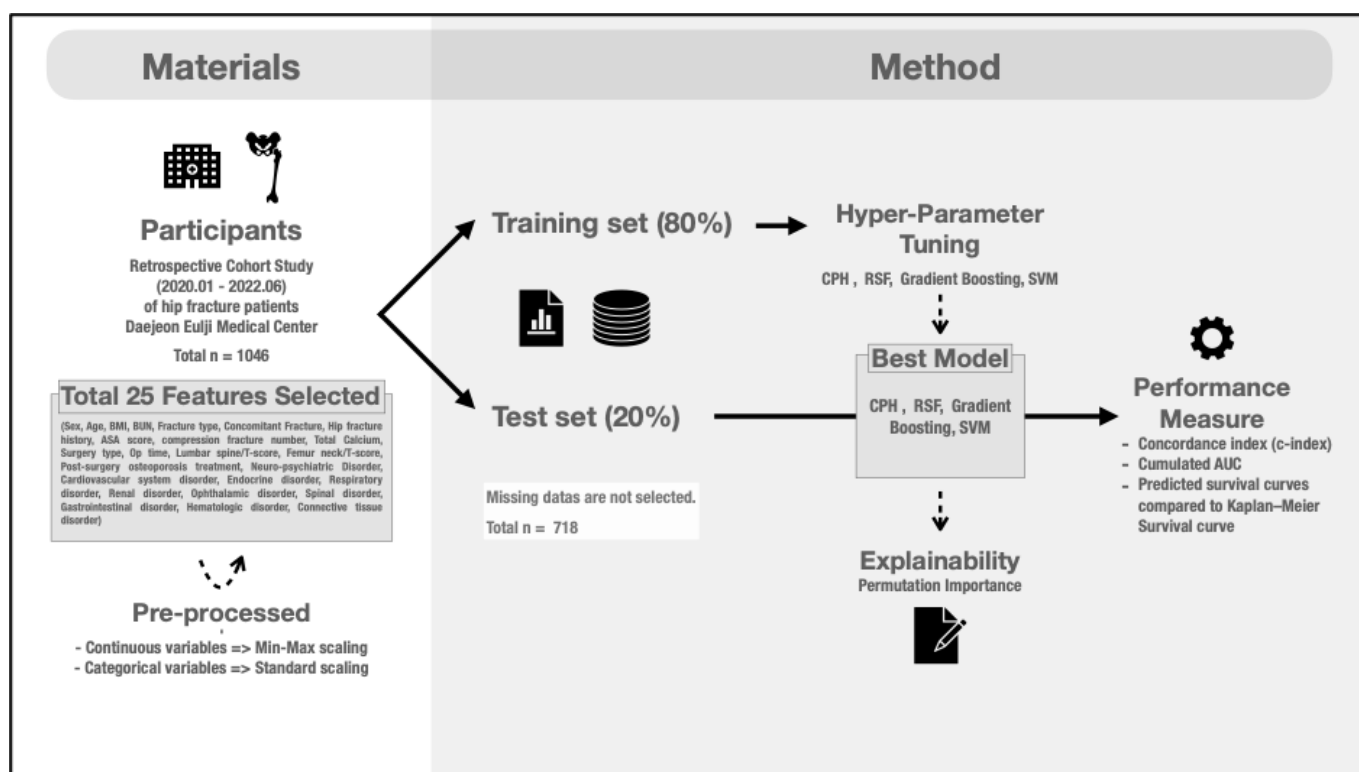
Model performance was evaluated using the Concordance Index (c-index), Area Under the Curve (AUC), and Kaplan-Meier Survival Curves. Statistical analyses used scikit-survival and scikit-learn libraries. Feature importance was assessed through Permutation Importance, with the best model selected based on overall performance.

Results

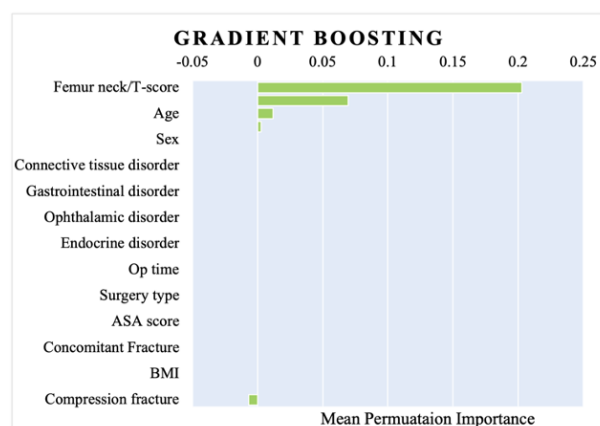
In the analysis of 718 hip fracture patients, hyperparameter tuning optimized machine learning models, with the GBM achieving the highest mean AUC of 0.868 (95% CI, 0.847–0.889). The RSF model had a mean AUC of 0.785 (95% CI, 0.764–0.806), the SVM 0.763 (95% CI, 0.742–0.784), and the CoxPH 0.736 (95% CI, 0.715–0.757). Feature importance analysis identified Femur neck/T-score, age, BMI, operation time, compression fractures, and total calcium as significant predictors. Feature selection improved the c-index for the RSF from 0.742 to 0.874 and the CoxPH from 0.717 to 0.915. The GBM and SVM models saw decreases in c-index after feature selection. Survival curves indicated that GBM and RSF models predicted lower probabilities of re-hospitalization compared to the Kaplan-Meier estimate, while the CoxPH's predictions closely matched the observed data.

Conclusions

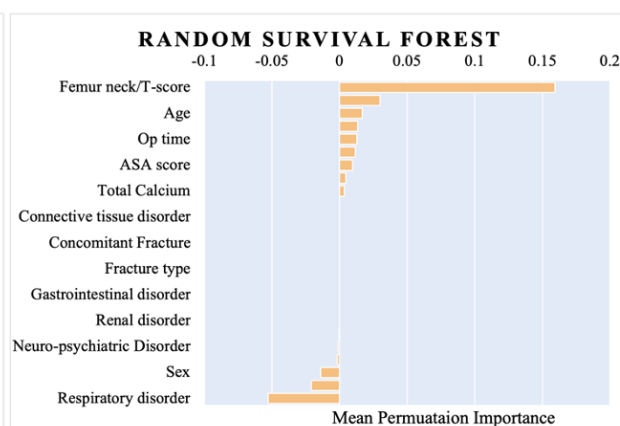
Our findings suggest that GBM is the most effective model for predicting rehospitalization in hip fracture patients, followed by RSF and SVM, with CoxPH being the least effective. The study highlights the critical role of features such as Femur neck/T-score, age, BMI, operation time, compression fractures, and total calcium in predicting re-hospitalization. Feature selection significantly impacted model performance, emphasizing the need for a comprehensive approach to enhance predictive accuracy.



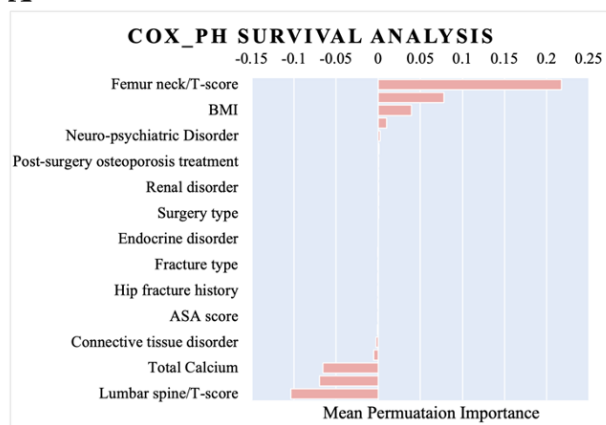
The whole flow diagram of the study.



A

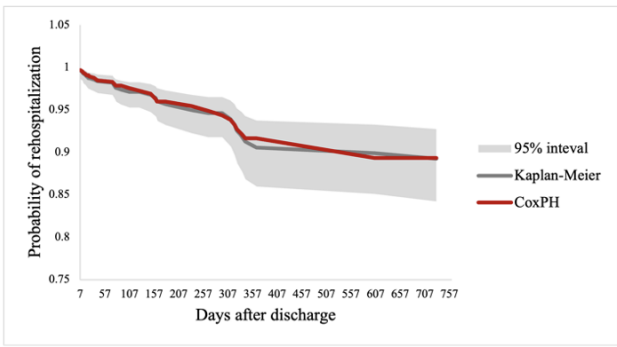
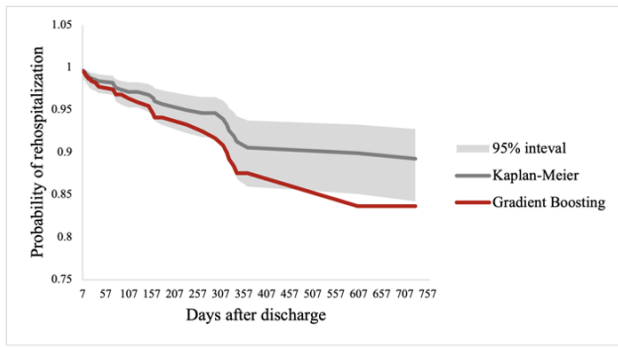


B



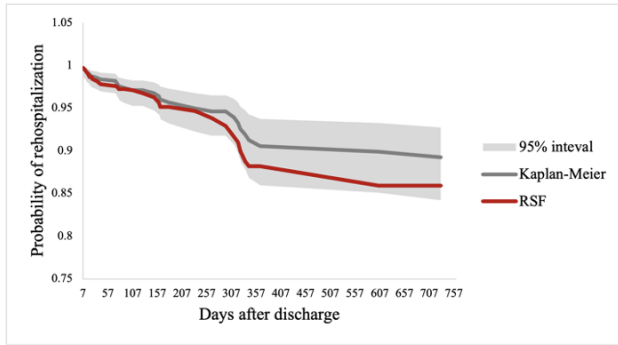
C

Mean Permutation Importance in Predictive Models



A

B



C

Survival Curves Comparison (Kaplan-Meier vs. Predictive Models)

Clinical Performance of Ultrasound Shearwave Elastography in Carpal Tunnel Syndrome

Jaewon Kim^{1*}, Min-Wook Kim¹, Jae Min Kim^{1†}

Department of Rehabilitation Medicine, Incheon St. Mary's hospital, The Catholic University of Korea¹

Introduction

Carpal tunnel syndrome (CTS) is a common neuropathy caused by compression of the median nerve at the wrist. Traditional diagnostic methods include nerve conduction studies (NCS) and electromyography (EMG). Shear wave elastography (SWE) is a non-invasive ultrasound technique that measures tissue stiffness and has potential utility in diagnosing CTS. This study aims to evaluate the effectiveness of SWE in diagnosing CTS.

Method

We recruited a normal control group and patients with CTS, performing NCS/EMG and ultrasound examinations of the median nerve on both wrists. Wrists were categorized into control and CTS groups based on NCS/EMG results using the AANEM classification. Data on pain intensity (NRS), BCTQ-SS/FS (Boston Carpal Tunnel Questionnaire – symptom severity/Functional Status scale), NCS/EMG findings, and ultrasound cross-sectional area (CSA) at the carpal tunnel inlet were collected. SWE measurements assessed the median nerve's elasticity in the longitudinal view around the carpal tunnel inlet (Figure 1).

Results

A total of 50 participants were included in the study, with 30 in the patient group and 20 in the control group. The study encompassed 99 wrists from the 50 patients, comprising 48 normal wrists and 51 wrists with CTS. Based on severity, the classification included 22 mild, 20 moderate, and 9 severe cases.

Comparing CSA, CTS wrists had significantly larger CSA compared to normal control wrists ($13.63 \pm 3.09 \text{ mm}^2$ vs $8.95 \pm 2.49 \text{ mm}^2$, p

When comparing elasticity, the CTS group had significantly higher elasticity compared to the normal control group ($106 \pm 47.22 \text{ kPa}$ vs. $60.96 \pm 21.8 \text{ kPa}$, p

When using the CSA x elasticity value for analysis, the severe group had significantly higher values compared to the mild group ($p = .006$). The ROC analysis for predicting severe cases yielded a cut-off value of 1225.97 (sensitivity 0.78, specificity 0.73, accuracy 0.77). (Figure 2)

There was a relatively weak linear relationship between CSA and elasticity variables, with an R^2 value of 0.26.

Additionally, the NRS and BCTQ-SS and BCTQ-FS showed weak correlations with elasticity ($R^2 = 0.05, 0.15, 0.10$, respectively).

Conclusion

SWE can aid in diagnosing CTS, with higher specificity and accuracy when combined with CSA measurements. This combination is particularly useful in screening and diagnosing severe CTS cases requiring surgical treatment.

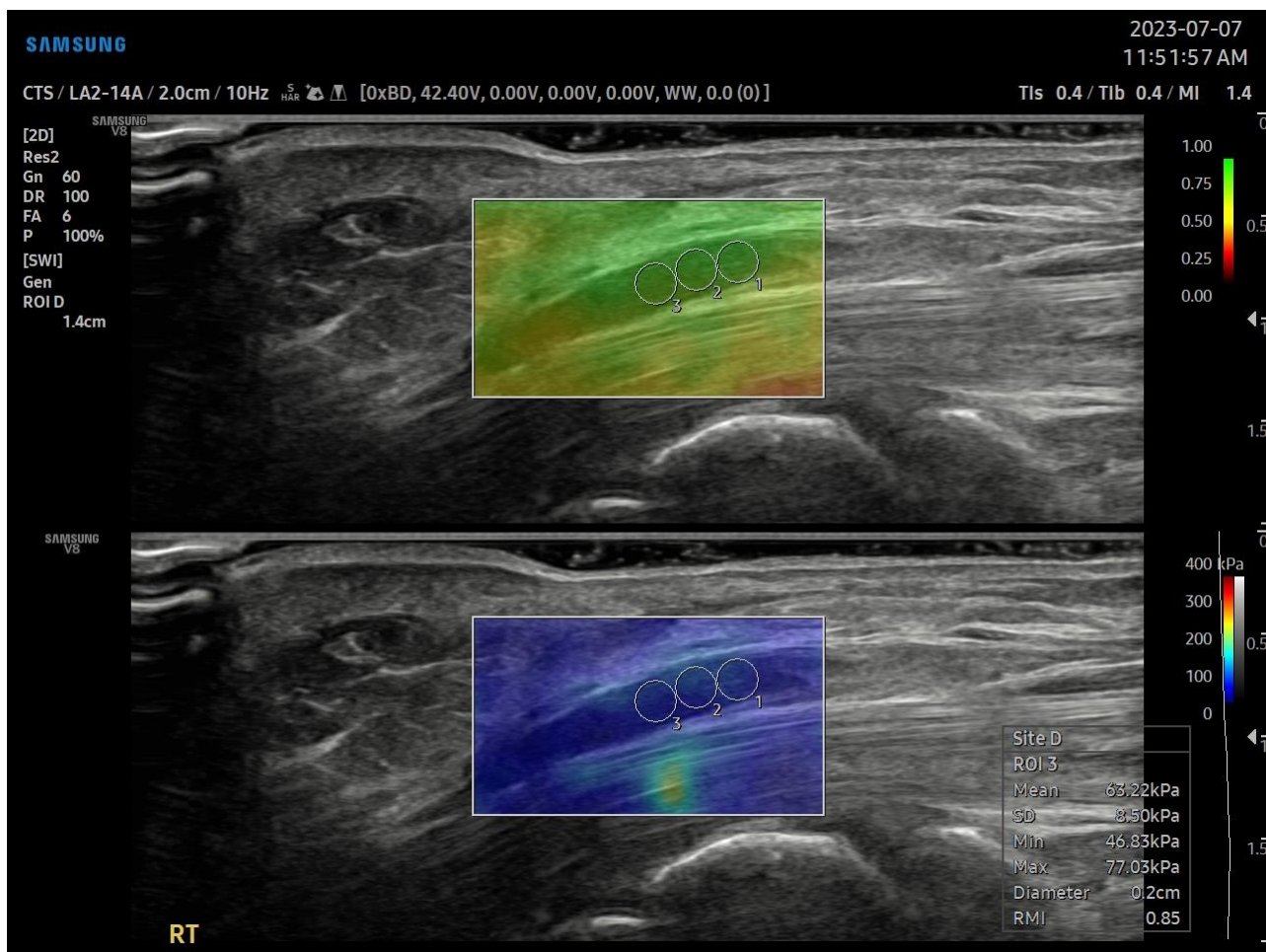


Figure 1. Elasticity measurement of median nerve by shear wave elastography

	CTS Patients				Controls (n=48)	P value (Controls vs Patient)
	Mild (n=22)	Moderate (n=20)	Severe (n=9)	Total (n=51)		
CSA(mm ²) (mean±SD)	12.49±2.67	14.32±2.96	14.89±3.35	13.63±3.09	8.95±2.49	<0.001*
Elasticity(kPa) (mean±SD)	95.52±32.63	105.79±47.98	133.74±62.27	106±47.22	60.96±21.80	<0.001*

Table 1. Cross-sectional area (CSA) and elasticity of normal control and carpal tunnel syndrome (CTS) group

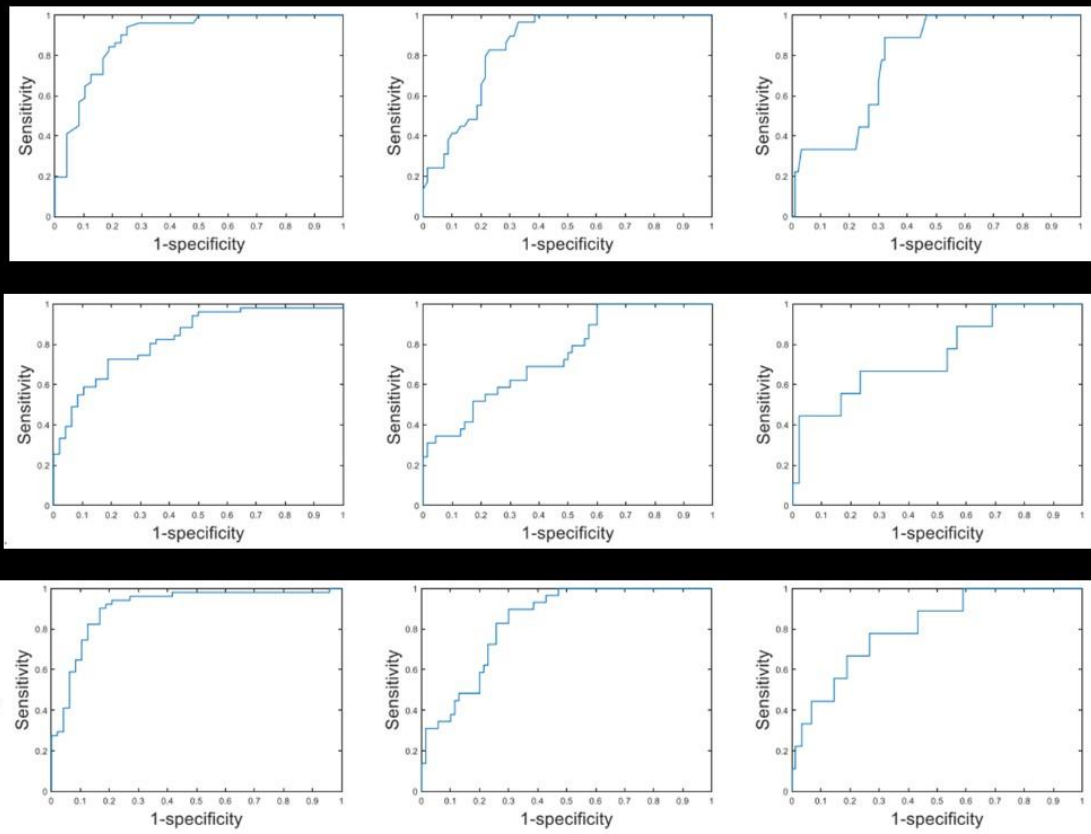


Figure 2. ROC curve of ultrasonographic measurement of cross sectional area (CSA), elasticity, CSA x elasticity

Hand Function and Activities of Daily Living in Ambulatory Patients with Charcot-Marie-Tooth Disease

Si Yun Kim^{1*}, Ji Hye Hwang^{1,3†}, Byung Ok Choi^{2,3}, Kyung hyup Koo¹, Sun Woo Kim¹

Department of Physical and Rehabilitation Medicine, Samsung Medical Center¹, Department of Neurology, Samsung Medical Center², Department of Medicine, Sungkyunkwan University School³

Background

Charcot-Marie-Tooth disease (CMT) leads to progressive distal muscle weakness and sensory loss, typically affecting the lower limbs but can also significantly impact the hands. While numerous studies have investigated the impact of CMT on lower limb function and associated rehabilitation interventions, there is relatively little research on hand function. Therefore, this study aims to evaluate hand function and activities of daily living (ADL) in ambulatory CMT patients.

Methods

Fifty-one ambulatory CMT patients were evaluated to assess hand power, fine motor skills, and functional performance related to ADLs, and all ambulatory CMT patients had a Functional Ambulation Category (FAC) score of 2 or higher (Table 1). The assessments included the Korean Modified Barthel Index (K-MBI), the Sollerman Hand Function Test, the Jebson Taylor Hand Function Test, grip strength measurements, and the Nine-Hole Pegboard Test.

Results

The evaluation of 51 ambulatory CMT patients showed that the general ADL index, K-MBI, decreased by 4.0% and the Sollerman Hand Function Test, which evaluates hand function in ADL, showed a reduction of 1.4%. However, grip strength measurements showed significant reductions ranging from 46.2% to 61.4%, with the greatest decline observed in lateral pinch strength, followed by tip pinch, tripod pinch, and power grasp. The Nine-Hole Pegboard Test results showed that patients took 70.3% longer with the dominant hand and 59.9% longer with the non-dominant hand to complete tasks, indicating a notable impairment in finger dexterity. The Jebson Taylor Hand Function Test showed that tasks took significantly longer, especially those involving pinch movements.

Conclusion

Ambulatory CMT patients maintain relatively good performance in basic ADLs, as measured by the K-MBI and Sollerman Hand Function Test, but detailed assessments reveal significant impairments in hand strength and fine motor skills. This indicates the necessity for comprehensive assessments and targeted rehabilitation interventions. This study can help to identify which hand functions are impaired in CMT patients and develop appropriate rehabilitation intervention plans.

Table 1. General characteristics

Number of participants		51
Age (years)		
Mean (SD)		37.39 (15.65)
Sex (n)		
Male		25
Female		26
Type CMT (n)		
CMT1		28
CMT2		12
CMTX		3
CMT4		2
Others		6
Functional ambulation category (n)		
Score	Category	
0	Nonfunctional ambulator	0
1	Ambulator, dependent on physical assistance – level I	0
2	Ambulator, dependent on physical assistance – level II	2
3	Ambulator, dependent on supervision	11
4	Ambulator, independent level surface only	27
5	Ambulator, independent	9

CMT = Charcot-Marie-Tooth disease

Biomechanical analysis in TF Amputees during Obstacle Crossing with Prosthetic knee made in Korea

Hee Seung, Yang^{1,1**}, Hoon Ki, Song^{1,1}, Seul Bin Na, Lee^{1,2}, Ye Dam, Bae^{1,2}, Chan hyeok, Jeong^{1,2}

Department of Rehabilitation Medicine, Veterans health system medical center¹, prosthetics & Orthotics center , Veterans health system medical center²

Objective

The purpose of this study is to evaluate the usability and stability of mechanical polycentric knee prosthesis new-developed in Korea by analyzing the biomechanical characteristics of new knee prosthesis compared with conventional prosthesis when crossing obstacles in unilateral transfemoral amputations.

Method

A total of 5 unilateral transfemoral amputation patients participated in this study. The walking across obstacles was carried out by wearing a conventional knee prosthesis (CKP) and a new-developed knee prosthesis (FIRST K1), respectively, and crossing wooden obstacles 10cm in height and thickness and 1m in width leading with the intact limb. Spatio-temporal, kinematic, kinetic, ground reaction force data was obtained through gait analysis using a 3D motion analysis system (Motion analysis®).

Results

As a result of spatio-temporal parameters, when wearing a new-developed knee prosthesis, the vertical distance from toe to obstacle and the horizontal distance from heel to obstacle were significantly increased (p

Conclusion

In this study, the new-developed mechanical polycentric knee prosthesis in Korea increases knee flexion in swing phase, which provides an advantage in securing a more sufficient space between the obstacle and the foot segment when crossing an obstacle. This suggests that the new-developed mechanical polycentric knee prosthesis (First K1) can improve walking stability when crossing obstacles for amputees, and it can contribute to improving the patient's daily activity and quality of life in the future. In addition, further research is needed to evaluate the impact of long-term use of First K1 and to investigate the recruitment characteristics of muscle activity together.

Acknowledgment This study was supported by Ministry of Trade, Industry and Energy Research Grant.

Safety and Feasibility of a Fabric-Type Knee Orthosis with Artificial Muscles for the Elderly

JungHyun Kim^{1*}, Sungbae Jo¹, Eunsu Lee¹, Woo Hyung Lee^{1,2}, Sung Eun Hyun^{1,2}, Yae Lim Lee^{1,2}, Seung Hwan Lee^{1,2}, Jeong Min Kim³, Cheol Hoon Park⁴, Seong Jun Park⁴, Kyungjun Choi⁴, Jeongae Bak⁴, Hyung-Ik Shin^{1,2†}

Department of Rehabilitation Medicine, Seoul National University Hospital¹, Department of Physical and Rehabilitation Medicine, PURME foundation NEXON Children's Rehabilitation Hospital², Department of Rehabilitation Medicine, Seoul National University College of Medicine³, Advanced Robotics Research Center, Korea Institute of Machinery and Materials⁴

Background

With the elderly population in South Korea projected to reach 46.4% by 2070, pedestrian safety among this demographic has become a significant concern, particularly given the higher incidence of accidents compared to the general population in 2022. Aging typically impairs reflexes, vision, and mobility, thereby increasing fall risks. Muscle strength is essential for maintaining effective gait. This protocol outlines a clinical trial to assess the safety and feasibility of a new fabric-type knee orthosis designed to mimic muscle function and enhance gait in the elderly.

Methods

This trial will evaluate the feasibility of a muscle-mimicking fabric-type knee orthosis (MMFKO) for elderly patients, registered on ClinicalTrials.gov under NCT06387459. Participants will receive training on orthosis usage and undergo comprehensive strength and balance assessments, including Muscle Mass Testing, Range of Motion (ROM), Berg Balance Scale (BBS), Timed Up and Go (TUG), and the Five Times Sit to Stand Test (5TSTS), to establish personalized training protocols. Training sessions will be conducted in three phases: 1) without the orthosis, 2) with the orthosis fitted but not powered on, and 3) with the orthosis fitted and powered on. Each session will last no longer than 30 minutes. Safety evaluations will include participant self-assessments of pain and skin condition, as well as monitoring of physiological and musculoskeletal changes. Assessments across three visits will measure metrics such as completion rate, dropout rate, participant feedback, the 10-Meter Walk Test, the 6-Minute Walk Test, gait analysis, and electromyography (EMG).

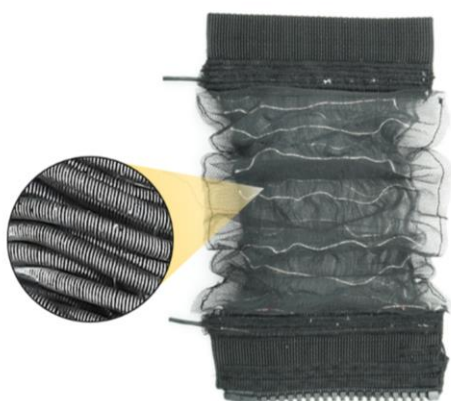
Results

While detailed results will be presented in future studies, we hypothesize that the muscle-mimicking fabric-type knee orthosis (MMFKO) will be safe and feasible for use among elderly patients. We anticipate demonstrating minimal adverse effects, such as pain or skin irritation, and high compliance with the training protocols. Furthermore, we expect to observe improvements in the participants' ability to use the orthosis effectively, contributing to better overall mobility and stability.

Conclusion

This innovative fabric-type knee orthosis shows potential for improving gait and lower limb function in elderly individuals. The clinical trial will provide critical data on the orthosis's safety and practicality, contributing valuable insights into enhancing mobility and reducing fall risks in the elderly. Positive outcomes could lead to advancements in rehabilitation strategies for the aging population.

Acknowledgment This research was supported by the Pioneer Research Center Program through the National Research Foundation of Korea funded by the Ministry of Science and ICT (Project No. 2022M3C1A3080598).



Evaluation during stand to sit activity in TF amputee with New Prosthetic Knee made in Korea

Hee Seung, Yang^{1,1**}, Hoon Ki Song^{1,1}, Hui Woo Choi^{1,2}, Pyung-Hwa Choi^{1,2}

Department of Rehabilitation Medicine, VHS medical center¹, Prosthetics & Orthotics Center, VHS Medical Center²

Introduction

The stand to sit movement should be converted to controlled smooth acceleration and deceleration through eccentric contraction of the muscle, which is difficult for lower limb amputee, and if performed only using the intact limb, excessive load is applied to the joint, which can lead to discomfort or failure of movement. First-K1, new-developed mechanical polycentric knee prosthesis made in Korea, has the advantage of being able to control movement with the wearer's voluntary control by applying the principle of operating based on the change in the angle of the knee by installing two piston-type eccentric rotating shafts on the upper body and rotating crankshaft to provide stability when weight is supported.

Objective

During stand to sit activity, the purpose of this study is to compare and analyze the change in knee joint motion and compensation movement with conventional prosthesis and First-K1 prosthesis using trunk and intact lower limb through 3D motion analysis

Methods

A total of 4 unilateral transfemoral amputation patients participated in this study. Using a 3D motion analysis system (Motion analysis®), the subject opened his feet shoulder-width and then sat down to the chair with both arms crossed in front of his chest. According to prosthesis type, We calculated trunk lateral bending and angular velocity of knee joint in frontal plane to find out the kinetic difference. and then, the vertical ground reaction force, impulse, and joint moment were calculated to find out the kinematic difference. In addition, the Symmetry index was analyzed according to the calculated variables of both lower extremities.

Results

Using First K1 prosthesis, in the stand to sit activity, the vertical ground reaction force and impulse showed to decrease on the intact side and increase on the amputee side. In addition, the symmetry index of the amount of impact on both lower extremities improved, all of which showed statistically significant differences.(p

Conclusion

In our study, it was found that the use of First K1 prosthesis in transfemoral amputated patients reduces the burden on the normal side as the impact is shifted to the amputation side in the stand to sit activity. However, it seems that research should be conducted on more transfemoral prosthesis user.

Acknowledgment This study was supported by Ministry of Trade, Industry and Energy and Korea Institute for Advancement of Technology Grant. Fund is Establishment of Track Record for A.I.-based Prosthetic Devices and Medical Auto-mobilities(P14770006)

Korean Translation and Psychometric Properties of the Prosthetic Limb Users Survey of Mobility

Jin-Hong Kim^{1*}, Sohye Jo¹, Brian J. Hafner³, Gangpyo Lee^{1,2†}

Rehabilitation Medical Research Center, Incheon hospital, Korea Workers' compensation and Welfare service, incheon, Republic of Korea¹, Department of Rehabilitation Medicine, Incheon hospital, Korea Workers' compensation and Welfare service, incheon, Republic of Korea², Department of Rehabilitation Medicine, University of Washington, Seattle, Washington, United States of America³

Aim

This study aimed to develop a Korean version of PLUS-M, obtain official certification, and analyse the psychometric properties of the PLUS-M 12-item Short Form (PLUS-M/SF12). This study provided an instrument that can accurately assess the mobility of individuals with lower limb amputations.

Method

1 Korean Translation - The process of Korean translation began with a consultation with the developer of the PLUS-M and included the first and second compatibility verification, back-translation, back-translation verification by the developer, and the final approval of the Korean version (Table 1).

2 Analysis of Psychometric Properties

2.1 Study participants

The inclusion criteria was as follows:

- 1) had undergone unilateral lower limb amputation at least 1 year prior
- 2) used a prosthesis indoors
- 3) could respond to questionnaires
- 4) voluntarily decided to participate in this study and signed informed consent before the study began

The exclusion criteria was as follows:

- 1) had bilateral lower limb amputations
- 2) had cognitive impairment
- 3) wore a prosthesis for aesthetic purposes
- 4) had limited housekeeping activities

2.2 variables measured

This study tested validity using different instruments, such as ABC, 2MWT, and TUG, to assess various characteristics related to mobility.

2.3 Outcome Measures of Efficiency

Construct validity, Reliability test (test-retest reliability), Internal consistency

3 Data analysis

Statistical analyses were performed using SAS ver. 9.4 (SAS Institute Inc., Cary, NC, USA). The participants' general characteristics were analysed using descriptive statistics and all correlation calculations.

Results

1 PLUS-M/SF-12 Korean Version (Table 2)

2 Psychometric Validation of PLUS-M/SF-12

2.1 General characteristics of participants

Out of 40 initial patients who agreed to participate in the study, 8 dropped out due to personal reasons. The final analysis included 32 male participants with unilateral lower limb amputations resulting from trauma (Table 3)

2.2 Construct validity

Data from 32 participants were analysed. PM had a high correlation with the ABC scores ($r = 0.88$, $P < 0.05$). PM exhibited a moderate correlation with 2MWT ($r = 0.58$, $P < 0.05$), but a weak correlation with TUG ($r = 0.40$, $P < 0.05$)

2.3 Test-retest reliability

The intra-rater correlation coefficient (ICC) calculated for the 32 participants who completed the PLUS-M/SF-12 twice was 0.91 [95% CI 0.82–0.95], which was excellent.

2.4 Internal consistency

The internal consistency of PLUS-M/SF-12 was analysed. Cronbach's α was 0.95 at the first test and 0.95 at the second test, demonstrating significantly excellent internal consistency.

Conclusion

This study translated the PLUS-M into Korean to account for cultural differences and demonstrated the reliability and validity of the translated instrument through psychometric verification procedures.

Acknowledgment This research was supported by the Korea Workers' Compensation & Welfare Service Research Grants in 2023

	Process	period	Study participants
PLUS-M English-Korean Translation			
Stage 1	PLUS-M translation agreement with the original version author	January, 2023	Original version author
Stage 2	PLUS-M Korean translation began	February, 2023	One Rehabilitation physician One Researcher
Stage 3	1 st and 2 nd English-Korean Translation Compatibility Verification	February, 2023	Two Physical therapists One Prosthetist & Orthotist
Stage 4	Reverse Translation	March, 2023	One Translation specialist
Stage 5	Reverse Translation Verification	April, 2023	Original version author
Stage 6	3 rd English-Korean Translation Compatibility Verification	May, 2023	Two Rehabilitation physician One Professor in the department of prosthetics and Orthotics
Stage 7	PLUS-M Translation Completion	June, 2023	Original version author
Analysis of psychometric properties of PLUS-M/SF-12			
Stage 1	IRB approved	August, 2023	
Stage 2	Survey and Data Analysis	August to December, 2023	

Study process and period of study

Items	Original English version	Korean version
Item 1	Are you able to walk a short distance in your home?	집안에서 짧은 거리를 걸을 수 있습니까?
Item 4	Are you able to step up and down curbs?	도로 가장자리의 경계석(연석)을 오르내릴 수 있습니까?
Item 7	Are you able to walk across a parking lot?	주차장을 가로질러 걸을 수 있습니까?
Item 14	Are you able to walk over gravel surfaces?	자갈길을 걸을 수 있습니까?
Item 19	Are you able to move a chair from one room to another?	의자를 방에서 다른 방으로 옮길 수 있습니까?
Item 20	Are you able to walk while carrying a shopping basket in one hand?	한 손에 장바구니를 들고 걸을 수 있습니까?
Item 21	Are you able to keep walking when people bump into you?	혼잡한 곳에서 사람들과 가볍게 부딪혀도 계속 걸어갈 수 있습니까?
Item 26	Are you able to walk on an unlit street or sidewalk?	불빛이 없는 도로나 보도를 걸을 수 있습니까?
Item 31	Are you able to keep up with others when walking?	다른 사람들과 보행속도를 맞춰 함께 걸을 수 있습니까?
Item 35	Are you able to walk across a slippery floor?	미끄러운 바닥에서 걸을 수 있습니까?
Item 37	Are you able to walk down a steep gravel driveway?	가파른 자갈길을 내려갈 수 있습니까?
Item 44	Are you able to hike about 2 miles on uneven surfaces, including hills?	언덕이 포함된 울퉁불퉁한 길에서 3km 정도 산책할 수 있습니까?

Korean version of PLUS-M/SF-12

Characteristics	
Age (year), mean (SD) [min-max]	52.22±13.86 [22-73]
Height (cm), mean (SD) [min-max]	170.7±5.7 [160-184]
Weight(kg), mean(SD)[min-max]	73.7±14.9 [58-130]
Duration of time since amputation (year), mean (SD) [min-max]	7.25±6.58 [1-26]
Sex, male	32 (100)
Cause of amputation	
Traumatic	32 (100)
Ischemic	0 (0)
Tumour, Infection	0 (0)
Level of amputation	
Transfemoral	18 (56.2)
Transtibial	14 (43.8)
Affected side	
Right/Left	10 (31.2)/22 (68.8)
Occupation	
Yes/No	11 (33.4)/21 (65.6)
Use of assistive device	
Yes/No	9 (28.1)/23 (71.9)

General characteristics of the participants (n = 32)

Muscle Regeneration Effects at Different Melittin Concentrations in Rabbit Atrophied Muscle

Byeong-Churl Jang¹, Eun Sang Kwon², Yoon-Jin Lee³, Jae Ik Jung⁴, Yong Suk Moon⁵, Dong Rak Kwon^{4**}

Department of Molecular Medicine, College of Medicine, Keimyung University¹, Department of Medicine, College of Medicine, Keimyung University², Department of Biochemistry, College of Medicine, Soonchunhyang University³, Department of Rehabilitation Medicine, Catholic University of Daegu School of Medicine⁴, Department of Anatomy, Catholic University of Daegu School of Medicine⁵

Objective

This research aimed to explore the healing impacts of Melittin treatment on gastrocnemius muscle wasting caused by immobilization with a cast in rabbits.

Methods

Twenty-four rabbits were randomly allocated to four groups (Figure 1). The procedures included different injections: 0.2mL of normal saline to Group 1 (G1-NS); 4μg/kg of Melittin to Group 2 (G2-4μg/kg Melittin); 20μg/kg of Melittin to Group 3 (G3-20μg/kg Melittin); and 100μg/kg of Melittin to Group 4 (G4-100μg/kg Melittin) (Figure 2). Ultrasound was used to guide the injections into the rabbits' atrophied calf muscles following two weeks of immobilization via casting. Clinical measurements, including the length of the calf, the compound muscle action potential (CMAP) of the tibial nerve, and the gastrocnemius muscle thickness, were assessed. Additionally, cross-sectional slices of gastrocnemius muscle fibers were examined, and immunohistochemistry and Western blot analyses were performed following two weeks of therapy.

Results

The mean regenerative changes, as indicated by clinical parameters, in Group 4 were significantly more pronounced than in the other groups ($p < 0.05$).

Conclusion

Melittin therapy at a higher dosage can more efficiently activate regeneration in atrophied gastrocnemius muscle compared to lower doses of Melittin or normal saline.

Acknowledgment This work was financially supported by the Basic Science Research Program through the National Research Foundation of Korea (NRF) funded by the Ministry of Education, Science, and Technology (MEST) (2022R1A2C2091162).

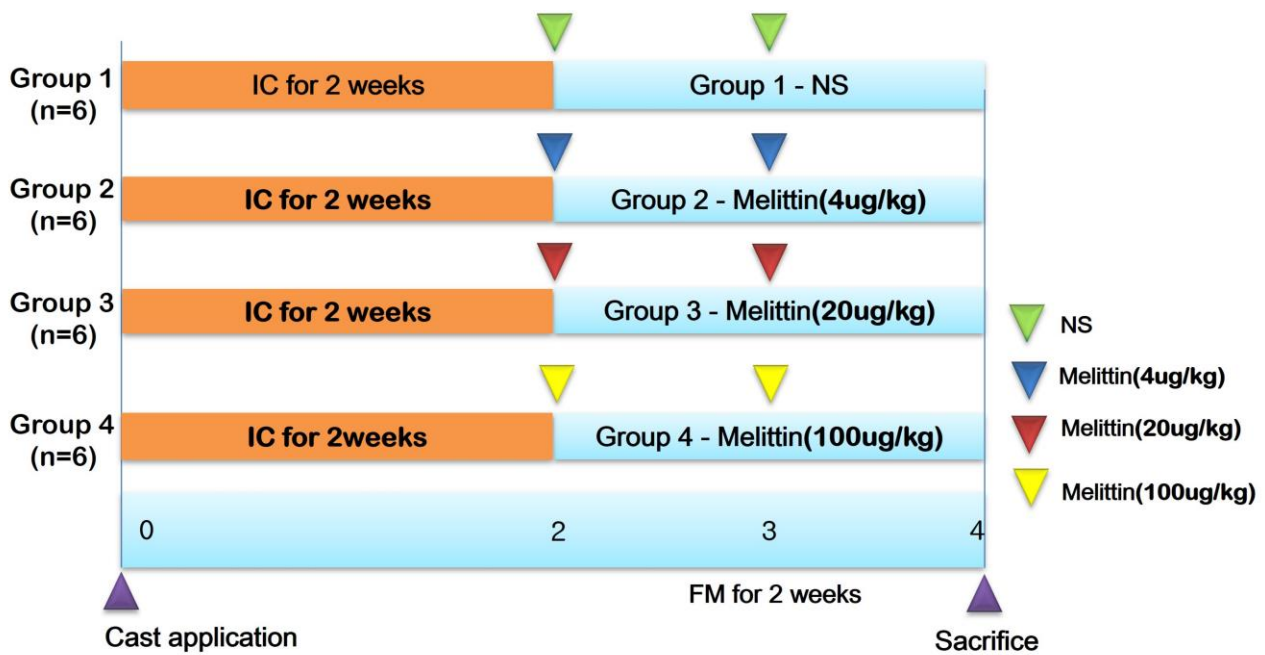


Figure 1. The study timeline involved 24 rabbits randomly assigned into four groups. Group 1 (G1) underwent immobilization by casting (IC) for two weeks, followed by daily injections of 0.2 mL normal saline for two weeks after cast removal (CR). Group 2 (G2) also experienced two weeks of IC, followed by daily injections of Melittin at a dose of 4 ug/kg for two weeks post-CR. Group 3 (G3) underwent the same initial two weeks of IC, followed by daily injections of Melittin at a dose of 20 ug/kg for two weeks after CR. Group 4 (G4) was subjected to two weeks of IC, followed by daily injections of Melittin at a dose of 100 ug/kg for two weeks post-CR. Definitions: IC, immobilized by cast; NS, normal saline; CR, cast removal.

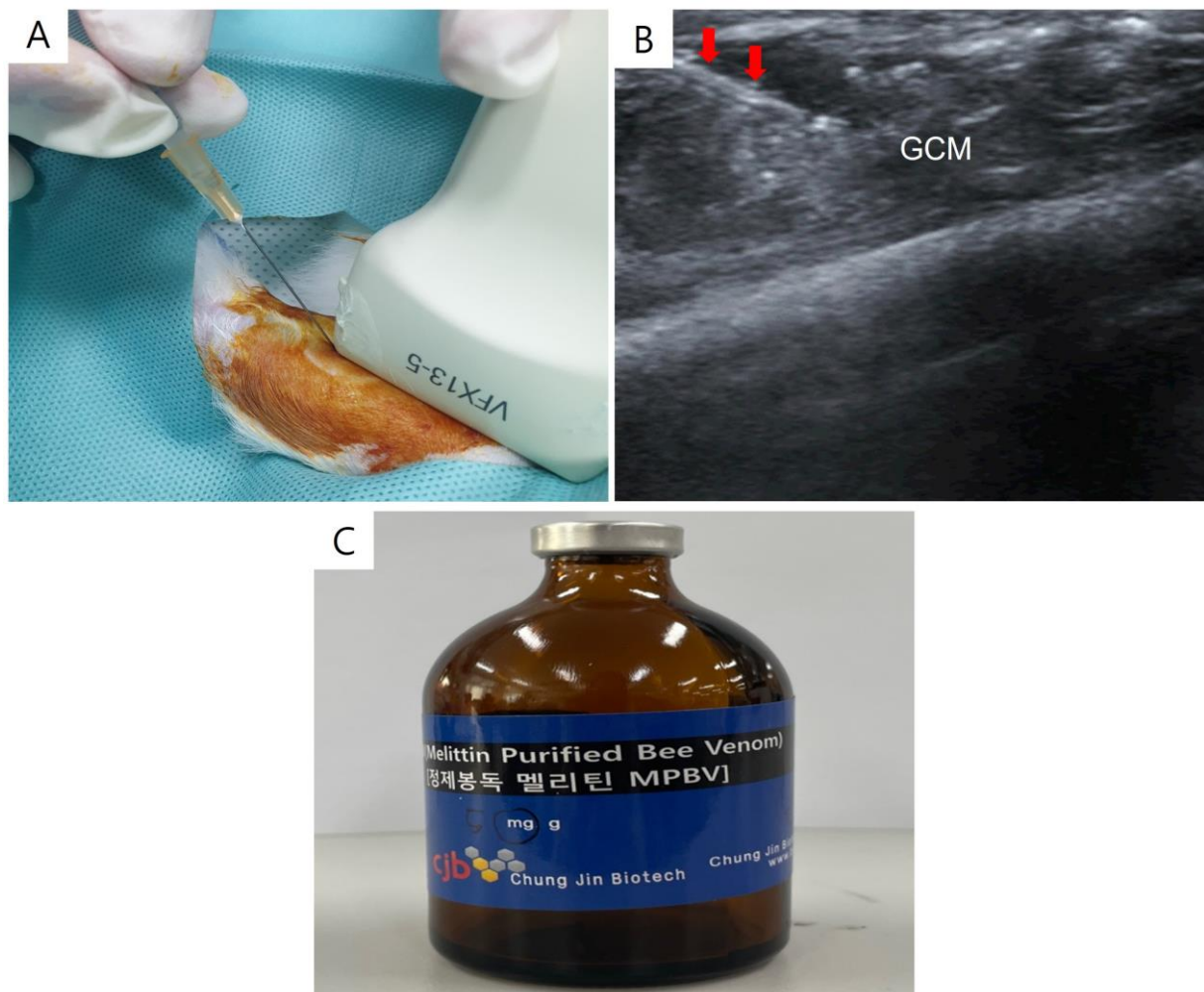


Figure 2. The longitudinal ultrasound image displays the process of injecting Melittin into a rabbit's right

gastrocnemius muscle. This procedure is guided by ultrasound, with the needle indicated by red arrows (A). The image also shows the gastrocnemius muscle (B) and the Melittin (C). GCM refers to the gastrocnemius muscle.

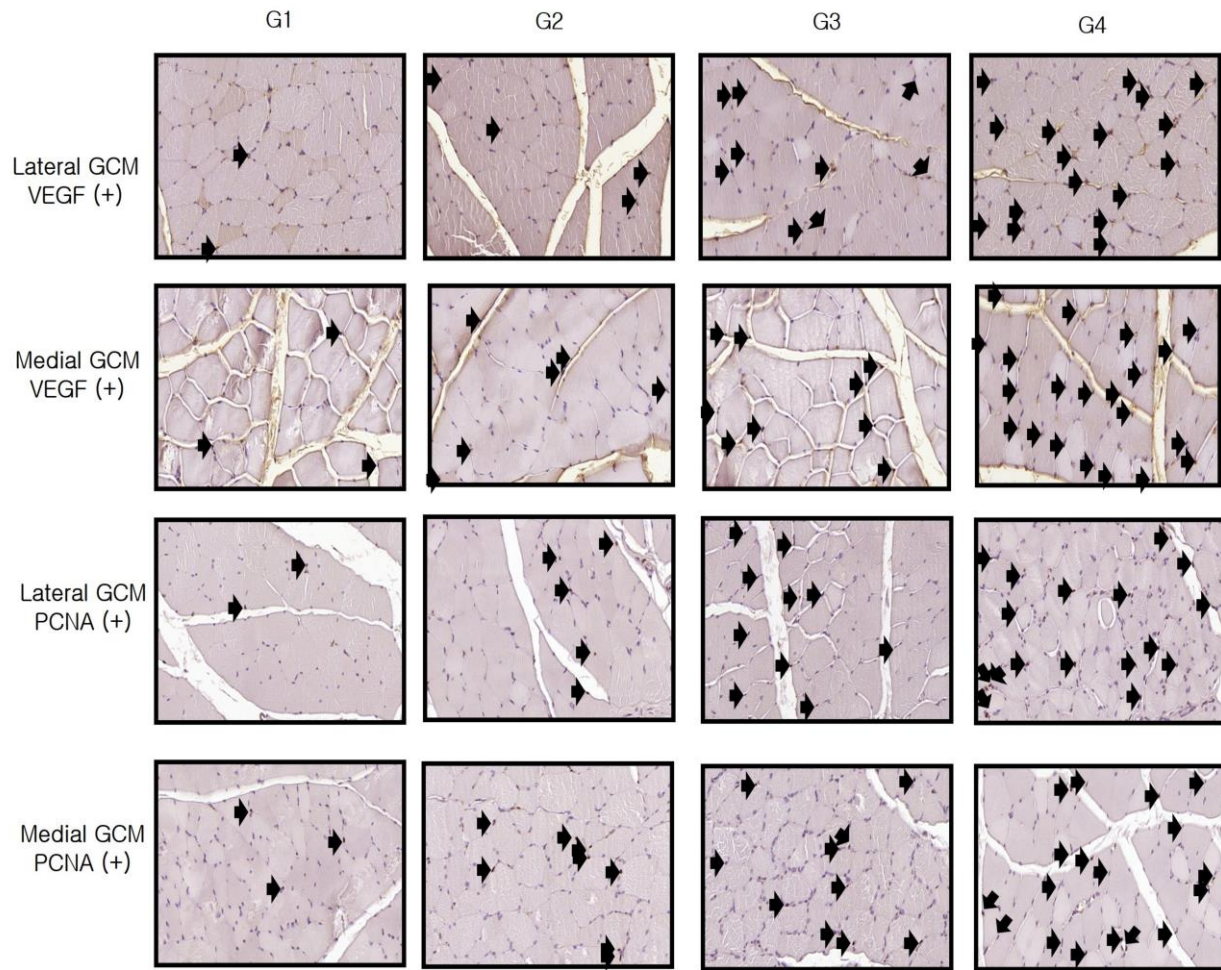


Figure 3. Immunohistochemical analysis of GCM (gastrocnemius muscle) fibers across the four groups involved examining immobilized GCM muscles stained with anti-VEGF and anti-PCNA antibodies. The number of cells or nuclei that were positive for VEGF and PCNA, identified by arrows, was counted, along with the total number of muscle fibers present in each image.

PLGA-Metformin-ICG Nanoparticles combined with Photothermal Therapy attenuate Joint inflammation

Su Hyun Lim¹, In Ah Kwon², Dongwoo Khang^{3†}, Youn Joo Kang^{4*†}

Department of Gachon Advanced Institute for Health Science & Technology (GAIHST), Gachon University, Incheon, 21999, South Korea¹, Lee Gil Ya Cancer and Diabetes Institute, Gachon University, Incheon 21999, South Korea², Department of Physiology, School of Medicine, Gachon University, Incheon 21999, South Korea³, Department of Rehabilitation Medicine, , Eulji Hospital, Eulji University School of Medicine, Seoul 01830, South Korea⁴

Objectives

Osteoarthritis (OA) and rheumatoid arthritis (RA). These diseases are characterized by persistent inflammation and hyperplastic invasive synovial formations in the joints. Inflammatory T cells and fibroblast-like synoviocytes (FLS) play a critical role on joint inflammation. Th-17 cells, a major type of inflammatory T cells, produce IL-17 and IL-22, cytokines that recruit neutrophils, monocytes, synovial fibroblasts and macrophages to the joints. This recruitment leads to increased joint inflammation and further production of Th-17 cells, creating a positive feedback loop. The significant reduction in joint inflammation in CIA mice model shows the importance of targeting Th-17 cells. Similarly, FLS in the inflamed synovium secrete inflammatory cytokines and proteases that degrade cartilage and lead to disease progression. Patients with arthritis develop a unique phenotype of FLS characterized by increased migration into the extracellular matrix, which exacerbates inflammation. This study aims to explore the therapeutic potential of targeting IL-22R and Th-17 cells using metformin-encapsulated polymeric nanoparticles in combination with photothermal therapy (PTT) to effectively reduce joint inflammation.

Materials and Methods

Polymeric nanoparticles were synthesized using poly(lactic-co-glycolic acid) (PLGA), metformin, and indocyanine green (ICG). The anti-inflammatory efficacy of metformin and ICG-encapsulated nanoparticles (PLGA-MET-ICG) combined with PTT was evaluated using fibroblast-like synoviocytes (FLS). The study included evaluation of physicochemical properties, real-time PCR and FACS analysis to measure the expression of IL-22R and Th-17-related markers.

Results

The combined treatment with PLGA-MET-ICG nanoparticles and photothermal therapy (PTT) effectively inhibits the polarization of Th-17 cells, thereby reducing joint inflammation and the associated inflammatory cytokine production in rheumatoid arthritis (Fig 1-a). The encapsulation of metformin and ICG in PLGA nanoparticles was confirmed by physicochemical analysis (Fig 1-b). FLS in which the expression of pro-inflammatory cytokines (IL-1 β , IL-6, TNF- α) was significantly reduced by treatment with PLGA-MET-ICG (Fig 1-c). Significantly, PLGA-MET-ICG combined with PTT significantly downregulated IL-22R expression (Fig 1-d). Th-17 cell differentiation in the spleen was subsequently reduced in the CIA mouse model (Fig 1-e).

Conclusion

This study demonstrates that targeting IL-22R and Th-17 cells using metformin and ICG-encapsulated polymeric nanoparticles in combination with PTT effectively attenuates joint inflammation. These findings highlight a novel therapeutic approach that combines the synergistic effects of drug repositioning and nanotechnology to more effectively treat joint inflammation.

Acknowledgment This work was supported by the Basic Science Research Program of the National Research Foundation of Korea (NRF- 2022M3A9H1014123 and NRF 2021R1F1A1056332).

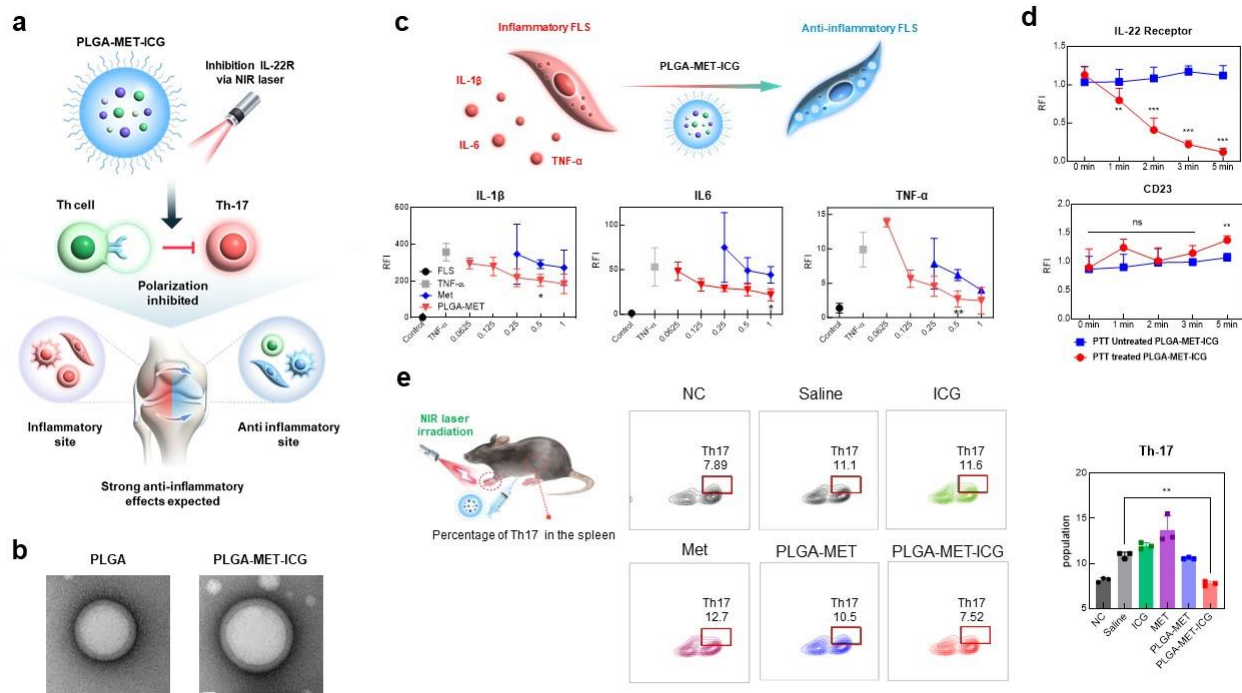


Figure 1

Highly Accurate AI Identification of 39 Rehabilitation Exercises Using IMU Data

Kyuwon Lee^{1*}, Shokhrukh Bibalaev², Yeji Jeong¹, Hyeon Hong¹, Jeong-Hyun Kim¹, Aehnon Lee¹, Hyeng-Kyu Park³, Seung-Don Yoo⁴, Shi-Uk Lee^{1,5†}

Seoul National University Boramae Medical Center, Department of Rehabilitation Medicine¹, AI Development Team, Rbiotech Co., Ltd.², Chonnam National University Hospital, Department of Rehabilitation Medicine³, Kyung Hee University Hospital at Gangdong, Department of Rehabilitation Medicine⁴, Seoul National University, Department of Physical Medicine & Rehabilitation, College of Medicine,⁵

Introduction

The advent of wearable technology has transformed the field of rehabilitation, offering objective measures of exercise performance. This study employs IMU sensor data to classify 39 types of musculoskeletal rehabilitation exercises using a Gated Recurrent Unit (GRU)-based deep learning model. Classifying these exercises accurately is crucial for monitoring patient adherence and the effectiveness of prescribed rehabilitation protocols.

Methods

IMU sensor data were collected from 86 individuals performing 39 different rehabilitation exercises. The raw data from the sensors were meticulously extracted and organized into an Excel format, ensuring systematic data for analysis (Figure 1). Several preprocessing steps were applied to prepare the data for modeling, including downsampling to standardize the time series lengths and normalization using a min-max scaler. A GRU-based model was then trained to classify the exercises. Key performance indicators such as test accuracy, precision, recall, and F1-score were used to evaluate the model's effectiveness.

Results

The GRU-based model demonstrated impressive performance, achieving a test accuracy of 98.6%. The model's precision, recall, and F1-score for each exercise class were also high, indicating robust classification capability across all exercise types (Table 1). Detailed performance metrics were tabulated (Table 2), showcasing the model's ability to handle a diverse set of movements with high accuracy.

Conclusion

The study confirms that IMU sensor data can be effectively used to classify a wide range of musculoskeletal rehabilitation exercises with high accuracy. This has significant implications for developing intelligent rehabilitation monitoring systems that provide real-time feedback to patients and clinicians. Future work will focus on expanding the dataset and exploring additional deep learning architectures to further enhance classification performance.

Discussion

This research highlights the potential of combining IMU sensor data with deep learning to improve rehabilitation outcomes. The high accuracy of the GRU model suggests that it can reliably distinguish between various exercises, which is essential for tailoring rehabilitation programs to individual patient needs. Additionally, the study underscores the importance of rigorous data preprocessing to ensure model effectiveness. Further research should investigate the application of this approach in real-world clinical settings and its impact on patient recovery trajectories.

Acknowledgment This research was supported by Culture, Sports and Tourism R&D Program through the Korea Creative Content Agency(KOCCA) grant funded by the Ministry of Culture, Sports and Tourism(MCST) in 2023(Project Name: Development of infrastructure linkage technology for community-based rehabilitation movements, Project Number: R202106001, Contribution Rate: 100%)

Table 1. List of Exercises and Their Corresponding Test Accuracies

No.	LIST OF EXERCISES	Accuracy
1	Anterior deltoid strength	1
2	Bent leg raise 2	0.99
3	Bird dog exercise	1
4	Bridge exercise	1
5	Crunch	0.99
6	Erector spinae exercise	0.97
7	Finger walk	1
8	Heel raise (in standing)	0.99
9	Heel slide (in sitting)	0.98
10	Hip abduction (in side-lying)	1
11	hip extension (in side-lying)	0.97
12	Hip flexion (with band in standing)	0.99
13	knee flexion (with gym ball)	0.99
14	Lawnmower exercise	0.99
15	Leg circling	0.98
16	Leg swing	0.99
17	Lunge exercise	1
18	Pectoralis minor stretching	0.95
19	Pendulum exercise	1
20	Posterior capsule stretching	0.99
21	Prone press-ups	1
22	Prone shoulder extension	0.97
23	reverse leg raise	0.99
24	Robbery exercise	0.98
25	Scapular active range of motion	0.97
26	Shoulder abduction (with band)	0.98
27	shoulder extension (with band)	0.95
28	shoulder external rotation (in side-lying)	1
29	shoulder external rotation (with band)	0.99
30	Shoulder flexion (in supine)	1
31	shoulder forward flexion (with band)	0.98
32	shoulder internal rotation (with band)	0.99
33	Side bridge	0.99
34	Side stepping	1
35	Sit to stand (reaching arms in front)	0.95
36	Squat	0.99
37	Straight leg raise	0.96
38	Tensor fascia latae stretching	0.99
39	Weight bearing & weight shifting	0.97

This table provides a detailed view of the model's performance across 39 different types of musculoskeletal rehabilitation exercises. The accuracies indicate how well the GRU-based model classified each exercise type, highlighting areas of high performance and potential opportunities for further improvement.

Table 1. This table provides a detailed view of the model's performance across 39 different types of musculoskeletal rehabilitation exercises. The accuracies indicate how well the GRU-based model classified each exercise type, highlighting areas of high performance and potential opportunities for further improvement.

Table 2. Performance Metrics for Each Class

No.	precision	recall	f1-score	support
1	0.99	0.99	0.99	200
2	0.97	0.99	0.98	189
3	0.99	1	1	165
4	0.99	1	0.99	191
5	1	0.99	1	230
6	0.98	0.97	0.98	188
7	0.99	1	0.99	174
8	0.99	0.99	0.99	148
9	0.95	0.98	0.96	165
10	1	1	1	158
11	0.98	0.97	0.97	91
12	0.98	0.99	0.98	91
13	1	0.99	0.99	214
14	0.99	0.99	0.99	178
15	0.96	0.98	0.97	109
16	0.98	0.99	0.98	155
17	1	1	1	215
18	0.98	0.95	0.96	131
19	1	1	1	173
20	0.99	0.99	0.99	195
21	1	1	1	185
22	1	0.97	0.99	110
23	0.96	0.99	0.98	198
24	0.99	0.98	0.99	174
25	0.99	0.97	0.98	169
26	0.98	0.98	0.98	129
27	0.98	0.95	0.97	102
28	1	1	1	164
29	0.97	0.99	0.98	128
30	0.99	1	1	163
31	0.98	0.98	0.98	128
32	0.99	0.99	0.99	143
33	1	0.99	1	185
34	0.98	1	0.99	186
35	0.99	0.95	0.97	182
36	0.95	0.99	0.97	192
37	0.99	0.96	0.97	183
38	0.97	0.99	0.98	192
39	1	0.97	0.98	93

The following table presents detailed performance metrics including precision, recall, F1-score, and support for each of the 39 classes. These metrics provide comprehensive insights into the GRU-based model's classification performance, helping to identify strengths and areas for improvement in recognizing various musculoskeletal rehabilitation exercises.

Table 2. The following table presents detailed performance metrics including precision, recall, F1-score, and support for each of the 39 classes. These metrics provide comprehensive insights into the GRU-based model's classification performance, helping to identify strengths and areas for improvement in recognizing various musculoskeletal rehabilitation exercises.

Calf Weakness and Its Association with Redundant Nerve Roots in Lumbar Spinal Stenosis

WONBIN KIM^{1*}, SUN G. Chung^{1†}

Department of Rehabilitation Medicine, Seoul National University Hospital¹

Abstract

Background: Redundant nerve roots (RNR) are often observed in imaging of lumbar spinal stenosis (LSS) patients, yet their clinical significance, particularly regarding calf weakness (CW), remains unclear. This study investigates the association between RNR and CW in LSS patients.

Methods

This retrospective study included 47 patients with LSS. The association between RNR and various factors, including CW, was analyzed using Fisher's exact test and logistic regression. Data were analyzed using SAS 9.4 and R 4.3.2 with the logistic package. Factors such as sex, age category, level of stenosis, KSL (Key stenotic level), shape, extension, and direction were evaluated for their association with RNR presence.

Results

Significant associations were found between RNR presence and several factors at the 5% significance level: level of stenosis ($p = 0.044$), CW ($p = 0.023$), KSL ($p < 0.001$), shape ($p < 0.001$), extension ($p < 0.001$), and direction ($p < 0.001$). Logistic regression indicated that the presence of CW increased the likelihood of RNR by approximately 7.73 times (95% CI: 1.51-77.78, $p = 0.012$). Other significant factors included KSL, shape, extension, and direction, each demonstrating strong associations with RNR presence. Due to separation issues and a small number of events, penalized maximum likelihood estimation (Firth method) was used for analysis.

Conclusions

The study highlights a significant association between CW and RNR in LSS patients. These findings suggest that CW can be a strong predictor of RNR presence, underscoring the need for clinicians to consider these factors in the diagnosis and management of LSS.

Keywords: Lumbar spinal stenosis, Calf weakness, Redundant nerve roots, Logistic regression, Penalized maximum likelihood estimation

Dose-Dependent Effects of Dexamethasone on Tendon-Derived Stem Cells: Implications for Tendon Differentiation Function

Yong-Taek Lee^{1,2*†}, Min-Jeong Kim³, Do Hyun Kwon², Kyung Jae Yoon¹, Chul-Hyun Park¹

Department of Physical and Rehabilitation Medicine, Kangbuk Samsung Hospital, Sungkyunkwan University School of Medicine¹, Medical Research Institute, Kangbuk Samsung Hospital, Sungkyunkwan University School of Medicine², Medicinal Bioconvergence Research Center, College of Pharmacy, Seoul National University³

Purpose

Tendinopathy presents a significant clinical challenge characterized by chronic pain and tendon dysfunction. Pathologic findings of tendinopathy show disorganization of collagen fibers and chondroid metaplasia, where tendon tissue undergoes cartilage-like changes. Tendon-derived stem cells (TDSCs) play a crucial role in tendon renewal and homeostasis, contributing significantly to the repair and maintenance of tendon structure. Impairment of TDSC function is linked to tendon degeneration and tendinopathy development. Corticosteroids are widely used in the treatment of tendinopathy, and its harmful effects on tendon tissue are well-documented. However, the mechanism remains unclear. The purpose of this study is to investigate the effect of dexamethasone treatment on TDSC function.

Subjects and Methods

In this in-vitro study, TDSCs were isolated from rat Achilles tendons and exposed to varying concentrations of dexamethasone (0, 0.1, 1, 10, 100, and 1000 nM) for 3 and 7 days. Flow cytometry analysis was used to confirm the successful isolation of TDSCs. Cell viability was assessed using MTT assays. RNA Expression of tenogenic markers (scleraxis, collagen type I, tenomodulin), chondrogenic marker (aggrecan), adipogenic marker (C/EBP), and osteogenic marker (ALP) were evaluated using reverse transcription polymerase chain reaction (RT-PCR) analyses.

Results

Flow cytometry analysis showed that the isolated TDSCs were positive for the stem cell marker CD90 and were negative for the hematopoietic marker CD45. This characterization confirms the successful isolation of TDSCs from rat Achilles tendons.

MTT assays showed dexamethasone significantly decreased cell viability in a dose-dependent manner. At day 7, higher dexamethasone concentrations were linked to reduced expression of all tenogenic markers (scleraxis, collagen type I, tenomodulin) (Figure 1, 2) and increased expression of chondrogenic marker aggrecan (Figure 3), adipogenic marker C/EBP, and decreased expression of osteogenic marker ALP. The increase in chondrogenic marker aggrecan suggests a shift towards chondroid metaplasia, aligning with pathologic findings in tendinopathy.

Notably, in tenogenic marker collagen type I, tenomodulin and chondrogenic marker aggrecan, the results from the 7-day experiment showed more pronounced effects compared to the 3-day experiment, indicating that the detrimental effects of dexamethasone on TDSCs are more significant with longer exposure durations.

Conclusion

These findings demonstrate the detrimental effects of dexamethasone on tendon health by impairing tenogenic pathways of TDSC function and promoting the chondrogenic pathway, which could contribute to tendon degeneration. While dexamethasone has therapeutic potential, its harmful effects necessitate careful consideration of dosage and application duration. This study provides insights for developing safer therapeutic protocols for tendinopathy using corticosteroids. Further in-vivo studies and clinical trials are necessary to validate these results.

Acknowledgment This work was supported by the National Research Foundation (NRF) of the Republic of Korea (NRF-2022R1A2C1010515).

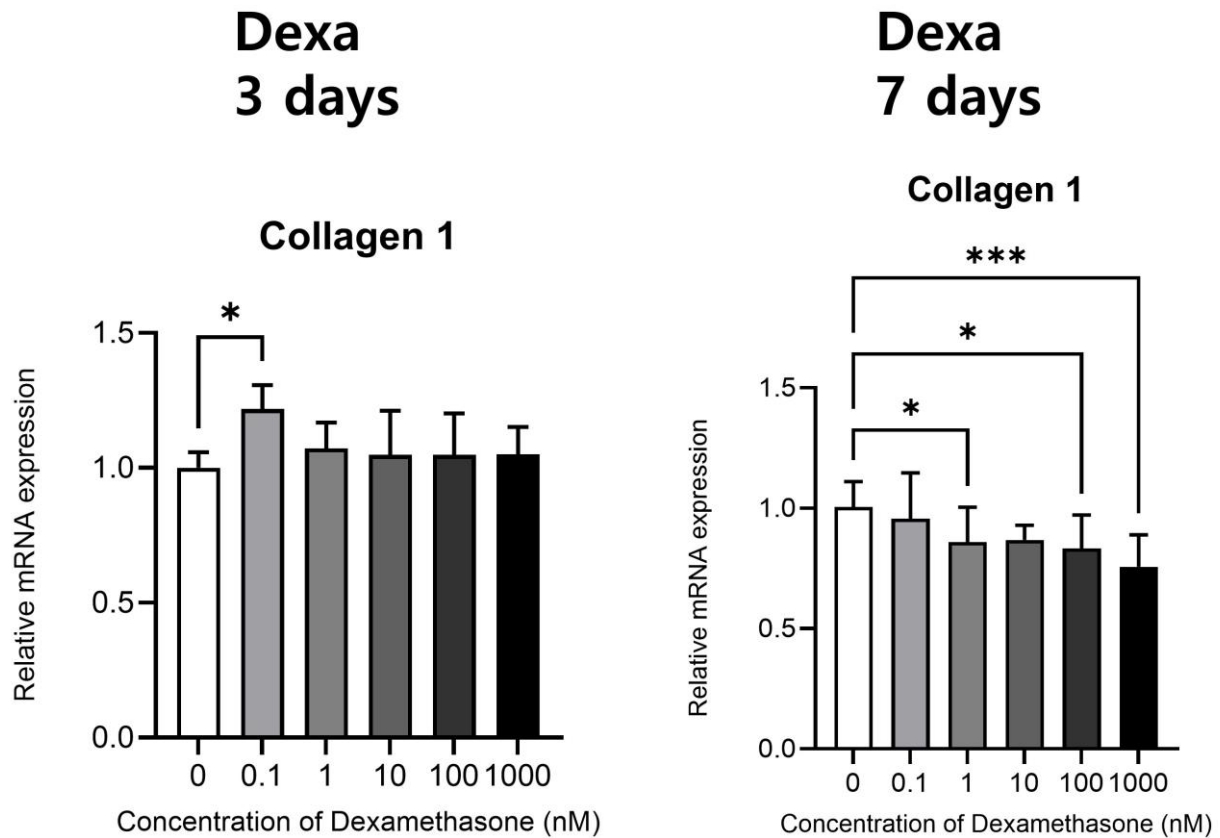


Figure 1: Effect of Dexamethasone on Tenogenic Marker (Collagen I). Relative mRNA expression levels of tenogenic marker Collagen I in TDSCs treated with varying concentrations of dexamethasone for 3 days and 7 days. A dose-dependent decrease in tenogenic marker Collagen I is observed. Notably, the results from the 7-day experiment showed more pronounced effects compared to the 3-day experiment. Data are represented as mean \pm SD. * $p < 0.05$, ** $p < 0.01$, *** $p < 0.001$ and **** $p < 0.0001$ Collagen I; collagen type I,

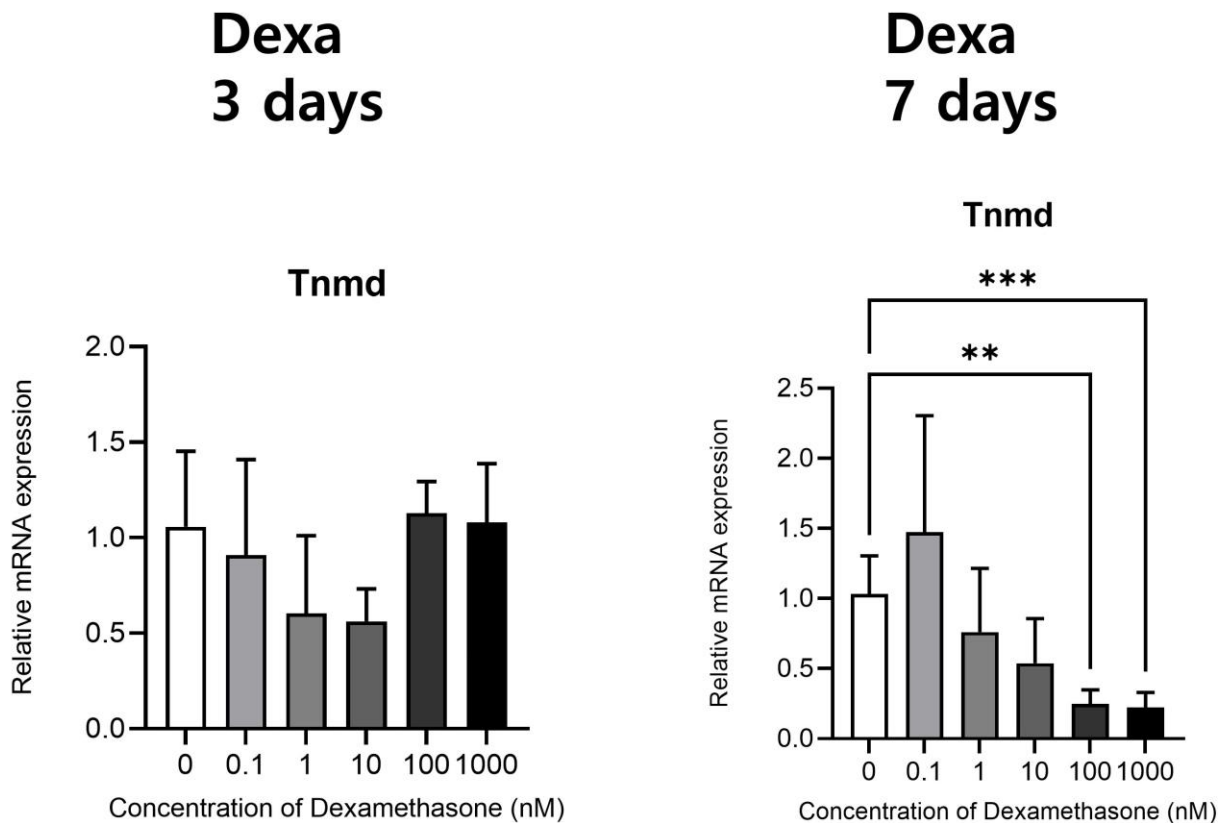


Figure 2: Effect of Dexamethasone on Tenogenic Marker (Tnmd). Relative mRNA expression levels of tenogenic marker Tnmd in TDSCs treated with varying concentrations of dexamethasone for 3 days and 7 days. A dose-dependent

decrease in tenogenic markers is observed. Notably, the results from the 7-day experiment showed more pronounced effects compared to the 3-day experiment. Data are represented as mean \pm SD. * $p < 0.05$, ** $p < 0.01$, *** $p < 0.001$ and **** $p < 0.0001$ Tnmd; tenomodulin,

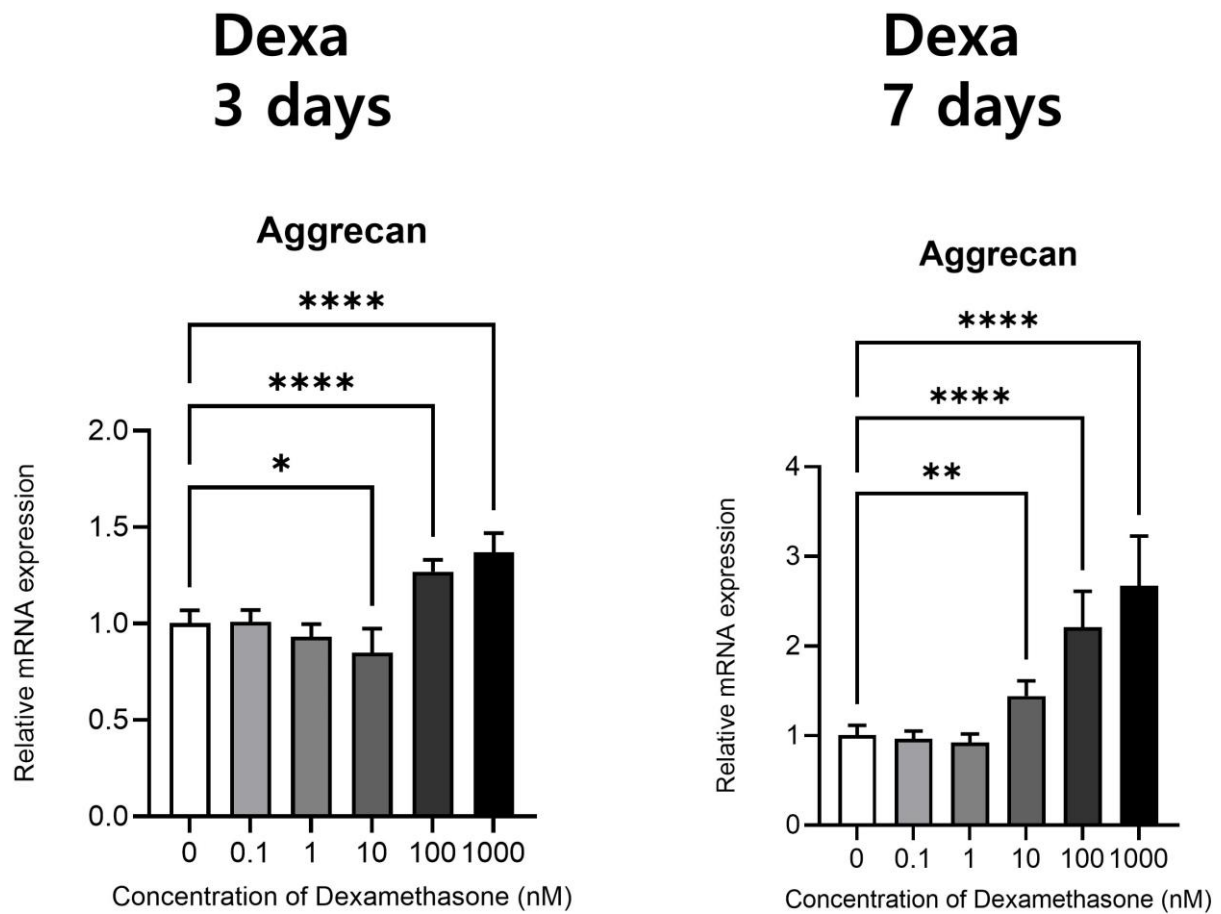


Figure 3: Effect of Dexamethasone on Chondrogenic Marker (Aggrecan) Relative mRNA expression levels of chondrogenic marker aggrecan in TDSCs treated with varying concentrations of dexamethasone for 3 days and 7 days. A dose-dependent increase in aggrecan is observed. Notably, the results from the 7-day experiment showed more pronounced effects compared to the 3-day experiment. Data are represented as mean \pm SD. * $p < 0.05$, ** $p < 0.01$, *** $p < 0.001$ and **** $p < 0.0001$

Characteristics of Dysphagia after Anterior Cervical Discectomy and Fusion

Yura Goh^{1*}, Hyun Jun Jang², Yoon Ghil Park¹, Sooin Lee¹, Joo Eun Park¹, Jinyoung Park^{1†}

Department of Rehabilitation Medicine, Gangnam Severance Hospital, Yonsei University College of Medicine, Seoul, Korea¹, Department of Neurosurgery, Spine and Spinal Cord Institute, Gangnam Severance Hospital, Yonsei University College of Medicine, Seoul, Korea²

Introduction

Anterior cervical discectomy and fusion (ACDF) is a type of neck surgery that involves removing a damaged disc to relieve pressure on the spinal cord or nerve roots and alleviate corresponding pain, weakness, numbness, and tingling. During this surgical procedure, structures involved in swallowing, such as the anterior neck muscles, nerves innervating these muscles, and the posterior pharyngeal wall, are inevitably damaged. As a result, swallowing dysfunction often accompanies the postoperative period. This study aims to observe and report on the patterns and severity of dysphagia that occur following ACDF.

Methods

This retrospective observational study screened patients who underwent VFSS due to dysphagia symptoms after ACDF between September 2023 and April 2024 in a single tertiary hospital. The VFSS protocol followed this order: semisolid (International Dysphagia Diet Standardisation Initiative [IDDSI] 3, 1 spoon), semisolid (IDDSI 2, 1 spoon), sesame porridge (IDDSI 4, 1 spoon), small liquid (IDDSI 0, 5 mL), and large liquid (IDDSI 0, 15 mL). If a serious aspiration event without cough reflex occurred, the VFSS was ceased in that step. The severity of swallowing problem was scored using the Videofluoroscopic Dysphagia Scale (VDS), which ranges from 0 to 100, with 0 indicating normal function. The severity of aspiration was rated using the Penetration-Aspiration Scale (PAS).

Results

A total of 11 VFSS videos from 11 patients were reviewed, along with their clinical medical records. The demographic, preoperative, perioperative, and postoperative characteristics are listed in Table 1. Six patients had myelopathy preoperatively. The average number of fixation levels was 2.4. The average period from surgery to VFSS was 2.1 days. By analysis of VFSS video, all patients had no abnormal findings in oral phase of swallowing, however, all 11 patients showed abnormal pattern in pharyngeal phase, resulting in the average VDS score 26.1 (Table 2). Specifically, 10 out of 11 patients showed decreased laryngeal elevation, 9 patients exhibited pharyngeal wall coating, and 8 and 7 patients had vallecular and piriform sinus residue after swallowing, respectively. The average PAS score was 2.2, with 6 patients showing penetration and 1 patient showing aspiration (Table 3). Mostly, the penetration or aspiration occurred during the swallowing event, while 1 patient exhibited a post-swallowing event.

Conclusions

Dysphagia after ACDF tends to be underestimated, leading clinicians to often overlook patients' discomfort. However, dysphagia is a disturbing symptom that can cause aspiration and is confined to the pharyngeal phase. Therefore, education on exercises and compensatory techniques is needed to manage the post-ACDF dysphagia based on its unique characteristics. Further data accumulation will aid in developing an effective strategy.

Table 1. Patients' characteristics

Characteristics (N=11)	N (%) or mean (SD)
1. Demographic characteristics	
Sex, N(%)	
Male	7 (63.6)
Female	4 (36.3)
Age, yr	60.2 (13.5)
Height, cm	163.9 (8.6)
Weight, kg	63.7 (7.7)
Body mass index, kg/m ²	21.3 (7.1)
2. Preoperative characteristics	
Diagnosis	
Herniated cervical disc	11 (100.0)
Ossification of posterior longitudinal ligament	1 (9.1)
Combined medical condition	
Diabete mellitus	5 (45.5)
Lesions in CNS	
Brain lesion	0 (0.0)
Myelopathy	6 (54.5)
Preoperative neurologic condition, N (%)	
Preoperative weakness	10 (90.9)
Preoperative sensory deficit	6 (54.5)
Preoperative dysphagia	0 (0.0)
3. Perioperative characteristics	
No. of fixation level	2.4 (0.5)
Fixation level, N (%)	
C3-4	2 (18.2)
C4-5	3 (27.3)
C5-6	2 (18.2)
C6-7	1 (9.1)
C4-5-6	1 (9.1)
C5-6-7	3 (27.3)
Operation duration, min	99.5 (31.4)
4. Postoperative characteristics	
Post-surgery to VFSS period	2.1 (0.8)

Table 1. Patients' characteristics

Table 2. Videofluoroscopic swallowing findings

Videofluoroscopic swallowing findings	Score, mean (SD)	No. of dysfunction (%)
Oral phase		
Lip closure	0.0 (0.0)	0.0 (0.0)
Bolus formation	0.0 (0.0)	0.0 (0.0)
Mastication	0.0 (0.0)	0.0 (0.0)
Apraxia	0.0 (0.0)	0.0 (0.0)
Tongue to palate contact	0.0 (0.0)	0.0 (0.0)
Premature bolus loss	0.0 (0.0)	0.0 (0.0)
Oral transit time	0.0 (0.0)	0.0 (0.0)
Pharyngeal phase		
Triggering of pharyngeal swallow	0.8 (1.8)	2 (18.2)
Vallecular residue	2.6 (2.2)	8 (72.7)
Laryngeal elevation	8.2 (2.7)	10 (90.9)
Pyriform sinus residue	2.9 (2.3)	7 (63.6)
Coating of pharyngeal wall	7.4 (3.6)	9 (81.8)
Pharyngeal transit time	0.6 (1.8)	1 (9.1)
Aspiration	3.8 (3.0)	7 (63.6)
Esophageal phase		
Esophageal peristalsis		7 (63.6)
VDS, oral phase subscore	0.0 (0.0)	
VDS, pharyngeal phase subscore	26.1 (8.4)	
VDS, total score	26.1 (8.4)	

Table 2. Videofluoroscopic swallowing findings

Table 3. Aspiration after ACDF

Parameters	N (%)
Penetration-aspiration scale (PAS) score	
1	4 (36.4)
2	5 (45.5)
3	1 (9.1)
4	0 (0.0)
5	0 (0.0)
6	0 (0.0)
7	1 (9.1)
8	0 (0.0)
Aspiration type	
Pre-swallowing aspiration	0 (0.0)
During-swallowing aspiration	6 (54.5)
Post-swallowing aspiration	1 (9.1)
Aspirate	0.0 (0.0)
Solid	0.0 (0.0)
Semisolid	0.0 (0.0)
Liquid	7 (63.6)
5 mL	1 (9.1)
15 mL	6 (54.5)

Table 3. Aspiration after ACDF

Effects of robot training on hand function and scars in patients with hand dysfunction after burns

Seung Yeol Lee², Yoon Soo Cho¹, Cheong Hoon Seo¹, Jisu Seo¹, So Young Joo^{1*†}

Department of rehabilitation medicine, Hangang Sacred Heart Hospital, College of Medicine Hallym University¹,
Department of rehabilitation medicine, College of Medicine, Soonchunhyang University Hospital, Bucheon²

Introduction

Hands are the most frequent burn injury sites. Appropriate rehabilitation is essential to ensure good functional recovery. The aim of this study was to investigate the effects of EMG driven robotic rehabilitation on hand functions and skin characteristics of patients with nerve damage caused by burns.

Methods

A randomized controlled, single blind trial recruited thirty six patients with hand dysfunction after burn injury. The participants were randomly allocated to experimental group (EG) and control group (CG) for 5 days a week and totally 60 sessions for 12 weeks. The EG received robotic assisted hand training with the EMG-driven exoskeleton hand robot (Hand of Hope[®].Rehab-Robotics Company) and conventional occupational therapy, 60 sessions over 12 weeks. The CG performed conventional occupational therapy, including hand range of motion (ROM) exercises and hand function training twice a day for 12 weeks. Outcome measures were as follows: 10-point visual analog scale for pain, Jebsen-Taylor hand function test, grip strength, Purdue Pegboard test, joint ROMs, ultrasound measurement of scar thickness, and skin characteristics before and immediately after 12 weeks of treatment.

Results

No significant inter-group difference was noted after the initial evaluation ($P > 0.05$). More significant improvements were found in the EG than in the CG in terms of the extension ROMs of hand joints, the JTT scores (writing, small, and light), and skin characteristics (skin distensibility) ($P < 0.05$). Other measured outcomes did not differ between the two groups after the treatment.

Conclusion

In this study, improvement in motor functions, joint ROMs, and skin characteristics were found in both groups (EG and CG groups). In EG including EMG-driven robotic training, significant improvement in joint ROMs due to increased scar distensibility was confirmed.

Acknowledgment Translational Research Program for Rehabilitation Robots (#NRCTR-EX24003), National Rehabilitation Center Ministry of Health and Welfare, Korea

Radiation-free thoracolumbar alignment screening device using real-time 3D depth camera

Doyoung Kim^{1*}, Sanghoon Shin¹, Min-Chul Paek¹, Sanghyun Jee¹, Jung Hyun Park^{1,2,3†}

Department of Rehabilitation Medicine, Gangnam Severance Hospital, Yonsei University College of Medicine, Seoul, Republic of Korea¹, Department of Integrative Medicine, The Graduate School, Yonsei University College of Medicine, Seoul, Republic of Korea², Department of Medical Device Engineering and Management, The Graduate School, Yonsei University College of Medicine, Seoul, Republic of Korea³

Introduction

Back pain is a prevalent issue among modern individuals, often linked to musculoskeletal disorders. It frequently results from poor posture which leads to histological damage and abnormal vertebral alignment. Assessment of spinal alignment is crucial and can be performed through physical examinations such as inspection, palpation or imaging techniques like X-ray, CT, and MRI. However, imaging modalities have inherent limitations. X-rays pose a radiation risk, while CT and MRI are spatially constrained and typically performed in a supine position, limiting their efficacy in spinal assessment. Recently, a real-time 3D depth camera has been developed to address these limitations. This study aims to evaluate the accuracy of the real-time 3D depth camera in assessing 'thoracolumbar alignment' by comparing its measurements with X-ray (EOS) imaging, particularly focusing on back pain, a common musculoskeletal complaint.

Material & Methods

From November 2023 to June 2024, EOS and 3D Depth Camera images sets were collected from patients at our Rehabilitation Medicine department. Using MG Solution's 'Motiphysio Expert' (Healthcare Device), 3D depth camera images were captured in four postures: Adam's posture, standing, back standing, and side standing (Figure 1). Vertebral Centroid Measurement (VCM) was employed to measure anterior-posterior (AP) and lateral vertebral alignment (Figure 2). VCM involves calculating the angle formed by an imaginary line connecting the centroids of vertebral bodies. EOS images provided centroid measurements for 17 vertebrae (12 for thoracic level, and 5 for lumbar level), while corresponding coordinates were derived from 3D depth camera datas. To enhance the accuracy of deep learning, the data set was augmented using subject data augmentation techniques. These amplified data were randomly allocated. Deep learning was performed on 80% of the amplified data, correlating depth images with EOS values to develop an algorithm for estimating thoracolumbar alignment in 3D depth camera images. The algorithm's effectiveness was validated using the remaining 20% of subjects through 'Pearson's correlation analysis.'

Results

We obtained data from a total of 580 sets of EOS and 3D depth camera images. We expanded the data fivefold to obtain a total of 2,900 data points with random allocation, and 80% of them were used for deep learning. Pearson correlation analysis revealed a high positive correlation between 3D depth camera images and EOS results for the remaining data, with correlation coefficients of 0.9780 for anterior spine prediction and 0.9230 for lateral spine prediction (Figure 3).

Conclusion

3D depth camera imaging exhibits a high degree of accuracy and concordance with EOS imaging in assessing thoracolumbar alignment. This technology offers a viable alternative for spinal alignment evaluation, free from the radiation exposure and spatial limitations inherent to traditional imaging methods.

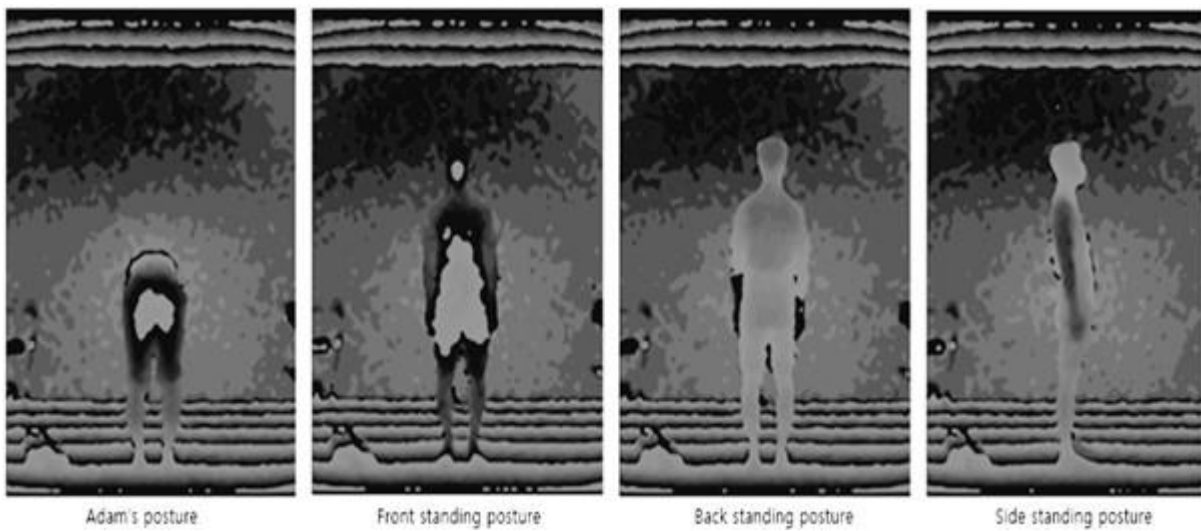


Fig 1. Four postures captured by the 3D depth camera (moiré image) from the 'Motiphysio Expert' (Healthcare Device)

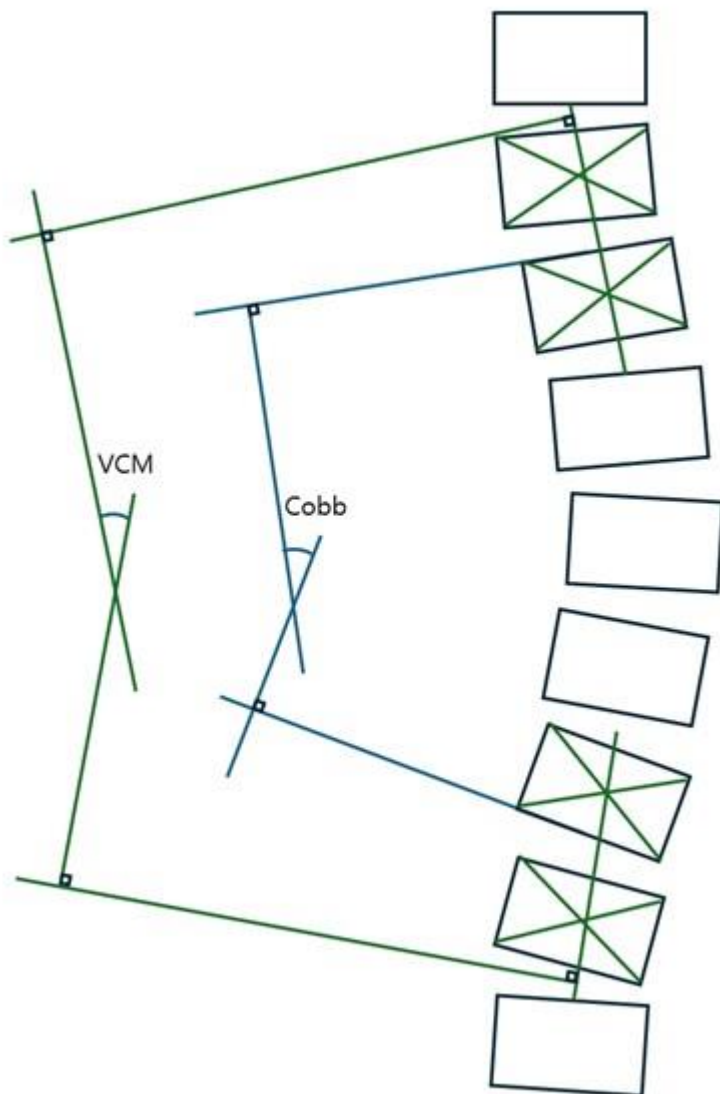
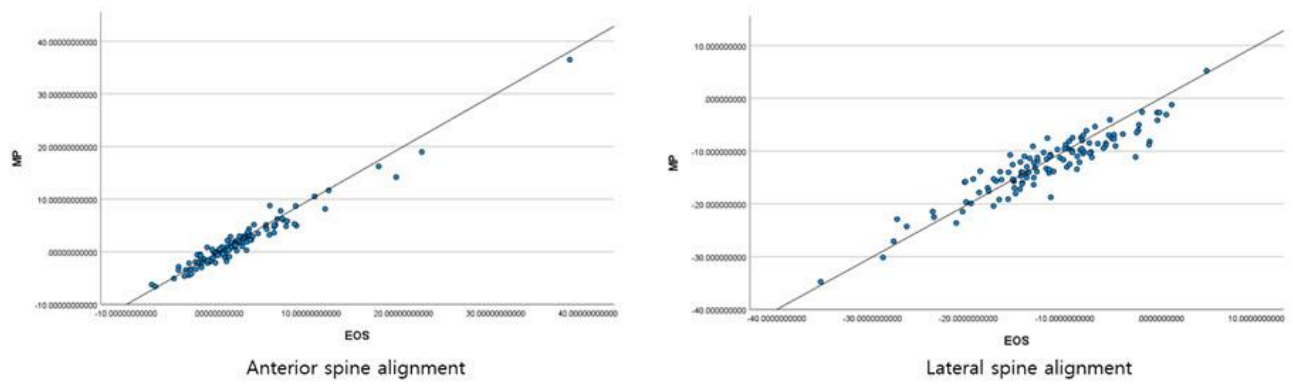


Fig 2. The Vertebral Centroid Measurement (VCM) method used for assessing thoracolumbar alignment



*MP: Motiphysio (3D depth camera)

Fig 3. Pearson correlation analysis between EOS and 3D depth camera images (moire images) for thoracolumbar alignment

Changes of muscle contractile properties after acute static stretching using TMG in sarcopenia

Jeong-Hun Bae^{1,2,3*}, Hyo-Seong Yeo^{2,3,4}, Jae-Young Lim^{2,3,4†}

Department of Health Science and Technology, Seoul National University¹, Department of Rehabilitation Medicine, Seoul National University Bundang Hospital², Aging & Mobility Biophysics Laboratory, Seoul National University Bundang Hospital³, Seoul National University Institute on Aging, Seoul National University⁴

Purpose

Sarcopenia refers to the progressive loss of skeletal muscle mass, strength, and function that occurs with aging. Static stretching is a type of stretching exercise where a muscle or group of muscles is gradually lengthened and it is commonly used to improve flexibility, increase range of motion in joints, and reduce muscle tension. However, effects of static stretching in contractile properties in aging muscle remain unclear. Therefore, the objective of the study was to investigate the changes of muscle contractile properties after acute static stretching using tensiomyography (TMG) in sarcopenia.

Method

Forty-six participants were divided into a young (age:20-35, n=20), a healthy old (age:60-85, n=20) and sarcopenia (age:60-85, n=6). Grip strength, physical performance and body composition assessments were performed. Muscle strength, power, endurance and eccentric force of lower limb were measured by isokinetic tests. TMG is a non-invasive method to determine contractile properties of skeletal muscles. TMG contractile properties measured were maximum radial displacement (Dm), delay time (Td), contraction time (Tc), sustain time (Ts) and relaxation time (Tr) on the left vastus lateralis (VL) and right biceps femoris (BF).

Results

Grip strength was significantly different between young and sarcopenia group. SPPB score was significant difference between young, healthy old and sarcopenia groups. Muscle strength, power and endurance were significantly lower in sarcopenia group compared with young and old group. Eccentric force was not significantly different in all groups. In young, healthy old, sarcopenia groups, a significant increase was observed in Dm of VL after static stretching. However, Dm of BF was not significantly different in all groups after static stretching. In young group, Ts and Tr of BF were significantly decreased. In healthy old group, a significant difference was found in Td, Tc and Ts of BF after static stretching. In sarcopenia group, Td and Tc of VL were significantly different after static stretching. Among all groups with aging and sarcopenia, Tc of VL was significantly different between young and old group. Dm and Vc of VL was significantly different between young and old, sarcopenia group. Tc, Dm, Vc were significantly different between young, old and sarcopenia group.

Conclusion

We found muscle strength, power and endurance were decreased in aging. Also, we found Dm was affected in VL in all groups after stretching. Therefore, acute static stretching is considered to alter VL muscle stiffness regardless of aging or sarcopenia.

			Pre(스트레칭 전)	Post(스트레칭 후)				Pre(스트레칭 전)	Post(스트레칭 후)				Pre(스트레칭 전)	Post(스트레칭 후)
Young	외측광근 (VL)	Td	23.43±3.18	23.38±1.70	Healthy old	외측광근 (VL)	Td	23.81±2.28	24.22±2.27	Sarcopenia	외측광근 (VL)	Td	23.39±1.63	<u>25.36±1.75*</u>
		Tc	24.56±2.92	25.12±3.95			Tc	<u>28.45±9.77**</u>	29.60±12.22			Tc	25.02±1.74	<u>27.44±2.24*</u>
		Ts	98.22±55.04	90.32±36.29			Ts	123.75±45.34	145.20±57.13			Ts	139.61±42.88	163.61±19.69
		Tr	64.26±54.61	60.18±35.39			Tr	83.82±43.84	103.33±57.67			Tr	102.72±38.74	118.50±23.06
		Dm	5.62±1.62	<u>6.11±1.57*</u>			Dm	<u>5.31±1.59#</u>	<u>5.64±1.74*</u>			Dm	<u>4.26±0.94#</u>	<u>5.29±1.46*</u>
		Vc	0.18±0.06	0.19±0.05			Vc	<u>0.16±0.06#</u>	0.17±0.06			Vc	<u>0.13±0.02#</u>	0.15±0.04
	대퇴 이두근 (BF)	Td	23.97±3.97	23.74±3.95		대퇴 이두근 (BF)	Td	25.14±2.72	<u>24.35±2.52*</u>		대퇴 이두근 (BF)	Td	26.33±1.12	26.23±1.40
		Tc	33.76±15.74	37.45±16.82			Tc	35.62±39.77	<u>39.77±12.81*</u>			Tc	<u>46.54±10.30##</u>	46.44±13.06
		Ts	229.36±54.49	<u>170.80±57.38*</u>			Ts	229.95±37.68	<u>186.77±28.39*</u>			Ts	209.05±23.21	197.61±46.75
		Tr	84.90±42.80	<u>50.21±28.14*</u>			Tr	81.26±29.43	67.41±32.82			Tr	95.75±28.74	84.96±51.50
		Dm	4.11±1.81	4.32±0.03			Dm	5.35±2.82	5.53±2.36			Dm	<u>9.47±3.07##</u>	9.89±3.50
		Vc	0.10±0.03	0.09±0.02			Vc	0.12±0.06	0.11±0.05			Vc	<u>0.16±0.06##</u>	0.17±0.05

* : significantly different between pre and post stretching

** : significantly different between young and old

: significantly different between young and old, sarcopenia

: significantly different between young, old and sarcopenia

Table 1. Comparison TMG contractile properties between pre and post stretching in young, old, sarcopenia groups

Effect of Wando Marine Healing Center Basic Program on Knee Osteoarthritis

Ji Woong Choi^{1*}, Jun Yup Kim¹, Tae Hoon Kim¹, Choong-Gon Kim², Si-Yoon Sung³, Mi Lyoun Kim⁴, Mi Jung Kim^{1,5}, Kyu Hoon Lee^{1,5}, Si-Bog Park^{1,5†}

Department of Rehabilitation Medicine, Hanyang University Medical Center, Seoul, Republic of Korea¹, Ocean Climate Response and Ecosystem Research Department, Korea Institute of Ocean Science and Technology, Busan, Republic of Korea², HUEN Therapy Laboratory, Suwon, Republic of Korea³, Wando County Office, Wando-gun, Jeollanam-do, Republic of Korea⁴, Department of Rehabilitation Medicine, Hanyang University College of Medicine, Seoul, Republic of Korea⁵

Introduction

Various marine-derived human healing resources have been reported to have anti-inflammatory and analgesic effects, and these effects have also been reported to show a correlation with serum biomarkers. In addition, the Wando Marine Healing Center, which opened for the first time in Korea in 2023, offers 5 basic programs and 10 premium programs, but their effectiveness has not yet been verified. Therefore, this study sought to investigate the clinical effects and related biomarker changes of 4 basic programs currently underway at the Wando Marine Healing Center.

Methods

This study was conducted as a randomized controlled trial to confirm the effectiveness of seaweed mud therapy and the basic program. The criteria for selection for the study were adults over 50 years of age who were independent walkers with pain in at least one knee that had lasted for more than 3 months. Additionally, to be eligible, they had to fall within the Kellgren-Lawrence (K-L) classification of osteoarthritis Grade 1 to 4 on radiological examination and be diagnosed with knee osteoarthritis based on 'clinical and imaging examination' criteria according to the American College of Rheumatology classification criteria. Study subjects who missed more than 40% of the intervention doses were regarded as the drop-out. The comparison between groups was made in two ways: one based on whether the mud therapy included seaweed ingredients, and the other based on whether the 4 basic programs (thalasso pool, seawater mist, mud therapy, and seaweed foam therapy) were included. A total of 41 subjects completed the clinical trial without dropping out. All study subjects were instructed to receive a total of 10 interventions over 2 weeks, 5 times a week, and the evaluation variables were as follows: 100 mm visual analog scale (VAS) pain score, Knee injury and Osteoarthritis Outcome Score-12 (KOOS-12), the 36-Item Short-Form Health Survey (SF-36), high sensitivity C-reactive protein (hs-CRP), interleukin-6 (IL-6), cartilage oligomeric matrix protein (COMP), tumor necrosis factor (TNF)- α .

Results

When only mud therapy was implemented without the basic program, there was no statistically significant difference in all evaluation variables depending on whether seaweed was added. However, when implemented together with the basic program, seaweed-added mud therapy improved the physical role limitation of SF-36 (Wilcoxon rank sum test, $P < 0.05$).

When mud therapy without seaweed was implemented, there was no statistically significant difference in all evaluation variables depending on whether the basic program was implemented. However, when mud therapy containing seaweed was performed, the basic program lowered CRP and TNF- α (Wilcoxon rank sum test, $P < 0.05$).

Conclusions

When used together, seaweed mud therapy and the basic marine healing program can improve physical role limitations and osteoarthritis biomarkers.

Acknowledgment Acknowledgments: This research was supported by "Efficacy/standardization technology development of marine healing resources and its life cycle safety management" of Korea Institute of Marine Science and Technology Promotion (KIMST) funded by the Ministry of Oceans and Fisheries (KIMST-20220027).

Pain and Musculoskeletal Rehabilitation

P-90

Establishment of a new treatment system using QR cords in taping patient experience

Won Bin Kim^{1**}

Department of Rehabilitation Medicine, Seoul National University Hospital¹

Abstract

Short Description of what will be discussed during the presentation (about 250 - 500 words)

Introduction

During the initial surge of coronavirus disease 2019 (COVID-19), which is sensitive to the spread of infectious diseases in the military, made it difficult to access medical care. Thus, we thought about how to use non-face-to-face medical care using digital devices. This study was undertaken to establish a new treatment system using QR cords in taping patient experience in military medical care.

Methods

We selected the 15 most common musculoskeletal diseases in the military based on medical records in military hospitals. Taping videos were produced for 15 diseases, and 14 additional "taping brochures for each disease" were also developed by supplementing the deficiencies in the video. The contents were organized based on taping books and papers, and the focus was on portability and readability. And in this cross-sectional study, we assessed a total of 160 patients (150 males and 10 females; average age 20.6±3.8 years) who underwent pain in musculoskeletal. All patients were surveyed on the knowledge and satisfaction of taping contents before and after taping education through QR code in mobile phone.

Results

Taping knowledge was 2.95 points out of 5 points, but it improved to 4.04 points out of 5 points. The items with the largest increase in the range of scores compared to the pre-level in taping knowledge are "Taping works to relieve pain by lifting the epidermis of the skin to promote blood circulation" and "It dries naturally when taping is wet and can be used for 3 to 5 days." And taping satisfaction improved from 3.82 to 4.32 points out of 5 points. The most popular taping contents by patients in three months were ankle sprain taping, followed by round shoulder and knee pain. This result correlated with the most prevalent musculoskeletal disease in the military.

Conclusion

This study demonstrated that a new treatment system using QR cords in taping patient influenced on the degree of knowledge in taping using skills, satisfaction and quality of life in patients with musculoskeletal disorders. Because functional ability after total knee arthroplasty is strongly associated with prevention of recurrence and reducing the pain, these results could be of importance in strengthening the military's combat capability and further national security.

Effect of wearable assist robot on reducing the burden of back muscle during squat and stoop lifting

Jeuhee Lee^{1,2*}, Dong-Wook Rha^{1,2}, Yebin Cho¹, Jehyun Yu¹, Taekyung Lee¹, Juntaek Hong^{1†}

Department and Research institute of Rehabilitation Medicine, Yonsei University¹, Department of Medical Device Engineering and Management, Yonsei University²

Introduction

Lifting heavy objects is a common cause of lower back pain and could also lead to muscle strain and other musculoskeletal problems. Recently, wearable assist robots have been developed to reduce the burden on weight-bearing muscles when lifting heavy objects. In this study, we aimed to analyze the effects of two types of assistance according to two different lifting postures, squat and stoop, while wearing a robotic device by comparing the sEMG activities of back and lower extremity muscles

Methods

A total of 18 healthy people (M=8, F=10) were enrolled in this study. Under 3 conditions (with a robot including stoop-assist-mode or squat-assist-mode; without a robot), all participants lifted an object weighing 20% of their body weight and lifting tasks consisted of 4 phases: Stand to Sit (St.->Si) without object, Si.->St. with object, St.->Si. with object, and Si.->St. without object. Each task was performed five times for a total of three sets, using two different lifting postures independently. For assistance mode, there are two types distinguished by assistive-torque profile regarding hip-joint bending angle depending on the two lifting postures and assistance modes appropriate for each lifting posture were provided. Wireless EMG sensors (Trigno, Delsys Inc.) were attached to the thoracic erector spinae (t-ES), lumbar erector spinae (l-ES), gluteus maximus (GM), biceps femoris (BF), and medial gastrocnemius (GCM) for measuring peak voluntary contraction activity during the tasks. For normalizing contraction values by each muscle, we used the average value of peak voluntary contraction without the robot as the reference value. Based on this value, we analyzed the difference of the peak voluntary contraction during 15 lifts in each condition.

Results

During stoop lifting, peak RMS measured at t-ES was significantly reduced when wearing the assist robot during the sitting phase, whether with or without the object (p

Conclusion

In this study, we analyzed the effects of two types of assistance provided by wearable robots and observed a significant reduction in peak RMS values during lifting tasks. These findings indicate that when assistive torque is appropriately adjusted according to lifting postures, the burden on back muscles as well as hip girdle muscles can be reduced in both squatting and stooping postures.

Impact of Sarcopenia on Functional Recovery Following Total Knee Replacement

Cho E Sim^{1*}, Mi Jin Hong^{1†}, Jong Bum Park¹, Yung Jin Lee¹, Dong Jin Chae¹, Seong-Eun Kim¹, Ji-Hwan Kwon¹, Byung Hak Oh², Hyun Jin Yoo²

Department of Rehabilitation Medicine, Konyang University College of Medicine¹, Department of Orthopedic Surgery, Konyang University College of Medicine²

Objective

Sarcopenia is characterized by an age-related decline in skeletal muscle mass and strength or a reduction in physical performance. Previous studies show knee osteoarthritis (OA) and sarcopenia often co-occur, sharing chronic low-grade inflammation as a common mechanism.

This study aimed to evaluate the post-surgical function of patients with knee OA who underwent total knee replacement (TKR) to determine function changes related to sarcopenia.

Methods

The study participants were patients aged 65 years and older who had knee OA and underwent surgery for TKR at OO University Hospital from February 2023. Before surgery, patients underwent baseline assessments including evaluations of functional and nutritional status, muscle mass, and obesity. Assessments was conducted using dual energy X-ray absorptiometry (DEXA) to assess body mass index (BMI), skeletal muscle index (SMI). Additionally, hand grip test, functional ambulation classification (FAC), the Western Ontario and McMaster universities osteoarthritis index (WOMAC), Charlson comorbidity index (CCI), hemoglobin and albumin level, geriatric nutritional risk index (GNRI), and medical history were evaluated.

Functional assessments were performed at 1-months, 6 months post-surgery using the short physical performance battery (SPPB), BBS, FAC, WOMAC, length of hospital stay, and discharge destination.

Results

Sarcopenic patients had a higher mean age, significantly lower BMI, SMI, hand grip strength, Hb level and GNRI compared to non-sarcopenic patients (Table 1).

Figure 1 and 2 showed trend of SPPB and BBS score at 1 month and 6 months post-surgery. In the no-sarcopenia group, there were significant changes in SPPB scores and BBS at 1 month and 6 months post-surgery ($p=0.004$ and $p=0.002$, respectively). Changes over time at 1 month and 6 months post-surgery were not significant ($p=0.176$), but there was a significant difference in changes over time between the groups based on the presence of sarcopenia ($p=0.004$).

In the sarcopenia group, there were significant changes in SPPB scores at 1 month and 6 months post-surgery ($p=0.006$), but no significant difference in BBS ($p=0.149$). No significant difference was observed between sarcopenic and non-sarcopenic participants for the 1-month follow-up BBS score and the 6-month follow-up BBS score ($p=0.063$).

Conclusion

Sarcopenic patients had a higher mean age and lower BMI, SMI, hand grip strength, Hb level, and GNRI compared to non-sarcopenic patients. Significant changes in SPPB and BBS scores were observed in the non-sarcopenia group, whereas the sarcopenia group showed no significant changes. Differences over time between groups were significant indicating that sarcopenia affects recovery. Future research will expand to a larger cohort and long-term follow-up to further investigate the relationship between TKR and sarcopenia.

	Total (n=25)	No sarcopenia (n=21)	Sarcopenia (n=4)	P value
Age (years), mean (SD)	72.56 (5.71)	71.14 (4.65)	80 (5.35)	0.002
Men, n (%)	6 (24)	10 (40)	0 (0)	1.000
BMI (kg/m ²), mean (SD)	26.06 (3.50)	26.92 (3.08)	21.53 (1.40)	0.003
SMI (kg/m ²), mean (SD)	6.68 (0.93)	6.94 (0.75)	5.29 (0.36)	0.000
WOMAC, mean (SD)	52.92 (17.52)	53.48 (18.24)	50 (14.90)	0.724
Hand grip strength (kg), mean (SD)	20.58 (7.73)	21.91 (7.57)	13.63 (4.36)	0.047
Length of hospital stay, days, mean (SD)	18.24 (12.81)	16.48 (6.037)	27.5 (30.51)	0.523
Discharge destination, n (%)				
Own home	22 (88)	19 (76)	3 (75)	0.796
Nursing home	3 (12)	6 (24)	1 (25)	
Previous FAC, n (%)				
1,2,3	1 (4)	1 (4.76)	0 (0)	0.790
4	6 (24)	5 (23.81)	1 (25)	
5	18 (72)	15 (71.43)	2 (50)	
Hb (g/dL), mean (SD)	12.72 (1.68)	13.11 (1.46)	10.68 (1.29)	0.005
GNRI, mean (SD)	114.02 (11.16)	116.29 (9.87)	102.10 (10.99)	0.016
Albumin, mean (SD)	4.35 (0.48)	4.39 (0.45)	4.12 (0.64)	0.299
Charlson comorbidity index, mean (SD)	1.24 (2.18)	1.43 (2.34)	0.25 (0.5)	0.333

Table 1. Comparison of subject characteristics

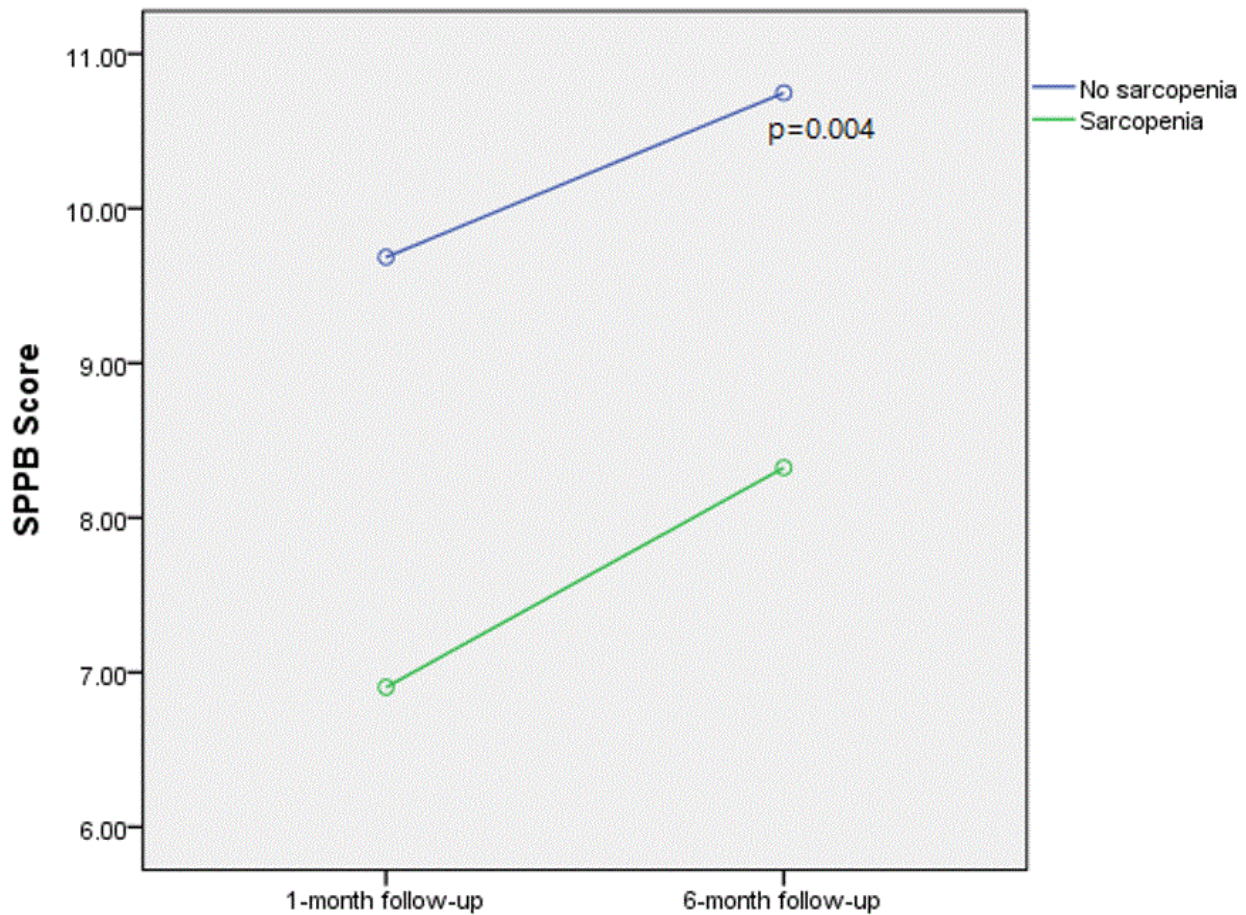
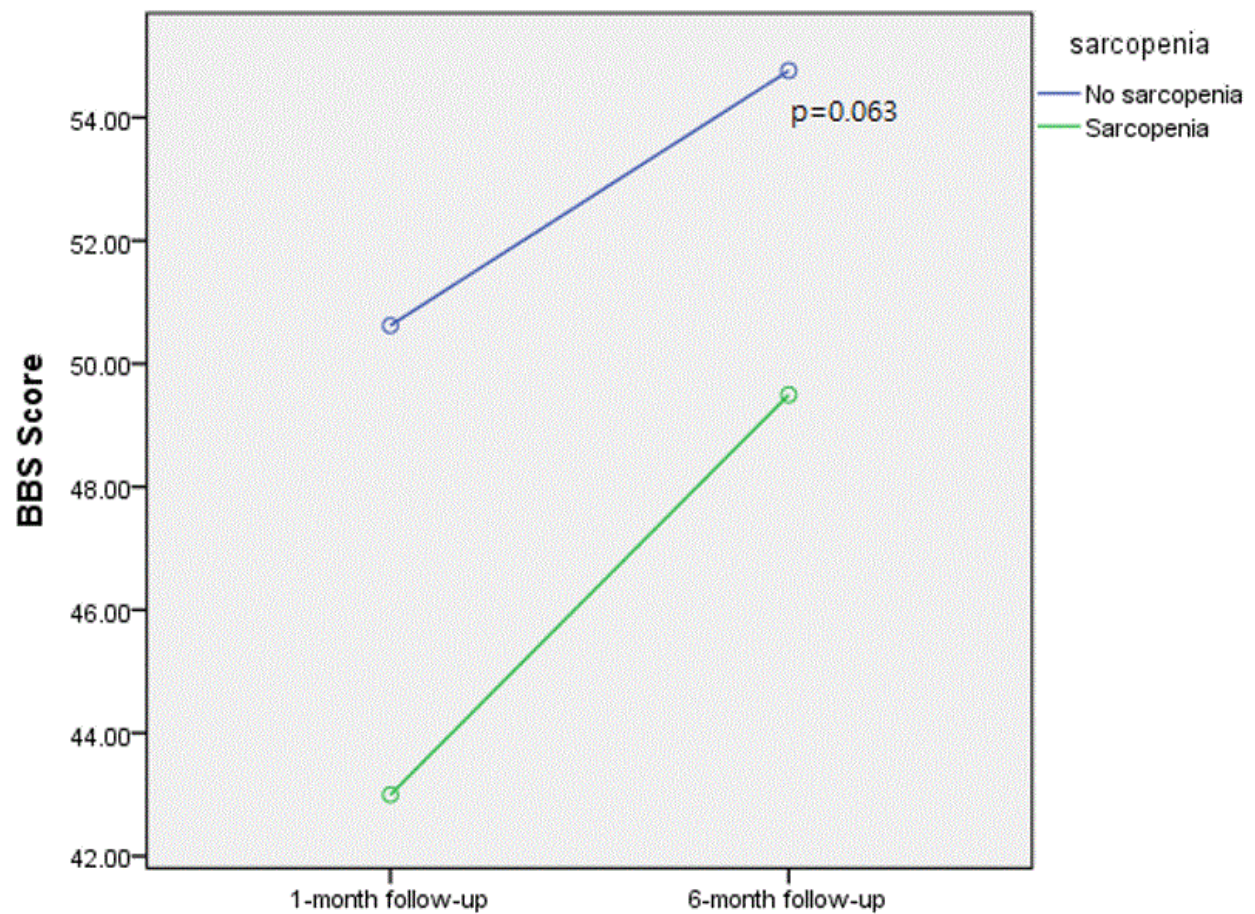


Fig 1. Trend of SPPB scores adjusted for age and gender (ANCOVA analysis) from total knee arthroplasty 1-month follow-up to 6-month follow-up



Covariates appearing in the model are evaluated at the following values: age = 72.5600

Fig 2. Trend of BBS scores adjusted for age and gender (ANCOVA analysis) from total knee arthroplasty 1-month follow-up to 6-month follow-up

Impact of Sarcopenia on Functional Recovery Following Hip Fracture Surgery

Cho E Sim^{1*}, Mi Jin Hong^{1†}, Jong Bum Park¹, Yung Jin Lee¹, Dong Jin Chae¹, Seong-Eun Kim¹, Ji-Hwan Kwon¹, Byung Hak Oh², Hyun Jin Yoo²

Department of Rehabilitation Medicine, Konyang University College of Medicine¹, Department of Orthopedic Surgery, Konyang University College of Medicine²

Objective

Sarcopenia, characterized by age-related loss of skeletal muscle mass and strength or reduced physical performance, has become increasingly relevant due to global aging trends. Older adults suffering from sarcopenia are more than three times more likely to fall. When the decline of muscle mass and function following a hip fracture is not regained during recovery, the risk for recurrence of fall-related fractures will rise.

This study aimed to investigate the differences in functional status after hip fracture surgery based on the presence or absence of early sarcopenia.

Methods

The study participants were patients aged 65 years and older who underwent hip fracture surgery at OO University Hospital from February 2023. Before surgery, patients underwent baseline assessments including evaluations of functional and nutritional status, muscle mass, and obesity. Assessments were conducted using dual energy X-ray absorptiometry (DEXA) to assess body mass index (BMI), skeletal muscle index (SMI). Additionally, hand grip test, bone mineral density (BMD), functional ambulation classification (FAC), hemoglobin and albumin level, geriatric nutritional risk index (GNRI), and medical history were evaluated.

Functional assessments were performed at 1-months, 6-month post-surgery using the short physical performance battery (SPPB), BBS, FAC, length of hospital stay, and discharge destination. We conducted a repeated measures ANCOVA to evaluate the differences in functional recovery over time based on the presence of sarcopenia.

Results

Hand grip strength was significantly lower in sarcopenic participants compared to non-sarcopenic participants (11.74 ± 5.47 kg vs. 18.15 ± 8.26 kg, $p=0.006$). Additionally, there was a significant difference in the distribution among FAC groups ($p=0.036$). No significant differences were observed in other characteristics such as age, BMI, and length of hospital stay (Table 1).

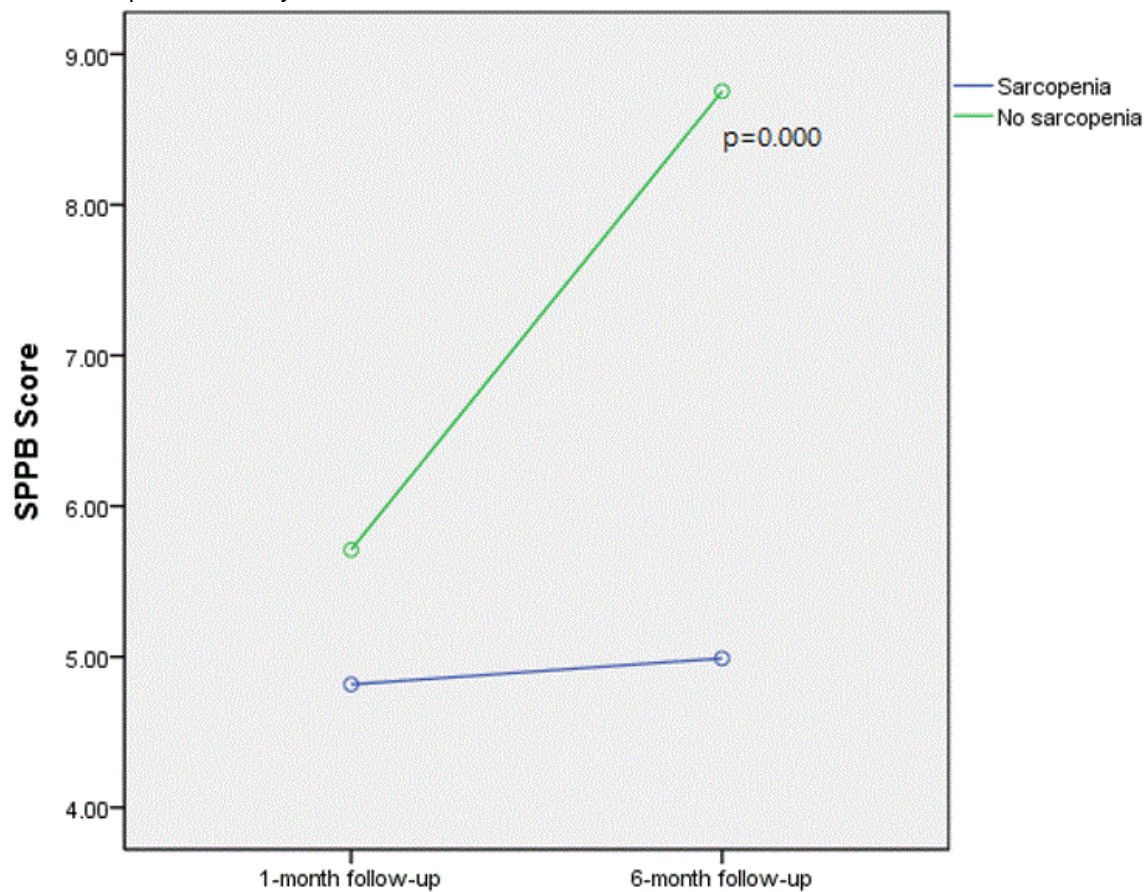
There was a significant difference in SPPB scores at 1-month and 6-month follow-ups between participants with sarcopenia and non-sarcopenic participants ($p=0.000$, Figure 1). No significant difference was observed between sarcopenic and non-sarcopenic participants for the 1-month follow-up BBS score and the 6-month follow-up BBS score ($p=0.106$, Figure 2).

Conclusion

Patients with sarcopenia undergoing hip fracture surgery had lower grip strength, slower functional recovery. Sarcopenic patients also had significantly lower SPPB scores at both 1-month and 6-month follow-ups, but no significant difference in BBS scores. Future research will recruit a larger cohort and include long-term follow-up to further explore these findings.

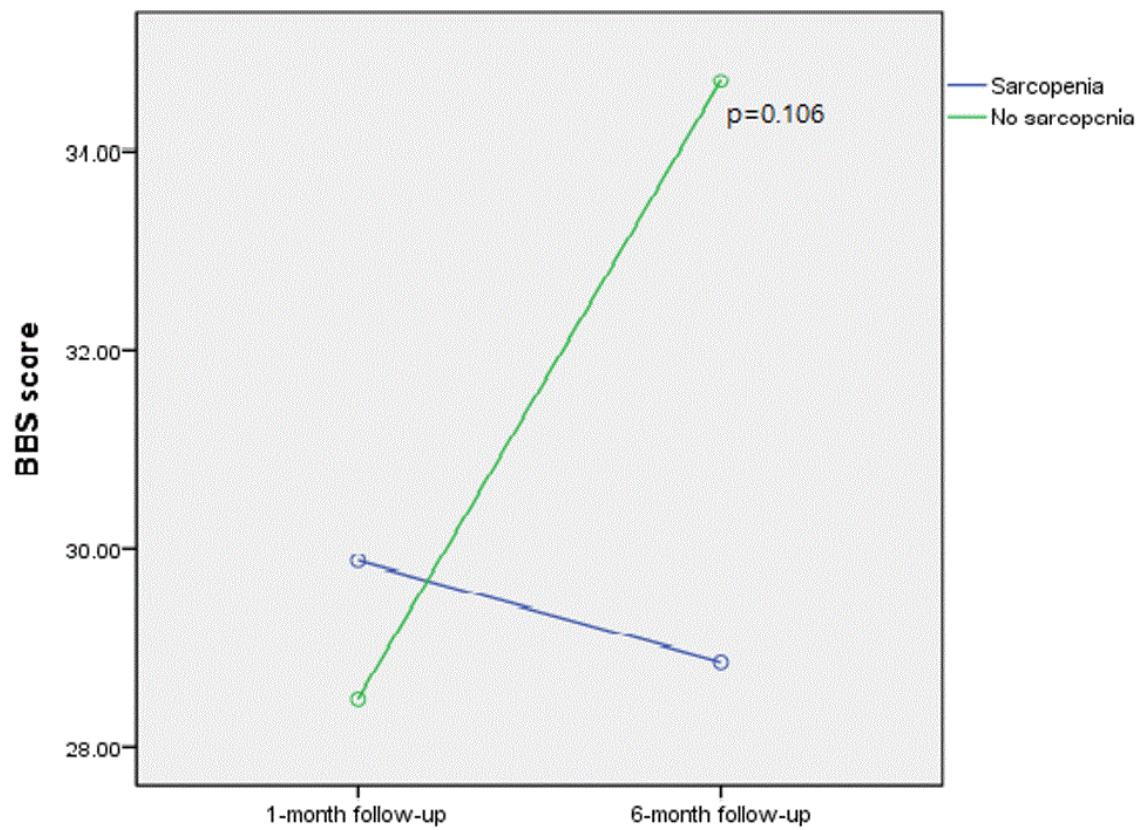
	Total (n=49)	No sarcopenia (n=19)	Sarcopenia (n=30)	P value
Age (years), mean (SD)	80.76 (7.27)	79.89 (7.59)	81.30 (7.14)	0.516
Men, n (%)	12 (24.49)	7 (36.84)	5 (16.67)	0.110
BMI (kg/m ²), mean (SD)	22.32 (3.42)	23.2 (3.26)	21.7 (3.45)	0.986
SMI (kg/m ²), mean (SD)	5.77 (0.91)	6.53 (0.68)	5.29 (0.67)	0.431
Fracture site (Rt.), n (%)	26 (56.06)	11 (57.89)	15 (50)	0.590
Type of fracture, n (%)				
Intertrochanter	29 (59.18)	15 (78.95)	14 (46.67)	0.074
Subtrochanter	1 (2.04)	-	1 (3.33)	
Femur neck	19 (38.78)	4 (21.05)	15 (50)	
Operation name, n (%)				
ORIF	13 (26.53)	5 (26.32)	8 (26.67)	0.067
CRIF	16 (32.65)	10 (52.63)	6 (20)	
Bipolar hemiarthroplasty	20 (40.82)	4 (21.05)	16 (53.33)	
Hand grip strength (kg), mean (SD)	14.23 (7.32)	18.15 (8.26)	11.74 (5.47)	0.006
Length of hospital stay, days, mean (SD)	17 (8.39)	15.42 (4.51)	18 (10.17)	0.304
Discharge destination, n (%)				
Own home	27 (55.1)	9 (47.37)	18 (60)	0.386
Nursing home	22 (44.9)	10 (52.63)	12 (40)	
Previous FAC, n (%)				
1,2,3	10 (20.4)	4 (21.05)	6 (20)	0.036
4	11 (22.45)	5 (26.32)	4 (13.33)	
5	28 (57.14)	10 (52.63)	18 (60)	
Hb (g/dL), mean (SD)	10.88 (1.80)	11.02 (2.02)	10.80 (1.67)	0.217
GNRI, mean (SD)	101.90 (10.82)	104.58 (12.02)	100.20 (9.81)	0.785
Albumin, mean (SD)	4.00 (0.49)	4.06 (0.50)	3.96 (0.48)	0.744
BMD (T-score), mean (SD)	-3.14 (1.19)	-2.58 (1.31)	-3.45 (1.01)	0.342

Table 1. Comparison of subject characteristics



모형에 표시되는 공변량은 다음 값을 사용하여 평가됩니다.: AGE = 80.7551, SEX = 1.7551

Fig 1. Trend of SPPB scores adjusted for age and gender (ANCOVA analysis) from post-fracture 1-month follow-up to 6-month follow-up



모형에 표시되는 공변량은 다음 값을 사용하여 평가됩니다.: AGE = 80.7551, SEX = 1.7551

Fig 2. Trend of BBS scores adjusted for age and gender (ANCOVA analysis) from post-fracture 1-month follow-up to 6-month follow-up

Measuring Range of Motion of Shoulder Joint using Multiple 3D RGB Cameras

Jun-Sang Han^{1*}, Jong Taek Lee³, Sang-Hyun Lee³, Eunhee Park^{2†}

Department of Rehabilitation Medicine, Kyungpook National University Hospital ¹, Department of Rehabilitation Medicine, Kyungpook National University Chilgok Hospital², School of Computer Science and Engineering, Kyungpook National University³

Introduction

The skeleton extracted from 2D RGB images has limitations in accurately measuring joint angles. The purpose of this pilot study is to measure the range of motion of joints in healthy adults by extracting a 3D skeleton from multiple RGB cameras.

Method

In the gait analysis laboratory equipped with 3D motion capture equipment, four RGB cameras were installed to simultaneously acquire 3D motion capture data and five RGB videos. The shoulder range of motion in five participants was measured by modifying each movement of the shoulder (flexion: 0-180°, extension: 0-60°, abduction: 0-180°, horizontal adduction: 0-130°, horizontal abduction: 0-40°, external rotation: 0-90°, internal rotation: 0-70°) in the frontal, sagittal, and axial planes in 20-degree increments.

Results

The performance evaluation of 3D pose estimation resulted in a Mean Per Joint Position Error (MPJPE) of 37.580 mm, and the Root Mean Squared Error (RMSE) in shoulder joint angle measurement was 9.82 degrees.

Conclusion

Multiple RGB cameras could be useful for measuring the range of motion and assessing the functional movement of clinically significant joints, such as the shoulder, elbow, wrist, hip, knee, and ankle.

Analgesic and Functional Improvement Effects of Marine Healing Program for Knee Osteoarthritis

Ji Woong Choi^{1*}, Jun Yup Kim¹, Tae Hoon Kim¹, Mi Jung Kim^{1,2}, Kyu Hoon Lee^{1,2}, Si-Bog Park^{1,2†}

Department of Rehabilitation Medicine, Hanyang University Medical Center, Seoul, Republic of Korea¹, Department of Rehabilitation Medicine, Hanyang University College of Medicine, Seoul, Republic of Korea²

Introduction

Relief of musculoskeletal pain and improvement of daily life functions using marine-derived human healing resources have been reported several times. However, because each healing center applies heterogeneous protocols, individual verification of effectiveness is necessary. Therefore, we wanted to investigate the effect on improving knee pain and daily life functions when applying the basic marine healing program, which has been in progress since 2023 at the Wando Marine Healing Center in Korea, to patients with knee arthritis.

Methods

In this prospective, pre-post comparative pilot study, subjects who met all of the following conditions were selected: adults aged 50 years or older with pain in at least one knee that had persisted for more than 3 months; Knee osteoarthritis was diagnosed based on 'clinical and imaging examination' criteria according to the American College of Rheumatology classification criteria.; Kellgren-Lawrence (K-L) classification of osteoarthritis Grade ranged from 1 to 4; More than 60% of intervention visits were implemented. A total of 41 people met the criteria and were included as subjects of analysis. They were instructed to receive a total of 10 interventions over 2 weeks, 5 times a week. There were a total of 4 groups according to the type of intervention as follows: Group 1) mud Therapy and basic program, group 2) seaweed mud therapy and basic program, group 3) mud therapy, and group 4) seaweed mud therapy. In these participants, the following variables were measured immediately before the beginning of the two-week interventions and immediately after the end of the two-week interventions: average knee pain score over the past week and current pain score at the time of evaluation using the 100 mm visual analogue scale pain scores of the more painful knee of both knees; Knee injury and Osteoarthritis Outcome Score (KOOS), a patient-reported questionnaire of knee-related symptoms over the past week, consisting of five subscales: pain, symptoms, functions of daily living (ADL), sports and recreation functions (Sport/Rec), and quality of life (QoL).

Results

Due to the small number of samples per group, all pre-post comparisons were conducted using the Wilcoxon signed rank test. The average knee pain score over the past week decreased significantly in groups 1, 2, and 4; however, the difference in knee pain scores at the time of evaluation was not significant. Among the KOOS subscales, knee pain significantly improved in group 4, and ADL significantly improved in all groups. The Sport/Rec subscale improved significantly in group 4, and the QoL subscale improved significantly in group 2.

Conclusions

Through this study, it was found that Wando Marine Healing Center's seaweed mud therapy can have a positive effect on knee pain, ADL, Sport/Rec, and QoL over the past week, and that the basic marine healing program can affect positively on knee pain and ADL over the past week.

Acknowledgment This research was supported by "Efficacy/standardization technology development of marine healing resources and its life cycle safety management" of Korea Institute of Marine Science and Technology Promotion (KIMST) funded by the Ministry of Oceans and Fisheries (KIMST-20220027).

Gait performance and brain activity are improved by gait automatization after robot training

So Young Joo^{1**}, Seung Yeol Lee², Yoon Soo Cho¹, Cheong Hoon Seo¹, Jisu Seo¹

Department of rehabilitation medicine, Hangeang Sacred Heart Hospital, College of Medicine Hallym University¹,
Department of rehabilitation medicine, College of Medicine, Soonchunhyang University Hospital, Bucheon²

Introduction

Patients with lower extremity burn injuries have decreased gait function. Gait dysfunctions are compensated by activation of executive areas such as the prefrontal cortex (PFC). Although robot-assisted gait training (RAGT) can improve gait function, the training mechanisms of RAGT are unknown. We aimed to determine the clinical effects of RAGT in patients with burns and investigate their underlying mechanisms.

Method

This single-blind, randomized controlled trial involved 54 patients with lower extremity burns. The RAGT group underwent RAGT using SUBAR[®] and conventional training. The control (CON) group underwent only conventional training. Gait-related cortical activity was measured using a functional near-infrared spectroscopy device before and after 8 weeks of training. Functional ambulation category (FAC) score, 6-minute walking test (6 MWT) distance, isometric force, and range of motion (ROM) of lower extremities were measured to evaluate physical function. The visual analog scale (VAS) score was used to rate subjective pain during gait. Results : The VAS score decreased and FAC score improved after 8 weeks of training in both groups. The 6 MWT scores, isometric strengths (the left knee flexor, right ankle plantar, and left ankle plantar flexors), and the ROMs (the right hip, left hip, right knee, and left knee extensions) of the RAGT group were significantly improved compared with those of the CON. PFC activation during the gait phase in the RAGT group decreased significantly compared with that of the CON.

Conclusions

In conclusion, this study demonstrated that robot training induces positive clinical effects in patients with lower extremity burns, and gait automatization may be involved in the training mechanisms of RAGT. To the best of our knowledge, this is the first study to observe the treatment mechanism through which robotic training improves gait function in patients with burns.

Acknowledgment Translational Research Program for Rehabilitation Robots (#NRCTR-EX24003), National Rehabilitation Center Ministry of Health and Welfare, Korea

Patient-friendly and Immediate Gait Classification Methodology for Hip OA Patients

Chang-Hwan Ahn¹, Young-Hwan Lim¹, Wiha Choi³, Tae-Du Jung^{1,2*†}

Department of Rehabilitation Medicine, Kyungpook National University Chilgok Hospital¹, Department of Rehabilitation Medicine, School of Medicine, Kyungpook National University², Department of Robotics and Mechatronics Engineering, DGIST³

Even with the same pathological conditions, patients' gait patterns can manifest in various forms. Classifying a patient's gait pattern is crucial for personalized rehabilitation. Many studies have been conducted to classify patients into 2 or 3 groups according to their gait patterns, and analyze the characteristics of each group before providing customized rehabilitation. In this study, a methodology for classifying the gait patterns of 16 patients with hip osteoarthritis (hip OA) is proposed. First, the ground reaction forces in 3 axes (anterior-posterior, medial-lateral, vertical) obtained from the force-plate in gait experiments are quantified for gait assessment using Pearson correlation coefficient in view of trend similarity and Symmetric Mean Absolute Percentage Error (SMAPE) in the view of scale similarity with healthy control. Second, Gaussian Mixture Models (GMM) are employed to cluster healthy controls and patients, and to cluster the patients into various groups based on these quantified measured value (3 Pearson correlation values and 3 SMAPE values). Lastly, the gait characteristics of each group are analyzed by comparing the kinetics (hip, knee, and ankle joint moment) and kinematics (hip, knee, and ankle joint angle) data of the clustered patients. This methodology allows for a convenient and immediate classification of gait patterns with comparable accuracy, as it relies solely on force-plate data, eliminating the need for external attachments such as infrared markers and electromyography.

Exercise prehabilitation affects residual force enhancement in hindlimb unloaded rat muscles

Hyo-Seong Yeo^{1,2,3*}, Jae-Young Lim^{1,2,3†}

Department of Rehabilitation Medicine, Seoul National University Bundang Hospital¹, Institute on Aging, Seoul National University², Aging & Mobility Biophysics Laboratory, Seoul National University Bundang Hospital³

Exercise prehabilitation (EP) has been attracting attention as a method to maintain skeletal muscle mass and function when muscle atrophy occurs. Residual force enhancement (RFE) is an intrinsic contractile muscle property that is related to muscle function. We investigated the effect of EP on passive force and RFE.

The study divided 25 Sprague–Dawley rats into control (CON, n = 9), hindlimb unloading (HU, n = 8), and exercise prehabilitation (EP, n = 8) groups. The HU group performed hindlimb unloading for 14 days and the EP group performed downhill running for 14 days before HU. Body (BW) and muscle (MW) weight were measured. Passive force and RFE were measured in the isolated soleus (SOL) and extensor digitorum longus (EDL) muscles. Western blot and histologic analysis were performed.

Body weight was highest in the CON group, whereas there was no difference between the EP and HU groups. SOL MW/BW was lower in the HU group than in CON, whereas EDL MW/BW did not differ among the groups. The physiological cross-sectional area (pCSA) was lower in the HU and EP groups than in the CON group in SOL. Peak passive normalized using the pCSA of the SOL was lower in the treatment groups than in the CON group. For the EDL, there were no between-group differences in pCSA and passive force. RFE was lower in the HU group compared to CON, whereas the EP group had higher RFE than the HU group in both the SOL and EDL.

Short-term EP may alleviate the reduction in RFE due to HU in both slow and fast twitch muscles. Therefore, short-term exercise intervention before surgery may have a positive effect on functional ability.

Acknowledgment This work was supported by the National Research Foundation of Korea (NRF) grant funded by the Korea government (MSIT) (NRF-2022R1A2C2010122).

New Method for Gait Pattern Assessment in Patient with Osteoarthritis

Young-Hwan Lim¹, Chang-Hwan Ahn¹, Wiha Choi³, Tae-Du Jung^{1,2*†}

Department of Rehabilitation Medicine, Kyungpook National University Chilgok Hospital¹, Department of Rehabilitation Medicine, School of Medicine, Kyungpook National University², Department of Robotics and Mechatronics Engineering, DGIST³

Through the quantification of gait ability, it becomes possible to assess the present level of gait proficiency and design a personalized rehabilitation program. In order to assess a patient's gait, both the trend and scale aspects of gait time-series data must be considered. This study introduces a methodology for evaluating gait in 3 patients with hip osteoarthritis (OA) by employing Pearson correlation coefficient for trend similarity and symmetric mean absolute percentage error (SMAPE) for scale similarity in view of kinematics and kinetics as preliminary study.

Effect of Wando Marine Healing Center Basic Program on Quality of Life in Knee Osteoarthritis

Tae Hoon Kim^{1*}, Jun Yup Kim¹, Ji Woong Choi¹, Mi Jung Kim^{1,2}, Kyu Hoon Lee^{1,2}, Si-Bog Park^{1,2†}

Department of Rehabilitation Medicine, Hanyang University Medical Center, Seoul, Republic of Korea¹, Department of Rehabilitation Medicine, Hanyang University College of Medicine, Seoul, Republic of Korea²

Introduction

Human therapy using marine-derived resources has long been used for various diseases, including skin diseases and arthritis, and its effectiveness has been reported through several studies. However, there is no research on what aspects of quality of life its use improves. Therefore, in this study, we sought to investigate the impact of a basic marine healing program on the quality of life in patients with knee osteoarthritis using the basic marine healing program currently underway at the Wando Marine Healing Center in Korea, which opened in 2023.

Methods

To be eligible for analysis after being selected for this prospective pre-post comparison pilot study, adults aged 50 years or older must have pain in at least one knee that has lasted for more than 3 months and have Kellgren-Lawrence (K-L) grade of osteoarthritis 1 to 4. The patient also had to be diagnosed with knee osteoarthritis based on 'clinical and imaging examination' according to the American College of Rheumatology classification criteria, and the study subject had to have completed more than 60% of intervention visits. Among the study subjects, 41 completed the intervention without dropping out. They were instructed to take the intervention 5 times a week, a total of 10 times over 2 weeks. There were 4 groups according to the type of intervention as follows: Group 1) mud therapy and basic program, group 2) seaweed mud therapy and basic program, group 3) mud therapy, group 4) seaweed mud therapy. The main evaluation variable was the 36-Item Short-Form Health Survey (SF-36), and its components were as follows: 1) Physical components: Physical Function (PF), Role Physical (RP), Bodily Pain (BP), General Health (GH), Physical Component Summary (PCS); 2) Mental components: Role Emotional (RE), Vitality (V), Mental Health (MH), Social Function (SF), Mental Component Summary (MCS). Statistical significance was defined at two-sided $P < 0.05$.

Results

All physical components showed no significant changes in any of the four groups. However, among mental components, VT, MH, SF, and MCS showed significant improvement in group 2, group 4, groups 1 and 2, and group 2, respectively.

Conclusions

Seaweed mud therapy and basic marine healing programs have a positive effect mainly on mental components of the quality of life of patients with knee osteoarthritis, and when these two interventions are implemented together, the quality of life of a wider range of mental components could be improved.

Acknowledgments This research was supported by "Efficacy/standardization technology development of marine healing resources and its life cycle safety management" of Korea Institute of Marine Science and Technology Promotion (KIMST) funded by the Ministry of Oceans and Fisheries (KIMST-20220027).

Maintaining Lumbar Lordosis to Prevent Scoliosis in Duchenne Muscular Dystrophy: A Longitudinal Study

Jeong Min Kim^{1*}, You Gyoung Yi², Hyung-Ik Shin^{3†}

PURME foundation NEXON Children's Rehabilitation Hospital, Department of Rehabilitation Medicine¹, Ewha Womans University Seoul Hospital, Department of Rehabilitation Medicine², Seoul National University Hospital, Department of Rehabilitation Medicine³

Objectives

Scoliosis is a major complication in patients with Duchenne muscular dystrophy (DMD). Once a loss of ambulation (LOA) occurs, scoliosis progresses rapidly. Previous studies suggested lumbar hyperextended posture significantly reduces the incidence of scoliosis. We aimed to investigate if portable seat devices supporting lumbar lordosis posture could reduce the incidence of scoliosis in DMD.

Materials and Methods

Twenty-four DMD patients were prospectively enrolled into the 'seat device group' from June 2018 to September 2019 (within 6 months of LOA, on steroid treatment). They were instructed to use their custom-made portable seat devices, which included lumbar pads, pelvic belts and chest straps to provide more stable lumbar lordosis and prevent sacral sitting. Designed for portability, these devices allowed use at home, school, or in wheelchairs, ensuring continuous support for lumbar lordosis (Fig 1). The seat devices were used for the first 3 years. Participants were followed up every 6 months up to 5 years. Whole spine radiographs in supine positions were obtained at each follow-up. Due to ethical issues, the control group was retrospectively recruited by reviewing medical records between August 2005 and July 2018.

Results

The demographic data of the patients is presented in Table 1. Among the 24 boys in the seat device group, two were excluded due to loss to follow-up, one due to discontinuation of steroid treatment, and seven due to low compliance (less than an hour per day). Thus, 14 boys were included in the analysis. The incidence of scoliosis in the seat device group was 35.7%, compared to 58.7% in the control group ($p=0.131$). The incidence of severe scoliosis (Cobb angle $\geq 40^\circ$) was 0% in the seat device group, compared to 6.5% in the control group ($p=1.000$). The final Cobb angle among patients who developed scoliosis was 18.9 degrees (IQR 16.5-35.8) in the seat device group, and 24.0 degrees (IQR 16.2-31.8) in the control group ($p=0.938$). Logistic regression analysis indicated that using a seat device was not a significant factor in the incidence of scoliosis 5 years after LOA ($p=0.138$). Additionally, the average time using the seat device was not a significant factor ($p=0.382$).

Conclusions

While the seat device group showed a lower incidence of scoliosis and severe scoliosis compared to the control group, the differences were not statistically significant. Additionally, the final Cobb angle among those who developed scoliosis was lower in the seat device group, but this was also not statistically significant. Therefore, the study does not provide conclusive evidence that maintaining lumbar lordosis with portable, custom-made seat devices significantly reduces the incidence of scoliosis in DMD patients. Future studies with larger sample sizes and improved seat device designs to enhance compliance are recommended to better assess the potential benefits.

Table 1. Demographic characteristics of participants

Characteristics	Seat device group (N=14)	Control group (N=46)	P-value
Age (years)	12.0 (11.0-13.3)	11.0 (10.0-12.0)	0.061
Average daily use of seat device (hours)	2.4 (2.1-4.1)	0.0 (0.0-0.0)	0.000*
Last follow up from LOA (months)	58.0 (54.8-63.3)	59.0 (55.0-60.0)	0.785

Values are presented as median (interquartile range)

* Significant at $p < 0.05$, by Mann-Whitney U test

Table 1. Demographic characteristics of participants

Figure 1. Custom-made portable seat device



Figure 1. Custom-made portable seat device. (a) Custom-made portable seat device designed for each participant, including lumbar pads to enhance lumbar lordosis, pelvic belts, and chest straps to prevent sacral sitting. The seat is equipped with a 5cm Roho cushion to reduce pressure on the ischial tuberosity. (b) Application of the seat device to a wheelchair, demonstrating its portability and adaptability to different settings. (c) A DMD patient sitting on a wheelchair equipped with the seat device at home, illustrating the device's use in various environments such as home, school, and other locations, ensuring continuous support for lumbar lordosis.

Developing Bimanual Task-Oriented Training Programs for Children with Unilateral Cerebral Palsy

Youngsub Hwang^{1*}, Jiyeon Tak¹, Jeong-Yi Kwon^{1†}

Department of Physical and Rehabilitation Medicine, Samsung Medical Center¹

Objective

To develop a tailored, task-specific, home-based upper limb training program for children with unilateral cerebral palsy (UCP) using the Delphi method, aiming to bridge the gap between therapy and practical daily life improvements.

Participants and Methods

A total of 65 experts, including 30 occupational therapists, 30 physical therapists, and 5 pediatric physiatrists, participated in the study. Foundational data from the Canadian Occupational Performance Measure (COPM) were collected in a previous RCT. Using COPM insights, daily challenges faced by children with UCP were categorized into self-care, productivity, and leisure following the Canadian Model of Occupational Performance and Engagement (CMOP-E). The study involved a two-round Delphi technique and an initial pilot survey. In Phase 1, an initial questionnaire analyzed challenges faced by 22 children with UCP, categorized under dressing, eating, hygiene, and other areas. Experts rated the importance of each goal on a 1–10 scale. The study team then refined the task list based on expert feedback. In Phase 2, preliminary therapeutic activities were developed, integrating expert insights to ensure alignment with the specific needs of children with UCP. These activities underwent pilot testing with ten pediatric therapy experts who provided feedback, leading to further refinements. A second pilot study assessed the validity of each activity, with ten experts scoring each on a 4-point scale. The Item Content Validity Index (I-CVI) was calculated, and activities with high content validity were retained. In Phase 3, the revised therapeutic activities were evaluated through two rounds of Delphi surveys by a panel of pediatric occupational therapists, physical therapists, and pediatric physiatrists. The experts rated the effectiveness and feasibility of activities, and a consensus was reached if there was ≥70% agreement among panelists and a mean importance score of ≥7.

Results

The initial COPM results of 22 children with UCP identified self-care tasks as critical, with dressing, feeding, and hygiene as the highest priorities. Consequently, 110 preliminary therapeutic activities were developed and refined through pilot testing. The Delphi process ultimately reached a consensus on 106 of 122 proposed activities. The final set of task-specific activities included a variety of self-care, productivity, and leisure tasks designed to be feasible within home settings.

Conclusions

This consensus-driven approach ensures that the therapeutic activities are both effective and applicable in real-world settings, addressing the need for evidence-based practices in home settings for children with UCP. The study highlights the importance of incorporating expert insights and systematic validation processes in developing home-based training programs that support improved daily functioning and independence for children with UCP.

Acknowledgment This research was made possible through the financial support of the National Research Foundation of Korea (NRF) grant, provided by the Korean government (Grant No. RS-2023-00278700).

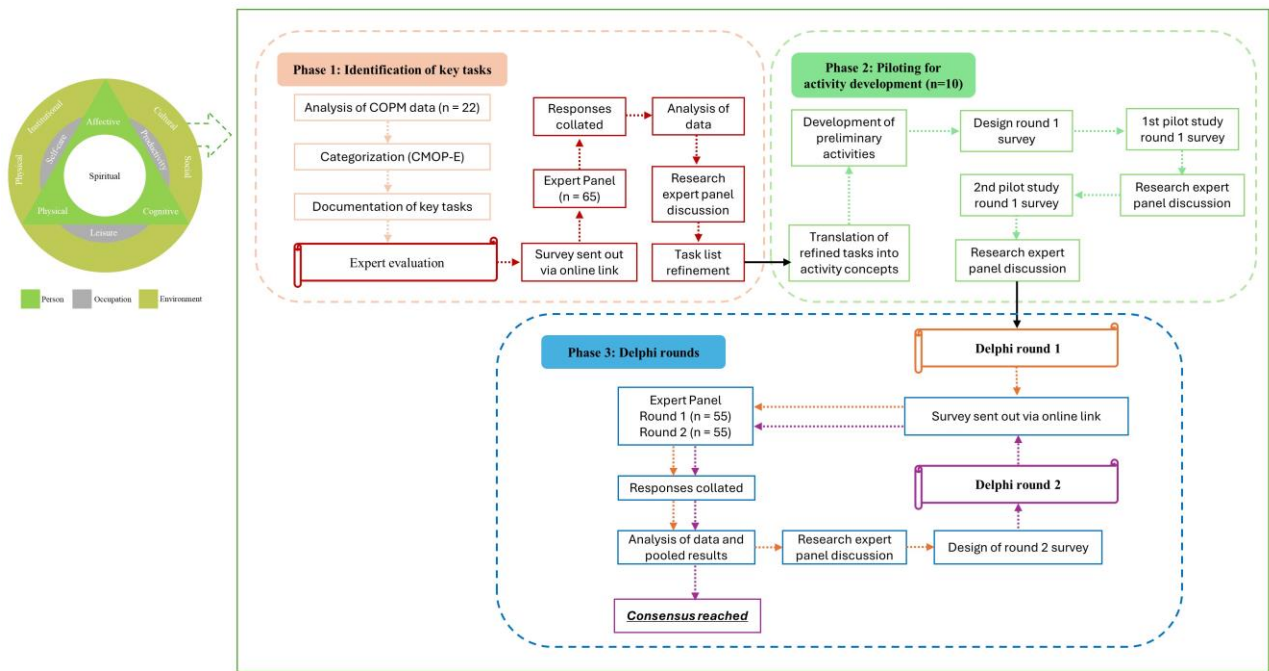


Figure 1. Development process of therapeutic activities for children with unilateral cerebral palsy. Phase 1 involved identifying key tasks based on Canadian Occupational Performance Measure (COPM) data from 22 children, followed by expert evaluation and task refinement. Phase 2 focused on piloting for activity development, including the initial activity development, preliminary pilot testing with expert feedback, and content validity assessment. Phase 3 utilized Delphi rounds, where a series of surveys were conducted to reach an expert consensus on the therapeutic activities.

A Study on Therapeutic Cervical Lateral Flexion Range of Motion Angles in Infants with Torticollis

Bumcheol Kim^{1*}, Dae-Hyun Jang¹, Jaewon Kim^{1†}

Department of Rehabilitation Medicine, Incheon St. Mary's hospital, The Catholic University of Korea¹

Introduction

Torticollis is a common musculoskeletal disorder in infants, characterized by a distinctive posture where the head is tilted to one side and rotated to the opposite side, sometimes accompanied by facial asymmetry. Cervical lateral flexion passive range of motion (PROM) exercise is an important therapeutic intervention. However, there is a lack of reference values for cervical lateral flexion PROM in infants, and information on age-specific neck lateral flexion AROM during growth is scarce. This study was conducted to determine these values in infants.

Methods

This study included infants under 12 months of age with normal gross motor development and muscle tone who visited the clinic for torticollis treatment. Videos of rehabilitation therapy performed by a therapist were collected from infants who visited the pediatric physical therapy clinic for torticollis treatment. The infants performed lateral flexion PROM exercises on both sides in sitting and supine positions, with each video recorded from a frontal view to ensure the infant's face was facing forward (Figure 1). The videos were divided into frames at 1-second intervals and analyzed as images. Among the frames, those showing full PROM exercises were selected and labeled for regions of interest (ROIs) on anatomical landmarks (eyes, nose, mouth, ears, and shoulders). The labeled frames were then analyzed using Python (version 3.10.6) with the numpy library (version 1.24.3) to measure the ROM angles. Vectors connecting the eyes and shoulders were extracted to calculate the angle values (Figure 2). The highest ROM value for each child was analyzed.

Results

A total of 95 infants were included. Among them, 18 (18.8%) were 4 months old, the most common age group. Torticollis was left-sided in 53 (55.8%) cases. Ten (10.4%) infants had congenital muscular torticollis confirmed by ultrasound showing fibromatosis colli. The age-specific cervical lateral flexion PROM values are described in Table 1. There were no significant differences in ROM values by age. However, ROM values in the sitting position were significantly higher than those in the supine position (mean (SD) 136.0 (9.4) vs 127.8 (6.4), $p < .001$).

Conclusion

This study was conducted to determine the reference values for cervical lateral flexion PROM in infants under 12 months of age. The values obtained from this study will serve as reference values for pediatric rehabilitation and provide a foundation for future research.



Figure 1. Lateral flexion passive range of motion exercises were recorded from a frontal view in both sitting and supine positions



Figure 2. The lateral flexion angle was calculated using lines connecting both eyes and both shoulders

Age (m)	1	2	3	4	5	6	7	8	11	12
Sitting position										
Mean	132.8	143.1	130.7	133.2	137.6	137.8	136.6	135.8	140.7	135.3
(SD)	(5.43)	(9.26)	(9.92)	(10.7)	(5.06)	(10.9)	(15.0)	(4.49)	(1.4)	(12.0)
Max	138.7	149.7	138.6	149.3	144.8	150.2	164.4	139.9	141.7	148.2
Supine position										
Mean	131.2	122.4	123.4	128.2	125.4	131.3	125	126.9	119.6	137.6
(SD)	(8.7)	(4.59)	(2.98)	(4.84)	(6.0)	(5.0)	(4.1)	(3.06)	(1.13)	(5.9)
Max	142.6	125.7	125.4	135.4	136.7	137.5	131.5	130.4	120.4	141.9

* High-quality images were difficult to obtain from 9-10 month-old infants due to poor cooperation

Table 1. Cervical lateral flexion passive range of motion angles in sitting and supine positions by age in months

Association Between Obesity and Activities of Daily Living Limitation in Children and Adolescents

Seong-Eun Kim^{1*}, Yung Jin Lee^{1†}, Jong Bum Park¹, Mi Jin Hong¹, Dong Jin Chae¹, Cho E Sim¹, Ji-Hwan Kwon¹

Department of Rehabilitation Medicine, Konyang University College of Medicine¹

Introduction

The ability to perform activities of daily living (ADL) is crucial for children's development. ADL disabilities can result from various health issues, yet most research focuses on specific conditions, leaving a gap in understanding ADL limitations in the broader pediatric population.

The prevalence of overweight/obesity in children and adolescents has increased due to various factors, becoming a significant public health issue. However, obesity prevalence among children with activity limitations remains unclear.

Objective

This study aimed to examine the relationship between obesity and ADL limitations in Korean children and adolescents, focusing on the impact of obesity on functional abilities and the influence of lifestyle and environmental factors.

Materials and methods

This cross-sectional study collected data from the KNHANES 2010–2015, conducted by the Korea Centers for Disease Control and Prevention (KCDC). We selected participants aged 3–18 years ($n = 8913$) who had completed surveys on ADL limitation, body mass index (BMI), waist circumference (WC), and sociodemographic data. Finally, 7601 participants were included in the study.

Statistical analyses, including chi-square test, t-test, and logistic regression, examined the relationship between ADL limitation and obesity, considering various factors.

Results

In our study population, the mean age was 11.1 years, and 159 (2.1%) patients had limitations in ADLs. As shown in Table 1, Those with ADL limitations had higher weight, BMI, and WC (49.0 kg, 20.2 kg/m², and 67.4 cm, respectively). There was a significant difference in residential area, household income, and paternal educational level.

Table 2 shows the variables related to ADL limitation. Overweight children had a higher likelihood of ADL limitation (OR, 1.76), even after adjusting for other socioeconomic factors (OR, 1.78). There was a significantly larger proportion of individuals from the lowest household income group (OR, 2.55), single-parent households (OR, 2.23), and when paternal education was below middle school (OR, 1.85).

As shown in Figure 1, the causes of ADL limitations included psychological disorders, mental retardation or developmental disorders, fractures or musculoskeletal disorders, cardiopulmonary disorders, language, visual or hearing problems, and others. Other causes include allergies, congenital myopathy, fever, fatigue, and infections.

Conclusions

This study identified factors influencing ADL limitations in children and adolescents and found a significantly higher prevalence of overweight children and adolescents with ADL limitations. Various causes of ADL limitation were identified, including psychological disorders, mental retardation, developmental disorders, and other health issues. These findings emphasize the association between being overweight and ADL limitations, highlighting the need for proper health intervention strategies for children and adolescents with ADL limitations.

Table 1. Characteristics of the participants

		ADL limitation			P value
		Total n=7601 n (%)	Yes n=159 n (%)	No n=7442 n (%)	
Age (years)	Mean (95% CI)	11.1 (10.9-11.3)	12.7 (11.8-13.7)	11.1 (10.9-11.2)	<.0001
Sex	Male	4033 (53.2)	96 (57.4)	3937 (53.1)	.368
	Female	3568 (46.8)	63 (42.6)	3505 (46.9)	
Weight (kg)	Mean (95% CI)	43.1 (42.4-43.7)	49.0 (44.5-53.5)	42.9 (42.3-43.6)	.002
BMI (kg/m ²)	Mean (95% CI)	19.1 (19.0-19.3)	20.2 (19.3-21.1)	19.1 (19.0-19.2)	.006
	Underweight	508 (6.7)	13 (5.2)	495 (6.7)	.092
	Normal	5615 (73.6)	107 (70.8)	5508 (73.6)	
	Overweight	693 (9.1)	24 (15.2)	669 (9.0)	
	Obesity	785 (10.6)	15 (8.9)	770 (10.7)	
Waist circumference(cm)	Mean (95% CI)	63.7 (63.3-64.1)	67.4 (64.6-70.3)	63.6 (63.2-64.0)	.002
Abdominal obesity	Present	573 (8.2)	10 (6.3)	563 (8.3)	.442
	Absent	7028 (91.8)	149 (93.7)	6879 (91.7)	
Residence area	Urban	6496 (83.6)	146 (93.8)	6350 (83.4)	.001
	Rural	1105 (16.4)	13 (6.2)	1092 (16.6)	
Household income	Q1	516 (8.4)	19 (18.3)	497 (8.2)	.007
	Q2	2062 (29.1)	37 (28.8)	2025 (29.1)	
	Q3	2729 (34.6)	59 (28.5)	2670 (34.7)	
	Q4	2294 (27.9)	44 (24.4)	2250 (28.0)	
Household members	parents	3384 (40.1)	84 (39.0)	3300 (40.1)	.059
	single parents	371 (5.7)	15 (12.1)	356 (5.6)	
	two-generations, others	3198 (45.1)	45 (39.4)	3153 (45.2)	
	three-generations	648 (9.1)	15 (9.5)	633 (9.1)	
Maternal education status	missing	294 (5.0)	7 (7.7)	287 (4.9)	.382
	middle school or less	360 (6.1)	11 (8.1)	349 (6.1)	
	high school or higher	6947 (88.9)	141 (84.2)	6806 (89.0)	
Paternal education status	missing	2311 (33.4)	60 (44.0)	2251 (33.2)	.021
	middle school or less	392 (6.5)	13 (10.5)	379 (6.4)	
	high school or higher	4898 (60.1)	86 (45.5)	4812 (60.4)	

BMI, body mass index; 95% CI, 95% confidence interval

The mean and 95% confidence interval for continuous variables were calculated using PROC SURVEYREG, frequency and percentages for categorical variables were computed using PROC SURVEYFREQ.

Table 1. Characteristics of the participants

Table 2. Association between covariates and ADLs limitation

		OR	95% CI	P value	adjusted OR ^a	95% CI	P value
BMI	Underweight	0.80	(0.42 -1.52)	0.49	0.70	(0.35 -1.38)	.31
	Normal	1.00		0.15	1.00		.11
	Overweight	1.76	(1.01 -3.05)	0.04	1.78	(1.02-3.10)	.04
	Obesity	0.87	(0.46 -1.64)	0.67	1.04	(0.53 -2.07)	.92
Abdominal obesity	Present	0.74	(0.35 -1.59)		0.65	(0.28 -1.49)	
	Absent	1.00		0.44	1.00		.28
Residence area	Urban	3.01	(1.56 -5.84)	0.00	3.17	(1.60 -6.26)	
	Rural	1.00			1.00		<.05
Household income	Q1	2.55	(1.25 -5.22)	0.01	2.26	(0.91 -5.61)	.11
	Q2	1.14	(0.66 -1.97)	0.65	1.15	(0.68 -1.95)	.68
	Q3	0.94	(0.57 -1.54)	0.80	0.95	(0.58 -1.57)	.81
	Q4	1.00		0.04			.33
Household members	parents	1.00		0.15	1.00		.66
	single parent	2.23	(1.06 -4.72)	0.04	1.58	(0.70 -3.55)	.29
	two-generations, others	0.90	(0.57 -1.41)	0.64	0.90	(0.58 -1.41)	.68
	three-generations	1.07	(0.58 -2.00)	0.82	1.15	(0.61 -2.16)	.66
Maternal education status	middle school or less	1.91	(0.97 -3.74)		1.09	(0.37 -3.27)	
	high school or higher	1.00		0.06	1.00		.46
Paternal education status	middle school or less	1.85	(1.04 -3.30)		1.42	(0.56 -3.61)	
	high school or higher	1.00		0.04			.88

BMI, body mass index; 95% CI, 95% confidence interval

The odds ratios and 95% confidence intervals were calculated using PROC SURVEYLOGISTIC.

^aThe adjusted odds ratio was calculated without variable selection; all covariates were included in the multivariable model.

Table 2. Association between covariates and ADLs limitation

Figure 1. The causes of ADL limitations

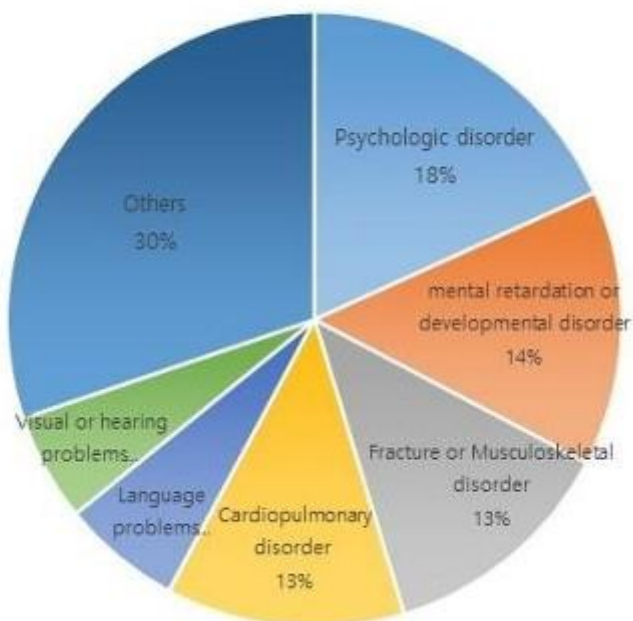


Fig 1. The causes of ADL limitations

Developing of Korean version of the Early Feeding Skills Assessment

Yebin Cho^{1*}, Hyeyeon Lee², Minhwa Park², Seon-ah Kim², Dong-wook Rha¹, Taekyung Lee¹, Juntaek Hong^{1†}

• Department and Research Institute of Rehabilitation Medicine, Yonsei University College of Medicine, Seoul, Korea¹, • Department of Pediatric Occupational Therapy, Severance Rehabilitation Hospital, Seoul, Korea²

Objective

The purpose of this study is to systematically develop a Korean version of the Early Feeding Skills Assessment (EFS), which comprehensively identifies and quantitatively compares feeding problems before, during, and after feeding in neonates and infants.

Method

The translation process followed the protocol presented by Feeding Flock, which has the authority to use EFS. (1) The forward translation of the original EFS from English to Korean was conducted by two pediatric occupational therapists with over 14 years of clinical experience. (2) The integration of the two Korean versions was carried out by two clinicians specializing in pediatric rehabilitation medicine, with over 5 and 20 years of experience. (3) The first Korean version was then back-translated into English by a professional translator (Enago) without medical knowledge. (4) The back-translation was reviewed by an expert from Feeding Flock to verify the accuracy and consistency of the translation. (5) The final Korean version of the EFS was developed through a cognitive interview process involving three neonatologists, three neonatal nurse practitioners, and two pediatric occupational therapists, each with over 15 years of clinical experience and independent of the translation process. Since the original EFS was revised during the translation process, the Korean version was updated in a traceable manner to reflect the most recent version.

Result

During the initial forward translation and integration process, discrepancies between Korean and English were resolved, such as modifying the term 'Feeding' in the title to better align with the evaluation age range, resulting in the first Korean version. In the back-translation verification process, any misinterpreted expressions were identified, and the accuracy of meaning transmission was reassessed. Clarification of terms, such as 'compression,' was provided to ensure a precise understanding of the definition. Additionally, domain titles such as 'Engagement' and 'Physiologic Stability', along with endnote terms such as 'furrowed brow', 'head bobbing', and 'suprasternal retraction', were revised by referring to words or phrases suggested from the Feeding Flock's expert, resulting in the second Korean version. During the cognitive interview process, terms that had not yet reached consensus in the previous stage, such as 'gulping', 'yelping' (indicative of swallowing coordination problems), and 'color change' (indicative of problems with physiologic stability) were further discussed, and the final Korean version was confirmed.

Conclusion

The Korean version of EFS developed through this study is expected to be widely and effectively utilized as a tool for assessing swallowing in neonates and infants in clinical settings in Korea. Future research should prioritize evaluating the reliability and validity of this version to establish its effectiveness in clinical practice.

Longitudinal Changes in Intelligence Quotient Across Age Groups: A Multi-Year Follow-Up Study

Bo Young Hong^{1**}, Soo Ho Lee¹, Youngdeok Hwang², Yeun-Jie Yoo¹, Mi-Jeong Yoon¹, Joon-Sung Kim¹

Department of Rehabilitation Medicine, St. Vincent's Hospital, College of Medicine, The Catholic University of Korea¹,
Paul H. Chook Department of Information Systems and Statistics, Baruch College, City University of New York²

Introduction

Cognitive development is a complex process influenced by genetic and environmental factors, encompassing various concepts and abilities. As individuals age, their cognitive functions evolve, and this development can be assessed through multiple standardized tests. One of the most commonly used tools for evaluating cognitive abilities is the Wechsler Intelligence Scale, which comprehensively measures intellectual functioning. However, the content and interpretation of these tests can vary significantly across different age groups, reflecting the dynamic nature of cognitive development.

This study aims to investigate the longitudinal changes in IQ (Intelligence quotient) across different age groups using multi-year follow-up data. By examining repeated measures of IQ over an extended period, we seek to identify patterns of cognitive development and decline, contributing to a deeper understanding of age-related variations in intelligence measured by the Wechsler Intelligence Scale.

Methods

We extracted data from patients who underwent intelligence testing at our institution's Department of Rehabilitation Medicine over 10 years and who had undergone at least three assessments. The IQ test results from 58 patients (186 test results) were analyzed, and cases where IQ values could not be computed were assumed to have an IQ score of zero.

The assessments used during this period included the following:

Korean Wechsler Preschool and Primary Scale of Intelligence (K-WPPSI) and K-WPPSI-IV

Korean Educational Development Institute - Wechsler Intelligence Scale for Children (KEDI-WISC)

Korean Wechsler Intelligence Scale for Children IV, V (K-WISC-IV, V)

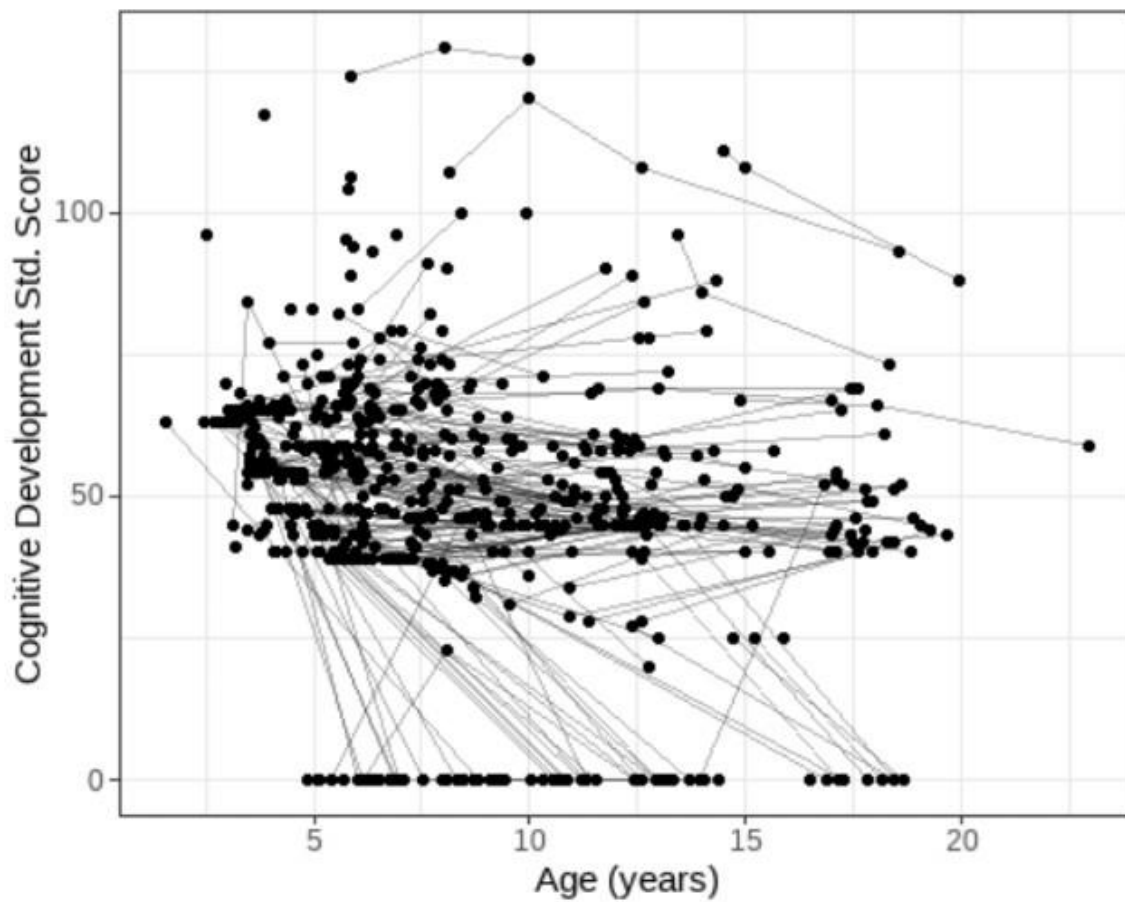
Korean Wechsler Adult Intelligence Scale-IV (K-WAIS-IV)

Results

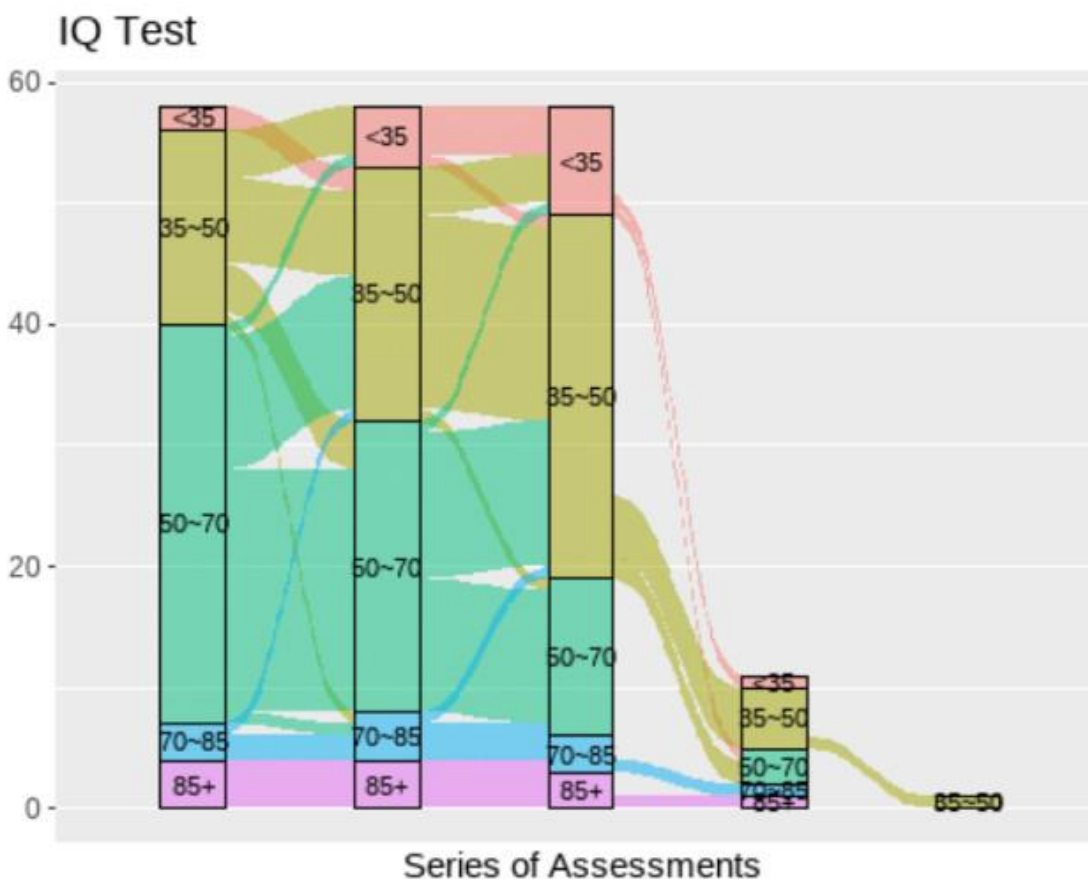
IQ scores were categorized into the following groups: Profound Intellectual Disability (IQ < 35), Moderate Intellectual Disability (35-50), Mild Intellectual Disability (50-70), Borderline Intellectual Functioning (70-85), and Normal (IQ > 85). Out of a total of 58 individuals, 56.9% remained in the same category as their previous assessment, 29.3% shifted to a lower category, and 13.8% moved to a higher category. Among those who experienced category shifts, one individual improved by two levels, while two individuals moved down by two levels; the remaining cases were within a one-level range of movement. The analysis revealed that, approximately after the age of 13, there were no significant changes in these categories. The differences in IQ scores by age were not statistically significant, with $p > 0.05$, indicating that IQ scores did not vary considerably across different ages.

Conclusion

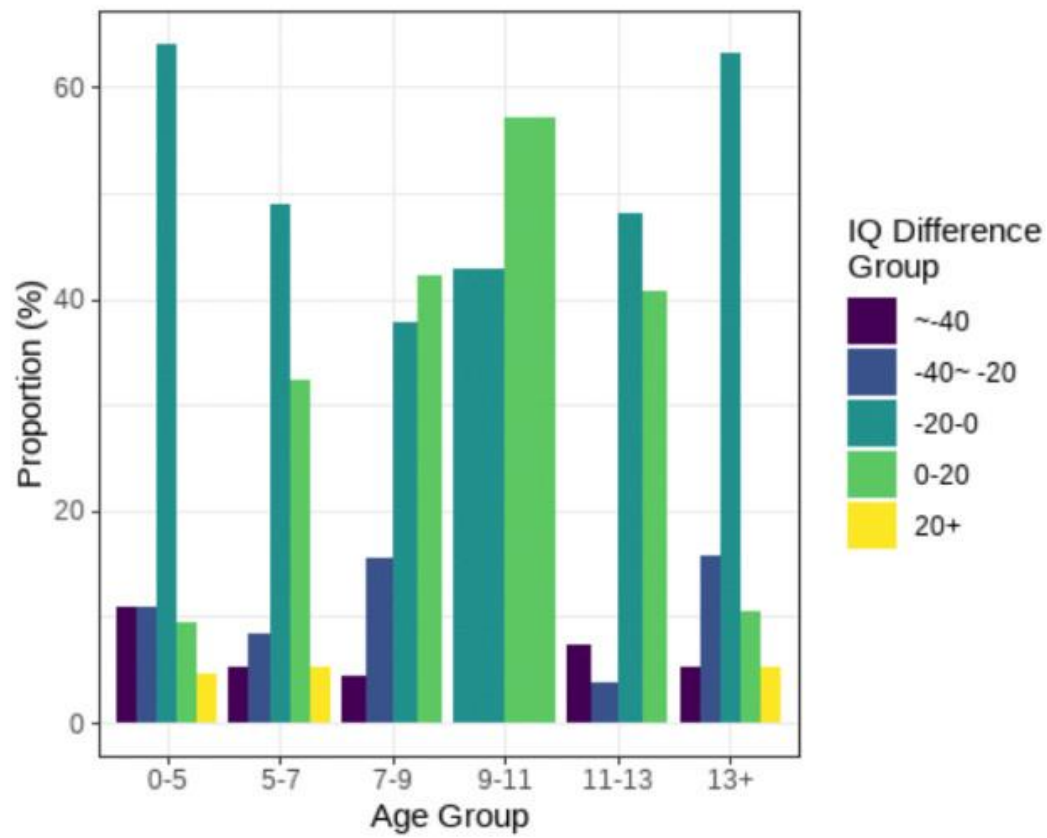
While individual IQ scores showed some fluctuations, there were no statistically significant differences in IQ scores over time. Before the age of 13, there was some movement between categories of intellectual disability (profound, moderate, mild) as well as between borderline and normal ranges. However, this movement decreased with increasing age.



Scatterplot of serial assessment of IQ



Movement of IQ category across the assessments



Difference of IQ according to the age

A protocol for digital healthcare providing at-home training in preterm infants

Soohyun Wi^{1,2*}, Moon Suk Bang¹, Hyung-Ik Shin¹, Sung Eun Hyun¹, Yae Lim Lee¹, Seung Hwan Lee¹, Woo Hyung Lee^{1†}

Department of Rehabilitation Medicine, Seoul National University Hospital¹, Biomedical Research Institute, Seoul National University Hospital²

Objectives

The birth rate of premature and very low birth weight infants, which are major risk factors for developmental delay and cerebral palsy, is continuously increasing, and early rehabilitation during the period of active brain plasticity is very important for a good prognosis. Since parents are a very important environmental factor that affects the survival and development of premature infants, expert monitoring is needed to provide a systematic and practical guide to developmental treatment for early intervention of non-specialist parents. We designed a digital health system protocol to provide an in-home developmental training guide for parent-centered early intervention of preterm or very low birth weight infants.

Materials and Methods

The study protocol is to investigate the feasibility and safety of home-based intervention for 6 months after discharge from the neonatal intensive care unit. After the hospital discharge, physiotherapist monitoring is conducted twice a week using a digital platform for parent-centered early intervention in the home. Parents record the developmental training process using a smartphone, and the therapist analyzes the video data to provide new training goals and guidelines.

Results

Developmental evaluation is performed as an outpatient visit at 0, 1.5, 4, 6, and 9 months of corrected age. The evaluation tools are the test of infant motor performance, General Movement Optimality Score, Motor Optimality Score-Revised, Hammersmith Infant Neurological Examination, Gross Motor Function Measure, and Bayley Scales of Infant and Toddler Development according to each corrected age.

Conclusions

This study protocol that parent-centered developmental training at home will increase the amount of rehabilitation dose for infants and maximize the effect of developmental training, thereby improving the prognosis for developmental delay and cerebral palsy.

Acknowledgment This work was supported by Seoul National University Hospital (04-2022-2050)

Utilizing Depth Cameras for Digital Mirrors in Pediatric Cognitive and Motor Therapy

Young-Hwan Lim¹, Chang-Hwan Ahn¹, Yu-Sun Min^{1,2*†}

Department of Rehabilitation Medicine, Kyungpook National University Chilgok Hospital¹, Department of Rehabilitation Medicine, School of Medicine, Kyungpook National University²

The innovative integration of depth cameras into digital mirrors presents a transformative approach to pediatric cognitive and motor therapy. This technology leverages real-time key point detection and visual feedback, offering significant advantages in rehabilitation settings. The purpose of this study is to explore the application of digital mirrors enhanced by depth cameras for the motor and cognitive rehabilitation of pediatric patients.

Our system employs depth cameras to capture the movements of pediatric patients in front of a digital mirror. This setup automatically detects key points on the patient's body, enabling precise motion tracking. The digital mirror then provides immediate visual feedback, which is crucial for effective motor learning and correction.

Depth cameras identify and track key points on the patient's body for accurate movement monitoring, and these movements are displayed instantly on the digital mirror for immediate correction and reinforcement. Additionally, interactive games enhance engagement and motivation, supporting both cognitive and motor rehabilitation. The gamified approach increases participation and enthusiasm, leading to enhanced engagement. Real-time feedback allows prompt adjustment of movements, resulting in improved motor skills. Additionally, the combination of visual stimuli and motor activities supports overall cognitive development.

Depth cameras in digital mirrors represent a promising advancement in pediatric motor therapy. This technology supports cognitive and motor rehabilitation through key point detection, visual feedback, and gamified learning. Future studies will refine the system and evaluate its long-term benefits in diverse pediatric populations.

A New Digital Solution for Rapid Motion and Gait Analysis in Pediatric Rehabilitation

Young-Hwan Lim¹, Chang-Hwan Ahn¹, Kim Deokseok³, Kim Hyo Joong³, Yu-Sun Min^{1,2*†}

Department of Rehabilitation Medicine, Kyungpook National University Chilgok Hospital¹, Department of Rehabilitation Medicine, School of Medicine, Kyungpook National University², AI Research Team, MTEG³

Gait analysis in pediatric rehabilitation patients is crucial for diagnosis, assessment, measurement of treatment outcomes, and planning of therapeutic interventions. However, traditional equipment faces challenges in pediatric settings, including difficulties in attaching markers to young patients, time and space constraints, and the need to follow specific protocols, limiting its widespread use.

The UDJET motion capture device is an advanced digital solution designed to swiftly perform motion and gait analysis for musculoskeletal disorders and central nervous system injuries. Utilizing four depth cameras, UDJET captures comprehensive motion data without the need for suits or markers, offering precise measurements of joint angles and velocities. The versatile setup, adaptable to various room sizes, maximizes spatial efficiency.

Using the UDJET program, we were able to analyze the gait speed, step length, stride, step width, and the kinematics of each lower limb joint(hip, knee, ankle) in pediatric rehabilitation patients. This innovation significantly benefits neurorehabilitation by providing reliable, efficient, and precise assessments of patient progress.

Pediatric Rehabilitation

P-110

Introducing EasyScope: A Novel Device for Enhanced Lower Limb Assessment and Rehabilitation Planning

Chang-Hwan Ahn¹, Young-Hwan Lim¹, Yu-Sun Min^{1,2*†}

Department of Rehabilitation Medicine, Kyungpook National University Chilgok Hospital¹, Department of Rehabilitation Medicine, School of Medicine, Kyungpook National University²

EasyScope is an innovative device designed to improve upon the traditional pedoscope by converting mirror-based images of the plantar surface into digital photographs. Additionally, it captures digital photos of the posterior aspect of both lower limbs in the coronal plane, allowing for efficient storage and subsequent analysis of medical images. This capability facilitates comprehensive evaluation through key point detection at the malleolus and knee level, enabling precise calculations of ankle joint movements and assessments of genu valgum and varum. EasyScope supports repeated measurements, making it possible to track improvements in ankle pronation and supination following therapeutic interventions. By providing detailed assessments of overall lower limb alignment, EasyScope enhances the efficiency of rehabilitation treatments and aids in the development of comprehensive treatment plans.

Effect of Botulinum Toxin Injection on Proximal Lower Limb Muscle in Low Functioning Cerebral Palsy

Jun Min Cha^{1*}, Jehyun Yoo¹, Juntaek Hong¹, Taekyung Lee¹, Jeuhee Lee¹, Yebin Cho¹, Dong-Wook Rha^{1†}

Department and Research Institute of Rehabilitation Medicine, Yonsei University College of Medicine¹

Introduction

Botulinum toxin type A (BoNT-A) injections are frequently administered into proximal lower limb muscles, such as the hip adductors or medial hamstrings, in low-functioning children with spastic cerebral palsy (CP) to alleviate spasticity, reduce pain, and facilitate caregiving by improving handling and positioning. However, unlike in ambulatory CP, there is limited research on the effectiveness of this intervention in improving functional outcomes in low-functioning CP children. This study aims to evaluate the efficacy of BoNT-A in improving gross motor function in low-functioning children with spastic CP.

Methods

This study is a retrospective observational study at a single tertiary hospital from March 2006 to May 2024. During the study period, a total of 3,609 BoNT-A injections were administered, of which 59 cases met the criteria for inclusion in this study. The inclusion criteria were preschool-aged children under 84 months of age, classified as Gross Motor Function Classification System (GMFCS) levels III, IV or V, with injections specifically targeting the medial hamstring and/or adductor muscles. Children who had received BoNT-A injection, nerve block, selective posterior rhizotomy (SPR), or orthopaedic surgery within one year prior to the study were excluded. Evaluations were conducted using the Gross Motor Function Measure (GMFM), and the study included only children with CP who underwent pre-injection assessments within one month before the injection and post-injection assessments between three weeks and four months after the injection.

Results

A total of 59 children with CP were included in the study (range 1.5–7y; mean 4.5y; 37M, 22F). According to the GMFCS classification, there were 14 children in level III, 16 children in level IV, and 29 children in level V. Assessments were performed using the GMFM-88, and the total score was then converted to GMFM-66. The GMFM-66 scores demonstrated statistically significant improvement post-BoNT-A injection compared to pre-injection in all GMFCS levels (p -value < 0.05). Additionally, the specific GMFM domains showing significant improvement varied by GMFCS level. In GMFCS level III children, who are capable of assisted gait, statistically significant improvements were observed primarily in GMFM domains D and E, which are associated with gait function (p -value < 0.05). In GMFCS level IV children, significant improvements were noted in domain C (p -value < 0.05). In GMFCS level V children, statistically significant improvements were observed in GMFM domains A, B, and C, which assess functional abilities in supine and seated positions (p -value < 0.05).

Conclusion

This study suggested that BoNT-A injections to proximal lower limb muscles improved gross motor function in low-functioning children with spastic CP.

Pediatric Rehabilitation

P-112

Identification, needs assessment and community intervention of the children with physical disability

Fatema Newaz^{1*†}

Assistant Professor, ¹

Purpose

Scope: Childhood disability is a global public health concern because of its long-term effects on physical and psychological well-being. Approximately 80% of childhood disabilities occur in low and middle income countries (LMIC). Despite substantial burden little is known about access to rehabilitation program, in total 78.2% never received rehabilitation. The WHO 2030 Agenda for SDG states that children with disability should have equal access to healthcare and rehabilitation. As Bangladesh is developing country rehabilitation is not a priority and has multiple challenges for rehabilitation team work.

Purpose: The primary goal is to train a group of people who will find out and evaluate the patient with physical disability living in community, provide a home-based exercise program with close monitoring with establish tele-rehabilitation.

Method

As a preliminary step, we intend to focus on zones such as Borura (Cumilla), Manikgonj Sadar, Kapashia to find out children with physical disability with current treatment status identification, diagnosis, treatment or rehabilitation status. This will assist us in creating register of children with physical disability along with assessment of need of these group. We will train a group of people known as therapeutic expander from the community for identification, assessment of need and easy rehabilitation procedure, assess therapy requirements and establish a CBR program in Bangladesh.

Conclusion

Inclusion in the society of person with physical disabilities as well as persons with special needs is crucial for Sustainable Development. In a country like us with many constraints, community based rehabilitation is time demanding that can be achieved by community intervention.

Physical Modality

P-113

Empowering Disabled Users: A Head-Mouth Controlled Mouse Interface for Improved Accessibility

Dr. Muhammad Umair Ahmad Khan PhD. ^{1**}, Muhammad Umair Ahmad Khan¹, Hafiz M Salman Ajmal¹, Marwa Maqsood¹, Shumaim Sajid¹, Zahid Shammass¹

Department of Biomedical Engineering UET Lahore Narowal Campus, .¹

Purpose

Purpose People with physical disabilities in their upper extremities face significant challenges using conventional gadgets due to limited movement and precision. This article proposes an alternative input method to address these issues by developing corresponding devices that enhance usability and accessibility.

Scope

The proposed interface utilizes an inertial measurement unit (IMU) to replace the traditional mouse. Head motions are used to move the mouse pointer, while buttons pressed by mouth trigger mouse clicks. The system is designed to navigate and interact with computing devices, providing a more accessible solution for users with physical disabilities in their upper extremities.

Method

The model consists of a headset and a mouthpiece. The headset is responsible for moving the cursor on the screen in response to head movements, while the mouthpiece performs click operations through mouth movements. To test the effectiveness of the device, five students with physical disabilities were selected to use the system. Their ability to use the computer and open different folders was observed and recorded.

Result

The testing demonstrated that the five students with physical disabilities were able to effectively use the proposed system. They successfully navigated the computer interface and opened various folders with ease. This indicates that the alternative input method significantly enhances the accessibility and usability of computing devices for individuals with upper extremity disabilities.

Conclusion

The developed interface, which uses head movements for cursor control and mouth movements for click operations, provides a viable alternative to traditional input methods for users with physical disabilities. The system's effectiveness, as demonstrated by the ease with which students used it to interact with computing devices, highlights its potential to improve the quality of life for individuals with upper extremity limitations. This innovative approach offers a promising solution for enhancing accessibility and independence for people with physical disabilities.

Rehabilitation Research in South Korea: Mapping Scientific Landscapes through a Scientometric Review

Eunjee Lee¹, Myungeun Yoo², Chan Woong Jang^{1†}, Gyu Jin Kim^{1*}

Department of Physical Medicine and Rehabilitation, Hallym University Sacred Heart Hospital¹, Department of Rehabilitation Medicine, Uijeongbu Eulji Medical Center²

Introduction

Established in 1972, the Korean Academy of Rehabilitation Medicine has significantly advanced the field in South Korea. This study aims to analyze research productivity, collaboration opportunities, and emerging patterns in South Korean rehabilitation research using scientometric methods.

Methods

We analyzed bibliometric data from the Web of Science Core Collection, focusing on original studies published between January 1, 2005, and June 30, 2024, indexed in the Science Citation Index Expanded, Social Science Citation Index, or Emerging Sources Citation Index, by authors affiliated with South Korean medical schools' rehabilitation departments. Queries were formatted as "OG=(University name) AND AD=(rehabilitation medicine OR physical medicine and rehabilitation OR physical and rehabilitation medicine)" or "ALL=(University name) AND AD=(rehabilitation medicine OR physical medicine and rehabilitation OR physical and rehabilitation medicine)." We conducted performance and science mapping analyses using Biblioshiny, CiteSpace, and VOSviewer.

Results

From 2005 to 2024, we found 4,974 rehabilitation research articles, with an 8.48% annual growth rate and 13.53 citations per article. There was a consistent rise in publications, citations, and authors until a peak in 2021 and 2022, followed by a decline likely due to COVID-19.

A co-authorship and institutional collaboration network (Figure 1) revealed ten distinct groups, with "Jang Sung Ho," "Kim Yun-Hee," and "Chang Won Hyuk" identified as pivotal authors. Key institutions in collaboration included "Seoul National University," "Yonsei University," and "Sungkyunkwan University."

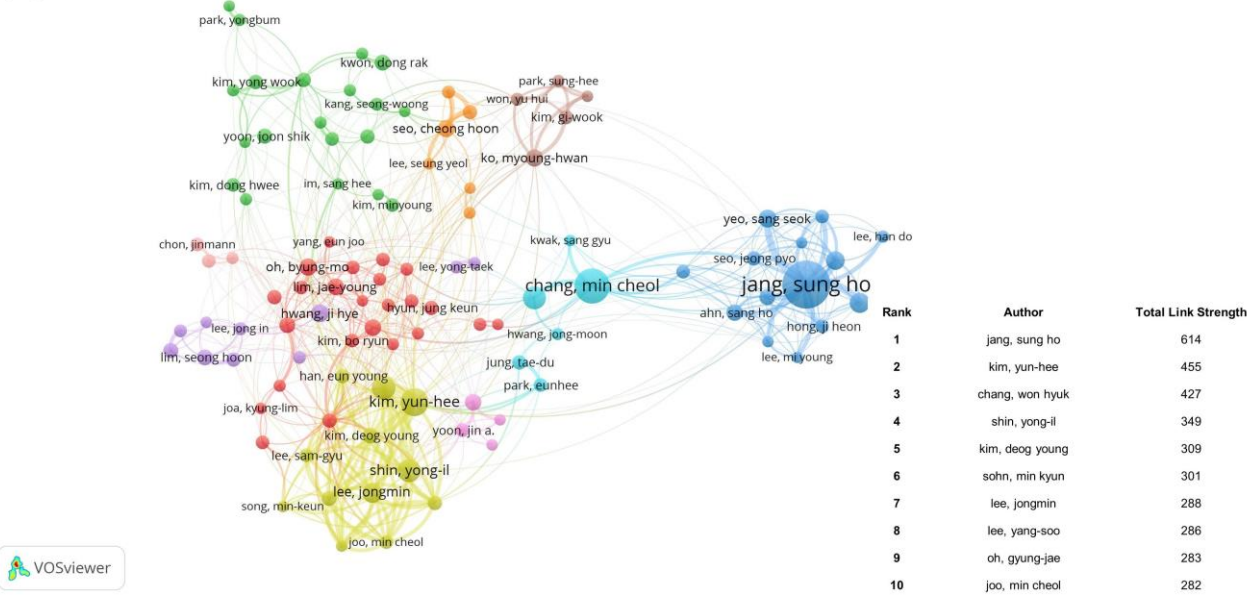
The keyword co-occurrence network (Figure 2) identifies four main research clusters: miscellaneous rehabilitation, stroke and diffusion tensor imaging, dysphagia, and cerebral palsy, with stroke being the primary focus. Cluster #2 centers on diffusion tensor imaging and predicting stroke recovery outcomes, with transcranial magnetic stimulation as a related topic. Cluster #4 focuses on gait in hemiplegic stroke patients, linked to cerebral palsy due to its gait connection. Cluster #3 centers on dysphagia, common in stroke patients, while Cluster #1 encompasses various rehabilitation topics outside stroke.

Keyword co-citation clustering (Figure 3) showed historical evolution and temporal distribution of the knowledge domain, with Clusters #7, #8, and #9 peaking around 2010-2012 and declining over the past decade. Cluster #6 emerged later but also declined recently, while Cluster #5, appearing around 2017, has maintained steady interest. No new significant research topics have emerged in recent years despite ongoing research using new technologies.

Conclusion

This study uses scientometric tools to map the intellectual growth of rehabilitation research in South Korea, aiding the scientific community in aligning studies with past developments and emerging agendas.

(A)



(B)

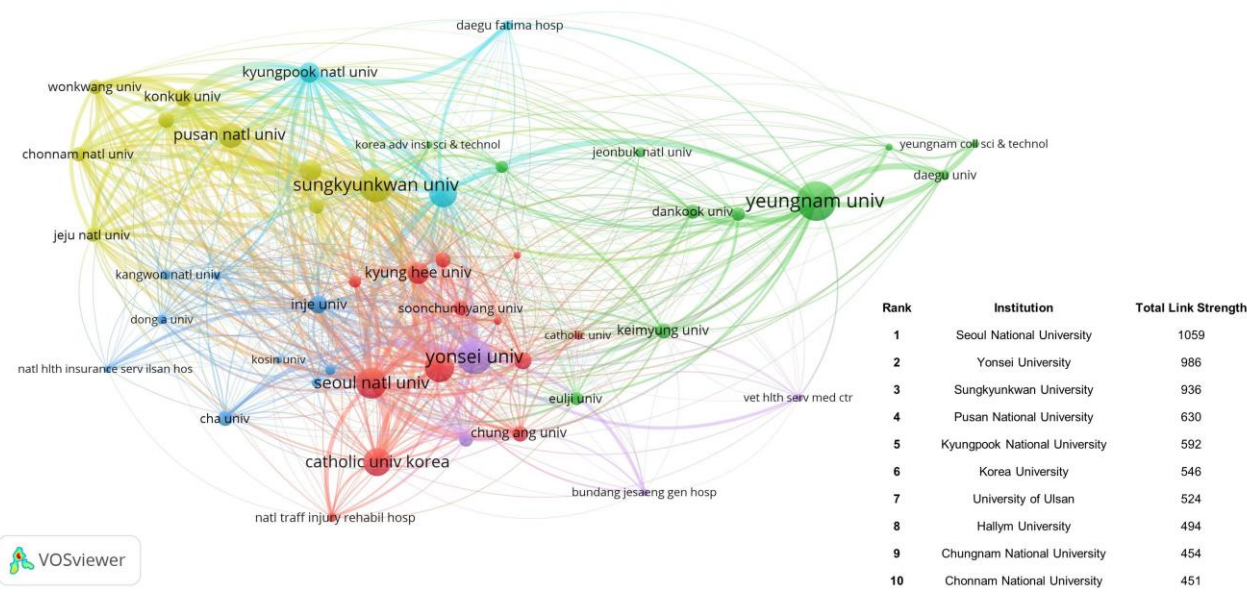


Figure 1. Collaborative network of co-authors (A) and institutions (B) of publications in South Korean rehabilitation research.

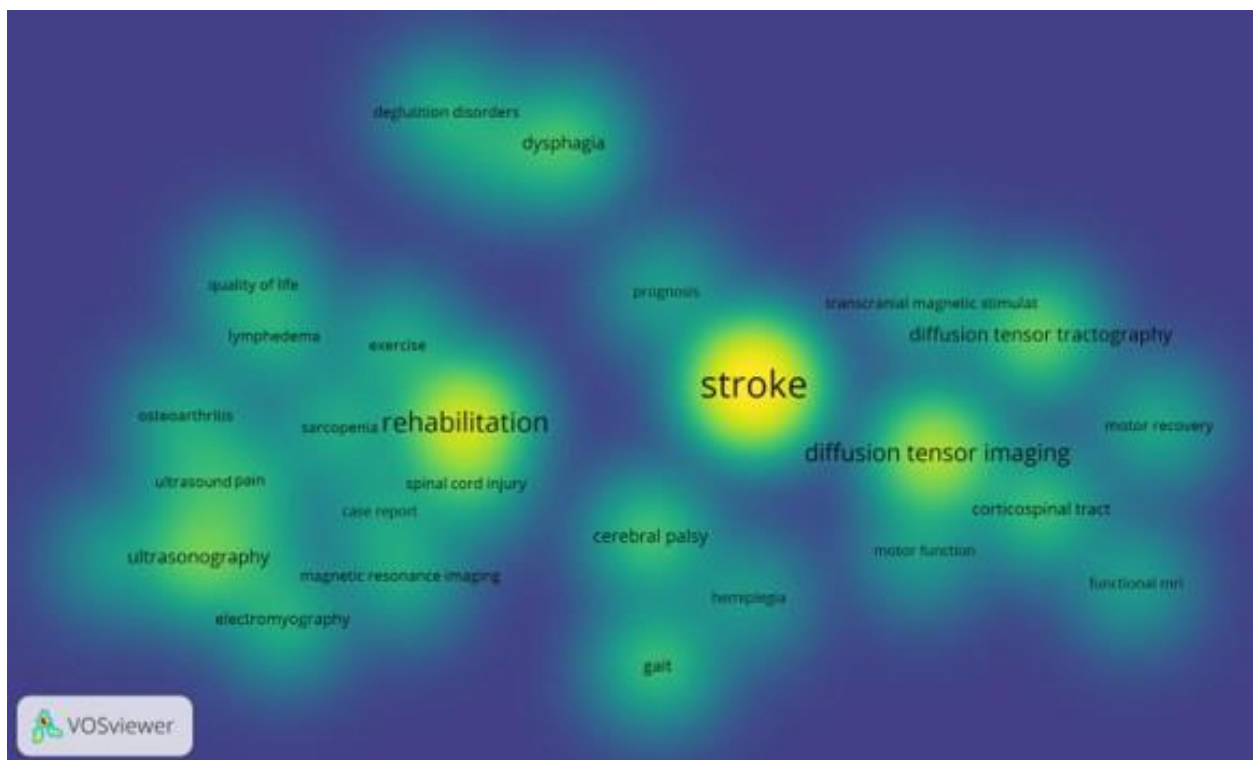


Figure 2. Keyword co-occurrence network using density visualization for publications in South Korean rehabilitation research.

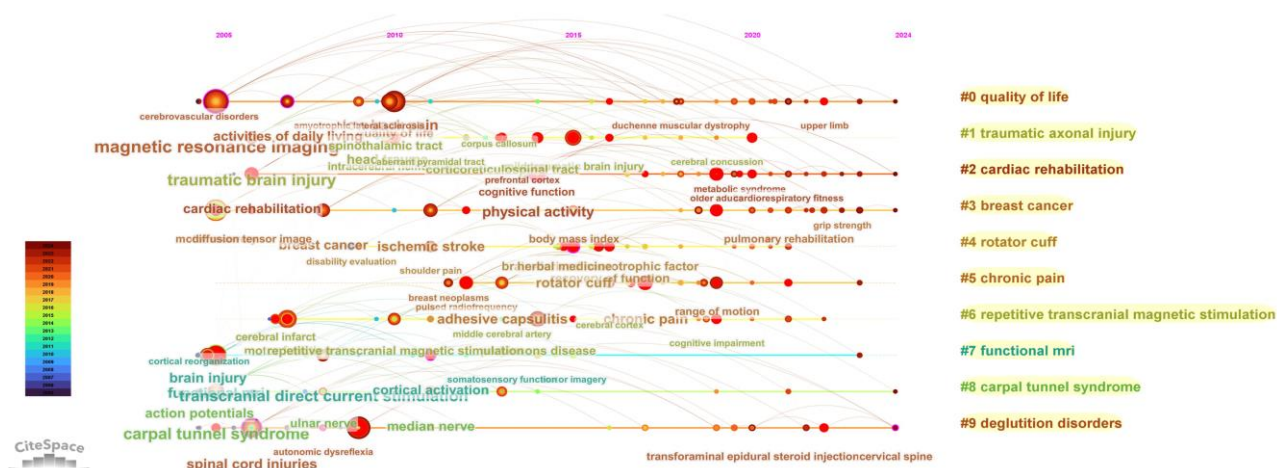


Figure 3. Timeline view visualization of keyword clusters in South Korean rehabilitation research.

Short-term Mortality and the Impact of Disability Type Following COVID-19 Among Disabled Individuals

Yoonjeong Choi^{1,2*}, Gi Hwan Bae³, Hyunji Lee⁴, Ja-Ho Leigh^{1,2,4†}

Department of Rehabilitation Medicine, Seoul National University Hospital¹, National Traffic Injury Rehabilitation Research Institute, National Traffic Injury Rehabilitation Hospital², Artificial Intelligence and Big-Data Convergence Center, Gil Medical Center³, Department of Rehabilitation Medicine, National Traffic Injury Rehabilitation Hospital⁴

Background

Since its emergence in 2019, the COVID-19 pandemic has resulted in numerous fatalities globally. Individuals with disabilities, who are mentally and physically vulnerable, face a significantly elevated risk of rapid mortality upon contracting COVID-19.

Objective: In this study, the risk of short-term mortality after COVID-19 infection among individuals with disabilities was determined and compared by disability type.

Methods

This is a national population-based study using the data from K-COV-N cohort, which is linked to the National Health Insurance Service (NHIS) and the Korea Disease Control and Prevention Agency (KDCA). We constructed a retrospective cohort including individuals with disabilities (n=2,729,089) registered in the NHIS system between 2020 and 2021. Information on COVID-19 infections was obtained from K-COV-N data, a cohort of individuals who infected with COVID-19 between January 2020 and March 2022. After excluding participants who transitioned from disabled to non-disabled or changed disability type, children or adolescents under 18 years of age, participants with missing values for variables, participants who died before baseline, and participants who were not matched by propensity score matching, 26,210 participants with COVID-19 infection and 1,928,650 controls without infection were finally selected as the study population. We used inverse probability of treatment weighting (IPTW) to mitigate selection bias, and Cox proportional hazards models to estimate the risk of mortality within 4 weeks after COVID-19 infection. Subgroup analysis were performed by severity of disability, types of disability, and the time of infection, respectively.

Results

The risk of death within 4 weeks of infection in the COVID-19-infected group before IPTW was 12 times that of the control group, and was similar after IPTW. Subgroup analysis by disability severity showed no difference in the risk of short-term mortality between mild and severe disability; however, in subgroups analysis by disability type, those with internal organs had the highest risk of short-term mortality and those with mental disabilities had the lowest risk. Subgroup analyses by the time of infection showed similar HRs for short-term mortality risk before and after the predominance of the SARS-CoV-2 Delta variant, but in the quarterly subgroup by 3-month period, the risk of short-term mortality was highest in the fourth quarter of 2020.

Conclusion

Although COVID-19 has transitioned to an endemic state, periodic outbreaks of respiratory infectious diseases continue to occur globally. Therefore, further research is needed to identify the factors that increase the risk of short-term mortality following COVID-19 infection among individuals with disabilities. Furthermore, policies should be implemented to prepare these vulnerable populations for respiratory epidemics.

Acknowledgment This study was supported by a grant from the Ministry of Land, Infrastructure and Transport (MOLIT) Research Fund (07-2024-5030). This study was conducted as part of the public-private joint research on the COVID-19 co-hosted by the KDCA and the NHIS. This study used the database of the KDCA and the NHIS for policy and academic research (NHIS-2022-1-699).

Table 1. Risk of mortality within 4 weeks after COVID-19 infection among people with disabilities

	Before IPTW			After IPTW		
	Hazard Ratios	95% CI	p-value	Hazard Ratios	95% CI	p-value
Crude model						
COVID-19						
None	reference			reference		
COVID-19 infection	11.00	10.41–11.63	< 0.0001	10.92	10.7–11.15	< 0.0001
Multivariable model ^a						
COVID-19						
None	reference			reference		
COVID-19 infection	12.14	11.48–12.85	< 0.0001	11.30	11.07–11.54	< 0.0001
Age						
18–34 yrs	reference			reference		
35–49 yrs	1.03	0.97–1.09	0.3449	1.04	1.03–1.07	< 0.0001
50–64 yrs	0.93	0.84–1.03	0.1793	0.76	0.74–0.79	< 0.0001
65–74 yrs	1.05	0.97–1.15	0.1952	1.18	1.16–1.21	< 0.0001
+75 yrs	0.97	0.93–1.03	0.4352	0.86	0.85–0.88	< 0.0001
Residence						
Seoul	reference			reference		
Gyeonggi-do	1.87	1.90–2.52	< 0.0001	2.68	2.39–3.00	< 0.0001
Daegu	3.51	2.68–4.61	< 0.0001	4.48	4.03–4.99	< 0.0001
Gyeongsangbuk-do	7.10	5.44–9.28	< 0.0001	12.06	10.85–13.41	< 0.0001
Other area	21.41	16.42–27.92	< 0.0001	36.84	33.17–40.94	< 0.0001

^a In the multivariable model, we only adjusted for the variables age and residence for which the absolute standardized difference was greater than 0.1 after IPTW compared to before IPTW among the baseline characteristics of age, gender, residence, household income, health insurance type, CCI group, disability severity, and disability type.

Table 1. Risk of mortality within 4 weeks after COVID-19 infection among people with disabilities

Table 2. Subgroup analysis by severity of disability or types of disability after IPTW

	Adjusted HR ^e	95% CI	p-value
By severity of disability			
Mild disability			
None	reference		
COVID-19 infection	11.02	10.73–11.34	< 0.0001
Moderate-to-severe disability			
None	reference		
COVID-19 infection	11.17	10.84–11.53	< 0.0001
By types of disability			
Physical disability ^a			
None	reference		
COVID-19 infection	10.96	10.66–11.28	< 0.0001
Sensory impairment ^b			
None	reference		
COVID-19 infection	10.71	10.32–11.13	< 0.0001
Mental disability ^c			
None	reference		
COVID-19 infection	7.99	7.29–8.77	< 0.0001
Internal organ disorder ^d			
None	reference		
COVID-19 infection	14.57	13.73–15.47	< 0.0001

^a Physical disability includes retardation, brain lesion disorders, speech disorders, facial disorders, and epilepsy.

^b Sensory impairment includes visual impairment and hearing impairment.

^c Mental disability includes intellectual disabilities, autism spectrum disorders, and psychiatric disorders.

^d Internal organ disorder includes kidney, heart, respiratory, liver, ostomy, and urostomy disorders.

^e We only adjusted for the variables age and residence for which the absolute standardized difference was greater than 0.1 after IPTW compared to before IPTW among the baseline characteristics of age, gender, residence, household income, health insurance type, CCI group, disability severity, and disability type.

Table 2. Subgroup analysis by severity of disability or types of disability after IPTW

Table 3. Subgroup analysis by the time of infection after IPTW

Time of COVID-19 infection	Adjusted HR ^a	95% CI	p-value
By SARS-CoV-2 Delta variant predominance			
Before SARS-CoV-2 Delta variant predominance (October, 2020–June, 2021)			
None	reference		
COVID-19 infection	10.85	10.33–11.39	< 0.0001
After SARS-CoV-2 Delta variant predominance (July, 2021–January, 2022)			
None	reference		
COVID-19 infection	11.37	11.12–11.63	< 0.0001
By quarter of a year during the study period			
4th quarter 2020 (October–December)			
None	reference		
COVID-19 infection	43.32	37.25–50.39	< 0.0001
3rd quarter 2021 (January–March)			
None	reference		
COVID-19 infection	8.16	7.64–8.73	< 0.0001
2nd quarter 2021 (April–June)			
None	reference		
COVID-19 infection	5.70	5.24–6.22	< 0.0001
3rd quarter 2021 (July–September)			
None	reference		
COVID-19 infection	6.91	6.50–7.36	< 0.0001
4th quarter 2021 (October–December)			
None	reference		
COVID-19 infection	12.10	11.81–12.40	< 0.0001

^a We only adjusted for the variables age and residence for which the absolute standardized difference was greater than 0.1 after IPTW compared to before IPTW among the baseline characteristics of age, gender, residence, household income, health insurance type, CCI group, disability severity, and disability type.

Table 3. Subgroup analysis by the time of infection after IPTW

Robot-Assisted Gait Training in Individuals with Spinal Cord Injury: A Meta-Analysis

Jong Mi Park^{1*}, Yong Wook Kim², Su Ji Lee², Ji Cheol Shin^{2†}

Department of Physical Medicine and Rehabilitation, Hallym University Sacred Heart Hospital, Hallym University College of Medicine, Anyang, Korea¹, Department and Research Institute of Rehabilitation Medicine, Yonsei University College of Medicine, Seoul, Republic of Korea²

Background

Spinal cord injury (SCI) can lead to significant impairments in sensory, motor, and autonomic functions below the level of the injury, resulting in muscle weakness, atrophy, gait disturbances, sensory dysfunctions, and autonomic dysfunction. Rehabilitation for SCI has traditionally focused on improving locomotion. With the introduction of robotic technologies such as the Lokomat in the late 1990s, robot-assisted gait training (RAGT) has gained prominence in clinical settings due to its ability to deliver high-intensity, repetitive movements consistently, reducing the physical demand on therapists. Various robotic systems, including exoskeleton treadmill training robots, wearable exoskeletons, and end-effector robots, have been developed to support gait training. Despite the widespread clinical adoption of RAGT, its efficacy remains debated, prompting this systematic review and meta-analysis to investigate the overall effectiveness of RAGT compared to conventional rehabilitation in SCI patients.

Methods

Adhering to PRISMA guidelines, a systematic search was conducted across multiple international and domestic databases until April 18, 2024. The meta-analysis included randomized controlled trials (RCTs) comparing RAGT with conventional rehabilitation methods. The meta-analysis employed a random effects model to determine the effect size as either mean difference (MD) or standardized MD (SMD). Evidence quality was evaluated using the Grading of Recommendations Assessment, Development and Evaluation (GRADE) approach.

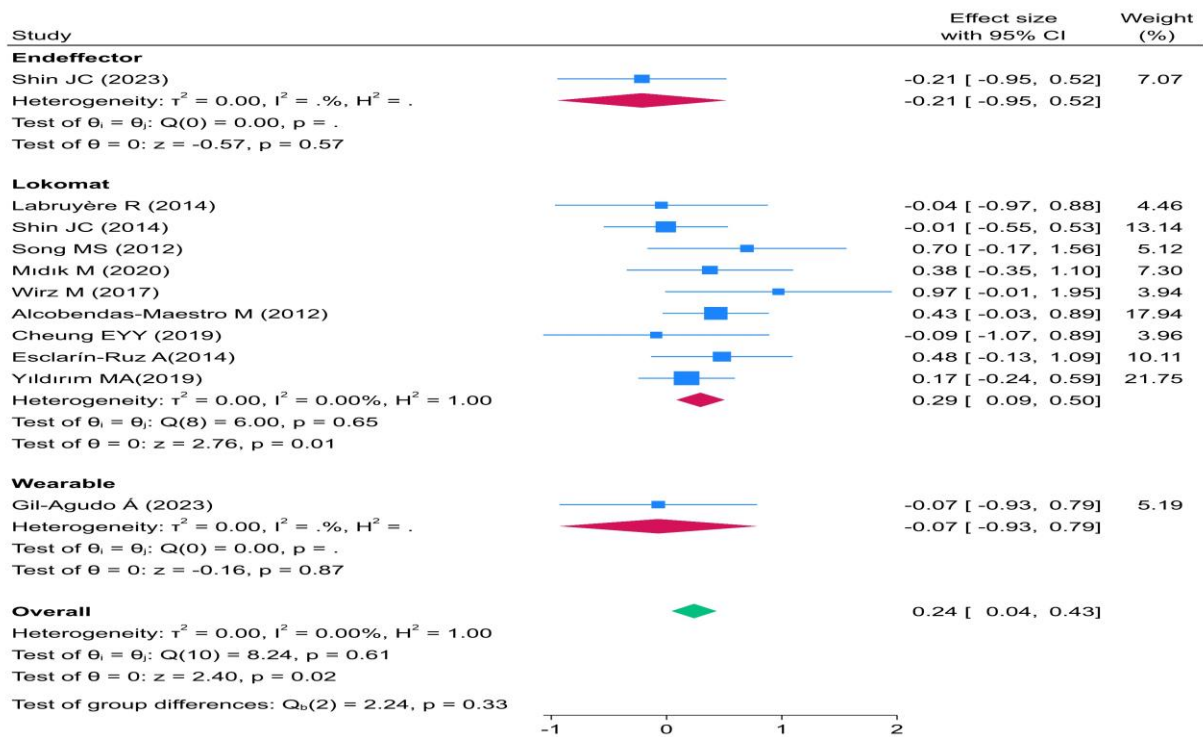
Results

A total of 23 studies with 690 participants were included. The overall pooled effect size for improvement in activities of daily living was (SMD 0.24, 95% confidence interval [CI], 0.04–0.43; GRADE: high, Figure 1.) favoring RAGT over conventional rehabilitation. Significant improvements were observed in muscular strength (MD, 0.23; 95% CI, 0.02–0.44; GRADE: high), walking index for SCI (MD, 0.31; 95% CI, 0.07–0.55; GRADE: moderate), and 6MWT distance (MD, 0.38; 95% CI, 0.14–0.63; GRADE: moderate) (Table 1). Subgroup analyses indicated that subacute patients and intervention periods exceeding 2 months demonstrated greater efficacy (Figure 2).

Conclusions

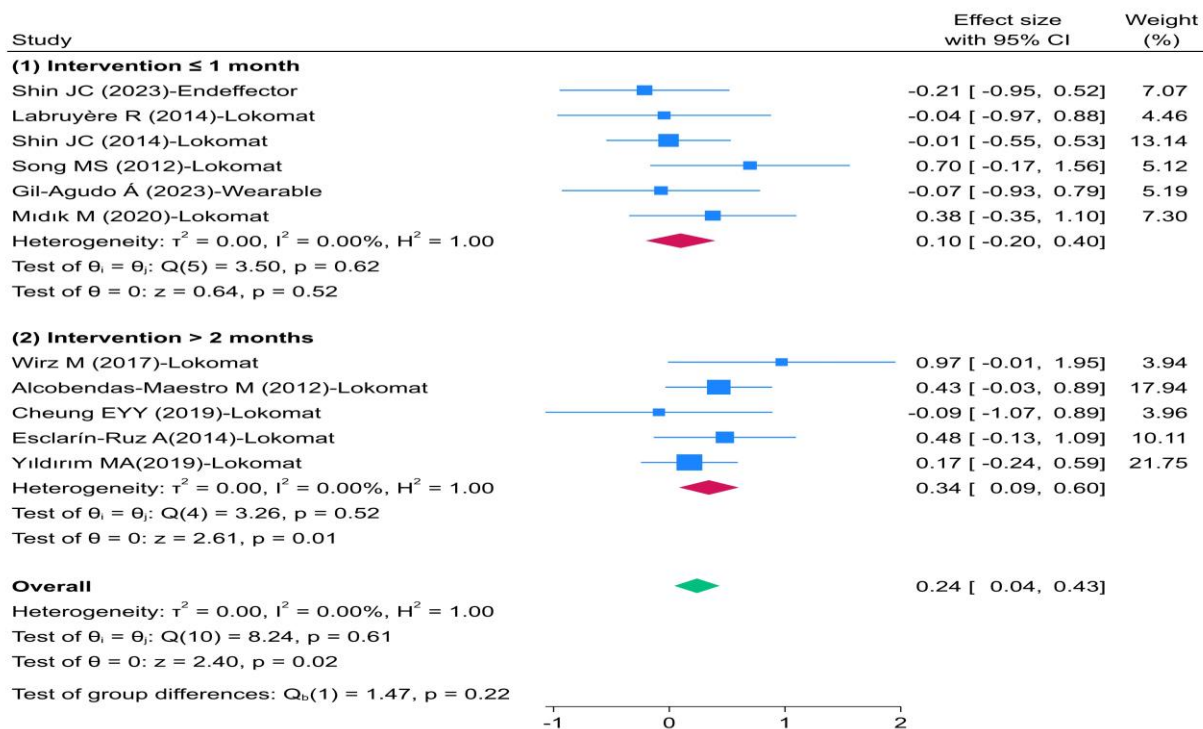
The findings indicate that RAGT significantly enhances activities of daily living, muscular strength, and walking abilities in individuals with SCI. The benefits are particularly notable in subacute patients and with longer intervention durations. Despite some heterogeneity and the small sample sizes of the included studies, RAGT presents a viable and effective rehabilitation option for SCI patients. Further research is needed to optimize treatment protocols and identify specific patient groups that would benefit the most from RAGT.

Acknowledgment This study was supported by the Special Research Fund for ARM Development of the Korean Academy of Rehabilitation Medicine in 2023.



Random-effects REML model

Figure 1. Meta-analysis of the effects of RAGT in patients with spinal cord injury (SCI) on Activities of daily living.



Random-effects REML model

Figure 2. Subgroup analysis of the effects of activities of daily living according to intervention period

		Summary of findings		Heterogeneity	Publication bias		Quality of evidence assessment (GRADE)				
Outcome measure		No. of patients	Effect size (95% confidence interval)	I ²	Egger's Test	Risk of bias ^a	Inconsistency ^b	Indirectness ^c	Imprecision ^d	Publication bias ^e	Quality of evidence ^f
		Experimental /Control (trials)									
Activities of daily living	FIM, SCIM, MBI	208/203 (11)	SMD 0.24 (0.04, 0.43) ^{***}	0%	0.950	Not Serious	Not Serious	Not Serious	Not Serious	None	High
Muscular strength	LEMS	184/187 (12)	MD 0.23 (0.02, 0.44) ^{***}	0%	0.592	Not Serious	Not Serious	Not Serious	Not Serious	None	High
Spasticity	MAS	73/75 (3)	MD -0.05 (-0.37, 0.28)	0%	0.952	Serious	Not Serious	Not Serious	Serious	None	Low
Balance	BBS	32/34 (3)	MD 0.44 (-0.18, 1.06)	33.42%	0.269	Not Serious	Serious	Not Serious	Serious	None	Low
Walking ability	WISCI	215/212 (10)	MD 0.31 (0.07, 0.55) ^{***}	30.67%	0.260	Serious	Not Serious	Not Serious	Not Serious	None	Moderate
	10MWT Speed (m/s)	172/176 (13)	MD -0.02 (-0.46, 0.42)	73.44%	0.521	Serious	Very Serious	Not Serious	Serious	None	Very low
	6MWT Distance (m)	134/134 (10)	MD 0.38 (0.14, 0.63) ^{***}	0%	0.256	Serious	Not Serious	Not Serious	Not Serious	None	Moderate
	Step length (m)	16/16 (2)	MD -0.15 (-0.84, 0.55)	0%	N/A	Not Serious	Not Serious	Not Serious	Serious	Suspected	Low
Body composition	Body mass (kg)	20/14 (2)	MD 0.02 (-0.67, 0.71)	0%	N/A	Not Serious	Not Serious	Not Serious	Serious	None	Moderate
	Lean tissue (kg)	20/14 (2)	MD 0.02 (-0.67, 0.72)	0%	N/A	Not Serious	Not Serious	Not Serious	Serious	None	Moderate
	Tissue fat (%)	20/14 (2)	MD 0.09 (-0.60, 0.79)	0%	N/A	Not Serious	Not Serious	Not Serious	Serious	None	Moderate
Cardiopulmonary Function	Forced expiratory volume in first second (FEV1) (L)	17/17 (2)	MD 0.49 (-0.20, 1.18)	0%	N/A	Not Serious	Not Serious	Not Serious	Serious	None	Moderate
	Forced vital capacity (L)	17/17 (2)	MD 0.33 (-0.35, 1.02)	0%	N/A	Not Serious	Not Serious	Not Serious	Serious	None	Moderate
	Heart Rate (beats/min)	17/17 (2)	MD 0.56 (-0.71, 1.30)	10.09%	N/A	Not Serious	Not Serious	Not Serious	Serious	None	Moderate
	Peak expiratory flow (L/s)	17/17 (2)	MD 0.26 (-0.41, 0.94)	0%	N/A	Not Serious	Not Serious	Not Serious	Serious	Suspected	Low

Table 1. Summary of the findings and quality of evidence assessment using the GRADE approach

Biomechanical Effects of Lumbar Fixation on Spine under Different Postures: A Finite Element Study

Won Mo Koo^{1*}, Seongho Woo¹, Kinam Park¹, Jong Min Kim¹, Jong-Moon Hwang¹, Byung Joo Lee^{1†}

Department of Rehabilitation Medicine, Daegu Fatima Hospital¹

Introduction

Lumbar lordosis is a unique structural feature of the normal human spine, which improves the ability to withstand gravity. In case of spinal instability due to various reasons, some patients undergo spinal fixation procedure. The fixation may have impact on lumbar lordosis and, therefore, on distribution of pressure applied to each spinal segment. In this study, we investigated the pressure change on vertebral components between normal model and post-lumbar spinal fixation model, utilizing finite element model (FEM) analysis.

Method

A 3D FEM centered on the lumbar spine was constructed for this study. The L1 to L5 lumbar vertebrae were modeled in detail, including the cortical bone (CB), annulus fiber (AF), and nucleus pulposus (NP). We analyzed the amount of stress applied to each component in every lumbar spinal segment during lumbar flexion motion. The motion was performed in four different postures; standing, erect sitting on a chair, slumped sitting on a chair, and sitting on the floor. Subsequently, we made a FEM for L4-5 fixated spine. The analysis of stress applied to the vertebral components for the fixated spine FEM was performed, in the same manner as normal model.

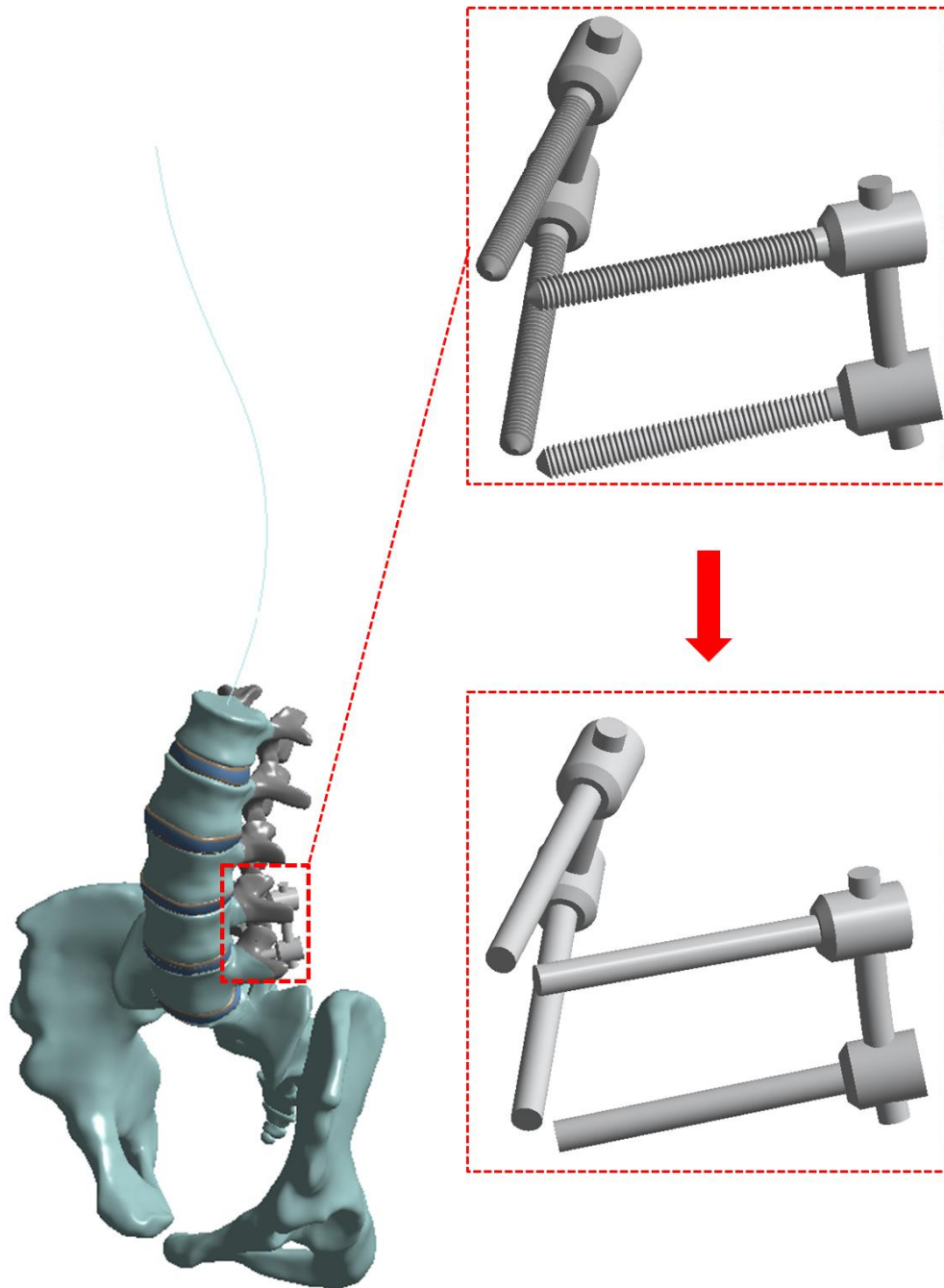
Result

The highest stress on the CB was introduced during slumped sitting on a chair. However, the highest stress on AF and NP was introduced while sitting on the floor. This tendency was similarly found on L4-5 fixated spine FEM. The stress on L4 CB, L5 CB, L4/5 AF, and L4/5 NP was reduced after L4-5 fixation. However, the stress on L3 CB, L3/4 AF, and L3/4 NP increased after the fixation.

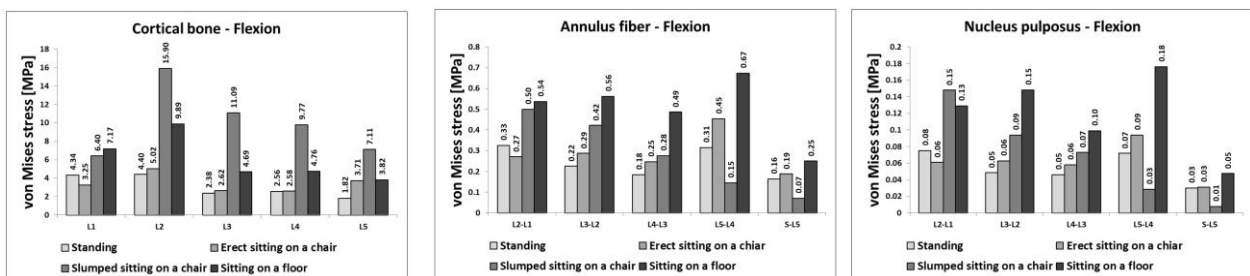
Conclusion

Slumped sitting on a chair or floor sitting posture aggravates stress on vertebral components. The fixation of lumbar spine provides decompressive effect on the corresponding vertebral components. However, the stress on the vertebral components above the fixation is increased.

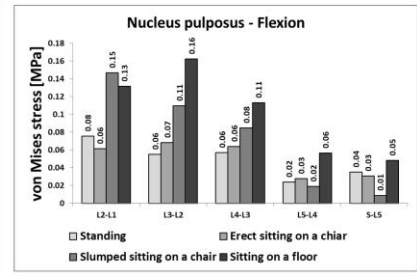
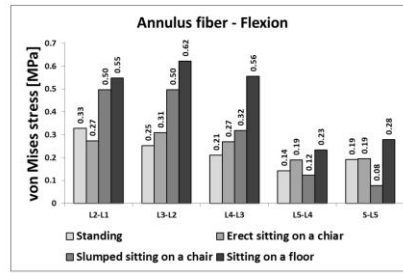
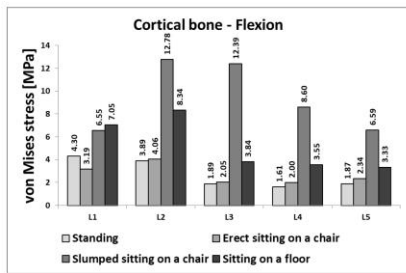
Acknowledgment The authors declare no conflict of interest.



Vertebrae body and implant finite element model



Stress on vertebral components in normal model



Stress on vertebral components in lumbar fixation model

Spinal Cord Injury Rehabilitation

P-118

Relationship between Carotid Blood Flow and Cognition, Orthostatic Hypotension in Cervical SCI

Jong Joon Lee^{1*}, Min Cheol Joo^{1†}

Department of Rehabilitation Medicine, Wonkwang University School of Medicine & Hospital¹

Objectives

The purpose of this study was to identify the occurrence of orthostatic hypotension in tetraplegia patients with cervical spinal cord injury and its association with internal carotid artery blood flow and cognitive impairment.

Methods

This study was conducted on patients who were admitted to the Department of Rehabilitation Medicine at our hospital for rehabilitation treatment after sustaining cervical spinal cord injuries from November 2021 to October 2023. Orthostatic hypotension was assessed by monitoring the occurrence of symptoms, systolic and diastolic blood pressure, and heart rate while the patient was in a supine position and after being maintained at a 50-degree angle on a tilt table for 5 minutes. The internal carotid artery blood flow was measured bilaterally in both the supine and tilt table positions using carotid duplex ultrasonography. The patients were classified into Group A, with a decrease in internal carotid artery blood flow of 21% or more, and Group B, without such a decrease. To assess cognitive function, the Korean version of the Mini-Mental State Examination (K-MMSE) and the Korean version of the Montreal Cognitive Assessment (MoCA-K) were administered.

Results

Forty-one patients with cervical spinal cord injuries participated in the study, with a mean age of 60.34 ± 11.97 years (Table 1). The mean scores for the Korean version of the Mini-Mental State Examination (K-MMSE) and the Korean version of the Montreal Cognitive Assessment (MoCA-K) in Group A were 22.69 ± 4.24 and 18.85 ± 6.28 , respectively, while in Group B, the scores were 25.53 ± 4.31 and 22.87 ± 5.71 , respectively. Independent sample T-tests showed that Group A had significantly lower scores than Group B ($p=0.047$, $p=0.048$) (Table 2). Meanwhile, the proportion of orthostatic hypotension symptoms and the actual diagnosis rate in each group were 42.31% and 76.92% for Group A, and 26.67% and 66.67% for Group B, respectively. Fisher's exact test did not show a significant association ($p=0.502$, $p=0.491$) (Table 3).

Conclusions

This study shows that patients with cervical spinal cord injury who experienced a significant decrease in internal carotid artery blood flow showed a notable decline in cognitive function. These findings suggest the necessity for appropriate diagnosis and therapeutic interventions to improve cognitive function in patients with cervical spinal cord injury.

Table 1. The demographic data and characteristics of spinal cord injury patients

		Group A (n=26)	Group B (n=15)
Age		59.54 ± 13.57	61.73 ± 8.80
Duration of injury, days		38.23 ± 20.58	28.93 ± 19.19
AIS grade	AIS A	3	0
	AIS B	2	1
	AIS C	9	4
	AIS D	12	10
Sex	Male	21	13
	Female	5	2
NLI	C1	0	1
	C2	2	1
	C3	5	0
	C4	13	8
	C5	6	5
HTN	(-)	16	10
	(+)	10	5
DM	(-)	22	12
	(+)	4	3
Dyslipidemia	(-)	21	9
	(+)	5	6
Heart disease	(-)	21	15
	(+)	5	0

* Group A; Δ ICA BFV $\geq 21\%$ * Group B; Δ ICA BFV $< 21\%$

Table 1. The demographic data and characteristics of spinal cord injury patients

Table 2. Association between carotid blood flow volume and cognitive function

Groups	Group A (N =26)	Group B (N =15)	P-value
K-MMSE	22.69 ± 4.24	25.53 ± 4.31	0.047*
MoCA-K	18.85 ± 6.28	22.87 ± 5.71	0.048*

* $P < 0.05$ * Group A; Δ ICA BFV $\geq 21\%$ * Group B; Δ ICA BFV $< 21\%$

Table 2. Association between carotid blood flow volume and cognitive function

Table 3. Association between carotid blood flow volume and orthostatic hypotension

		Group A (n=26)	Group B (n=15)	P-value
Presyncopal Symptoms	(+)	11 (42.31)	4 (26.67)	0.502
	(-)	15 (57.69)	11 (73.33)	
Orthostatic Hypotension	(+)	20 (76.92)	10 (66.67)	0.491
	(-)	6 (23.08)	5 (33.33)	

* $P < 0.05$ * Group A; Δ ICA BFV $\geq 21\%$ * Group B; Δ ICA BFV $< 21\%$

Table 3. Association between carotid blood flow volume and orthostatic hypotension

Factors Influencing Paralytic Ileus Without Herniation According to Types of Spinal Cord Injury

Won Mo Koo^{1*}, Seongho Woo¹, Jong-Moon Hwang^{1†}, Myung-Gwan Kim^{2,3†}

Department of Rehabilitation Medicine, Daegu Fatima Hospital¹, Department of Biomedical Informatics, Graduate School of Medicine, CHA University², Institute for Biomedical Informatics, Graduate School of Medicine, CHA University³

Introduction

Spinal cord injury alone causes health problems. However, complications from spinal damage can further reduce the patient's quality of life. Management of various health behaviors after spinal injury can be a factor that can reduce the occurrence of complications. This study aimed to identify the status of the occurrence of complications of Paralytic Ileus Without Herniation due to spinal injury and the factors that affect it, and to explore factors that can reduce the occurrence of complications after spinal injury.

Methods

For this study, we utilized the National Health Insurance Corporation big data and used SAS as the analysis program. Patients with trauma disease codes among spinal injuries from 2009 to 2019 were extracted, and patients with other disease codes were excluded, and patients with cervical, thoracic, and lumbar disease codes were extracted. In addition, patients with missing major information, patients under the age of 19, patients without examination records or patients with outcome events were excluded, and the final number of patients subject to analysis was 584,266. Chi-square test and multiple logistic regression were performed for the analysis. Through this, the odds ratio according to factors that Paralytic Ileus Without Herniation will occur within 5 years of spinal injury was calculated for each spinal injury type.

Results

Paralytic bowel obstruction without hernia differed according to spinal injury. The proportion of cases with minor thoracic injury was higher. And when we looked at the factors affecting paralytic bowel obstruction without hernia by spinal injury, more complications occurred in women than in men when there was thoracic or lumbar injury. There was no correlation with increasing age, and the risk of developing complications due to cervical, thoracic, and lumbar injuries increased when living in a rural area rather than a metropolitan area. Depending on the severity of the disability, the more severe the disability, the more complications there were due to cervical, thoracic, and lumbar injuries. Although there was a low correlation with cervical spine injury depending on BMI, the incidence of complications increased with increasing BMI for thoracic spine injury and lumbar spine injury. Regarding smoking and drinking, it is necessary to interpret it in reverse as a possibility that these activities may occur in cases where there are no complications due to cervical, lumbar, or thoracic injuries. High-intensity, medium-intensity, and walking exercise were factors that generally lowered the occurrence of complications.

Conclusion

It has been shown that engaging in beneficial health behaviors such as physical activity reduces the risk of developing Paralytic Ileus Without Herniation, a complication of spinal injury. When spinal injury occurs, it may be difficult to engage in physical activity due to physical discomfort. Nevertheless, continuous physical activity and proper health behavior

Acknowledgment This research was supported by a grant of the Korea Health Technology R&D Project through the Korea Health Industry Development Institute (KHIDI), funded by the Ministry of Health & Welfare, Republic of Korea (grant number : HR22C1832).

Table 1. Characteristics of Subjects According to Types of Spinal Cord Injury

Variables	Spinal Cord Injury								p - value χ ² (p)
	Cervical spine (S10-19)		Thoracic spine (S20-29)		Lumbar spine (S30-39)		Total		
	N	(%)	N	(%)	N	(%)	N	(%)	
Gender, n (%)									
Male	79,182	52.97%	88,421	63.05%	165,447	56.17%	333,050	57.00%	<.001
Female	70,290	47.03%	51,814	36.95%	129,112	43.83%	251,216	43.00%	
Age									
< 20 years	181	0.12%	76	0.05%	371	0.13%	628	0.11%	<.001
20-39 years	49,529	33.14%	36,607	26.10%	90,144	30.60%	176,280	30.17%	
40-64 years	87,955	58.84%	79,958	57.02%	168,794	57.30%	336,707	57.63%	
≥ 65 years	11,807	7.90%	23,594	16.82%	35,250	11.97%	70,651	12.09%	
Residence area									
Metropolitan area	28,638	19.16%	24,510	17.48%	50,564	17.17%	103,712	17.75%	<.001
Metropolitan City	37,414	25.03%	35,798	25.53%	77,764	26.40%	150,976	25.84%	
Provincial area	83,420	55.81%	79,927	57.00%	166,231	56.43%	329,578	56.41%	
Severity of Disability									
Not applicable	143,611	96.08%	132,038	94.15%	281,158	95.45%	556,807	95.30%	<.001
Mild (Grades 4-6)	4,455	2.98%	6,214	4.43%	10,001	3.40%	20,670	3.54%	
Severe (Grades 1-3)	1,406	0.94%	1,983	1.41%	3,400	1.15%	6,789	1.16%	
BMI									
<18.5	5,155	3.45%	4,402	3.14%	8,901	3.02%	18,458	3.16%	<.001
18.5-22.9	58,429	39.09%	53,066	37.84%	107,843	36.61%	219,338	37.54%	
23.0-24.9	35,992	24.08%	35,088	25.02%	72,413	24.58%	143,493	24.56%	
≥25.0	49,896	33.38%	47,679	34.00%	105,402	35.78%	202,977	34.74%	
Smoking									
Not Smoking	89,089	59.60%	73,096	52.12%	170,731	57.96%	332,916	56.98%	<.001
Past Smoking	21,275	14.23%	22,006	15.69%	43,523	14.78%	86,804	14.86%	
Current Smoking	39,108	26.16%	45,133	32.18%	80,305	27.26%	164,546	28.16%	
Drinking									
Month <3	72,329	48.39%	63,875	45.55%	144,761	49.14%	280,965	48.09%	<.001
Month 4-7	35,824	23.97%	29,708	21.18%	67,535	22.93%	133,067	22.78%	
Month ≥8	41,319	27.64%	46,652	33.27%	82,263	27.93%	170,234	29.14%	
High-intensity physical activity									
No	87,763	58.72%	81,702	58.26%	173,533	58.91%	342,998	58.71%	<.001
Yes	61,709	41.28%	58,533	41.74%	121,026	41.09%	241,268	41.29%	
Moderate-intensity physical activity									
No	79,160	52.96%	75,437	53.79%	157,092	53.33%	311,689	53.35%	<.001
Yes	70,312	47.04%	64,798	46.21%	137,467	46.67%	272,577	46.65%	
Walking									
No	41,332	27.65%	41,299	29.45%	83,117	28.22%	165,748	28.37%	<.001
Yes	108,140	72.35%	98,936	70.55%	211,442	71.78%	418,518	71.63%	
Total	149,472		140,235		294,559		584,266		

Table 1. Characteristics of Subjects According to Types of Spinal Cord Injury

Table 2. Paralytic Ileus Without Herniation Within 5 Years Based on Types of Spinal Cord Injury

Variables	Spinal Cord Injury								p -value χ2(p)
	Cervical spine (S10-19)		Thoracic spine (S20-29)		Lumbar spine (S30-39)		Total		
	N	(%)	N	(%)	N	(%)	N	(%)	
Paralytic Ileus Without Herniation (K56)									
No	147,673	98.80%	138,202	98.55%	290,843	98.74%	576,718	98.71%	<.001
Yes	1,799	1.20%	2,033	1.45%	3,716	1.26%	7,548	1.29%	
전체	149,472	100.0%	140,235	100.0%	294,559	100.0%	584,266	100.0%	

Table 2. Paralytic Ileus Without Herniation Within 5 Years Based on Types of Spinal Cord Injury

Table 3. Factors Influencing Paralytic Ileus Without Herniation Within 5 Years Based on Types of Spinal Cord Injury

Variables	Paralytic Ileus Without Herniation(K56)							
	Cervical spine (S10-19)		Thoracic spine (S20-29)		Lumbar spine (S30-39)		Total	
	Crude OR (95% CI)	P	Crude OR (95% CI)	P	Crude OR (95% CI)	P	Crude OR (95% CI)	P
Gender, n (%)								
Male	ref		ref		ref		ref	
Female	1.085 (0.988 - 1.19)	.087	1.202 (1.1 - 1.314)	<.001	1.078 (1.01 - 1.15)	.0233	1.099 (1.05 - 1.15)	<.001
Age								
< 20 years	ref		ref		ref		ref	
20-39 years	1.647 (0.23 - 11.78)	.619	0.634 (0.088 - 4.577)	.652	1.668 (0.415 - 6.702)	.471	1.396 (0.522 - 3.737)	0.506
40-64 years	2.192 (0.307 - 15.657)	.434	1.027 (0.143 - 7.392)	.979	2.275 (0.567 - 9.132)	.247	1.968 (0.736 - 5.263)	0.177
≥65 years	4.548 (0.635 - 32.578)	.132	2.109 (0.293 - 15.189)	.459	4.553 (1.133 - 18.295)	.033	4.044 (1.511 - 10.82)	0.005
Residence area								
Metropolitan area	ref		ref		ref		ref	
Metropolitan City	0.975 (0.832 - 1.143)	.754	1.095 (0.939 - 1.278)	.248	0.996 (0.892 - 1.113)	.950	1.018 (0.942 - 1.101)	0.651
Provincial area	1.48 (1.297 - 1.689)	<.001	1.556 (1.364 - 1.777)	<.001	1.401 (1.273 - 1.541)	<.001	1.462 (1.368 - 1.563)	<.001
Severity of Disability							0	
Not applicable	ref		ref		ref		ref	
Mild (Grades 4-6)	1.833 (1.486 - 2.262)	<.001	1.619 (1.359 - 1.928)	<.001	1.76 (1.53 - 2.025)	<.001	1.746 (1.585 - 1.924)	<.001
Severe (Grades 1-3)	2.238 (1.602 - 3.126)	<.001	2.531 (1.978 - 3.237)	<.001	2.11 (1.699 - 2.621)	<.001	2.29 (1.979 - 2.65)	<.001
BMI								
<18.5	ref		ref		ref		ref	
18.5-22.9	0.834 (0.657 - 1.058)	.134	0.78 (0.621 - 0.98)	.033	0.872 (0.73 - 1.041)	.123	0.837 (0.742 - 0.945)	.004
23.0-24.9	0.8 (0.626 - 1.023)	.076	0.753 (0.596 - 0.952)	.018	0.773 (0.644 - 0.927)	.006	0.775 (0.685 - 0.878)	<.001
≥25.0	0.782 (0.614 - 0.995)	.045	0.736 (0.584 - 0.926)	.009	0.793 (0.664 - 0.948)	.011	0.775 (0.686 - 0.875)	<.001
Smoking								
Not Smoking	ref		ref		ref		ref	
Past Smoking	0.948 (0.824 - 1.092)	.462	0.889 (0.784 - 1.009)	0.068	0.948 (0.862 - 1.042)	.264	0.939 (0.878 - 1.004)	0.064
Current Smoking	1.077 (0.967 - 1.198)	.177	0.792 (0.716 - 0.876)	<.001	0.895 (0.829 - 0.967)	.005	0.913 (0.865 - 0.962)	.001
Drinking								
Month <3	ref		ref		ref		ref	
Month 4-7	0.808 (0.717 - 0.911)	.001	0.628 (0.555 - 0.711)	<.001	0.769 (0.706 - 0.837)	<.001	0.739 (0.696 - 0.785)	<.001
Month ≥8	0.871 (0.779 - 0.973)	.015	0.719 (0.65 - 0.795)	<.001	0.836 (0.774 - 0.903)	<.001	0.816 (0.773 - 0.86)	<.001
High-intensity physical activity								
No	ref		ref		ref		ref	
Yes	0.836 (0.76 - 0.921)	<.001	0.717 (0.654 - 0.786)	<.001	0.809 (0.757 - 0.866)	<.001	0.79 (0.754 - 0.829)	<.001
Moderate-intensity physical activity								
No	ref		ref		ref		ref	
Yes	0.779 (0.709 - 0.856)	<.001	0.751 (0.686 - 0.821)	<.001	0.797 (0.746 - 0.851)	<.001	0.779 (0.744 - 0.816)	<.001
Walking								
No	ref		ref		ref		ref	
Yes	0.775 (0.702 - 0.855)	<.001	0.722 (0.66 - 0.791)	<.0001	0.785 (0.733 - 0.841)	<.001	0.763 (0.728 - 0.801)	<.001

Table 3. Factors Influencing Paralytic Ileus Without Herniation Within 5 Years Based on Types of Spinal Cord Injury

Spinal Cord Injury Rehabilitation

P-120

Alterations in Resting-State Neural Networks on the Severity of Neuropathic Pain after SCI

Jung-Sang Han^{1*}, Jang Woo Park³, Tae-Du Jung², Yongmin Chang^{4,5,6}, Eunhee Park^{2†}

Department of Rehabilitation Medicine, Kyungpook National University Hospital¹, Department of Rehabilitation Medicine, Kyungpook National University Chilgok Hospital², Korea Radioisotope Center for Pharmaceuticals, Korea Institute of Radiological & Medical Sciences³, Department of Radiology, Kyungpook National University Hospital⁴, Department of Molecular Medicine, School of Medicine, Kyungpook National University⁵, Department of Medical & Biological Engineering, Kyungpook National University⁶

Introduction

Neuropathic pain (NP) following spinal cord injury (SCI) is refractory to pain control strategies, and the underlying neuronal mechanisms remain poorly understood. This study aimed to determine the brain regions engaged in maintaining a spontaneous resting state and the link between those regions and the severity of NP in patients with incomplete SCI.

Method

Seventy-three subjects (41 patients and 32 age- and sex-matched healthy controls) participated in this retrospective study. Regarding the neurological level of injury, patients with incomplete SCI experienced at-level or below-level NP. The severity of NP was evaluated using a visual analog scale (VAS), and patients were divided into mild and moderate–severe NP groups based on VAS scores. Graph theory and fractional amplitude of low-frequency fluctuation (fALFF) analyses were performed to compare resting-state functional magnetic resonance imaging (fMRI) analysis results among the three groups. Graph theory analysis was performed through a region of interest (ROI)-to-ROI analysis and then fALFF analysis was performed in the brain regions demonstrating significant differences among the three groups analyzed using the graph theory. We evaluated whether the brain regions showing significant differences using graph theory and fALFF correlated with the VAS scores.

Result

Patients with moderate–severe NP showed reduced node degree and fALFF in the left middle frontal gyrus compared with those with mild NP and healthy controls. Furthermore, patients with severe NP demonstrated increased average path lengths and reduced fALFF values in the posterior cingulate gyrus.

Conclusion

This study found that changes in intrinsic oscillations of fMRI signals in the middle frontal gyrus and posterior cingulate gyrus were significant considering the severity of NP.

Spinal Cord Injury Rehabilitation

P-121

Factors predicting the employment status for spinal cord injury dwelling in Republic of Korea

Kyungah Song^{1,1*}, Onyoo Kim^{2,2†}, Suin Jang^{3,3}

Dept. of Spinal Cord Injury Rehabilitation, National Rehabilitation Center¹, Dept. of Spinal Cord Injury Rehabilitation, National Rehabilitation Center², Dept. of Clinical Research on Rehabilitation, National Rehabilitation Center³

Objectives

Spinal cord injury (SCI) often results in to permanent disability, functional impairment, and a range of health complications, posing considerable obstacles for employment among persons with SCI. Although some studies have identified correlations between demographic characteristics, personal factors, physical and environmental factors, and employment outcomes for persons with spinal cord injuries, research examining these relationships in South Korea is scarce. Therefore, this study aimed to explore the various factors influencing paid employment among persons with SCI in Korean society, categorized into demographic characteristics, spinal cord injury lesions, personal and psychological health issues, activity and participation, independence, quality of life, and environmental factors, in order to generate evidence that could form the basis of future research.

Methods

A total of 892 individuals with SCI aged 19 years and above, residing in the local community and having completed the International Spinal Cord Injury Community Survey (InSCI Survey) in 2017, were included in the analysis. Participants with congenital causes of spinal cord injury, neurodegenerative diseases, peripheral nerve injuries, or without community experience were excluded. The survey consisted of 125 self-reported items. Given the large number of variables, the study employed random forest, a machine learning technique involving decision trees.

Results

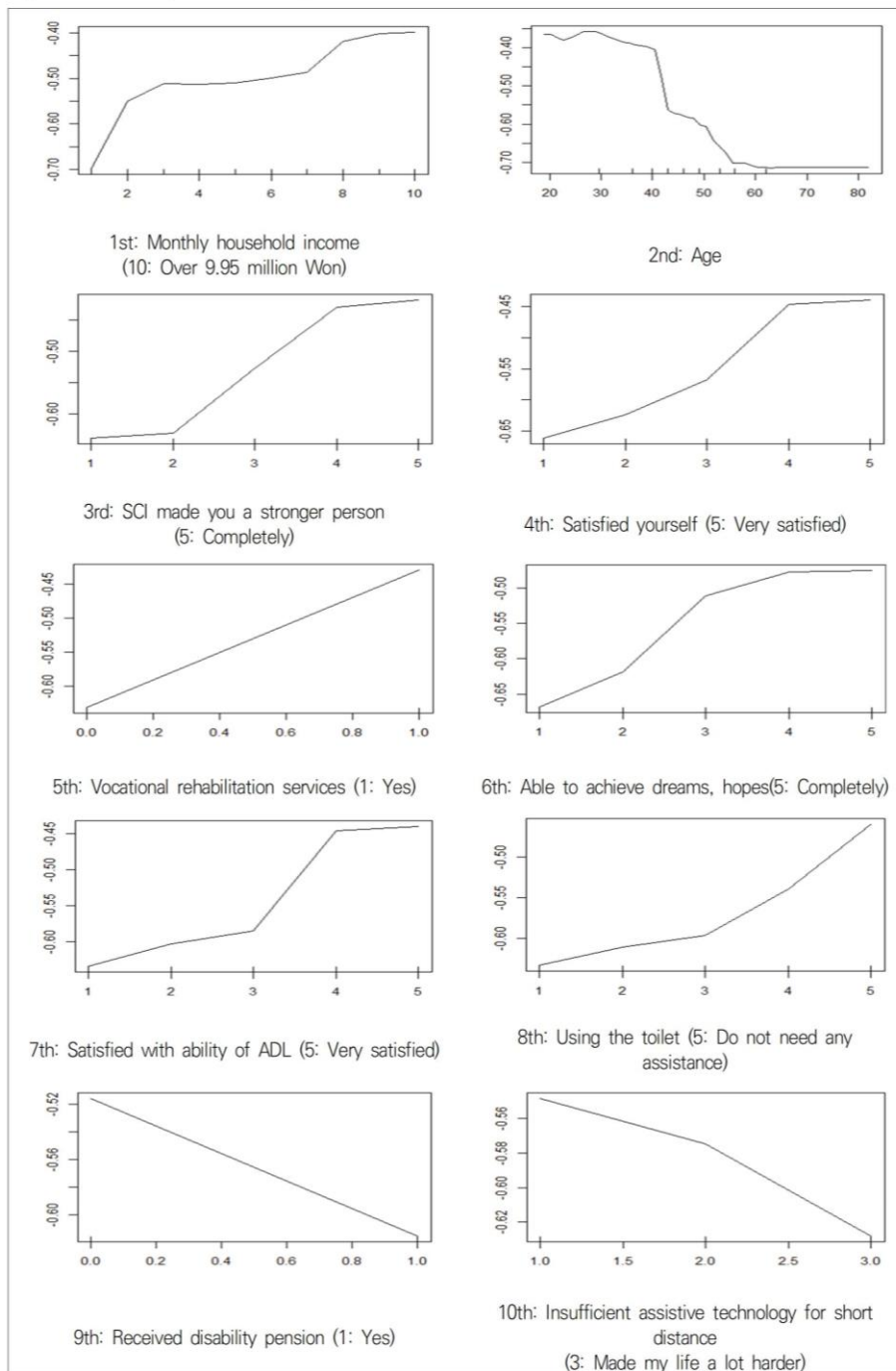
The data from 538 respondents who provided responses regarding their employment status were analyzed, excluding non-respondents. The sample characteristics included male gender (75.1%), unmarried status (53.9%), living with family (90.1%), receiving daily living assistance (84.8%), educational attainment of high school diploma or lower (56.1%), paraplegia (57.2%), complete injury (58.7%), and predominantly traumatic injury causes (93.1%). The mean age was 46 years, and the average duration of spinal cord injury was 15.25 years. A higher probability of paid employment was observed in respondents with a higher average monthly household income, younger age, higher self-efficacy, higher life satisfaction and quality of life, receipt of vocational rehabilitation services, no disability pension, independence in daily activities, less difficulty in activity participation, absence of sleep problems as a secondary health issue, higher educational attainment, and unmarried status.

Conclusion

This study is significant to the field by employing the random forest method to examine the impact of various factors on paid employment among persons with spinal cord injuries in South Korea, utilizing data from a large-scale dataset. The predictive factors identified in this study can serve as foundational data for finding strategies to support employment among persons with SCI in Korea. Further research is required, particularly focusing on essential job environments necessary for sustained employment among this population.

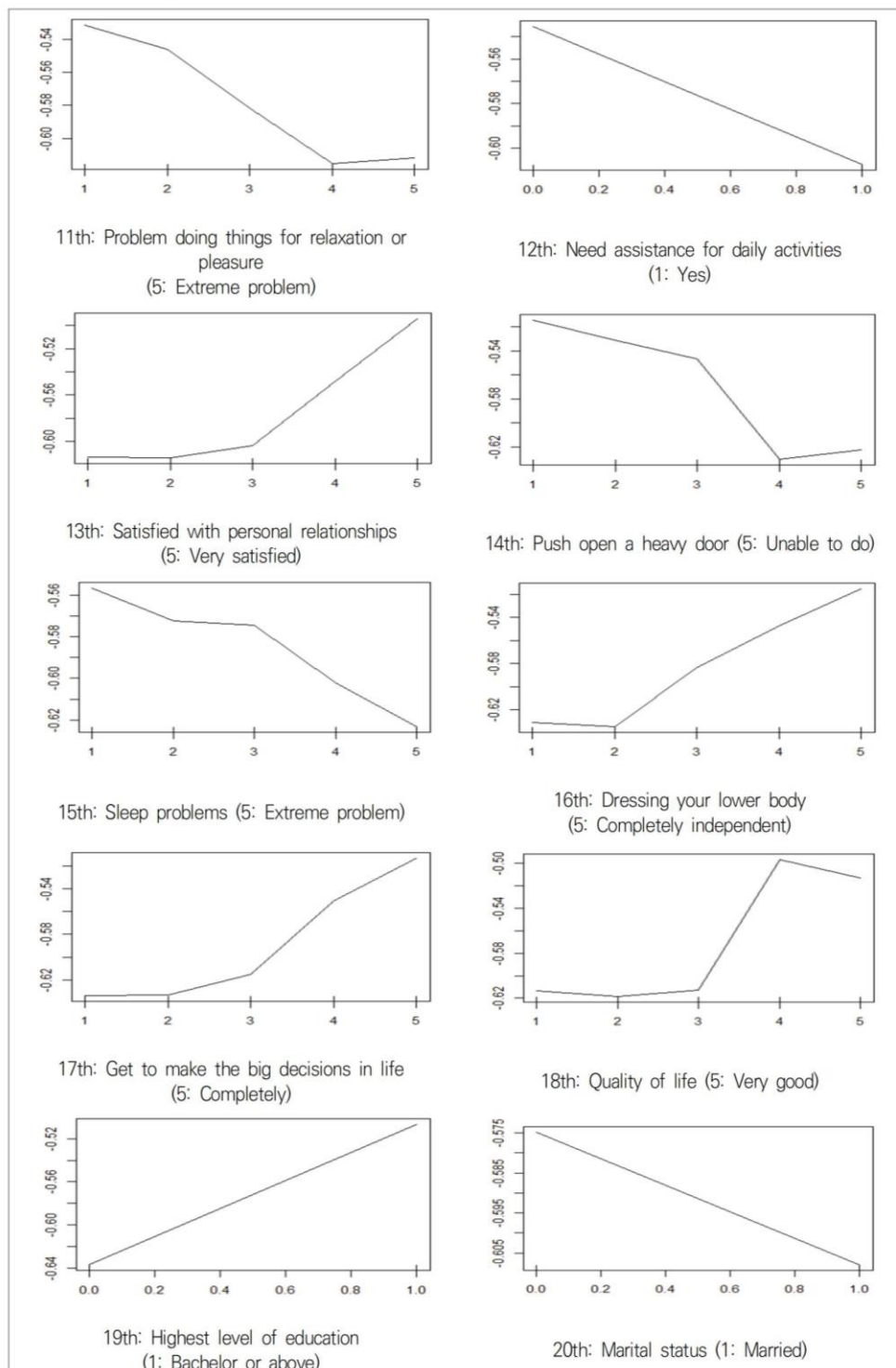
Acknowledgment 본 연구는 국립재활원에서 자체 진행한 연구로 설문조사에 참여해주신 연구자 및 한국척수장애인협회 협조에 감사드립니다.

[Figure 1] Partial Dependence Plots (1st-10th)



Partial dependency plot showing the top 20 contributing explanatory variables(1st-10th)

[Figure 2] Partial Dependence Plots (11th-20th)



Partial dependency plot showing the top 20 contributing explanatory variables(11th-20th)

Comparison of the prevalence of metabolic syndrome between men with spinal cord injury and the gene

Jisun Lim^{1*}, Kimin Yun², Sunmin Nam², Onyoo Kim^{2†}

Department of Clinical Research on Rehabilitation, National Rehabilitation Center¹, Department of Rehabilitation Medicine, National Rehabilitation Center²

Introduction

To compare the prevalence of metabolic syndrome (MetS) between men with traumatic spinal cord injury (TSCI) and the general population (GP) using healthcare data.

Methods

Among individuals aged ≥ 20 years who underwent routine health check-ups covered by the Republic of Korea National Health Insurance Service in 2019, we selected men with TSCI and age-matched male individuals from the GP at a 1:10 ratio. MetS was defined according to the National Cholesterol Education Program criteria, with the waist circumference (WC) threshold for abdominal obesity based on the Asian criteria provided by the International Diabetes Federation. Accordingly, individuals who met three or more of the following criteria were considered to have MetS: abdominal obesity ($WC \geq 90$ cm), hypertriglyceridemia [triglycerides (TG) level ≥ 150 mg/dL or medication use], low high-density lipoprotein (HDL)-cholesterol (HDL-cholesterol level < 40 mg/dL), high blood pressure (BP) (systolic BP ≥ 130 mmHg and/or diastolic BP), and hyperglycemia [fasting plasma glucose (FPG) level ≥ 100 mg or medication use].

Results

The baseline characteristics and 1:10 matched results of the GP and TSCI groups are presented in Table 1. The neurological level of injury (NLI) for spinal cord injury patients was as follows: cervical (72.54%), lumbar (17.55%), and thoracic (9.91%). No significant difference was noted in the mean age between the TSCI group (59.70 ± 13.23 years) and GP group (59.70 ± 13.25 years) ($p > 0.95$). The mean body mass index (BMI) was significantly lower in the TSCI group (24.37 kg/m²) than in the GP group (24.63 kg/m²) ($p = 0.05$) (Table 1). In addition, the prevalence of MetS tended to increase with age, but interestingly, it decreased in those aged ≥ 70 years; however, this reduction was considerably lower in the TSCI group (0.78%) than in the GP group (3.19%) (Fig. 1).

Conclusions

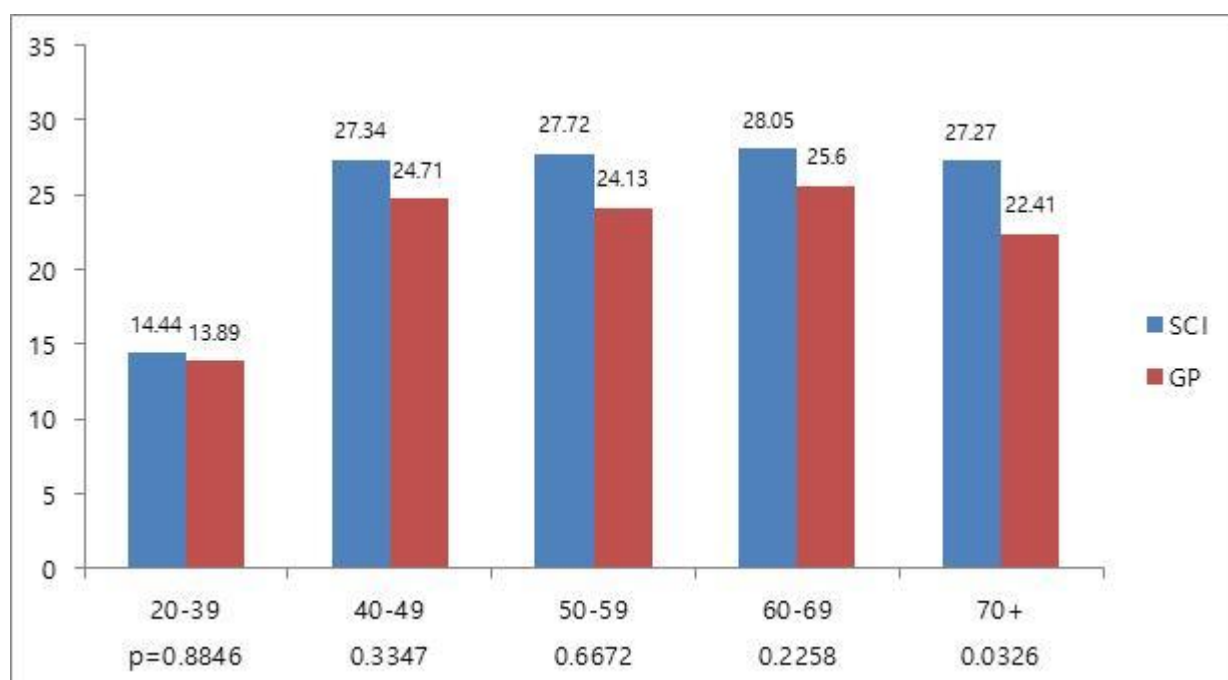
Despite having a lower average BMI, patients with TSCI had a greater WC, a measure of abdominal obesity, than individuals in the GP, suggesting that these patients with TSCI have higher accumulation of visceral fat within the abdominal cavity, which is a risk factor for MetS. Moreover, the prevalence of MetS was higher in patients with TSCI than in individuals in the GP, and the trend of prevalence in these groups varied across age groups. Therefore, managing MetS in patients with TSCI requires tailored approaches compared with that in individuals in the GP, highlighting the need for further research.

Acknowledgment NRCRSP-24TB04

Table 1. The results of the 1:10 matching for SCI and GP based on gender and age

Characteristics	SCI N=1,544		GP N=15,440		P-value
	Mean (SD)	N(%)	Mean (SD)	N(%)	
Age (years)	59.70 (13.23)		59.70(13.25)		0.9557
20-39		90(5.83)		900(5.83)	
40-49		278(18.01)		2,780(18.01)	
50-59		285(18.46)		2,850(18.46)	
60-69		517(33.48)		5,170(33.48)	
70+		374(24.22)		3,740(24.22)	
BMI (kg/m ²)	24.37 (3.30)		24.63 (3.09)		0.0005
WC (kg/m ²)	86.59 (8.98)		85.81(8.22)		<.0001
Metabolic syndrome		415(26.88)		3,730(24.16)	0.0177
NLI					
Cervical		1,120(72.54)			
Thoracic		153(9.91)			
Lumbar		271(17.55)			

The results of the 1:10 matching for SCI and GP based on gender and age



The Prevalence and Trends of Metaboic syndrome by Age

Spinal Cord Injury Rehabilitation

P-123

Urodynamic Evaluation of Neurogenic Bladder in Patients with Spinal Cord Injury

Byung Chan Lee^{1*†}, Yeonjae Lee¹, Jeemyung Han¹, Lyekyung An², Onyoo Kim³

Department of Physical Medicine and Rehabilitation, Chung-Ang University Hospital¹, Department of Rehabilitation Medicine, National Rehabilitation Center², Department of Spinal Cord Injury Rehabilitation, National Rehabilitation Center³

Study Design

Retrospective cross-sectional survey of Korean patients with spinal cord injury (SCI) within 6 months post-injury.

Objective

To evaluate urodynamic parameters and identify unfavorable urodynamic findings in patients with neurogenic bladder due to spinal cord injury (SCI) during the acute to subacute stages of the disease based on the post-injury time interval.

Setting

National Rehabilitation Center, Seoul, Korea

Methods

Data from urodynamic tests performed on SCI patients within 6 months post-injury were collected. Based on the time interval from injury to testing, the recruited patients were divided into three groups: 0–90 days, 91–135 days, and 136–180 days. Based on these groups, urodynamic test parameters and incidence of unfavorable urodynamic findings (detrusor overactivity [DO], high detrusor pressure exceeding 40 cmH₂O during the filling phase, low compliance of the bladder, underactive or acontractile bladder, and detrusor-sphincter dyssynergia [DSD]) were compared.

Results

Analysis of urodynamic study (UDS) findings in 191 patients with acute to subacute SCI, revealed that unfavorable urodynamic findings were observed within 3 months after injury in both complete and incomplete SCI. The UDS test results and incidence of unfavorable outcomes based on the interval between injury and examination showed no significant statistical differences over time.

Conclusion

The urodynamics of SCI patients suggest that unfavorable urodynamic results are common in the acute to subacute stages of SCI.

Acknowledgment This study was supported by a Chung Hie Oh & Jin-Sang Chung research grant of Korean Academy of Rehabilitation Medicine for 2023.

Table 1. Basal Demographics of Including Participants

Variables	Complete N (%) or M (SD)	Incomplete N (%) or M (SD)	Value (<i>p</i>)
Sex			0.025 ^a (.873)
Male	45 (71.4)	90 (70.3)	
Female	18 (28.6)	38 (29.7)	
Age	45.63 (16.02)	55.30 (15.92)	-3.936 ^c (<.001)
AIS			191.000 ^a (<.001)
A	34 (54.0)	0 (0.0)	
B	29 (46.0)	0 (0.0)	
C	0 (0.0)	34 (26.6)	
D	0 (0.0)	94 (73.4)	
Neurological level			11.694 ^a (.003)
Cervical	25 (39.7)	68 (53.1)	
Thoracic	33 (52.4)	36 (28.1)	
Lumbar	5 (7.9)	24 (18.8)	
Etiology of injury			2.274 ^a (.132)
Traumatic	44 (69.8)	75 (58.6)	
Non-Traumatic	19 (30.2)	53 (41.4)	
Date between injury and UDS			1.973 ^a (.373)
0-90	11 (17.5)	34 (26.6)	
90-135	33 (52.4)	61 (47.7)	
135-180	19 (30.2)	33 (25.8)	
Voiding method			35.468 ^a (<.001)
Foley	22 (34.9)	25 (19.5)	
Suprapubic	1 (1.6)	2 (1.6)	
CIC	33 (52.4)	34 (26.6)	
Spontaneous Voiding	4 (6.3)	64 (50.0)	
Combined methods ^d	3 (4.8)	3 (2.3)	
Bladder medication			0.052 ^a (.974)
Not used	38 (60.3)	75 (58.6)	
1	16 (25.4)	34 (26.6)	
2	9 (14.3)	19 (14.8)	

AIS, American Spinal Injury Association Impairment Scale; UDS, Urodynamic Study; CIC, Clean Intermittent Catheterization

^a: Pearson's chi-squared test; ^b: Fisher's exact test; ^c: Student's *t* test. **Bold** is statistically significant (*p*<.05).

^d: Spontaneous or Crede voiding + intermittent catheterization

Table 1. Basal Demographics of Including Participants

Table 3. Results of Urodynamics in Participants across Time-interval Subgroups.

Variables	Date between injury and UDS			H ^a	p
	0-90 (N=11)	90-135 (N=33)	135-180 (N=19)		
Complete					
Bladder capacity	546.82 (143.36)	488.03 (145.25)	561.58 (124.69)	4.623	.099
Bladder compliance	45.86 (35.12)	69.85 (91.47)	81.77 (82.41)	1.707	.426
VV	0.00 (0.00)	11.82 (40.27)	7.89 (34.41)	1.833	.400
PVRU	523.64 (219.97)	470.00 (167.46)	553.16 (130.30)	4.805	.090
Max Pdet at filling	17.27 (14.89)	29.56 (25.05)	24.12 (20.37)	1.986	.370
Max Pdet at voiding	8.73 (6.97)	16.14 (16.46)	16.21 (15.74)	1.092	.579
Variables	Date between injury and UDS			F ^b	p
	0-90 (N=34)	90-135 (N=61)	135-180 (N=33)		
Incomplete					
Bladder capacity	503.26 (106.48)	506.48 (122.11)	506.18 (159.80)	0.007	.993
Bladder compliance	75.28 (95.47)	91.85 (102.90)	135.75 (154.08)	2.462	.089
VV	68.82 (135.62)	122.62 (192.64)	66.36 (137.06)	1.760	.176
PVRU	414.12 (183.97)	369.75 (221.89)	432.42 (233.02)	1.039	.357
Max Pdet at filling	23.62 (20.08)	24.42 (24.21)	25.96 (28.81)	0.080	.924
Max Pdet at voiding	20.07 (21.65)	26.62 (25.03)	24.09 (26.92)	0.768	.466

UDS, Urodynamic Study; VV, Voided Volume; PVRU, Post-voided Residual Urine; Max Pdet at filling, Maximal Detrusor Pressure at the Filling Phase; Max Pdet at voiding, Maximal Detrusor Pressure at the Voiding Phase

^a: Kruskal-Wallis test, ^b: One-way ANOVA

Table 3. Results of Urodynamics in Participants across Time-interval Subgroups.

Table 4 Results of Unfavorable Urodynamic Findings in Participants across Time-interval Subgroups.

Completeness	Date between injury and UDS			Value (<i>p</i>)
	0-90 (N=11)	90-135 (N=33)	135-180 (N=19)	
Detrusor function at filling				
DO	6 (54.5)	20 (60.6)	9 (47.4)	0.861*
Normal	5 (45.5)	13 (39.42)	10 (52.6)	(.650)
Bladder compliance				
Low	4 (36.4)	10 (30.3)	1 (5.3)	5.741 ^b
Normal	7 (63.6)	23 (69.7)	18 (94.7)	(.053)
Detrusor pressure over 40cmH ₂ O at the filling phase				
Yes	1 (9.1)	10 (30.3)	7 (36.8)	2.649 ^b
No	10 (90.9)	23 (69.7)	12 (63.2)	(.233)
Detrusor function at voiding				
DU or Acontractile	11 (100.0)	32 (97.0)	19 (100.0)	1.240 ^b
Normal	0 (0.0)	1 (3.0)	0 (0.0)	(1.000)
Urethral function at voiding				
DSD	4 (36.4)	12 (36.4)	5 (26.3)	0.603*
Normal	7 (63.6)	21 (63.6)	14 (73.7)	(.740)
Incompleteness	Date between injury and UDS			Value (<i>p</i>)
	0-90 (N=34)	90-135 (N=61)	135-180 (N=33)	
Detrusor function at filling				
DO	18 (52.9)	27 (44.3)	15 (45.5)	0.696*
Normal	16 (47.1)	34 (55.7)	18 (54.5)	(.700)
Bladder compliance				
Low	7 (20.6)	12 (19.7)	8 (24.2)	0.276*
Normal	27 (79.4)	49 (80.3)	25 (75.8)	(.871)
Detrusor pressure over 40cmH ₂ O at the filling phase				
Yes	7 (20.6)	11 (18.0)	7 (21.2)	0.171 *
No	27 (79.4)	50 (82.0)	26 (78.8)	(.918)
Detrusor function at voiding				
DU or Acontractile	33 (97.1)	54 (88.5)	27 (81.8)	4.024 ^b
Normal	1 (2.9)	7 (11.5)	6 (18.2)	(.120)
Urethral function at voiding				
DSD	12 (35.3)	24 (39.3)	15 (45.5)	0.733*
Normal	55 (64.7)	37 (60.7)	18 (54.5)	(.693)

UDS, Urodynamic Study; DO, Detrusor Overactivity; DU, Detrusor Underactivity; DSD, Detrusor-Sphincter Dyssynergia

^a: Pearson's chi-squared test; ^b: Fisher's exact test.

Table 4 Results of Unfavorable Urodynamic Findings in Participants across Time-interval Subgroups.

Biomechanical Insights into ACDF: Comparing Flexible Cage System to Conventional Implants

Seongho Woo^{1*}, Kwangohk Jun¹, Won Mo Koo¹, Kinam Park¹, Myeong Geun Jeong², Kyoung Tae Kim², Jong Min Kim¹, Byung Joo Lee¹, Jong-Moon Hwang^{1†}

Department of Physical Medicine and Rehabilitation, Daegu Fatima Hospital¹, Department of Rehabilitation Medicine, Keimyung University, Dongsan Hospital²

Introduction

Anterior cervical discectomy and fusion (ACDF) is commonly used to treat cervical spondylosis when non-surgical treatments fail. Conventional cage and plate (CCP) implants (Figure 1), though effective, are associated with complications such as postoperative dysphagia, adjacent segment degeneration, and soft tissue injury. A novel Flexible Cage System (FCS) prototype by Medyssey (Figure 1) has been developed to address these issues. This study employs finite-element modeling to compare the von Mises stress distribution in bone, disc, endplate, and cage between CCP and FCS implants, aiming to provide insights into their biomechanical properties and clinical implications.

Methods

A three-dimensional finite element method (FEM) analysis was conducted, including the C3 to T1 vertebrae, cortical and cancellous bones, intervertebral discs, endplates, and posterior elements. The model was created using ANSYS SpaceClaim software, with the cage system positioned between the C5 and C6 vertebrae. Mesh sizes were set to 0.7mm for the cage system and 1mm for the rest of the model. A vertical load of 73.6 N and a moment of 1.0 Nm were applied to simulate neck bending, with the T1 vertebra fixed. The study evaluated maximum von Mises stress in the cortical bone, cancellous bone, upper and lower endplates, and intervertebral discs across reference (no surgery), CCP, and FCS models.

Results

The FCS model exhibited higher von Mises stress concentrations in the endplates and screws compared to the CCP model (Table 1, Figure 2). For example, the FCS model showed a 142.06% increase in stress in the C4-5 upper endplate compared to the reference model, while the CCP model showed a 52.74% increase. Similar trends were observed in other spinal components, indicating higher stress concentrations in the FCS model.

Conclusion

The FCS implant aims to mitigate complications associated with CCP implants, such as postoperative dysphagia and extended surgical times. However, the FCS implant introduces higher von Mises stress concentrations in the endplates and screws, potentially leading to increased subsidence rates and implant instability. The design differences between the FCS and CCP implants result in uneven stress distribution, which can be problematic, especially in patients with compromised bone quality. Careful consideration of patient-specific factors, such as age, bone quality, and cervical spine alignment, is crucial when selecting an implant for ACDF surgery. The FCS implant's design may require more precise surgical techniques to mitigate the risk of subsidence. Despite potential benefits, including reduced operative times and blood loss, the higher stress concentrations associated with the FCS implant necessitate careful patient selection and surgical precision. Future research should focus on long-term clinical outcomes of FCS implants in diverse patient populations and a broader range of spinal levels.

Acknowledgment This work was supported by the National Research Foundation of Korea(NRF) grant funded by the Korea government(MSIT) (No. 2022R1F1A1066508)

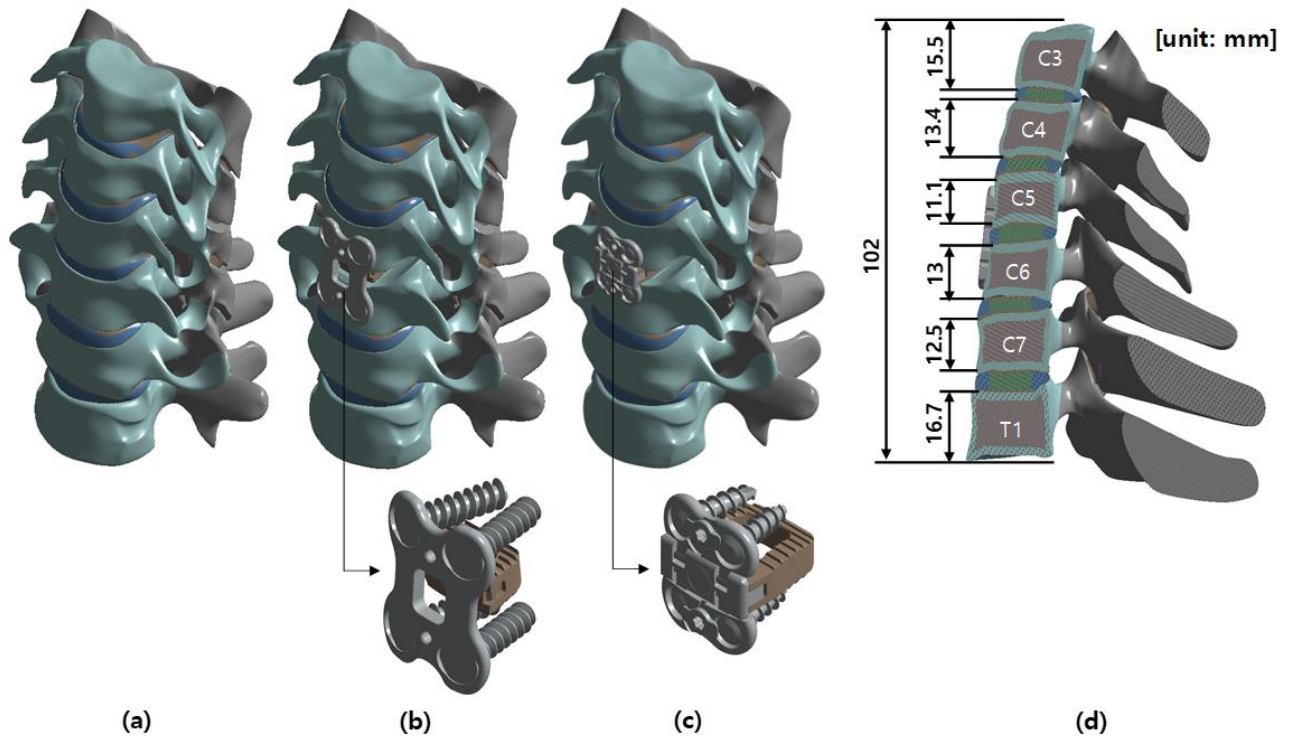


Figure 1. Analysis model; (a) Reference model, (b) CCP implant model, (c) FSC model, (d) Section view of the CCP implant model

Component	von Mises stress on each model (Mpa) (% of von Mises stress with reference)		
	Reference	CCP	FSC
C4-5 Endplate upper	3.946	2.081 (52.74%)	5.606 (142.06%)
C4-5 Endplate lower	2.505	1.736 (69.30%)	2.875 (114.77%)
C4-5 Annulus fibrosus	1.844	4.400 (238.61%)	2.084 (113.02%)
C4-5 Nucleus pulposus	0.013	0.275 (2116.54%)	0.222 (1707.69%)
C6-7 Endplate upper	1.744	1.731 (99.25%)	2.829 (162.21%)
C6-7 Endplate lower	1.646	1.422 (86.39%)	2.537 (154.13%)
C6-7 Annulus fibrosus	1.154	3.920 (339.69%)	1.915 (165.94%)
C6-7 Nucleus pulposus	0.005	0.179 (3580.00%)	0.012 (240.00%)
C5 Cortical bone	9.337	22.525 (241.24%)	8.385 (89.80%)
C6 Cortical bone	8.228	17.925 (217.85%)	9.079 (110.34%)
C5 Cancellous bone	0.060	0.183 (305.00%)	0.055 (91.67%)
C6 Cancellous bone	0.112	0.305 (272.32%)	0.116 (103.57%)
Cage		103.610	54.384
Screw		69.074	16.876

Table 1. von Mises stress results at each structure in three different models.

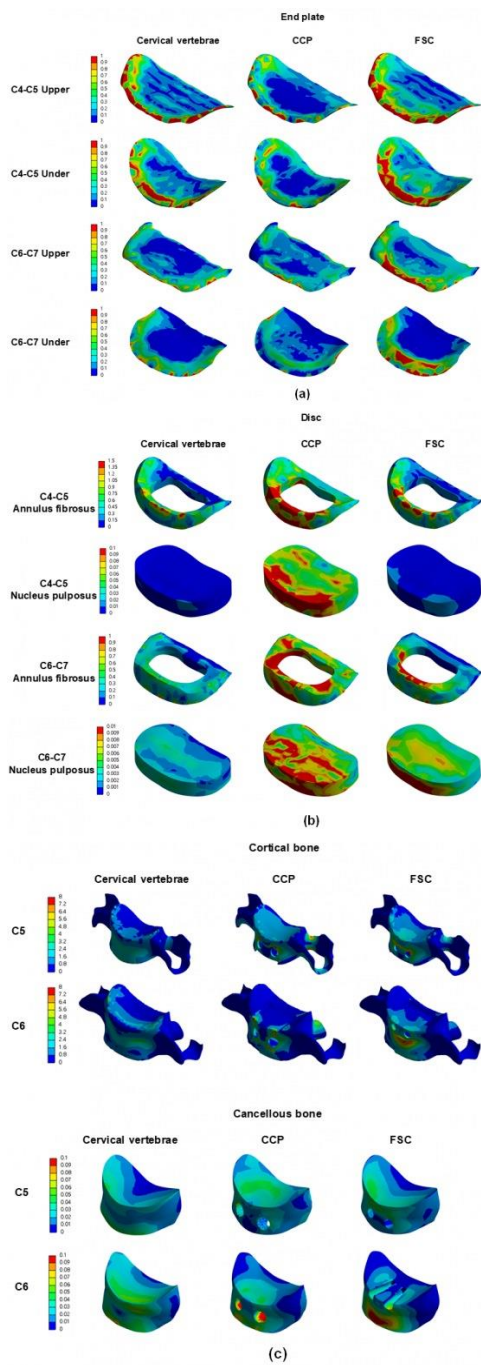


Figure 2. von Mises stress results at each structure in three different models (Unit: MPa), (a) upper and lower endplate, (b) intervertebral disc, (c) cortical and cancellous bone.

Spinal Cord Injury Rehabilitation

P-177

Efficacy of an exercise program for individuals with spinal cord injury in a community setting

Sungchul Huh^{1,2,3**}, Sung-Hwa Ko^{1,2,3}, Hyun-Yoon Ko^{3,4}, Yuna Kim², Jung-Lim Lee²

Department of Rehabilitation Medicine, Pusan National University Yangsan Hospital¹, Research Institute for Convergence of Biomedical Science and Technology, Pusan National University Yangsan Hospital², Department of Rehabilitation Medicine, Pusan National University School of Medicine³, Department of Rehabilitation Medicine, Parkside Rehabilitation Hospital⁴

Objective

To evaluate the efficacy of a community-based structured exercise program in enhancing physical, functional, and psychological outcomes for individuals with spinal cord injury (SCI).

Design: Randomized controlled trial comparing exercise group with usual care group.

Setting

One university-affiliated rehabilitation hospital.

Participants: Fifty-seven participants with chronic SCI who can walk more than 10 meters.

Interventions: Supervised 20-session program focusing on flexibility, aerobic, and strengthening exercises for 8 weeks.

Main outcome measures: Primary outcomes included EuroQol-5 Dimensions 5-Level and 6-minute walk test, while secondary outcomes assessed Spinal Cord Independence Measure III, Berg Balance Scale, timed up and go, grip strength, 30-second sit to stand test, sit and reach test, Beck Anxiety Inventory, Beck Depression Inventory, and bioelectrical impedance analysis.

Results

The exercise group showed significant improvements in balance and walking capacity compared with the usual care group. The adherence rate was remarkably high at 89.6%, suggesting the feasibility of community exercise programs for this population. However, no significant changes were observed in psychological and quality of life measures.

Conclusion

Community-based structured exercise programs can significantly improve physical outcomes for individuals with SCI and are met with high adherence and satisfaction rates. This trial contributes to the evidence base supporting the integration of structured exercise into long-term care strategies for SCI, potentially informing policy changes and healthcare practices to facilitate sustained physical activity and societal participation for the SCI population.

Acknowledgment This work was supported by The National Research Foundation of Korea grant funded by the Korean government (Ministry of Science and ICT) (No.2023M3I2A1009022). Informed consent was obtained from all participants involved in the study. Written informed consent for publication of results is waived, subject to the privacy provisions contained in that consent form.

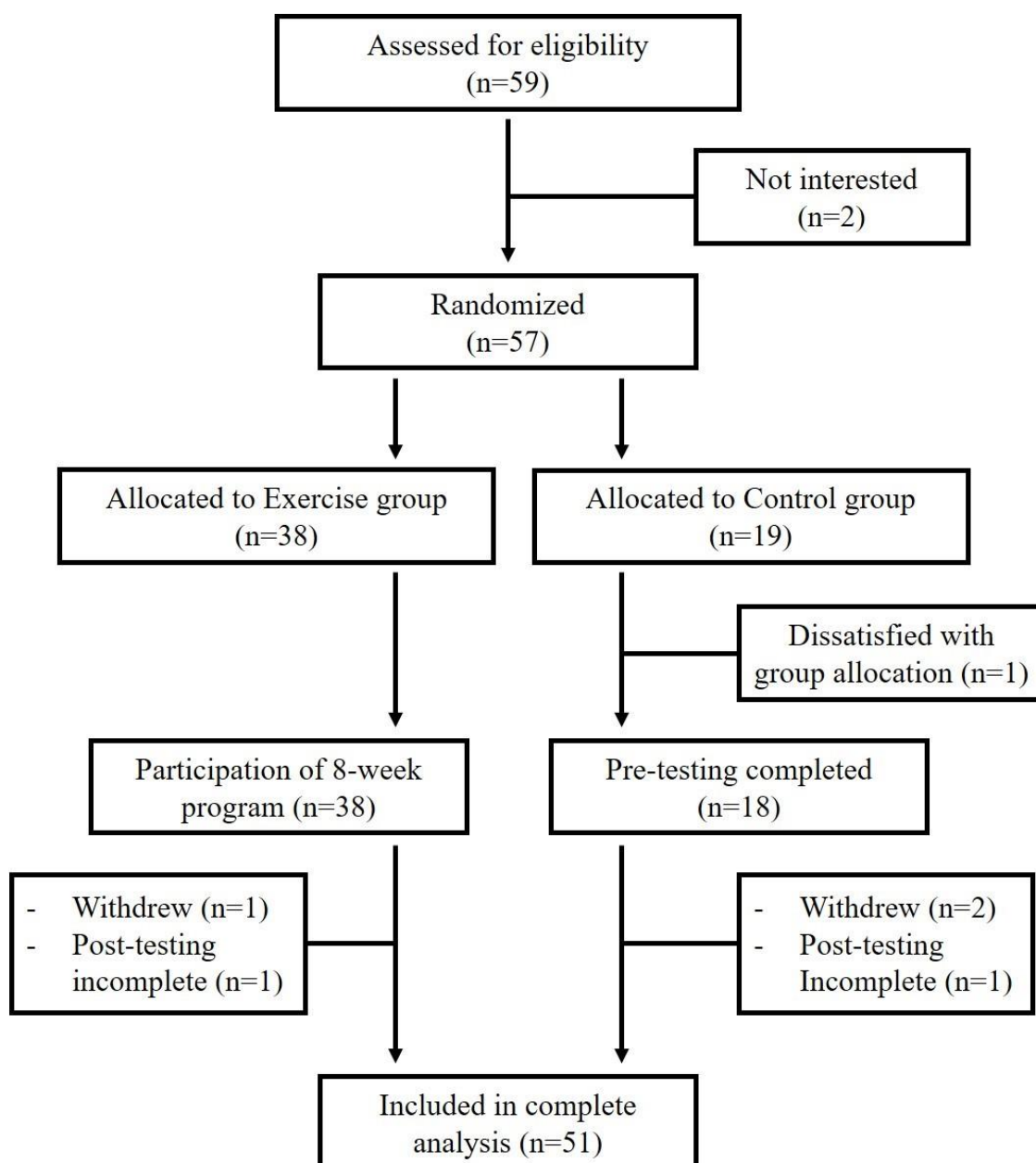


Figure 1. Consolidated Standards of Reporting Trials diagram.

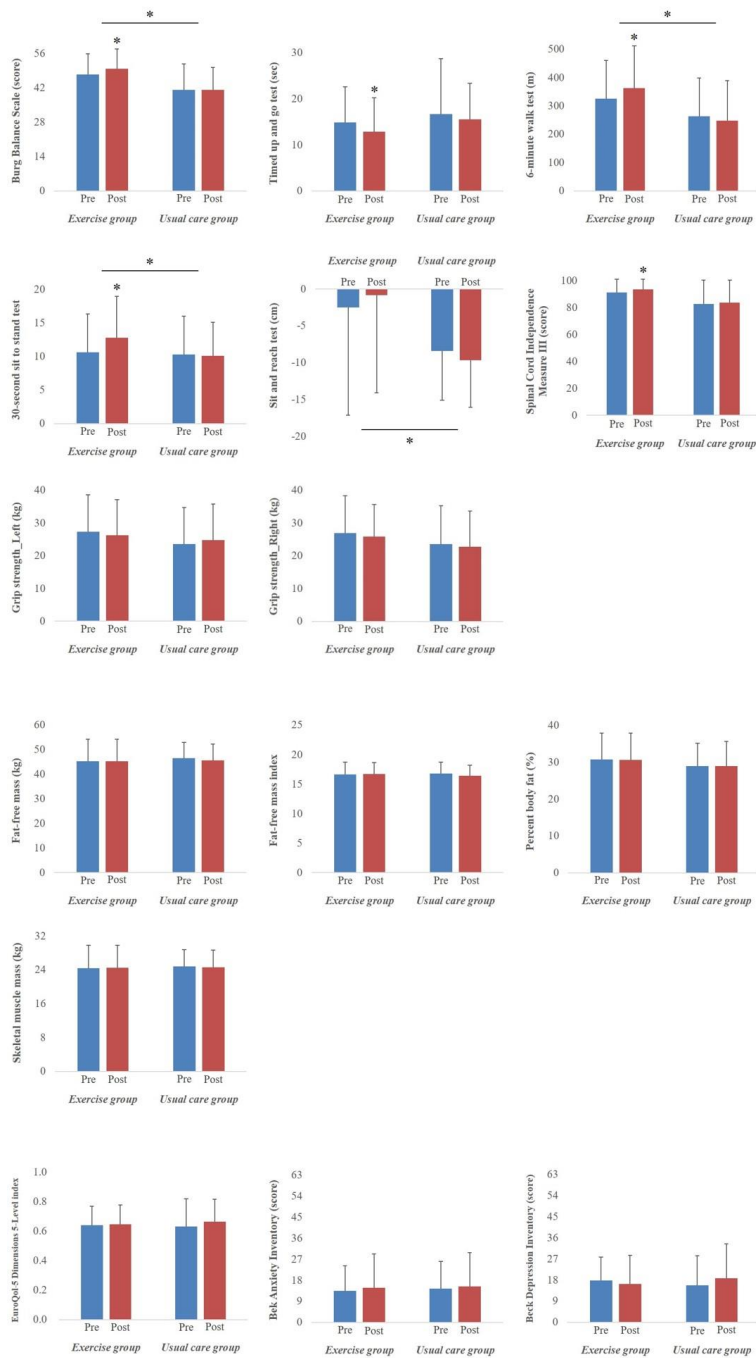


Figure 2a. Physical and functional outcome measures before and after the exercise program; Figure 2b. Bioelectrical impedance analysis outcome measures before and after the exercise program.

Table 2. Outcome measures before and after the 8-weeks exercise program

	Exercise group (n=36)				Usual care group (n=15)				Effect size (95% C.I.)	ANCOVA p
	Pre	Post	Difference (95% C.I.)	p	Pre	Post	Difference (95% C.I.)	p		
BBS	47.33±8.52	49.83±8.04	2.50 (1.29, 3.71)	.000*	41.07±10.71	41.20±9.15	0.13 (-2.88, 3.14)	.926	0.56 (-0.05, 1.18)	.006*
TUG (sec)	14.85±7.80	12.85±7.39	-2.00 (-3.00, -1.01)	.000*	16.73±12.01	15.58±7.80	-1.15 (-6.01, 3.70)	.618	-0.16 (-0.76, 0.44)	.280
6MWT (m)	325.95±134.34	363.56±148.08	37.61 (15.69, 59.53)	.001*	263.02±136.19	247.37±141.98	-15.65 (-34.46, 3.16)	.096	0.91 (0.29, 1.55)	.005*
30-STST	10.64±5.71	12.78±6.19	2.14 (0.95, 3.33)	.001*	10.33±5.67	10.13±4.97	-0.20 (-2.03, 1.63)	.818	0.67 (0.06, 1.29)	.026*
SRT (cm)	-2.49±14.61	-0.84±13.21	1.64 (-0.15, 3.43)	.071	-8.40±6.67	-9.67±6.39	-1.27 (-3.83, 1.29)	.306	0.57 (-0.04, 1.19)	.011*
Grip strength, left (kg)	27.32±11.25	26.26±10.85	-1.06 (-3.11, 0.98)	.299	23.51±11.23	24.82±11.00	1.31 (-1.39, 4.02)	.316	-0.41 (-1.02, 0.20)	.309
Grip strength, right (kg)	26.95±11.40	25.89±9.84	-1.06 (-2.93, 0.80)	.255	23.58±11.70	22.82±10.88	-0.76 (-3.14, 1.62)	.504	-0.06 (-0.66, 0.54)	.776
SCIM III	91.39±9.92	93.58±7.72	2.19 (0.09, 4.30)	.042*	82.87±17.86	83.87±16.75	1.00 (-2.15, 4.15)	.507	0.19 (-0.41, 0.80)	.070
EQ-5D-5L	0.64±0.13	0.65±0.13	0.01 (-0.04, 0.05)	.794	0.63±0.19	0.66±0.15	0.03 (-0.04, 0.11)	.368	-0.16 (-0.77, 0.44)	.497
BAI	13.58±10.71	14.89±14.40	1.31 (-1.64, 4.25)	.375	14.47±11.64	15.47±14.41	1.00 (-1.65, 3.65)	.431	0.04 (-0.56, 0.64)	.868
BDI	17.86±9.94	16.39±12.10	-1.47 (-4.39, 1.44)	.312	15.67±12.71	18.73±14.75	3.07 (-2.48, 8.61)	.256	-0.49 (-1.11, 0.11)	.134
Bioimpedance analysis										
FFM	45.25±9.11	45.39±8.88	0.14 (-0.39, 0.66)	.597	46.49±6.56	45.67±6.58	-0.82 (-2.16, 0.52)	.209	0.53 (-0.09, 1.17)	.111
FFMI	16.64±2.07	16.70±1.94	0.06 (-0.14, 0.26)	.549	16.76±1.94	16.44±1.76	-0.32 (-0.80, 0.16)	.177	0.57 (-0.06, 1.20)	.070
PBF	30.71±7.17	30.59±7.35	-0.12 (-0.81, 0.57)	.725	28.99±6.17	29.01±6.60	0.02 (-1.39, 1.43)	.974	-0.06 (-0.69, 0.55)	.860
SMM	24.41±5.44	24.55±5.30	0.15 (-0.17, 0.46)	.352	24.81±3.94	24.59±4.07	-0.22 (-0.90, 0.46)	.492	0.37 (-0.25, 1.00)	.264

BBS, Berg Balance Scale; TUG, Timed Up and Go; 6MWT, 6-Minute Walk Test; 30-STST, 30-Second Sit to Stand Test; SRT, Sit and Reach Test; SCIM III, Spinal Cord

Independence Measure III; EQ-5D-5L, EuroQol-5 Dimensions 5-Level; BAI, Beck Anxiety Inventory; BDI, Beck Depression Inventory; FFM, Fat-Free Mass; FFMI, Fat-Free Mass Index; PBF, Percent Body Fat; SMM, Skeletal Muscle Mass.

† Values are mean±s.d. *p<0.05

† BBS ranges from 0 to 56, where 56 is the best possible score; SCIM III ranges from 0 to 100, where 100 is the best score; EQ-5D-5L index score ranges from -0.59 to 1, where 1 is the best possible health state; BAI and BDI range from 0 to 63, where 63 is worse.

Table 1. Outcome measures before and after the 8-weeks exercise program.

Developed an AI-based CrossFit Exercise Multi-Management Monitoring System

Hyun Jong Lee^{1*}, Jea Hak Kim², Jun Pil Shin², Jung Hwan Kim^{2†}

Department of Clinical Research for Rehabilitation, National Rehabilitation Center¹, Department of Rehabilitation Exercise, National Rehabilitation Center²

introduction

CrossFit is a high-intensity workout system that combines strength and aerobic exercises in a short period, yielding various benefits such as weight loss, fat reduction, muscle development, and improved cardiovascular function. Additionally, CrossFit exercises are often performed in groups, fostering a sense of competition and collective solidarity through participant interaction. Such workouts can be highly beneficial for the rehabilitation of exercise with disabilities. However, high-intensity exercise programs come with a risk of injury. To prevent this, ideally, each user should have a personal instructor, which is practically unfeasible. Therefore, this study developed a system using artificial intelligence technology that allows one instructor to care for multiple users.

method

To enable real-time analysis of users' movements during exercise, we developed an AI system using Google's Mediapipe model. The exercise program was designed with five representative rehabilitation exercises for individuals with disabilities: squats, arm curls, chest presses, lateral raises, and dips. These five exercises, inspired by CrossFit, are divided into zones where users perform them sequentially within a short time. A monitoring system was created for each zone, allowing users to see their movements. Cameras, positioned at a 30-45 degree angle from the user's exercise zones, analyze the movements. Additionally, a separate monitor for the instructor was installed on the exercise equipment, allowing the instructor to oversee multiple users simultaneously.

Results and Considerations

This study developed an AI-based CrossFit exercise multi-management monitoring system that enables one instructor to care for multiple users during CrossFit exercises for individuals with disabilities. Test results showed that users were more satisfied as they could see their movements in real-time through the personal monitoring system. Instructors also found the system convenient, as they could manage multiple users simultaneously via the monitor on the exercise equipment. Future clinical trials with individuals with disabilities are planned to verify the effectiveness of the developed system.

Acknowledgment This study was supported by a grant from the Rehabilitation Research & Development Support Program (NRCRSP-24TB02) National Rehabilitation Center, Ministry of Health & Welfare, Korea.

Effect of Programed Walking Exercise Using Bo Fit® in Younger Adults

SuHyun Lee^{1*}, Eunmi Kim¹, Jinuk Kim², Dokwan Lee³, Hwang-Jae Lee³, Yun-Hee Kim^{1,4†}

Department of Physical and Rehabilitation Medicine, Sungkyunkwan University School of Medicine¹, Center for Neuroscience Imaging Research, Institute for Basic Science², Bot Fit T/F, New Biz T/F, Samsung Electronics³, Department of Rehabilitation Medicine, Myongji Choonhey Rehabilitation Hospital⁴

Purpose

The purpose of this study was to investigate the effect of programed walking exercise using a wearable hip exoskeleton, Bot Fit® on muscle strength, muscle effort, and the kinematics of the pelvis in younger adults.

Methods

In this study, a wearable hip exoskeleton, Bot Fit® (Samsung Electronics, Suwon, Republic of Korea) which provide assistive/resistive torque during walking was used. We designed three parallel experimental conditions and randomly assigned participants to one of three groups; those assigned to exercise using an interval program of Bot Fit (Interval group), those who used a power program of Bot Fit (Power group), and a control group who exercised without Bot Fit. The interval program repeated rapid walking in resistance mode and slow walking in assistance mode with Bot Fit, while the power program repeated rapid walking in resistance mode and rapid walking in assistance mode with Bot Fit. A total of 45 young adults participated in 18 exercise-intervention sessions over six weeks, and all participants were assessed at two-time points; before and after the 18 exercise sessions. Muscle strength was measured by maximum voluntary contraction (MVC) and muscle effort was calculated as %MVC using surface electromyography (sEMG) at the bilateral rectus femoris (RF), the biceps femoris (BF), the right rectus abdominis, and the lumbar erector spinae (LES) muscles. Kinematics of the pelvis (anterior-posterior tilt, up-down obliquity, and intra-extra rotation) and pelvic symmetry index (SI) were measured using a wireless G-Walk wearable sensor. In addition, the number of steps, distance, energy expenditure, and average HR during 30 min of exercise were measured using a Samsung Galaxy Watch 4 linked to a mobile phone Bot Fit® application.

Results

Significant improvements in the MVC of the left BF were seen in the Interval group, while the Power group showed significant changes in the MVC of the bilateral BF after Bot Fit® exercise. Muscle effort during the total gait cycle decreased significantly in the right BF in the Interval group and in the right LES and bilateral BF in the Power group after Bot Fit® exercise. In contrast, the control group showed no significant muscle effort change. The SI of pelvic tilt tended to increase in post- compared to pre-time points in the Interval and Power groups (by 23.80% and 23.04%, respectively), but this change was statistically significant only in the Interval group. Both the Interval and Power groups showed greater total number of steps, distance, energy expenditure, and average heart rate compared to the control group.

Conclusion

Results of this study confirmed the beneficial effect of programed walking exercise using the Bot Fit® on muscle strength of trunk and lower extremities, muscle effort, and pelvic movement symmetry in younger adults. Personalized exercise programs can be provided for younger adults using various resistance or assistance modes of robotic device with the Bot Fit

Acknowledgment This study was supported by Samsung Electronics (S-2023-0600-000-1) and by the Korea Medical Device Development Fund grant funded by the Korean government (Ministry of Science and ICT, Ministry of Trade, Industry and Energy, Ministry of Health & Welfare, and Ministry of Food and Drug Safety) (KMDF-RS-2022-00140478).

The Validity and Reliability of the Load Cell-based Hand Dynamometer in Healthy Adults.

Gun Seo Jung^{1*}, Jang Hyuk Cho¹, Soyoung Lee¹, Jong-Moon Hwang², Seongho Woo², Kyoung Tae Kim^{1†}

Department of Rehabilitation Medicine, Keimyung University Dongsan Hospital, Keimyung University School of Medicine, Daegu, Republic of Korea¹, Department of Rehabilitation Medicine, Daegu Fatima Hospital, Daegu, South Korea²

Aim

Hand grip strength has been utilized as a representative measure of overall muscle strength. Two of the gold standard hand dynamometers are the Takei (Takei Scientific Instruments, Japan) and the Jamar (Patterson Medical, USA). However, the Takei, being a spring-type, has the disadvantage of hysteresis (the phenomenon where energy is consumed due to internal friction, preventing it from returning to its original state). Jamar, which is a hydraulic-type, has the disadvantage of handle rigidity. InGrip® (InBody, Korea) uses a both load cell and incorporated spring which does not affect the results, thus compensating for the shortcomings of two dynamometers. We aimed to evaluate the validity and reliability of InGrip® by comparing it with the Takei.

Method

A total of 119 community-dwelling healthy adults (61.6±8.3 years old) participated, consisting of 34 males (28.6%) and 85 females (71.4%). Participants tried to grip the dynamometer with their maximum force for 3~5 seconds, alternating between both hands twice on each side, with a minimum 30 second interval between each trial. Takei and InGrip® were evaluated in random order, with minimum 10-minute interval. The maximum grip strength among L1(first trial of left hand), R1(first trial of right hand), L2(second trial of left hand), R2(second trial of right hand) was used. To verify the test-retest reliability of each dynamometer, L1 was compared with L2, and R1 with R2. The paired t-test was used for comparing the means of the two dynamometers. Pearson correlation analysis was conducted to check the correlation between the two dynamometers. Level of agreement between two dynamometer was evaluated using Bland–Altman plots. The interclass correlation coefficient(ICC), standard error of measurement(SEM), minimal detectable change(MDC) were used to assess the test-retest reliability of the two devices. Statistical significance was set at p

Results

There were no significant differences between the two dynamometers ($p>0.05$). The correlation coefficient was 0.944 overall, 0.926 for men, and 0.740 for women respectively (p

Conclusion

The InGrip® showed good agreement with the Takei and excellent test-retest reliability. In the future, a study to confirm whether hysteresis occurs compared to Takei during long-term use, as well as a validation study with Jamar, will be necessary.

Acknowledgment This work was supported by the Korea Medical Device Development Fund grant funded by the Korea government the Ministry of Science and ICT (Project Number: 1711179413, RS-2022-00164620)

Table 1. Correlation between the Takei and the InGrip® for hand grip strength measurement.

	Takei (kg)	InGrip® (kg)	r
All (n=119)	27.1±8.3	26.9±8.5	0.944**
Male (n=34)	37.0±8.3 [^]	37.1±8.6 [^]	0.926**
Female (n=85)	23.1±3.7 [^]	22.8±3.6 [^]	0.740**

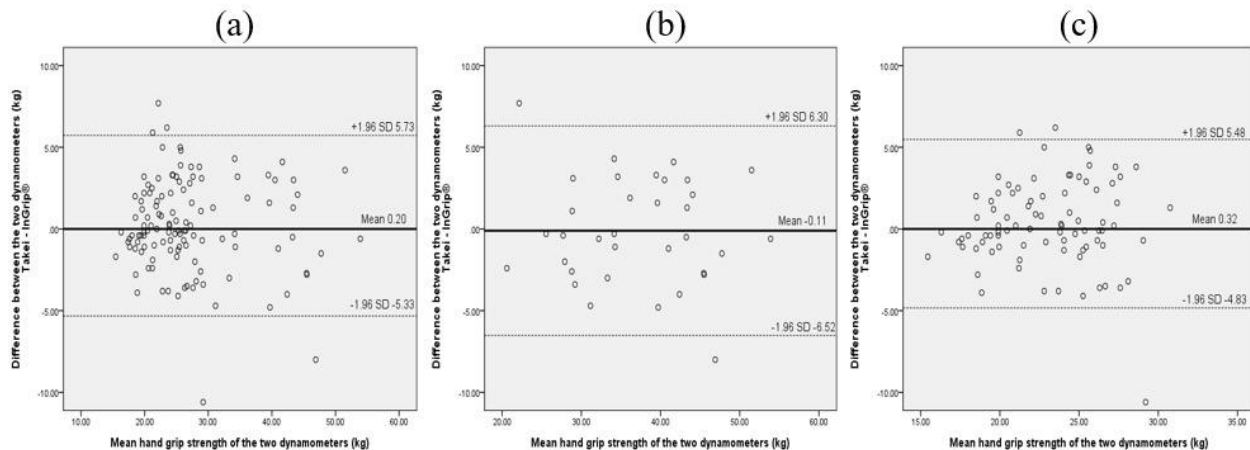
All data are presented as mean±SDs

r; correlation coefficient

**p<0.01, [^]p<0.01 between genders

Correlation between the Takei and the InGrip® for hand grip strength measurement.

Figure 1. Bland-Altman plot comparing between the Takei and the InGrip® in (a) all participants, (b) male, (c) female.



Bland-Altman plot comparing between the Takei and the InGrip®.

Table 2. Test–retest reliability of the Takei and the InGrip® for hand grip strength measurement.

	ICC(95%CI)	SEM	SEM%	MDC	MDC%
Left hand in Takei	0.967**(0.946-0.979)	0.48	2.02%	1.34	5.60%
Right hand in Takei	0.983**(0.973-0.989)	0.26	1.01%	0.73	2.81%
Left hand in InGrip®	0.984**(0.977-0.989)	0.26	1.07%	0.72	2.96%
Right hand in InGrip®	0.983**(0.976-0.989)	0.27	1.07%	0.72	2.80%

ICC; Intraclass Correlation Coefficient, SEM; Standard Error of Measurement,

MDC; Minimal Detectable Change.

**p<0.01

Test-retest reliability of the Takei and the InGrip® for hand grip strength measurement.

Terson syndrome secondary to subarachnoid hemorrhage

Hyo Jeong Lee^{1*†}, Hyun Ho Kim¹

Department of Rehabilitation Medicine, Bundang Jesaeng Hospital ¹

Introduction

Terson syndrome is defined as intraocular hemorrhage (IOH) in the context of severe subarachnoid hemorrhage (SAH) and is a significant treatable cause of vision loss. Early detection in the emergency department can prevent permanent visual impairment and allow patients to maximize their rehabilitation potential.

Case presentation

A 49-year-old male with SAH was stupor no history of trauma. He underwent endovascular treatment with coiling of middle cerebral artery bifurcation on left and external ventricular drainage with mannitol injections in order to lower intracranial pressure. Also physician checked the transcranial doppler every day. Serial brain CT finding was suggestive of retinal hemorrhage manifested by a retinal nodularity (figure 1).

After ten days, his mental state was almost back to normal, although he frequently had visual loss and impairment in his right eye's visual field. A funduscopy and ocular ultrasonography examination conducted after 20 days indicated vitreous hemorrhage, Terson syndrome (figure 2). Ten days later, he had operation in right eye with vitrectomy pars planar under topical anesthesia and a subconjunctival injection of lidocaine. Following the procedure, he recovered quickly and his visual acuity was normal. He kept working on strengthening his right ankle.

Discussion

Terson syndrome is not a rare complication of SAH, with a high incidence and worse prognosis. On the other hand, Terson syndrome is a serious illness that highlights the connection between ophthalmological and neurological health. A thorough management plan and early diagnosis are essential for bettering patient outcomes. Patients who may have experienced intraocular bleeding should keep considering conservative measures like vitrectomy and routine monitoring.

Acknowledgment The authors declare that they have no conflicts of interest concerning this article.

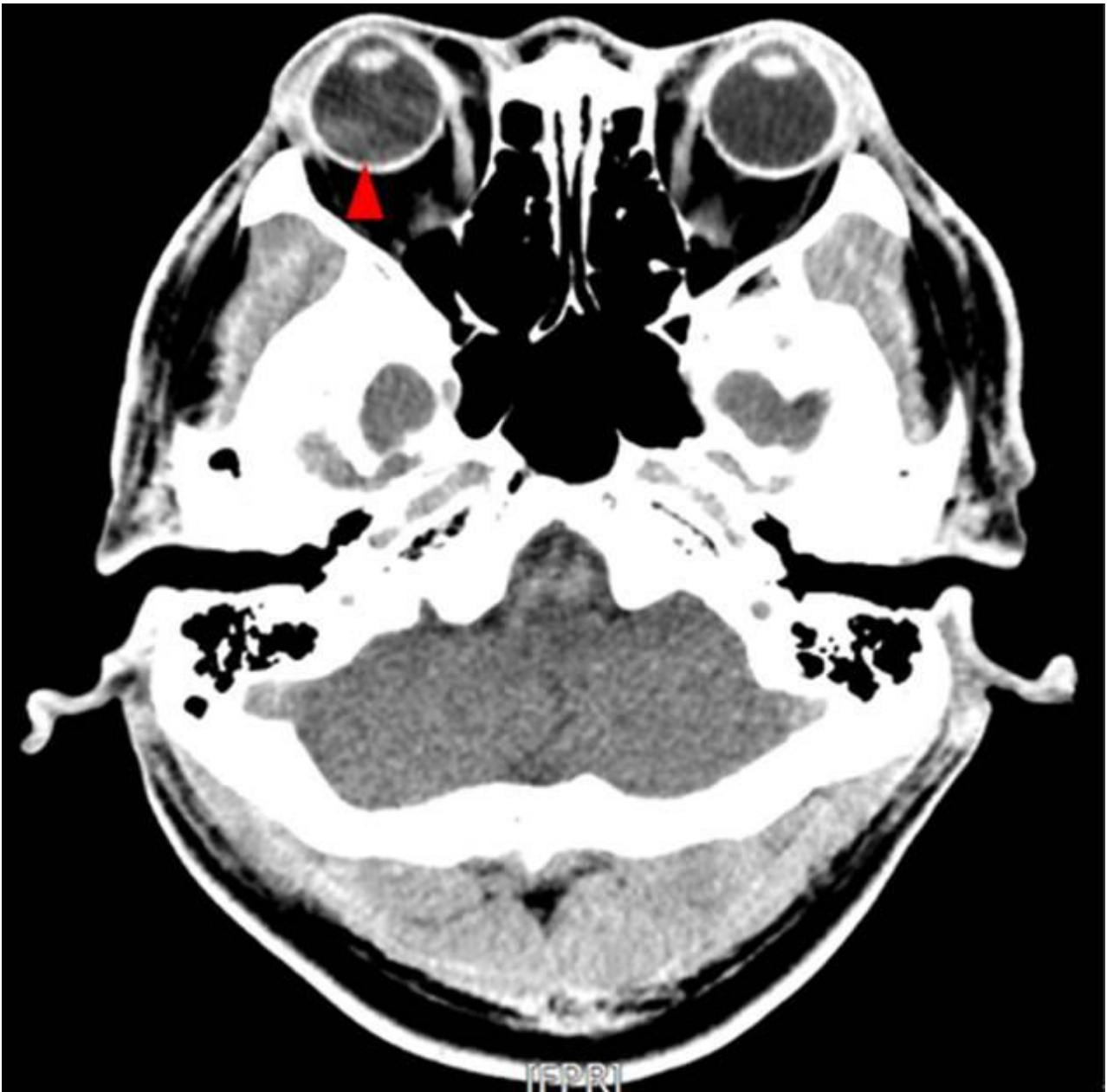


Figure 1. CT finding was suggestive of retinal hemorrhage manifested by a retinal nodularity (within 1 day).

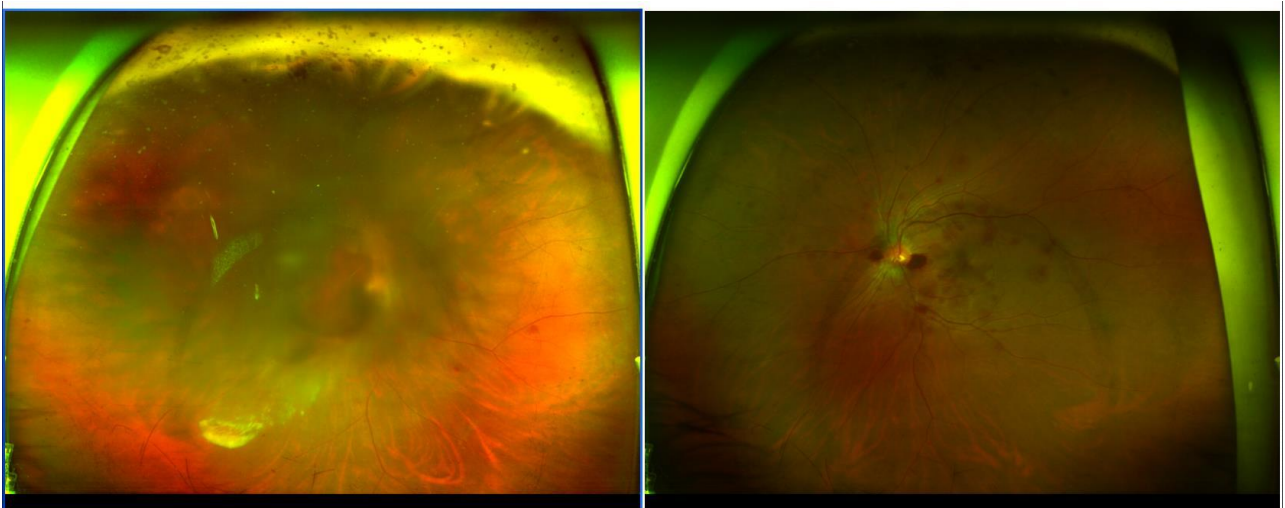


Figure 2. Funduscopy exam OD/OS. OD, showing a large area of subretinal and vitreous hemorrhage

Meige Syndrome Caused by Bi-pallidal Ischemic Lesions : a Case Report

So-youn Chang^{1*}, Eun Jin Park¹, Ja Eun Koo¹, Eun Joo Lee¹, Sun Jae Won¹, Youngkook Kim^{1†}

Department of Rehabilitation Medicine, Yeouido St. Mary's hospital, College of Medicine, The Catholic University of Korea, Republic of Korea¹

Background

Meige syndrome is a rare focal dystonic movement disorder characterized by involuntary muscle contractions leading to stereotyped and repetitive face, mouth, and neck movements. These symptoms may gradually progress over time, significantly impacting the patient's quality of life. Most cases are idiopathic, with unknown causes, but environmental triggers like psychological stress, drug exposure, or physical trauma can influence secondary Meige syndrome. We present a patient with blepharospasm and oromandibular dystonia following bi-pallidal ischemic lesions.

Case Description

A 73-year-old woman presented that for several years, involuntary muscle spasms around both eyes and the mouth would begin when she opens her eyes, accompanied by dystonic movements of the head in a vertical direction, spreading to the cheeks. These symptoms have progressively worsened over the past year, leading to a referral from the neurosurgery department to our department for an electromyography (EMG) examination. The motor conduction study from the frontalis, nasalis, orbicularis oculi, and orbicularis oris muscles showed normal onset latencies and amplitudes of the bilateral facial nerves. Normal responses were observed in the blink reflex test with bilateral supraorbital nerve stimulation. However, abnormal reflexes of the orbicularis oris (delayed latencies) were detected on bilateral supraorbital nerve stimulation with co-recording from the orbicularis oculi and orbicularis oris muscles. Dual-channel EMG revealed involuntary non-simultaneous contraction of the bilateral orbicularis oculi and oris muscles, particularly during eye-opening efforts. Magnetic resonance imaging (MRI) and angiography revealed symmetrically T2 high signal lesions at bilateral globus pallidus, which were suspected to be indicative of old infarction. Detailed history taking showed that the patient was diagnosed with cerebral infarction in 2017, has been on antiplatelet medication, and reported that symptoms appeared after that. She had received three Botox injections at another hospital without significant improvement. On physical examination, blepharospasm started with eye opening, followed by gradual onset of oromandibular dystonia and vertical head dystonic movements, more pronounced on the left side. Laboratory tests, including those for metabolic diseases and a copper study, were normal. There were no family members with similar symptoms, no other neurological signs, and depressed or hysterical traits. Subsequently, she received an additional Botox injection but still experienced no relief.

Conclusion

This rare case was presumably predisposed to developing Meige syndrome due to an ischemic insult at the bi-pallidum. Recent research has demonstrated that deep brain stimulation at the pallidum may be an effective treatment for this syndrome, indicating that the pallidum may play a role in the pathogenesis of Meige syndrome.

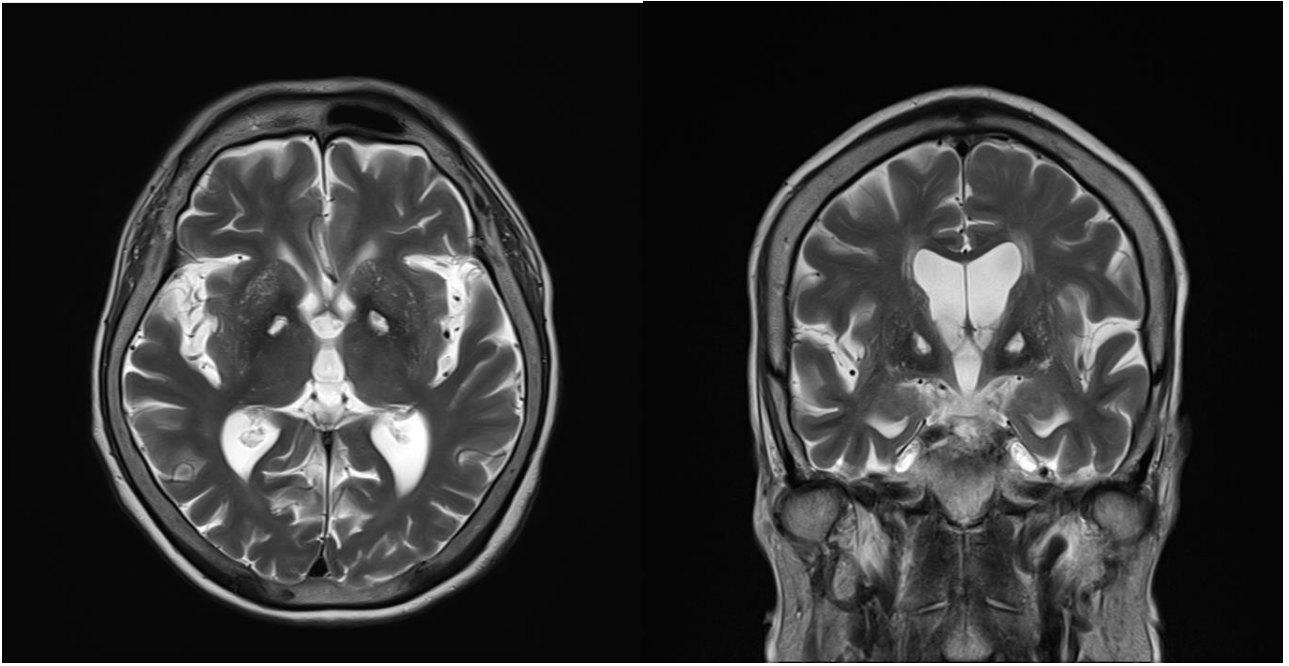
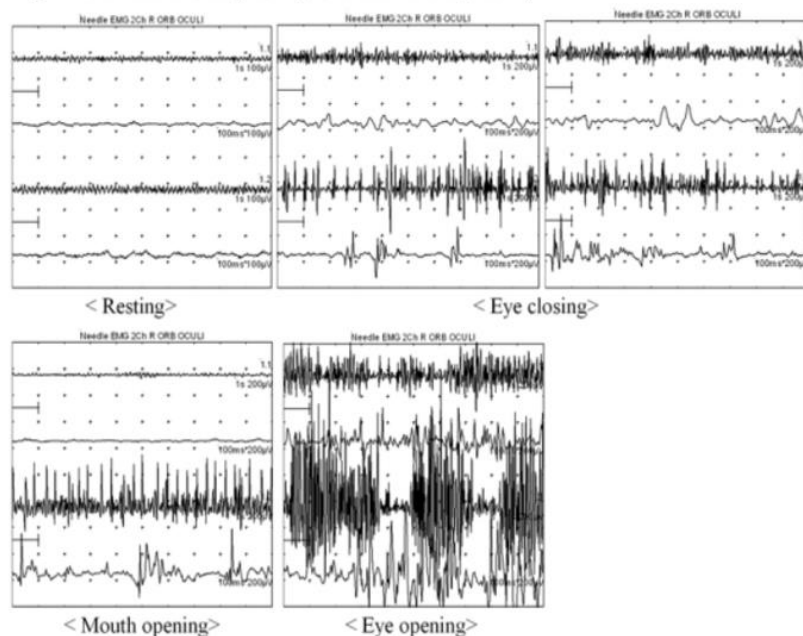


Figure 1. Magnetic resonance imaging shows T2 high signal lesions at bilateral globus pallidus.

Right : Orbicularis oculi (Above), Orbicularis oris (Below)



Left : Orbicularis oculi (Above), Orbicularis oris (Below)

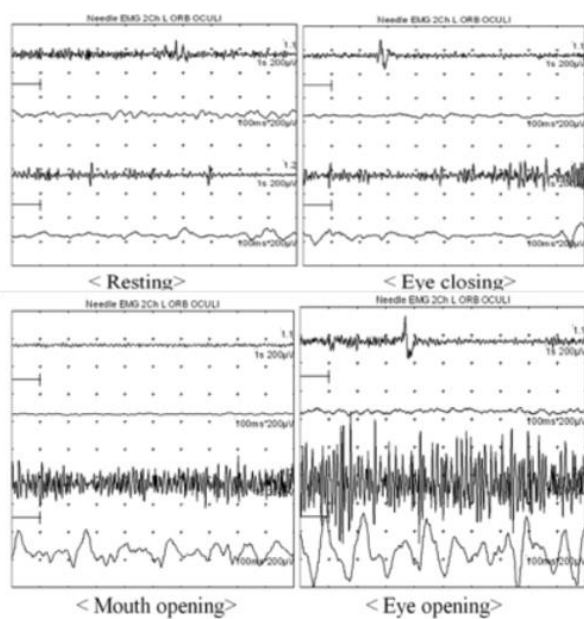


Figure 2. Dual-channel EMG reveals involuntary non-simultaneous contraction of the bilateral orbicularis oculi and oris muscles, during eye-opening efforts.

Effect of low frequency rTMS on fluent aphasia and cognitive impairment in chronic stroke patient

Jae-Hwan-Choi¹, Yeon-Hee Choi², Ji-Young Lee³, Kang-Jae Jung¹, Jae-Hyung Kim^{1*†}

Department of Physical Medicine & Rehabilitation, Daejeon Eulji University Hospital ¹, Speech therapy Section, Daejeon Eulji University Medical Center², Occupational therapy Section, Daejeon Eulji University Medical Center³

Introduction

There are so many studies investigated the effects of rTMS on non-fluent aphasia rehabilitation. Naeser et al., applied low-frequency rTMS to the non-lesioned hemisphere over a 2-week period as a therapeutic intervention for non-fluent motor aphasia and reported clinical improvement of language function. However, there are very rare reports that document the therapeutic application of low-frequency rTMS in post-stroke patients with sensory-dominant aphasia and its clinical effects. We reported that the effect of rTMS on fluent aphasia and cognitive impairment in a patient with chronic stroke event.

Case report

The subject was a right handed 75-year-old man diagnosed with cerebral hemorrhagic infarction in 2008. He was transferred to emergency room for back pain, speech disturbance with cognitive impairment. He had a medical history of hypertension, hyperlipidemia, and atrial fibrillation. After one week from onset of the back pain, he was referred to rehabilitation department for comprehensive rehabilitation. The patient's motor power was recorded at 4/5 at both the upper and lower extremities and he could gait under supervision, indoor level. The patient had 54 of Berg balance scale score. The score of modified Barthel index was measured at 89/100, reflecting partial dependency in personal hygiene, bathing, feeding, stair climbing, and ambulation. The score of K-MMSE was 12/30, indicating problems with attention, memory, and language. The global deterioration scale was stage 5 (moderately severe cognitive decline). The evoked potential tests revealed dysfunction in the motor evoked potential, auditory evoked potential, and somatosensory evoked potential pathways. The Brain MRI showed regional irregular cystic cerebromalacia, atrophy, peripheral dark hemosiderin deposit, surrounding reactive gliotic change at the left temporo-parietal cortex, white matter area, with secondary dilated left occipital horn (Figure 1). He was diagnosed with Wernike aphasia by the Korean version of the Western Aphasia Battery (K-WAB).

rTMS protocol: For 2 weeks, 10 times of rTMS was applied over the posterior superior temporal gyrus of non-dominant hemisphere. The 8-figured coil was placed over CP5 (according to the 10-20 electroencephalograph system) for 15 minutes at an intensity of 90% of threshold with 1Hz frequency.

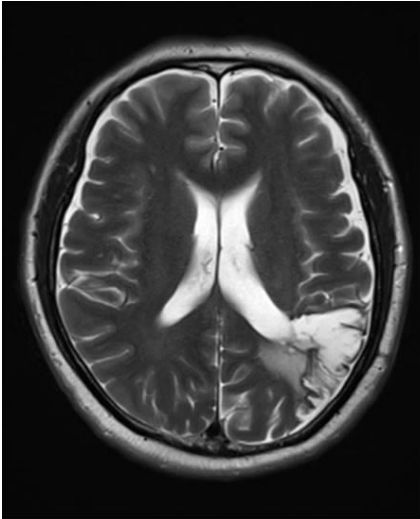
Results

After 2 weeks treatment, rTMS elicited a meaningful enhancement of reading function, and verbal comprehensive function by K-WAB assessment (Table 1). In the cognitive function test using the Cognitive Screening Assessment System (CoSAS), improvement was observed. Total score of CoSAS was improved from 70.3 to 83.7. (Figure 2).

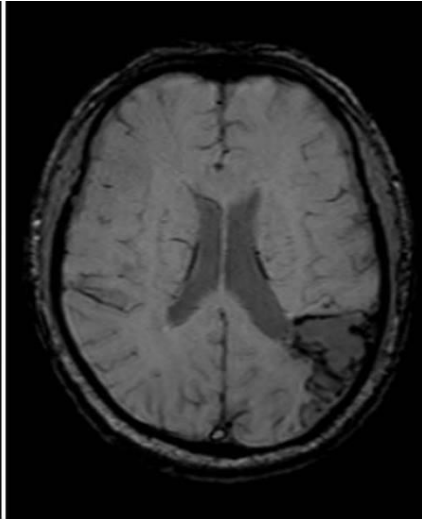
Conclusion

Our results show that the low frequency rTMS on the posterior superior temporal gyrus of non-dominant hemisphere can be helpful for fluent sensory aphasia and cognitive impairment in patient with chronic stroke event.

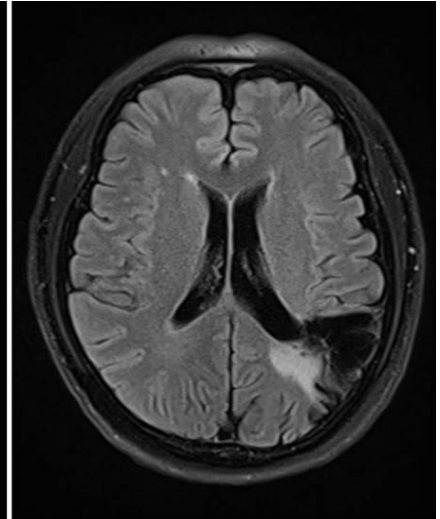
Acknowledgment There were no financial support.



(A)



(B)



(C)

Brain MRI axial images show old hemorrhagic infarction from (A) diffusion weighted imaging with apparent diffusion coefficient mapping, (B) susceptibility weighted Imaging, and (C) T2 FLAIR image.

		Pre-rTMS	Post-rTMS
spontaneous speech	information	4	8
	fluency	7	7
	total	11	15
auditory verbal comprehension	yes/no question	21	33
	auditory word recognition	2	11
	sequential commands	4	4
	total	27	48
repetition	total	0	0
naming	object naming	0	0
	word fluency	0	0
	sentence completion	0	0
	responsive speech	0	1
	total	0	1
reading	sentences	0	2
	commands	0	0
	word-objection matching	0	1
	word-picture matching	0	2
	picture-word matching	0	6
	verbal-word matching	0	3
	spoken word-written word	0	0
	spelling mix	0	0
	spelling detachment	0	0
	total	0	14
writing	writing on request	0	2
	written output	0	0
	writing to dictation	0	0
	writing of words	0	0
	writing & number	0	9
	syllable & number	0	0
	copying of a sentence	0	10
	total	0	21
aphasia quotient		24.7	36.8
language quotient		12.4	25.4

The results of Korean Western Aphasia Battery (K-WAB), conducted before and after rTMS.



(A)

(B)

CoSAS results (A) before rTMS, and (B) after rTMS

The trans-Cranial Direct Current Stimulation with simulation after craniectomy for consciousness

Seong Hoon Lim^{1,2*†}, Tae-Woo Kim³, Donghyeon Kim⁴, Hyungtaek Kim⁴, Sun Im⁵, Kyoung Hyun Park¹

Department of Rehabilitation Medicine, Seoul St. Mary's Hospital, College of Medicine, The Catholic University of Korea¹, Institute for Basic Medical Science, Catholic Medical Center, College of Medicine, The Catholic University of Korea², Department of Rehabilitation Medicine, National Traffic Injury Rehabilitation Hospital³, Research Institute, NEUROPHET, Inc⁴, Department of Rehabilitation Medicine, Bucheon St. Mary's Hospital, College of Medicine, The Catholic University of Korea⁵

Transcranial direct current stimulation (tDCS) has been used for the restoration of awareness in patients with a minimal consciousness state (MCS). Until now, tDCS were contraindicated in brains that had undergone craniectomy. We present a case with prolonged MCS over 1 year, who had severe brain damage, ventriculoperitoneal (VP) shunt, and craniectomy, which was treated with tDCS after simulation with the patient's brain magnetic resonance image (MRI).

A 22-year-old man with prolonged consciousness disorder over 1 year, due to traumatic brain injury, had underwent decompressive craniectomy and VP shunt, admitted our clinic (PANEL A). his revised coma recovery scale (CRS-r) score was 8 (A1V1M3O1C0Ar2).

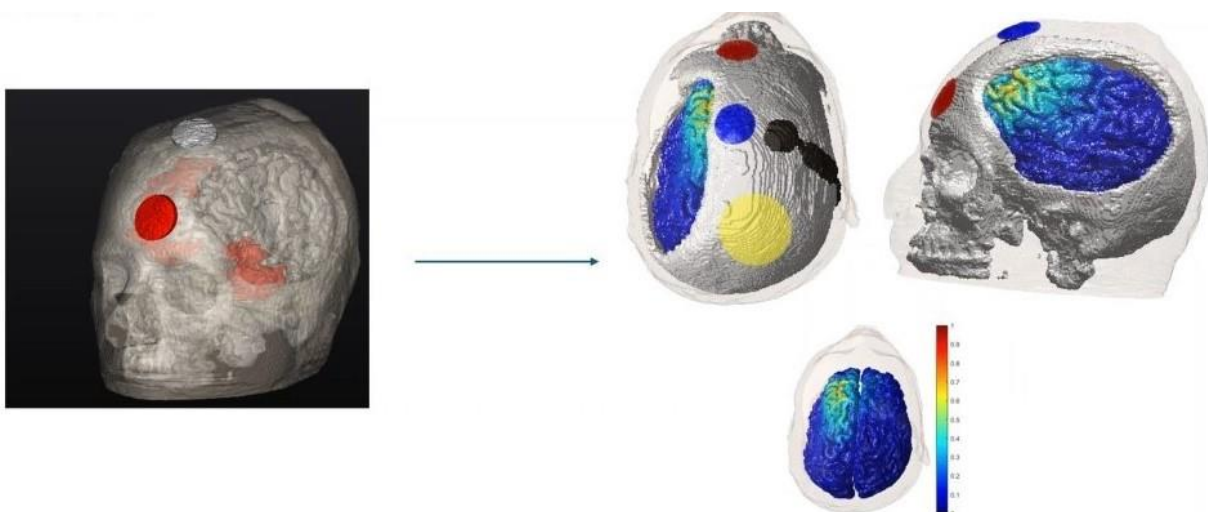
The parents wanted to provide neuromodulation treatment for their son, and since he needed a craniectomy, we wanted to find a safe method through simulation. The enorm of the cerebral cortex was targeted at 0.2-0.3V/m, which was calculated from previous our clinical trial for MCS with intact skulls. Our simulation was taken for target to the left dorsolateral prefrontal cortex via Neurophet's tES Lab based on the patient's MRI, may stimulated prefrontal cortical-striatopallidal-thalamo-cortical loop(PANEL A).. In addition, the stimulation location was intended to minimize unexpected problems in patient by positioning of electrodes on scalp with skull remaining. After the patient treated with forty optimized tDCS sessions, she woke up with a CRS-r score of 12 (A2V3M3O2C0Ar2). And, he stated to partial oral feeding with puree and liquid.

After severe traumatic brain injury, craniectomy may be an unavoidable neurosurgical treatment. This case provides evidence that patients with craniectomy can undergo successful tDCS treatment with simulation.

Acknowledgment This work was supported by the Promotion of Innovative Businesses for Regulation-Free Special Zones funded by the Ministry of SMEs and Startups (MSS, Korea) (P0020624).



lateral plain X-ray



electric simulation of patient

Robot-Assisted Hand Rehabilitation: A Case Series Investigating the Alleviating Post-Stroke Pain

Jihyun Park^{1*†}, Yeon Jun Kim¹, Yeong Jae Kim¹, Yongkyun Jung¹, Soo Jin Jung¹

Department of Rehabilitation Medicine, Hallym University Dongtan Sacred Heart Hospital¹

Background

Post-stroke pain affects approximately half of the patients and can manifest in various forms in upper extremities, including hemiplegic shoulder pain, central post-stroke pain, and painful spasticity. Given that most post-stroke pain involves mixed and combined mechanism, pain control and alleviation remain mysterious and complex. Robot-assisted upper-extremity rehabilitation has been studied for hemiplegic post-stroke patients, with the aim of stimulating early motor recovery based on the hypothesis of neuroplasticity. Unlike most previous studies that focused on the effect of upper limb function recovery, this study seeks to explore new possibilities that robot-assisted hand therapy can offer as a pain control modality, highlighting its potential to integrate post-stroke rehabilitation.

Method

This study is a case series study to investigate the effects of robot-assisted hand rehabilitation therapy (RT) for post-stroke central pain. “Hand of Hope” (Rehab-Robotics Company, Hong Kong) —an EMG- driven robot-assisted hand rehabilitation device— was used for the intervention. The robot-assisted hand rehabilitation includes continuous passive motion, hand opening, reaching and grasping training with EMG biofeedback. Training was conducted for 30 minutes per session, for a total of 10 sessions. The primary outcome measure is the Visual Analog Scale (VAS) score for subjective pain. Secondary outcomes include Box and Block Test (BBT) for fine motor function and Modified Ashworth Scale (MAS) for spasticity. Each outcome was assessed before and after the treatment.

Results

Seven participants with post-stroke pain were included. Primary outcome results showed a trend of pain relief (figure 1). Fine motor function increased after RT. Improvement of BBT (figure 2) score and improving trend in spasticity checked by MAS score (figure 3) were found after RT.

Conclusion: EMG-driven robot-assisted hand rehabilitation may alleviate post-stroke pain. The results provide preliminary evidence suggesting a potential pain relief effect of robot-assisted hand rehabilitation therapy in patients with stroke. Although the study results did not significantly differ from conventional therapy, positive effects can still be anticipated. With a sufficient number of participants recruited for future studies, further research is needed to confirm these findings definitively.

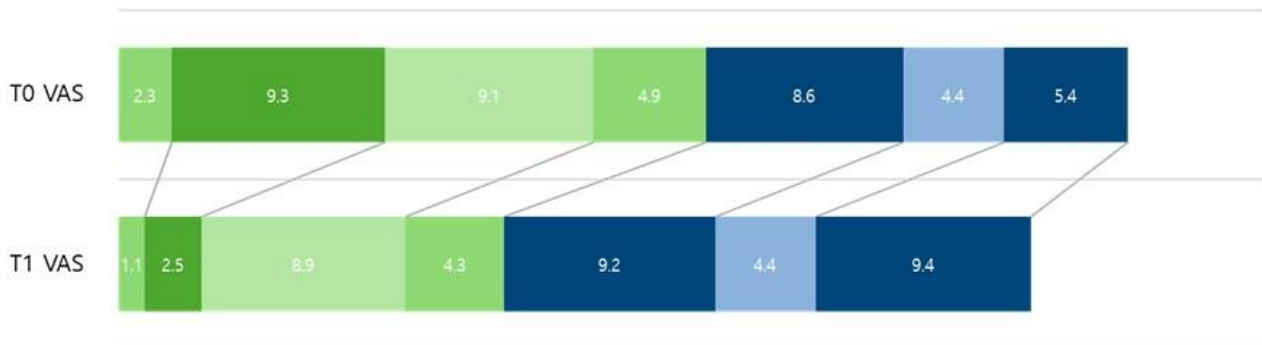


Figure 1. Visual Analog Scale (VAS) score during exercise before(T0) and after(T1) robot-assisted hand rehabilitation

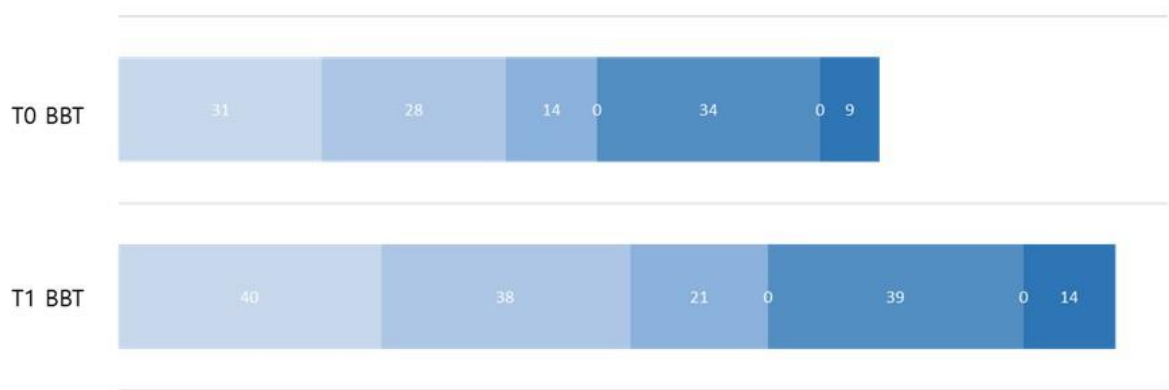


Figure 2. Box and Block Test (BBT) score of affected arms before(T0) and after(T1) robot-assisted hand rehabilitation



Figure 3. MAS score of upper extremities(UE), sum of finger flexors, wrist flexors and elbow flexors, before(T0) and after(T1) robot-assisted hand rehabilitation

Central Pontine Myelinolysis Initially Presented with Dysphagia: A Case Report

Byung Chan Lee^{1*†}, Minjae Jeong¹, Kyeongil Min¹, Myung Woo Park¹

Department of physical medicine and rehabilitation, Chung-Ang University Hospital¹

Introduction

Central pontine myelinolysis is a type of osmotic demyelination syndrome that can occur due to rapid correction of hyponatremia. It is predominantly known to affect the white matter of the pons. Symptoms typically manifest several days after the correction of hyponatremia and can range from dysphagia, dysarthria, spastic quadriparesis, and pseudobulbar paralysis to severe conditions such as locked-in syndrome or coma. Here, we present a case of a patient who visited the outpatient rehabilitation department with dysphagia and dysarthria and was eventually diagnosed with central pontine myelinolysis.

Case Report

A 65-year-old male patient presented to the outpatient rehabilitation department with complaints of dysarthria and dysphagia. The patient reported that the symptoms began two months ago, and over these two months, he experienced prolonged mealtimes and a weight loss of about 5 kg. His medical history included hypertension and dyslipidemia, and he had undergone surgery for gastric cancer 12 years prior.

Eight weeks before his visit, the patient was treated for hyponatremia at another hospital. Six weeks before his visit to our emergency department due to dysphagia and general weakness, blood lab results showed normal levels of sodium (137 mEq/L) and potassium (3.9 mEq/L), with no significant abnormalities other than mild anemia (hemoglobin 10.1 g/dl).

Physical examination revealed no abnormalities in cranial nerve examination, but hyperreflexia of all extremities and mild spasticity in the right lower limb were observed. To further investigate the patient's hyperreflexia, dysphagia, and dysarthria, we planned VFSS, EMG/NCS, and brain MRI.

The VFSS test showed aspiration with reflex cough (PAS 8) on a small amount of fluid (Figure 1). EMG/NCS showed no abnormalities. Brain MRI revealed a lesion with signal hyperintensity in the central pons on T2 flair and diffusion-weighted images (thick white arrow, Figure 2). Therefore, the patient was diagnosed with dysphagia due to central pontine myelinolysis.

For supportive care, we prescribed the patient on dysphagia treatment and compensatory techniques using thickeners. However, the dysphagia symptoms persist, and the patient remains under follow-up.

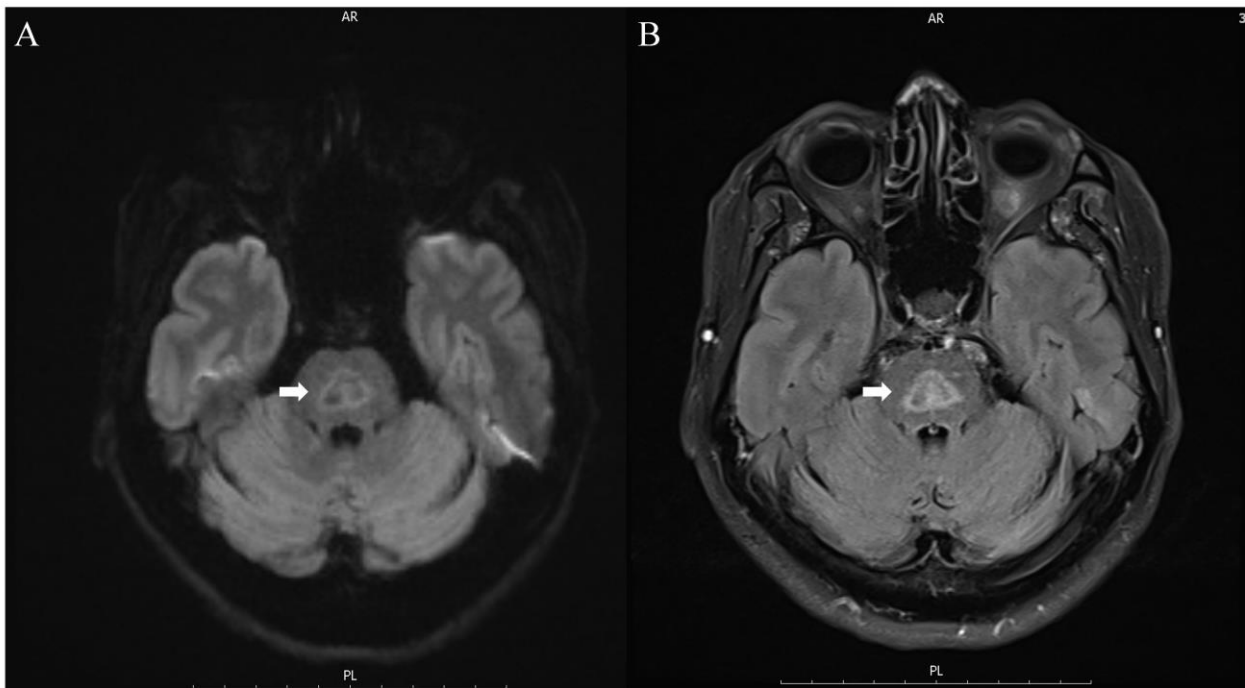
Conclusion

When a patient presents with dysphagia and dysarthria, central pontine myelinolysis, though rare, should be considered. Accurate neurological examination and diagnosis through imaging modalities could be essential.

Acknowledgment None.



Figure 1 demonstrates aspiration of a small amount of fluid in the VFSS.



T2 FLAIR and diffusion-weighted MRI showed high signal intensities in the pons, suggesting central pontine myelinolysis.

Influence of UCB and rhEPO combination therapy on biomechanical gait parameter in a stroke patient

HyeongMin Jeon^{1*}, Seyoung Shin¹, Eun-Hye Chung¹, Se-Young Bak¹, Heegoo Kim¹, Hongsok Baek¹, MinYoung Kim^{1†}

Department of Rehabilitation Medicine, CHA Bundang Medical Center, CHA University School of Medicine¹

Objective

To reveal the effect of allogeneic umbilical cord blood (UCB) multi-dose treatment combined with recombinant human erythropoietin (rhEPO) on gait parameters using 3D motion analysis in a 62-year-old chronic stroke patient case.

Methods

Subject: A 62-year-old male, 2 years and 8 months after the cerebral infarction onset with left hemiparesis (Baseline Functional Ambulation Category 4).

Intervention: After checking blood type and Human Leukocyte Antigen type matching, the allogeneic umbilical cord blood was administered intravenously twice. The patient received twice of 2 cord blood units ($> 2 \times 10^7$ /kg cell number/kg) each 4 weeks apart. rhEPO (Espogen Prefilled INJ, 10000 IU/ml) 500 IU per kg was administered subcutaneously or intravenously 2 hours before the cord blood infusion, 4 days and 7 days after the infusion.

Motion analysis: An eight-camera three-dimensional motion capture system (Qualisys., Sweden) sampled at 100 Hz was used to collect the gait data. Three force plates (9260AA6; Kistler., Switzerland) embedded in the walking path were used to collect the force data while walking at 1,000 Hz. A set of Helen Hayes markers were attached to the subjects. The subjects walked 3 times in a 10 m \times 4.5 m walkway at a comfortable speed. The collected data were analyzed by performing inverse dynamics using Visual 3D software (c-motion inc., Boyds, MD, United States) to obtain kinetic and kinematic data. Pre-assessment was performed within 1 week prior to UCB administration and post-assessment was performed immediately after completion of second UCB and rhEPO treatment.

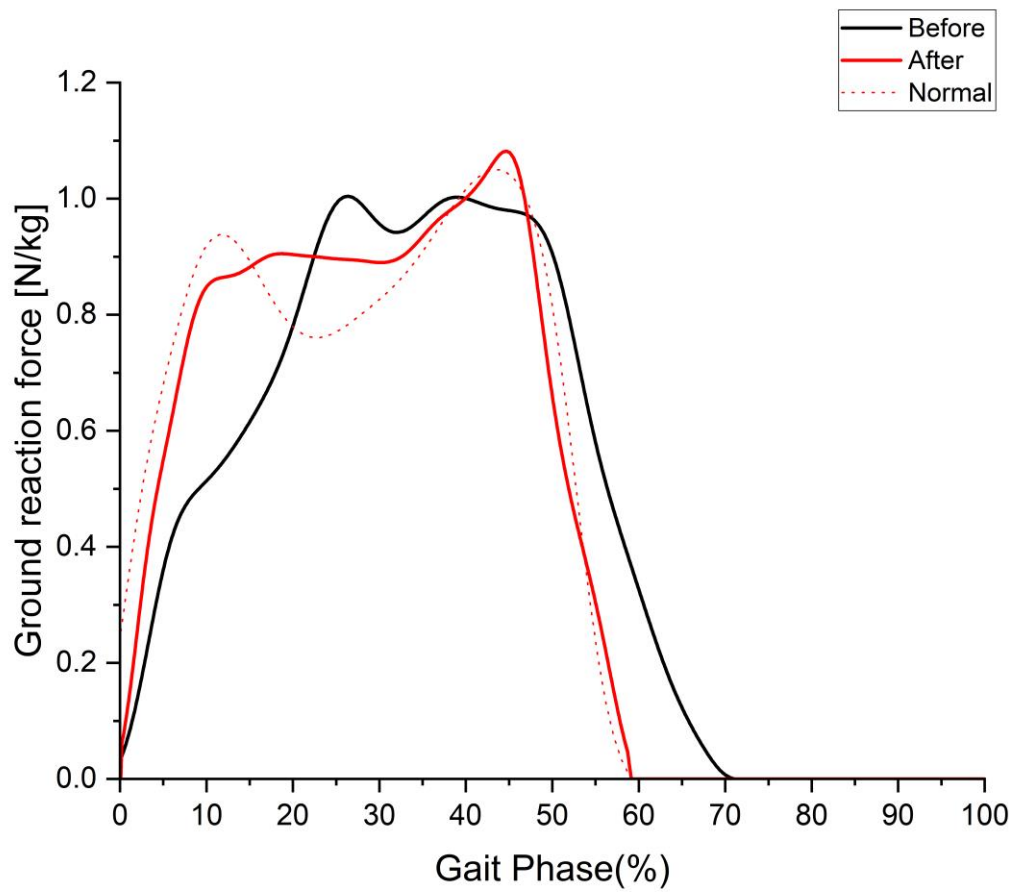
Results

Subject had a BBS of 48, TIS of 16, and MMT (affected side) of 580 prior to UCB administration. The stride time on the affected side did not change significantly, around 1.8 seconds before and after, but the proportion of stance phase (before: $69.1 \pm 3.4\%$, after: $60.6 \pm 0.4\%$) approached the normal proportion of 60%. The pre-treatment ground reaction force (GRF) pattern of the affected side showed no clear second peak, but the post-treatment GRF pattern showed two clear peaks. Pelvic mobility range in transverse plane increased from pre: 1.43 ± 0.12 deg[°], post: 2.82 ± 0.20 deg[°]

Conclusion:

After UCB treatment, we revealed that the gait pattern was recovered similar to that of normal people through stance phase ratio and GRF pattern, and we would like to further study the gait changes of stroke patients with UCB treatment through detailed analysis of more patients and joints.

Acknowledgment This research was supported by a grant of the Korea Health Technology R&D Project through the Korea Health Industry Development Institute (KHIDI), funded by the Ministry of Health & Welfare, Republic of Korea (grant number: HI16C1559, RS-2023-00262005)



Comparison of ground reaction forces during walking before and after UCB treatment

Cerebrolysin Use in the Treatment of Hypoxic-Metabolic Encephalopathy: a Case Report

Joo-ee Jung¹, Hyun Im Moon^{1**}

Department of Rehabilitation Medicine, Bundang Jeseang Hospital¹

Introduction

Finding neuroprotective agents to counteract the deleterious effects of hypoxia on neuronal cells successfully is one of the most critical targets of clinical research since preclinical studies have identified potential neuroprotective strategies. We introduce case report that describe our experience with adjunctive therapy for hypoxic-metabolic encephalopathy (HME) after an overdose of sleeping pills, using cerebrolysin - a multimodal agent has been suggested to promote neuroprotection and neuroregeneration after stroke and traumatic brain injury.

Case presentation

81-year-old female patient who usually takes depressive drugs and sleeping pills (the exact dosage of the drug was unknown), but she did not wake up after sleeping, so she visited emergency room and was hospitalized under the diagnosis of hypoxic ischemic encephalopathy at that time. At the time of transfer to our hospital, she was considered as a vegetative state (VS) in which only eye opening is possible and communication or instruction is not followed at all. Neurologist stated that the possibility of recovery was not significant based on electroencephalogram (EEG) and brain positron emission tomography (PET). Cerebrolysin (20ml) was administered during for 14 days and methylphenidate (10mg) was added per oral. After 14 days, her eye opening time was increased and she more frequently responded to the verbal command. We used Cerebrolysin (20ml) one more cycle for 14 days after 1 week interval. Physical rehabilitation was carried out during whole hospitalization period. Her response was improved. At discharge, the patient was conscious, and verbal communication was possible with occasional non-logic periods. Her long-term memory was preserved, so she could answer accurate information about her family or her personal life.

Conclusion

Cerebrolysin has effects such as protecting nerve cells, promoting nerve regeneration, and reducing oxidative stress, which can be useful for helping recovery after brain damage. There is still insufficient evidence that Cerebrolysin is effective in patients with HME. Although specific studies on HME are lacking, there are studies that have shown positive effects on other types of brain injury or recovery after stroke. Although there is no clear evidence that the improved patient's consciousness and cognitive function in this case are due to cerebrolysin, this is a case that showed that cerebrolysin can be safely used in HME patients as well. Further research and clinical trials will be helpful to provide clearer answers.

Rare Complications of Antiepileptic Drugs in an Elderly Stroke Patient: A Case Report

Hae-Yeon Park^{1**}, Jisoo Park¹, Dongwook Song¹, Seung Yup Song¹, Geun-Young Park¹, Sun Im¹

Department of Rehabilitation Medicine, Bucheon St. Mary's Hospital, College of Medicine, The Catholic University of Korea¹

Introduction

The use of antiepileptic drugs (AEDs) is essential in the management of seizures, especially in patients with a history of stroke. However, AEDs can have significant adverse effects that complicate patient care. This case report presents an 83-year-old female diagnosed with stroke who developed ileus and hyponatremia as adverse effects of levetiracetam and valproic acid, respectively.

Case Report

A 83 year-old female was admitted to the hospital with the diagnosis of left parietal lobe infarction. She had a past medical history of hypertension, and gastric adenocarcinoma which was surgically treated six years ago. Electroencephalography (EEG) showed phase reversal rhythm in the bilateral temporal area, leading to the prescription of levetiracetam 500 mg twice daily for seizure prevention. To evaluate dysphagia, a videofluoroscopic swallow study (VFSS) was conducted. However, she subsequently experienced poor bowel movement, as seen on abdominal X-ray. Management strategies to improve bowel movement, including bowel massage and enemas, were not effective. After a thorough review of her medications, we decided to switch from levetiracetam to valproic acid due to the rare complication of intestinal obstruction associated with levetiracetam. Following the medication change, her bowel movements improved, as confirmed by serial X-rays (Figure 1). However, on the third day after starting valproic acid, she developed hyponatremia with a sodium level of 127 mEq/L. The only recent change was the addition of valproic acid. A literature review indicated that valproic acid could be associated with hyponatremia. Therefore, valproic acid was switched to lamotrigine, and two days later, her sodium levels improved.

Conclusion

This case highlights the rare but serious complications associated with the use of levetiracetam and valproic acid in an elderly poststroke patient. Levetiracetam was associated with ileus, necessitating a switch to valproic acid, which subsequently caused hyponatremia. The patient's condition improved following the discontinuation of the offending drugs. This case emphasizes the need for careful selection and monitoring of antiepileptic medications in elderly stroke patients, particularly those with complex medical histories. Clinicians should be aware of these potential adverse effects and further studies are needed to better understand the mechanisms of these side effects and to develop strategies for safer AED use in elderly poststroke patients.



A day after VFSS



6 days after VFSS



9 days after VFSS



**11 days after VFSS
2 days after discontinuation
of levetiracetam**



**3 days after discontinuation
of levetiracetam**

Figure 1. Serial abdominal X-rays of the patient

Successful Extubation of a Brainstem Tumor Patient Through ICU Rehabilitation: A Case Report

Jae Sik Seo¹, Seon Jun Yoon¹, Bo Kyung Ha³, Seung Heon Cha⁴, Myung-Jun Shin^{1,2}, Myung Hun Jang^{1,2*}, Yong Beom Shin^{1,2†}

Department of Rehabilitation Medicine, Biomedical Research Institute, Pusan National University Hospital, Busan, Korea¹, Department of Rehabilitation Medicine, Pusan National University School of Medicine, Busan, Korea², Department of Nursing, Regional Trauma Center, Busan, Korea³, Department of Neurosurgery, Pusan National University Hospital, Pusan National University School of Medicine, Busan, Korea⁴

Introduction

Brainstem cavernous malformations (BCMs) exhibit higher morbidity and mortality compared to other cerebral cavernous malformations. Issues such as tetraplegia and respiratory distress are contributing factors to weaning and extubation failure. This case report presents a patient who successfully underwent extubation following strategic rehabilitation treatment in the ICU after surgery.

Case presentation

A 38-year-old female patient presented with gait disturbances that began approximately one week prior and was admitted to the ICU due to cardiac arrest. An MRI revealed a hemorrhage in the spinal cord, leading to the diagnosis of a BCM, for which she underwent craniotomy and hematoma evacuation.

Preoperatively, the physical examination indicated locked-in syndrome due to the mass lesion, and the negative inspiratory force (NIF) was significantly reduced at -10 cmH₂O while intubated. Post-surgery, it was crucial to enhance the recovery of respiratory muscles and improve the ability to clear secretions to prevent pulmonary complications and achieve successful extubation. To accomplish this goal, mobilization and chest physiotherapy were implemented in the ICU.

Alongside these interventions, periodic neurological assessments were conducted, measuring NIF as indicators of weaning and peak expiratory flow (PEF) as indicators of secretion clearance. Ultrasound (US) evaluations were also performed. The physical examination revealed that the recovery of strength in the left upper and lower extremities was slower compared to the right side. One-week post-surgery, chest X-ray showed elevation of the left hemi-diaphragm, and diaphragm US indicated a lack of contraction on the left side (Fig 1).

To facilitate respiratory muscle recovery, inspiratory muscle training was conducted, along with positioning and lung recruitment maneuvers to resolve atelectasis, as well as mechanical insufflation-exsufflation. Extubation was performed when the desired PEF value was achieved (Fig 2). Preventing the deterioration of atelectasis in the left lung was essential, and post-extubation management included the application of non-invasive ventilation via a full-face mask.

Subsequently, the patient's dysphagia improved, allowing for the initiation of oral feeding. After three additional weeks of rehabilitation without any respiratory complications, she was discharged.

Conclusion

ICU rehabilitation can greatly assist in the patient's rapid recovery and prevention of complications. As demonstrated in this case, implementing a goal-oriented rehabilitation strategy through continuous respiratory function assessment allows for high-quality rehabilitation, ultimately ensuring better patient outcomes.

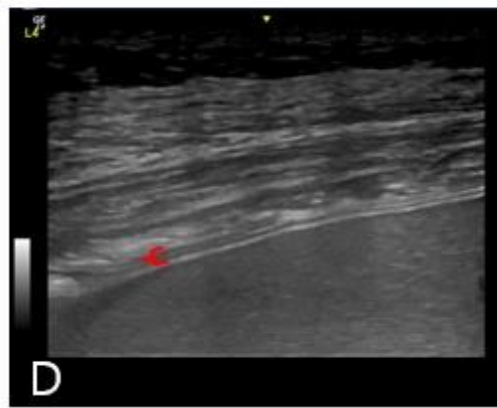
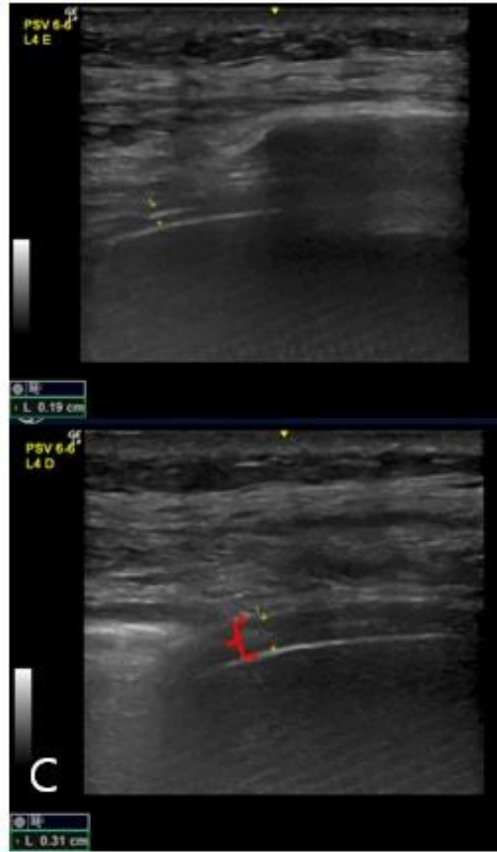


Figure 1. (A) CXR, on POD1. (B) Elevation of the left diaphragm on POD 7. (C) Changes in the left diaphragm thickness during DB by US on POD 1. (D) Absence of contraction of the left diaphragm during DB on POD 7. *CXR, Chest x-ray, POD, postoperative day, DB, deep breathing, US, ultrasound

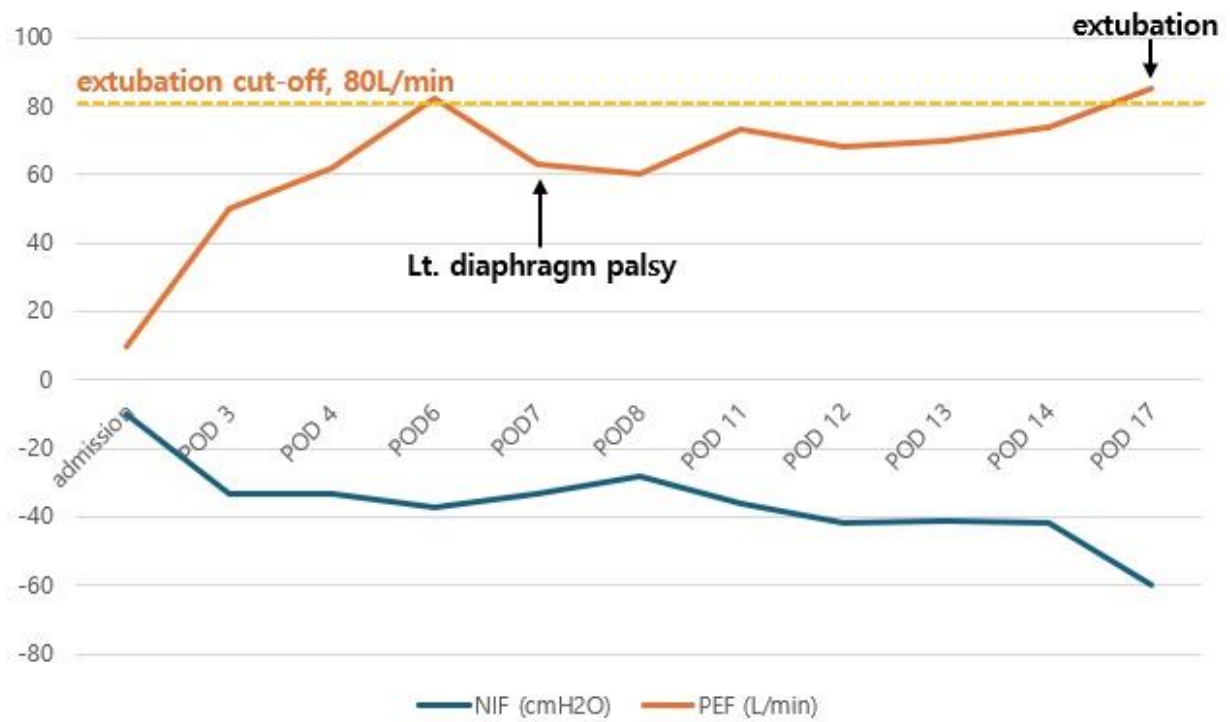


Figure 2. Serial pulmonary function assessments measured up to extubation.

Post-Radiation Cervical Spine Inflammation Mimicking Metastasis in Hypopharyngeal Carcinoma

Sun Im ^{1**}, Jisoo Park¹, Seung Yup Song¹, Dongwook Song¹, Geun-Young Park¹, Hae-Yeon Park¹

Department of Rehabilitation Medicine , Bucheon St Mary's Hospital, College of Medicine, The Catholic University of Korea, Seoul, Republic of Korea¹

Introduction

Radiation therapy (RT) is a common treatment modality for head and neck cancers. However, it can lead to complications that mimic disease recurrence, posing diagnostic challenges. This case report details a patient with hypopharyngeal carcinoma who developed severe neck pain post-surgery and chemoradiotherapy (CCRT), with imaging findings suggestive of metastasis but ultimately diagnosed as post-RT inflammation of the cervical spine.

Case Presentation

55-year-old male patient with a diagnosis of hypopharyngeal carcinoma (pT2N0M0, RM(+)) underwent surgical resection followed by adjuvant CCRT. The radiation regimen included 6572 cGy to the tumor bed, 6045 cGy to the whole hypopharynx, and 5580 cGy to the bilateral neck (levels II-IV) over 31 fractions using VMAT IMRT, completed over 45 days. Six and a half months post-CCRT, the patient presented with severe neck pain. The pain showed a progressive nature and showed little response to NSAID, analgesics or morphine prescription. Tenderness of the posterior neck with limitation of range of motion observed in the cervical spine observed. The patient complained of pain exacerbation at night time. Imaging studies, including PET, bone scan (Fig 1.), and MRI, showed abnormal signal changes in the cervical spine (Fig 2.), raising suspicion of metastatic disease.

MRI revealed abnormal bone marrow signal intensity changes at the C3, C4, and C5 vertebral bodies, anterior epidural soft tissue changes, mild to moderate prevertebral soft tissue swelling, and several degenerative changes, including mild retrolisthesis and stenosis. The differential diagnosis included bone metastasis, tumor extension, infection, and RT-induced inflammation

Despite initial suspicions of metastasis, follow-up confirmed the final diagnosis as post-RT inflammation of the cervical spine. The patient was managed with supportive care including steroid pulse therapy and antibiotics with improvement of pain.

Conclusion

RT is a critical component of head and neck cancer treatment but is associated with various complications, the most common being mucositis, xerostomia, lymphedema, and trismus. Recognizing and managing these complications, particularly distinguishing between inflammatory changes and disease recurrence, is essential for optimal patient care.

This case underscores the importance of considering RT-induced changes of the cervical spine in the differential diagnosis when evaluating post-treatment complications in head and neck cancer patients. Accurate differentiation between metastatic disease and post-RT inflammatory changes is crucial to avoid unnecessary interventions and guide appropriate management.

Acknowledgment not applicable



Fig 1. PET scan reveals increased trace uptake in the cervical spine.



Fig 2. MRI scan reveals Anterior epidural soft tissue change and enhancement at C3-4.

Neurolymphomatosis of the Brachial Plexus Mimicking Peripheral Neuropathy of Bilateral Upper Limb: A Case Report

Eunseok Choi^{1*}, Yeon Soo Lee^{1†}

Department of Rehabilitation Medicine, The Catholic University of Korea Daejeon St. Mary's Hospital ¹

Background

Neurolymphomatosis (NL) is defined as peripheral or cranial nerve, nerve roots or plexus infiltration by malignant lymphocytes, most strongly associated with non-Hodgkin's lymphoma. NL should be considered in any patient with the malignant disease presenting with unexplained symptoms of peripheral neuropathy. And differential diagnosis from paraneoplastic, metabolic, nutritional and chemotherapy-related neuropathy or leptomeningeal metastasis is important because of its possibility of response to a specific chemotherapy. EMG can define the presence of peripheral neuropathy but MRI is the investigation of choice, and on STIR/T2WI, infiltrated nerves appear hyperintense of the lymphoma and peritumoral edema. We report a case of NL with bilateral brachial plexus involvement. Early MRI study diagnosed NL and clinical improvement occurred by MRI and FDG-PET CT follow-up after proper chemotherapy.

Material & Methods

These case illustrates the clinical manifestations of NL of bilateral brachial plexus, in which electrodiagnosis abnormality of upper extremities were proven.

Results

A 78 years-old female visited the outpatient clinic because of tingling and numbness of both upper extremities for 2 months. She had been diagnosed as diffuse large B-cell lymphoma (BLDL) stage 3 and received CHOP (cyclophosphamide-doxorubicin-vincristine-prednisolone) chemotherapy. Neurological examination revealed mild weakness (Good grade) of grasping in left hand and positive Tinel sign at both carpal tunnel areas. Otherwise, no motor/sensory deficits were found. EMG study showed distal symmetric sensorimotor polyneuropathy of both upper extremities. MR neurography revealed hyperintensity on T2 and STIR sequences, focal and diffuse bilateral brachial plexus enlargement with fascicular disorganization. Gadolinium enhancement showed high grade FDG activity along the bilateral brachial plexus on FDG-PET CT. Dramatic Improvement was found by MRI and FDG-PET CT follow up after CHOP treatment.

Conclusions

NL should be considered as one of rare causes of unexplained peripheral neuropathy and early investigation with dedicated MRI and PET-CT imaging can lead to proper management of the disease.



Neurolymphomatosis of brachial plexus before anti-cancer treatment



Neurolymphomatosis of brachial plexus 10 days after anti-cancer treatment

A case of infected polycystic liver disease presenting with dyspnea

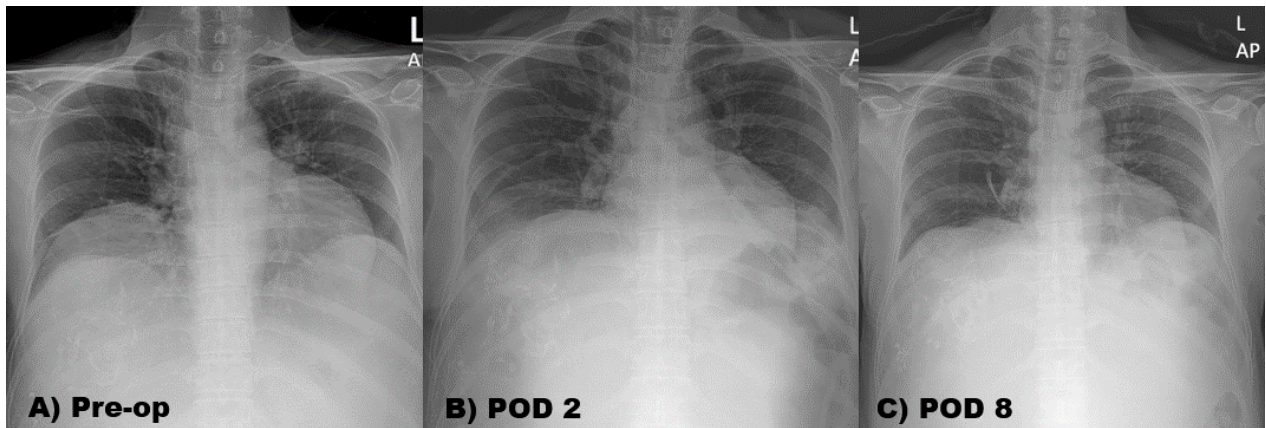
Da-Sol Kim ^{1,3**†}, Mi-Rin Lee^{2,3}, Gi-Wook Kim^{1,3}, Yu Hui Won^{1,3}, Sung-Hee Park ^{1,3}, Myoung-Hwan Ko^{1,3}, Jeong-Hwan Seo^{1,3}

Department of Physical Medicine and Rehabilitation , Jeonbuk National University Hospital ¹, Department of Surgery Division of HBP-Transplantation-Vascular, Jeonbuk National University Hospital², Research Institute of Clinical Medicine - Biomedical Research Institute, Jeonbuk National University Hospital³

Polycystic liver disease (PLD) is a genetic condition characterized by the presence of more than 20 liver cysts. It is categorized into three types: the AD genotype with isolated PLD, the AD genotype with polycystic kidney disease (PKD), and the AR genotype with PKD. Although most individuals are asymptomatic, 2-5% may experience a variety of symptoms with varying severity. Abdominal symptoms can include abdominal pain, abdominal distension, early satiety, and esophagogastric reflux. In rare cases, respiratory symptoms such as dyspnea can occur. Treatment options for PLD include: drug therapy (Somatostatin analogue), aspiration with sclerotherapy, and surgical treatment (Laparoscopic fenestration, hepatic resection, and liver transplantation). This case report focuses on a 63-year-old female patient whose primary symptom was shortness of breath. Following surgical treatment and respiratory rehabilitation, her respiratory symptoms resolved, and her lung capacity significantly increased.



APCT of pre-operation at portal phase. The CT shows polycystic liver and kidney diseases.



CXR f/u. After the operation and rehabilitation, the lung was expended.

	Pre-operation	POD 3	POD 13	POD 22
FVC at supine	Not testable due to severe dyspnea	700ml	1850ml	1900ml
FVC at sitting		1010ml	2280ml	2100ml
MIP		31(42.6%)	76(104.5%)	70(96.2%)
MEP		39(41.9%)	81(87.0%)	106(113.85)
Hand grip(R:L)		14:16kg	20:23kg	20:23kg
PCF		130L/min	250L/min	410L/min
6mWT		147m	297m	405m

Pulmonary function tests, hand grips, and 6mWT f/u

Advantages of Wearable Robotics for Balance Training in COPD Rehabilitation: A Case Report

Han Eol Cho^{1,2**}, Won Ah Choi^{1,2}, Ji Hyun Kwon^{1,2}

Department of Rehabilitation Medicine, Gangnam Severance Hospital¹, Research Institute of Rehabilitation Medicine, Yonsei University College of Medicine²

Objective

Chronic Obstructive Pulmonary Disease (COPD) often leads to muscle weakness and impaired balance, increasing fall risk. This study aims to investigate the impact of wearable robot-assisted exercise on balance improvement in a COPD patient.

Case Report

A 75-year-old male with COPD, bronchiectasis, chronic kidney disease, and bilateral carpal tunnel syndrome was assessed. He showed significant muscle weakness, balance impairment, and difficulty with walking and hand use. Evaluations included Manual Muscle Testing (MMT), Short Physical Performance Battery (SPPB), a stair climbing test, and the 6-Minute Walk Test (6MWT). The intervention combined standard COPD rehabilitation with wearable robot-assisted training using the Angel Legs M. This exoskeleton uses sensors under the feet to aid joint torque, controlled by a backpack computer. Exercises included weight shifting, squats, and box step-ups, followed by over-ground robot-assisted exercise training, twice a week for one month. After one month, the patient showed significant improvements in muscle strength and balance. The SPPB score and 6MWT distance did not change, but the Berg Balance Scale (BBS) score improved. The patient could control his descent into a chair better, reducing fall risk. Stair climbing time decreased, and he could climb stairs without resting and with improved posture. Reports indicated better daily activities and high satisfaction.

Conclusion

Wearable robotics can enhance balance and functional capacity in COPD patients. This case suggests integrating robot-assisted exercises into rehabilitation programs can significantly improve muscle strength, balance, and daily functions. Further research with larger samples is needed to confirm these findings and explore long-term benefits.

Case Report: Pulmonary Rehabilitation Strategies and Outcomes Following Lung Transplantation

Jecheon Seong^{1*}, Yunjee Lee¹, Yun Jung Lee^{1†}

MyongJi Hospital, Department of Rehabilitation Medicine¹

Introduction

Lung transplantation is often the final option for patients with end-stage pulmonary diseases, such as Interstitial Pneumonia with Autoimmune Disease (IPD), who have severely reduced exercise capacity and quality of life (QOL). To maximize recovery and benefits, pulmonary rehabilitation is essential. This case report introduces our hospital's pulmonary rehabilitation program for lung transplantation patients.

Case Presentation

A 66-year-old delivery driver with idiopathic pulmonary fibrosis, diagnosed a year ago, presented with exertional dyspnea. After a COVID-19 infection in November 2023, he experienced severe respiratory distress. On home oxygen therapy at 4 liters per minute, he was dependent in daily activities due to dyspnea. He underwent lung transplantation on January 5, 2024, with VA ECMO insertion.

Two weeks before surgery, on December 22, 2023, the patient was admitted for pre-surgical evaluation and prehabilitation. Assessments included a 6-minute walk test (6MWT) and manual muscle testing (MMT) to evaluate functional capacity, and a thorough physical exam to identify musculoskeletal issues. Motor power was normal; however, he could only walk 10 meters during the 6MWT despite 4 liters of oxygen due to dyspnea. Prehabilitation involved managing respiratory secretions, breathing techniques, and core muscle strengthening.

Post-surgery, extubation occurred on January 9, 2024. Immediate bedside rehabilitation included secretion management, breathing techniques, and sit-to-stand training. Intensive rehabilitation started after weaning off the high-flow nasal cannula, including aerobic and resistance exercises. Thorough physical examinations were conducted due to the risk of nerve injury and thromboembolic events.

On January 23, 2024, the Berg Balance Scale score was 48, indicating a low fall risk. A 6MWT showed a walking distance of 272 meters with no SpO₂ decrease without supplemental oxygen. Maximal expiratory pressure and inspiratory pressure were 64 and 89 cmH₂O, respectively. The patient was discharged with an independent gait and no need for supplemental oxygen, and was referred to our outpatient clinic for follow-up.

Conclusion

Pulmonary rehabilitation is crucial for lung transplantation recovery, addressing declines in exercise capacity and quality of life. This case report demonstrates our hospital's pulmonary rehabilitation program's effectiveness. Prehabilitation prepared the patient for surgery, and post-surgery rehabilitation focused on respiratory management and exercise, significantly improving recovery. The patient showed notable gains in functional outcomes, highlighting the importance of comprehensive rehabilitation in optimizing recovery.

	Pre-test	Post-test
Total exercise time	1 minutes	
Borg scale	4	7
SpO2 (%)	93 (%)	83 (%)
Heart rate	101	123
Whether the test was discontinued	Yes	
Post-test symptoms	Dyspnea	
Total walking distance	10m	

Fig 1. 6-minute walk test (23.12.26)

	Pre-test	Post-test
Total exercise time	6 minutes	
Borg scale	0	3
SpO2 (%)	96 (%)	98 (%)
Heart rate	96	101
Whether the test was discontinued	No	
Post-test symptoms	None	
Total walking distance	272m	

Fig 2. 6-minute walk test (24.01.23)

	Measurement	Reference range	Predicted value (%)	Predicted value
MEP (cmH2O)	64	>63	120	54
MIP (cmH2O)	89	>52	93	95

Fig 3. MIP and MEP evaluation (24.01.23)

Case Report: Cardiac Rehabilitation in a 75-Year-Old Patient with CABG Surgery

Jecheon Seong^{1*}, Yunjee Lee¹, Yong Kyun Kim^{1†}

MyongJi Hospital, Department of Rehabilitation Medicine¹

Introduction

Cardiac rehabilitation is crucial for patients post-coronary artery bypass graft (CABG) surgery. This structured program improves cardiovascular health, functional capacity, and quality of life. Among its components, the warm-up exercise phase is significant. It prepares patients for intensive activities, providing physiological and psychological benefits. This report highlights the importance of warm-up exercises in cardiac rehabilitation and discusses considerations for implementing rehabilitation programs in CABG patients.

Case Presentation

A 75-year-old male presented with exertional dyspnea and was using nitroglycerin therapy. He underwent PCI on February 2, revealing near-total stenosis in the left main artery and diffuse stenosis in the middle right coronary artery. Subsequently, he was referred for CABG.

Preoperative pulmonary rehabilitation began on February 5, including pursed lip breathing, diaphragm breathing, and incentive spirometer use. Off-pump coronary artery bypass surgery was performed on February 13. Postoperatively, on February 15, ICU rehabilitation included passive range of motion exercises, diaphragm exercises, rib cage expansion exercises, and lung segmental breathing exercises. Arm exercises were avoided due to the sternotomy. The patient was transferred to the general ward on February 22 and started low-intensity rehabilitation with an ergometer due to deconditioning from pneumonia and a catheter-induced infection. Continuous EKG monitoring was implemented to watch for arrhythmias and autonomic dysfunction. On March 18, the patient initiated standing and high walker-assisted indoor gait training. The session featured a 5-minute warm-up comprising stretching and tension-free ergometer use, followed by two 10-minute intervals of walking training separated by a 5-minute rest period. The session concluded with cool-down exercises using the AirDyne machine. After a 5-minute rest, the session ends with a stability check. During the session, the patient achieved a distance of up to 200 meters with the assistance of the high walker.

On March 21, due to low compliance, warm-up exercises were omitted. During gait training, the patient experienced syncope after 5 meters of walking. EKG monitoring showed sinus rhythm with a heart rate drop to 40 bpm. The patient was stabilized with rest and inotropic support. He was then discharged with the capability for indoor walking.

Conclusion

At our institution, we implement breathing exercises and continuous EKG monitoring for CABG patients, with structured warm-up and cool-down phases. This case highlights the importance of warm-up exercises, as their omission led to a significant adverse event. Tailoring rehabilitation programs and ensuring compliance through education on warm-up exercises, along with continuous EKG monitoring, are essential to prevent incidents and improve recovery and quality of life.

Activity	Time	Workload	METS	HR	RPE	Systolic	Diastolic	SPO2	AvgHR	MinHR	MaxHR	%THR
* Rest	05:00											
* Warmup	05:00											
* Treadmill	15:00											
* Rest	10:00											
* Treadmill	15:00											
* AirDyne	05:00											
* Recovery	05:00											

Fig 1. Cardiac rehabilitation protocol

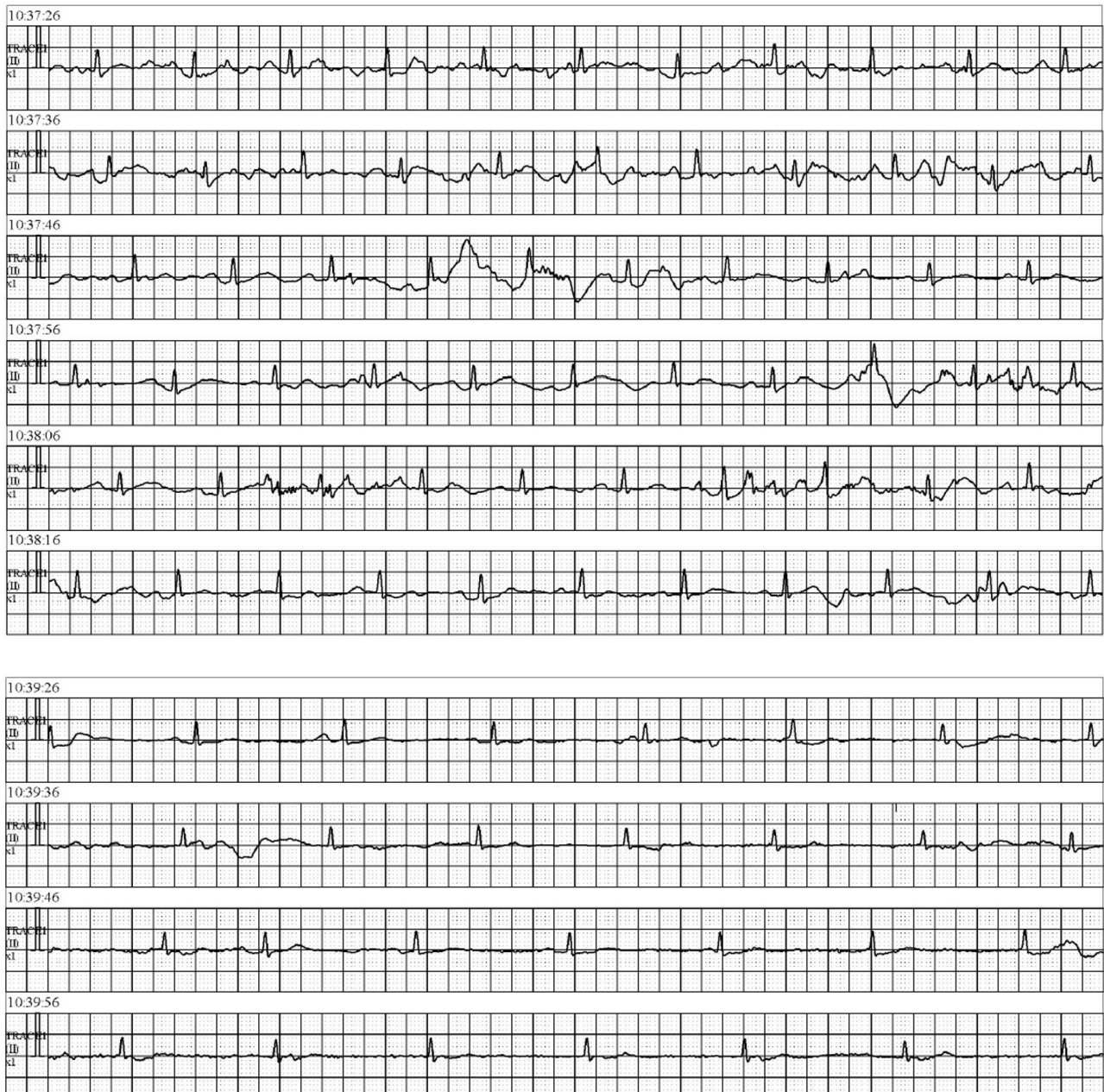


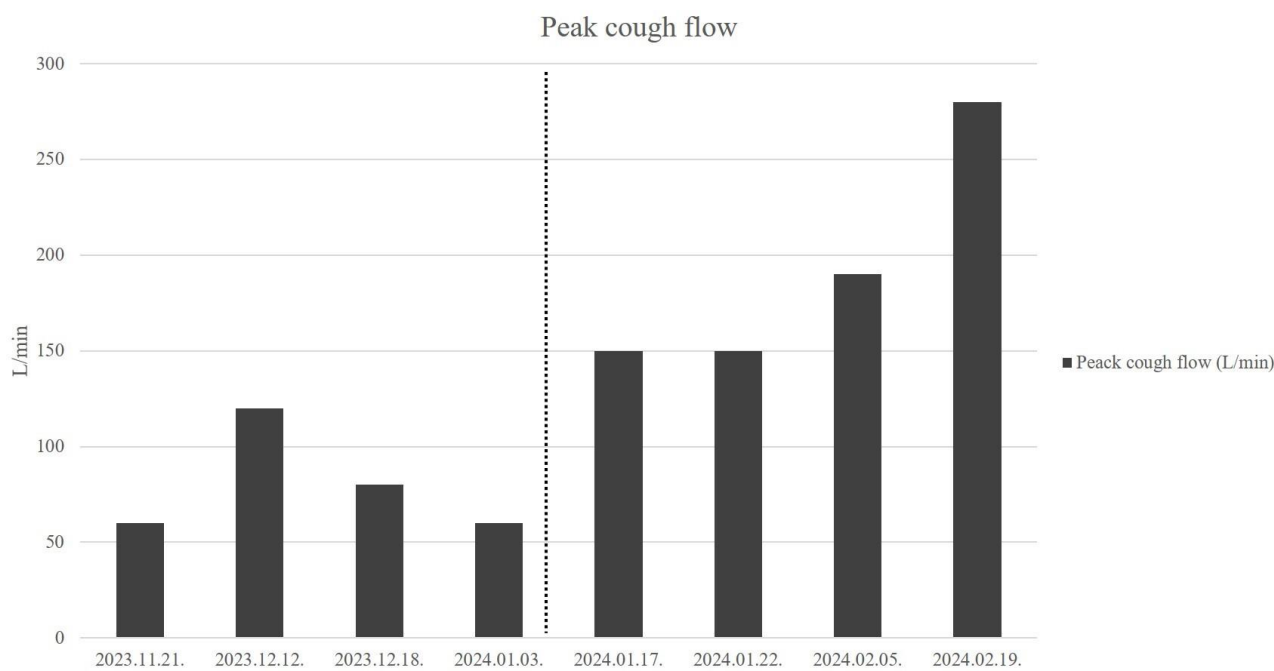
Fig 2. EKG at the time of syncope

The effect of aerobic exercise on spinal cord injured patient with tracheostomy: A case report

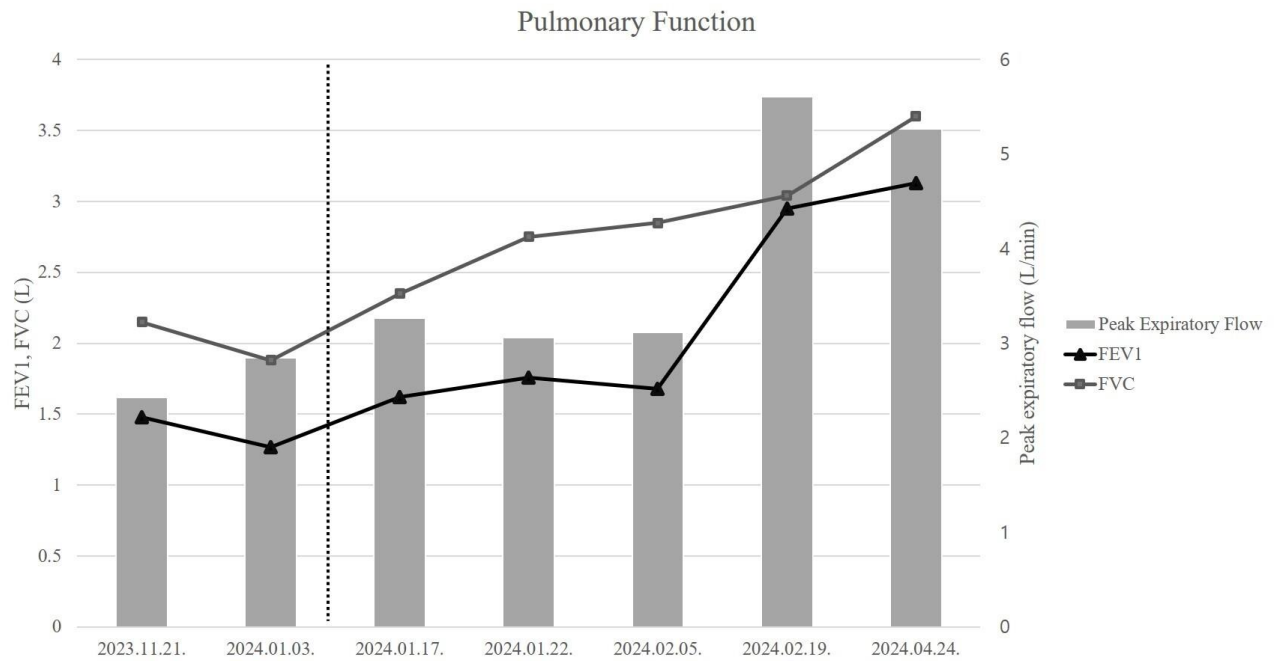
Sang-Pil Son^{1*}, Hyo-Sik Park^{1†}

Eulji Hospital, Eulji University, Department of Rehabilitation Medicine¹

Aerobic exercise is widely recognized for its benefits in improving pulmonary function across various clinical populations. Individuals with spinal cord injury (SCI) often experience respiratory complications, such as reduced lung function, necessitating interventions like tracheostomy. We report a case of a 19-year-old SCI patient who underwent tracheostomy following a traffic accident. Despite conventional rehabilitation, the patient's cough flow remained inadequate for decannulation. Subsequent implementation of moderate to high-intensity aerobic exercise resulted in significant improvements in peak cough flow, leading to successful decannulation. This case highlights the potential of aerobic exercise as an adjunctive therapy for respiratory rehabilitation in SCI patients with tracheostomy. Further research is warranted to explore the efficacy of aerobic exercise in improving respiratory parameters and enhancing the quality of life in this population.



Changes in the Peak cough flow in the patient. Left of the dashed line represents the values before aerobic exercise, while the right side represents the values after aerobic exercise.



Changes in the forced vital capacity (FVC), forced expiratory volume in one second (FEV1), and peak expiratory flow (PEF) in the patient. Left of the dashed line represents the values before aerobic exercise, while the right side represents the values after aerobic exercise.

Altered mental status related to Cefepime-Induced Encephalopathy: Case Series

Jisoo Park^{1*}, Dongwook Song¹, Seung Yup Song¹, Geun-Young Park¹, Hae-Yeon Park¹, Sun Im^{1†}

Department of Rehabilitation Medicine, The Catholic University of Korea Bucheon St. Mary's Hospital ¹

Background

Cefepime, a fourth-generation cephalosporin, can cross the blood-brain barrier, leading to neurotoxicity. Symptoms typically appear within 2 to 6 days of starting cefepime and resolve with discontinuation. However, the symptoms may be subtle and not easily detected. This case series highlights the neurological complications associated with cefepime in elderly patients with severe underlying conditions.

Case Presentation

Case 1:

An 83-year-old female with chronic kidney disease, diabetes, hypertension, and dementia contracted COVID-19. Treated with remdesivir for 10 days, she sequentially received ceftriaxone, minocycline, piperacillin/tazobactam, levofloxacin, and cefepime for 7 days, adjusted for renal function. Shortly after starting cefepime, the patient developed severe disorientation and confusion. Cefepime was continued until her transfer to our hospital. A change to meropenem improved her neurological status but induced neutropenia and anemia, necessitating a return to cefepime. The patient's delirium and altered mental status worsened after reinitiating cefepime. An extensive workup, including electroencephalography (EEG), revealed triphasic waves indicative of metabolic encephalopathy likely related to cefepime. Cefepime was discontinued and replaced with levofloxacin 750 mg every other day. A follow-up EEG showed improvement in brain wave abnormalities, and her cognitive status subsequently improved.

Case 2:

An 87-year-old female with hypertension and chronic kidney disease was being treated for subcortical infarction at a rehabilitation hospital. Despite several weeks of piperacillin/tazobactam, her fever persisted, leading to her admission to our hospital's infectious disease department, where she was prescribed with cefepime. Shortly thereafter, she exhibited decreased limb movement and rapid consciousness decline. A brain MRI showed no new lesions that could be attributable to the acute deterioration, but an EEG indicated moderate to severe diffuse cerebral dysfunction with triphasic waves, suggestive of metabolic encephalopathy. Cefepime was replaced with levofloxacin 750mg every other day. A follow-up EEG six days later showed significant improvement, and her cognitive function subsequently improved.

Conclusion

Cefepime is often prescribed for severe infections in the geriatric population. Cefepime-induced encephalopathy (CIE), though rare, is a reversible condition but challenging to diagnose as it can mimic other neurological disorders. Early recognition and discontinuation of cefepime are crucial for recovery. These cases highlight the importance of considering CIE in patients with sudden cognitive decline, especially those with chronic kidney disease and concurrent cerebral infarctions. Clinicians should be vigilant in distinguishing between neurological changes due to underlying conditions and those induced by antibiotics like cefepime, ensuring accurate diagnosis and appropriate management.

A Case of Severe Dysphagia due to Deep Neck Infection: Effect of dysphagia rehabilitaiton

Da-Sol Kim^{1,2**}, Gi-Wook Kim^{1,2}, Yu Hui Won^{1,2}, Sung-Hee Park^{1,2}, Myoung-Hwan Ko^{1,2}, Jeong-Hwan Seo^{1,2}

Department of Physical Medicine and Rehabilitation, Jeonbuk National University Hospital ¹, Research Institute of Clinical Medicine - Biomedical Research Institute, Jeonbuk National University Hospital ²

This case study involves a 78-year-old male patient who developed dysphagia following a deep neck infection that required extensive surgical intervention including abscess tonsillectomy and cervical drainage. Imaging revealed the infection affecting multiple neck spaces. Despite treatment, the patient experienced severe dysphagia, along with tongue muscle weakness, and restricted jaw and laryngeal movement. Videofluoroscopic examination (VF) conducted on postoperative day 16 showed significant impairments in laryngeal elevation and upper esophageal sphincter opening. The patient underwent a regimen of neck stretching exercises targeting suprahyoid and infrahyoid muscles, along with passive exercises for the hyoid and larynx. These interventions aimed to alleviate dysphagia by addressing potential neck contracture scars resulting from the infection and surgeries. By postoperative day 52, significant improvements were noted in laryngeal elevation and upper esophageal sphincter opening during VF. Specifically, there was notable progress in the movement of the hyoid bone. In conclusion, this case study highlights the efficacy of neck stretching and passive exercise of the hyoid and larynx in improving dysphagia secondary to deep neck infections. The observed enhancements in laryngeal function and hyoid movement suggest that these rehabilitative interventions can effectively mitigate the effects of neck contracture and scar formation caused by inflammation and surgical procedures. This underscores the importance of tailored rehabilitation strategies in managing dysphagia in such complex cases.

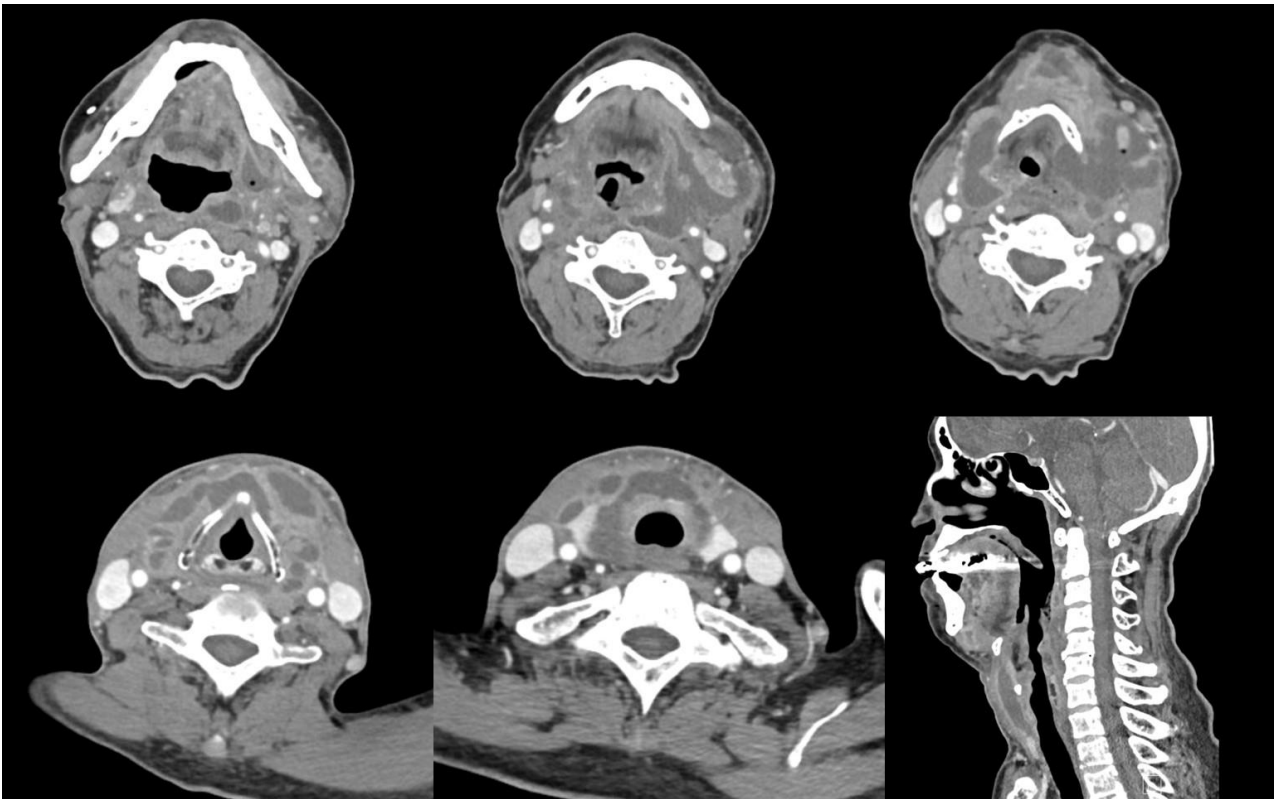


figure 1. neck CT before operation

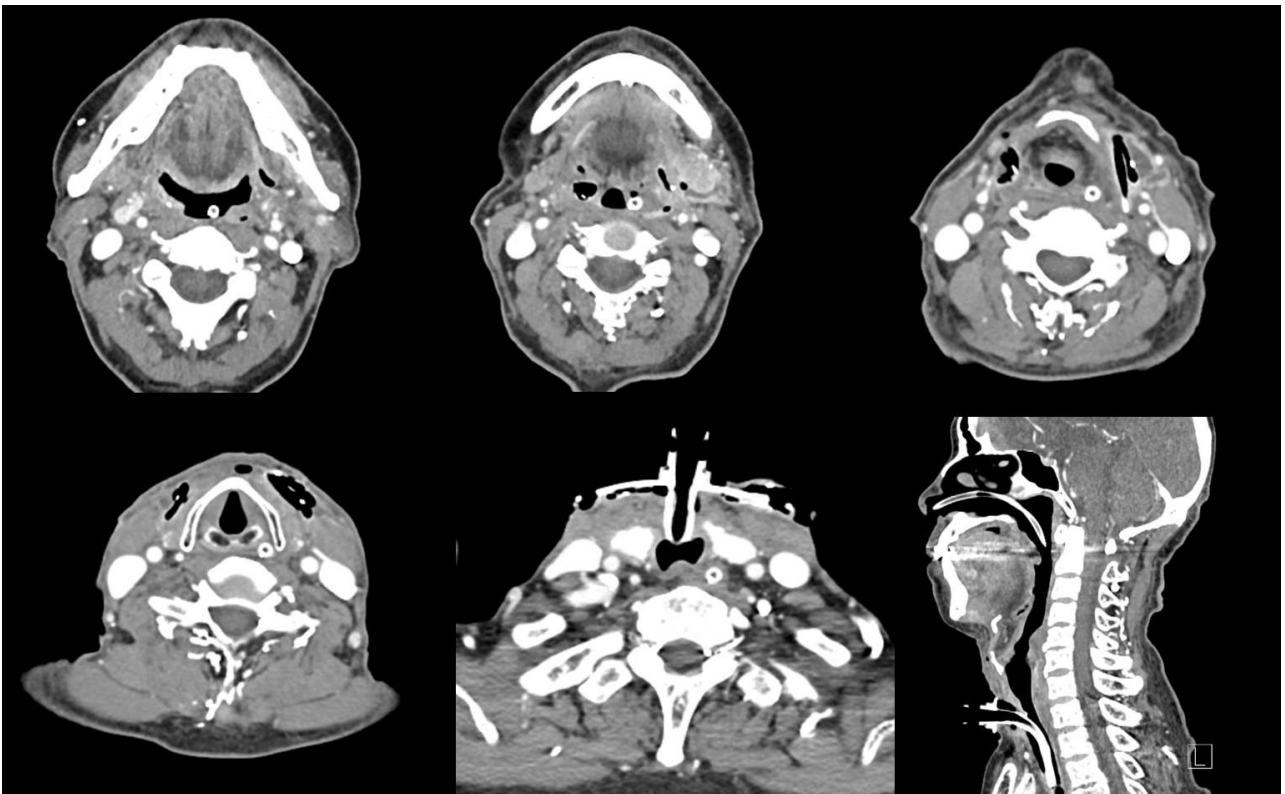


figure 2. f/u neck CT at POD 15

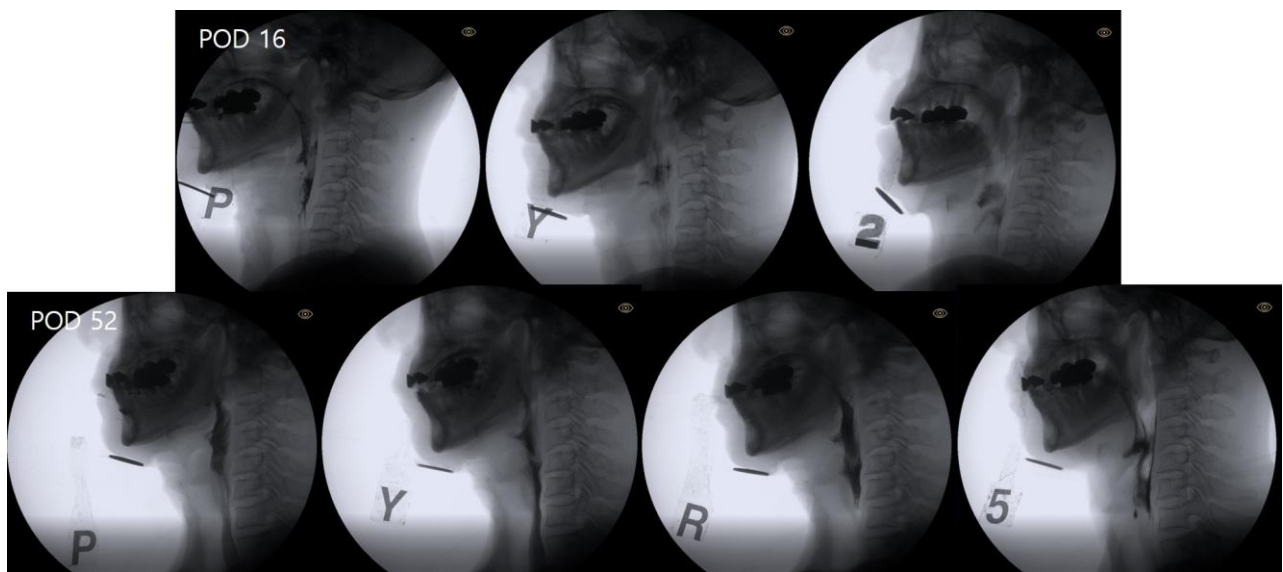


figure 3. VFSS f/u at POD 16 and 52

Pelvic Hematoma and Bilateral Lumbosacral Plexopathy Combined with Unilateral Femoral Neuropathy.

Ji Seon Hong^{1*†}

Department of Rehabilitation Medicine, Yonsei University Wonju College of Medicine¹

Introduction

Pelvic hematoma is a rare cause of femoral neuropathy or lumbosacral plexopathy. Most published cases focus solely on isolated femoral neuropathy or lumbosacral plexopathy and lack detailed neurological and electromyographic findings and long-term outcomes. This case report discusses bilateral lumbosacral plexopathy combined with unilateral femoral neuropathy in a patient who underwent a cesarean section along with anticoagulation therapy in extracorporeal membrane oxygenation (ECMO).

Case Report

A 35-year-old woman at 26 weeks of gestation with no significant past medical history presented to the emergency room on January 6, 2022, with dyspnea and was diagnosed with severe acute respiratory distress syndrome (ARDS) associated COVID-19. After intrauterine fetal death was confirmed via abdominal ultrasound, a cesarean hysterotomy was performed. Despite high-flow O₂ therapy, the patient did not show improvement and was placed on ECMO. During the ECMO weaning process, an abdomen-pelvis contrast-enhanced computed tomography (CT) study revealed a 17x10 cm right pelvic cavity hematoma and a left iliopsoas hematoma (Figure 1) and percutaneous catheter drainage was performed. At that time, Muscle assessment using the standard Medical Research Council (MRC) scale revealed weakness in both lower extremities, graded between 0 to 2. Following the improvement of ARDS, the patient was transferred to the Department of Rehabilitation Medicine.

At the time of transfer, the patient's muscle strength was graded as 2 to 3 in the right lower extremity and 0 to 3- in the left side. An electrophysiologic study performed on March 24, 2022, confirmed bilateral lumbosacral plexopathy (Table 1). The patient underwent rehabilitation including neuromuscular electrical stimulation, gait training, resistance training, and range of motion exercises. Serial electrophysiological studies performed at 6, and 13 months from onset demonstrated improved right lumbosacral plexopathy nearly up to the normal range, although some residual lesions remained on the left side. At thirty months after onset, electrophysiological studies demonstrated recovery to near-normal levels, except for persistent left femoral neuropathy (Table 2). The patient exhibited weakness in the left knee extensor (MRC grade 4-) and sensory abnormalities in the saphenous nerve area but was able to ambulate on flat ground without assistive devices.

Discussion

This case presents a rare instance of bilateral lumbosacral plexopathy and unilateral femoral neuropathy in a patient with a high risk of bleeding. It suggests that aggressive hematoma evacuation and comprehensive rehabilitation therapy can significantly enhance recovery outcomes. Furthermore, it is necessary to recognize that patients with a high risk of bleeding, such as those undergoing ECMO and requiring sedation, are susceptible to neuropathy and thorough monitoring of these patients to promptly identify and address any neurological complications.

Acknowledgment None

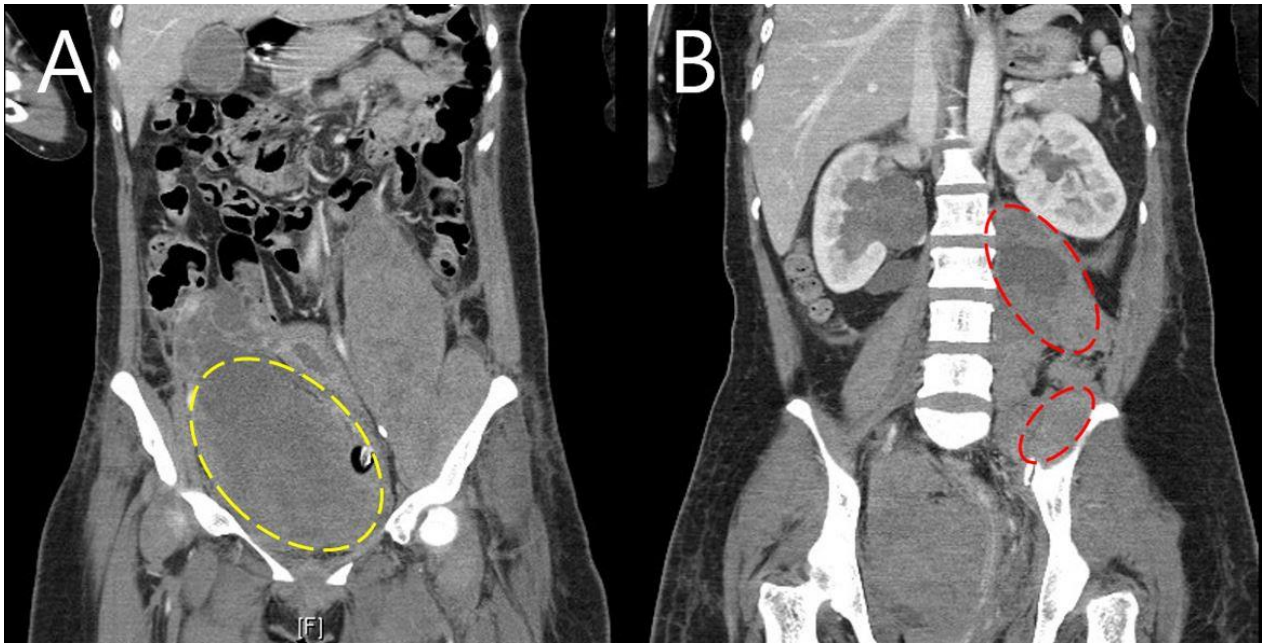


Figure 1. Contrast-enhanced abdomen-pelvis CT reveals a huge pelvic hematoma(yellow circle) and left iliopsoas muscle hematoma(red circle).

Nerve	Stimulation	Right			Left		
		Latency (ms)	Amplitude (mV/uV)	CV (m/s)	Latency (ms)	Amplitude (mV)	CV (m/s)
Motor							
Peroneal at EDB	Ankle	2.60	1.77		5.32	0.94	
	Fibular head	9.17	1.93	44.1	11.7	0.71	45.4
Peroneal at TA	Popliteal fossa	2.15	3.8		3.42	1.39	
Tibial at AH	Ankle	3.13	13.5		3.04	16.2	
	Popliteal fossa	10.2	9.9	41.0	9.79	13.1	43.0
Femoral at VM	Inguinal ligament	4.03	5.8		No response		
Sensory							
Superficial peroneal	Lateral leg	No response			No response		
Sural	Calf	2.00	4.9		No response		
Saphenous	Medial knee	Not assessed			Not assessed		

Table 1. Summary of nerve conduction study at 2 months from onset. Amplitudes are measured in millivolts (mV) for motor responses and microvolts (μ V) for sensory responses. CV, conduction velocity; EDB, extensor digitorum brevis; TA, tibialis anterior; AH, abductor hallucis; VM, vastus medialis; AM, adductor magnus.

Nerve	Stimulation	Right			Left		
		Latency (ms)	Amplitude (mV/uV)	CV (m/s)	Latency (ms)	Amplitude (mV)	CV (m/s)
Motor							
Peroneal at EDB	Ankle	1.58	5.4	-	2.83	7.3	-
	Fibular head	8.09	4.4	46.1	8.59	6.6	51.5
Peroneal at TA	Popliteal fossa	1.92	6.6	-	1.81	19.8	-
Tibial at AH	Ankle	2.79	17.8	-	2.98	25.9	-
	Popliteal fossa	8.98	14.1	41.0	10.0	18.7	51.3
Femoral at VM	Inguinal ligament	3.43	35.5	-	5.97	1.69	-
Sensory							
Superficial peroneal	Lateral leg	1.44	9.3		1.79	23.0	
Sural	Calf	1.69	5.2		1.60	19.7	
Saphenous	Medial knee	1.33	5.5		No response		

Table 2. Summary of nerve conduction study at 6 months (right side) and 30 months(all studies on left side, saphenous nerve study on right side) from onset.

Case Report: Rhabdomyolysis associated neuropathy

Jecheon Seong^{1*}, Yunjee Lee¹, Aram Kim^{1†}

MyongJi Hospital, Department of Rehabilitation Medicine¹

Introduction

Rhabdomyolysis, marked by rapid muscle breakdown and release of muscle cell contents into the bloodstream, can cause severe complications like acute kidney injury. It is often triggered by trauma, strenuous exercise, drugs, or toxins. Peripheral neuropathy is a known complication of rhabdomyolysis, usually linked to compartment syndrome or prolonged immobilization. However, it can also result from other mechanisms, such as toxins. This report aims to enhance the understanding of rhabdomyolysis-associated neuropathy and highlight the need to consider toxin-mediated mechanisms as pathophysiology.

Case Presentation

A 49-year-old male visited our emergency department on July 30, 2023, after being found vomiting at home following heavy drinking. Initial examination revealed no extremity swelling, but lab results indicated rhabdomyolysis with a creatine kinase level of 27,039. He was admitted to the nephrology department. During his stay, right foot drop was noted, with motor strength grade 2 in the right dorsiflexor (DF) and decreased sensation below the ankles. A nerve conduction study (NCS) was performed on August 26, 2023. Sensory NCS showed low amplitude in the right sural nerve and no response in both superficial peroneal nerves (SPN). Motor NCS revealed low amplitude and slow conduction velocity in the left common peroneal nerve (CPN) at the extensor digitorum brevis (EDB) and no response in the right CPN. The right tibial nerve showed delayed latency, low amplitude, and slow conduction velocity. He received electrical stimulation therapy at the right CPN and gait training. After discharge, he was referred to our outpatient clinic. On January 24, 2024, motor strength had improved (Grade 4 in right DF) with hypoesthesia only below the right ankle. Sensory NCS showed no response in the right SPN, right deep peroneal nerve, and right plantar nerve, with low amplitude in the right sural nerve, and no abnormalities on the left side. Motor NCS indicated recovery of the right CPN, but low amplitude findings persisted in the right CPN at the EDB and right tibial nerve. A needle exam showed abnormal spontaneous activity in the right tibialis anterior and right extensor hallucis longus, with polyphasic motor units in the right tibialis anterior, peroneus longus, gastrocnemius, and extensor hallucis longus. The above electrophysiologic study findings are compatible with right common peroneal and tibial neuropathy with improvement.

Conclusion

This case report describes a patient who developed peripheral neuropathy after rhabdomyolysis, suggesting a toxin-mediated cause, without compartment syndrome or immobilization. Tibial nerve injury in this case, an uncommon complication of immobilization, suggests that clinicians must consider peripheral nerve lesions with toxin-induced inflammation mechanisms in rhabdomyolysis patients with weakness even without compartment syndrome or immobilization.

Sensory NCS

Nerve / Sites	Rec. Site	O. Lat ms	Sig.	O.P Amp μ V	Sig.	Distance cm	Onset Vel m/s	Sig.
L Superficial peroneal - Ankle								
Calf	Ankle	2.71	Normal	7.35	Normal	12	44.31	Normal
Calf	Ankle	2.73		8.96		12	43.97	
R Superficial peroneal - Ankle								
Calf	Ankle	NR	NR	NR	NR			
Calf	Ankle	NR		NR				
L Deep peroneal - Ankle								
Ankle	Ankle	2.58	Normal	4.29	Normal	12	46.45	Normal
Ankle	Ankle	2.65		4.32		12	45.35	
R Deep peroneal - Ankle								
Ankle	Ankle	NR	NR	NR	NR			
Ankle	Ankle	NR		NR				
L Sural								
Leg	Ankle	2.44	Normal	7.14	Normal	12	49.23	Normal
Leg	Ankle	2.48		8.02		12	48.40	
R Sural								
Leg	Ankle	2.83	Normal	3.75	Low	12	42.35	Normal
Leg	Ankle	2.63		2.85		12	45.71	
L Plantar - Ankle								
Medial	Ankle	2.42	Normal	6.12	Normal	12	49.66	Normal
Medial	Ankle	2.54		5.44		12	47.21	
Lateral	Ankle	2.50	Normal	5.56	Normal	12	48.00	Normal
Lateral	Ankle	2.54		5.23		12	47.21	
R Plantar - Ankle								
Medial	Ankle	NR	NR	NR	NR			
Medial	Ankle	NR		NR				
Lateral	Ankle	NR	NR	NR	NR			
Lateral	Ankle	NR		NR				

Fig 1. Sensory NCS (24.01.24)

Motor NCS

Nerve / Sites	Muscle	O.Lat ms	Sig.	O.P Amp mV	Sig.	Distance cm	Velocity m/s	Sig.
L Peroneal - EDB								
Ankle	EDB	4.85	Normal	4.75	Normal			Normal
Fib Head	EDB	11.65		4.50		31	45.64	
R Peroneal - EDB								
Ankle	EDB	4.73	Normal	0.36	Low			Delayed
Fib Head	EDB	13.08		0.36		31	37.11	
Pop Fossa	EDB	14.71		0.32		9	55.38	
L Tibial - AH								
Ankle	AH	3.52	Normal	11.17	Normal			Normal
Pop Fossa	AH	11.73		8.00		36	43.86	
R Tibial - AH								
Ankle	AH	4.08	Normal	2.82	Low			Normal
Pop Fossa	AH	13.02		2.30		36	40.28	
L Peroneal - Tib Ant								
Fib Head	TA	2.77	Normal	5.19	Normal			Normal
Pop Fossa	TA	4.35		5.03		9	56.84	
R Peroneal - Tib Ant								
Fib Head	TA	2.42	Normal	4.26	Normal			Normal
Pop Fossa	TA	4.21		4.24		9	50.23	

Fig 2. Motor NCS (24.01.24)

EMG Summary Table										
Muscle	Spontaneous						MUAP			Interference
	IA	Fib	PSW	Fasc	H.F.		Amp	Dur.	PPP	Pattern
R. Vastus medialis	Normal	None	None	None	None	None	Normal	Normal	Normal	Full
R. Rectus femoris	Normal	None	None	None	None	None	Normal	Normal	Normal	Full
R. Adductor longus	Normal	None	None	None	None	None	Normal	Normal	Normal	Full
R. Tibialis anterior	Increased	2+	2+	None	None	None	Increased	Increased	Poly	Full
R. Peroneus longus	Normal	None	None	None	None	None	Normal	Increased	Poly	Full
R. Gastrocnemius (Medial head)	UC	UC	UC	UC	UC	UC	Increased	Increased	Poly	Full
R. Biceps femoris (short head)	Normal	None	None	None	None	None	Normal	Normal	Normal	Full
R. Biceps femoris (long head)	Normal	None	None	None	None	None	Normal	Normal	Normal	Full
R. Gluteus maximus	Normal	None	None	None	None	None	Normal	Normal	Normal	Full
R. Tensor fasciae latae	Normal	None	None	None	None	None	Normal	Normal	Normal	Full
R. Extensor hallucis longus	Increased	1+	1+	None	None	None	Normal	Increased	Poly	S to P
R. Lumbar paraspinals (low)	Normal	None	None	None	None	None	Normal	Normal	Normal	None
R. Lumbar paraspinals (mid)	Normal	None	None	None	None	None	Normal	Normal	Normal	None

Fig 3. Needle EMG (24.01.24)

Right arm weakness suggesting post-polio syndrome of unilateral upper limb: A case

Sujeong Choi^{1*}, Eun Sang Yoon¹, Jongkyu Kim^{1†}

Department of Physical Medicine & Rehabilitation, Seoul Medical Center¹

Introduction

Post-polio syndrome is a late complication of poliomyelitis. Up to 50% of poliomyelitis survivors experience late weakness of the involved leg(s). Studies on post-polio syndrome described late weakness of poliomyelitis-involved legs. However, there has been even no case report about arm involvement in post-polio syndrome. We experienced a unilateral arm weakness, which was diagnosed with post-polio syndrome of the arm, and we reported it.

Case

A 65-year-old woman visited complaining of right arm weakness for several years. Three years ago, the patient was diagnosed with right C5 radiculopathy with electromyography and had a cervical vertebra laminectomy. Immediately after the surgery, the weakness recovered slightly but recurred. Two years ago, the patient was diagnosed with normal pressure hydrocephalus and had ventriculoperitoneal shunt surgery, but right arm weakness was not recovered.

The patient had a history of poliomyelitis and was paraplegic. The patient did not know how many limbs were affected by poliomyelitis. Subjectively, the patient complained of weakness only on the right shoulder flexor and elbow flexor, suggesting C5 involvement. The motor powers below the elbow were evaluated as normal. (Table 1)

Our clinical impressions were as follows;

C5 radiculopathy, right

brachial plexopathy, right

post-polio syndrome, right upper limb

We did an electromyography study. A nerve conduction study there showed both carpal tunnel syndrome and left cubital tunnel syndrome. The right deltoid, biceps brachii, triceps brachii, and flexor carpi radialis muscles showed giant motor unit action potentials in needle electromyography. The left biceps brachii muscle showed long-duration polyphasic motor unit action potential. (Table 2) We concluded that these results are long-lasting sequelae of anterior horn cell disease on the right upper arm, suggesting poliomyelitis sequelae. With clinical correlation, we diagnosed post-polio syndrome of the right upper limb.

Conclusion

We experienced a rare case of post-polio syndrome of the unilateral upper limb and reported it.

Table 1. Manual motor test of upper limbs

	Shoulder		Elbow		Wrist		Fingers	
	flexor	extensor	flexor	extensor	flexor	extensor	flexors	extensors
Right	F	F	F	N	N	N	N	N
Left	N	N	N	N	N	N	N	N

Manual motor test of upper limbs

Table 2, Needle electromyography results.

Side	Muscle	Fibs	PSWs	Polyphasic	Giant MUAP	MUAP amp
Right	Deltoid	-	1+	-	+	5.4 mV
	BB	-	-	-	+	5.3 mV
	TB	-	-	-	+	11 mV
	FCR	-	-	-	+	6.2 mV
	EDC	-	-	-	-	
	APB	-	-	-	-	
	FDI	-	-	-	-	
Left	Deltoid	-	-	-	+	13.7 mV
	BB	-	-	+	-	
	TB	-	-	-	+	12.8 mV
	FCR	-	-	-	-	
	EDC	-	-	-	-	
	APB	-	-	-	-	
	FDI	-	-	-	-	

abbreviations; Fibs, fibrillations, PSWs, positive sharp waves, MUAP, motor unit action potential, amp, amplitude, BB, biceps brachii, TB, triceps brachii, FCR, flexor carpi radialis, EDC, extensor digitorum communis, APB, abductor pollicis brevis, FDI, first dorsal interossei

Needle electromyography results.

Iatrogenic Deep Peroneal Neuropathy Following Clamshell Osteotomy with Intramedullary Nailing

Su Jeong Choi^{1*}, Eun Sang Yoon¹, Hee dong Park^{1†}

Department of physical medicine & Rehabilitation , Seoul Medical Center¹

Case

A 64-year-old male, previously independent in mobility and activities of daily living, presented with varus deformity, pain, and a sensation of shifting fixation devices in his right leg. He had a history of right tibiofibular fracture treated with two Ender nails 40 years prior. Recent X-rays revealed callus formation, angulation deformity, and malunion. He underwent elective clamshell osteotomy with intramedullary (IM) nailing.

On the first postoperative day, the patient reported difficulty dorsiflexing his right big toe and decreased sensation in the first web space, consistent with isolated extensor hallucis longus (EHL) muscle weakness. Due to persistent motor weakness and sensory impairment, a consultation was requested from the Department of Orthopedics. On postoperative day 82, electromyography (EMG) and nerve conduction studies (NCS) were performed.

Physical examination revealed an absent right EHL tendon and complete paralysis (grade 0) of the muscle. The right extensor digitorum brevis (EDB) muscle appeared atrophied compared to the left.

Motor NCS revealed no compound muscle action potential (CMAP) from the right peroneal nerve. The right tibialis anterior (TA) recording showed decreased CMAP amplitude. Sensory NCS demonstrated reduced amplitude of the right superficial peroneal sensory nerve action potential (SNAP), though within lower normal limits. The deep peroneal SNAP was absent on the right. F-wave study showed no response from the right peroneal nerve.

EMG findings revealed denervation potentials at rest in the TA and EHL muscles, with 3+ positive sharp waves (PSWs).

The TA showed long polyphasic potentials on minimal effort, but a full interference pattern on maximal effort. In the EHL, normal motor units were absent during minimal effort, and maximal volitional contraction attempts were unsuccessful. The EDB also showed denervation potentials at rest with 1+ PSWs and a reduced interference pattern on maximal effort.

These findings are consistent with an isolated acute deep peroneal nerve injury proximal to the tibialis anterior motor branch. This case presentation highlights a potential complication of the surgical procedure. Suspected causes include direct nerve injury, muscle or tendon injury, compartment syndrome, and postoperative swelling.

Notably, this case demonstrates pronounced weakness and denervation of the EHL compared to other muscles innervated by the deep peroneal nerve. While isolated EHL weakness can occur after procedures like high tibial osteotomy, it may also be due to variations in neural innervation and blood supply to the EHL.

Conclusion

To mitigate such complications, it is crucial to utilize fluoroscopic imaging during surgery to accurately identify and avoid anatomical areas at risk when placing fixation devices. Additionally, careful attention must be paid to avoid excessive retraction of neurovascular structures during the operation.

Esophageal diverticulum and fissure formation related with displaced hardware in cervical spine

Nami Han^{1*†}, Hyun-dong Kim¹, Hee-sung Nam¹

Department of Rehabilitation Medicine, Inje University Busan Paik Hospital¹

Introduction

Implanted hardware to cervical spine can interrupt swallowing function by disturbing physiologic motion of adjacent soft tissue. Mostly, mass effects of implanted materials are claimed to be a main cause. Here, we report a case of structural failure induced by a prolonged displacement of a hardware in cervical spine.

Case Report

A 46-year-old woman was referred for videofluoroscopic swallowing study (VFSS) with a symptom of foreign body sensation during swallowing. She complained that the symptom provoked regardless of types of dietary contents, however it was somewhat prominent during swallowing solid diet. Coughing during or after swallow was not observed and her voice didn't show any change. She had past history of cervical spine operation, which was an anterior stabilization with plate and screw in C4/5/6 levels 3 years earlier. In July 2022, a fracture of screw was found after a slip down, and regular follow up was continued for the fixation material. In November 2023, she had an injury of slip down from a few steps of stairs and symptoms of foreign body sensation and choking, neck pain, and tingling sensation of right arm started. She visited a local hospital, took a simple x-ray of cervical spine, and the broken screw and displacement of plate was found. She was transferred to our institution for surgical management. From the pre-op VFSS, esophageal passage was somewhat narrow at upper esophagus and widened at mid esophagus. No aspiration or penetration was found. During the surgical removal of the hardware, the operator reported massive adhesion between the hardware and adjacent soft tissue. After the surgery, patient experienced odynophagia and parenteral feeding was decided. At the follow up VFSS on the 8th post-operation date, a unique pattern of food regurgitation in prevertebral space up to C3 level was observed. The upward regurgitation lied at the identical location of previously removed hardware and started from an esophageal diverticulum suspiciously. Next day, endoscopy revealed a perforation in large diverticulum and clipping of the laceration carried out. At the 3rd VFSS after 4 weeks of parenteral feeding, the diverticulum was still existed and no food leakage was observed around the clipping area. Oral feeding with soft diet started and no abnormal finding except remained diverticulum was found at the 4th VFSS after 4 weeks of oral feeding.

Discussion

The location of diverticulum was at the level of inferior end of fixation material. It means the focused expansion pressure can be made at the end level of mass effect. After removal of the mass effect, the motion of soft tissue increases so that the extraction force to esophagus can become stronger. The extraction force can result in laceration or perforation to the weak wall of diverticulum. For the evaluation of structural problem of esophagus, VFSS can show instant structural abnormality avoiding mass leakage of food content to injured structure.

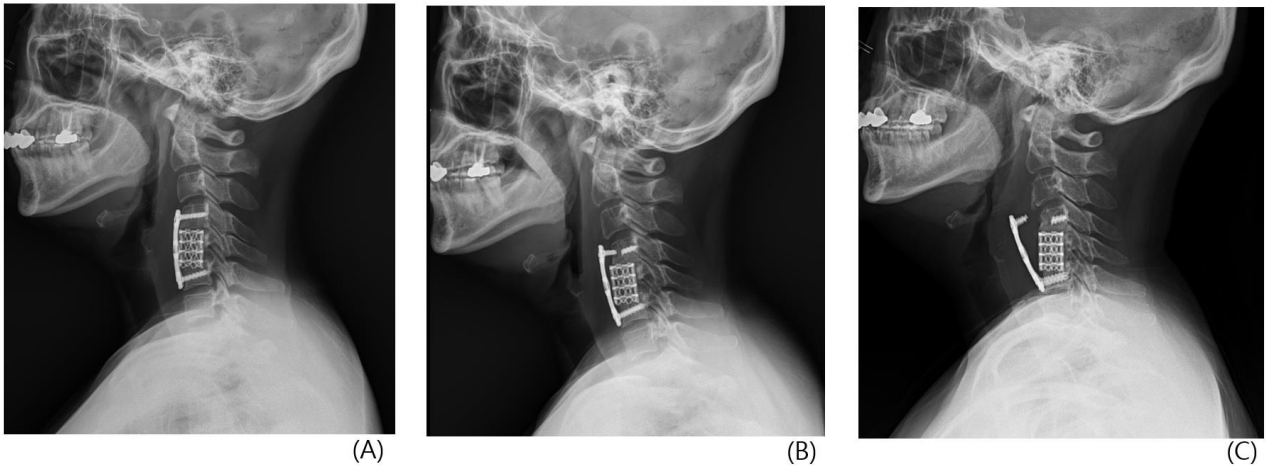


Fig 1. Simple X-ray of cervical spine. Sturdy placement of anterior stabilization with plate & screw in C4/5/6 (A). Fracture of upper screw was noted after 1st slip down in 2022 (B). Far displacement of plate in 2024, after 1 year from 2nd slip down (C).

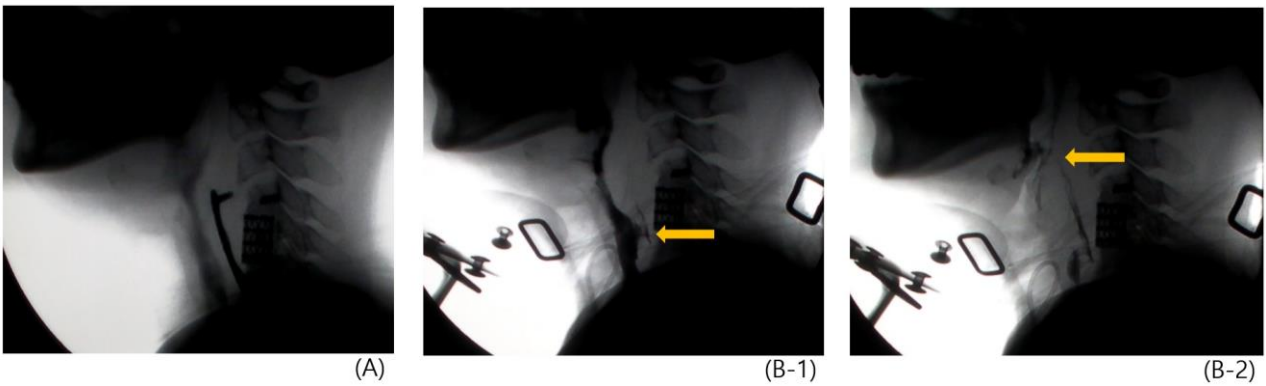


Fig 2. Videofluoroscopic swallowing study (VFSS) findings. Pre-operative VFSS showed patent esophageal passage with some narrowed diameter along displaced plate (A). Local dilatated esophageal contour and a yellow arrow indicating leakage point in the VFSS of post-operation (B-1). Food leakage and regurgitation extended up to C3 level (Yellow arrow) showing the identical passage with previous hardware location (B-2).

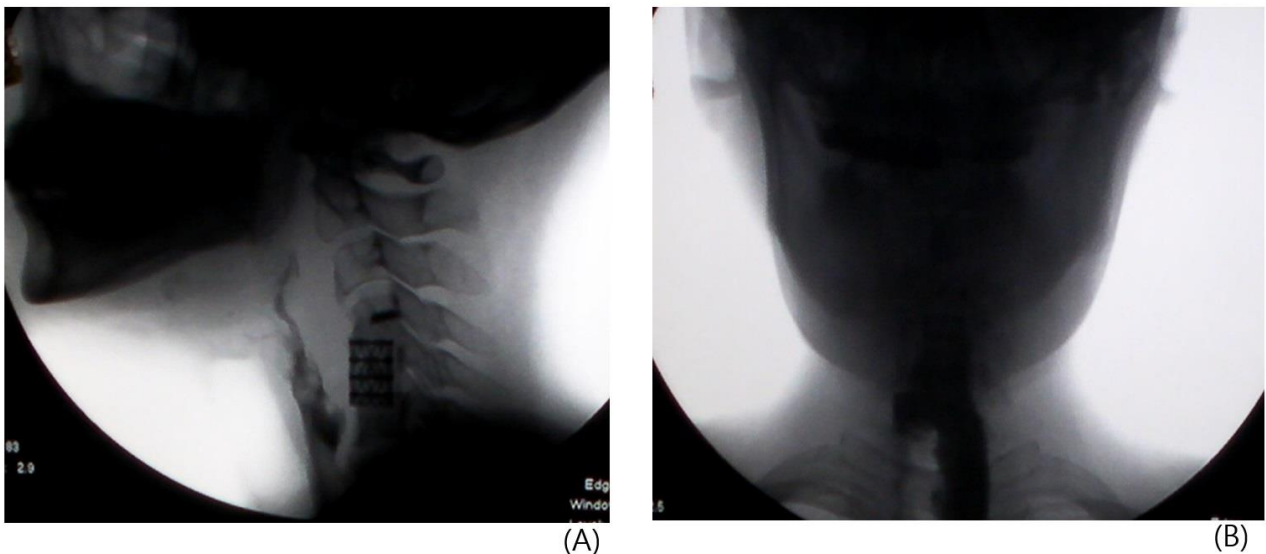


Fig 3. Follow-up VFSS findings after 1 month since oral feeding started. Food leakage and regurgitation in the prevertebral space disappeared, but dilated esophageal contour still observed (A). A-P view of VFSS revealed the outline of large esophageal diverticulum filled with dye content (B).

Lymphocele after Complex Decongestant Therapy in a Patient with Lymphedema: A Case Report

Dong Jin Chae^{1*}, Yung Jin Lee^{1†}, Jong Bum Park¹, Mi Jin Hong¹, Cho E Sim¹, Seong-Eun Kim¹, Ji-Hwan Kwon¹

Department of Rehabilitation Medicine, Konyang University College of Medicine¹

Introduction

Complex Decongestive Therapy (CDT) has long been an effective treatment for lymphedema caused by lymph flow retention, as it improves lymphatic flow. However, CDT can exacerbate lymphocele, potentially posing new challenges in treating lymphedema patients with lymphocele. The authors aim to highlight the correlation between CDT and lymphocele, and emphasize the need for research to prevent such side effects.

Case report

A 52-year-old man has had discomfort in his left leg for about 40 years, with no diagnosis from previous other hospital evaluations, including a biopsy. Swelling began in his left lower extremity in 20s, but he did not receive treatment. After 30 years, he visited Department of Rehabilitation of Medicine for evaluation about progressing symptoms. On physical examination, left lower extremity's manual muscle test was good grade with no other neurologic symptoms. Leg circumference was measured for both sides, which were above knee 10cm 43/47cm, below knee 25cm 36/42cm, ankle 24/31cm. The complementary exams showed no deep vein thrombosis, left and right saphenous vein insufficiency, and collateral and perforating vein with reflux to the popliteal vein. Lymphoscintigraphy (Figure 1.) was performed, it revealed dermal backflow of left lower extremity and asymmetric left inguinal lymph nodes, a stage I lymphedema was diagnosed. The patient was treated with compression stockings and CDT, which was administered once a week for about 7 months. Over the course of treatment, swelling improved in areas, above and below the knees, except the ankle. Three months after beginning CDT, a painless and soft mass was found in the left inguinal area, which continued to enlarge as the therapy progressed. Upon ultrasonography, it was diagnosed as a 3.9 x 2.3 x 5.4cm sized lymphocele (Figure 2.). Without prior imaging, it was unclear if the lymphocele was pre-existing. Since there were no symptoms like pain or discomfort, invasive treatment was not pursued. CDT was discontinued, but the patient continues using compression stockings and medication. We informed the patient that continuous follow-up is necessary for the lymphocele after stopping CDT and active intervention would be needed if any additional discomfort arises.

Conclusion

Lymphocele, a fluid collection with fibrous walls, often develops in the pelvic or paraaortic regions after surgery, with a prevalence ranging from 0% to 58.5% due to underdiagnosis as most cases are asymptomatic. One case report suggested CDT might contribute to lymphocele enlargement by improving lymph flow, but there is still insufficient research on whether CDT alone can cause lymphocele formation.

The authors highlight the need for further research on the correlation between CDT and lymphocele in patients receiving lymphatic treatment. It is also essential for physicians to inform patients about this potential side effect and the importance of regular monitoring.

Lymphocintigraphy
(2hr)

ANT



POST



Lymphocintigraphy
(3hr)

ANT



POST

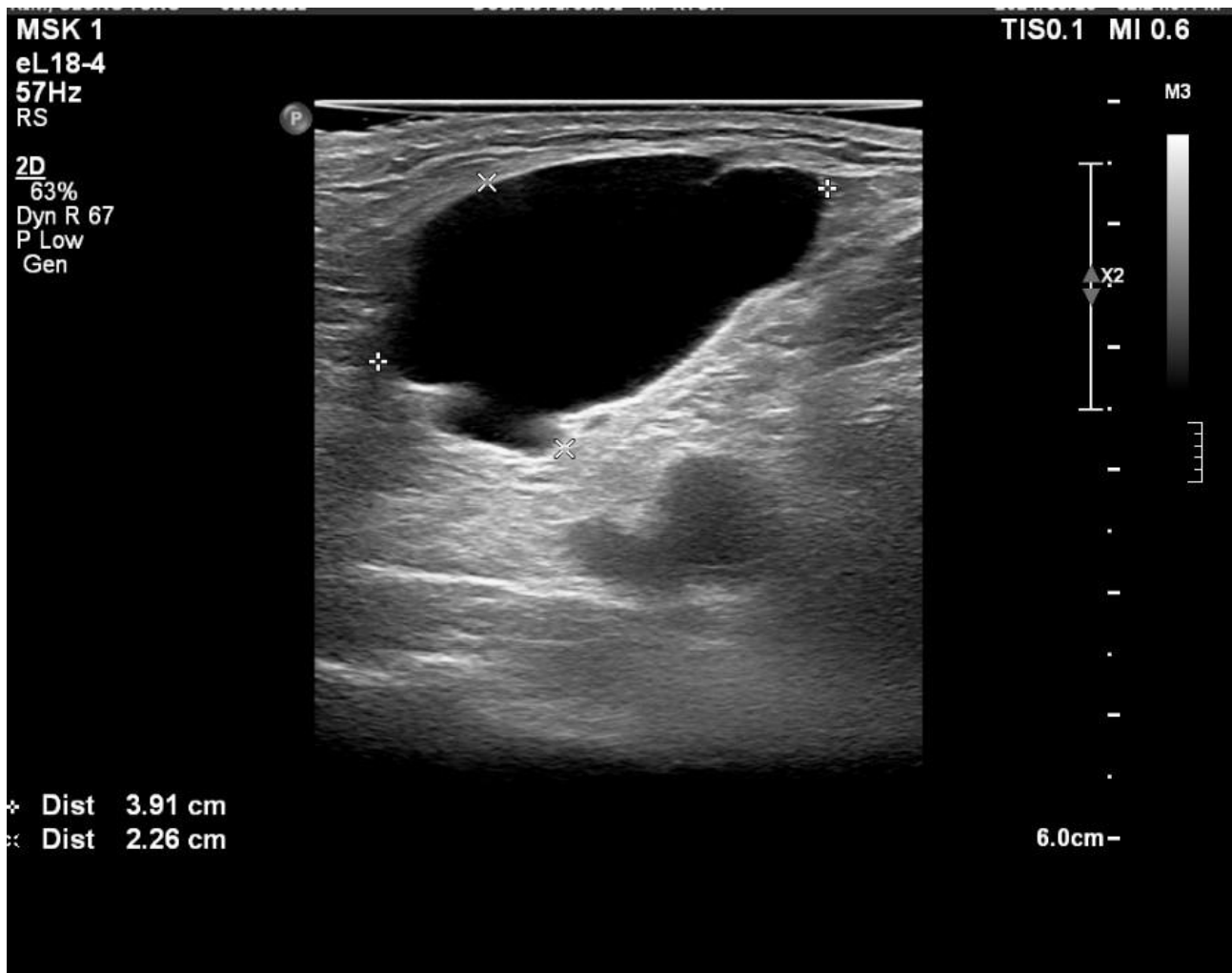


Lymphoscintigraphy

+

+

+



Ultrasonography shows a 3.9 x 2.3 x 5.4 cm sized septated subcutaneous cystic mass, likely lymphocele, at left inguinal area

Effective Fascia Hydrorelease for Chronic Iliotibial Band Tendinopathy after Fascia Lata Harvest

Soo Jin Jung¹, Yeon Jun Kim¹, Yeong Jae Kim¹, Yongkyun Jung¹

Department of Rehabilitation Medicine, Dongtan Sacred Heart Hospital¹

Patient

A 51-year-old woman with chronic iliotibial band tendinopathy after the fascia lata harvest

Case Description

The patient reported experiencing lateral thigh pain and gait discomfort that had gradually developed over the past year. Previously diagnosed with left Bell's palsy, she underwent temporalis tendon transfer surgery leading to severe facial contracture, and later facial reconstructive and muscle reconstruction surgeries with a fascia lata graft and facelift. Despite a year of pain medication, her symptoms did not significantly improve. Femur and lumbar spine x-rays showed no remarkable findings. Left thigh ultrasonography revealed increased vascularity near the iliotibial band and increased stiffness in the shear wave findings with adhesions around the operation site. An ultrasound-guided fascia hydrorelease was performed around the iliotibial band, using a mixture of 1% lidocaine and 20mg triamcinolone, totaling 10cc. The patient reported an immediate decrease in pain following the injection, and no acute complications were observed after the procedure.

Assessment/Results

At 8 weeks post-injection, the patient showed a significant reduction in pain from visual analogue scale 8 to 1 and reported that her gait felt much more comfortable.

Discussion

This is the first reported case, to our knowledge, of successful fascia hydrorelease for iliotibial band tendinopathy after a huge fascia lata harvest. Fascial tissues, dense with nociceptors and nerve endings, have viscoelastic properties affecting receptor activation leading to pain upon stretching. After undergoing fascia hydrorelease, the patient reported a decrease in pain, as well as enhanced functionality of the iliotibial band, which is essential for pelvic stability and posture. This technique, notably effective in South Korea, demands further research due to a lack of agreement on medication, injection schedules, and specific usage guidelines.

Conclusion

Hydrorelease may be a favorable therapeutic option for tendinopathy emerging at the donor site following graft procedures.

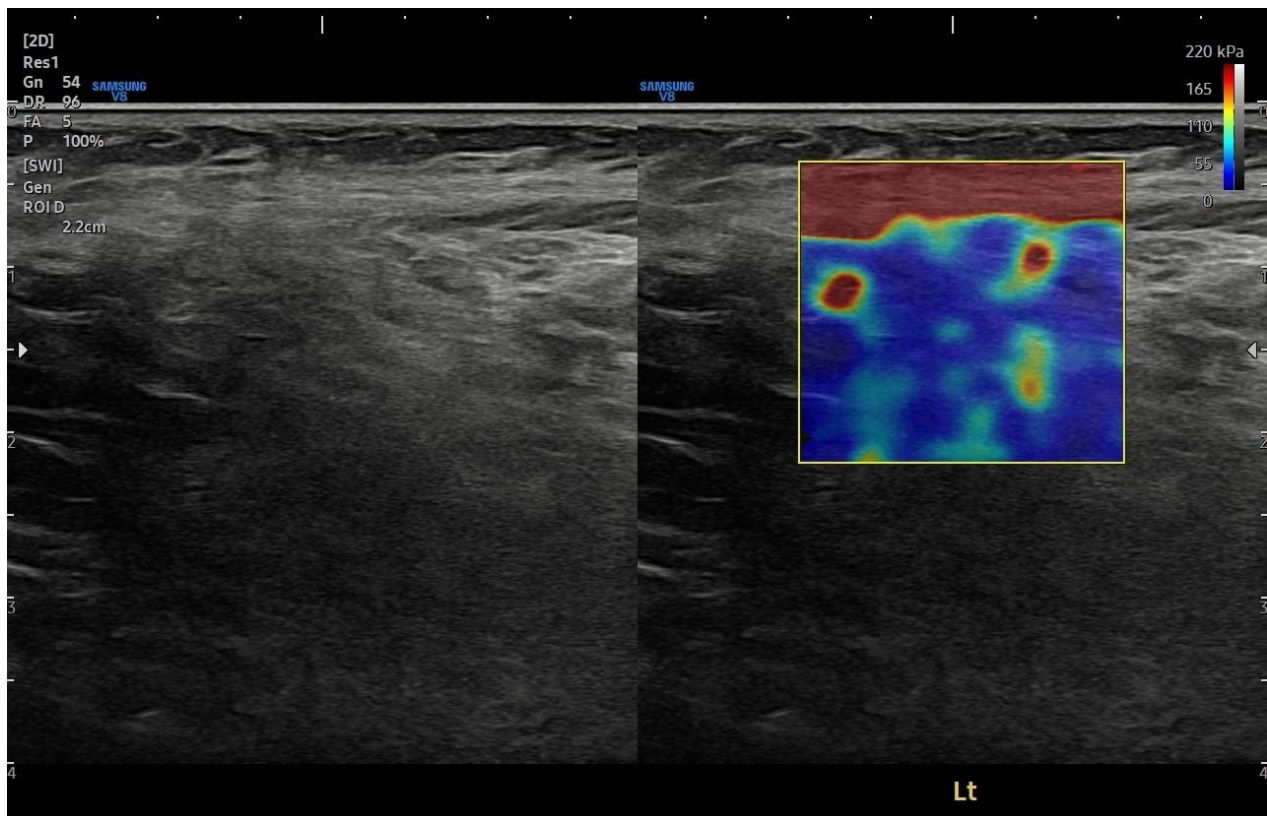


Fig 1. Semiquantitative evaluation of the left iliotibial band stiffness by shear wave elastography. On B-mode ultrasound, no structural changes were visible in the tendon. Increased stiffness in the shear wave was observed in the adhesion areas around the operation site.

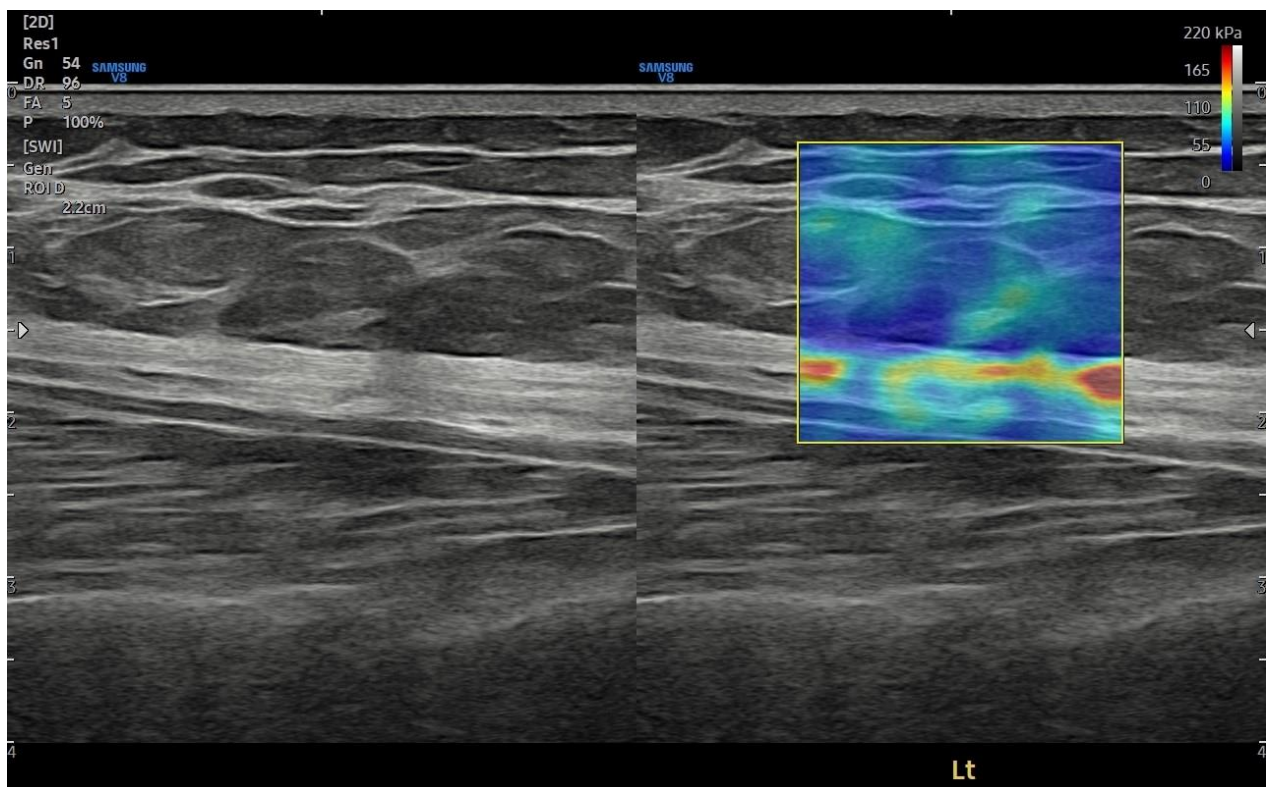


Fig 2. Semiquantitative assessment of tendon stiffness by shear wave elastography(SWE) revealed a yellow-green (intermediate- tissue rigidity) and blue (soft-tissue rigidity) SWE color chart.



Fig 3. The left femur X-ray showed normal findings.

A Case of Spinal Cord Injury after Cardiac Arrest following an Intra-articular Shoulder injection

Kyung Eun Nam^{1*}, Ah Yeon Lee¹, Jong In Lee^{1†}

Department of Rehabilitation Medicine, Seoul St. Mary's Hospital, College of Medicine, The Catholic University of Korea, Seoul, Republic of Korea. ¹

Background

Local anesthetics (LAs) are commonly used in musculoskeletal injection treatments. Although LAs are relatively safe with proper use, there does exist the incidence of local anesthetic system toxicity (LAST) and, very rarely, allergy. LAST syndrome is associated with several life-threatening events which most often involve the cardiovascular and neurologic systems.

Case report

A 55-year-old female patient with no known underlying conditions experienced seizure-like movements 15 minutes after receiving a shoulder intra-articular injection (total volume 15cc, no information of LAs concentration). She was subsequently found in cardiac arrest and received CPR en route to the hospital emergency room. After achieving return of spontaneous circulation (ischemic time 38min), therapeutic temperature management was performed. After regaining consciousness, her cognitive function was intact; however, motor weakness in both lower extremities (grade II~III) was noted, leading to further investigations. She showed paresthesia below T12 dermatome, no upper motor signs, flaccid legs, and urinary retention (self-voiding 0cc, residual urine 800cc). Spine MRI showed symmetric high SI with enhancement and diffusion restriction in bilateral central grey matter below T6, and no definite evidence of myelitis was observed in the CSF study. Initial EEG showed continuous normal voltage, and bilateral ischemic change in both basal ganglia, compatible with anoxic injury, was observed in the brain MRI. Based on the physical examination and imaging results, bilateral lower extremity weakness was related to the spinal cord injury (AIS D, NLI T11) due to spinal cord infarction. She received comprehensive rehabilitation therapies including strengthening, sitting balance training, weight-bearing and shifting training, and activities of daily living Training. At the time of discharge (about 1 month after onset), the Berg Balance Scale changed from 2 to 5, and the K-MBI score improved from 19 to 30. The neurogenic bladder symptoms also improved and were managed with oral medication alone without catheterization.

Discussion

We experienced a patient with spinal cord injury after cardiac arrest following a shoulder intra-articular injection. A primary cause of LAST syndrome includes increased plasma levels of LAs. The serum concentration of LAs is dictated by either accidental intravascular injection or systemic absorption if an appropriate dose is administered. Systemic toxicity is associated with several risk factors, including drug selection (dosing), age (pediatric and geriatric), coexisting disease (cardiac, metabolic, and renal dysfunction), and procedure (ultrasound guidance). Clinicians must always make efforts to reduce the risk of LAs toxicity. Despite the very low incidence, the LAST syndrome should be kept in mind during musculoskeletal injection procedures.

May-Thurner Syndrome with Recurrent Deep Vein Thrombosis: A Case Report

Ji-Hwan Kwon^{1*}, Jong Bum Park^{1†}, Yung Jin Lee¹, Mi Jin Hong¹, Dong Jin Chae¹, Cho E Sim¹, Seong-Eun Kim¹

Department of Rehabilitation Medicine, Konyang University College of Medicine¹

Introduction

May-Thurner syndrome (MTS), also known as iliac vein compression syndrome or Cockett's syndrome, is a condition that the left common iliac vein is compressed between the right common iliac artery crossing over it and the lumbar vertebral body, leading to venous outflow obstruction. Symptoms can range from asymptomatic to chronic venous hypertension, venous occlusion, and deep vein thrombosis (DVT) depending on the degree of venous obstruction. In this article, we report a case of May-Thurner syndrome with recurrent DVT in left lower extremity.

Case report

The 73-year-old woman with history of spontaneous subarachnoid hemorrhage (SAH) that occurred in July 2022 was admitted to the Department of Rehabilitation Medicine after 11 months of stroke onset for rehabilitation. She was diagnosed with pulmonary thromboembolism (PTE) and DVT in both lower extremities three months after the onset of SAH. She started taking rivaroxaban 20mg once daily and discontinued the medication after taking medication for about 6 months without any recurrence. On the day of admission, there were findings of swelling and warmth in the left lower extremity. Therefore, D-dimer levels and imaging studies were performed. The D-dimer level was elevated at 1.09ug/mL (normal range: 0.0-0.5ug/mL), and findings of DVT were observed in the left popliteal, superficial femoral, and external iliac veins on lower extremity CT angiography. Also, it was observed that the left iliac vein was compressed between the right iliac artery and the vertebral body. (Figure 1) In the chest CT performed, to rule out PTE, no PTE was observed. A diagnosis of May-Thurner syndrome was made based on previous test and consultation with the Cardiovascular Thoracic Surgery department. The patient started taking rivaroxaban 20mg once daily and Vitis vinifera Ext. 150mg twice daily. After starting drug therapy, the swelling in the left lower limb showed an improving trend. (Table 1) Accordingly, while maintaining the previous medication therapy, the patient began applying compression stocking with left leg elevation as an adjunctive measure, and continues up to now.

Conclusion

For physicians who frequently encounter bedridden patients, DVT may be a relatively common condition. As a result, there is a risk of overlooking cases with secondary causes such as, and in cases of MTS that may require angioplasty, stent placement, or even surgical intervention in addition to anticoagulation therapy, the condition can be fatal. Therefore, in cases of DVT in the iliofemoral venous territory, especially when it occurs on the left side, suspicion of MTS can be meaningful, and additional studies such as CT angiography, venography, in addition to ultrasound, may be necessary.



Fig 1. Axial CT image shows that the left iliac vein is compressed between the right iliac artery and the vertebral body.

Date	Rt.(cm)	Lt.(cm)	Difference(Lt.-Rt.)
1st day of hospitalization	40	45	+5
15th day of hospitalization	39	41	+2
21st day of hospitalization	39.5	40.3	+0.8

Table 1. Difference between circumference of both thighs (measured 5cm above the patella)

A rare case of Geminin and Delta Like Canonical Notch Ligand 1 gene mutation–related SCTS

Junhwan Lee^{1*}, Byung-Ju Ryu^{1†}, Yunhee Kim¹

Department of Physical medicine and Rehabilitation, Sahmyook Medical Center¹

Abstract

Spondylotarsal synostosis syndrome (SCTS) is a rare genetic disorder characterized by vertebral fusion, short stature, and skeletal anomalies. Previously linked to mutations in the filamin B gene, this report presents a unique case of a 28-year-old male with SCTS associated with mutations in the Geminin (GMNN) and Delta Like Canonical Notch Ligand 1 (DLL1) genes. The patient exhibited persistent neck and shoulder pain, radioulnar synostosis, cervical spine anomalies (scoliosis and agenesis of the posterior arch of C1), and a history of polydactyly. This is the first documented instance of SCTS involving these genetic mutations.

Introduction

Spondylotarsal synostosis (SCTS) is a rare genetic disorder affecting bone development, characterized by vertebral fusion, short stature, scoliosis, and carpal and tarsal bone abnormalities. Additional features may include facial dysmorphism, dental enamel hypoplasia, joint laxity, cleft palate, and hearing impairment. Mutations in the filamin B gene (FLNB) cause SCTS in an autosomal recessive manner.

This report documents the first case of SCTS caused by mutations in GMNN and DLL1 genes. Informed consent for the use of the patient's clinical details and images was obtained.

Case Report

A 28-year-old male presented with persistent neck and shoulder pain. He had radioulnar synostosis (RUS), limiting forearm rotation, and a history of surgically corrected polydactyly. Physical examination showed normal muscle strength and sensation but limited neck rotation (30° to the right, 35° to the left). X-rays confirmed RUS and cervical scoliosis. A CT scan revealed agenesis of the posterior arch of C1.

Genetic analysis using DNA from the patient's blood revealed mutations in GMNN (c.611A>T, p.Asp204Val) and DLL1 (c.289G>C, p.Gly97Arg).

Discussion

This is the first reported case of SCTS associated with GMNN and DLL1 mutations rather than FLNB. FLNB mutations, typically autosomal recessive, cause SCTS by disrupting protein amounts and functionality, leading to vertebral fusion. GMNN regulates DNA replication during the cell cycle's S phase and is crucial for proper embryonic and tissue development. Mutations in GMNN are linked to developmental abnormalities like Meier-Gorlin syndrome.

DLL1, part of the Notch signaling pathway, is vital for embryonic development and tissue differentiation. DLL1 mutations affect bone formation and spinal irregularities through Notch signaling. The roles of GMNN and DLL1 mutations in posterior arch agenesis and RUS are not fully understood, necessitating further research.

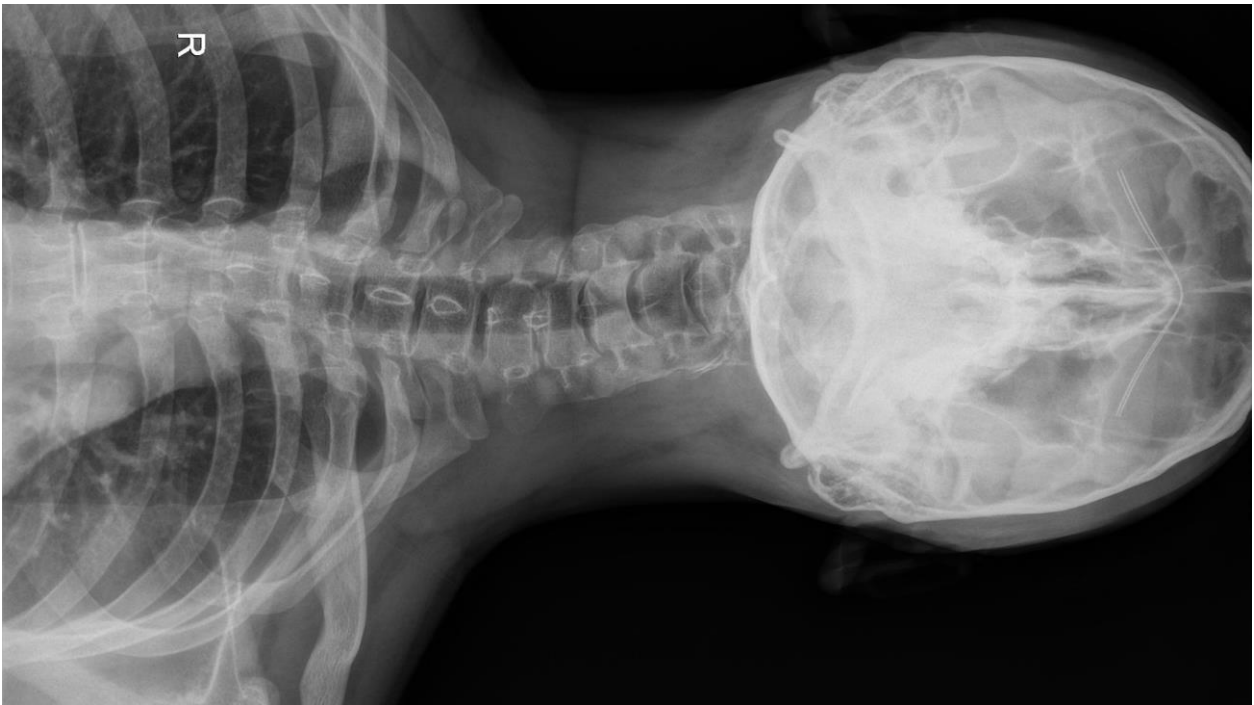
This case highlights the novel association of SCTS with GMNN and DLL1 mutations, presenting with agenesis of the posterior arch of the atlas, RUS, and polydactyly. Further investigation is required to understand these genetic mutations' impact on skeletal development and their functional implications.

Acknowledgment 1. Isidor B, Cormier-Daire V, Le Merrer M, Lefrancois T, Hamel A, Le Caignec C, et al. Autosomal dominant spondylotarsal synostosis syndrome: phenotypic homogeneity and genetic heterogeneity. *Am J Med Genet A* 2008;146a:1593-7. 2. Krakow D, Robertson SP, King LM, Morgan T, Sebald ET, Bertolotto C, et al. Mutations in the gene encoding filamin B disrupt vertebral segmentation, joint formation and skeletogenesis. *Nat Genet* 2004;36:405-10. 3. Yang CF, Wang CH, Siong H'ng W, Chang CP, Lin WD, Chen YT, et al. Filamin B Loss-of-Function Mutation in Dimerization Domain Causes Autosomal-Recessive Spondylotarsal Synostosis Syndrome with Rib

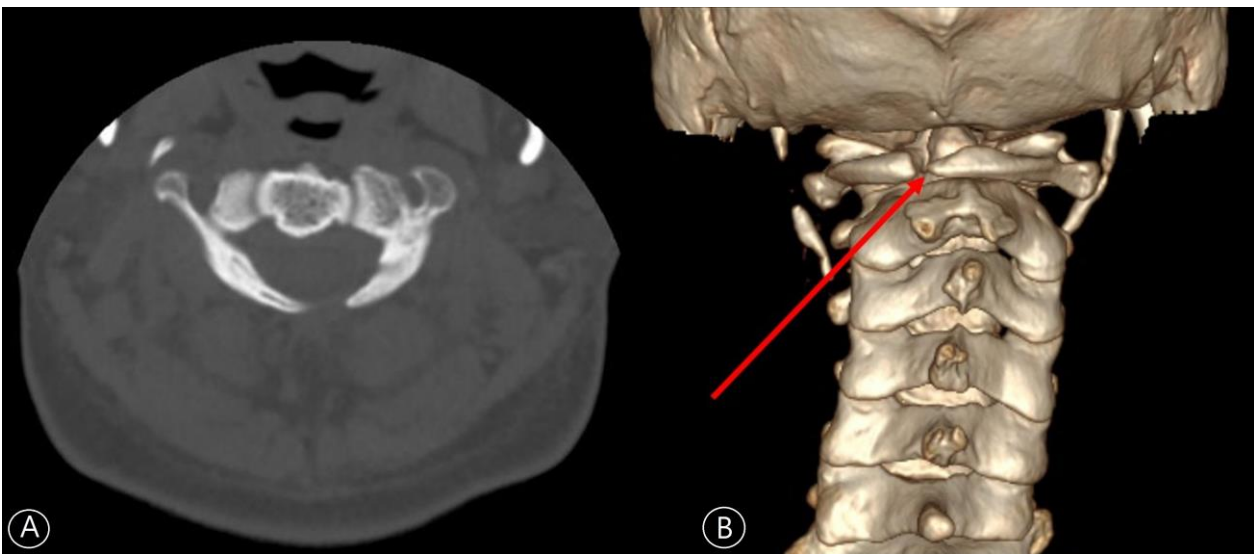
Anomalies. *Hum Mutat* 2017;38:540-7. 4. McGarry TJ, Kirschner MW. Geminin, an Inhibitor of DNA Replication, Is Degraded during Mitosis. *Cell* 1998;93:1043-53. 5. Burrage LC, Charng WL, Eldomery MK, Willer JR, Davis EE, Lugtenberg D, et al. De Novo GMNN Mutations Cause Autosomal-Dominant Primordial Dwarfism Associated with Meier-Gorlin Syndrome. *Am J Hum Genet* 2015;97:904-13. 6. Arzate D-M, Valencia C, Dimas M-A, Antonio-Cabrera E, Domínguez-Salazar E, Guerrero-Flores G, et al. Dll1 haploinsufficiency causes brain abnormalities with functional relevance. *Frontiers in Neuroscience* 2022;16. 7. Luo Z, Shang X, Zhang H, Wang G, Massey PA, Barton SR, et al. Notch Signaling in Osteogenesis, Osteoclastogenesis, and Angiogenesis. *Am J Pathol* 2019;189:1495-500. 8. Shen F, Yang Y, Li P, Zheng Y, Luo Z, Fu Y, et al. A genotype and phenotype analysis of SMAD6 mutant patients with radioulnar synostosis. *Mol Genet Genomic Med* 2022;10:e1850. 9. Kornak U, Mundlos S. Genetic disorders of the skeleton: a developmental approach. *Am J Hum Genet* 2003;73:447-74. 10. Cameron-Christie SR, Wells CF, Simon M, Wessels M, Tang CZN, Wei W, et al. Recessive Spondylocarpotarsal Synostosis Syndrome Due to Compound Heterozygosity for Variants in MYH3. *Am J Hum Genet* 2018;102:1115-25.



Picture shows a thumb scar from polydactyly surgery in childhood (arrow).



Lateral view of the right elbow X-ray showingdemonstrating the fusion of the proximal radius and ulna.



AP view of the C-spine X-ray revealing scoliosis.

Hypovolemic shock caused vascular injury following a lumbar minimally invasive procedure

Kyung Eun Nam^{1*}, Kyung Hyun Park¹, Jong In Lee^{1†}

Department of Rehabilitation Medicine, Seoul St. Mary's Hospital, College of Medicine, The Catholic University of Korea, Seoul, Republic of Korea.¹

Background

The lumbar foraminoplasty is a novel surgical option for addressing lumbar stenosis and radicular pains which have not responded to conservative treatment options. The procedure involves the removal of a selected portion of the bone and ligament to widen the foramen and allow for easy passage of the compressed nerve. There has been a growing enthusiasm towards definite management in the form of a foraminoplasty. Although high success rates have been reported in the literature, complications and failures are often associated with patient indications or technical variables.

Case report

A 76-year-old female on clopidogrel for an old cerebrovascular accident underwent percutaneous foraminoplasty (left L34,L45,L5S1, right L34, L45) for back pain. An hour after the procedure, the patient developed left flank pain and hypotension (SBP 81mmHg, DBP 52mmHg). Two intravascular injections of ephedrine (1st 4mg, 2nd 20mg) were administered, but hypotension persisted, leading to transfer to the emergency room. Blood tests related to coagulation such as platelet count, prothrombin time, and partial thromboplastin time showed normal findings, but significant anemia (hemoglobin 6.1 mg/dL) was observed. CT scan revealed a large amount of hematoma, especially in the left posterior pararenal space (Fig 1.). There were no signs of bleeding in the pancreas or spleen and no definite abnormalities in both kidney, liver, and gallbladder. Active arterial bleeding was suspected, and an emergency angiography was performed. Active bleeding from the left 4th lumbar artery and left iliolumbar artery was detected, and immediate trans-arterial embolization was performed without immediate complication. While receiving care in the intensive care unit, her medical condition gradually stabilized. 1 week after the onset, the physical examination revealed left proximal and distal lower extremity weakness (grade 3) and radiating pain, which were absent before the procedure. She received physical therapy for 1 week and was discharged with motor improvement from grade 3 to grade 4.

Discussion

The lumbar arteries are small blood vessels originating from the abdominal aorta that are mostly distributed in L1-L4 pairs. They traverse the posterolateral side of the vertebral body and are divided into 3 branches in front of the intervertebral foramen. The branches of the lumbar arteries can be damaged by spinal canal decompression or transforaminal endoscopic surgery. The iliolumbar artery is the first branch of the posterior trunk of the internal iliac artery. It turns upward behind the obturator nerve and the external iliac vessels. However, there are variations in the location and origin of branches of the iliolumbar artery, and this increases the risk of complications during spinal procedures. Small vessel injuries such as lumbar artery and iliolumbar artery during spinal procedures is uncommon but can cause serious life-threatening consequences if they occur.

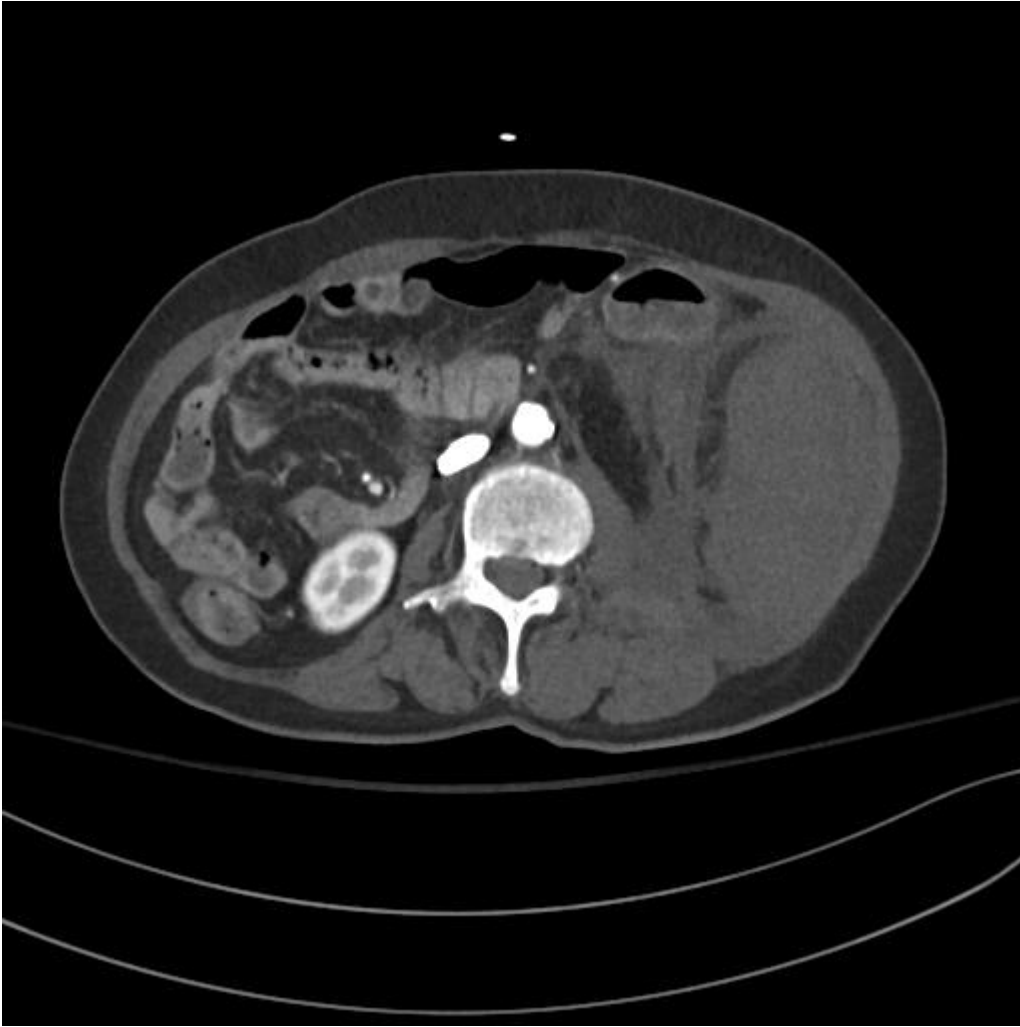


Fig 1. Large amount of hematoma in the left posterior pararenal space

Management strategy for brachial plexus injury following neck dissection in a thyroid cancer patient

Jinyoung Park^{1*}, Yura Goh¹, Sooin Lee¹, Joo Eun Park¹, Yoon Ghil Park^{1†}

Department of Rehabilitation Medicine, Gangnam Severance Hospital, Yonsei University College of Medicine, Seoul, Korea¹

Introduction

Brachial plexus injury is one of the complications of neck dissection surgery in patients with thyroid cancer. This study describes a case of iatrogenic brachial plexus injury negative for magnetic resonance imaging (MRI) but presented abnormalities on electromyography. Furthermore, we suggest intramuscular electrical stimulation as an effective treatment option.

Case report

A 35-year-old female, who underwent thyroid cancer surgery two months ago, visited the outpatient clinic with complaints of left neck and shoulder pain, along with weakness and limited range of motion (ROM) in her left shoulder. The surgical procedures included bilateral total thyroidectomy with central compartment neck dissection and a modified radical neck dissection (MRND) on the left side. The numeric rating scale (NRS) pain score was 6 out of 10. Physical examination revealed limitation in the active ROM in the left shoulder joint: flexion (90°), abduction (90°), and external rotation (20°). Under the impression of brachial plexus injury, an electrodiagnostic study was performed at POD 53. The motor and sensory conduction studies were normal for bilateral axillary, dorsal scapular, and suprascapular, accessory nerves. However, needle electromyography revealed abnormal spontaneous activities in the left deltoid, supraspinatus, rhomboid, and sternocleidomastoid muscles, suggestive of an incomplete left brachial plexus injury (probably upper trunk lesion). Accordingly, to identify the exact lesion and the extent of the injury, MRI was taken on POD 57. There was no significant signal change in the brachial plexus. However, while the trunk level of the right brachial plexus appeared loose with a concave shape at the top, the left side looked tight, with the top being almost straight or convex (Figure 1). Additionally, distortion and edematous signal intensity were observed in the left neck muscles. The electrophysiological abnormality of the left brachial plexus is thought to be a secondary tension injury caused by edema and hypercontraction of the neck muscles. Therefore, intramuscular electrical stimulation was performed using a stimulator (Clavis, Alpine Biomed ApS, Denmark) under ultrasound guidance to relax the levator scapulae, scalene, sternocleidomastoid, and upper trapezius muscles. Square waves with 2 mA intensity and 0.2 ms pulse width were applied at a frequency of 2 Hz for 5 seconds at each stimulating point. Immediately after the treatment, the active ROM of left shoulder was improved: flexion (170°), abduction (160°), and external rotation (70°).

Conclusion

The incomplete brachial plexus injury, negative on MRI but positive on electrodiagnostic study, poses treatment challenges. High suspicion for secondary traction injury due to muscle changes is crucial in thyroid cancer patients after radical neck lymph node dissection. Targeting muscles rather than nerves may be key, with intramuscular electrical stimulation considered effective.

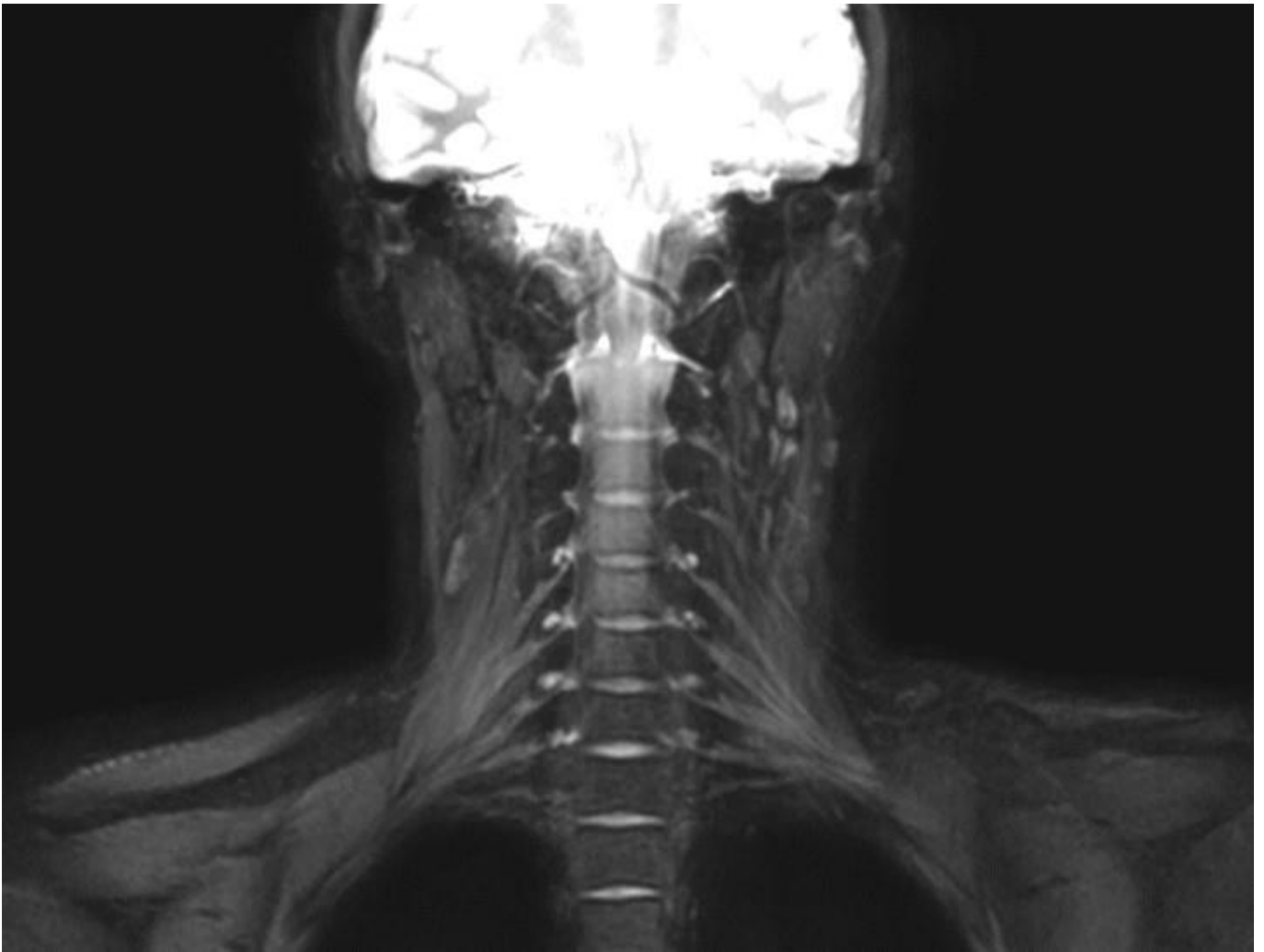


Figure 1. Magnetic resonance image of brachial plexus. There is no significant signal change in the left brachial plexus. Rather, at the trunk level of the right brachial plexus, it appeared loose with a concave shape at the top, while the left side appeared tight, with the top nearly straight or convex.

Bilateral Foot Drop Caused by L3-L4 Spinal Central Canal Stenosis

Heesung Nam^{1*}, Hyun dong Kim¹, Nami Han^{1†}

Department of Rehabilitation Medicine, Inje University Busan Paik Hospital¹

Introduction

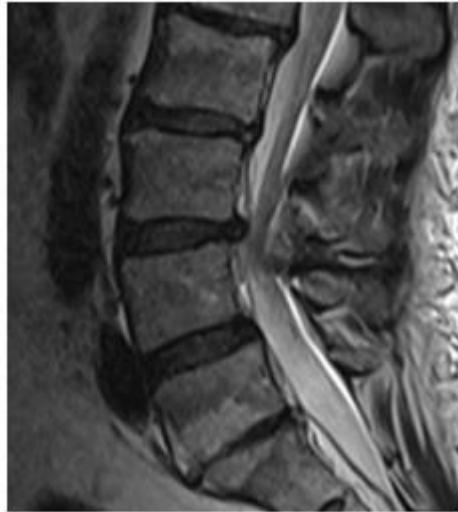
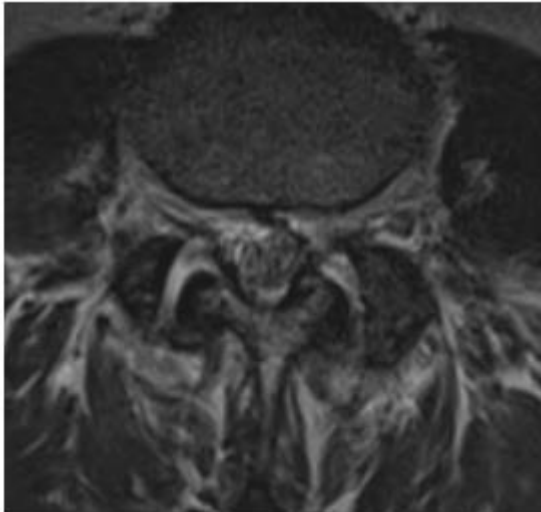
Foot drop is a general term for difficulty lifting the front part of the foot and it is a quite common symptom of degenerative lumbar diseases. Disc herniation and spinal canal stenosis are the two most common diseases causing foot drop. It is well known that the L4-L5 segment is the most commonly involved spinal level followed by the L5-S1 segment. Here, we present a sudden onset of bilateral foot drop caused by L3-L4 spinal canal stenosis.

Case report

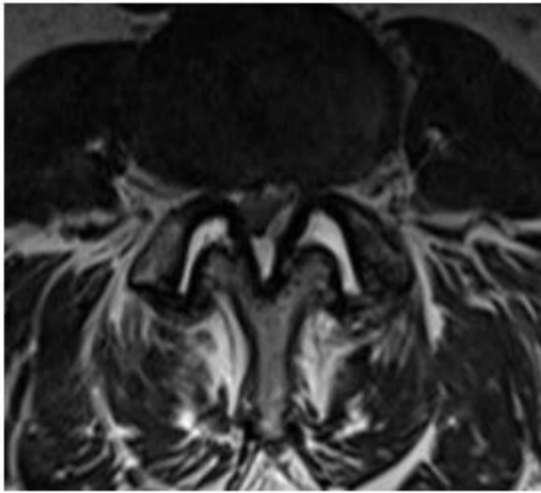
A 54-year-old woman visited a neurosurgical clinic with a history of progressive symptoms of radiating pain in her right leg and right foot drop for 2 weeks. She had a medical history of hypertension, bilateral carotid artery stenosis and severe obesity (Body mass index 40). At admission for further evaluation, motor examination revealed 2/5 strength in the right ankle dorsiflexion and 1st toe dorsiflexion on the manual muscle test. Sensory examination revealed a reduction of light touch and pinprick on the right L5 distribution. Magnetic resonance imaging (MRI) of her lumbar spine revealed moderate spinal central canal stenosis at L3-L4 (Fig1). Electrodiagnostic study showed 1+ fibrillations and positive sharp waves in right lumbar paraspinalis and extensor hallucis longus (EHL), extensor digitorum brevis (EDB) and we diagnosed right L5 radiculopathy. Neurosurgical doctor hesitated to operate because of the difference between the MRI-confirmed lesion and the Electrodiagnostic study-confirmed lesion and the patient's obesity. So she was transferred to the department of rehabilitation for non-surgical treatment. Her symptoms progressed after falling down during hospitalization, presenting bilateral foot drop (1/5 strength in both ankle and 1st toe D/F) Follow-up Electrodiagnostic study showed 2+ fibrillations and positive sharp waves at bilateral Tibialis anterior (TA), EHL, peroneus longus, EDB, and along L4-L5 lumbar paraspinalis and we diagnosed bilateral L5 radiculopathy. A newly taken lumbar MRI showed aggravated central canal stenosis at L3-L4 (Fig 2). Bilateral laminectomy and posterolateral fusion at L3-L4 were then performed (Fig 3). After 2 months of surgery, motor weakness had improved at bilateral ankle and 1st toe from 1/5 to 4/5 and at bilateral hip flexors from 3/5 to 4/5, enabling independent gait after 6 months of surgery.

Discussion

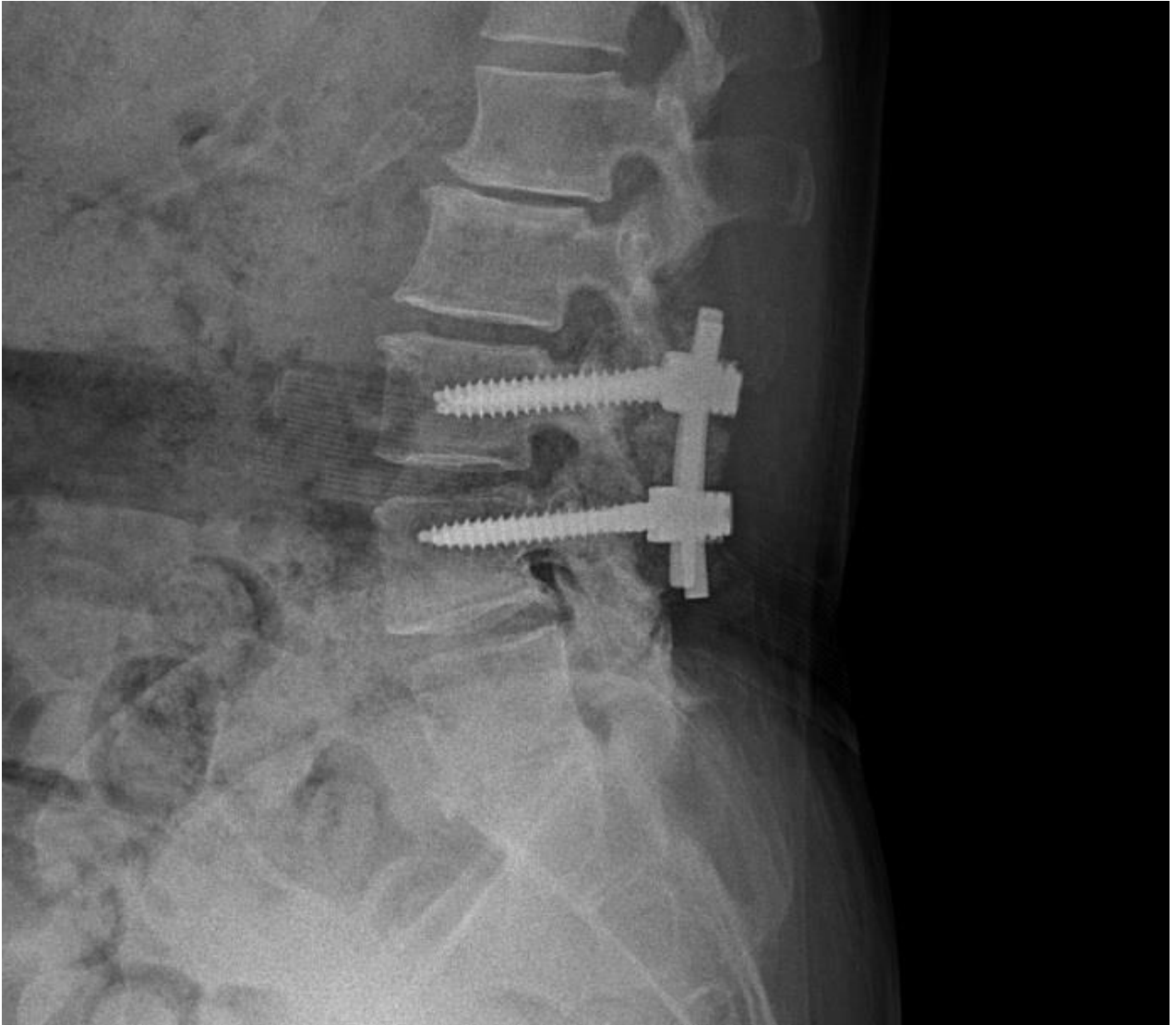
This case is unique because bilateral foot drop was caused by Electrodiagnostic study-proven compression of the traversing L5 nerve root at the L3-L4 level, without any anatomical variation of the nerve root. In cases of sudden onset of bilateral foot drop, a central lesion or peripheral polyneuropathy like Guillaine-Barre Syndrome is usually considered first. Spine lesions at the upper lumbar level may be overlooked due to their prevalence. However, as proven in this case, the traversing L5 nerve root can be compressed along the upper pathway leading to bilateral foot drop.



Lumbar spine MRI T2 image. L3-L4 spinal stenosis was observed.



Lumbar spine MRI T2 image. L3-L4 spinal stenosis was aggravated after fall down.



Lumbar spine X-ray, lateral view. posterolateral fusion at L3-L4.

Sjogren syndrome causing Leriche syndrome in a woman with bilateral leg pain: a case report

Gun Seo Jung^{1*}, Kyoung Tae Kim¹, Soyoung Lee¹, Jang Hyuk Cho^{1†}

Department of Rehabilitation Medicine, Keimyung University Dongsan Hospital, Keimyung University School of Medicine, Daegu, Republic of Korea¹

Background

Leriche Syndrome is a rare and critical vascular condition, that causes the progressive atherosclerotic obliteration of the terminal part of the abdominal aorta, iliac arteries and femoropopliteal vessels. This disease is frequently unrecognized or misdiagnosed, the exact prevalence and incidence are also unknown. Sjogren syndrome is a systemic autoimmune disease commonly presenting with dryness involving the eyes and mouth due to inflammation. Atherosclerosis risk increases in patients with systemic autoimmune diseases, there were few data on Sjogren syndrome.

Case presentation

A 69-year-old female patient was referred to our clinic from the Department of Rheumatology due to progressive and constant cramping pain and intermittent claudication in bilateral extremities for 6 months. She reported Sjogren syndrome, taking celecoxib and hydroxychloroquine for 4 years. The patient denied other medical conditions as hypertension, hyperlipidemia, hyperglycemia, and smoking. Motor and sensory examination revealed normal. Nerve conduction studies of her lower extremities performed were normal and symmetrical. Magnetic resonance imaging revealed a protruded intervertebral disc at the L4 and L5 vertebral levels, but no obvious stenotic findings was seen in spinal canal. She underwent conservative managements including physical therapy, caudal approach epidural steroid injection, and pregabalin medication. However, the pain was refractory to those managements.

The ankle-brachial index was 0.44 on the right side and 0.51 on the left side, indicating bilateral vascular disease. Abdominal contrast-enhanced computed tomography angiography showed occlusion from the infrarenal abdominal aorta to bilateral common iliac arteries, with collateral pathways. Based on the clinical and radiographic findings, a diagnosis of aortoiliac occlusive disease, also called Leriche syndrome was made. She underwent an aorto-biiliac bypass surgery and showed no other complication in Department of Vascular Surgery.

Discussion and conclusion

Atherosclerosis could be caused and accelerated by inflammation of arteries' wall, however, the exact immune mechanisms are still unknown. The association between Sjogren syndrome and atherosclerosis haven't been explained for now, and the pathophysiology of atherosclerosis in Sjogren syndrome are also yet be discovered. More studies need to be conducted to find the pathophysiology of atherosclerosis in Sjogren syndrome with Leriche syndrome or vascular event.



fig 1. Abdominal contrast-enhanced computed tomography angiography

Cellulitis Following Ethanol Injection in a Hemiplegic Patient: A Case Report

JEONG SEOB KIM^{1*}, SUK BONG YUN^{1†}

Department of Rehabilitation Medicine, Presbyterian Medical center¹

Introduction

Cellulitis is an infection of the skin and underlying tissues, commonly caused by bacterial infections, trauma or lacerations, skin damage following surgical procedures, chronic edema, and inflammatory reactions due to drug injections. This case report discusses the rare complication of cellulitis spreading to distant sites following muscle injection with 99.5% ethanol for the improvement of ankle clonus, which is unique and noteworthy in itself.

History and Examination

A 48-year-old female patient presented with right-sided hemiplegia due to T-SAH and T-SDH, necessitating hospitalization for rehabilitation. While ambulatory with the aid of a Q-cane, she experienced significant ankle clonus on the right, impairing her gait. During hospitalization, ethanol injections were administered into the tibialis posterior and gastrocnemius muscles, resulting in improvement of the ankle clonus. However, three days post-injection, the patient developed swelling, erythema, and fever in the right calf and foot. Laboratory tests revealed a white blood cell count of 13,000/ μ L and a CRP level of 14 mg/dL. A foot CT scan confirmed cellulitis findings on the top of the toes.

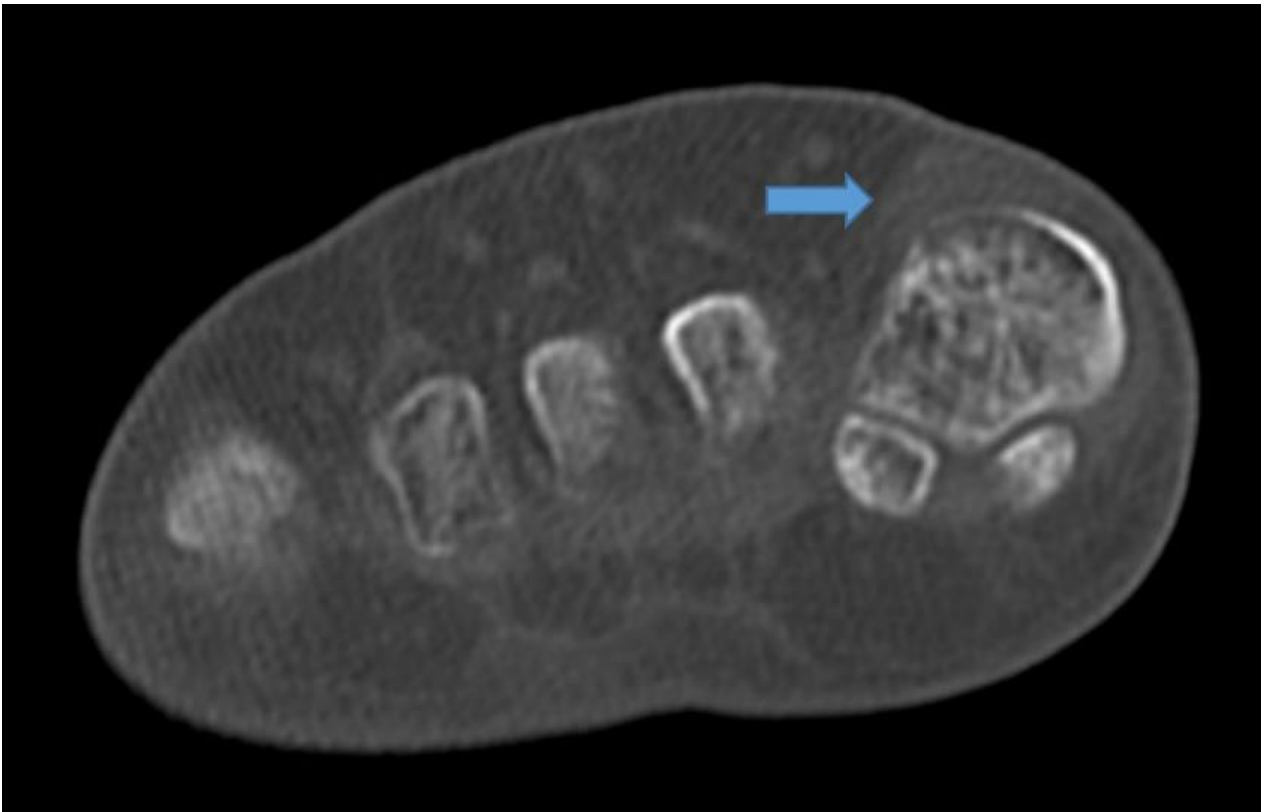
Discussion

Cellulitis can arise from various causes, and in this case, it occurred as a rare complication following muscle injection. Particularly in hemiplegic patients, limited muscle movement may impede adequate blood circulation and lymphatic drainage, facilitating the spread of cellulitis from the calf, where ethanol was injected, to the foot. The cellulitis that developed post-injection originated from the site of ethanol injection in the calf but rapidly disseminated to the foot due to restricted mobility and compromised immune function associated with hemiplegia.

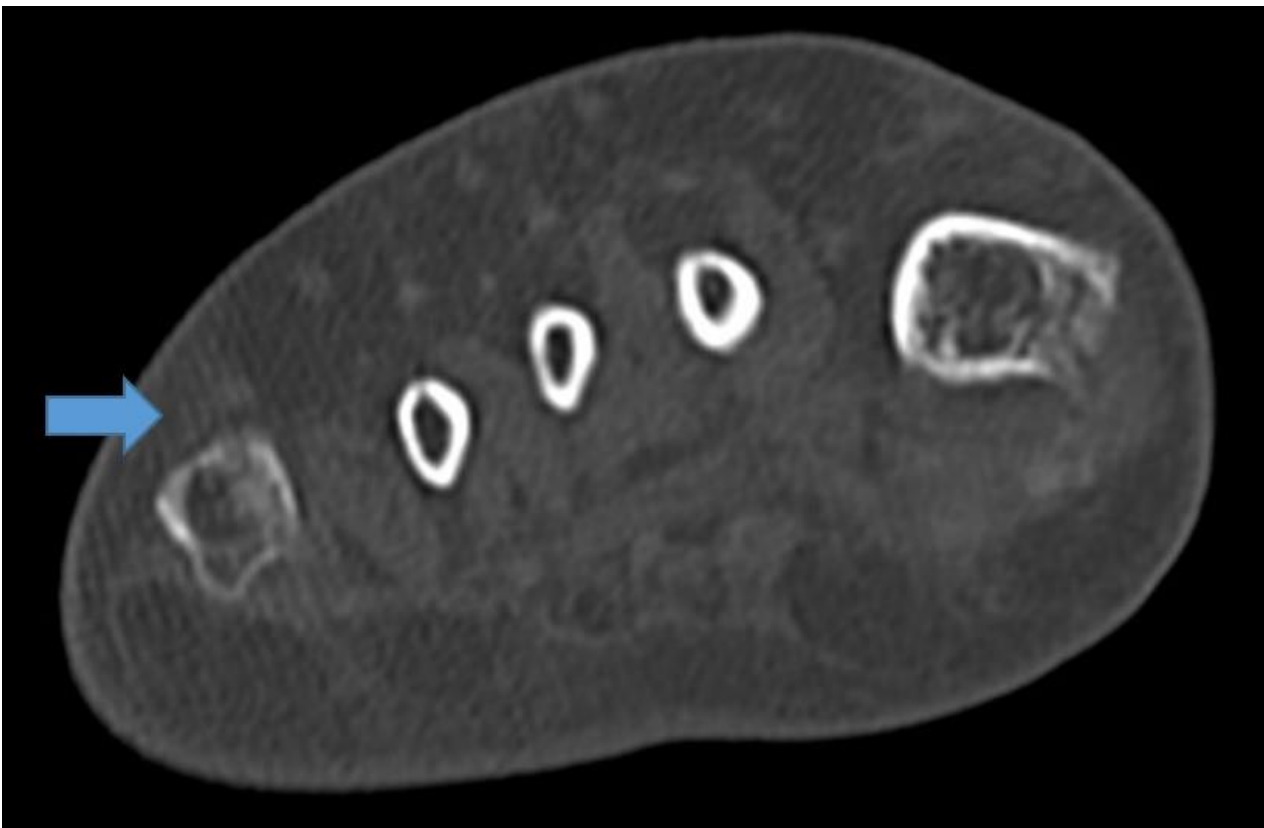
Treatment of cellulitis following ethanol injection involves the use of various antibiotics, and in this case, clarithromycin was chosen for its efficacy against skin pathogens such as *Streptococcus* and *Staphylococcus aureus*. Clarithromycin, a widely recognized antibiotic for these bacteria, contributed to the improvement of the patient's symptoms. Particularly in hemiplegic patients, there is a risk of compromised immune responses to bacterial infections, necessitating prompt diagnosis and appropriate antibiotic therapy.

Conclusion

This case report highlights a unique pathway of cellulitis development following muscle injection with ethanol, emphasizing the rapid spread from the calf to the foot due to impaired muscle movement and immune function in a hemiplegic patient. Effective treatment with clarithromycin resulted in symptom improvement, underscoring the importance of early diagnosis and appropriate antibiotic management in preventing complications. Such cases provide valuable insights into the potential complications of muscle injections in rehabilitation medicine. Continuous monitoring and evaluation of the patient's treatment course will contribute to optimizing cellulitis management strategies.



CT scan: blue arrow indicates cellulitis on the big toe.



CT scan: blue arrow indicates cellulitis on the little toe.

A 42-year-old Patient with Renal Cell Carcinoma Presenting as Low Back Pain: A case report

Jong Ha Lee¹, Dong Hwan Yun¹, Jinmann Chon¹, Yunsoo Soh¹, Ga Yang Shim¹, Seongmin Choi¹, Min-Su Kim¹, Hong Jun Kim², Yewan Park³, So-Woon Kim⁴, Myung Chul Yoo^{1**}

Department of Physical and Rehabilitation Medicine, College of Medicine, Kyung Hee University¹, Division of Medical Oncology-Hematology, Department of Medicine, , College of Medicine, Kyung Hee University², Department of Internal Medicine, Kyung Hee University Medical Center³, Department of Pathology, College of Medicine, Kyung Hee University⁴

Purpose

Renal cell carcinoma (RCC) is the most common renal neoplasm, accounting for 2.4% of all cancers in Korea. Although the usual clinical manifestations of RCC include flank pain, hematuria, and palpable mass, RCC is generally characterized by a lack of early warning signs and is mostly discovered incidentally in advanced stage. This case report describes a 42-year-old Korean man diagnosed with giant RCC who presented with simple back pain.

Patient concerns: The clinical manifestation of a 42-year-old Korean man was chronic back pain.

Diagnoses

Contrast-enhanced computed tomography showed a 19.1-cm sized heterogeneous enhancing mass on the right kidney and tumor thrombosis extending into inferior vena cava.

Intervention

Due to the large size of the tumor and extensive tumor thrombosis, the multidisciplinary team decided to administer neoadjuvant chemotherapy and an anticoagulant. Following 12 cycles of treatment with nivolumab and cabozantinib, he underwent a right radical nephrectomy with an adrenalectomy and tumor thrombectomy.

Outcomes

Treatment was successful and post-treatment he started a cancer rehabilitation program. He was followed-up as an outpatient and no longer complains of back pain.

Lessons

RCC can manifest clinically as back pain, with diagnosis being difficult without appropriate imaging modalities. RCC should be included in the differential diagnosis of patients with low back pain, even at a young age.

Acknowledgment This work was supported by a National Research Foundation of Korea (NRF) grant funded by the Korean government (MSIT) (RS-2024-00346622).



Figure 1. Abdominal radiography, anterior-posterior view, of this patient, showing a mass-like opacity (arrow) in the right abdomen.



Figure 2. Abdominal computed tomography, axial view, of this patient, showing a heterogeneous enhancing mass (arrow) replacing the right kidney with nephromegaly (long diameter, 19.1 cm), with the mass extending into the renal pelvis and proximal ureter, suggesting a malignant renal tumor.

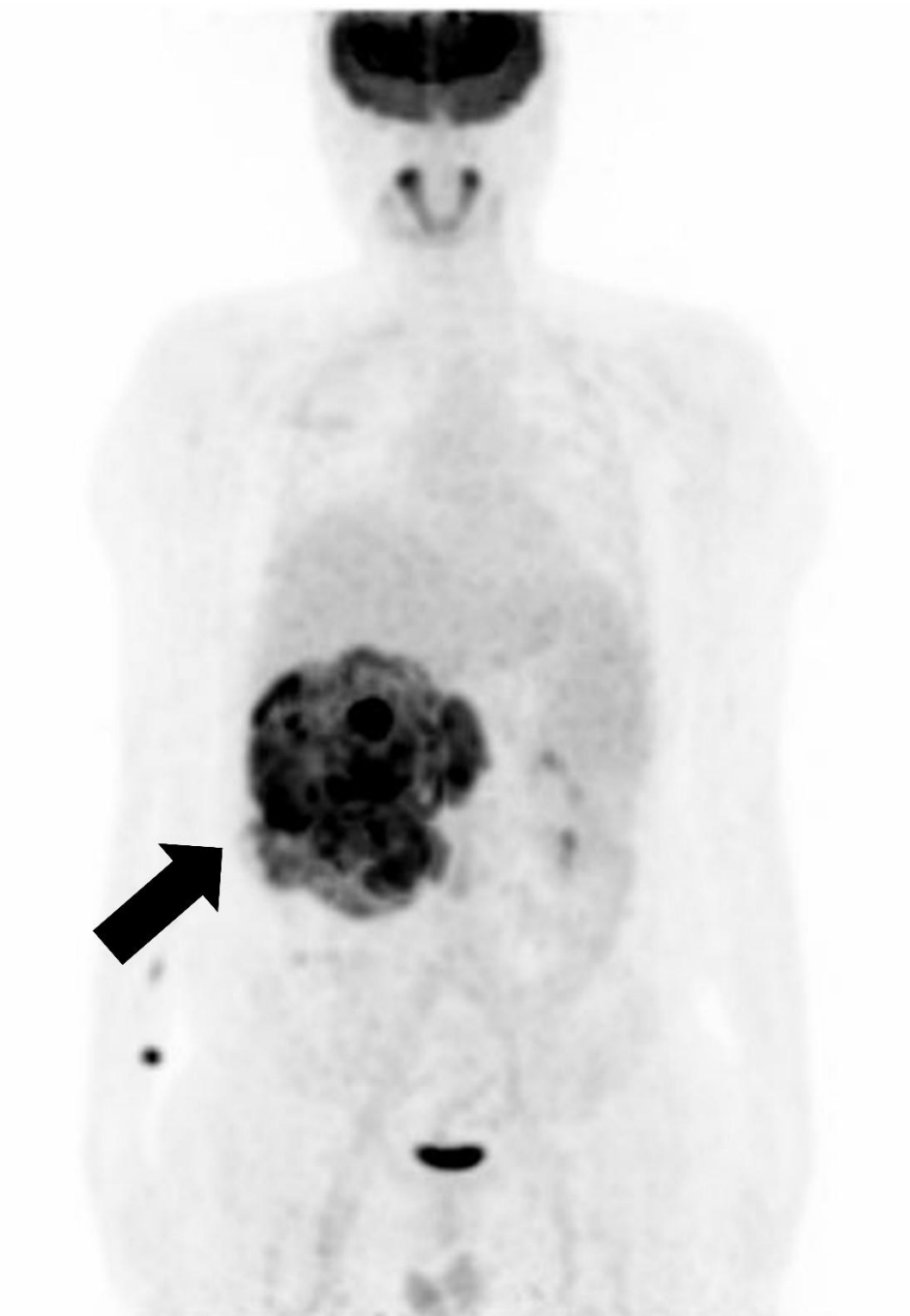


Figure 3. Whole-body positron emission tomography/computed tomography, anterior-posterior view, of this patient, showing a huge hypermetabolic lesion in the right kidney with maximum standardized uptake values of 13.3 (arrow), consistent with RCC, and involving the proximal ureter. Probable metastatic lymph nodes were detected in the retrocaval and aortocaval areas, along with tumor thrombosis in the right renal vein and inferior vena cava.

Successful Conservative Management of Plantar Fasciitis: A Case Report for Rehabilitation Medicine

JEONG SEOB KIM^{1*}, SUK BONG YUN^{1†}

Department of Rehabilitation Medicine, Presbyterian Medical Center¹

Introduction

Plantar fasciitis is an inflammatory condition of the plantar fascia, leading to severe heel pain, especially noticeable during the first steps in the morning or after prolonged standing or walking. This case report examines the effectiveness of conservative treatment methods for a 45-year-old female patient, Ms. L, with plantar fasciitis in her right foot. The report highlights the successful combination of various treatments to alleviate pain and enhance the patient's quality of life.

History and Examination

Ms. L began experiencing plantar fasciitis symptoms in her right foot during winter, characterized by severe heel pain during the first steps in the morning and recurring pain after prolonged standing or walking, exacerbated by cold weather. Initial diagnosis revealed inflammation and tension in the plantar fascia of her right foot. An initial treatment plan included stretching exercises for the plantar fascia and Achilles tendon, strengthening exercises, rest, and cold compresses.

Discussion

Plantar fasciitis can be caused by overuse, improper footwear, obesity, and structural foot abnormalities, leading to stress and inflammation in the plantar fascia. Treatment options range from conservative methods like rest, cold compresses, stretching exercises, physical therapy, and NSAIDs to more aggressive approaches such as steroid injections, acetic acid iontophoresis, extracorporeal shock wave therapy (ESWT), and surgery.

Conservative treatment was chosen for Ms. L due to the initial non-severity of her symptoms, the lower side effects compared to invasive treatments, and the potential for patient self-management. The initial lack of significant pain improvement after two weeks led to a revised treatment plan incorporating acetic acid iontophoresis, taping, and manual therapy, alongside continued home exercises.

Four weeks into the revised treatment plan, Ms. L's pain in her right foot significantly reduced, with her visual analogue scale (VAS) pain score dropping from 7 to 3. Continuing with rehabilitation exercises and supplementing with vitamin C and glucosamine sulfate, her pain nearly disappeared after eight weeks, achieving a VAS score of 0. Ms. L could resume daily activities without significant discomfort.

Conclusion

Ms. L's case demonstrates the high effectiveness of conservative treatment for managing plantar fasciitis in the right foot. The combination of initial and mid-term treatments led to a gradual decrease in pain, ultimately allowing her to live pain-free. This multi-faceted approach, involving stretching, strengthening exercises, rest, cold compresses, acetic acid iontophoresis, taping, and manual therapy, offers a valuable reference for treating other patients with plantar fasciitis in rehabilitation medicine.



Calcaneal spur



Plantar fasciitis taping techniques

Evaluation of a New Hybrid Brace for Scoliosis: Usability tests and Finite Element Analysis

Doyoung Kim^{1*}, Sanghoon Shin¹, Min-Chul Paek¹, Sanghyun Jee¹, Hae Won Choi², In Seok Han², Chan Woong Jang³, Sang Kuy Han², Jung Hyun Park^{1,4,5†}

Department of Rehabilitation Medicine, Gangnam Severance Hospital, Yonsei University College of Medicine, Seoul, Republic of Korea¹, Korea Institute of Industrial Technology, Ansan Gyeonggi-do, Republic of Korea², Department of Physical Medicine and Rehabilitation, Hallym University Sacred Heart Hospital, Hallym University College of Medicine, Anyang, Republic of Korea³, Department of Integrative Medicine, The Graduate School, Yonsei University College of Medicine, Seoul, Republic of Korea⁴, Department of Medical Device Engineering and Management, Yonsei University College of Medicine, Seoul, Republic of Korea⁵

Introduction

Scoliosis, characterized by a three-dimensional deformity of the spine and rib cage, is often managed with orthotic hard braces to prevent curve progression and minimize deformity. Effective treatment hinges on developing more comfortable braces to enhance compliance and outcomes. This study aims to assess a novel hybrid soft brace for scoliosis treatment using usability testing and a subject-specific finite element (FE) analysis.

Materials and Methods

The soft hybrid brace (The Spinamic®, version 2.0 beta, VNTC., Ltd., Seoul, Korea), designed for better fit and comfort, features a thoracic-hump band, lumbar band, and pelvic belt (Figure 1). It includes textile multi-layer pressure sensors that measure and transmit pressure data via Bluetooth, adjusting pressure according to the patient's body shape. First, we performed usability tests using this brace on patients with moderate scoliosis. Then, a subject-specific finite element (FE) analysis was conducted using a digital X-ray model of a single patient (a 15-year-old male) with a Cobb angle of 18.97°. The patient-specific spine model was adapted to reflect individual anatomy and material properties were drawn from existing literature. Pressures were applied at three locations on the FE model: thoracic apex, hump (9th-11th rib), and lumbar apex (L2-L5). Simulated scoliosis correction was evaluated at each site and particularly focusing on pressure applied at various parts of the thoracic apex (upper, middle, and lower) based on severity (Figure 2).

Results

For the 11 patients wearing the new soft hybrid brace, the usability tests showed an average Cobb angle correction from $34.0 \pm 5.0^\circ$ to $26.6 \pm 3.4^\circ$ (a 22.9% improvement) (Table 1). The FE model simulations demonstrated Cobb angle corrections of 14.1° (24.4% improvement) when pressure was applied to the upper thoracic apex, 13.1° (29.4% improvement) for the middle thoracic apex, and 11.8° (36.4% improvement) for the lower thoracic apex. The most significant correction was achieved when pressure was applied to the lower part of the thoracic apex at FE model. X-ray images verified the FE model's predictions, showing a reduction in the Cobb angle from 18.9° to 9.7° (a 51.1% correction) when wearing the hybrid brace. The FE analysis demonstrated that the correction effects predicted by the model closely matched the actual results, revealing optimal pressure application areas (lower thoracic apex) for maximum corrective impact.

Conclusion

The new soft hybrid brace showed initial corrective performance comparable to established hard braces. This study highlights an effective evaluation methodology for predicting the therapeutic efficacy of newly developed hybrid braces for scoliosis via initial performance assessments and customized finite element modeling. By targeting areas requiring relatively low pressure, this approach could lead to optimal scoliosis correction, improving both comfort and treatment outcomes.

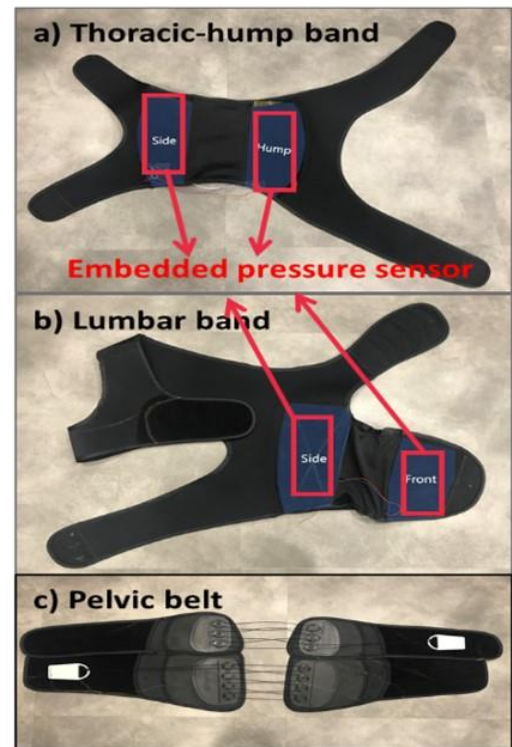


Fig 1. A new soft hybrid brace comprising a mixture of fabric and plastic plate developed for patients with scoliosis

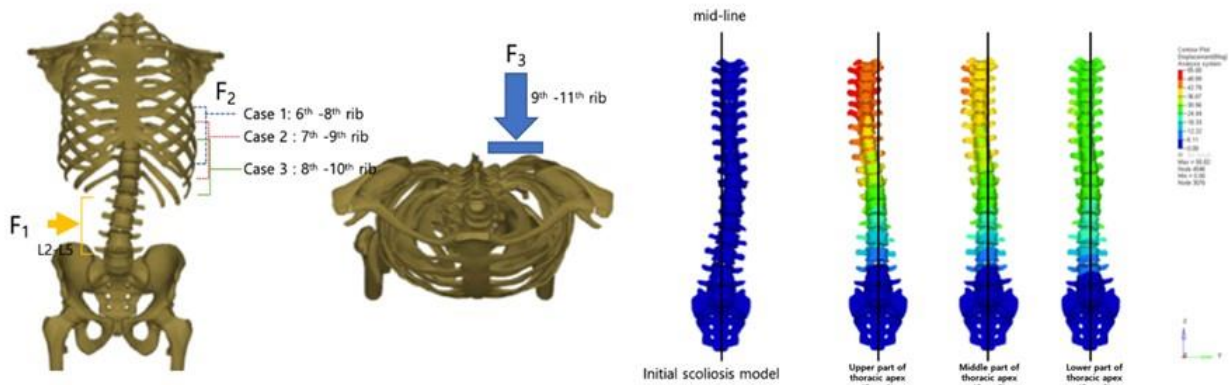


Fig 2. Boundary and loading conditions for corrective analysis & contour plot of displacement results

Patient number	Cobb angle (°)		correction rate (%)
	prior to wearing brace	post wearing brace	
1	9.1	17.8	6.6
2	31.8	26.9	15.4
3	15.1	12.5	17.4
4	22.0	15.9	27.8
5	44.7	37.5	16.1
6	39.2	34.4	12.3
7	58.9	31.5	46.6
8	44.1	40.6	8.0
9	43.6	34.5	21.0
10	46.5	31.6	32.1
11	18.9	9.7	48.7
Average	34.0	26.6	22.9

Table 1. Comparisons of Cobb angles between prior to and post wearing soft hybrid brace

White-Sutton syndrome arising from a de novo missense mutation in POGZ : a case report

Hye Jung Park^{1*}, Ah Yeon Lee¹, Myungshin Kim², Joo Hyun Park^{1†}

Department of Rehabilitation Medicine, Seoul St. Mary's Hospital, College of Medicine, The Catholic University of Korea¹, Department of Clinical Laboratory Medicine, Seoul St. Mary's Hospital, College of Medicine, The Catholic University of Korea²

Introduction

White-Sutton syndrome(WHSUS) is a neurodevelopmental disorder characterized by a wide range of developmental delay, and/or intellectual disability, as well as autistic features. WHSUS is also associated with low muscle tone, feeding difficulties, vision problems, hearing loss, seizures, and distinct facial features.

We present a case of a 3-year-old male with a de novo POGZ (Pogo transposable element with ZNF domain) gene mutation (c.1954T>A, heterozygous), showing variant degree of development delay, especially in motor and expressive communication area, as well as findings of diffuse tensor tractography.

Case Report

A 4-months-old boy was referred to our department of rehabilitation medicine for evaluation of possible developmental delay. He was born at full term with a birth weight of 2120g by cesarean section delivery and admitted to the neonatal intensive care unit for 5 days due to intrauterine growth retardation. Persistent failure to thrive was noted, with weight-for-height particularly below the 5th percentile. K-DST(Korean Developmental Screening Test for Infants & Children) indicated that follow-up and further testing were needed for motor, cognitive, language, and social domains. From that time, he continued with physical and occupational therapy, and later, speech therapy.

Assessments of the patient using the Bayley III, Sequenced language scale for infants (SELSI) and Preschool Receptive-Expressive language Scale (PRES) are presented in the tables below (Table 1-1, 1-2). He began independent walking at 17 months of age. Brain MRI performed at age of 18 months showed no definite structural abnormality. However, in diffusion tensor tractography, the left corticoreticular pathway(CRP) and corticopontocerebellar tract(CPC) from the left cortex to the right cerebellum were not reconstructed compared to contralateral side. Tract volume estimates for the left corticospinal tract(CST) and right arcuate fasciculus(AF) were significantly decreased in the patient compared with tract volume estimates from the other side (Fig 1).

Chromosomal microarray analysis (CMA) showed no significant deletion or duplication of genes. However, in targeted next generation sequencing (NGS), mutation of POGZ gene (c.1954T>A) was detected. Subsequent segregation study of his unaffected parents revealed no identical mutation in any of them, implying the mutation is de novo (Table 2). Though it is not yet known as pathogenic mutation, considering the fact that the patient was also presented with other clinical features of WHSUS, the mutation is highly likely pathogenic.

Conclusion

The POGZ gene plays a crucial role in the development and function of the brain. We present a case of a de novo POGZ gene mutation associated with developmental delay, especially in motor and communication skills. Additional evaluation is planned to assess the intellectual disability and autistic spectrum disorder that can occur in WHSUS.

Acknowledgment This research was supported by a grant of the Korea Health Technology R&D Project through the Korea Health Industry Development Institute (KHIDI), funded by the Ministry of Health & Welfare, Republic of Korea (grant number : HR22C160504)

Developmental evaluation (The Bayley III)	9months 2days		15months 7days		24months 19days	
	DAE (months)	Composite Score	DAE (months)	Composite Score	DAE (months)	Composite Score
Cognitive	7	85	17	110	25	100
Receptive communication	5.33	89	11	89	21	86
Expressive communication	9		14		19	
Fine motor	6	70	12	76	26	100
Gross motor	7		10		23	
Social-emotional	-	95	-	85	-	100
Adaptive behavior	-	84	-	92	-	93

DAE; Developmental age equivalent

Table 1-1. Developmental evaluation using the Bayley III scales of Infant Development.

Speech evaluation	SELSI (24 months of age)		PRES (34 months of age)	
	DAE	Quotient	DAE	Quotient
Receptive communication	22 months	91.7	41 months	120.6
Expressive communication	20 months	83.3	36 months	105.6

DAE; Developmental age equivalent

Table 1-2. Speech evaluation by using Sequenced language scale for infants (SELSI) and Preschool Receptive-Expressive language Scale (PRES)

Table 1-1. Developmental evaluation using the Bayley III scales of Infant Development, Table 1-2. Speech evaluation by using Sequenced language scale for infants (SELSI) and Preschool Receptive-Expressive language Scale (PRES)

	<i>POGZ</i> c.1954T>A	<i>KMT2D</i> c.2534G>A
Patient's father		
Patient's mother		
The patient		

*Colored section means mutation was detected

Table 2. Findings of targeted next generation sequencing (NGS) in the patient's family. The POGZ gene which is known to be related to White-Sutton syndrome (WHSUS), is only found in the patient.

Table 2. Findings of targeted next generation sequencing (NGS) in the patient's family. The POGZ gene which is known to be related to White-Sutton syndrome (WHSUS), is only found in the patient.

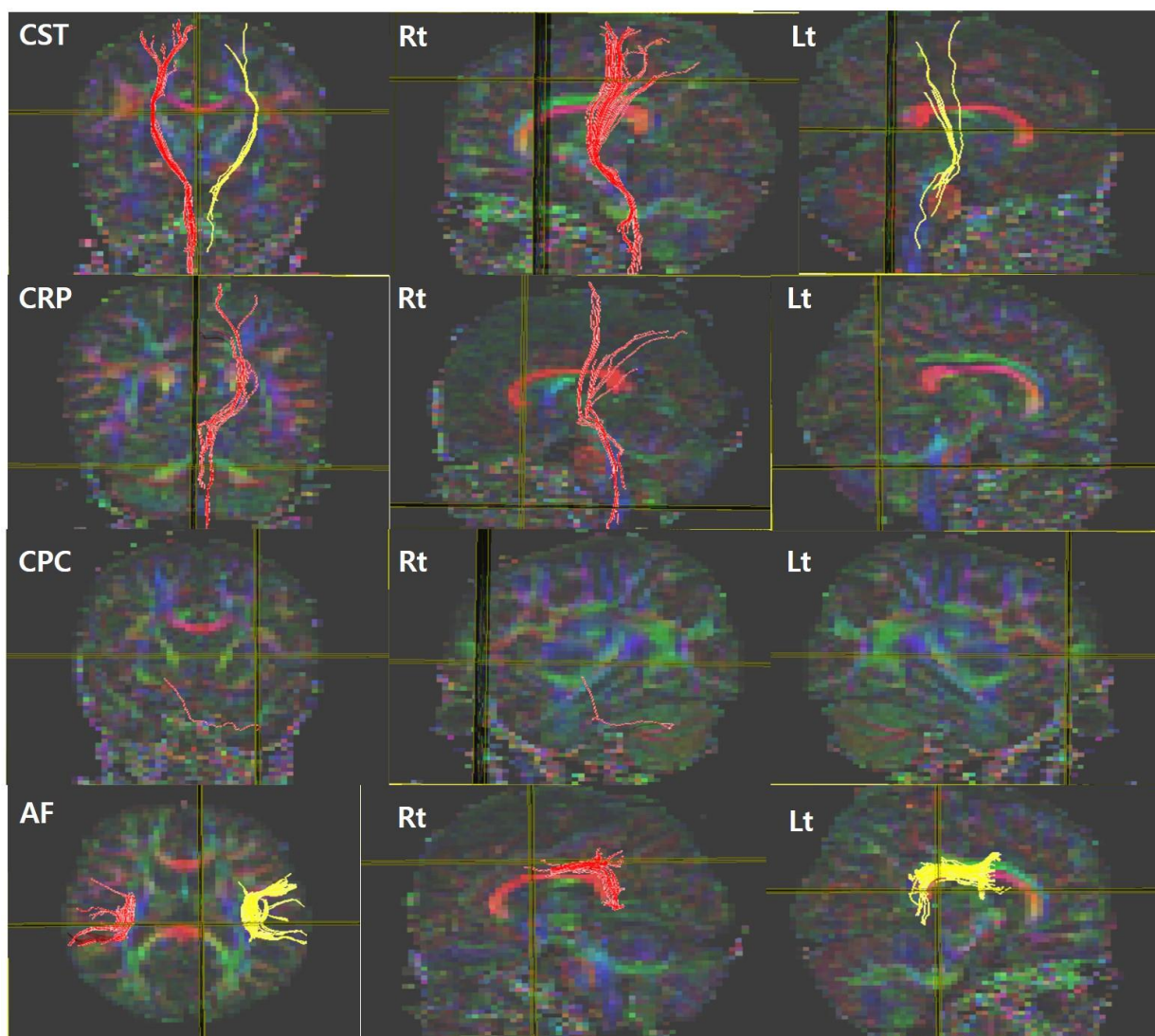


Fig1. Diffusion tensor tractography

Novel NUS1 Mutation in a child with neurodevelopmental Disorder and Ataxia

Seung Jun Lee^{1*}, Hyun Jung Lee^{1†}, So Young Lee¹, Jun Hwan Choi¹

Department of Rehabilitation Medicine, Jeju National University Hospital¹

Introduction

Neurodevelopmental disorders (NDDs) encompass a broad spectrum of conditions characterized by developmental deficits that can significantly impair personal, social, academic, or occupational functioning. Recent advancements in genomic technologies, such as Whole Genome Sequencing (WGS) and Whole Exome Sequencing (WES), have significantly enhanced our ability to identify genetic mutations underlying NDDs. Among the numerous genes implicated in these disorders, the NUS1 gene has garnered particular attention due to its critical role in neurological function and development. This report describes a case involving genetic abnormalities contributing to a severe neurodevelopmental disability with ataxia.

Case report

The patient, a 9-year-old girl, initially presented with global developmental delays observed since infancy and later developed ataxia and tremors. She was born at gestational age 40 weeks, weighing 3.3 kg, via vaginal delivery with no perinatal complications. In early childhood, she began experiencing seizures. At age 7, she was assessed to have moderate intellectual disability and mild to moderate autism. Due to observed hand tremors and ataxia, a brain MRI was attempted but was unsuccessful due to sedation challenges and the chromosomal Microarray Analysis (CMA) revealed genomic duplications at loci 2q34.q35 and 20q13.33 (Figure 1). The 2q34q35 region duplication is classified as a variant of uncertain significance (VUS), which is noted in clinical reports to be associated with intellectual disability and behavioral abnormalities. Additionally, the 20q13.33 duplication is known for its role in maintaining proper electrical activity of neurons, related to neonatal seizures. These findings align with the patient's symptoms of intellectual disability, seizures, and autism but do not fully explain the symptoms of tremors and ataxic gait. During the outpatient visit, the patient's mother also displayed tremors and dysmetria in both hands, decreased motor coordination abilities. This prompted simultaneous WGS for both the mother and the child, and CMA for the mother. This extensive sequencing effort revealed a novel deletion mutation in the NUS1 gene, found in both the mother and the daughter (Figure 2). Unlike her daughter, the mother's CMA results were normal. Pathogenic or likely pathogenic NUS1 gene variants have been associated with neurological symptoms such as psychomotor retardation, refractory epilepsy, myoclonus, tremor, ataxia, and dystonia.

Conclusion

In this case, While CMA provided initial insights into large-scale genomic duplications, it did not detect the finer-scale mutation in NUS1. WGS was essential to uncover the precise small-scale deletion that was critical for an accurate diagnosis. The discovery of a novel NUS1 mutation in this familial case provides insights into the genetic underpinnings of NDDs and underscores the utility of advanced genetic testing in clinical practice.

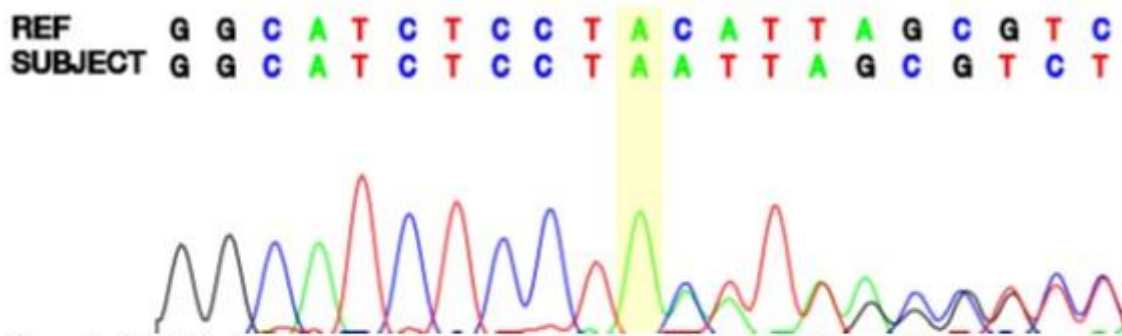


Figure 2. Identification of the heterozygous likely pathogenic NUS1 mutation in the patient and her mother.

The sequencing chromatogram displays the nucleotide sequence surrounding the mutation site. The highlighted yellow region indicates the position of the c.393del mutation (p.Tyr131Ter). The alignment of the reference (REF) and subject (SUBJECT) sequences illustrates the heterozygous deletion observed in the patient.

The sequencing chromatogram displays the nucleotide sequence surrounding the mutation site. The highlighted yellow region indicates the position of the c.393del mutation (p.Tyr131Ter). The alignment of the reference (REF) and subject (SUBJECT) sequences illustrates the heterozygous deletion observed in the patient.

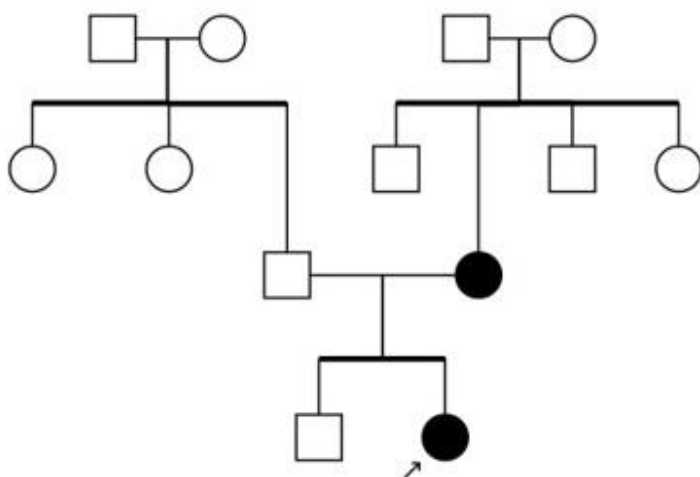


Figure 3. Pedigree chart of the family.

The chart shows the inheritance pattern of the identified NUS1 mutation. The filled symbols represent affected individuals, and the arrow indicates the proband. The mother's symptoms included tremor, dysmetria, ataxia, and intellectual disability.

The chart shows the inheritance pattern of the identified NUS1 mutation. The filled symbols represent affected individuals, and the arrow indicates the proband. The mother's symptoms included tremor, dysmetria, ataxia, and intellectual disability.

Leigh syndrome in an infant: case report

Se Hee Jung^{1**†}, Yu-ri Lee¹, Yeonggi Song¹, Ji Hee Jeon¹, Hee Young Cha¹

Department of Rehabilitation Medicine, Seoul National University College of Medicine¹

A 4-month-old girl was brought to an outpatient clinic. Her mother was told that her baby had a spasticity while she saw a pediatrician. The girl could not control her neck and tended to rotate her neck to the right side. The passive range of motion of her neck was symmetric both in tilting and rotation. Her Moro reflex was asymmetric. Her muscle tone was within normal range in limbs but was variable. Her axial muscle tone was decreased. On Bayley Scales of Infant and Toddler Development, every area showed extremely delayed development. She underwent brain magnetic resonance imaging, which revealed no definite abnormality. When she was followed-up one month later, she showed significant motor developmental delay with dyskinetic limb movement pattern and poor axial control and axial muscle tone. She also had abnormal visual gaze and abnormal General Movements such as poor repertoire and absent fidgety movements. As having more distinctive abnormality since last visit which was not supported by brain MRI findings, we consulted her to a department of clinical genetics. The genetic test confirmed that she had a Leigh syndrome. At 21 months of age, she shows a severe dystonia both in limbs and axial muscles. She has a severe developmental delay in every aspect even with a comprehensive physical and occupational therapy.

Encephalomyelopathy and axonal polyneuropathy in Influenza A virus infection

Yumi Ha ^{1*}, Jeongyi Kwon ^{1†}

Department of Rehabilitation Medicine, Samsung Medical Center ¹

Influenza A is a disease that can be life-threatening and can lead to multiple organ failure. It can cause respiratory problems like ARDS (Acute Respiratory Distress Syndrome) and also affect the brain, spine, and peripheral nervous system.

A 16-year-old boy presented with dyspnea and fever and was diagnosed with Influenza A. He was admitted to the intensive care unit due to desaturation. Despite the insertion of ECMO (Extracorporeal Membrane Oxygenation), he showed ventricular fibrillation and cardiac arrest but achieved spontaneous circulation after 20 minutes of cardiopulmonary resuscitation. An echocardiogram revealed hypertrophic cardiomyopathy and detection of the MYH7 gene mutation. He received CRRT (Continuous Renal Replacement Therapy) for oliguria and underwent steroid pulse therapy and intravenous immunoglobulin therapy due to a suspected cytokine storm.

One month after admission, the patient was found to have quadriparesis, with significant weakness in his legs. Nerve conduction studies and electromyography confirmed motor-dominant axonal polyneuropathy. MRI revealed atrophy of the brain and spinal cord, along with ventricular enlargement. By six months, muscle strength in all limbs except the right lower limb had improved to fair or better.

Prolonged use of a mechanical ventilator, repetitive unsuccessful weaning trials, and ongoing CO₂ retention led to the use of fluoroscopy and ultrasound to evaluate the diaphragm, revealing bilateral diaphragmatic paralysis. After seven months of intensive physical rehabilitation, including respiratory rehabilitation training, he was able to undergo walking training with assistive devices and use a home ventilator with a mask only during sleep, without tracheostomy at the time of discharge.

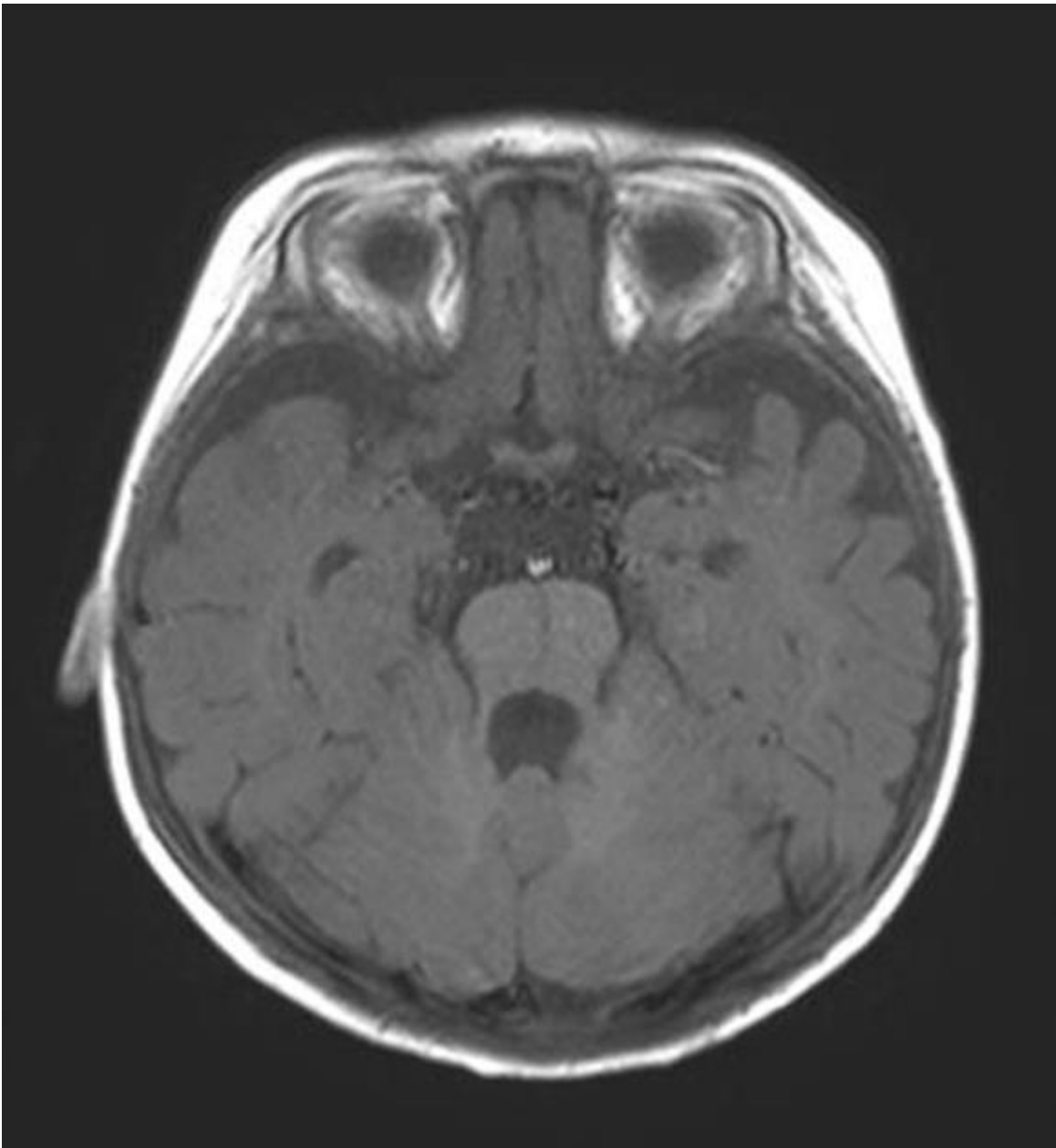
It is important to recognize that influenza can affect various parts of the nervous system, including the phrenic nerve, potentially leading to fatal or persistent disability. Therefore, it is crucial to carefully monitor the patient from multiple angles and explore diagnostic and treatment methods through a multidisciplinary approach.

Joubert syndrome in an infant: case report

Se Hee Jung^{1**}, Jeong-Uk Kim¹, Jeong Soo Lee¹, Ju-young Kang¹, Yeo Jin Lee¹

Department of Rehabilitation Medicine, Seoul National University College of Medicine¹

A 7-month-old girl was brought to an outpatient clinic. She could not make a secure eye contact until 4 months of age. She turned her head rapidly while she tried to look at an object. Her conjugate eye movement, saccade, smooth pursuit and vergence were all intact. There was no nystagmus, hyper- or hypotropia, Eso- or exotropia. However, she showed a definite oculomotor apraxia. She could not sit alone or come to sit. Her truncal control was poor. She could stay prone on both forearms only for short time. She did not have spasticity or increased muscle tone. She underwent brain magnetic resonance imaging, which revealed a molar tooth sign. She was diagnosed with Joubert syndrome. After the diagnosis, she has been on rehabilitation therapy. At 21 months of age, she has a gross motor developmental delay but her fine motor, language, and social development is relatively within normal range.



Her brain MRI shows a molar tooth sign.

How could Brainbridge-Ropers Syndrome Developmental delay be recognized?: A Case Report

Jin Hee Jung ¹, Sung Hyun Kim^{1**}

Department of Rehabilitation Medicine, Bundang Jesaeng Hospital¹

Introduction

Brainbridge-Ropers syndrome (BRPS) is a rare genetic condition that results from a change in function of a gene called additional additional sex combs like 3 (ASCL3). It is characterized by failure to thrive, global developmental delay, feeding problems, hypotonia, profound speech delays, and intellectual disability and dysmorphic features. Although several cases have been reported so far, they share these non-specific symptoms. In this report, we present the first reported case of BRPS in Korea.

Case presentation

He first visited our outpatient clinic at 12 months with developmental delay. He had no problems feeding, but overall hypotonia and head lagging were observed. The boy showed an overall low postural tone and appears to maintain a supported sitting posture with a kyphotic posture. He showed longish face with a prominent forehead, temporal narrowing and arched eyebrows. Deep tendon reflex was brisk, ankle clonus was not visible, and no other reflexes were observed.

According to the Bayley scales III performed at 12 months, overall developmental delay was confirmed at 5 months in cognitive ability, 5 months in language, 5 months in fine motor skills, and 5 months in gross motor skills. Brain MRI, chromosome microarray, and SMA gene test were performed but there were no specific findings.

He received intensive rehabilitation from 12 months to 4 years of age, receiving physical therapy and occupational therapy once daily, and cognitive therapy and speech therapy once a week. According to the Bayley scales III conducted at 24 months, He was confirmed at 10 months in cognitive ability, 10 months in language, 10 months in fine motor skills, and 9 months in gross motor skills. He still showed hypotonia and tried to stand up and maintain his position, but he quickly tried to sit down. When provided with an interesting object, crawling was possible, but it was difficult to maintain interest.

At 4 years old, he could stand up and walked on his own, but his balance was very unstable. It was possible to stack about 3 cubes, but it was difficult to draw a circle, and although pointing was possible, there was no meaningful speech at all.

Conclusion

If overall developmental delay and hypotonia are observed, Brainbridge-Ropers Syndrome disease should be suspected.

Introducing Angel Legs M20: A Wearable Robotic Solution for Lower Limb Rehabilitation in NMD

Chang-Hwan Ahn¹, Young-Hwan Lim¹, Yu-Sun Min^{1,2*†}

Department of Rehabilitation Medicine, Kyungpook National University Chilgok Hospital¹, Department of Rehabilitation Medicine, School of Medicine, Kyungpook National University²

Angel Robotics` product, Angel Legs M20, is a wearable robotic device designed to assist gait training for patients with lower limb paralysis due to neuromuscular disorders such as cerebral palsy, spinal cord injury, stroke, spina bifida, developmental disorders, and muscular diseases. Unlike conventional rehabilitation robots that operate on a treadmill with pre-programmed trajectories, Angel Legs M20 utilizes an `overground` training method, allowing patients to walk on the ground while receiving necessary assistance to supplement their strength, thereby enhancing patient engagement and rehabilitation outcomes. The device is equipped with six training programs, including standing, sitting, standing up, flat-ground walking, stair climbing, and squatting, and features 20 adjustable levels of assistance to tailor the training to the patient`s functional status.

In patients with Guillain-Barré Syndrome (GBS), we measured gait parameters, gait variability, gait asymmetry, and cyclogram using the Angel leg robot. Gait training with the Angel leg robot may serve as a valuable strengthening exercise, potentially aiding in the recovery of GBS patients. Particularly for pediatric patients with lower limb weakness, this approach is expected to significantly enhance motivation during exercise.

Rehabilitation of ventilator-dependent spinal muscular atrophy type II until return to home: A case report

Mr. Ferdian Musthafa MD. ^{1**†}, Ferdian Musthafa¹

Brawijaya University, ¹

Purpose

Spinal muscular atrophy (SMA) is a genetic neuromuscular condition characterized by progressive muscle weakness and atrophy due to the loss of lower motor neurons. The prognosis varies depending on the type of SMA. Respiratory complications are the primary cause of death in SMA. This study aims to contribute to the understanding of effective rehabilitation strategies for SMA type II patients, demonstrating the importance of multidisciplinary care and the potential for patients to return home with ongoing respiratory support.

Scope

focusing on the patient's initial condition, diagnostic findings, rehabilitation strategies, outcomes, and the broader implications of managing SMA type II

Methods

An 11-year-old female child with SMA type II was diagnosed by genetic testing and had respiratory failure on the ventilator. The patient had complained of tetraparesis since 2 years old. Physical examinations reveal unconsciousness due to sedation, rhonchi in the lung, decreased physiological reflex, hypotonus, and also contracture on her knee and ankle. Laboratories results were leucocytosis and alkalosis metabolic. A chest x-ray showed pneumonia, atelectasis, and scoliosis. The pediatric logistic organ dysfunction (PELOD) score was 7, and the pediatric sequential organ failure assessment (pSOFA) score was 9. Current planning included proper positioning, gradual mobilization, passive breathing exercises, secret mobilization, airway clearance, passive range of motion (PROM) exercises, and knee and ankle stretching.

Results

After 4 months in intensive care, the patient was fully conscious. Respiratory support is provided by bilevel positive airway pressure on the tracheostomy. The revised Hammersmith scale (RHS) is 5. Pediatric quality of life (PedsQL): 28. Although the patient had total dependent activities daily (ADL) provided by her parents, she was discharged with continued respiratory support.

Conclusion

SMA type II is a progressive neuromuscular disease with a poor prognosis. Patients can survive in intensive care and be discharged with respiratory support if they receive appropriate interventions, rehabilitation, and total support from their caregivers

Rehabilitation challenge in pediatric patients after diabetic coma in intensive care: a case report

Mr. Ferdian Musthafa MD. ^{1**}, Rosalyna Pudji Hapsari¹

Brawijaya University, .¹

Purpose

Diabetic ketoacidosis (DKA) is a common complication of acute hyperglycemia in children with diabetes mellitus type I. DKA can cause cerebral edema and, in rare cases, diabetic coma. This condition can have a cognitive and emotional impact on their recovery and rehabilitation. This study presented the rehabilitation challenge of early mobilization in the intensive care unit.

Scope

The scope of this study is centered on the rehabilitation and recovery of a pediatric patient with severe DKA, highlighting the importance of early psychological intervention and a multidisciplinary approach to rehabilitation.

Method

Methods A 13-year-old girl with severe diabetic ketoacidosis who had already had a tracheostomy regained consciousness after 1 month of intubation. She had complained of a cough and a secret from the tracheostomy. Physical examination revealed minimal rhonchi on the right medial and lower lobes and the left upper and medial lobes, a decrease in manual muscle testing (MMT) at 2/2 and 3/2, and mobilization of the patient still at 45 degrees. The random blood glucose was 186. The chest x-ray showed pneumonia and a left pleural effusion. A head CT scan revealed an acute infarct at the left capsule externa. Current planning included early mobilization, active assistive range of motion (AAROM), breathing exercises, and clapping. The Barthel index was 4 (total dependent). The patient refused to undergo mobilization and training.

Result

Results The patient consulted a psychiatrist and was diagnosed with an organic mood disorder. Although mobilization was delayed, the patient gradually mobilized after cognitive behavior therapy and reinforcement from her parents. She was now able to walk with a walker. The Barthel index was 15. And MMT was 4/3/4/3.

Conclusion

A holistic approach to rehabilitation for pediatric after-coma Diabetes involves a comprehensive and multidisciplinary strategy that addresses the physical, emotional, and cognitive needs of the patient.

Rehabilitation Strategies for Femur Fractures in Complete Spinal Cord Injury

Min Cheol Ha^{1*}, Seongeun Park¹, Su Ji Lee¹, Ji Cheol Shin^{1†}

Department and Research Institute of Rehabilitation Medicine, Severance Hospital, Yonsei University College of Medicine, Seoul, Republic of Korea¹

Femoral fractures in patients with complete lower limb paralysis are challenging due to impaired weight-bearing and muscle function, which can lead to prolonged recovery or nonunion despite surgery. This case report aims to discuss strategies used to promote bone healing and enhance functional independence in patients with bilateral femur shaft fractures with complete spinal cord injuries.

In Case 1, a 45-year-old male with L4 burst fracture, cauda equine injury, complete paraplegia, and bilateral femur shaft fractures is described. In Case 2, an 18-year old male with C6/7 dislocation, complete tetraplegia, bilateral sciatic nerve injuries and femur shaft fractures is described. Both cases underwent intramedullary nailing at other institutions; however, upon admission to our rehabilitation center, neither had achieved bone union (Figure 1A, 1B). Our rehabilitation treatment emphasized a weight reduction orthosis with specialized components, coupled with electrical stimulation therapy and a tilt table standing program. Both cases achieved successful bone union and improved functional independence (Figure 2A, 2B).

This case report highlights effective strategies for promoting bone union and functional recovery in patients with bilateral femur fractures and complete lower limb paralysis. Prolonged immobility and altered bone metabolism pose challenges for delayed healing. A weight reduction orthosis was crucial for achieving stable weight-bearing, complemented by electrical stimulation therapy to stimulate muscle contraction and periosteal response for those with complete lower limb paralysis. These interventions aimed to expedite bone healing beyond natural processes. This case underscores the importance of effective strategies in managing complications such as fractures in individuals in complete lower limb paralysis who are unable to achieve adequate weight bearing.



Fig 1. A. Case 1 initial femur fracture x-ray. B. Case 2 initial femur fracture x-ray.

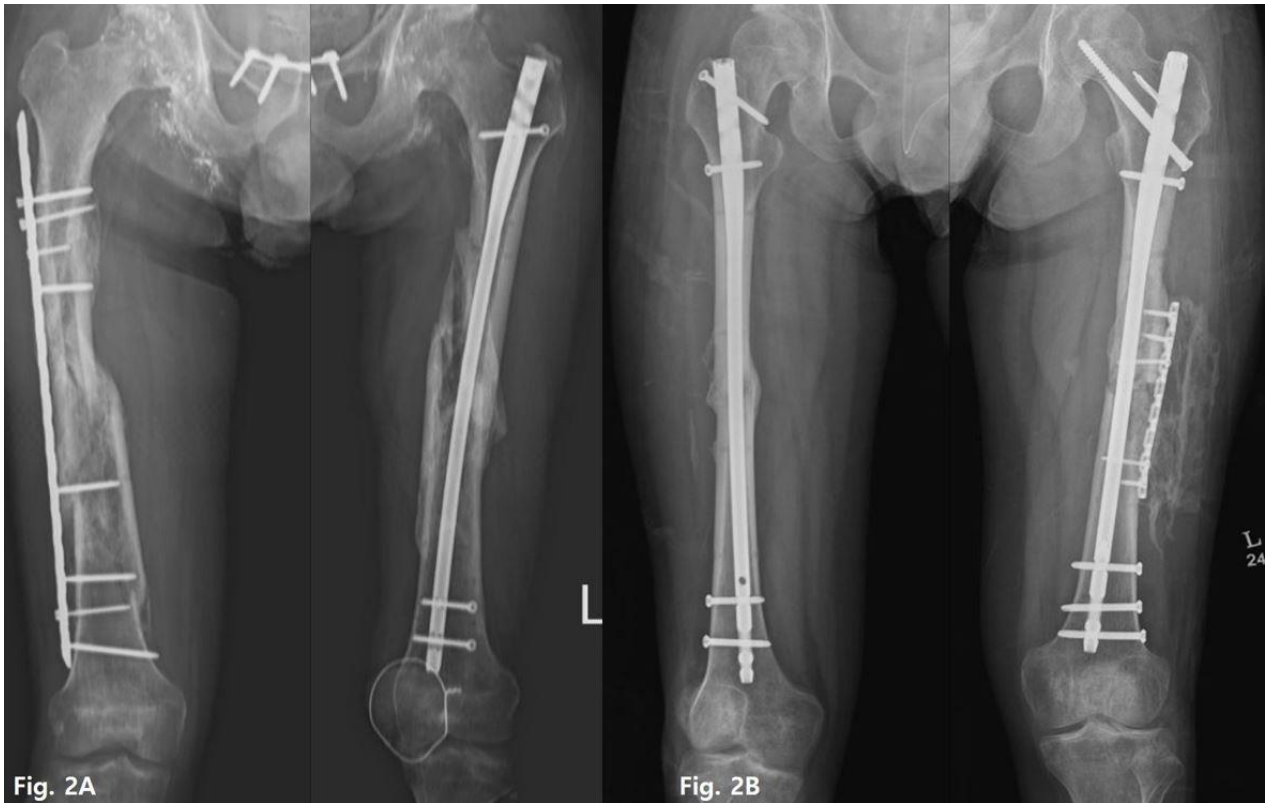


Fig 2. A. Case 1 follow up femur fracture x-ray. B. Case 2 follow up femur fracture x-ray.

Spinal Cord Infarction with Concurrent Stroke and Myocardial Infarction in Atrial Fibrillation

Hae-Yeon Park^{1**}, Jisoo Park¹, Jisun Bae¹, Dongwook Song¹, Sun Im¹, Geun-Young Park¹

Department of Rehabilitation Medicine, Bucheon St. Mary's Hospital, College of Medicine, The Catholic University of Korea¹

Introduction

Atrial fibrillation is a well-known risk factor for thromboembolic events. However, the simultaneous occurrence of embolic stroke, myocardial infarction, and spinal cord infarction in a single patient is rare and uncommon in clinical practice. This case report discusses a 66-year-old man who presented with these concurrent embolic events.

Case report

A 66-year-old man with a past medical history of hypertension, diabetes, and dyslipidemia arrived at the hospital presenting with left hemiplegia with MRC grade IV muscle strength. He was diagnosed with a right middle cerebral artery territory embolic infarction. During the evaluation to determine the cause, he was also diagnosed with atrial fibrillation. An echocardiogram revealed akinesia in the basal to mid-inferolateral region of the left ventricular (LV) wall and hypokinesia in the basal to mid-anterior, anterolateral, basal inferior, apicolateral, anterior, and apical cap regions of the LV wall. These findings suggested a recent ST-elevation myocardial infarction (STEMI) in the posterior wall, and the patient underwent coronary angiography with percutaneous coronary intervention.

Around that time, the patient also complained of sudden paraplegia accompanied by severe back pain. A physical examination revealed reduced deep tendon reflexes without any pathological reflexes. Both lower extremities exhibited grade zero muscle strength, but there were no definite sensory deficits. Lumbar spine MRI showed no definite abnormal findings, and an electrodiagnostic study showed normal results. However, an evoked potential study indicated a central nervous system lesion at the spinal level. Based on the physical examination and evoked potential test results, a spinal cord diffusion MRI was performed. MRI revealed segmental T2 high signal intensity with diffusion restriction at the T11-L1 level of the spinal cord, primarily affecting the anterior cord, symmetrically and bilaterally (Figure 1). In consultation with the neurosurgery department, the patient was advised to continue with the novel oral anticoagulant that had already been prescribed for atrial fibrillation.

Conclusion

This case emphasizes the rare and challenging presentation of simultaneous embolic stroke, myocardial infarction, and spinal cord infarction in a single patient with atrial fibrillation. The patient's presentation with multiple embolic events required a comprehensive diagnostic approach, including echocardiography, MRI (brain and spine), and electrodiagnostic studies, to identify the underlying causes and the extent of the embolic events. This case highlights the importance of considering multiple potential embolic sources in patients with atrial fibrillation and stresses the need for careful monitoring and prompt intervention to address the diverse and severe complications that may arise.

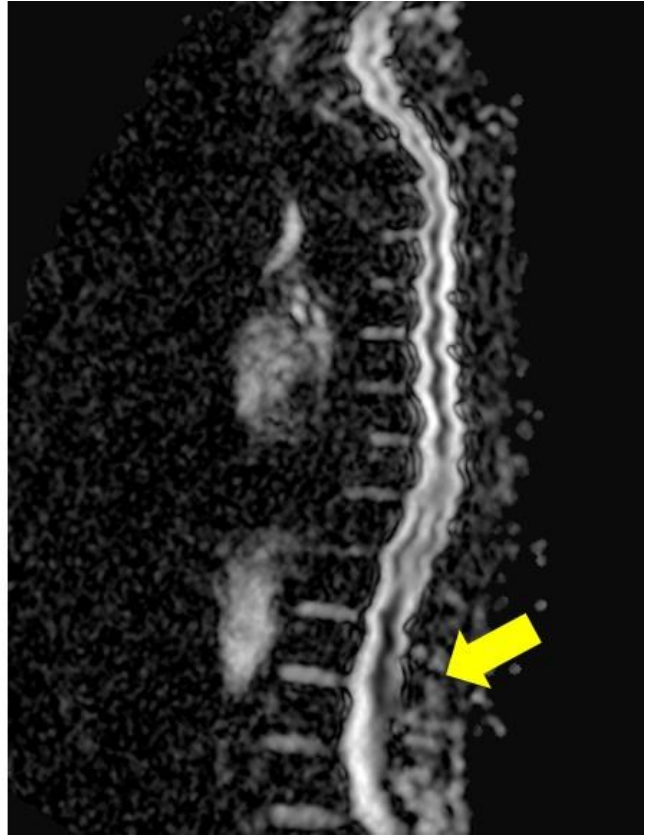


Figure 1. Images of spinal cord diffusion MRI of the patient, showing diffusion restriction at the T11-L1 level of the spinal cord.

Application of Upper Limb Assistive Devices for Function Recovery in Cervical Spinal Cord Injury

Jung Eun Lim^{1*}, Duk Youn Cho¹, Onyoo Kim^{2†}

National Rehabilitation Research Institute, National Rehabilitation Center and Hospital¹, Department of Rehabilitation Medicine, National Rehabilitation Center and Hospital²

Objective

Patients with cervical spinal cord injury (SCI) often face issues of muscle weakness in the upper limb proximal region and reduced range of motion in the joints. While various rehabilitation training and assistive devices are utilized to improve upper limb function, there is a lack of devices specifically designed to assist the proximal upper limb muscles such as the shoulder and elbow. Mobile arm support (MAS) is primarily used for patients with muscle weakness due to neuromuscular disorders, but it can also be utilized as a tool for daily life independence in spinal cord injury patients. The purpose of this study is to assess the effectiveness of applying MAS to cervical spinal cord injury patients for functional recovery.

Methods

Cervical SCI patients with more than one year post-onset were trained using an exoskeleton-type upper limb assistive device, the Wilmington Robotic Exoskeleton (WREX), in the form of MAS. Participants wore the WREX on their right arm and performed tasks included in the Jebsen Taylor Hand Function Test (JTHFT). The intervention consisted of six sessions conducted over two weeks, with each session lasting 30 minutes and conducted three times per week. Evaluation was performed before training and after six sessions using JTHFT and Manual Muscle Testing (MMT) of the shoulder region. Results were analyzed based on the outcomes of the right arm.

(Fig 1. Wilmington Robotic Exoskeleton)

Results

A total of 20 participants took part in this study. The distribution based on the American Spinal Injury Association Impairment Scale (AIS) was as follows: AIS A (9 participants), AIS B (3 participants), AIS C (4 participants), and AIS D (4 participants), with neurological injury levels ranging from C2 to C6. JTHFT scores improved from 8.86 ± 14.64 before training to 9.24 ± 15.21 after training. MMT showed improvements in shoulder flexion (from 2.75 ± 1.02 to 2.90 ± 1.07), extension (from 3.00 ± 0.97 to 3.25 ± 0.96), abduction (from 2.85 ± 1.09 to 3.00 ± 0.97), and adduction (from 2.65 ± 1.04 to 2.90 ± 1.17).

(Fig 2. Average of Jebsen Taylor Hand Function Test)

(Fig 3. Average of Manual Muscle Testing)

Conclusions

This study demonstrates that the WREX assistive device effectively aids cervical SCI patients with upper limb proximal muscle weakness. The results indicate overall improvements in upper limb function and shoulder strength. Despite difficulties in upper limb functional use due to proximal muscle weakness in cervical SCI patients, MAS was found to be beneficial for this patient population regardless of hand function. These findings underscore the potential of MAS training in enhancing independence and quality of life for cervical SCI patients.

Acknowledgment This study was supported by a grant (NRCTR-IN21002) of the Translational Research Center for Rehabilitation Robotics, Korea, Korea National Rehabilitation Center, Ministry of Health and Welfare, Korea.



Fig 1. Wilmington Robotic Exoskeleton

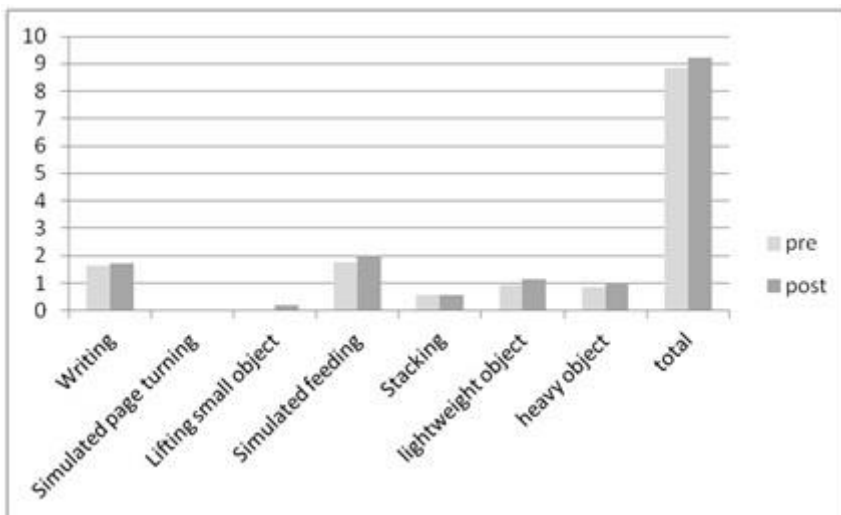


Fig 2. Average of Jebsen Taylor Hand Function Test

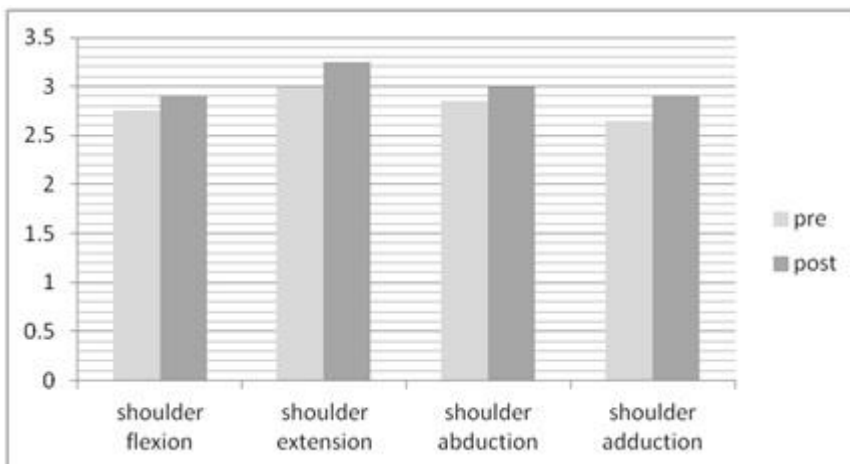


Fig 3. Average of Manual Muscle Testing

Cervical Cord Injury with Brain Injury Following Playing Bubble Soccer; a Case Report

Byeong Seong Kang¹, Sun Geon Yoon², Dongseok Yang^{3*†}

Department of radiology, Ulsan University Hospital ¹, Department of neurosurgery, Ulsan University Hospital ²,
Department of rehabilitation medicine, Ulsan University Hospital ³

Introduction

Bubble soccer, a variation of traditional soccer, is growing in popularity worldwide. In this full-contact sport, players encased in large, air-inflated suits that provide protection while allowing full-contact play. Despite being marketed as one of the safest sports by bubble soccer companies, it has a relatively higher injury risk compared to other soccer variations. Here, we report the first case of a patient with a complete C4 cord injury combined with a subdural hematoma following bubble soccer. Case presentation: During a company game, a 36-year-old male collided head-on with an opponent. We analyzed in detail using video footage. The collision occurred when the patient's head impacted the opponent's head as they leaned forward to bump each other. After the collision, the patient fell backward, and the posterior part of his head hit the ground. His suit collapsed completely at the point of impact (Figure -1A). He immediately lost consciousness and motor function in all four limbs. He was transferred to a regional trauma center of a tertiary hospital. Initial examination revealed complete tetraplegia at the C4 level. Initial brain CT images revealed a subdural hematoma with a skull fracture (white arrow) in the left frontal area (Figure- 1B). Sagittal CT image showed a C4 teardrop fracture. The axial view showed reduced anteroposterior diameter of the spinal canal with a fracture of the posterior vertebral body (Figure -2A). Sagittal T2 T2-weighted magnetic resonance (MR) image showed hypointensity of the central cord (light blue arrow) with hyperintensity of the peripheral cord at the C4 level. Sagittal T2 short inversion time inversion-recovery (STIR) MR images showed hyperintense intramedullary edema from the C4 level to the upper part of the C5 level, with central hypointense hemorrhage at mid-C4(light blue arrows). Axial T2 MR images showed a mixed signal lesion with central hypointensity and peripheral hyperintensity. Axial STIR images showed two dark spots in the central medullary area (light blue arrows) surrounded by hyperintensity, with fractures of both laminae (red arrows). One day postonset, the patient underwent a C4 corpectomy with anterior fusion of the C3 and C5 vertebral bodies. By day 10 postonset, he was able to breathe without ventilator support and was transferred to the department of rehabilitative medicine by 3week postonset. Over a 15-day period, the patient's pulmonary function improved significantly: forced vital capacity increased from 26% to 50%; forced expiratory volume in one second increased from 19% to 54%; and peak cough flow improved from 70 L/min to 140 L/min. Two months postonset, his tracheotomy was decannulated. Despite these improvements, no neurological recovery was observed up to six months postonset. Conclusion: This case highlights the potential for severe cervical cord and head injuries following bubble soccer.



Fig.1A

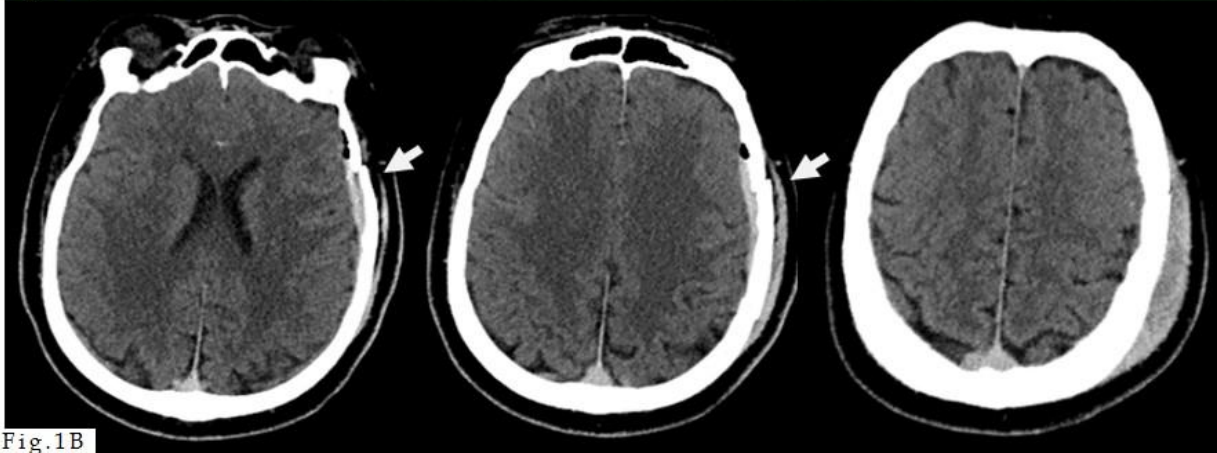


Fig.1B

Video footage indicated the collision occurred when the patient's head impacted the opponent's head as they leaned forward to bump each other. After the collision, the patient fell backward with his knees flexed, and the posterior part of his head hit the ground. Despite wearing a large inflated bubble suit, the suit collapsed completely at the point of impact (Fig. 1A). Brain CT showed a subdural hematoma with a skull fracture (white arrow) in the left frontal area (Fig. 1B).

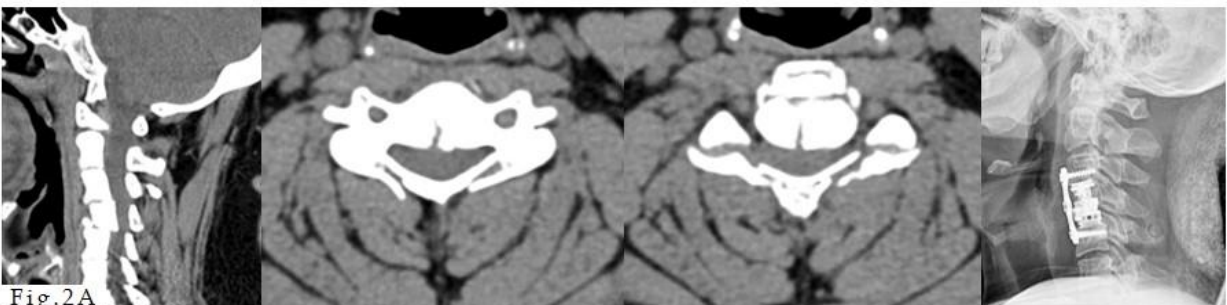


Fig.2A

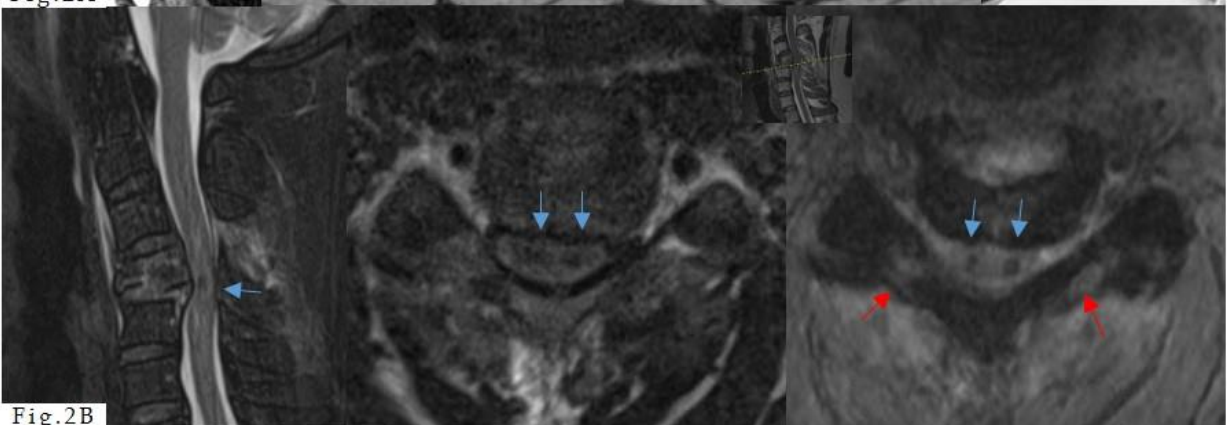


Fig.2B

Cervical CT on the sagittal view showed a C4 teardrop fracture. The upper C4 column was displaced posteriorly relative to the lower column. The axial view indicated a reduced spinal canal anteroposterior diameter and widening with a fracture of the posterior vertebral body. Cervical lateral view showed a C4 corpectomy with anterior fusion of the C3 and C5 vertebral bodies (Fig. 2A). Sagittal T2 short inversion time inversion-recovery (STIR) images showed hyperintense intramedullary edema from the C4 level to the upper part of the C5 level, with central hypointense hemorrhage at mid-C4 (light blue arrows). Axial T2 MRI showed a mixed signal lesion with central hypointensity and peripheral hyperintensity. Axial STIR images showed two dark spots in the central medullary area (light blue arrows) surrounded by hyperintensity, with fractures of both laminae ((red arrows) (Fig. 2A)).

Successful Extubation of a Brainstem Tumor Patient Through ICU Rehabilitation: A Case Report

Jae Sik Seo¹, Seon Jun Yoon¹, Bo Kyung Ha³, Seung Heon Cha⁴, Myung-Jun Shin^{1,2}, Myung Hun Jang^{1,2*}, Yong Beom Shin^{1,2†}

Department of Rehabilitation Medicine, Biomedical Research Institute, Pusan National University Hospital, Busan, Korea¹, Department of Rehabilitation Medicine, Pusan National University School of Medicine, Busan, Korea², Department of Nursing, Regional Trauma Center, Busan, Korea³, Department of Neurosurgery, Pusan National University Hospital, Pusan National University School of Medicine, Busan, Korea⁴

Introduction

Brainstem cavernous malformations (BCMs) exhibit higher morbidity and mortality compared to other cerebral cavernous malformations. Issues such as tetraplegia and respiratory distress are contributing factors to weaning and extubation failure. This case report presents a patient who successfully underwent extubation following strategic rehabilitation treatment in the ICU after surgery.

Case presentation

A 38-year-old female patient presented with gait disturbances that began approximately one week prior and was admitted to the ICU due to cardiac arrest. An MRI revealed a hemorrhage in the spinal cord, leading to the diagnosis of a BCM, for which she underwent craniotomy and hematoma evacuation.

Preoperatively, the physical examination indicated locked-in syndrome due to the mass lesion, and the negative inspiratory force (NIF) was significantly reduced at -10 cmH₂O while intubated. Post-surgery, it was crucial to enhance the recovery of respiratory muscles and improve the ability to clear secretions to prevent pulmonary complications and achieve successful extubation. To accomplish this goal, mobilization and chest physiotherapy were implemented in the ICU.

Alongside these interventions, periodic neurological assessments were conducted, measuring NIF as indicators of weaning and peak expiratory flow (PEF) as indicators of secretion clearance. Ultrasound (US) evaluations were also performed. The physical examination revealed that the recovery of strength in the left upper and lower extremities was slower compared to the right side. One-week post-surgery, chest X-ray showed elevation of the left hemi-diaphragm, and diaphragm US indicated a lack of contraction on the left side (Fig 1).

To facilitate respiratory muscle recovery, inspiratory muscle training was conducted, along with positioning and lung recruitment maneuvers to resolve atelectasis, as well as mechanical insufflation-exsufflation. Extubation was performed when the desired PEF value was achieved (Fig 2). Preventing the deterioration of atelectasis in the left lung was essential, and post-extubation management included the application of non-invasive ventilation via a full-face mask.

Subsequently, the patient's dysphagia improved, allowing for the initiation of oral feeding. After three additional weeks of rehabilitation without any respiratory complications, she was discharged.

Conclusion

ICU rehabilitation can greatly assist in the patient's rapid recovery and prevention of complications. As demonstrated in this case, implementing a goal-oriented rehabilitation strategy through continuous respiratory function assessment allows for high-quality rehabilitation, ultimately ensuring better patient outcomes.

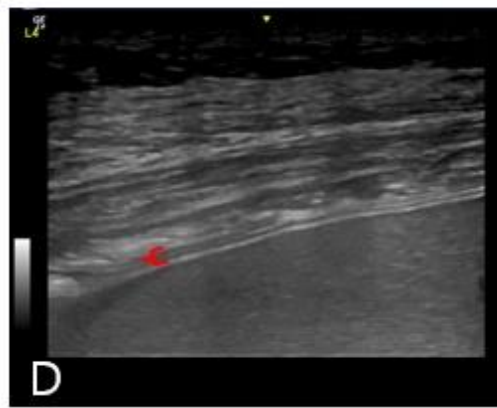
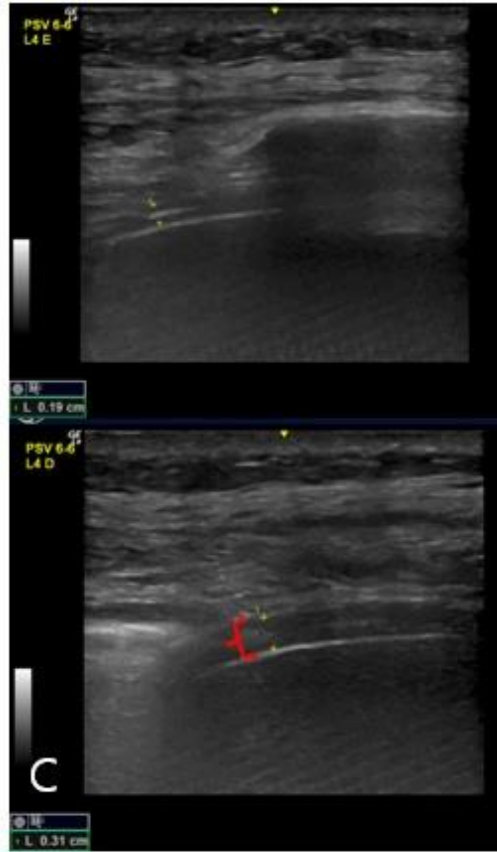
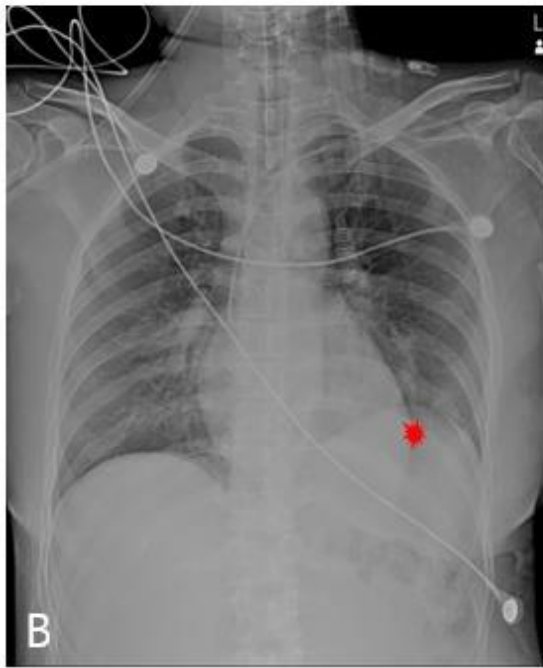


Figure 1. (A) CXR, on POD1. (B) Elevation of the left diaphragm on POD 7. (C) Changes in the left diaphragm thickness during DB by US on POD 1. (D) Absence of contraction of the left diaphragm during DB on POD 7. *CXR, Chest x-ray, POD, postoperative day, DB, deep breathing, US, ultrasound

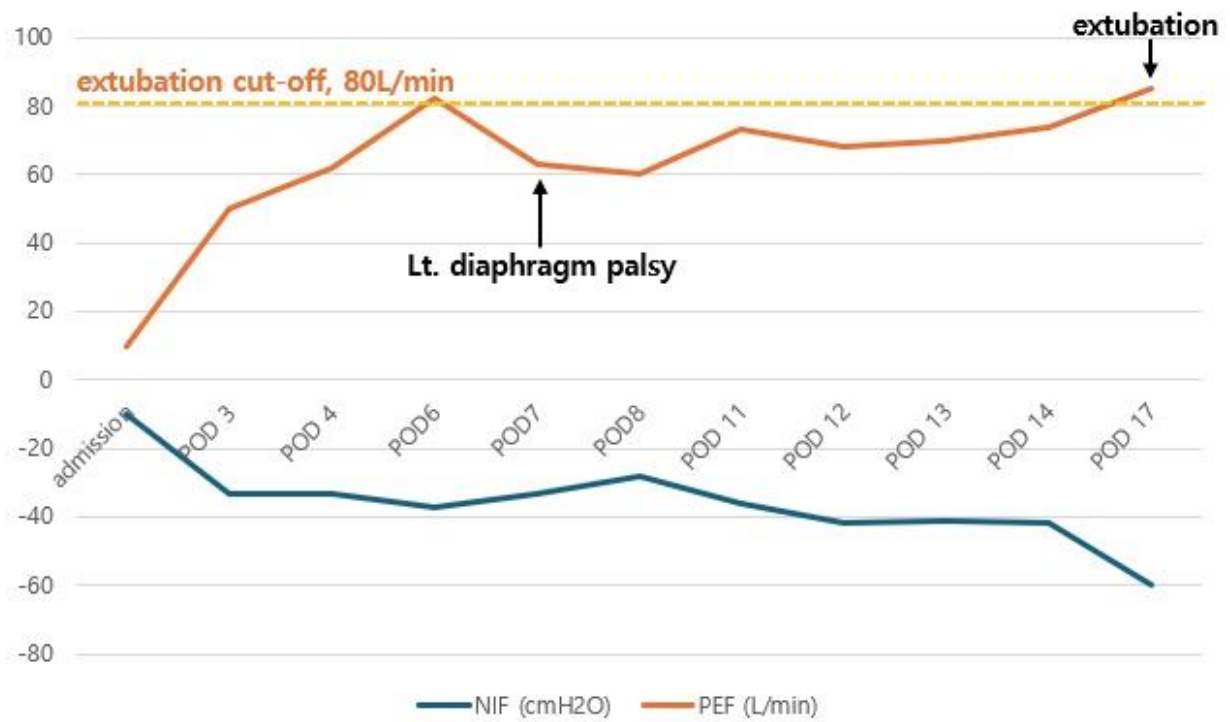


Figure 2. Serial pulmonary function assessments measured up to extubation.